RUSSIAN GEOGRAPHICAL SOCIETY

FACULTY OF GEOGRAPHY,
LOMONOSOV MOSCOW STATE UNIVERSITY

INSTITUTE OF GEOGRAPHY,
RUSSIAN ACADEMY OF SCIENCE

Vol. 12 2019 No. 02

GEOGRAPHY ENVIRONMENT SUSTAINABILITY

Special Issue «Climate-vegetation interaction:
natural processes versus human impact»

Issue Guest Editors: Elena Yu. Novenko,
Pavel E. Tarasov, Alexander V. Olchev

EDITORIAL BOARD

CONTENTS

CONTENTS

SPECIAL ISSUE

Maria A. Pitukhina[1], Oleg V. Tolstoguzov[2*] and Irina Chernyuk[3]
[1] Petrozavodsk State University, Budget Monitoring Center, Petrozavodsk, Russia
[2] Karelian Research Center of Russian Science Academy, Institute of Economy, Petrozavodsk, Russia
[3] independent researcher, researcher at Institute of Baltic Studies in Finland (2010-2012)
*** Corresponding author:** olvito@mail.ru

RUSSIAN-SPEAKING DIASPORA IN FINLAND AS A PUBLIC DIPLOMACY TOOL

ABSTRACT. The article deals with complex studies of the Finnish case particularly migrants' inclusion analysis into local cultural and political environments (as conditions to cultural and political environment stability) as well as public diplomacy impact evaluation of an important «soft power» tool where migrants role is rather high. Authors scrutinize migrants' interaction with the environment, outline cause-and-effect links of this interaction, and unveil external factors that influence the respondents' political behavior. The research method is based upon interviews, which result in respondents' typology development, political information channels were defined, and the influence of education and social inclusion upon political communication was characterized. This method helps to perceive migrants' integration policy at example of Finland, the fourth most attractive country in the world in accordance with the Migrant Integration Policy Index. Finnish experience could be highly useful for Russia in terms of both national migration policy development. The resulting characteristics of migrants' political communication might be of high interest in terms of migration policy regulation and understanding the issue of migration quotas, help to predict structural changes in society, also to provide the basis for making decisions on the effective use of public diplomacy tools.

KEY WORDS: sustainable development, political communication, migration policy, integration policy, migrants' survey, public diplomacy

CITATION: Maria A. Pitukhina, Oleg V. Tolstoguzov and Irina Chernyuk (2019) Russian-speaking diaspora in Finland as a public diplomacy TOOL. Geography, Environment, Sustainability, Vol.12, No 2, p. 6-17
DOI-10.24057/2071-9388-2018-31

INTRODUCTION

In 2017 the number of migrants reached 258 million people. Over the past 17 years the total number of migrants has increased from 173 million by 49% according to the International migration report (Un.org 2017). The growth of migrants' mobility and the impact of migration flows on almost all countries' development include the international migration issue.

Migrants' studies (including surveys) are highly important in terms of migration policies analysis in the European countries. They are performing migrants' surveys regularly for accessing migrants' living conditions, political preferences etc. The best foreign practice has shown that migrants' studies are highly important in terms of society structural changes projection.

Migrants not only affect population dynamics, change its structure, but also to some extent influence local community life: the larger the proportion of migrants, the greater their impact on the local community.

In order to obtain up-to-date information on both state and socio-cultural perspectives a competent migration policy development is highly necessary taking into account different aspects of globalization phenomenon.

Therefore, it is necessary to research migrants' inclusion mechanisms in local cultural and political environment as a condition for socio-cultural sustainability as well as public diplomacy as the most important «soft power» tool where migrants' role is rather high.

The goal of the article is both to research on problems dealing with the Russian-speaking diaspora in Finland as well as public diplomacy tools (media analysis, social networks, social groups) aimed at migrants' integration policy upgrading in local communities.

Nowadays (both in Russia and in the world) the research is not enough devoted to migrants' political communication.In particular, in Russia political communication isscrutinized in the following areas: power as a political communication (Timofeeva 2010), political communication theory (Timofeeva 2012), sociology of political communication (Diligensky 1994), psychological aspects of political communication (Zimichev 2010;Olshansky 2001;Shestopal 2002;Yurev et al. 2005), information security impact on political communication (Panarin 2012), political communication as a way to deploy political order events (Anohina andMalakanova 2001); political communication as an independent phenomenon not as a function, but as a process (Solov'iev 2002); use of information and communication technologies (Zazaeva 2012).

Based upon a wide- known theoretical approaches in the field of migration - the so-called general migration theory (E.Ravenstein, Stoufer, E.Lee etc.), we shall consider the Russian-speaking diaspora integrating problems in Finland as well as some public diplomacy tools as a soft power resource (J.Nye) (E.Ravenstein 1889; S.Stoufer 1940; E.Lee 1966; J.Nye 1989). The issues of migrants' integration in local communities are unveiled in papers of S.Abashin, E.Varshaver, A. Rocheva, V.Mukomel etc. (S.Abashin 2012; E.Varshaver, A. Rocheva 2016; V.Mukomel 2011).Papers of St.Petersburgsociologists (O.Brednikova, O.Tkach, O.Zaporozhets) shall be also mentioned in terms of cross-border practices and neighborhood phenomenon analysis by the examples of Finland and Russia (Kaizer, O.Brednikova 2004).

MATERIALS AND METHODS

Official statistics both of the UN andnational statesis widely applied (Un.org 2017; EUROSTAT 2013 etc.). Migrants' survey is the most important tool that allows to identify structural changes in society and to evaluate reasons for these changes (EuropeanSocialSurvey.org 2014). Migrants' surveys allow to supplement and provide more detailed information on statistics obtained from public information sources.

The research is also dealing with Migrants Integration Policy Index developed according to Barcelona Center for International Affairs and Migration Policy Group. This method embraces 7 areas of migrants' integration – labour market mobility, family reunion, education, political participation, long-term residence, access to nationality, anti-discrimination (according to Migrant integration policy index). Migrant integration policy index helps us to evaluate migrants' rights and wellbeing, analyze state migration policy, state's responsibility as well as develop recommendations on migrants' integration policy. This article deals with the one of the 7th integration areas in accordance with the Migrant integration policy index – migrants' political participation, in particular, Russian migrants' political communication in Finland (our case).

The research is based upon interviews, which result in respondents' typology development, political information channels were defined, and the influence of education and social inclusion upon political communication was characterized. Thus, for example, in Finland, migrants' personal data upon age, gender, country of origin, immigration country,

religion, marriage, date of entry is obtained from a variety of sources accumulated in one information system "Population Information System" under Statistical Agency of Finland. Information on migrants is accumulating from different confessions' parishes, hospitals and the Migration Service of Finland. In Finland, migrants need to obtain ID card necessary for work or medical assistance, and for this each migrant has to undergo a mandatory registration procedure in "Population Information System". Every year "Population Information System" staff is serving migrants and thus checking their residential address. In 2014 it turned out that 99% of migrants have the same address. Each month the information system generates final reports on changes occurred for the last month - «Population statistics service». At the end of each quarter the information system provides provisional statistics on population changes for the year («Quarterly population statistics»). Statistics on migrants is published annually: in electronic form in May and in paper form in June of each year («Population structure and vital statistics by municipality»).

Migrants' surveys allow to supplement the information system data from open sources and is used to achieve the following objectives:
1) to access detailed information on various parameters
2) to identify migrants sentiments
3) to define migrant problems
4) to get information that demands the response (for example, which materials migrants are reading).

The authors developed a questionnaire in order to achieve the research goal. The questionnaire included 30 questions and was divided into five main categories: political information sources, political dialogue, use of sources of information through the Internet, political participation, social status etc. Secondary questions were related to international news, national government, economic news, community events, and editorial columns of the local news.

RESULTS

Europe remains migrants' most attractive region. Largest migrants groups consist mostly of people coming from the Middle East and Africa. At the same time, migration is being characterized with irregularity: migrants' distribution across Europe can be characterized with both low and high concentrations. Rather different situation is being witnessed in Northern Europe.

Increase in both migrants' flows and concentrations reduces naturally the share of a recipient community: there is a significant increase of Arab origin population in France, of Turkish-Arab origin in Germany, of Indopakistan and-Arab origin in the UK.

Hereby we apply the Pareto rule in order both to analyze and evaluate influencing factor effectiveness. Migrants' excess of over 20% is known as a threshold after which socio-cultural relations structure changes significantly. The interval amounting to "10-20%" is a transition zone. It shows migrants increasing influence till a critical value. This is not an exact criterion, but rather a mnemonic rule that identifies an important meaning, namely a serious shift in a social environment.

Fig. 1-5 below provides data (Un.org 2017) for various European countries and regions, hatching corresponds to focus areas.

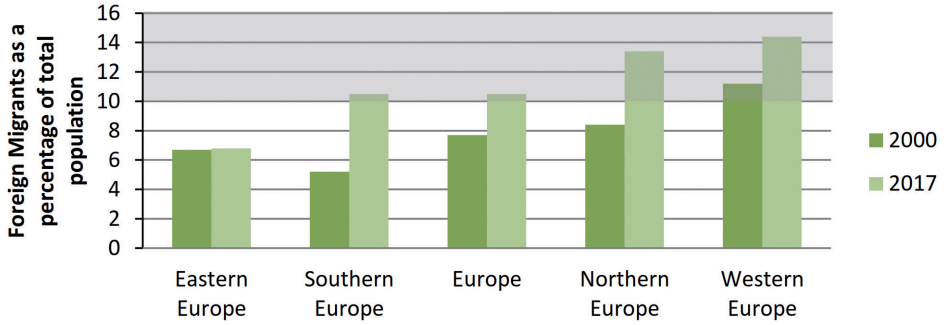

Fig. 1. Foreign migrants as a percentage of total population of Europe

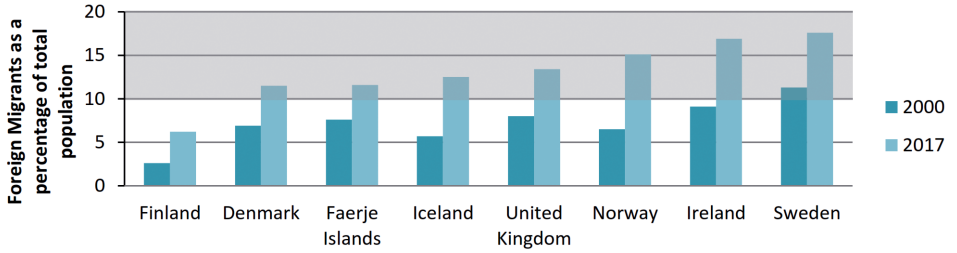

Fig. 2. Foreign migrants as a percentage of total population of Northern Europe

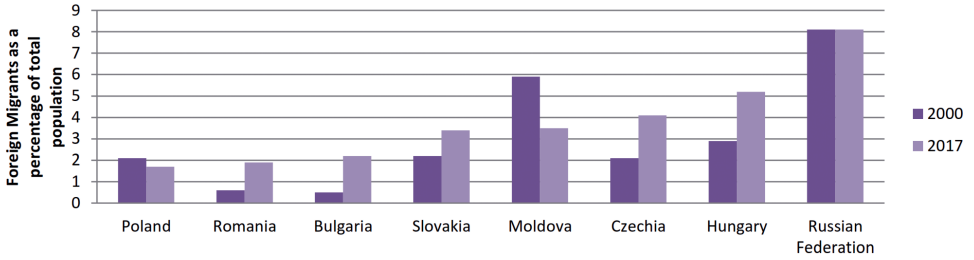

Fig. 3. Foreign migrants as a percentage of total population of Eastern Europe

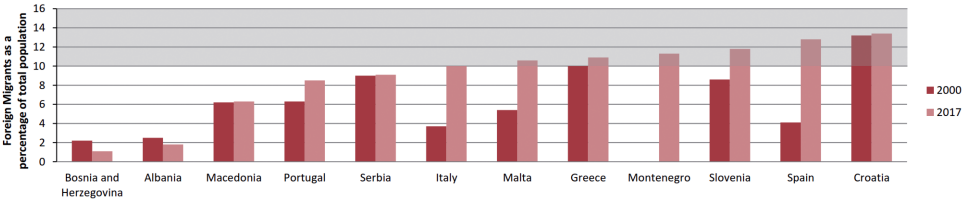

Fig. 4. Foreign migrants as a percentage of total population of Southern Europe

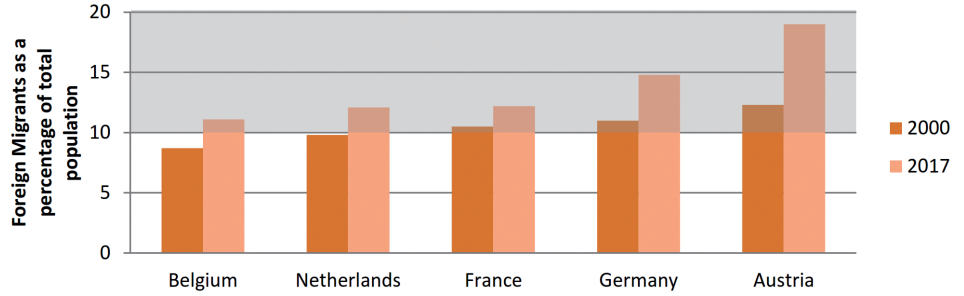

Fig. 5. Foreign migrants as a percentage of total population of Western Europe

There are three groups of countries to be shaped based upon Fig. 1-5 mentioned above. The first group of countries are without any significant migration challenges (migrants make up less than 10% of the recipient community in Finland and Central Eastern Europe), second group where migration challenges are pretty visible (migrants make up 10-15% in Croatia, Spain, Slovenia, Iceland, Denmark) and a third group, where migration challenges are highly critical (more than 15% of migrants in Germany, Sweden, Ireland, Austria, Norway).

Figures show that serious difficulties in trend preserving are being witnessed in Western and Northern Europe (in accordance with Pareto rule), while Northern Europe alongside with Southern Europe are showing much higher migrants' growth rates.

Finland stands out quite separately out of a number of some other Northern Europe countries, which is undoubtedly an interest for the research. Finland borders with Russia possessing a large diaspora of the Russian-speaking population (29,000 people) which turns out to be a serious public diplomacy resource in promoting "Russian world" abroad. Migration policy in Finland is considered to be highly adaptive, balanced, primarily preserving national interests and human capital. While analyzing reasons for Finland's success we are highlighting the main aspects - high human capital quality of foreign migrants coming to Finland, successful information dissemination for migrants coming to Finland, successful migrants' integration in a Finnish labour market.

Therefore, this region is highly attractive both from the point of view of migration impact upon local community as well as taking into account multiple economic and cultural ties with Russia. Therefore, it is important to explore some possibilities for public diplomacy tools application using Russian diaspora resource.

Among Northern Europe countries' Finland is of the great interest as a neighboring country having a large number of migrants from Russia, and as a country that pursues a successful migration policy aimed at local community sustainability. Finland's Future of Migration 2020 Strategy (Ec.europa.eu 2013) has been recently adopted and announces the following principles:
- Diversity will be valued as Finland's internationalization continues.
- Equality and equal opportunities will apply to everyone.
- Migration will enhance the wellbeing of the population and boost Finland's competitiveness.
- Migrants will be able to use their skills and contribute to the future development of society.
- Migration will be foreseeable and controlled.

Starting from the 1st of January 2015 an updated Finnish Non-Discrimination Act(Finlex.fi 2014) came into force authorizing the Non-Discrimination Ombudsman. Nowadays in Finland there are Non-Discrimination Ombudsman, Equality Ombudsman and Ombudsman for children, all three institutions are also aimed at migration policy regulation.

In accordance with Finnish statistics Russians were the largest migration group till 2010 (29 500) according to Statistics Finland (Stat.fi 2013). Nowadays the situation has changed. Russians (29 800) are the second largest groups after Estonians (38 000) (International Migration Outlook 2013). Today migration flow in Finland is mainly represented with 2 largest groups of migrants – 49% of Estonians and 39% of Russians according to International Migration Outlook (Oecd-ilibrary.org 2013).

For the last 5 years (2010-2015) migration outflow has dried out from Russia to Finland. For a long period starting from 1990-ies and till 2010 (about 20 years) basic reasons for active labour migration in Finland were: Inkeri Finns repatriation, international marriages, and refugees. However currently Finnish immigration policy is changing drastically–foreign labour migration flows from Russia are significantly reducing. One of the basic reasons is that Finnish government has fully stopped Inkeri Finns repatriation from Russia starting from the 1 July 2011. As a result Finnish migration policy has changed significantly.

Currently Russian diaspora in Finland is not studied well though, especially Russian migrants peculiar political communication traits. In this term, these characteristics are highly valuable from the point of view of migration policy regulation.

Russian migrants are the second largest group of migrants in Finland influencing potentially the political process. Here we have in mind that Russian migrants in Finland have a very strong instrument of influence - right to vote at municipal elections. According to the Finnish law – the Election Act (Finlex.fi 2016) – any citizen of any state has a right to take part in municipal elections. There is however additional two conditions which are living in the municipality in which the

vote is held (at least 51 days before election day) and stay in Finland for at least two years.

Let's consider Russian migrants' living in Finland survey results in order to identify their political communication characteristics. The research of Russian migrants organized in Finland is a qualitative one and allows both to develop and prepare basis for the more in-depth study. The aim of the research is to identify Russian migrants' relations with politics.

In general, 122 respondents took part in interviews. No doubt obtained data demands further approval by quantitative data but this research is mainly qualitative and aimed at analyzing interaction of the target group with an ambient environment.

Respondents were selected in accordance with the snowball effect. The respondent profile is presented with a Russian migrant living in Finland for more than 3 years, of Russian nationality, of full legal age. Age, education level and income level were not taken into consideration. The interview also revealed some additional characteristics of the sample.

After interview it became clear that 45%of respondents were not interested in politics ("idle respondents"), 45% - became "active respondents" were actively using political communication channels (media, social networks, internet, TV, social circles (family, job)). 10% of respondents were rather negative towards politics ("blocking respondents"): "I am interested only in my close people, I do not see any reason to spend my time on politics".13% of respondents participated in municipal voting. Finnish law is ensuring migrants' participation in municipal elections – "for those migrants who live at least 2 years in Finland and at least 51 days in the commune in order to involve them in the processes of integration" according to Election Act.

The most popular expression that served as a motive for respondents' typology was "try to follow up all the news". Thus, the respondents ranged from actively watching political events «to be in the swim» to never participating in elections, signing/ creating petitions "because that doesn't help", and never be interested in news but participating in elections "of course it's my duty, I have to vote" or "it is necessary to do something, chose if you remain silent this will happen all the time". In summary, 3 main types of respondents could be identified based upon their interest in politics: active, idle and blocking.

Active respondent. Most active respondents have aspiration to compare different sources of information, interest in politics of both Finland and Russia, as well as international and local political issues. Those, whose interest in political issues is high, can be divided to two further groups:
- those, who actually like to discuss politics with peers;
- and those, who are actively looking for political news but they are not that open to discussions and consider this knowledge only for their personal development.

Moreover, willingness to compare different sources of information often correlate with higher education.

Idle respondents are those, who would listen about political issues in the general daily news flow but would not try to find information about political topics themselves. They would listen to political discussion and even might slightly participate to it but would not initiate it themselves. Politics for them is a parallel world to which they never seek to interfere, but always watch it how it changes.

Blocking respondent. Mentioning politics brings negative emotions to members of this group. They generally have a skeptic approach towards political affairs. They would not participate to political discussions and would try to avoid them.
Thus, respondents' answers gave us an opportunity to categorize migrants' in accordance with the above mentioned types, and also to allocate channels of political information for migrants.

There were outlined 4 main channels of receiving political information by Russian migrants in Finland – internet, TV,

newspapers and social circles. It should be noted that information obtained by Russian migrants living in Finland is performed through a wide range of channels. However, it should also be mentioned another peculiar feature. Thus, for some respondents who don't know Finnish language or possess low knowledge itis difficult to access news in Finnish. Despite this, it is still believed that the most favorable conditions for migrants are established in Finland which is actively working on migrants' integration including Russian migrants also.

This is also proved by a wide range of news presented in Russian, for example, Internet news resources "YLE" and "Spectrum", information portals «Russian.fi», "Fontanka.fi", "Russian Finland", radio news in Russian language – "Sputnik".

Thus, the variety of sources from which the respondents received information on political events is reduced to the following basic 4 channels:
1.Newspapers (both printed and electronic) are divided in 3 groups:
- Russian newspapers: «Novaya gazeta», «Argumenty I facty», «Snob»;
- Finnish daily newspaper «Aamulehti» (second popular newspaper in Finland after «HelsinkinSanomat» and «TurunSanomat»);
- Finnish resources in Russian language «Spector» и «YLE».
2. Television - respondents prefer watching Russian channels such as ORT, NTV, RTR, TNT, Channel 5, the channel "Spas". Respondents particularly noted such political programs browsing as «K Bariery» on RTR channel and «Pyaterkapoekonomike» on «Spas» channel.
3. Internet sources used by respondents in order to learn political news - Newsru.com, Yandex.ru, Euronews, Facebook, Vkontakte, Odnoklassniki.
4. Small groups - another popular method of respondents political communication with co-workers and family members.
Migrants' surveys results draw the following conclusion - newspapers (in electronic and printed form) were used by active and idle respondents. There is also a study outlining that newspapers reading as well as participation in discussions motivate to participate in political activities (Sotirovic and McLeod 2001). At the same time it prevents from entertainment television programs viewing. Thus, according to the results people with higher interest in political events prefer to read newspapers and analytical articles, but refuse to participate in any political activity. Those who prefer TV programs to newspapers are trying to participate in the elections.

Different channels influence upon political communication intensity was also studied. Frequency of turning to different information sources (number of days per year when sources were viewed in relation with the total number of days) was used as an indicator characterizing migrants' political communication intensity. Thus, "1" is presented as a maximum (daily frequency) and minimum is corresponding to "0.03" which is several times per year.

The Fig. 6 shows the mean intensity of migrants' political communication depending on the type of source.

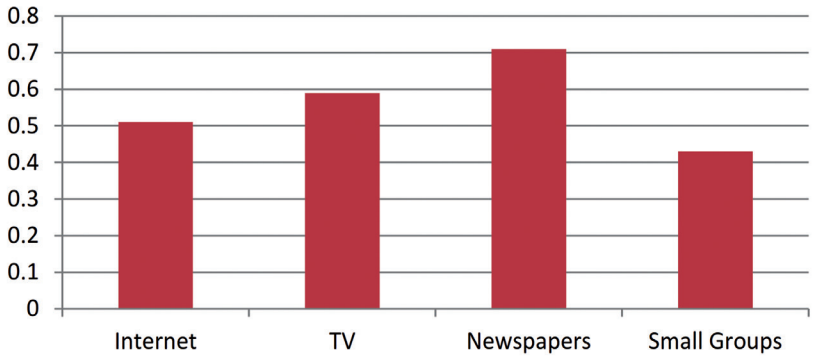

Fig. 6. Political communication intensity of Russian migrants in Finland based upon information channels

It is visible from the Fig. 6 that political communication is getting more intensive when a migrant gets information from newspapers. In part this might be due to predominant position of Finnish newspapers that usually publish much details on municipality/city life in Finland. Second place goes to TV, third –to Internet.

Migrants' survey results showed that migrants' political communication evaluation is highly important since it allows to identify the underlying trends in political preferences, to obtain information for a rapid response in certain cases as well as identify areas where migrant needs support or assistance.

DISCUSSION

The article is analyzing interaction of the target group with ambient environment, cause-and-effect relationship together with factors influencing respondents' behavior are outlined. Besides, migrants' interviews dealing with political communication trends will help to perform the projections of various shifts in the society.

According to study of Mutz and Mondak (2006), the most likely place for the policy debate is a working place. However, data obtained under the interview indicates that the situation has some limitations for Russian migrants in Finland. In the workplace, both in mixed teams (with Russian and Finnish colleagues) and in teams where only Russian migrants work there are some discussions on political topics. Colleagues discuss political events not only in Russia and Finland but also on international arena; however, in companies with international staff political themes often get avoid.

The probability of discussion upon conflicting topics is much higher within the family members, since the level of trust is high. In the workplace, employees often prefer to avoid such issues, though it is not an absolute rule, and if there's trusting relationship between colleagues it is quite possible to exchange opinions.

Under the interview it was also defined that the role of small groups has an impact on Russian migrants' political communication in Finland.

Under the interview, the correlation between level of integration into the host society and choice of an interesting event in Russian and Finnish societies was found. For example, young migrants (students, young migrants in a labour market), who grew up in Finland and are fluent in Finnish language, have a higher degree of social inclusion, which allows them to understand more easily what is happening in political arena.

Senior migrants often lack language skills, socialization experience in the new society (no work, no new education), often prefer to concentrate on Russian political events, obtaining information mainly from Russian media. However, this is not a widespread rule. In Finland there are Russian migrants who are active in the pre-retirement and retirement age. They continue to familiarize themselves with the host society, and to stay up to date with its main events. For some Russian migrants Finnish news daily newspaper "Aamulehti" is the main source of information, and they read it, even if you have to use the dictionary constantly.

Migrants survey's results confirmed previously identified relationship between level of education and breadth of political interests (see Hillygus 2005; Price and Zaller 1993) and have showed that migrants with higher education seek to educate a wider range of political topics. They used a wider range of information, including analytical programs and magazines. These respondents refer to news critically and compare news from various sources. The results of conducted migrants' interviews confirm this relationship again. Thus, "active" respondents with higher education are more eager to talk about information analysis from different (or even multilingual) sources ("I compare information from different sources, in particular, the Finnish sources – YLE, Russian news channels in Internet, British sources, then I can skype with my friends and ask how it is in reality").

Thus, the analysis of a wide range of news gives a clearer picture of the situation in a political world, and can provide a more solid basis for political communication and political participation later.

The research also proved the fact that migrants' social inclusion into host society is highly dependent on language knowledge. For confirmation of the hypothesis a causal analysis of the social inclusion impact upon political communication intensity was conducted. As an indicator, which characterizes Russian migrants' social inclusion we use factor of foreign languages knowledge, including Finnish and English. The final indicator for political communication intensity became the frequency of interaction with information sources (access to Internet sources, reading newspapers, watching TV, small group discussion etc.)

Knowledge of Russian language is accepted as a minimum factor of migrants' social inclusion. Knowledge of one foreign language (English or Finnish) correlated to average value of migrants' social inclusion. The maximum value of the factor is the knowledge of two or more foreign languages.

Fig. 7 below shows migrants' political communication intensity depending on foreign language knowledge.

Fig. 7 shows that migrants' political communication intensity is higher if a migrant knows one or more foreign languages, accordingly, he/she has an opportunity to get acquainted with a wide range of multilingual sources.

These results confirm the theory Sotirovich and McLeod (2001) that: "Education provides both knowledge and skills to work with information, and therefore, improves access to political process, at least, makes political participation more likely".

The survey results have showed that workers with higher education in general, seek to familiarize with a wide spectrum of political topics, and thus analyze events critically (see also (Kyhä 2011).

CONCLUSION

Complex studies of the Finnish case were performed dealing with migrants' inclusion into local cultural and political environments (as conditions to cultural and political environment stability) as well as public diplomacy impact of an important «soft power» tool where migrants role is rather high.

In this research we've investigated some unknown features of Russian migrants' political communication in Finland. We've identified some characteristics of political communication by applying interview method. The main factors that would influence interpersonal communication in politics among Russian migrants in Finland are explored.

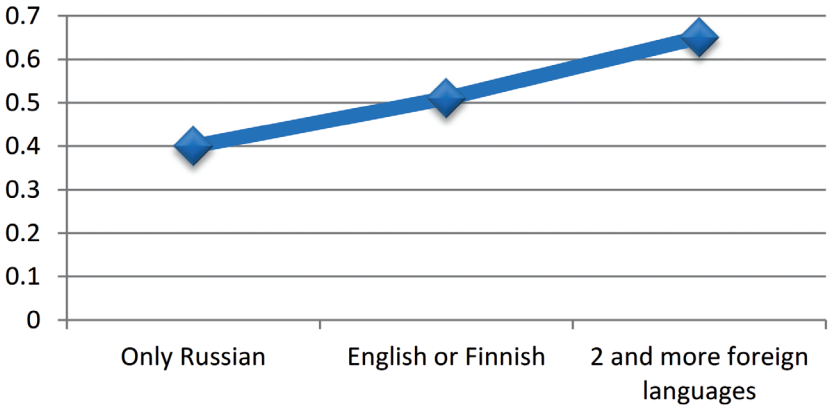

Fig. 7. Political communication intensity of Russian migrants in Finland depending on foreign language knowledge

Theoretically the research allowed both to analyze such an important aspect of migration policy as migrants' political communication and identify its key features.

It is worth noting that research has proved the fact that migrants' social inclusion into society is heavily dependent upon foreign language skills. The following characteristics of migrants' political communication were outlined as a result of survey data processing:
- respondents are distributed according to the following types of political communication: «active» – 45%; «idle» – 45%; «blocking» – 10%;
- relationship is found between level of education and both quantity and quality of media sources accessed by respondents, for example, only migrants with higher education accessed analytical journals;
- positive correlation between number of foreign languages and migrants' political communication intensity is found;
- following priorities for the use of political information sources among migrants is identified: Internet – 64%; TV – 45%, newspapers – 27%; small groups – 18%;
- impact of various information channels on political communication intensity of Russian immigrants in Finland is estimated;
- role of small groups in migrants' political communication is discovered.

So, at the workplace and, in particular, in companies with an international team, despite the presence of small groups (colleagues), political topics are shot out by tolerant reasons. On the contrary, political situation is discussed more frequently within the family.

The resulting characteristics of migrants' political communication might be of high interest in terms of migration policy regulation and understanding the issue of migration quotas. The findings would also help to predict structural changes in society, to assess the level of radicalization in society, provide the basis for making decisions on the effective use of public diplomacy tools. The growth of anthropogenous mobiles (movement of people, influence of cultures) is a phenomenon with many security contexts: it aggravates interethnic and interreligious contradictions between different ethno-cultural groups of the population, increases social tension, defragments the local community through the formation of ethnic enclaves.

ACKNOWLEDGMENTS

Within the framework of the RAS Presidium program «No.I.53 on fundamental scientific research within the framework of Fundamental Scientific Research Program of State Academies of Sciences for 2013-2020 «as well as the RFBR project» Live, work or go? Youth-well-being and viability (post) of extractive Arctic industrial cities in Finland and Russia".

REFERENCES

Abashin S. (2012). Central Asian Migration: Practices, Local Communities, Transnationalism, Ethnographic Review, 4, pp. 3-13. (In Russian).

Anohina N.V. and Malakanova O.A. (2001). Political communication. In: E.D. Meleskina, ed., Political process: main aspects and ways of analysis. Moscow: Infra-M., pp. 213-234. (In Russian).

Brednikova O. (2017). (Not) Return: Can Migrants Become Ex? Ethnographic review, 3, pp.32-47. (In Russian).

Cidob.org (2018). Barcelona Center for International Affairs Official Website. [online] Available at: http://www.cidob.org/en/ [Accessed 6 Jun. 2018].

Diligensky G.G. (1994). Social-political psychology. Moscow: Nauka. (In Russian).

Ec.europa.eu (2013). Finland's Future of Migration 2020 Strategy. [online] European Website on Integration. Available at: https://ec.europa.eu/migrant-integration/librarydoc/finland-future-of-migration-2020-strategy [Accessed 6 Juny 2018].

Epp.eurostaec.europa.eu (2013). EUROSTAT Official Website. [online] Available at: http://epp.eurostat.ec.europa.eu/tgm/table.do?tab=table&init=1&language=en&pcode=tps00024&plugin=1 [Accessed 14 Dec. 2015].

EuropeanSocialSurvey.org (2014). European Social Survey Official Website. [online] Available at: http://www.europeansocialsurvey.org/data/themes.html?t=immigration [Accessed 27 Jan. 2018].

Finlex.fi (2014). New Non-Discrimination Act entered into force. [online] Ministry of Justice of Finland Official Website. Available at: http://www.finlex.fi/fi/laki/kaannokset/2014/en20141325.pdf [Accessed 06. Jun. 2018].

Finlex.fi (2016). Election Act (714/1998; amendments up to 361/2016 included). [online] Ministry of Justice of Finland Official Website. Available at: http://www.finlex.fi/fi/laki/kaannokset/1998/en19980714.pdf [Accessed 27 Jan. 2018].

Hillygus D. (2005). The Missing Link: Exploring the Relationship between Higher Education and Political Engagement. Political Behavior, 27 (1), pp. 25-47.

Kaiser M., Brednikova O. (2004). Transnationalism and translocality (comments on terminology), Migration and the national state, pp. 133-146. (In Russian).

Kyhä H. (2011). Educated immigrants in employment markets. A study on higher educated immigrants' employment opportunities and career starts in Finland. [online] Doria. Available at: https://www.doria.fi/handle/10024/72519 [Accessed 27 Jan. 2018].

Lee E. (1966). A Theoryof Migration, Demography, 3, pp. 47–57.

Mukomel V. (2011). Migrant Integration: Challenges, Politics, Social Practices, The Russian World,1, pp. 34-50. (In Russian).

Mipex.eu (2015). Migrant Integration Policy Index Official Website. [online] Available at: http://www.mipex.eu/ [Accessed 14 Dec. 2015].

Migpolgroup.com (2015). Migration Policy GroupOfficial Website. [online] Available at: http://www.migpolgroup.com/ [Accessed 14 Dec. 2015].

Mutz D. and Mondak J. (2006). The Workplace as a Context for Cross-Cutting Political Discourse. The Journal of Politics, 68 (1). pp. 140-155.

Nye J. (1989). Interdependence and the changing international policy, World economy and International relations, 12, pp. 72-76. (In Russian).

Oecd-ilibrary.org (2013). International Migration Outlook. [online] OECD Official Website. Available at: https://www.oecd-ilibrary.org/social-issues-migration-health/international-migration-outlook-2013_migr_outlook-2013-en [Accessed 6 Juny 2018].

Olshanskij D.V. (2001). Fundamentals of political psychology. Ekaterinburg: Delovaja kniga. (In Russian).

Panarin I.N. (2012). Media, propaganda and information wars. Moscow: Pokolenie. (In Russian).

Price V. and Zaller J. (1993). Who Gets the News? Alternative Measures of News Reception and Their Implications for Research, Public Opinion Quarterly, 57 (2). pp. 133-164.

Ravenstein E. (1889). The Laws of Migration: Second Paper, Journal of the Royal Statistical Society, 52, pp. 241–305.

Shestopal E.B. (2002). Psychology of power perceptions. Moscow: SP Mysl'. (In Russian).

Solov'ev A. (2002). Political communication: to the issue of theoretical identification, Political studies, №3, pp. 5-18. (In Russian).

Sotirovic M. and McLeod J. (2001). Values, Communication Behavior, and Political Participation. Political Communication, 18 (3), pp. 273-300.

Stat.fi, 2013. Statistics Finland Official Website. [online] Available at: https://www.stat.fi/til/index_en.html [Accessed 14 Dec. 2015].

Stouffer S. (1940).Intervening Opportunities: A Theory Relating Mobility and Distance, American Sociological Review, 5, pp. 845–867.

Timofeeva L.N. (2010). Power as political communication: materials of the methodological seminar. Moscow: Publishing House RAPS. (In Russian).

Timofeeva L.N., ed. (2012). Political communicative theory: theory, methodology and practice. Moscow: Publishing House RAPS. (In Russian).

Varshaver E., Rocheva A. (2014). Migrant Communities in Moscow: mechanisms for the emergence, functioning and maintenance, UFO, 3 (127). (In Russian)

Un.org (2017). International Migration Report 2017. [online] United Nations, Department of Economic and Social Affairs, Population Division Official Website. Available at: http://www.un.org/en/development/desa/population/migration/publications/migrationreport/docs/MigrationReport2017.pdf [Accessed 6 Juny 2018].

Yurev A.I., Anisimova T.V. and Samushova I.A. (2005). Issues of psychological-political speech communications in contemporary Russia, Vestnik SPbGU, Series 6, №3, pp.121-129. (In Russian).

Zazaeva N.B. (2012). Political communications in contemporary Russia, Power, №7, pp. 63-66. (In Russian).

Zimichev A.M. (2010). Psychology of political struggle. Moscow: Lomonosov. (In Russian).

Received on July 9th, 2018 Accepted on May 17th, 2019

Alexandra V. Starikova[1*]
[1] Institute of Geography, Russian Academy of Sciences, Moscow, Russia
*** Corresponding author:** a.v.starikova@igras.ru

SPATIAL BEHAVIOR OF STUDENTS AND THEIR ROLE IN POLARIZED DEVELOPMENT: COMPARATIVE STUDIES OF YAROSLAVL OBLAST AND BAVARIA

ABSTRACT. The article deals with the analysis of student educational migration and its role in origin of spatial contrasts at the territory of Russian early developed regions. In the paper ongoing processes are considered on the case of Yaroslavl oblast at the intra- and interregional levels and compared to processes abroad on the case of German federal state of Bavaria. The results are based on examination of official statistical data, surveys among students (disclosing their spatial behavior during the study and after degree completion) and expert interviews with university spokespersons. Migration bonds of Yaroslavl universities as well as space-time features of educational migration (average distances, time costs, transportation means) in Yaroslavl oblast and Bavaria are revealed. The study found that educational migration (together with other population mobility types) plays an important role in spatial polarization at the research territory due to importance of Yaroslavl as big educational centre for northern part of Non-Chernozem zone (Vologda, Arkhangelsk, Kostroma oblasts and Komi Republic). School-leavers from small cities and countryside come to the regional capital for bachelor's degree completion, next they try to go to Moscow, St. Petersburg or other largest cities not only to get masters' degree, but also in search of life conditions improvement. They want to change place of permanent residence and to have a career on perspective labor market.

KEY WORDS: educational migration, higher education institutions, early developed regions, spatial polarization, Yaroslavl oblast, Bavaria

CITATION: Alexandra V. Starikova (2019) Spatial Behavior Of Students And Their Role In Polarized Development: Comparative Studies Of Yaroslavl Oblast And Bavaria. Geography, Environment, Sustainability, Vol.12, No 2, p. 18-28
DOI-10.24057/2071-9388-2019-49

INTRODUCTION

In modern Russia polarization of space is closely related to the increase of spatial mobility and concentration of population into large and largest cities due to Russia's incomplete urbanization and attractiveness of large centers' labor markets for intra- and interregional migrants (Nefedova and Treivish 2019). Most often, administrative centers and their suburbs in Russian regions are the only centers of population growth against the background of steady population decline in the intraregional periphery (Mkrtchyan 2018). Such strengthening of socio-economic space polarization is especially characteristic of Non-Chernozem early developed regions,

their small and medium-sized cities and countryside primarily suffering from intensive migration outflow of young people (Mkrtchyan 2019). School leavers aim to get into education institutions in large cities (including for living conditions improvement and adaptation to local labor market before a degree getting), so one can consider educational migration as one of urbanization stages. In such circumstances, relevance of educational migration researches and role of young people mobility and their spatial behavior in contrasts' intensification at intra- and interregional levels is increasing.

Literature review shows that educational migration compared to other migration types rarely becomes the main topic of researches, although many authors write about their role in migration processes' intensification and about urgency of such studies (Meusburger 1998, Katrovskiy 2003 etc.). Migrations with educational purposes are considering more often by sociologists, demographers and economists: mostly they highlight university students' mobility and such its aspects as demographic resources of educational migration (Pismennaya 2010), migration plans of school leavers and graduates (Varshavskaya and Chudinovskikh 2014), academic mobility (Kostina 2014). Researches abroad also pay special attention to academic mobility patterns (Cornet 2015), among other often discussed topics are international migration of students and its geographical structure (Kelo et al. 2006).

According to Katrovskiy (2003) educational migration analysis need to be conducted from the standpoint of geographical approach due to geographical synthesis potential in the problems' generalization in the area of territorial organization of education. Consideration of the spatio-temporal characteristics, territorial structure and scale of migration are of top priority for early developed regions because it allows to determine the significance of educational migration for their socio-economic development.

The process of educational migration is studied by Russian authors in the context of international migration, special attention is paid to the prospects of Russian universities in teaching foreigners and their adaptation to the new environment (Dementieva and Giniyatova 2012, Study migration from CIS and Baltic countries 2012). Internal educational migration is analysed by cases of separate universities and rarely by cases of regions (Voronezh and Tomsk oblasts, North Caucasus). There are also series of works dedicated to youth migration including school leavers and students (Kashnitsky, Mkrtchyan and Leshukov 2016; Mkrtchyan 2017, 2019; etc.). Special place among the publications is occupied by the fundamental study of German geographer P. Meusburger (1998) devoted to geography of knowledge, science and education (including issues related to educational mobility).

Educational migration across Bavaria borders was considered by German researches in the context of economic and social state of students in old and in new federal states of Germany (Middendorff et al. 2013). Internal migration of students was examined by R. Rödel (2010) based on data about origin of first-year students in local universities.

The urgency of educational migration studies is increasing also due to the process of strengthening the role of universities as "engine" of territorial development and their influence on local labor markets (Katrovskiy 2003). In the current research author aimed at analysing of spatio-temporal features of student educational migration and their behavior within the time geography framework. This scientific direction has appeared in the Lund School of T. Hägerstrand in the 1960–70s. (Hägerstrand 1970). At the heart of time geography understanding of space-time organization of people's activities lies, when individuals are forced to move constantly within the framework of a daily, weekly or annual cycle: between home, work, places of rest, study, etc. As distinct from other works of Russian authors in the research the ongoing processes (on the case of Yaroslavl

oblasts) are considered at the intra- and interregional levels and compared to processes in foreign countries (on the case of Bavaria) in order to understand if foreign realities will be prospects for early developed regions evolution.

MATERIALS AND METHODS

In Russian statistical sources intra- and interregional migration links (including commuters flows) cannot be directly traced that's why their use is possible only with some restrictions: it is considered in detail by Kashnitsky, Mkrtchyan and Leshukov (2016). Some higher education institutions in their yearbooks and other documents provide information about non-resident students, but it is not enough for detailed analysis. Under such conditions, the main data source about educational migration is surveys of students and expert interviews with university spokespersons: it makes possible to identify the features of migration processes at regional level, flows structure and migration behaviour of students.

As case for the research Yaroslavl oblasts was selected. It is one of the most industrially developed regions in Central Russia. Here there are large-scale facilities (including high-tech ones), forming the demand for highly skilled workers. Such specialists are educated in numerous local higher education institutions that attract both local and non-resident (from other Russian regions and from abroad) students. In the base of the research is a survey of students (190 people in 2018) of three universities in Yaroslavl: P.G. Demidov Yaroslavl State University, Yaroslavl State Pedagogical University named after K.D. Ushinsky and Yaroslavl State Medical University (such set of education institutions is associated with role of classical, medical and pedagogical universities for regional development). The survey was carried out in the form of a questionnaire, respondents answered questions from three blocks: about their social and financial situation, life in the city and plans for the future. In the same period interviews with experts were conducted. Also, data on the residence of part-time students (1509 people) of the Yaroslavl branch of Academy of labour and social relations (head institution – in Moscow) were analysed.

As case abroad German federal state of Bavaria was chosen. Among other federal states it is distinguished by low cross-border educational mobility and at the same time very high mobility in the Bavaria territory (Starikova 2017). The share of commuters among students is here even higher than among workers (Böhme 2007). The main feature of educational migration bonds in Bavaria are their regionality (Starikova 2017) that largely is in line with the current trends to higher education regionalization (Katrovskiy 2003) going in our country. On the other hand, in Bavaria there is developed transport infrastructure, tax benefits and state support to students as good basis for such migration type. Data about educational migration has obtained from different official statistical sources, the primary of them are regularly published population microcensus results (Erwerbstätige sowie Schüler und Studierende nach Pendlereigenschaften in Bayern… 2017). Some indices for general presentation of Yaroslavl oblast and Bavaria are given in Table 1.

RESULTS AND DISCUSSION

Since the 1990s. importance of migration for Russian early developed regions is increasing due to its possibility redistributing human capital and smoothing down negative effects of natural population decline and aging. In the Yaroslavl oblast today the processes of economic and social desertification are underway in the countryside and peripheral areas. In some years net migration rate compensated here for up to 20% of the natural decline of population (over 15% in 2017), but nowadays it is focused on city of Yaroslavl and the surrounding Yaroslavl district (here locates the main part of regional center's suburbs). In such situation issues of youth people mobility (including their spatial behavior during educational migration) come to the fore in the light of local problems solving.

Table 1. Area, population and students' number of Yaroslavl oblast and Bavaria

Index	Yaroslavl oblast	Bavaria
Land area (sq. km)	36.2	70.5
Population (thousands, 2018)	1265.9	12997.2
Administrative center or capital (Population, thousands, 2018)	Yaroslavl (608.7)	München (1539.3)
Number of students (thousands, 2017–18 academic year)	31.3	388.9
Number of students per 10000 inhabitants (2018)	247	299

Yaroslavl as one of the largest cities of Non-Chernozem zone (its population exceeds 600 thousand people) congregates young people not only from its region, but also from remote areas (for example, the distance between Yaroslavl and Vorkuta is over 3000 km, between Yaroslavl and Arkhangelsk is almost 1000 km). Among main attractors for young people are local higher education institutions. Yaroslavl oblast in the Central Federal District ranks 4th (after Moscow, Moscow oblast and Voronezh oblast) in terms of higher education institutions number (24 at the beginning of the 2017–18 academic year) and 7th (after Moscow, Smolensk, Kaluga, Bryansk, Vladimir and Voronezh oblasts) by the number of branches. Most of higher education institutions locate in Yaroslavl (over 90% of students in the region study here); there are also higher education institutions in Rybinsk (over 9%) and Tutaev. At the beginning of the 2017–18 academic year the total number of students in Yaroslavl oblast was 31.3 thousand people. It is important to note that Yaroslavl attractiveness determines due not only to its own attractors: proximity to Moscow is of particular importance (Yaroslavl is only 300 km away from it). For many young people Russia's capital is viewed as the final goal of their migratory movements chain and Yaroslavl is only a springboard to its achievement.

The overwhelming majority of students are Russians (97.2% in 2017) with predominating of the Yaroslavl oblast residents (87.7%; more than half of them are from administrative centre – 56.4%, there are also residents of Rybinsk – about 7.0%, Rostov – 4.5%, Pereslavl-Zalessky – 2.5%, Uglich – 2.1% and Danilov – 2.0%). More than 20% of the students are from rural areas. A small number of foreign students represent a few dozen countries, about 44.5% originate from Tajikistan and else 10.9% from Turkmenistan. The most popular educational programs for foreigners are offered in State Aviation Technical University named after P.A. Solovyov (in Rybinsk and Tutaev), agricultural academy, technical and medical universities (all in Yaroslavl).

The territorial structure of interregional educational migrations was determined using the data about residence place of Academy of Labor and Social Relations' part-time students. Comparison of the results with the survey among full-time students of other institutions and interviews with spokespersons allowed to reveal main migrant-supplying regions. Traditionally strong migration ties are with Yaroslavl universities in the cities and districts of the Arkhangelsk oblast (35.5% of interregional educational migrants, primarily from Arkhangelsk, Velsk, Velskiy and Plesetsky districts, Nyandoma). Significant migrants' part is supplied by neighbouring Kostroma (almost 12%; from different areas but rarely from the administrative centre), Vologda (almost 10%, mainly from Cherepovets and Vologda), Ivanovo (about 5%) oblasts and Komi Republic (approx. 6.5%). About 12% are residents of the Moscow capital region (Moscow and Moscow oblast), who are attracted by the education costs in the branch of Academy of Labor and Social

Relations compared to the head university. The results of the survey and expert interviews let to talk about Yaroslavl role as an important educational centre in Non-Chernozem zone (especially for Vologda, Arkhangelsk, Kostroma oblasts and Komi Republic). Thus, by the share of university entrants to the architectural and construction faculty of Yaroslavl State Technical University in 2017 the same regions stood out (Vologda – 10% of university entrants, Kostroma – 10–11%, Arkhangelsk – less than 10%, Komi – about 5%, a little less – from Ivanovo, Moscow and Tver oblast).

Migration ties are actively maintaining within the framework of cooperation in the field of personnel training programs between technical and vocational education organizations (primarily, these are pedagogical and medical colleges) and universities. For example, Association of continuing professional education at the head of the Yaroslavl State Pedagogical University operates for several decades and units 22 pedagogical colleges from the Yaroslavl oblast, all neighboring regions, as well as from the Arkhangelsk and Kirov oblasts and Komi Republic.

The structure of migration links is also determined by the position of Yaroslavl on the Northern Railway, which direction corresponds to the main migrant-supplying regions. For Yaroslavl State Medical University, both the connections formed in the Soviet era due to process of university location (they trained specialists for certain regions, institutions in Yaroslavl served the northern part of European Russia) and modern agreements on the creation of joint departments for targeted training of specialists (today there are two such departments – in cities Vologda and Kostroma). Regions and cities, which are the main suppliers of educational migrants, also provide Yaroslavl oblast with commuters and approximately in the same ratio (Kondakova 2017), which indicates the necessity and prospects of educational migration studies.

More than 1/3 of the respondents indicated that after study completion they want to stay in Yaroslavl (to live and work, less often – to study) (Fig. 1): most of them are residents of other Russian regions (57%). Among reasons that push students from neighboring regions to stay in Yaroslavl, experts denote higher incomes, climate, proximity to Moscow, relatives settled here or nearby. Significant share of the respondents (1/5) associate their future with life in another major city: they try to get into Moscow or St. Petersburg, less popular are cities of the Russian South (Krasnodar, Sochi, Rostov-on-Don) and administrative centers (like Kazan, Ryazan, Vologda).

Along with the territorial structure of educational migration, spatio-temporal features of this population mobility type were analyzed. In contrast to other Russian researches educational migration is considering compared to processes abroad (by the example of Bavaria).

Non-resident students make trips to their places of permanent residence during the year (Fig. 2): over 75% of them doing it with a certain rhythmicity, the other visit home occasionally (1–2 times a month, half-yearly, in summer, etc.).

High trips' frequency is peculiar to students permanently living in the Yaroslavl oblast. They move between places of residence and studying 1–2 times a week (and more often) and spend weekends at home (so more than half of intraregional migrants do). Students from other regions have a chance to visit their families mainly for weekends (respondents from Ivanovo, Vladimir, Kostroma, Vologda, Arkhangelsk oblasts and Komi Republic say about such practice) or holidays. The share of students returning home for the weekends decreases with the growth of the distance between their settlement and city of Yaroslavl (of course, transportation, direct routes' presence and need to make connections could matter), at the same time the share of non-residents spending holidays at home increases.

Fig. 1. Distribution of respondents' answers to the question «What are you going to do after you graduate?»

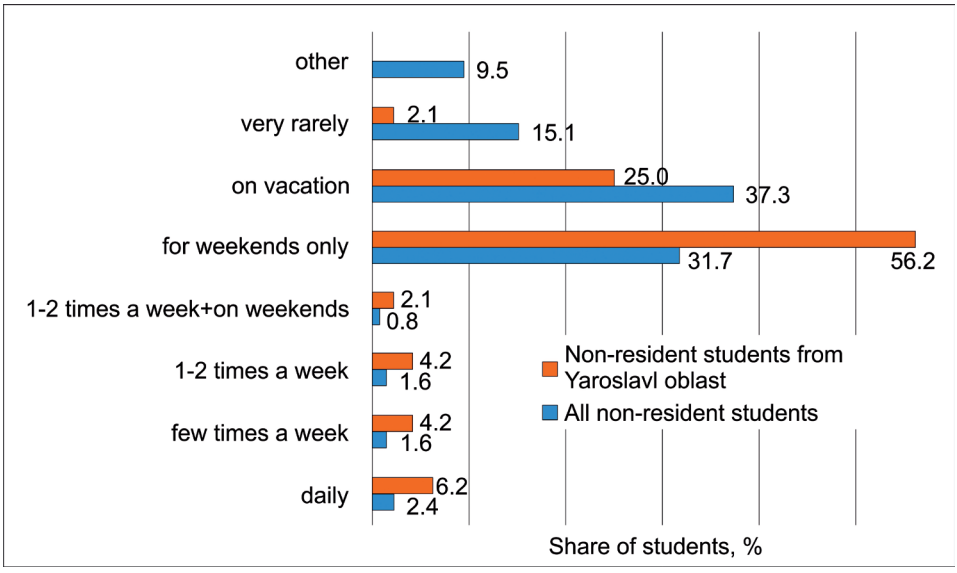

Fig. 2. The frequency of home visiting by non-resident students, 2018

Time in educational migration processes plays an important role: it depends on both distance (between house and education institutions) and choice of transportation means. Nearly half of the respondents use rail transport, most of them are non-Yaroslavl oblast residents. More than a quarter of the respondents use intercity buses. These are students from the Yaroslavl oblast and neighboring regions. Another quarter gets to their homes by private cars or hitchhike. The mobility of students is largely influenced by their financial capacities (trip costs is often significant for family budget), so young people prefer to visit their homes rarely or to look for a cheaper transport (car-pooling and services like BlaBlaCar; long-distance trip by train instead of flight, etc.).

If we talk about Germany one can suppose that students' time costs on the trip to the university are less than in Russia (considering high level of transport accessibility on its territory). It is more profitable for them to travel every day rather than to move closer to their university or other high school due to many municipalities impose taxes on those who rent accommodation here, so students bear additional costs. Available German statistics allow us to look at the spatio-temporal features of daily educational migration and accordingly to compare it with processes in Russia.

Both in the Yaroslavl oblast and in the federal state of Bavaria, universities are usually located in large cities, and the number of daily trips participants decline as the distance to education institution increases. However, there is a clear difference in the distribution of migration participants shares depending on the distance (Fig. 3). Differences in the average radiuses of trips are pronounced: in Yaroslavl oblast radiuses of one-way trip are almost two times shorter than in Bavaria (11.8 km and 22.3 km, respectively; radiuses are calculated as the weighted average according to Fig. 3).

In case of Yaroslavl oblast direct dependence of commuters share among students on the trip distance is revealed: the greater distance between home and university, the less young people overcoming it. Most of the respondents live near their education institution, for more than 67% of them one-way trip is less than 10 km, time costs are also small (less than half an hour). The second group is formed by students (a little more than 1/4 of the respondents) traveling 10–25 km daily, the share of the rest is slightly more than 6%. This distribution may be caused due to many of respondents have an opportunity to live near the university in dormitories (1/3 of students for whom the distance of commuting is less than 10 km) or renting apartments nearby (1/4). In Bavaria, the share of young people living in the area of their universities is also high, but the proportion of students living at a sizeable distance (more than 25 km) is much higher. Shares of commuters, covering distances over 10 km, decline slightly with distances increasing, and those who travel over 50 km become even more.

These indicators reflect differences in the level of population spatial mobility due to several factors. In Bavaria transport accessibility of universities is significantly higher, besides local authorities provide financial support to students ready to make long trips to places of their study. But unlike Russia it is harder for students to get a room in university campuses (always there is a big queue here). In Russian conditions, providing of non-residents with a dormitory is a traditional practice, at the same time it is much more difficult to get to the university by public transport from remote places and to offset financial costs by scholarship and part-time job.

Regarding to time costs, for Russian and German students the average travel time to the place of study practically coincides

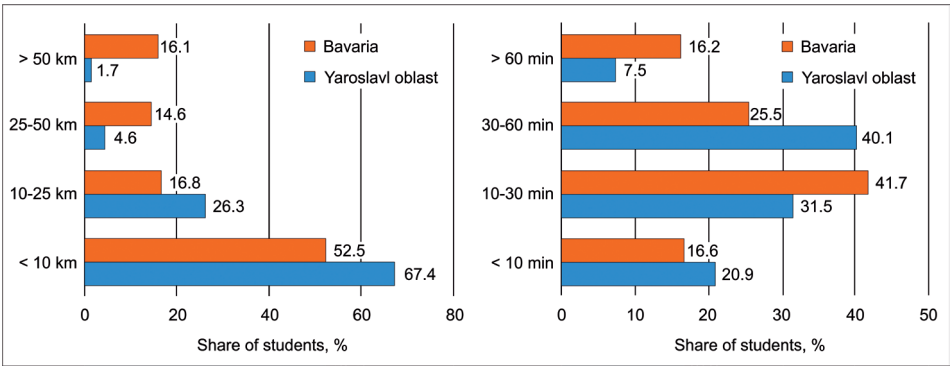

Fig. 3. Trip distances (left) and time costs (right) during students daily educational migration in Yaroslavl Oblast (2018) and Bavaria (2016)

(31.6 and 33.8 minutes, respectively; obtained according to Fig. 3 as the weighted average). Nevertheless, among students of Yaroslavl universities, the share of people traveling 30–60 minutes on their trip is especially big (and significantly more than in Bavaria). This time is spending to move within the city, and not on long-distance interregional travels. In Bavaria, a similar proportion of students need for 10–30 minutes (both on intra-city trips and on moving from the suburbs); those who ready to spend more than an hour to reach the university are much more (primarily due to the developed transport infrastructure).

In the city students of Yaroslavl universities use bus and trolleybus routes, rarely – taxis: over 57% of respondents gives preference to public transport (Fig. 4). It is bounded with the fact that most of respondents (including non-residents) live in Yaroslavl during the study period and doesn't have a need to go to the city daily. Respondents (2.7%) leaving regional center for holidays and weekends prefer suburban transport. Personal cars due to financial costs are using only 13.3% of students (almost 2 times less than in Bavaria). Almost a quarter of respondents goes on foot by the route to the university or its significant part. Bavarian students have no marked preferences. Urban public transport isn't so popular (it is chosen by just over 30%), although it is possible to use specially organized routes. The share of students using private cars (due to higher standard of living) and suburban transport (because of higher value of average commuting radiuses) is naturally high. In Bavaria there are a lot of cyclists among commuters (17.1% in the federal state versus 3.1% in the Yaroslavl oblast). It connects not only with the Germans' thrift, healthy lifestyle practicing and preservation of the environment, but also with mild natural conditions (one can ride a bike throughout the year, including winter), as well as the widespread infrastructure for cyclists (in our country it isn't enough).

CONCLUSIONS

The socio-demographic situation in Yaroslavl oblast is in line with problems of other European Russia early developed regions. It relates with population decline and migration outflow of working-age residents from small cities and rural areas into large center and its suburbs: in other words, into Yaroslavl and its district. Educational migration together with other migration types plays significant role in intensification of spatial contrasts at the intra- and interregional levels due

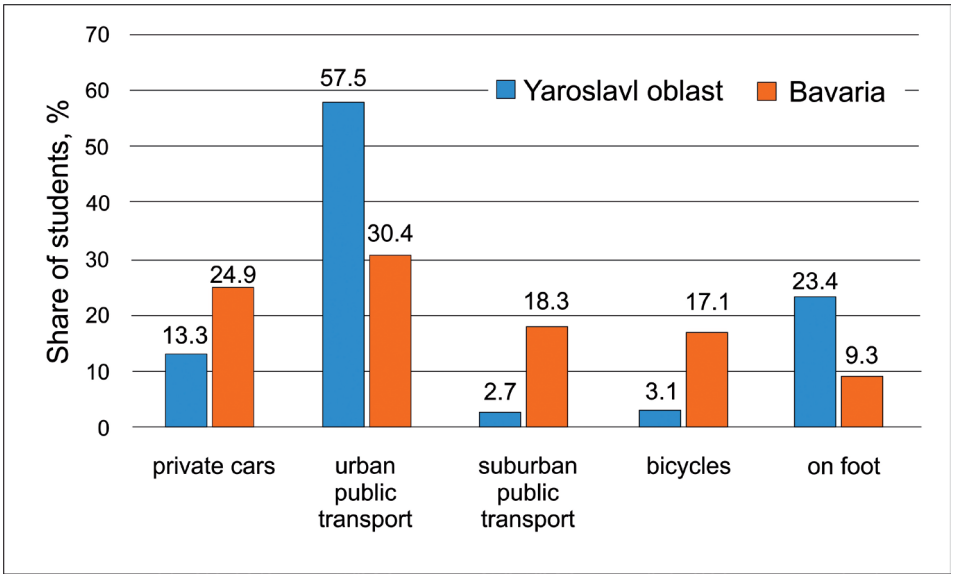

Fig. 4. Main transportation means for daily trips from home to university in Yaroslavl Oblast (2018) and Bavaria (2016)

to importance of Yaroslavl as educational center for northern part of Central Russia and often as a springboard for further migration to Moscow.

Arkhangelsk, Vologda and Kostroma oblasts as well as Komi Republic are the main interregional educational migrant-suppliers for Yaroslavl and its universities. Speaking about intraregional migration one can note that approximately half of Yaroslavl students are the dwellers of this center. The proportion of residents from other cities of its region is also large, 1/5 of students comes from the countryside. Spatial behavior of these young people is predominantly focused on large cities. If school-leavers from small cities and rural settlements usually go to the regional center, after completion of a bachelor's degree in Yaroslavl they strive to continue education in largest centers – Moscow and rarely in St. Petersburg (less often to move in capitals of other regions or southern Russia's cities). The main goal of graduates isn't only to get masters' degree, but also to change place of permanent residence with improving economic, social and living conditions compared to those in their own settlements.

Student spatial behavior during educational migration is characterized by different rhythm. The high trips' frequency (usually 1–2 times a week) is revealed for the residents of Yaroslavl oblast. With the growth of remoteness between places of residence and study and depending on the transport accessibility share of students going home for the weekends decreases, at the same time the share of those who spending at home only holidays increases. The average radiuses of daily educational migration in the Yaroslavl oblast is half as much as the same indicator for Bavaria with close indicator of average time per trip. This is because most of Yaroslavl students live in a dormitory near universities and don't need to go from remote areas with low transport accessibility. Among Bavarian students the share of long-distance commuters is several times higher than for Yaroslavl students because of developed infrastructure, state financial support for such migrants and the high cost of apartments renting near universities. At Russian students the most popular transportation means are trains (for young people living outside the region), buses (for students from the Yaroslavl oblast and neighboring regions) and private cars; for daily educational migration they prefer urban public transport. Bavarian students have no pronounced priorities, but among them there are much more car enthusiasts, passengers of suburban transport and cyclists. The comparison shows that in early developed regions of Non-Chernozem zone educational migration (students' spatial behavior included) is a factor of spatial contrasts' intensification under continuing urbanization while in Bavaria this type of return migration increases uniformity of human activity distribution on its territory under suburbanization and deurbanization processes. Evolution of early developed regions in line with German experience is attractive, but it is concerned primarily with solving their typical infrastructural and economic problems, improvement of living standards and creating of self-realization opportunities for youth people in small cities and rural areas.

ACKNOWLEDGEMENTS

The study was financially supported by the Russian Scientific Foundation (project N 19-17- 00174 "Early developed regions under socio-economic polarization and shrinkage of active space in European Russia" for the Institute of Geography, Russian Academy of Sciences).

REFERENCES

Böhme M. (2007). Ausbildungsmarkt und Ausbildungsmobilität in Bayern. IAB regional. IAB Bayern. Nr. 01.

Cornet F. (2015). Student Mobility in European Higher Education. J. Higher Education and Lifelong Learning, №22, pp. 57–66.

Dementieva S. and Giniyatova E. (2012). Educational Migration to the Tomsk Polytechnic University: Mechanisms and Practices of Effective Adaptation. Bulletin of the Tomsk Polytechnic University. Economy. Philosophy, Sociology and Cultural Studies, History, vol. 321, №6, pp. 187–190. (in Russian).

Erwerbstätige sowie Schüler und Studierende nach Pendlereigenschaften in Bayern 2016. Statistische Berichte. Ergebnisse der 1%-Mikrozensuserhebung 2016, (2017). Bayerisches Landesamt für Statistik, Fürth.

Hägerstrand T. (1970). What about people in regional science? Papers of the Regional Science Association, vol. 24, pp. 7–21.

Kashnitsky I., Mkrtchyan N. and Leshukov O. (2016). Interregional Youth Migration in Russia: a Comprehensive Analysis of Demographic Statistical Data. Educational Studies, №3, pp. 169–203.

Katrovskiy A. (2003). Territorial Organization of Higher Education in Russia: Monograph. Smolensk: Oikumena. (in Russian).

Kelo M., Teichler U. and Wächter B. (eds.) (2006). EURODATA – Student mobility in European higher education. Bonn: Lemmens Verlags- & Mediengesellschaft.

Kondakova T. (2017). Features of the Modern Socio-Economic Development of Rural Areas in the Yaroslavl Oblast. Geography and Ecology in the school of the XXI century, №1, pp. 19–29. (in Russian).

Kostina E. (2014). Academic Mobility of Students of Higher Education in Russia: a Cross-cultural Approach. Philosophy of education, №6(57), pp. 64–76. (in Russian).

Meusburger P. (1998). Bildungsgeographie: Wissen und Ausbildung in der räumlichen Dimension. Heidelberg, Spektrum Akademischer Verlag.

Middendorff E., Apolinarski B., Poskowsky J., Kandulla M., Netz N. (2013). Die wirtschaftliche und soziale Lage der Studierenden in Deutschland 2012. 20. Sozialerhebung des Deutschen Studentenwerks, durchgeführt durch das HIS-Institut für Hochschulforschung. Bonn/Berlin.

Mkrtchyan N. (2017). The youth migration from small towns in Russia. Monitoring of Public Opinion: Economic and Social Changes, №1, pp. 225–242.

Mkrtchyan N. (2018). Regional Capitals and Their Suburbs in Russia: Net Migration Patterns. Bulletin of the Russian Academy of Sciences. Geography, №6, pp. 26–38. (in Russian).

Mkrtchyan N. (2019). Migration in Rural Areas of Russia: Territorial Differences. Population and Economics, №3(1), pp. 39–51.

Nefedova T., Treivish A. (2019). Urbanization and Seasonal Deurbanization in Modern Russia. Regional Research of Russia, vol. 9, №1, pp. 1–11.

Pismennaya E. (2010). Educational Migration to Russia: Role in Socio-Economic and Demographic Development. Bulletin of higher education institutions. Sociology. Economy. Politics, №1, pp. 76–78. (in Russian).

Rödel R. (2010). Zugereiste oder Einheimische? Die Herkunft von Erstsemestern an bayerischen Hochschulen. Bayern in Zahlen, №12, pp. 561–567.

Starikova A. (2017). Educational Migration in Bavaria: Features and Role in the Formation of the Migration Patterns in the Region. Scholarly Papers of V.I. Vernadsky Crimean Federal University. Geography, Geology, vol. 3, №2, pp. 173–185. (in Russian with English summary).

Study migration from CIS and Baltic countries: potential and prospects for Russia (2012). Moscow: Fund «Eurasia Heritage». (in Russian).

Varshavskaya E. and Chudinovskikh O. (2014). Migration plans of graduates in regional universities of Russia. Herald of the Lomonosov Moscow State University. Geography, №3, pp. 36–58. (in Russian).

Received on April 28th, 2019 Accepted on May 17th, 2019

Jiri Chlachula[1,2*]
[1] Institute of Geoecology and Geoinformation, Adam Mickiewicz University, Poznan, Poland
[2] Laboratory for Palaeoecology, Tomas Bata University in Zlin, Czech Republic
*** Corresponding author:** altay@seznam.cz

GEO-TOURISM PERSPECTIVES IN EAST KAZAKHSTAN

ABSTRACT. Eastern Kazakhstan and the adjacent Gorno Altai of southern Siberia encompass very mosaic landscapes across all the geographic and geomorphic zones enclosing numerous (pre-)historic monuments, some of them being a part of the UNESCO World natural and cultural heritage. Excepting the high-mountain ranges (Rudno and Southern Altai, Narym, Tarbagatay and Dzhungarskiy Alatau) surrounding the territory, the interior open arid steppes characterized by a broken relief of the granite-built Central Kazakhstan Hills as well as the barren rocky semi-deserts in the SE parts of the land remain largely unexplored and tourism-uncovered. The extraordinary topographic diversity was generated by complex geological processes associated with the Cainozoic orogenesis and the changing Quaternary climates. Geo-tourism focusing on the most exquisite landscape forms (geo-sites) and geological formations is a new trend in the country with still minor activities that take advantage of the region's supreme geo-heritage potential. The unquestionable touristic-recreational attractiveness of this geographically marginal area of Central Asia (historically a part of the Russian Empire's Tomsk Gubernia) reflects unique natural features – both geomorphic and biotic – including orographic, hydrologic, climatic, mineral and pedogenic, as well as rare endemic plants and wildlife in addition to the colourful national Kazakh and Russian traditions. In spite of these predispositions, an introduction of a vital, sustainable geo-tourism in East Kazakhstan is impeded by the limited accessibility to the region due to an insufficient year-round transport infrastructure and poor local accommodation facilities in addition to the restricting boarder-zone entry regulations.

KEY WORDS: East Kazakhstan, topography diversity, Altai, geo- and cultural heritage, geo-tourism.

CITATION: Jiri Chlachula (2019) Geo-Tourism Perspectives In East Kazakhstan. Geography, Environment, Sustainability, Vol.12, No 2, p. 29-43
DOI-10.24057/2071-9388-2018-78

INTRODUCTION

Geo-tourism is a new phenomenon in Kazakhstan despite the major potential linked to the extraordinary relief diversity of this largest country of Central Asia (2 724 900 km^2). In some other developing countries and emerging economies, this environmental sector plays an increasing role as a part of a sustainable development with international geo- and eco-tourism promotions and publicity (e.g., Czerniawska and Chlachula 2018). As a novel form of the global tourism industry, geo-tourism generally means tourism of geologically interesting places – geographical loci

and relief features in terms of acting processes (such as mountain orogeny and glaciations, regional metamorphism, erosion, sedimentation) and resulting forms (alpine peaks, geological formations, rocky outcrops, deposits, minerals, palaeontology occurrences, etc.) (Downing 2011; Downing and Newsome 2010). The territory of East Kazakhstan with the major mountain systems (Southern Altai, Tarbagatay, Alatau), and the continental depressions (the Bukhtarma and Zaisan/Black Irtysh Basins) include the most picturesque and physiographically unique landscapes and geo-sites. The broader regional topographic configuration (Fig. 1) mirrors a long and complex geological history and sequenced (palaeo)-environmental transformations seen by relief features of geomorphic processes related to the Quaternary climate evolution with periodic glaciations in conjunction with the regional tectonics (Deviatkin 1981; Aubekerov 1993; Galakhov and Mukhametov 1999).

The past climate shifts that sculptured the present relief are evidenced by well-preserved palaeo-landscape forms in the mountain, steppe and semi-desert areas, as well as by deeply stratified sedimentary geology, palaeoecology and geoarchaeology records indicating long-term atmospheric variations in temperature and humidity (Akhmetyev et al. 2005). Spectacular glaciofluvial terraces in the mountain valleys indicate presence of a system of the ice-dammed lakes that were subjected to periodic cataclysmic drainages during the final stages of deglaciation and considered as the most dramatic geomorphic events in the latest Earth geological history (Rudoy and Baker 1993; Herget 2005). Alpine valleys, upland plateaus, enigmatic rocky canyons, sand dune fields, deep ravines amid of undulating steppe terrains are just some of the most characteristic landscape features (Fig. 2a-f). High-resolution loess-palaeosol sections, enclosing sequenced environmental archaeology data from the Pleistocene human occupation sites, provide evidence of a rather pronounced natural dynamics for the last ca. 130 000 years (Chlachula 2010).

The geo-tourism focus is on visiting and learning these places, adding to ecotourism aimed at biotic diversity (flora & fauna). In essence, it contributes to better awareness of nature-friendly actions, environmental protection, education and landscape preservation. The most interesting loci (geo-sites) are subjected to mapping in terms of environmental management and a geo-heritage evaluation still highly unexplored on the national level (Mazbayev 2016). The major protected areas such as the Katon-Karagay Nature Park, being the major NP in Kazakhstan (643 477 ha), and the Lake Markakol Nature Reserve among others enhance the regional natural value. East Kazakhstan and the adjoining Gorno Altai (southern Siberia) are also known for the World-unique archaeological sites and historical monuments (Chlachula 2018). The combination of pristine nature and the traditional culture makes the country most appealing for local as well as foreign visitors (Saparov and Zhensikbaeva 2016; Zhensikbayeva et al. 2017, 2018). This study presents an insight on the East Kazakhstan landscapes integrating distinctive physio-geographic features with rich cultural monuments, providing in unity a most promising geo-contextual milieu for the modern geo-tourism development by taking into account the regionally specific natural, historical, cultural and modern socio-economic aspects.

The East Kazakhstan Geography, Geology And Environments

The district of East Kazakhstan / Восточно-казахстанская область (283 000 km^2; population 1.4 mil.), the administrative centre Ust'-Kamenogorsk (315 000), belongs to the most progressing and historically developed parts of the Republic of Kazakhstan due to the rich natural resources, the mineral-processing industry, the transport network with the country's most vital communication links to the neighboring West Siberian Omsk and Altai Regions of the Russian Federation (Fig. 1). Climate is strongly continental (MAT –4°C) with very pronounced seasonal temperatures. The uneven annual (rainfall and snow) precipitation, ranging from 150

Fig. 1. Geographic location and relief diversity of East Kazakhstan with the most attractive physiographic geo-tourism areas and discussed geo-sites: 1 The West Altai Nature Reserve; 2 The Katon-Karagay State National Park (Fig. 2a-b, 3a,c,f); 3 The Lake Markakol Nature Reserve (Fig. 2c); 4 The arid zone of the Zaisan Basin and the Tarbagatay Range (Fig. 2e-f, 3d); 5 The Shingistau and Kalba Ranges (Fig. 2d, 3b); 6 The East Kazakhstan Highlands (Fig. 3e)

mm in the most arid eastern semi-deserts to 1300 mm on the NW flanks of Rudno (Rudnyy) Altai in the North, together with the great regional relief diversity predisposes a marked vegetation zonality (Chlachula 2007).

The territory is of a broken physiographic configuration of undulating parklands, adjoining the western steppes, and aligned (N-E-S) by the Altai, Tarbagatay and Alatau Mountain ranges (reaching to 4500 m asl.) (Fig. 1). A complex geological history is manifested by past and large-scale geomorphic processes of granitic and gneissic bedrock weathering, erosion and mass sediment transfer in the central Bukhtarma and Zaisan Basins linked to neotectonics and climate change over the past millions of year (Chupakhin 1968; Mikhailova 2002; Yegorina 2002). The broader regional geology is structured by the Proterozoic metamorphic rocks mantled by the Palaeozoic, Devonian, Carboniferous and Palaeogene formations of volcanogenic and sedimentary (sandstone, limestone) origin filling the interior syncline depressions. Karstic cavities are developed in the Palaeozoic limestones (Nekhoroshev 1967). The igneous and metamorphic geological bodies host rich mineral resources – metallic and non-metallic, including the occurrences of semi-precious and precious gemstones (emeralds, garnets, opals, beryl, tourmalines, granates and crystal quartz among other crystalline minerals) and the varieties of decorative stones (such as variegated microcline quartz and jasper) used in the jeweller, artistic and decorative stone-processing industry as well as building construction (Pacekov et al. 1990; Chernenko and Chlachula 2017). The known regional mineral provenience sites are largely bound to the exposed outcrops and shallow sub-surface deposits extracted by a small-scale mining.

The majestic alpine relief (>2000 m altitude) was shaped by periodic Quaternary glaciations accompanied by succeeding fluvial erosion and gravity slope processes particularly active in the mountain valleys. The changing cold/warm Late Pleistocene (130 000–12 000 yr BP) intervals contributed to formation of desert and parkland-steppe ecosystems during the warm stages, and periglacial arid steppes during the cold stages with glaciations of the East Kazakhstan mountains and loess deposition on the western foothills. The best-preserved landform features date to the Last Glacial stage (24 000–12 000 yr BP). The pronounced palaeoclimate dynamics is eloquently manifested by the preserved Last Glacial topography with most unique geo-sites in the principal valleys – the former ice-dammed lake basins (Butvilovskiy 1985) (Fig. 2a). Stratified, up to 30 m thick aeolian sand and wind-blown silt sedimentary records mantle the present smoothened topography and the palaeo-relief forms (Chlachula 2003; Bábek et al. 2011). East Kazakhstan is a dynamic geomorphic region due to the co-acting continental plate tectonics along the main central Eurasian orogenic belt (Velikovskaya 1946; Svarichevskaya 1965). The climate-driven regional relief restructuring continues until today giving rise to new and most interesting geo-settings. The present territorial aridification evident by active sand dune formation and mass-sediment transfer (Fig. 2f). leads to progressing regional desertification and the steppe ecosystem instability.

Geo-Tourism And Cultural Heritage

The great geo-diversity of the mosaic landscapes of the East Kazakhstan mountains and parkland-steppes is completed by the extraordinary cultural heritage jointly accentuating the touristic values of this still marginally exposed geographic area. The broader region was occupied from the earliest stages of the prehistory manifested by various cultures and traditions leaving behind numerous archaeological monuments as testimony of once flourishing ancient settlements (Chlachula 2018). In East Kazakhstan, the early cultural sites are recurrently associated with picturesque relief forms and places. The past environmental conditions and physio-geographic configurations regulated the sequenced prehistoric occupation as well as historical settlements on this territory

Fig. 2. The East Kazakhstan landscapes and natural geo-sites. a: Abraded granite boulders on top of the glacio-fluvial terrace resulting from a cataclysmic release of the Last Ice glacier-dammed ablation-water lake at the foot of the Southern Altai Range (Zhambul, Katon-Karagay District); b: Proterozoic monolithic granite rocks sculptured by wind-erosion encountered in the mid-altitude (1500-2200 m asl.) Altai Mountain area (Arshaty, Katon-Karagay District); c: Lake Markakol filling a 30 m-deep tectonic depression with picturesque surroundings of the nature reserve (Markakol District); d: Lakes Sibinskiye - a popular recreation site in the Kalba Range built by weathered granite formations; e: Mesozoic, iron-mineral colored and stratified clayey bedrock at Kiin-Kerish shaped into canyons and badlands amid of the Zaisan Basin semi-desert, indicative of past humid and hot tropical climates, and sealing fragmented Jurassic fauna (dinosaur) skeletal records (Kurchum District); f: Active, up to 300 m-high sand dunes (Aygyrkum Sands) along the Kazakh–Chinese border limits resulted from a massive and long-term aeolian sediment accumulation (ca. 40x15 km) with asand-drifting from the interior basin (Zaisan District)

known under the historical name *Sary-Arka* (Saparov et al. 2018). Past climates regulated the occupation dynamics and predetermined formation of specific glacial and non-glacial ecosystems.

The mapped archaeological localities in the East Kazakhstan Region unearthed in diverse geo-settings and geo-contexts indicate a much earlier human inhabitation predating the post-glacial prehistoric cultures. The oldest (Palaeolithic) sites bear witness of the Pleistocene hominine occupancy of this geographic area during the preceding interglacials and interstadials and environmental adjustment to Pleistocene ecosystems. The uncovered Middle Pleistocene sites documented by expedient stone industries (cobble-tools) discarded on the elevated riverine terraces and dry floors of continental basins, and currently wind-exposed within gravel pavements represent the most ancient vestiges of the early human dispersal in this poorly investigated territory (Chlachula 2010). Cave sites and rocky abris with the Middle to Final Palaeolithic findings from West and Southern Altai mountain valleys and the adjoining rocky foothills bear witness to montane adaptations of the last Ice-Age hunting-gathering populations (Fig. 3a). The prehistoric rock-art, rich burial complexes and ritual sites hidden in sheltered mountain valleys and the river-cut canyons inform on the later Holocene-age (Neolithic and Eneolithic) ethnics (Fig. 3b). The most eloquent cultural records are associated with the Bronze Age (late 4th–early 1st Millennium BC) and especially the early historical times (6th Century BC–9th Century AD). The latter are represented by stone-laid royal burial mounds (kurgans) (Fig. 3c), ritual structures, and rock-engraved petroglyphs assigned to the Scythian Period (6th–2nd Centuries BC), being the most famous early cultural relics and a part of the UNESCO World heritage (Polosmak 2001; Samashev 2001, 2011; Gorbunov et al. 2005). The geographical distribution of the mapped archaeological sites displays a broad topographic range of the previously occupied and/or exploited landscapes (Chlachula 2018) (Fig. 3d-e). All these loci have major potential not just for scientific research, but also for inclusion into the cultural and geo-heritage promoting programs and the related environmental management actions.

The linguistic evidence completing the material culture records points to a rather complex and chronologically long historical development (Konkashpayev 1959; Kenesbayev et al. 1971). This is best-reflected by the names of the major East Kazakhstan rivers and the mountains (hydronyms and oronyms, respectively), with the latter (Altai, Tarbagatay, Alatau) of a definite Mongolian provenance (Saparov et al. 2018). Etymology of the main physiographic entities delivers some insights on the past population shifts in northern Central Asia throughout the millennia since the most ancient Indo-European inhabitants through the Bronze and Iron Ages (3rd and 1st Mill. BC) until the historical period (2nd Mill. AD) represented by nomadic and territorially mobile to semi-sedentary ethnics. This knowledge can be implemented into geo-tourism activities and has an unquestionable national culture-historical significance.

Geo-Tourism Potential Of East Kazakhstan

The multi-facetted geography of East Kazakhstan has all predispositions for eco- and geo-tourism taking into account the pronounced regional climate seasonality, the overall natural beauty and comfort with favourable hydro-geological conditions (mineral waters, balneology loci, radon-gas thermals) and the attractive landscapes underlining, together with the rich cultural heritage, the immense touristic and recreational capacity of the region. The integration of all these aspects provides foundation for the specific tourism sectors and their implementation onto the Kazakhstan landscapes (Mazbaev 2016). Viability and sustainability of the specific tourism activities can be assessed by evaluating each of the particular physical and human geography constituents (i.e., terrain, climate, hydrology, biodiversity, therapeutic resources among other variables) (Inskeep 1994; Wimbledon and

Fig. 3. The East Kazakhstan landscapes and cultural-heritage geo-sites. a: A Stone Age site located on an exposed granitic promontory at the margin of the former glacial lake providing evidence of a Final Pleistocene human colonization of the deglaciated Bukhtarma River valley (Zhambul, Katon-Karagay District); b: A Neolithic and Bronze Age Ak-Bauyr cultic site with rock-art grottos (Kalba Range); c: Excavation (2006) of a rich "royal" burial mound (kurgan) of the Iron Age Pazyryk culture (6th-2nd C. BC) at Berel' (Katon-Karagay District) with mummified bodies preserved in permafrost; d: A medieval circular sacral place made of dry-bricks in the middle of the desert (Shilikty, Zaisan District) providing a vivid testimony of ancient tribal settlements; e: The scenic rocky steppe landscape with hidden valleys and raised plateaus was a place of refuge as well as sanctuaries since the prehistoric times (the East Kazakhstan Highlands, Shar District); f: The "Austrian Road" built in 1915-16 across the Sarym-Sakty Range at ca. 1500-2200 m asl. connecting the Bukhtarma Valley (N) with the Black Irtysh Basin (S)

Smith-Meyer 2012; Yegorina et al. 2016) and the site accessibility, transport possibilities and visitors accommodation conditions. Each of the selected geo-sites of Saryarka may then be considered by its uniqueness among other relief places, its spatial occurrence (concentration) within the particular area, its diversity and complexity in respect to other geo-relief features and the state of physical preservation. The natural and past-present cultural diversity confirms the uniqueness of the geographic area for various tourism activities and free-time recreation (Chikhachev 1974; Yerdavletov 2000; Geta et al. 2015).

The specific geographical aspect of East Kazakhstan is its location in the border zone adjoining the other (Russian, Mongolian and Chinese) nature protection reserves and national parks. The broader area encompasses several major physiographic units of the "Great Altai" including the Gorno Altai-Sayan Mountain Region, the Altai Region, the Mongolian Altai, the Chinese Altai (Kanas NP), and eight Kazakh districts In East Kazakhstan, five explicit nature-recreational areas can be defined by the regional ortho-climatic characteristics: the Zyryan (Rudno Altai), Katon-Karagay, Lake Markakol, Kurchum and Kalba/Shyngystau (Fig. 1) with pristine taiga, tundra, desert and rocky steppe habitats hosting rich endemic and elsewhere rare biota with unique floral and faunal communities. The particular natural conditions predisposed by the geomorphic settings and the arid-zone atmospheric regime gave rise to the variety of ecosystems reflecting the geographic and climatic zonality of the territory (Chlachula 2007, 2011).

The Kazakh Altai formed by the E-W aligned mountain ranges (Southern Altai, Sarym-Sakty, Narym, Kurchum) is connecting through the Tarbagatay massif (2992 m) and the Saur Range (3816 m) to the Dzhungarskiy Alatau (4464 m) in the South. These orogenic systems are characterized by the erosional northern slopes – uplifted relics of old plateaus (>3000 m asl.) with a decreasing topographic gradient (3900–2300 m asl.). The territory of the Southern Altai (3485 m asl.) is included in the globally most significant geo-ecological regions hosting unique geo-ecosystems with many varieties of rare and endemic flora and fauna. The Katon-Karagay State National Park is the largest among the protected natural areas and biosphere reserves in the country (est. in 2001). In view to the broken physiography the region also offers good opportunities for adventure tourism (rafting, paragliding, horse-riding and alpinism) (Fig. 2a-c) (Swarbrookeet al. 2003). Overall, the KKSNP has the best preconditions for the geo-tourism industry in the frame of the regional eco-tourism management highly competitive with other mountain regions of the World (Newsome and Bowling 2010; Harns et al. 2017; Ilieş et al. 2017; Saarinen et al. 2017). Together with a more stationary recreation, such as at the Lakes Sibinskiye surrounded by granite hills sculptured by weathering of the Kalba Range (Fig. 2d), these activities contribute to the rural socio-economic sustainability.

A largely forested, lower-elevation relief (800–2200 m asl.) of Rudno Altai encloses the East Kazakhstan territory from the North adjoining the Russian Gorno Altai. Scenic, wind-eroded rocky formations sculptured into granite bedrock centred in the West Altai Nature Reserve (86 122 ha) and the adjoining mountain ranges is the most distinctive landform component of the regional physiography (Fig. 2b). Lake Markakol (1449 m asl.), filling the tectonic depression enclosed by the Sarytau Range (3373 m) and the Azutau Mountains (2300 m) in the middle of the eponymous nature reserve, is renown for the great diversity of plants and animals (mainly birds, fish and insect) (Mitrofanov and Petr 1999; Chlachula 2007) (Fig. 2c). The rather specific and very different geo-relief diversity is encountered in the south-eastern (Kurchum) area of vegetation-free (semi-)desert with badlands (Fig. 2e) and salty evaporates marshes of the Zaisan Depression fed by the Kaldzhyr and Black Irtysh Rivers. The dry barren rocky and gravel-pavement steppes transgressing into the rising foothills with closed patchy forests in riverine canyons are gradually replaced by the rising partly forested slopes

of the Tarbagatay and Alatau Mountains. Natrium- and silica-enriched mud deposits of the Mynshunkyr ('a thousand of pits') site have unique therapeutic properties.

In spite of the wide spectrum of the countryside beauty, these touristic zones of eastern Kazakhstan are still being very marginally visited. Until now, only c. 2000–3000 people come to Lake Markakol and the Kaldzhyr River area during the peak season in summer and early fall (Saparov and Zhensikbayeva 2016).

DISCUSSION: FUTURE PERSPECTIVES

The mountain regions encompass some of the major ecosystems on the Earth. They also comprise the most significant mineral, natural and geo-tourism resources (Dunets 2011; Sherba et al. 2000; Melinte-Dobrinescu et al. 2017; Bouzekraoui et al. 2018). The national and internationally-based tourism represents one of the most emerging and profitable sectors of global industry. The regional attractiveness is considered as the principal proviso of geo-tourism. Even formerly geographically marginal and less-accessible places have become increasingly open to visitors and the organized tourism stimulating a further infrastructure and facilities development. This is particularly true for the geo-environmentally-oriented activities (e.g., Mihalič 2000; Goessling and Hall 2005; Mason 2015). Eastern Kazakhstan, with the major alpine mountain systems constituting the extreme NE frontiers of the Republic of Kazakhstan, offers major tourism opportunities, particularly in respect to geo-tourism and eco-tourism that can well compete with other geomorphically most diverse places in the World (Dowling 2009; 2011; Brilha 2016). The natural sites are supplemented by unique anthropogenic landscape construction elements, such as the "Austrian road" built during the I. World War (in 1914-1916) by the imprisoned Austrian solders (Fig. 3f), as well as other relief features that constitute a part of the modern regional history and human work imprinted onto the landscape. Nevertheless, because of the limited logistics and the special border-zone entry regulations, this area still represents one of the most underdeveloped, pristine and most attractive places for sustainable tourism and recreation in Central Asia.

In terms of the modern geo-tourism promotion (Asrat and Zwolinski 2012), field mapping and documentation should not be confined just to the geo-sites listed by UNESCO such as Plateau Ukok (Molodin et al. 2004). Other prominent and regionally specific geo-relief locations should be enclosed with assessment of their attractiveness. Interdisciplinary Quaternary (geological, geomorphologic, hydrological and present climate-change) studies represent a constituent contextual part of the Eastern Kazakhstan geo-diversity documentation in terms of the acting natural processes, their dynamics and chronology, allowing for reconstruction of the regional physiographic history and the present relief formation. The distinct Last Ice Age mountain topography attest to pronounced intensity of these processes and marked climatic fluctuations since the Last Glacial (Chlachula 2001, 2010). A progressing retreat of the mountain glaciers reinforced by global warming observed across the broader Altai area (Surazakov et al. 2007; Chlachula and Sukhova 2011; Narozhniy and Zemtsov 2011) exposes new landforms in the recently deglaciated alpine zone. These actions may generate major geo-environmental risks and geo-hazards subjected to monitoring, including the status of preservation of permafrost-sealed and most unique cultural sites (Hahn 2006; Jakobson-Tepfer 2008). A geo-archaeological survey adds to improved knowledge and better awareness of the regional prehistory as well as protection of the Altai (pre-) historical monuments (Cheremisin 2006). Landscape mapping and GIS visualization constitute a background for the spatial distribution assessment of specific geo-sites as well as biotopes and plant species in the frame of the regional eco-tourism (Hovorkova and Chlachula 2012). Legal regulations should be implemented to prevent destruction of unique geo-sites and geoarchaeology monuments by industrial activities (infrastructure development, mining, building construction, etc.) or human behavior.

The future geo- and eco-tourism resort development in East Kazakhstan is bound to naturally supreme places (such as the salty mud spa at Mynshunkyr, the radon-gas spa at Lake Yazovoye, Rakhmanovskye Klyuchi, Sibinskiye Lakes, Shul'ba Lake, canyon Kiim-Kerish, Aygyrkum dunes, etc.) combined by the traditional economy facilities such as red-deer farms aimed at the pantocrine/blood extract production from velvet antlers used as a traditional medicine or horse-milking farms). A complex regionally-specific physiographic assessment is prerequisite for evaluation of future tourism perspectives (Mazbaev 2016). In spite of the major biotic and geo-sites potential, the introduction of a vital and sustainable tourism in the area is hindered by the insufficient, mostly unpaved road network (with some roads without maintenance during the winter season), inadequate local accommodation facilities, as well as the special boarder-zone entry regulations. Helicopter transport can be used as a faster, yet more costly alternative to the road (car/bus) transportation. Only the airport in Ust'-Kamenogorsk / Oeskemen (Fig. 1) can be used for international flight arrivals. The Irtysh River with local ferries is a good option for a leisure-time yet geographically most cognitive riverine route to Lake Zaisan via the tributary Bukhtarma Lake reservoir. The relatively rising living standard and wages in the main industrial cities of East Kazakhstan, such as Ust'-Kamenogorsk, contribute to expansion of the present tourism industry into the commercial geo-tourism and recreation geography.

CONCLUSION

Geography of the Republic of Kazakhstan, situated in the North of Central Asia, inspires a lot of scientific as well as commercial attention because of the spectacular landscapes with many World-unique geo-sites found across all the physio-geographic zones. Their extreme diversity mirrors a wide range of geomorphic processes acting on the territory over the past millions of year in linkage with the Cainozoic orogeny and Quaternary climate change. The complex geological history sculptured the present topography of East Kazakhstan by generating the most attractive relief forms and locations enclosing the ancient archaeological sites and historical monuments with the permafrost-sealed royal burial mounds of the Iron-Age Pazyryk Culture being the most famous. Yet, there has been a marginal activity promoting the country's supreme geo-heritage and the geo-tourism potential due to the limited accessibility with a poor infrastructure, and the restricting entry regime of the present Kazakh-Russian-Chinese border zone. Study of climate variations affecting the relief structure and the associated semi-desert, parkland-steppe and the alpine zone biodiversity is most essential for understanding the current geo-environmental transformations over the territory and pre-determining integration of geo-tourism as a part of the national economic development.

ACKNOWLEDGEMENTS

The conducted geography and geo-heritage investigations in East Kazakhstan were a part of field studies coordinated by the author and supported by the Czech Ministry of Environment, the Amanzholov East Kazakhstan State University, Ust'-Kamenogorsk and the Irbis ngo.

REFERENCES

Akhmetyev M.A., Dodonov A.E., Sotnikova M.V. (2005). Kazakhstan and Central Asia (Plains and Foothills). In: Velichko, A.A., Nechaev, V.P. (Eds), Cenozoic Climatic and Environmental Changes in Russia. Geological Society of America, pp.139–161.

Asrat A., Zwolinski Z. (2012). Geoheritage: from geoarchaeology to geotourism. Editorial. Quaestiones Geographicae 31(1), 5–6.

Aubekerov B. Zh. (1993). Stratigraphy and paleogeography of the plain zones of Kazakhstan during the Late Pleistocene and Holocene. Development of Landscape and Climate in Northern Asia in Late Pleistocene and Holocene 1, 101–110. Nauka, Moskva (in Russian).

Bábek O., Chlachula J., Grygar J. (2011). Non-magnetic indicators of pedogenesis related to loess magnetic enhancement and depletion from two contrasting loess-paleosol sections of Czech Republic and Central Siberia during the last glacial-interglacial cycle. Quaternary Science Reviews 30, 967–979.

Bouzekraoui H., Barakat A., Elyoussi M., Touhami F., Mouaddine A., Hafid A., Zwoliński Zb. (2018). Mapping geosites as gateways to the geotourism management in Central High-Atlas (Morocco). Quaestiones Geographicae 37(1), Bogucki Wydawnictwo Naukowe, Poznań, pp. 87–102.

Brilha J. (2016). Inventory and quantitative assessment of geosites and geodiversity sites: a review, Geoheritage 8(2), 119–134.

Butvilovskiy V.V. (1985). Catastrophic releases of waters of glacial lakes of the south-eastern Altai and their traces in relief. Geomorphology 1985(1), 65–74 (in Russian).

Cheremisin D.V. (2006). Frozen tombs in the Altai Mountains: strategies and perspectives. Archaeology, Ethnology and Anthropology of Eurasia 27(1), 157–159.

Chernenko Z.I., Chlachula J. (2017). Precious and decorative non-metallic minerals from East Kazakhstan: geological deposits and present utilisation. Proceedings, 17th International Multidisciplinary Scientific Geoconference SGEM, Sofia, 29.06.- 05.07.2017. Vol. 17, Issue 11: Science and Technologies in Geology Exploration and Mining, STEF92 Technology Press, Sofia, pp. 447–454.

Chikhachev P.A. (1974). Travel in East Kazakhstan. Nauka, Moskva, 317p (in Russian).

Chlachula J. (2001). Pleistocene climates, natural environments and palaeolithic occupation of the Altai area, west Central Siberia. In Lake Baikal and Surrounding Regions (S. Prokopenko, N. Catto, J. Chlachula, Eds.), Quaternary International 80-81, 131–167.

Chlachula J. (2003). The Siberian loess record and its significance for reconstruction of the Pleistocene climate change in north-central Asia. In: Dust Indicators and Records of Terrestrial and Marine Palaeoenvironments (DIRTMAP) (E. Derbyshire, Editor). Quaternary Science Reviews 22 (18-19), 1879–1906.

Chlachula J. (2007). Biodiversity Protection of Southern Altai in the Context of Contemporary Environmental Transformations and Sustainable Development. Sector 2–3 (East Kazakhstan). Final Report Field Studies 2007, Irbis, Staré Město, 152 p.

Chlachula J. (2010). Pleistocene climate change, natural environments and Palaeolithic peopling of East Kazakhstan, In: Eurasian Perspectives of Environmental Archaeology (J. Chlachula, N. Catto, Eds.), Quaternary International 220, 64–87.

Chlachula J. (2011). Biodiversity and environmental protection of Southern Altai. Studii Sicomunicari, Stiintelenaturii 27(1), 171–178.

Chlachula J. (2018). Environmental context and adaptations of the prehistoric and early historical occupation of the Southern Altai (SW Siberia – East Kazakhstan). Archaeological and Anthropological Sciences, 11(5), 2215-2236 doi.org/10.1007/s12520-018-0664-0.

Chlachula J., Sukhova M.G. (2011). Regional manifestations of present climate change in the Altai, Siberia. Proceedings, ICEEA 2nd International Conference on Environmental Engineering and Applications, Shanghai, China (August 19-21, 2011). In: International Proceedings of Chemical, Biological and Environmental Engineering. Environmental Engineering and Applications, Edited by Li Xuan, Vol. 17, pp. 134–139, IACSIT Press, Singapore.

Chupakhin V. (1968). Physical Geography of Kazakhstan. Alma-Ata. «Mektep» Press, 260 p. (in Russian).

Czerniawska J., Chlachula J. (2018). The Field Trip in the Thar Desert. Landform Analysis 35, 21–26.

Deviatkin E.V. (1981). The Cainozoic of the Inner Asia. Nauka, Moskva, 196 p.

Dowling, R.K. (2009). Geotourism's contribution to local and regional development. In: de Carvalho C, Rodrigues J (Eds) Geotourism and local development, Camar municipal de Idanha-a-Nova, Portugal, pp. 15–37.

Dowling R.K. (2011). Geotourism's global growth. Geoheritage 3(1), 1–13.

Dowling R.K., Newsome D. (2010). Global Geotourism Perspectives. Goodfellow Publishers, Woodeaton, Oxford.

Dunets A. N. (2011). Tourist and Recreational Complexes of Mountain Region, Altai State University Press, Barnaul, 150 p.

Dyachkov B.A., Mayorova N.P., Chernenko Z.I. (2014). History of East Kazakhstan geological structures development in the Hercynian, Cimmerian and Alpine cycles of tectonic genesis, Part II. Proceedings of the Ust-Kamenogorsk Kazakh Geographical Society, D. Serikbaev East Kazakhstan State Technical University Press, Ust-Kamenogorsk, pp. 42–48 (in Russian).

Galakhov V.P., Mukhametov P.M. (1999). Glaciers of the Altai. Nauka, Novosibirsk, 136 p.

Geta R.I., Yegorina A.V., Saparov K.T., Zhensikbaeva N.Z. (2015). Methods for Assessing the Recreational Potential of the Kazakhstan Part of Altai on the Basis of Information Theory, In: Academy of Natural Sciences. International Journal of Experimental Education (Moscow) 2015, 10–14.

Goessling S., Hall C.M. (2005). Tourism and Global Environmental Change. Ecological, Social, economic and political interrelationship. Routledge Publishers, London–New York, 331 p.

Gorbunov A., Samashev Z, Severskiy E. (2005). Treasures of Frozen Kurgans of the Kazakh Altai. Materials of the Berel' Burial Ground. Il'-Tech-Kitap, 114 p.

Hahn J. (2006). Impact of the Climate Change on the Frozen Tombs in the Altai Mountains, Heritage at Risk 2006/2007, 215–217.

Harms E., Sukhova M., Kocheeva N. (2016). On the concept of sustainable recreational use of natural resources of cross-border areas of Altai, Journal of Environmental Management and Tourism 2(14/7), 158–164.

Herget J. (2005). Reconstruction of Pleistocene ice-dammed lake outburst floods in Altai Mountains, Siberia. Geological Society of America, Special Publication, 386 p.

Hovorkova M., Chlachula J. (2012). Methods and Visualisation of Geographic Information System in Southern Altai. News of the Department of the National Geographic Society in the Altai Republic, University of Gorno Altai, Gorno Altaisk, 2012(3), 42-48.

Ilieş M., Ilieş G., Hotea M., Wendt J.A. (2017). Geomorphic attributes involved in sustainable ecosystem management scenario for the Ignis-Gutai Mountains Romania. Journal of Environmental Biology 38(5), 1121–1127.

Inskeep E. (1994). National and Regional Tourism Planning: Methodologies and Case Studies, New York, Rutledge, 249 p.

Jakobson-Tepfer E. (2008). Culture and Landscape of the High Altai. In: Preservation of the Frozen Tombs in the Altai Mountains, UNESCO, pp. 31–34.

Kenesbayev S.K, Abdrakhmanov A.A., Donidze G.I. (1971). Place Names of Kazakhstan, their research, writing and transcription. Proceedings of the Academy of Sciences of the KazSSR. Public Series 4, 73–74.

Konkashpayev G.K. (1959). Kazakh folk geographical terms. Proceedings of the Academy of Sciences of the KazSSR. Geographical Series 3, p.7 (in Russian).

Mason P. (2015). Tourism Impacts, Planning and Management. Routledge, Oxon, UK. 253 p.

Mazbaev O.B. (2016). Geographical Bases of Territorial Development of Tourism in Republic of Kazakhstan, Ph.D. Thesis, Al-Farabi Kazakh National University, Almaty, 138 p. (in Russian).

Melinte-Dobrinescu M.C., Brustur T., Jipa D., Macaleț R., Ion G., Ion E., Popa A., Stănescu I., Briceag, A. (2017). The Geological and Palaeontological Heritage of the Buzău Land Geopark (Carpathians, Romania). Geoheritage 2017(9), 225–236.

Mihalič T. (2000). Environmental management of a tourism destination: a factor of tourism competitiveness. Tourism Management 21(1), 65–78.

Mikhailova N.I. (2002). Environmental Evolution of East Kazakhstan in Cainozoic Period. In: Regional Components in System of Ecological Education, Ust-Kamenogorsk, pp. 88–93 (in Russian).

Mitrofanov V.P., Petr T. (1999). Fish and fisheries in the Altai, northern Thien-Shan, and Lake Balkhash (Kazakhstan). In: Petr, T. (Ed.), Fish and Fisheries in the High Altitudes (Asia). FAO Fisheries Technical Papers, Rome, Vol. 385, pp. 149–167.

Molodin V.I., Polosmak N.V., Novikov A.V., Bogdanov E.S., Slyusarenko I.Yu., Sheremisin D.V. (2004). Archaeological Monuments of the Plateau Ukok (Gorno Altai). IAET SB RAS, Novosibirsk, 255 p. (in Russian).

Narozhniy Y., Zemtsov V. (2011). Current State of the Altai Glaciers (Russia) and Trends Over the Period of Instrumental Observations 1952–2008, AMBIO 40, 575.

Nekhoroshev V.P. (1967). Eastern Kazakhstan. Geological Structure, In: Sidorenko A.V., Nedra M. (Eds.), Geology of the USSR, Volume 41, Nauka, Moskva–Leningrad, 467 p. (in Russian).

Newsome D., Dowling R.K. (Eds.) (2010). Geotourism: The Tourism of Geology and Landscape. Goodfellow Publishers, Woodeaton, Oxford.

Pacekov U.M., Jukova A.A., Alekseyev A.G., Artemeva E.L. (1990). Minerals of Kazakhstan, IGS AS KazSSR, Alma Ata, 196 p. (in Russian).

Polosmak N.V. (2001). Inhabitants of Ukok. Infolio, Novosibirsk, pp. 334.

Rudoy A.N., Baker, V.R. (1993). Sedimentary effects of cataclysmic late Pleistocene glacial outburst flooding, Altay Mountains, Siberia. Sedimentary Geology 85, 53–62.

Saarinen J., Rogerson C.M., Hall C.M. (2017). Geographies of tourism development and planning, Tourism Geographies 19(3), 307–317.

Samashev Z. (2001). Archaeological Monuments of the Kazakh Altai. Institute of Archaeology, Almaty, 108p (in Russian).

Samashev Z. (2011). Berel'. Ministry of Education and Science, Archaeological Institute, Taimas Press, Astana, 236 p.

Saparov K., Chlachula J., Yeginbayeva A. (2018). Toponymy of the Ancient Sary-Arka (North-Eastern Kazakhstan). Quaestiones Geographicae 37(3), 37–54.

Saparov K.T., Zhensikbayeva N.Z. (2016). Evaluation of the Natural Resource Potential of the Southern Altai. Vestnik, D. Serikbayev East Kazakhstan State Technical University, Scientific Journal (Ust-Kamenogorsk), pp. 66–71.

Sherba G.N., Bespayev X.A., Dyachkov B.A. (2000). Large Altai (Geology and Metallogeny). RIO VAC RK, Almaty, 400 p. (in Russian).

Surazakov A.B., Aizen V.B., Aizen E.M., Nikotin S.A. (2007). Glacier changes in the Siberian Altai Mountains, the Ob river basin, (1952–2006) estimated with high resolution imager. Environmental Research Letters 2(4), 1–7.

Svarichevskaya I. (1965). Geomorphology of Kazakhstan and Central Asia. Nauka, Leningrad (in Russian).

Swarbrooke J., Beard C., Leckie S., Pomfret G. (2003). Adventure Tourism, the New Frontier, in: Oxford, Butterworth-Heineman, 354 p.

Velikovskaya E.M. (1946). Relief Development of the Southern Altai and Kalba and Deep Gold Placers. Bulletin of the Moscow Institute of Petrology, Geology Section, 21(6), 57–77 (in Russian).

Wimbledon W.A.P., Smith-Meyer S. (Eds.) (2012). Geoheritage in Europe and Its Conservation. Oslo, ProGEO, 405 p. ISBN 978-82-426-2476-5.

Yegorina A.V. (2002). Physical Geography of East Kazakhstan, Ust-Kamenogorsk, EHI Press, 181 p. (in Russian).

Yegorina A., Saparov K.T., Zhensikbayeva, N. Z. (2016). The Structure of the Geo-Cultural Space of Southern Altai as a Factor of Tourist-Recreational Development. Vestnik, KNU, Scientific Journal. Almaty, pp. 214–219.

Yerdavletov S.R. (2000). Geography of Tourism: History, Theory, Methods, Practice.Textbook. Almaty, 336 p. (in Russian).

Zhensikbayeva N., Saparov K.., Atasoy E., Kulzhanova S., Wendt J. (2017). Determination of Southern Altai geography propitiousness extent for tourism development, in: GeoJournal of Tourism and Geosites 9(2), 158–164.

Zhensikbayeva N.Z., Saparov K.T., Chlachula J., Yegorina A.V., Atasoy A., Wendt J.A. (2018). Natural potential of tourism development in southern Altai. GeoJournal of Tourism and Geosites IX/1 (21), 200–212. ISSN 2065-0817.

Received on December 13th, 2018 Accepted on May 17th, 2019

Viktor Krechik[2], Stanislav Myslenkov[1,2,3*], Maria Kapustina[2]
[1] Lomonosov Moscow State University, Moscow, Russia
[2] Shirshov Institute of Oceanology, Russian Academy of Sciences, Moscow, Russia
[3] Hydrometeorological Research Centre of the Russian Federation, Marine forecast division, Moscow, Russia
***Corresponding author:** stasocean@gmail.com

NEW POSSIBILITIES IN THE STUDY OF COASTAL UPWELLINGS IN THE SOUTHEASTERN BALTIC SEA WITH USING THERMISTOR CHAIN

ABSTRACT. The article gives an analysis of a unique data of the thermistor chain, which installed on the D-6 oil platform in the coastal zone of the Baltic Sea. In total 10 temperature sensors were installed at different depths with a recording interval of 1 min, the depth at the installation site was 29 m. Based on satellite data, ship measurements and thermistor chain observation the characteristics and dynamics of the sharp decrease in water temperature which registered in the south-eastern Baltic Sea (Gdansk Bay area), during June 5-12, 2016 are analyzed. The temperature decreasing caused by the simultaneous action of at least two factors: wind-driven Ekman upwelling and advection of cold water. Scales of temporal and spatial variability of water temperature in a coastal zone of the south-eastern Baltic Sea near the coast of the Kaliningrad region are described. This event led to the considerable SST (sea surface temperature) drop by more than 8 °C for two days. The rate of reduction of its temperature during certain upwelling periods can reach 0.3-0.4 °C per hour, but the maximum warming rate between phases varies from 0.25 to 0.28 °C per hour. This dramatically changed the conditions of the thermal balance of the sea surface. The width of the upwelling, as seen in the SST data, was about 25 km. Satellite data were supplemented with data of a thermistor chain and CTD measurements. The high correlation between water temperature variability and changes in wind parameters: when the wind speed has decreased and its direction has changed, the response of the vertical thermal structure has occurred very quickly, sometimes within 1 hour. Thermistor chain data allow to evaluate the vertical temperature distribution and get more detailed analysis of temporal variability and short pulsations of upwelling.

KEY WORDS: coastal water; SST; satellite data; wind; Baltic Sea; upwelling; thermistor chain

CITATION: Viktor Krechik, Stanislav Myslenkov, Maria Kapustina (2019) New possibilities in the study of coastal upwellings in the southeastern Baltic Sea with using thermistor chain. Geography, Environment, Sustainability, Vol.12, No 2, p. 44-61
DOI-10.24057/2071-9388-2018-67

INTRODUCTION

Coastal upwelling is one of the most significant factors in the variability of surface water temperature near the coast (Kahru et al. 1995), and the most important vertical water exchange mechanism in the coastal zone of the sea (Esiukova et al. 2017; Hela 1976). In the conditions of two-layer stratification that is typical for the Baltic Sea, this phenomenon plays a key role in the balance of nutrients within the upper layer of the water column (Svansson 1975). In addition, after the first spring phytoplankton bloom, when the nutrients in the surface layer are depleted, coastal upwelling is sufficient to maintain the bloom (Siegel et al. 1999).

The first documented scientific observation of the effect of upwelling on the properties of the surface layer in the Baltic Sea was performed by Alexander von Humboldt in 1834 (Leppäranta and Myrberg 2010). In the second half of the 20th century observations of the temperature variability in the coastal zone were carried out on the basis of instrumental measurements and were of a local nature (Simons 1978; Walin 1972). A new stage in the study of sea surface temperature (hereafter SST) and upwelling began in the late 1980s when remote sensing data became widely used. During this period, a lot of studies of bioproductivity and upwelling phenomena were performed on the basis of satellite images of the Baltic Sea area (Horstmann 1983; Bychkova and Viktorov 1987; Gidhagen 1987). Later, when a large array of sea surface temperature maps was accumulated, statistical work on SST appeared both for the entire Baltic Sea (Lehmann and Myrberg 2008; Lehmann et al. 2012) and for its regions (Kreżel et al. 2005; Kowalewski and Ostrowski 2005).

Coastal upwelling within the investigated area occurs quite often (Bychkova et al. 1988; Lehmann et al. 2012; Kozlov et al. 2012) and is observed during the northern, northeastern and eastern winds (Kowalewski and Ostrowski 2005). From 2000 to 2014 135 upwelling events that occurred in the studied area during the period of stable thermal stratification (May-October) were identified (Esiukova et al. 2017).

Thus, satellite data are effectively used to detect and study upwelling. Their big advantage is a large spatial coverage. However, there are a number of shortcomings. Firstly, due to the high cloudiness typical of certain seasons for the Baltic Sea, these data are very irregular in time (Zhelezova et al. 2018). Secondly, satellite images may only provide a representation of a thin surface layer, and data about the state of water column deeper layers remains inaccessible (Elachi and van Zyr 2006).

Currently, the water temperature vertical structure in the Baltic Sea are mainly obtained when making sections with discrete oceanographic stations or using towed CTD-probes (Krechik and Gritsenko 2016; Kapustina et al. 2017; Demidov et al. 2011; Stepanova et al. 2015; Chubarenko et al. 2013; Demchenko and Chubarenko 2012; Zhurbas et al. 2012). In the southeastern part of the Baltic Sea, a large amount of such data are obtained during the research vessels' cruises and the industrial environmental monitoring of the Kravtsovskoye oil field (Sivkov et al. 2012). As part of the monitoring, measurements of meteorological characteristics are carried out on the D-6 platform (Stont et al. 2012), and measurements of waves and currents have been carried out periodically (Ambrosimov et al. 2013). Monitoring of the temperature and salinity is based on CTD measurements from the surface to the bottom once a month (Sivkov et al. 2012). Such data allow us to identify spatial heterogeneity, seasonal and inter-annual variability of water temperature.

The thermistor chains are used for investigation of the propagation parameters of internal waves and the high-frequency variability of water temperature (Gemmrich and van Haren 2002; Van Haren et al. 2005; Serebryanyy et al. 2014) and also to study different-scale effects of vertical mixing and stratification (Gemmrich and van Haren 2001; Brookes et al. 2013) all over the world.

Such method of observation is little used in the Baltic Sea (Massel 2015), but the studies which based on the thermistor chains data show good results and effectivity of these devices (Sellschopp 1991; Morozov et al. 2007; Van der Lee and Umlauf 2011).

There are first results of analysis data, which received from thermistor chain installed in southeastern part of the Baltic Sea on D-6 platform in 2015, presented in articles (Myslenkov et al. 2017a,b). The thermistor chain data allow us to study the vertical structure of the temperature distribution at different time scales, including the hourly scale (Myslenkov et al. 2017a). Comparison of in situ measurements with remote sensing data carried out for this region showed that the systematic error of satellite data did not exceed +0.25 °C in all cases and was no more than +0.14 °C when strong diurnal warming was not taken into account (Myslenkov et al. 2017b). Thus, our data set represents a rather rare occasion for the joint application of remote sensing data and in situ data to study upwelling.

The purpose of this study is to describe and analyze the upwelling parameters recorded in the summer of 2016 near the coast of the Kaliningrad region, based on satellite imagery and in situ measurements. New possibilities of using the thermistor chain in the study of upwelling are presented.

DATA AND METHODS

SST was obtained in the study area from the multi-sensor Earth remote sensing data, distributed by CMEMS (Copernicus Marine Environment Monitoring Service), with spatial resolution 0,02 * 0,02 degree and L3 processing level. This data were averaged daily. The data were obtained from different scanners: AVHRR/3 (MetOp-B, NOAA-18 and NOAA-19), MODIS (Terra and Aqua), VIIRS (Suomi NPP) and AMSR-2 (GCOM-W1). Non-corrected products are 24 hourly syntheses centered at 00 UTC. Quantum-GIS software was used to process and analyze the data.

For the joint analysis of satellite and thermistor chain data, the Level-2 SST images downloaded from NASA OceanColor website (https://oceancolor.gsfc.nasa.gov) were used. The analysis was carried out on the basis of data from spectroradiometers MODIS, based on the Terra and Aqua satellites, as well as the spectroradiometer VIIRS, based on the Suomi NPP satellite. The spatial resolution of the data was 1 km in the nadir for MODIS and 0.75 km in the nadir for VIIRS and the swath' width were 2330 and 3000 km, respectively. At the first stage, the images covered the thermistor chain location was selected, regardless of the position of the satellite track. Then the location of the satellite data points relative to the location of the measuring device was checked. The QGIS software was used for this procedure. The data points located from the thermistor chain at the distance exceeded the double spatial resolution of the MODIS spectroradiometer were not taken into account. At the second stage, the difference between the SST data and the temperature measured by the thermistor chain was calculated. Next, a filter based on the three sigma rule (Pukelsheim 1994) was applied. The author of the work (Lehmann 2013) showed that for gross measurement errors, which act randomly, this rule works poorly. For this reason, the confidence interval was reduced from 99.73 to 95%. The boundaries of the confidence interval were determined by the expression $X_{mean} \pm 1.96\sigma$.

The data of the thermistor chain which installed on the offshore ice-resistant fixed platform (hereafter OIFP) D-6 (Fig. 1) were used. D-6 is located in the coastal zone 22 km offshore of the Curonian Spit (Southeastern Baltic Sea). The thermistor chain consists of 10 "Starmon mini" sensors located at the depths of –0.9, 0.15, 1, 3, 5, 8, 10, 13, 24, 28 m. The depth at the installation site is 29 m. In the event of a strong wave, the first two-three sensors were periodically in the air, but these data can be filtered because of the sharp increase in the temperature dispersion. The time step of temperature measurements is 1 min; accuracy is +/- 0.025 °C.

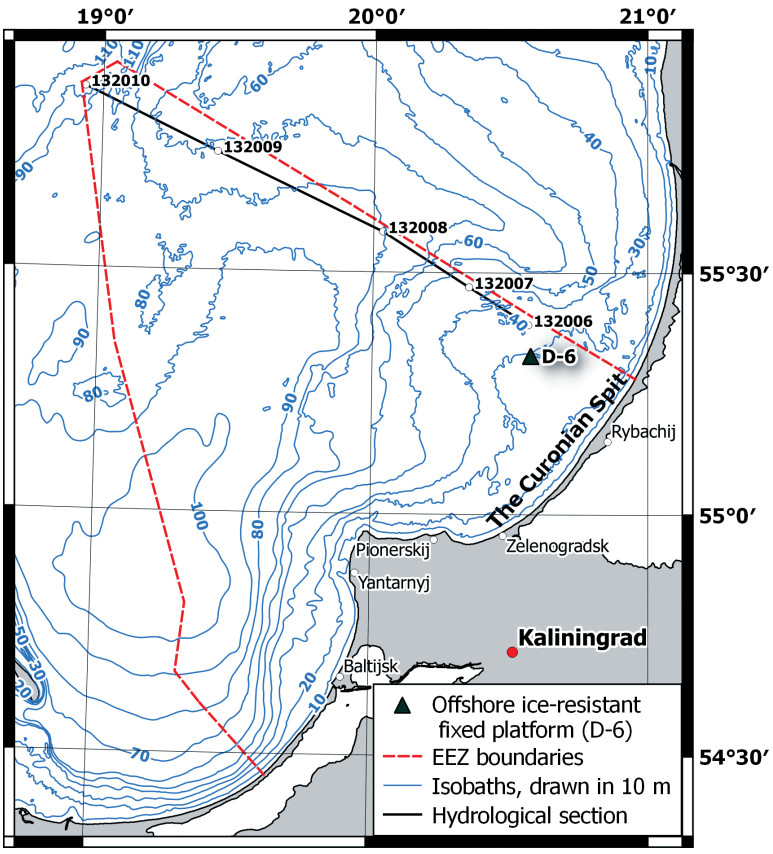

Fig. 1. The study area and stations location

The vertical temperature distribution on the hydrological section (stations 132006-132010, Fig. 1)) was measured using a CTD90M probe, produced by Sea & Sun Technology, Germany. The soundings were made from the surface to the bottom in the mode of the free sliding probe along the hawser. The lowering speed of the instrument was from 0.7 to 1 m/s with a measurement frequency of 4 Hz. This method makes it possible to record changes in the parameters with a high resolution. The measurements were carried out during the 132nd cruise of the research vessel Professor Shtokman (11-16 of June 2016).

Meteorological data were received by the meteorological station KRAMS-4-03, which is located on the OIFP D-6. The height of the sensors is 27 m above the sea. The station automatically measures and records the following parameters: air temperature and relative humidity, wind speed and direction, atmospheric pressure, cloud height, meteorological optical visibility range. Only data on wind speed and direction were used in this study.

Wind speed and direction data over the all study area were obtained from the high-resolution reanalysis NCEP/CFSR (Climate Forecast System Version 2) (2011-2016) (Saha et al. 2014; CISL... 2015). The wind's parameters were obtained at 10 meters height with a spatial resolution of ~ 0.2 °. To improve the quality of visualization, the data are presented with a spacing of ~0.4 ° and a time step of 3 hours.

RESULTS

All available sea temperature data (satellite, hydrological section) was used to study the sharp decrease in water temperature which had been observed since June 4 till

12, 2016 along the coast of the Curonian Spit. However, the basic information for analysis was obtained by the thermistor chain installed on the D-6 platform. According to these data, in May 2016 an intensive warming of the upper water layer was observed in the southeastern Baltic Sea. Thus, at the beginning of June, the water surface temperature was about 19–20 °C. At the same time the upper mixed layer (UML) thickness was not great, and at the depth of 13 m the temperature varies from 10 to 11 °C (Fig. 2). Since June 4 till 11, the surface temperature had been dropped to 8.2 °C and then, its values increased again to 20 °C by June 26. The amplitude of the temperature was more than 10 °C. It is the unique and extreme event for the summer period in this region. Due to the availability of high temporal resolution water temperature data at the different depths obtained by the moored thermistor chain, it became possible to make a deep analysis of this event.

In the coastal zone, similar temperature dropping is usually associated with upwelling (Lehmann and Myrberg 2008). However, it is well-known that a decrease in temperature could be caused by various reasons, such as atmospheric cooling effects, advection of colder waters and upwelling events (as wind-driven or eddy-driven). Apparently, in the studied case, the temperature decreasing could be caused by the simultaneous action of at least two factors from those, which listed above: wind-driven upwelling and advection. As far as upwelling is a complex dynamic process, it should be considered as a whole.

Let us consider a relatively short period of time since June 1 till 16, 2016 in more details. The water column had been well stratified and the surface layer temperature varied from 15.67 to 18.79 °C before the upwelling event started. At the time of the cooling started, the sea surface temperature at the observation point was 18.55 °C. Strong NNE wind, blowing since the last half of 3 till 5 of June caused the formation of an upper mixed layer. Simultaneously with changing of the wind direction to the northern, there was the temperature dropping, registered by the thermistor

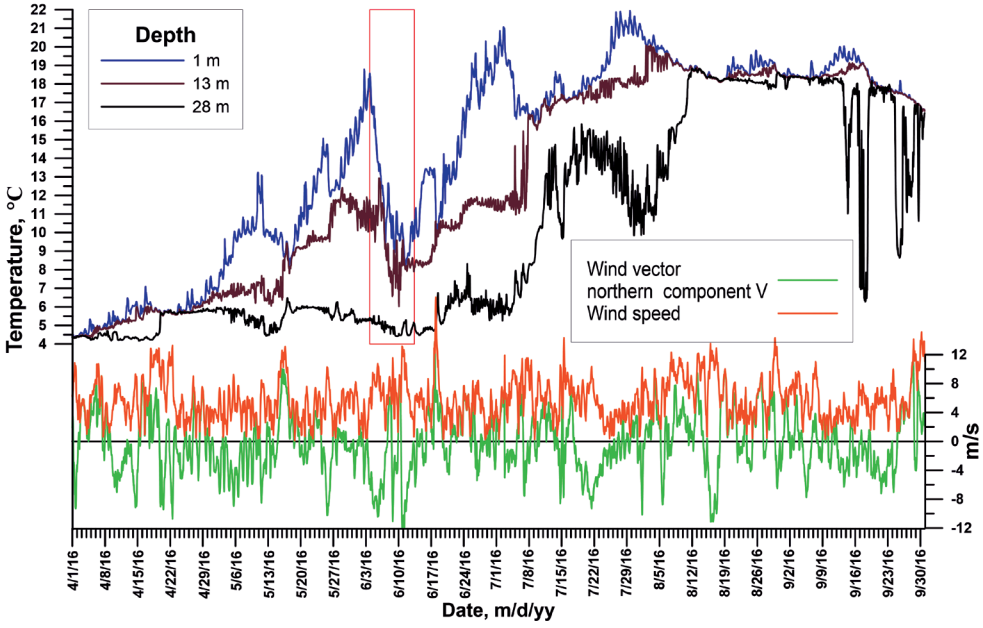

Fig. 2. The water temperature at the upper, medium and near-bottom layers according to the data of the thermistor chain during April 1–September 30, 2016, and the northern wind component and also wind speed according to NCEP/CFSR reanalysis near the D-6 platform. The red frame shows the period of the studied event

chain. By the end of June 5, UML thickness was about 10 m and the temperature decreased by 5.31 °C. The average cooling rate of the UML was about 0.1°C per hour. At the water depths of 24 and 28 m, no significant changes were recorded (Fig. 3).

The reaction of coastal waters in the study area on the wind direction changing was confirmed by remote sensing data. On the satellite image on June 6 the cold water jets were well-identified. The SST map showed three such regions: in the north of the study water area, along the Curonian Spit coast and near the western coast of Kaliningrad region (Fig. 4). Taking into account the direction of the wind, blowing along the coast, the presence of such jets is a typical occurrence of the Ekman origin upwelling event. The presence of different areas (from north to the south) where the same events have been recognized is evidence of this type of upwelling origin. It should be noted that a cold water jet pressed to the shore and observed in areas where the coast extends from north to south direction.

Due to the northern wind impact had been continued, the average rate of cooling of the water column increased to 0.16 °C per hour at the beginning of June 7. The thickness of the UML reached 13 m, and its temperature dropped to 9.6 °C. The temperature dropping has been lasting for 25 hours. Then the wind speed had decreased and at 2 am on June 7, the stratification began to recover. Later, the wind changed the direction to the west and water temperature started to increase (Fig. 3). On June 8 the values of water temperature started to show the recession again. The average rate of cooling was about 0.16 °C per hour. However, at this time, the southeastern wind was observed over the water area, which couldn't lead to the formation of coastal upwelling either under the forcing of the Ekman transport or the downsurge. This situation was also well demonstrated by the fact that there was no cold water in the surface layer along the western coast of the Kaliningrad region. Consequently, here we have seen no coastal upwelling, but rather the advection of a cold water stream from the neighbour water areas. Apparently, due to the long

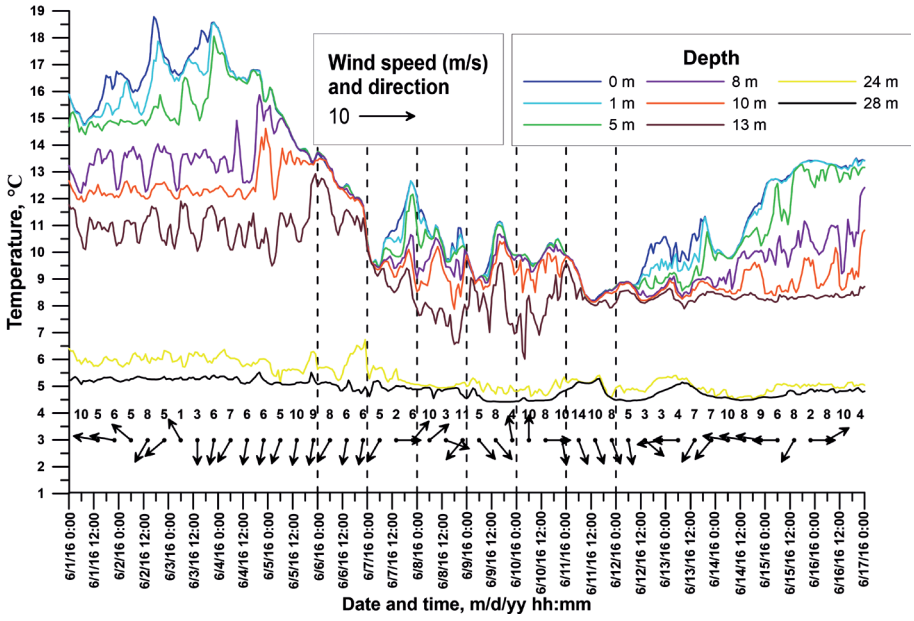

Fig. 3. The water temperature at different depths according to the data of the thermistor chain during 01-16.06.2016, and the wind speed and direction at the D-6 platform (marked every 8 hours). Intermittent vertical lines indicate the time of the shown satellite images

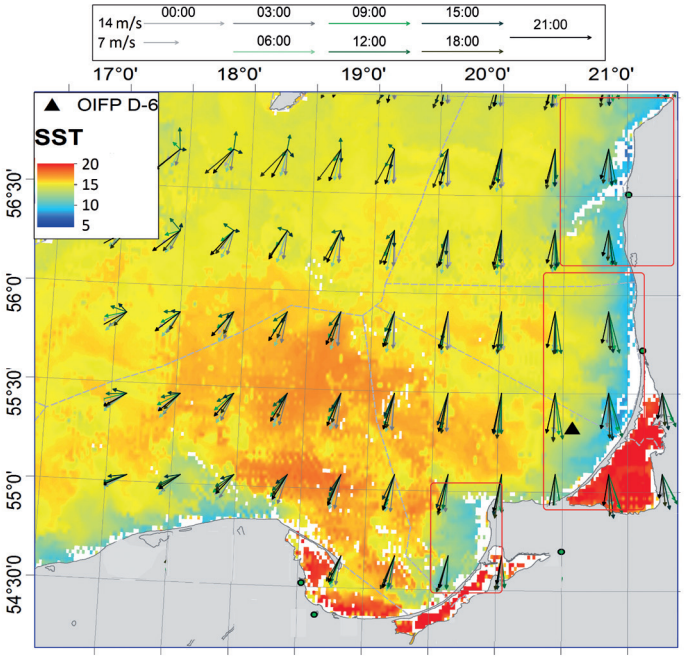

Fig. 4. Wind speed and direction (3 hourly arrows, NCEP/CSFR reanalysis) on June 5, 2016 and SST on June 6, 2016 (coloured contours with SST in °C, satellite data). Top panel: sample arrows indicating 14 m/s and 7 m/s winds, colour coded for the synoptic hours of observation. The red frames mark the locations of the Ekman origin upwelling event occurrence

exposure of the west and south-west winds in combination with the aspect of the coastline, a positive sea level anomaly was formed here. The coastal level anomaly caused the formation of a compensation off-shore current. This current began to deliver cold water in the south-western direction to the OIFP D-6 (Fig. 5).

On the night of June 9, the NE wind leads to the beginning of the second phase of upwelling. The thickness of the UML increased, and the SST decreased (Fig. 3). At 4 a.m. on June 9, the direction of the wind changed to the north-west and the upwelling stopped. The temperature of the surface layer increased. Thermal stratification appeared in the water column again (Fig. 3).

On June 10, the thermal stratification of the water column increased (Fig. 3). In the first half of the day a southerly wind was observed above the area, and then the direction of the wind veered to the west. From 7 p.m. the wind speed increased to 10-12 m/s and direction changed to northerly. This led to the beginning of the third phase of upwelling. Since the beginning of June 11, the temperature of the surface layer has been rapidly decreasing to 8.14 °C (11th of June at 10:54). The temperature decreased on average 0.13 °C per hour. Then its slow growth was noted (Fig. 3).

On June 11, because of the rather strong cloudiness above the Gdansk Basin, it was not possible to obtain a high-quality satellite image. However, we can recognize a decrease in the SST values of the open part of the sea. There was a noticeable increase in the area of coastal waters with lower temperatures north towards of the D-6 platform (Fig. 6).

The hydrological section performed in this period (Fig. 7) shows that the vertical temperature distribution in the Gdansk Basin consisted of two layers. The surface temperature of the open sea varies between 14-14.8 °C. In the coastal zone from an isobath of 50 m, where the upwelling

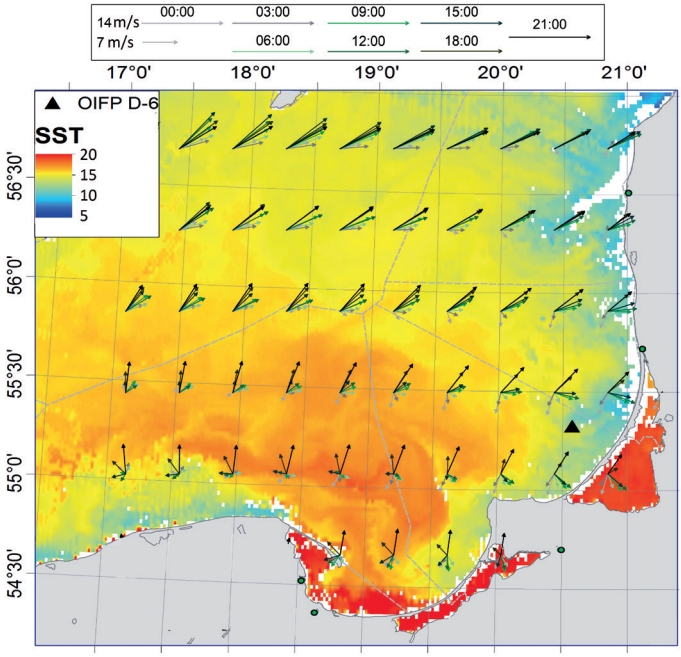

Fig. 5. Wind speed and direction (3 hourly arrows, NCEP/CSFR reanalysis) on June 7, 2016 and SST on June 8, 2016 (coloured contours with SST in °C, satellite data). Top panel: sample arrows indicating 14 m/s and 7 m/s winds, colour coded for the synoptic hours of observation

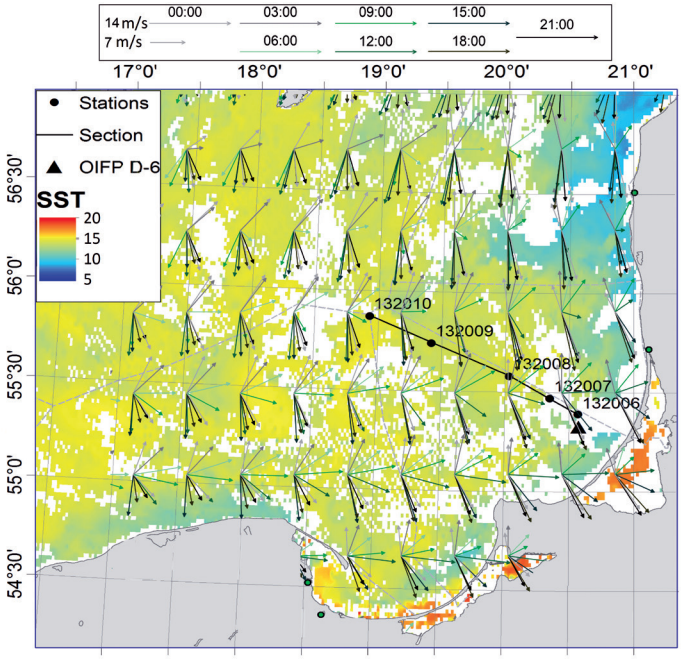

Fig. 6. Wind speed and direction (3 hourly arrows, NCEP/CSFR reanalysis) on June 10, 2016 and SST on June 11, 2016 (coloured contours with SST in °C, satellite data). Top panel: sample arrows indicating 14 m/s and 7 m/s winds, colour coded for the synoptic hours of observation

occurred, the surface layer temperature varied from 9.6 (station 132006) to 12.4 °C (station 132007). The upper boundary of the seasonal thermocline penetrated down to 18 m, and its thickness reduced from 14 to 8 m due to the rising of the upper part. Gradients in the thermocline core also decreased from 0.6-0.8 °C/m to 0.2-0.3 °C/m towards the shore.

According to the thermistor chain data, the upwelling in the study area lasted until 10 a.m. on June 12 (Fig. 3). Then the wind direction changed and the warming of the water column began. From June 12 10:00 onwards, SST (surface thermistor) reached values greater than 10 °C. Thermal stratification was well traced to a depth of 8 m. Below this depth, there was a quasihomogeneous layer, which thickness was more than 5 m. On June 13, the water column was thermally stratified in the same way. The surface layer had warmed up and at 7 p.m. on June 13 the SST values in the area of the D-6 platform increased to 11.36 °C. (Fig. 3). Then, under the influence of the northeast wind, the temperature dropped to 9.79 ºC on June 14 at 7:27 am. It should be noted that the reaction of the water column began only when the wind speed had increased up to 8 m/s. Despite the fact that the wind of the same direction at a speed of 5-7 m/s had been blowing during 6 hours over the water area before it. Then the warming up of the water continued and since the end of June 15 till the beginning of June 17, the temperature of the water column varied from 13.13 to 13.47 ºC (Fig. 3).

The processes described above could be characterized in some numerical indicators, such as the thickness of the UML, the sea surface temperature minimum and maximum, the rate of temperature variability, the weather and etc. The detailed description of the hydrometeorological conditions in the study area separately for each day is contained in Table1.

The information contained at Table 1 clearly demonstrates that in contrast to satellite data, the thermistor chain allows to estimate the vertical structure of water, as well as the dynamics of temperature changes during various events with a high resolution. At the same time, satellite data allows as to see the dynamics of coastal upwelling over a large water area and observe the same event on a different spatial and temporal scale. And meteorological data is critically necessary for the correct interpretation of remote sensing data and in-situ measurements.

DISCUSSION

Any research aimed at estimation and analyzing new possibilities, methods and techniques for studying natural phenomena should cover a number of questions dedicated to their effectiveness. One of

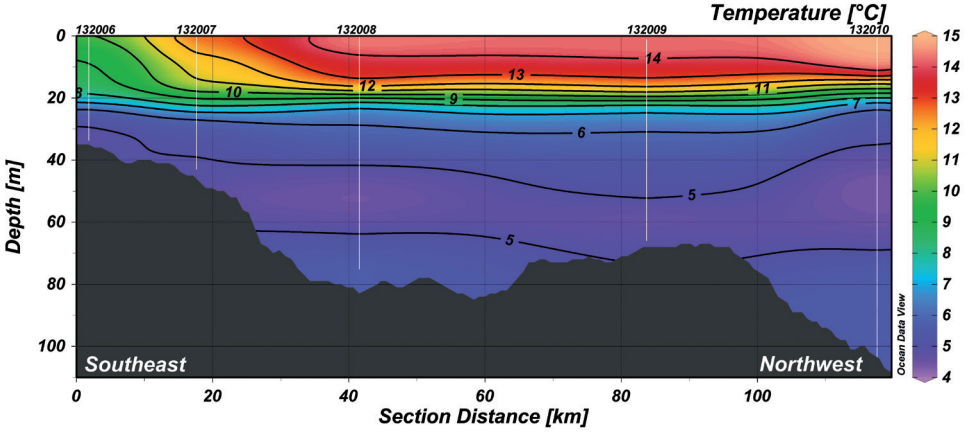

Fig. 7. Vertical temperature distribution on June 11 at the hydrological section. The location of the section is shown at Fig. 1 and Fig. 6

Table 1. Hydrometeorological conditions for the period from 5 to 13 of June 2016

Date (DD. MM)	Meteorological conditions	Characteristics of the surface layer					
		According to thermistor chain data (average temperature gradient)			According to remote sensing data		
		UML thickness	Temperature changes (for horizons 1 and 5 m.)	Average rate of temperature decreasing / increasing, (°C / hour) (1 and 5 m.)	SST of the open sea (°C)	SST of the upwelling zone (°C)	SST of the D6 platform area (°C)
5.06	NNE with speed 5-11 m/s (maximum at 3 p.m.)	Increasing from 5 m. to 8 m. (4 a.m.), than to 10 m. (7 p.m.)	Decreasing from 16 (0:00) to 13.3 °C (10 p.m.)	-0.11; -0.11	17-18	10-11	14-15
6.06	NNE, 3-13 m/s	10 m.	Decreasing from 13.5 °C (0:00) to 9.9 °C (11 p.m.)	-0.16; -0.17	16-17	9-10	13-14 (Fig. 4)
7.06	NNE, NE 2-5 m/s	13 m. (0:00-6 a.m.)	Increasing from 9.6 (0:00) to 12.6 °C (7 p.m.)	0.16; 0.16	15-16	10-11	12-13
7.06	From 11 a.m. direction changes to W-SW, 1-6 m/s	Up to 1 m. (7 a.m. - 6 p.m.)					
		5 m. (7 p.m.-11 p.m.)	Decreasing to 11.4 °C (11 p.m.)	-0.30; -0.34			
8.06	Till 12 p.m. SW, 7-10 m/s, than W, 2-8 m/s	Increasing from 5 m. (0:00-2 a.m.) to 8 m. (3 a.m.-8 a.m.), than to 10 m. (9 a.m.-2 p.m.)	Decreasing from 11.6 °C (0:00) to 9.9 °C (5 p.m.)	-0.15; -0.14	15-17	11-13	13 (Fig. 5)
8.06	From 6 p.m. NNE, 7-13 m/s	Decreasing to 5 m. (3 p.m.-11 p.m.). Increasing to 8 m (9 p.m.), than - 10 m.	Decreasing to 9.5 °C (11 p.m.)	-0.08; -0.07			
9.06	To 4 a.m. NNE, 2-7 m/s.	10-13 m. (0:00 - 8 a.m.)	Decreasing from 9.3°C (0:00) to 8.9 °C (3 a.m.)	-0.21; -0.25	15	9-12	11-12
	From 5 a.m. NW-NNW, 5-8 m/s	8 m. (9 a.m.-3 p.m.),	Increasing from 8.9 °C (4 a.m.) to 11.1 °C (2 p.m.)	0.21; 0.21			
9.06	From 8 p.m. - S, 1-6 m/s	10 m. (4 p.m. - 11 p.m.)	Decreasing to 9.8 °C (at 11 p.m.)	-0.18; -0.18			

10.06	Till 11 a.m. S-SSW, 7-10 m/s	8 m.	Decreasing from 9.8°C (0:00) to 9.6°C (5 a.m.)	-0.05; -0.06	14-15	11-12	10-11
10.06	From 12 p.m. W-NW, up to 12 m/s.		Increasing from 9.6 °C (at 6 a.m.) to 10.5 °C (6 p.m.)	0.08; 0.08			
	From 7 p.m.-N, 9-12 m/s.		Decreasing from 10.4°C (7 p.m.) to 9.8°C (11 p.m.)	-0.14; -0.14			
11.06	NNW-N, 9-14 m/s	10 m. (0:00-6 a.m.)	Decreasing from 9.8 °C (at 0:00) to 8.2 °C (at 11 a.m.).	-0.12; -0.13	13-14	11	12 (Fig. 6)
		13 m. (7 a.m.-5 p.m.), than 10 m. (6 p.m.-11 p.m.)	Increasing to 8.8°C (11 p.m.)	0.05; 0.06			
12.06	NW-NNW, 3-7 m/s	Decreasing from 13 m. (0:00-10 a.m.) to 0 m. (11 a.m.-11 p.m.)	Increasing from 8.8 °C (at 0:00) to 10.5°C (at 10 p.m.)	0.06; 0.03	13-14	10-11	11
12.06	At 7 p.m. NNE-E, 1-3 m/s.						
13.06	ENE-E, 3-4 m/s	0 m.	Decreasing from 10.6 °C (at 0:00) to 9.7 °C (at 9 a.m.)	-0.08; -0.03	14-15	12-13	11-12
13.06	From 10 a.m. direction changes to NNE -NE, 7-8 m/s	1-5 m. (4 p.m.-11 p.m.)	Increasing to 11.3°C (5 p.m.)	0.10; 0.18			

the main objectives of similar studies is the validation of new and generally accepted methods and the estimation of the difference between their results. The idea of comparing remote satellite data with contact measurements is not new. However, in the framework of this study the joint analysis of different time scale data was performed. We have made validation of the satellite data with the thermistor chain data. To increase the time resolution of the remote sensing data the information obtained by three different satellites was analyzed. The preliminary data set included not only the acquisition data received directly over the OIFP (2 times a day) but also images containing SST data near the D-6 platform. It is known that the spatial resolution of satellite data deteriorates from the nadir to the edge of the swath. For this reason, we took into account the data in which the distance from the thermistor chain to the centre of the nearest pixel did not exceed 2 km. Then the second stage of data filtering was carried out. The procedure is described in detail in the "Materials and Methods" section. The statistical estimation of the data set is shown in Table 2, and the results of the data comparison are shown in Fig. 8.

The maximum statistical indicators values are shown in bold and the minimum one is shown in underline.

Table 2. The statistical estimate of the distance from the SST map value point to the point of the thermistor chain installation and the difference between the remote sensing data and in-situ measurements

Characteristic	Statistical indicator	Aqua	Terra	Suomi	All satellites
Distance from the OIFP to pixel center	Average	**1.03**	0.77	0.51	0.75
	Median	**1.04**	0.65	0.42	0.73
	Standard deviation	**0.42**	0.36	0.36	0.43
	Minimum	0.25	**0.4**	0.15	0.15
	Maximum	1.7	**1.83**	1.42	1.83
	Count	18	19	21	58
The difference between satellite and in-situ data (SST-thermistor chain)	Average	**0.54**	-0.03	0.11	0.19
	Median	**0.62**	0.15	0.07	0.37
	Standard deviation	1.12	**1.55**	1.01	1.25
	Minimum	-1.75	**-2.92**	-2.70	-2.92
	Maximum	**3.09**	2.9	1.55	3.09
	Count	18	19	21	58

It is known that the results of remote sensing are applicable to the upper thin layer of water (skin-layer), with a thickness of 10-100 μm. And this temperature differs from the surface temperature in the oceanographic point of view due to the fact that most SST in situ measurements are made at a depth of up to one meter (Siegel et al. 2008) The thermistor chain measurements on the OIFP D-6 were obtained at a depth of several decimeters to one meter depending on the state of the sea surface and sea level anomaly. However, the Table 1 shows that the absolute value of the difference between satellite data and contact measurements did not exceed 3.09 °C, and statistical indicators reflecting the central value of the data set were less than half a degree Celsius (0.19 °C for the average and 0.37 °C for the median). All other things being constant, the Aqua satellite showed the worst results, the Terra satellite has quite good results. The Suomi satellite proved to be the best of all; its standard deviation of the difference between SST and thermistor chain measurements was 1.5 times less than Terra's one. It is impossible to assert with confidence that this fact is related to the difference in the used spectroradiometers (MODIS and VIIRS). Probably, such results were provided with a higher spatial resolution of VIIRS than other devices. The average deviation of this satellite from the location of the D-6 platform was 0.51 km. It is interesting that due to the location of the track of the Terra satellite relative to the OIFP, its average deviation from the point of contact measurements was less than its spatial resolution (Table 1).

The Fig. 8 showed the comparison of the remote sensing data and the in-situ measured temperature values. The one minute time resolution of the thermistor chain allowed making the intercomparison with such time resolution. As can be seen from Fig. 8, most of the values of the two data

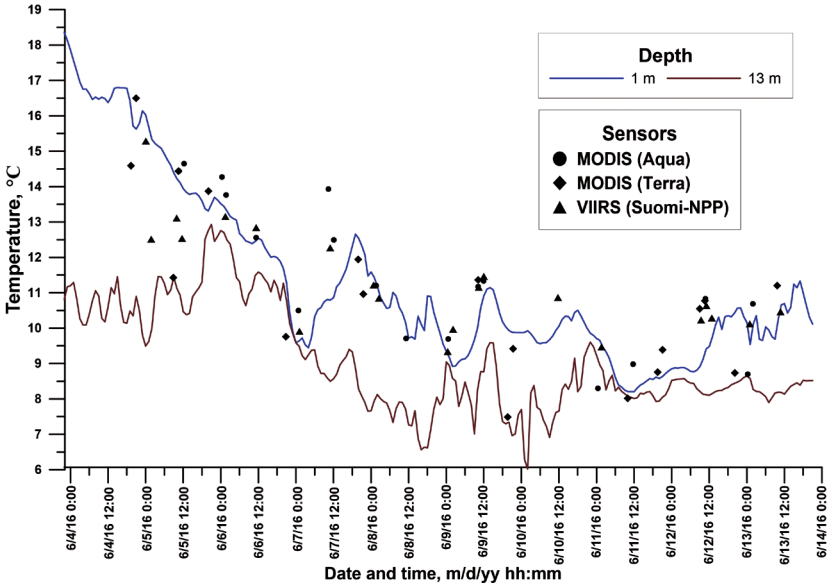

Fig. 8. The comparison of the SST data and the temperature values were obtained by the thermistor chain

samples coincide within about 1 ºC. These results should be recognized as quite good in view of the fact that the satellite acquisition results for this period were obtained under conditions of the thermal structure variability of surface waters, the variable wind speed and sea-surface conditions. All of these are negative physical effects that could create strong differences between the thermal skin-layer and the depth of several decimeters (Robinson 2004).

The intercomparison of SST maps and the thermistor chain measurements demonstrates that despite the representativeness of satellite data for a thin skin-layer, remote sensing data could be used for the surface layer temperature estimation. Due to the fact that satellite imagery shows the dynamics of the processes in general, these data could also be used to study the variability of the temperature of the upper part of UML on a scale exceeding the diurnal one. The lack of data on cloudy days and the long acquisition event interval do not allow to make the analysis of high-frequency temperature variability.

CONCLUSIONS

Based on satellite data, ship measurements and thermistor chain observation the characteristics and dynamics of the sharp decrease in water temperature registered during June 5-12, 2016 in south-eastern Baltic Sea (Gdansk Bay area) are considered. This event led to the considerable SST drop by more than 8 °C for two days. The temperature decreasing caused by the simultaneous action of at least two factors: wind-driven Ekman upwelling and advection of cold water. The temperature decreasing has an impulse character and included several phases. In first phase it was a strong north-north-easterly wind within 2 days which caused Ekman upwelling. A clear response of the temperature to a change in the wind stress was fixed through to the thermistor chain data. In the second phase it was no coastal upwelling, but rather the advection of a cold water stream from the neighbour water areas. All this phases was occurrence in the SST field of the coastal zone arises with the beginning of the first phase and is preserved until the end of the last one. The rate of reduction of its temperature during certain upwelling periods can reach 0.3-0.4 ºC per hour, but the maximum warm-

ing rate between phases varies from 0.25 to 0.28 ºC per hour.

At depths of 30-50 m, the compensatory rise of cold waters leads to the rising of the seasonal thermocline and causes a reduction of the vertical temperature gradients in its core by 2-3 times. This process promotes vertical mixing, as well as the formation of frontal zones in the coastal waters. The movement of cold water offshore by means of Ekman transport ensures their advection to the open sea, reducing the temperature of its surface. So during the upwelling observed from 5 to 12 June 2016 the surface layer temperature in the open sea in the study area dropped by 3-4 °C. In the vicinity of the D-6 platform, the maximum SST amplitude reached 10.22 °C.

An important result of this study is the high correlation between water temperature variability and changes in wind parameters: when the wind speed has decreased and its direction has changed, the response of the vertical thermal structure has occurred very quickly, sometimes within 1 hour. Such a situation was observed during the period of Ekman upwelling occurrence, but during the periods of advection occurrence such feature was not traced. It is impossible to identify such associations using the remote sensing data, due to the limitations caused by the orbital characteristics of the satellites and the large temporal resolution of the data.

However, one should not consider the thermistor chain as a universal tool for studying the coastal upwelling events that could replace satellite data or other devices and methods of in-situ measurements. But the thermistor chain using allows us to look inside the phenomenon and study its vertical structure and small-scale processes. It makes possible to supplement the existing ideas about temperature variability and correctly interpret the measurement results. At the same time, the coastal upwelling is a multifactorial process and for its study and analysis, an integrated approach is required which allow making the simultaneous observation of the same event on different spatial and temporal scales. That is why the simultaneous using of the remote sensing data which illustrate the dynamics of the coastal upwelling over a large area and measurements with a high resolution is important. There is the same situation with meteorological data. It's necessary to have simultaneous measurements of the thermistor chain and the weather station for the understanding of the processes occurring within the upwelling phenomenon and their cause-and-effect relationship. At the same time, the reanalysis data show us the meteorological situation in the entire water area of the study area and beyond. Of course, for a correct comprehensive analysis of the upwelling process and its origin, it is necessary to observe the currents. The absence of such data in the presented study is undoubtedly a negative fact. It is also very promising to continue research in this area is the usage of three moored thermistor chains, located in the shape of a triangle at a distance of several kilometres from each other. This modification will make it possible to observe the processes of water advection along and across the shelf, as well as a vertical structure variability during upwelling events more better.

ACKNOWLEDGEMENTS

This research was performed in the framework of the state assignment of IO RAS (Theme No.0149-2019-0013). The part of work in analysis thermos-chain data were obtained within the RSF grant (project No.14-50-00095). Authors are grateful to LLC "Lukoil-KMN" (Kaliningrad) for assistance in the installation of equipment and organization of data acquisition process.

REFERENCES

Ambrosimov A.K., Kabatchenko I.M., Stont Z.I., Yakubov S.K. (2013) Seasonal characteristics of waves in the southeastern part of the Baltic Sea in 2008-2009. Russian Meteorology and Hydrology, 38, (3), pp. 191-198. DOI:10.3103/S1068373913030084.

Brookes J.D., O'Brien K.R., Burford M.A., Bruesewitz D.A., Hodges B.R., McBride C., and Hamilton D.P. (2013). Effects of diurnal vertical mixing and stratification on phytoplankton productivity in geothermal Lake Rotowhero, New Zealand. Inland Waters, 3(3), 369-376. DOI: 10.5268/IW-3.3.625

Bychkova I.A., Viktorov S.V., Shumakher D.A. (1988). A relationship between the large-scale atmospheric circulation and the origin of coastal upwelling in the Baltic Sea. Russian Meteorology and Hydrology, 10, pp. 91–98 (in Russian).

Bychkova I. and Viktorov S. (1987). Use of satellite data for identification and classification of upwelling in the Baltic Sea. Oceanology, 27(2), pp. 158-162.

Chubarenko I.P., Afonov V.V., Chugaevich V.Ya., Krechik V.A. (2013). Water dynamics above the sloping bottom due to an intense summer heating. Russian Meteorology and Hydrology, 1, pp. 66-78. DOI:10.3103/S1068373913010068.

CISL Research Data Archive (2018). NCEP/NCAR Reanalysis Project. [online] Available at: http://rda.ucar.edu/ [Accessed 26 Oct. 2018].

Demchenko N.Yu. and Chubarenko I.P. (2012). Spatiotemporal variability of thermal front features in the Baltic Sea 2010-2011. Oceanology, №6 (52), pp. 790-797. DOI:10.1134/S0001437012060021.

Demidov A.N., Myslenkov S.A., Gritsenko V.A., Chugaevich V.Ya., Sultanov P.A., Pisareva M.N., Silvestrova K.P., Polukhin A.A. (2011). Specific features of water structure and dynamics within the coastal part of the Baltic Sea near the Sambian Peninsula. Moscow State University Bulletin. Series 5. Geography, 1, pp. 41–47 (in Russian with English summary).

Elachi Ch., and Jakob J. Van Zyl (2006). Introduction To The Physics and Techniques of Remote Sensing, 2nd Edition. John Wiley & Sons. DOI:10.1063/1.2811643.

Esiukova E.E., Chubarenko I.P., Stont Zh.I. (2017). Upwelling or differential cooling? Analysis of satellite SST images of the Southeastern Baltic Sea. Water Resources, 44 (1), pp. 69-77. DOI:10.1134/s0097807817010043.

Gemmrich J.R. and Van Haren H. (2001). Thermal fronts generated by internal waves propagating obliquely along the continental slope. Journal of physical oceanography, 31(3), 649-655. DOI: 10.1175/1520-0485(2001)031<0649:TFGBIW>2.0.CO;2

Gemmrich J.R. and Van Haren H. (2002). Internal wave band eddy fluxes above a continental slope. Journal of marine research, 60(2), 227-253. DOI: 10.1357/00222400260497471

Gidhagen L. (1987). Coastal upwelling in the Baltic Sea—Satellite and in situ measurements of sea-Surface temperatures indicating coastal upwelling. Estuarine, Coastal and Shelf Science, 24 (4), pp. 449–62. DOI:10.1016/0272-7714(87)90127-2.

Hela I. (1976). Vertical velocity of the upwelling in the sea. Commentationes physico-mathematicae, 46(1), pp. 9-24.

Horstmann U. (1983). Distribution patterns of temperature and water colour in the Baltic Sea as recorded in satellite images: indicators for phytoplankton growth. Kiel: Institut für Meereskunde an der Universität Kiel. DOI:10.3289/ifm_ber_106.

Kahru M., Håkansson B., Rud O. (1995). Distributions of the sea-Surface temperature fronts in the Baltic Sea as derived from satellite imagery. Continental Shelf Research, 15 (6), pp. 663–79. DOI:10.1016/0278-4343(94)e0030-p.

Kapustina M.V., Krechik V.A., Gritsenko V.A. (2017). Seasonal variations in the vertical structure of temperature and salinity fields in the shallow Baltic Sea off the Kaliningrad region coast. Russian Journal of Earth Sciences, 17 (1). pp. 1-7. DOI: 10.2205/2017ES000595.

Kowalewski M. and Ostrowski M. (2005). Coastal up- and downwelling in the southern Baltic. Oceanologia, 47(4), pp. 435-475.

Kozlov I.E., Kudryavtsev V.N., Johannessen J.A., Chapron B., Dailidienė I., Myasoedov A.G. (2012). ASAR imaging for coastal upwelling in the Baltic Sea. Advances in Space Research, 50 (8), pp. 1125-137. DOI:10.1016/j.asr.2011.08.017.

Krechik V.A. and Gritsenko V.A. (2016). Thermal structure of the coastal waters of the Baltic sea near the north coast of the Kaliningrad region. Processes in Geomedia, 5, pp. 77-84 (in Russian with English summary).

Krężel A., Ostrowksi M., Szymelfenig M. (2005). Sea surface temperature distribution during upwelling along the Polish Baltic coast. Oceanologia, 47(4), pp. 415-432.

Lehmann A. and Myrberg K. (2008). Upwelling in the Baltic Sea-A review. Journal of Marine Systems, 74, pp. 3-12. DOI:10.1016/j.jmarsys.02.010.

Lehmann A., Myrberg K., Höflich K. (2012). A statistical approach to coastal upwelling in the Baltic Sea based on the analysis of satellite data for 1990–2009. Oceanologia, 54 (3), pp. 369-93. DOI:10.5697/oc.54-3.369.

Lehmann R. (2013). 3 σ-Rule for Outlier Detection from the Viewpoint of Geodetic Adjustment. Journal of Surveying Engineering, 139(4), 157-165. DOI: 10.1061/(ASCE) SU.1943-5428.0000112.

Leppäranta M. and Myrberg K. (2010) Physical oceanography of the Baltic Sea. Chichester, U.K.: Springer/Praxis Pub. DOI:10.1007/978-3-662-04453-7_2.

Massel S.R. (2015). Internal Gravity Waves in the Shallow Seas. GeoPlanet: Earth and Planetary Sciences. Springer Int. Publ, Switzerland. DOI:10.1007/978-3-319-18908-6.

Morozov Ye.G., Shchuka C.A., Zapotylko V.S. (2007). Towed spectra of internal waves on a pycnocline in the Baltic. Doklady Earth Sciences, 412 (4), pp. 552-554. (in Russian with English summary).

Myslenkov S.A., Krechik V.A., Bondar A.V. (2017a). Daily and seasonal water temperature changes in the coastal zone of the Baltic Sea measured by thermistor chain. Ecological Systems and Devices, 5, pp. 25–33. (in Russian with English summary).

Myslenkov S.A., Krechik V.A., Soloviev D.M. (2017b). Water temperature analysis in the coastal zone of the Baltic Sea based on thermistor chain observations and satellite data. Proceedings of Hydrometcentre of Russia, 364, pp. 159–169 (in Russian with English summary).

Pukelsheim F. (1994). The three sigma rule. The American Statistician, 48(2), 88-91. DOI:10.1080/00031305.1994.10476030.

Robinson I.S. (2004). Measuring Ocean from Space: The Principals and Methods of Satellite Oceanography. Springer,Berlin, 668 pp.

Saha S., Moorthi S., Wu X., Wang J., Nadiga S., Tripp P., Behringer D., Hou Y., Chuang H., Iredell M., Ek M., Meng J., Yang R., Mendez M.P., van den Dool H., Zhang Q., Wang W., Chen M., Becker E. (2014). The NCEP Climate Forecast System Version 2. J. Climate, 27, pp. 2185–2208. DOI:10.1175/JCLI-D-12-00823.1

Sellschopp J. (1991). Stochastic ray tracing in thermoclines. In Ocean Variability & Acoustic Propagation (pp. 293-312). Springer, Dordrecht. DOI: 10.1007/978-94-011-3312-8_23

Serebryany A.N. and Khymchenko E.E. (2014). Observations of internal waves at Caucasian and Crimean shelves of the Black Sea in summer 2013. Current problems in remote sensing of the Earth from space, 11 (3), pp. 88-104. (in Russian with English summary).

Siegel H., Gerth M., Neumann T., Doerffer R. (1999). Case studies on phytoplankton blooms in coastal and open waters of the Baltic Sea using Coastal Zone Color Scanner data. International Journal of Remote Sensing, 20 (7), pp. 1249-1264. DOI:10.1080/014311699212713.

Siegel H., Gerth M., Tschersich G. (2008). Satellite–Derived Sea Surface Temperature for the Period 1990–2005. State and Evolution of the Baltic Sea, 1952–2005: A Detailed 50–Year Survey of Meteorology and Climate, Physics, Chemistry, Biology, and Marine Environment. pp. 241-264.

Simons T.J. (1978). Wind-driven circulations in the southwest Baltic. Tellus, 30 (3), pp. 272-83. DOI:10.3402/tellusa.v30i3.10341.

Sivkov V.V., Kadzhoyan Yu.S., Pichuzhkina O.Ye., Feldman V.N. (2012). Oil and environment of the Kaliningrad region. Kaliningrad: Terra Baltika. (in Russian).

Stepanova N.B., Shchuka S.A., Chubarenko I.P. (2015). Structure and evolution of the cold intermediate layer in the southeastern part of the Baltic sea by the field measurement data of 2004-2008. Oceanology, 55, (1), pp. 25-35. DOI:10.1134/S0001437015010154.

Stont Zh.I., Gushchin O.A., Dubravin V.F. (2012). Storm winds in the southeast Baltic according to the data of the automatic meteorological station in 2004-2010. Proceedings of the Russian Geographical Society, 144 (1), pp. 51-58. (in Russian with English summary).

Svansson A. (1975). Interaction between the coastal zone and the open sea. Finnish marine research, 239, pp. 11–28.

Van der Lee E.M. and Umlauf L. (2011). Internal wave mixing in the Baltic Sea: Near–inertial waves in the absence of tides. Journal of Geophysical Research: Oceans, 116(C10). DOI: 10.1029/2011JC007072.

Van Haren H., Groenewegen R., Laan M., Koster B. (2005). High sampling rate thermistor string observations at the slope of Great Meteor Seamount. Ocean Science, 1(1), 17-28. DOI: 10.5194/os-1-17-2005.

Walin G. (1972). Some observations of temperature fluctuations in the coastal region of the Baltic. Tellus, 24 (3), pp. 187-98. DOI:10.3402/tellusa.v24i3.10633.

Zhelezova E., Krek E., Chubarenko B. (2018) Characteristics of the polynya in the Vistula Lagoon of the Baltic Sea by remote sensing data. International Journal of Remote Sensing, [online], pp. 1-12. Available at: https://www.tandfonline.com/doi/abs/10.1080/01431161.2018.1524181. DOI: 10.1080/01431161.2018.1524181.

Zhurbas V., Elken J., Paka V., Piechura J., Väli G., Chubarenko I., Golenko N., Shchuka S. (2012). Structure of unsteady overflow in the Slupsk furrow of the Baltic Sea. Journal of Geophysical Research, 117 (C4), pp. C04027. DOI:10.1029/2011JC007284.

Received on November 16th, 2018 Accepted on February 20th, 2019

Maria B. Kireeva[1*], Vladislav P. Ilich[1], Natalia L. Frolova[1], Maksim A. Kharlamov[1], Aleksey A. Sazonov[1], Polina G. Mikhaylyukova[1]
[1] Faculty of Geography, Lomonosov Moscow State University, Moscow, Russia
***Corresponding author:** kireeva_mb@mail.ru

ESTIMATION OF THE IMPACT OF CLIMATIC AND ANTHROPOGENIC FACTORS ON THE FORMATION OF THE EXTREME LOW-FLOW PERIOD IN THE DON RIVER BASIN DURING 2007-2016

ABSTRACT. The Don River is the largest river in the southwestern part of European Russia and the second largest river system in European Russia. The Don River basin is one of the most water deficient regions in Russia and the long term average water usage in the basin amounts to 45%. The period 2007-2016 was the longest long-term low-flow period observed, with an estimated total water resources deficit of 40.4 km^3 over 8 years. The main reason for this deficit were anomalously warm winters (2-4 degrees over average) with a low degree of soil frost penetration. This resulted in low spring flood volume (37% of the average) due to heavy seepage losses combined with thin snow cover. A similar low-flow situation was observed in 2014, when the drought caused great damage to ecosystem of Tsimlianskoye water reservoir and the River Don. Most of the fish breeding grounds had dried up by May 2014. This caused the number of round fish whitebait to drop 5-10 times below the 2002-2014 average. Inland shipping and hydropower industry also sustained losses of 42 million euro (according to interview from State Shipping company) due to low water level. This study shows that the main reasons for the 2007-2016 extreme hydrological drought are exceptional hydro-climatic conditions and anthropogenic transformations in the watershed, such as urbanisation growth and afforestation. The analysis shows that the main cause in water deficit is associated with the left tributaries of Don – Khoper and Medveditsa, while the flow in Upper Don remained more or less normal. The results can be interpreted as a "warning sign" to reduce water consumption in these sub-basins to avoid similar drought situations in future.

KEY WORDS: low-flow period, hydrological hazards, hydrological droughts, Don River, climatic factors, anthropogenic factors, runoff formation

CITATION: Maria B. Kireeva, Vladislav P. Ilich, Natalia L. Frolova, Maksim A. Kharlamov, Aleksey A. Sazonov, Polina G. Mikhaylyukova (2019) Estimation of the impact of climatic and anthropogenic factors on the formation of the extreme low-flow period in the Don River basin during 2007-2016. Geography, Environment, Sustainability,
DOI-10.24057/2071-9388-2017-28

INTRODUCTION

The clustering of years of a high and low water discharge in a river are a distinctive feature of fluctuations in the river runoff characteristics, especially during the low-flow period of the year. The term "low-flow" is determined by characteristics of a period with low discharges, accompanied by various types of social, economic and environmental damage (Alekseevskiy and Frolova 2011). The concept of "low-flow" used in this study is closely connected to the concept of "hydrological drought" (Hydrometeorological Risks 2008), which differs from the atmospheric, soil, agricultural and water use drought (Bolgov et al. 2005).

For the Don River basin located in the southern European part of Russia the clustering of floods and low water levels is particularly clear (Shiklomanov 1979; Dzhamalov 2013). The observed increase in the occurrence frequency of such extreme events is related to climatic changes (Semenov 2009; Semenov et al. 2015). However, while the duration of floods rarely exceeds several months, low-flow periods can last for several years (Dmitrieva 2011). In addition, since the 1950s, the high needs for water availability, driven by the population growth, have led to a sharp increase in the human impact (runoff regulation, water withdrawal, water transfer to neighbouring basins) on the hydrological regime of the rivers in the Don basin. Thus, I.A. Shiklomanov noted (Shiklomanov 1979) that in 1975 the irretrievable water consumption was 8-10 km3 per year, which is approximately equal to one third of the annual runoff of the Don River in its estuary. In terms of runoff losses, the additional evaporation from the water surface of ponds and reservoirs and the water abstraction for municipal and domestic water supply and agriculture (Alekseevskiy and Frolova 2011) are important factors. For example, the area of irrigated land increased from 35.000 ha in the 1940s and 1950s to 511.000 ha in 1975. Similar conclusions about unconstrained water use in the Don River basin in 1970s -1980s were obtained other studies (Koronkevich et al. 1990; Scheme of complex... 2013). Thus, according to most of the past studies performed during the Late Soviet period (1980s-1990s) the industry and agriculture was expected to grow continue growing at the same rate. These projections would have led to twice as much water abstractions by the beginning of the twenty-first century. However, the collapse of the Soviet Union led to a reduced growth of water management activities and these projections were not confirmed. Nevertheless, the Don basin is currently one of the most water-stressed regions in Russia (Alekseevskiy 2013). In addition, significant changes in seasonal runoff in the Don basin were observed, which also have an impact on the low-flow periods (Kireeva et al. 2015; Dmitrieva 2013, 2014).

The increased occurrence of low water levels in recent years has been observed in many European countries and around the world (Van Lenen et al. 2016; Bordi et al. 2009). For example, the summer of 2015 was extremely dry in Europe and at the same time an extreme low-flow period was also observed in the Don basin, which has similar hydro-climatic conditions as the countries of south-east Europe (Van Lenen et al. 2016).

To gain more insights into the characteristics of extreme low-flow periods, this paper presents a comprehensive analysis of the 2007-2016 low-flow in the Don basin.

MATERIALS AND METHODS

ERA Interim reanalysis data (V2) was used in this paper, to study the contribution of climatic variability to the formation of low-flow period. ERA Interim is a third-generation reanalysis created by the European Centre for Medium-Range Weather Forecasts (ECMWF official website [online]). The reanalysis data is publicly available and include

series from 1979 to the present. The data is available in grid format with a spatial resolution of 0.75° x 0.75°, which covers the surface of the entire planet (Mouat and Lancaster 2008).

Different versions of the reanalysis data have different errors in the air temperature and the precipitation magnitudes. Typically, reanalysis temperature data has a smooth field structure and a high degree of spatial correlation of adjacent values. Due to this, for example, when comparing air temperature data obtained from the Lipetsk weather station and the data obtained reanalysis (here – ERA-Interim V2), the square of the coefficient of determination (R^2) is 0.99 (Fig. 1A). In the case of total precipitation, the R^2 is reduced to 0.53 (Fig. 1B). These differences are likely due to the large distance (about 40 km) between

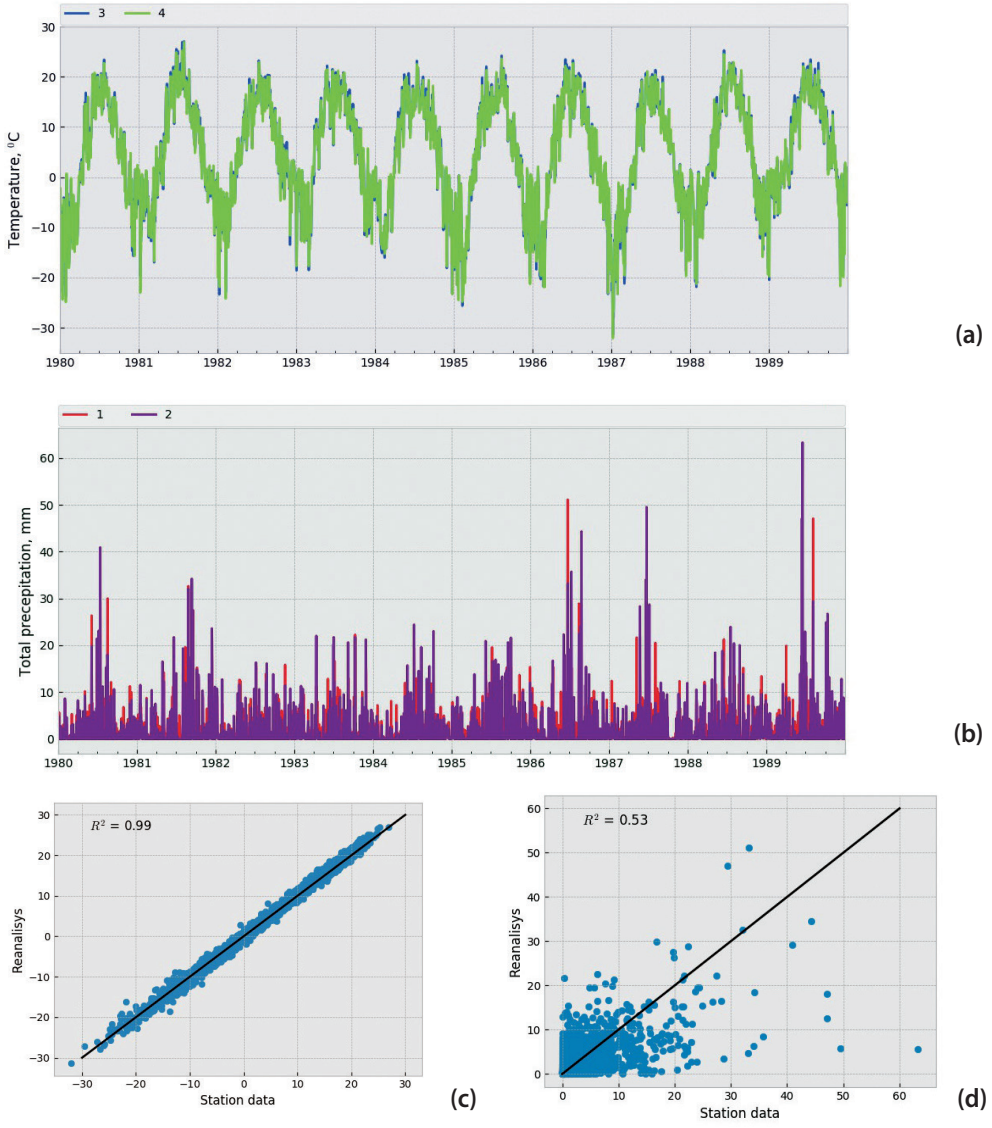

Fig. 1. Comparison between the observation data of temperature (A, C) and precipitation (B, D) at the Lipetsk meteorological station and the reanalysis data for the period from 1980 to 1990. Blue (3) and red (1) indicates data obtained from the weather stations; green (4) and violet (2) indicate reanalysis data

the weather station and the nearest grid point of the reanalysis grid and the uneven distribution of precipitation at small scales. When averaging over larger areas errors cancel each other. Thus, we consider the analyses of the tendencies in precipitation characteristics calculated from reanalyze data as a good approximation, as the data show shows the main pattern and differences between sub-regions clearly.

In this study, daily records of precipitation and air temperature were taken from the model, available in the NetCDF format from 1979 to 2016 (ERA-Interim 2005; ERA-40 2005). The coarse reanalysis data (0.75° x 0.75°) were interpolated to a 0.125"x 0.125" grid (Official site CDO [online]), using the CDO (Climate Data Operators [online]) utility developed at the Max Planck Institute for Meteorology.

The data was then divided into two periods: 1979-2006 and 2007-2016. The former period is used as a reference period. The latter period was chosen, as it is representative of the extreme low-flow period in the Don basin. Based on the reanalysis data for the catchment area of the Don River and its tributaries the key meteorological indicators that are suspected to have affected the runoff formation in the catchment were chosen. Then the anomalies compared to the reference period, were calculated (Table 1).

The absolute changes of characteristics (ΔC_{abs}) were obtained by subtracting the long-term average of the reference period $\overline{P_1}$ (1979 – 2006) from the long term average value of the low-flow period $\overline{P_2}$ (2007 – 2016) (Eq. 1)

$$\Delta C_{abc} = \overline{P_2} - \overline{P_1} \quad (1)$$

The relative changes of the characteristics (ΔC_{rel}) in percents (%) were calculated as the difference between the low-flow period ($\overline{P_2}$) and the reference period ($\overline{P_1}$), relative to the average value of the reference period ($\overline{P_1}$), multiplied by 100 (Eq. 2):

$$\Delta C_{rel} = \frac{\overline{P_2} - \overline{P_1}}{\overline{P_1}} \quad (2)$$

The statistical significance of the detected changes was assessed at the 95% confidence level using a Student's t-test.

Table 1. Meteorological indicators used in the analysis

Meteorological indicator	Reference period	Low-flow period
number of days with negative air temperature	1979 – 2006	2007 – 2016
total sum of negative air temperatures in 'degree' values	1979 – 2006	2007 – 2016
duration of the winter period* in days	1979 – 2006	2007 – 2016
average air temperature during the winter period*	1979 – 2006	2007 – 2016
number of thaw episodes during the winter period**	1979 – 2006	2007 – 2016
total solid precipitation for the winter period*	1979 – 2006	2007 – 2016
total liquid precipitation for the winter period*	1979 – 2006	2007 – 2016
total liquid precipitation for the summer period***	1979 – 2006	2007 – 2016

**winter period = the time interval from the moment of the first transition of air temperature through 0°C to the moment of the last transition of air temperature through 0°C*
*** number of thaw = the number of temperature transitions through 0°C*
****summer period = the time interval between two winter periods*

The hydrological characteristics in this study were estimated at 14 representative hydrological stations located at the main tributaries of the Don River (Fig. 2).

One of the most important characteristics of low-flow period is the water deficit. Usually it can be calculated as difference between mean value of the annual runoff volume (averaged for all years of low-flow period) and runoff of 50% occurrence (for the all period of observation). In this work we also decided to use normalized values of deficit to make them comparable with each other.

To analyze the spatio-temporal distribution of this deficit, equation (3) was used:

$$D_{lfp} = \frac{\overline{W}_{lfp} \cdot -W_{50\%}}{W_{50\%}} \quad (3)$$

where D_{lfp} is the runoff deficit for the low-flow period, $\overline{W}_{lfp}$. is the average annual runoff for the low-flow period and W50% is the runoff of 50% occurrence (for all the period of observation).

The anthropogenic influences can also contribute significantly to changes in river runoff. During extreme low-flow periods, an increasing water use can be

Fig. 2. Location of the hydrological stations selected for the analysis. Gauges with extra data include two watersheds, which used for analyzes of land cover transformation

observed, for example, in agriculture (Koronkevich 1990). This increases the water abstractions, which can further exacerbate the water supply deficit. In addition, the transformation of the catchment area surface can have an indirect impact on the formation of low-flow periods. One of the most popular methods for the catchment land cover estimation is processing remote sensing data of the Earth (Mouat and Lancaster 2008; Sheeja et al. 2011). In this study, the data on land cover transformation, water withdraw, and sewage were used from the past studies (Kireeva et al. 2017; State water kadastre 1990-2013) to analyze the direct anthropogenic impact, and the results of processing the composition of satellite images LANDSAT for the selected time periods of 1985, 1995, 2005 and 2015 were used to estimate the indirect anthropogenic impact.

RESULTS

The low-flow period of 2007-2016 is characterized by fewer days with negative air temperatures during the cold period, i.e. more days with positive air temperatures when compared to the reference period 1979-2006 (Fig. 3). The warmest winter in the region occurred in 2007 and 2013-2014. In the eastern and southern parts of the Don basin, there are ~10 to 15 days less compared to the reference period 1979-2006. The greatest changes are found in the western part of the basin, with 15 - 30 more days with positive air temperatures, which accounts to about 20 - 25% (Fig. 3 B). For the whole basin, except the south-east territory, the change is statistically significant.

Apart from the decrease in the number of days with negative temperatures described above, there was also a decrease in the total sum of negative temperatures compared with the reference period (not shown). In the western part of the basin, the relative decrease of this parameter accounts to 20-25%, while in the north-east part to 5-10%.

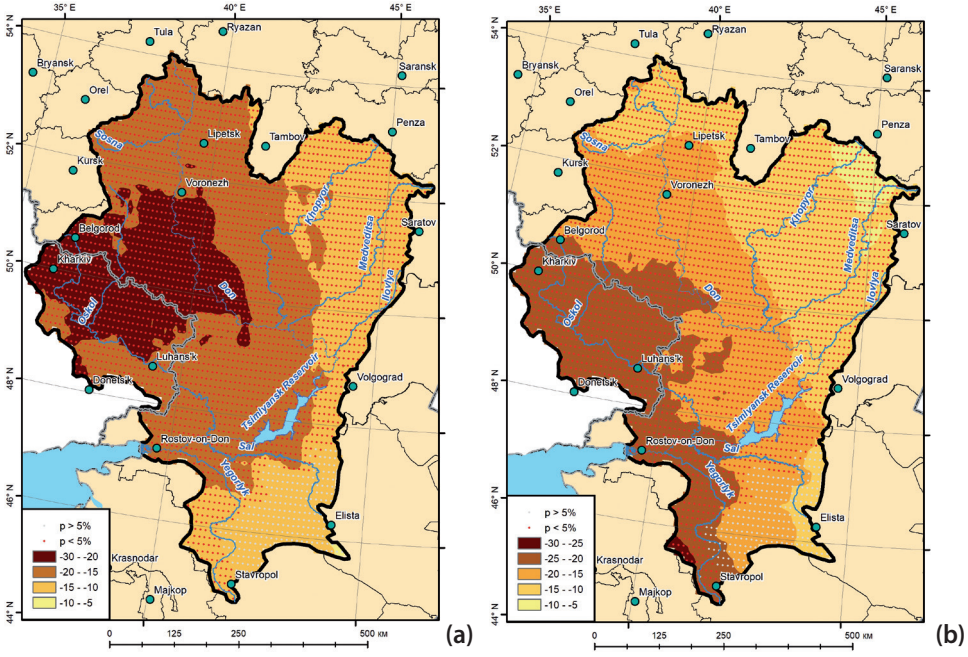

Fig. 3. Difference in the number of days with negative temperatures. Absolute difference (ΔC_{abs}) in days (A) and relative difference (ΔC_{rel}) in percent (B). Dots denote change above the 95% confidence level (t-test)

Fig. 4 shows the decrease in the duration of the winter period. In most parts of the basin, the absolute reduction ranged from 10 to 15 days, which accounts to an approximate 5-10% decrease relative to the reference period. The smallest changes of 0-5 days (up to 5%) are found in the northern and southern parts of the basin. The highest changes are located in the northwestern part of the basin in the vicinity of Lipetsk, Voronezh and Belgorod. In these regions, the duration of the winter period decreased between 15 to 20 days, i.e. about 10-15%. Most of the central part of the watershed shows statistical significant changes, while on the north and south-east part the changes between the periods are non-significant. The average air temperature for the winter period increased throughout the entire basin (not shown). The increase ranged between 0.25-1.5 °C over the entire period 2007-2016, with some extreme years (2011, 2014, 2015), in which the temperature anomalies reached up to 3-4 °C in winter.

The recorded warming during the winter period had also an impact on the amount of solid precipitation. In general, solid precipitation decreased throughout the basin over the years 2007-2016 (Fig. 5A). The smallest changes are found in the eastern and southern parts of the basin. The amount of solid precipitation decreased by 10-20% in these regions during the winter period. In the north-eastern part, the changes amount to 0-10%. The greatest changes are observed in the central and western parts, where the amount of solid precipitation decreased by (20-50 mm), which is about 20-35%. Simultaneously, the total amount of liquid precipitation also changed, for example, only 40-60 mm per year were recorded throughout the basin in 2014 and 2015 (not shown).

The decrease in the amount of solid precipitation was partially compensated by an increase in the amount of liquid precipitation (Fig. 5 B) in some regions during the winter period. Liquid precipitation increased by 10-40% (10-40 mm) in the northern part of the

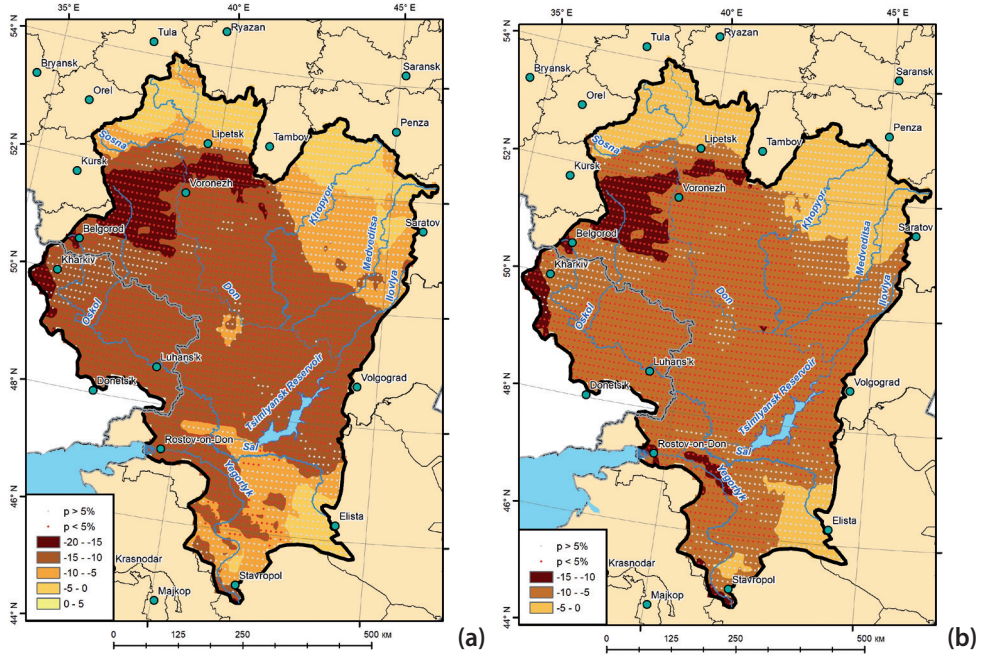

Fig. 4. Difference in the length of the winter period (see Table 1). Absolute difference (ΔC_{abs}) in days (A) and relative difference (ΔC_{rel}) in percent (B). Dots denote change above the 95% confidence level (t-test)

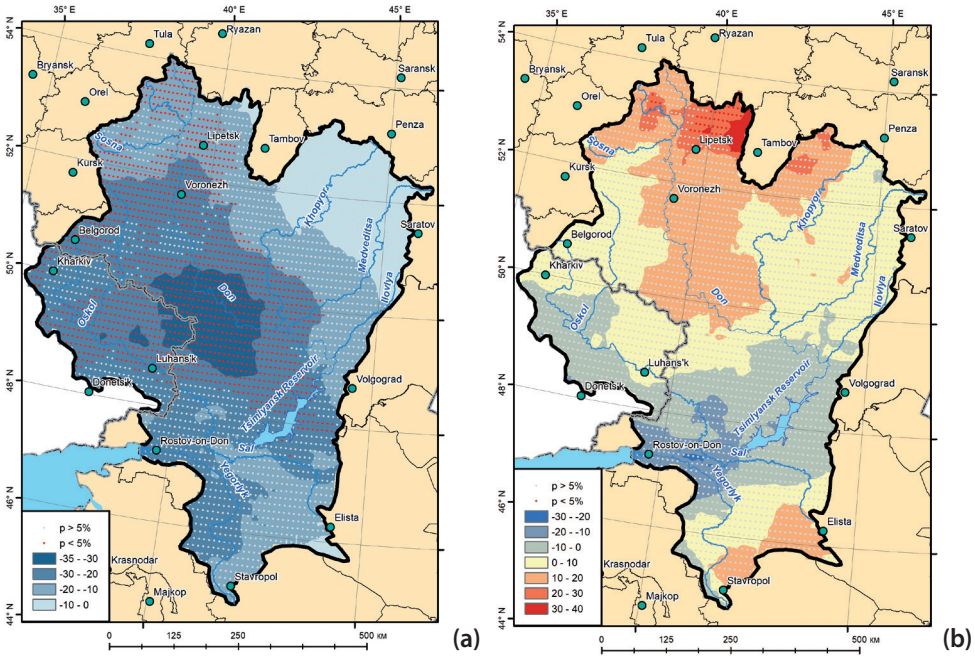

Fig. 5. Relative difference (ΔC_{rel}) in percent in the amount of solid (A) and liquid (B) precipitation for the winter period. Dots denote change above the 95% confidence level (t-test)

basin and 10-20% (10-20 mm) in the southern part. In the central part of the basin (near the Tsimlyansk Reservoir), the relative decrease of liquid precipitation ranges between 10 and 20% (up to 20 30 mm).

A change in the amount of liquid precipitation during the summer period was the most noticeable change over the past 10 years (Fig. 6). The largest changes can be found in the northern and in parts of the central region of the basin, where the precipitation amount has decreased by 20-25% (-80-120 mm). Here the changes are statistical significant. The northeastern region (Medveditsa river basin) exhibits similar changes. Here liquid precipitation for the summer period decreased by 80-100 mm, but the relative change amounts to more than 25 %. The smallest changes are found in the vicinity of the Tsimlyansk Reservoir and at the mouth of the Medveditsa River with a decrease of 20-60 mm (i.e. 5-10%).

In the previous sections the changes of the meteorological indicator were analysed to identify possible influences on the runoff formation in the catchment. However, transformations of the catchment surface area (e.g. land use changes) and the economic use of the water resources might have exacerbated the low-flow situation. Therefore, an analysis of economic activity in the "pilot" basins at the Khopyor River at the gauging section of Novokhopyorsk and the Don River at Liski was carried out.

In the Khopyor basin, an increase in forest cover from 10.0% to 16.8% and a slight increase in urban areas was observed between 1985 and 2015 (Fig. 7A). The increasing area of water bodies (including artificial reservoirs and rivers) in the 1980s and 1990s was followed by a decline in the early 2000s. From 2007 to 2014 the area decreased almost twice as much (from 0.90 to 0.49%). The direct water abstraction (equals water withdraw minus sewage) from the river system does not seem to play an important role in the formation of a wa-

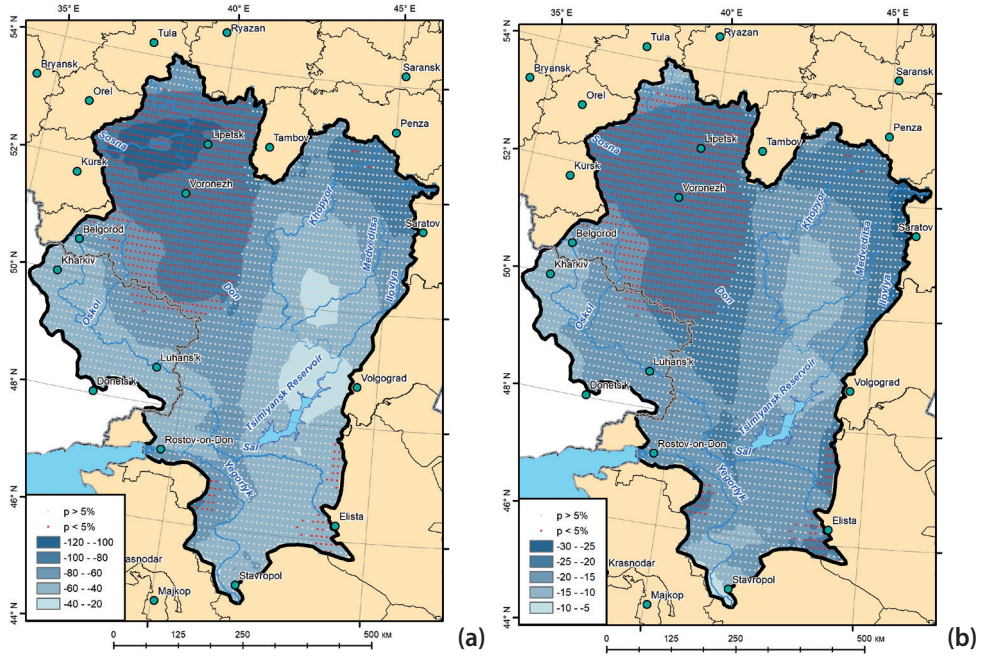

Fig. 6. Difference in liquid precipitation for the summer period (see Table 1). Absolute difference (ΔC_{abs}) in mm (A) and relative difference (ΔC_{rel}) in percent (B). Dots denote change above the 95% confidence level

ter deficit. Even in 1992, when runoff of 90% occurrence (less than 2 km^3) was observed, and the water abstraction volume was much higher than now, the water abstraction volume was just 6 % from total runoff (Fig. 7A). During last 20 years, the water abstractions fluctuate around 0.6-0.8% of total runoff (Fig. 7A).

Even for the shorter analyzing intervals (for the satellite images) of the Liski station (1998 to 2014), an increase in the forest cover is evident from 1.2 to 5.2% of the total catchment area (i.e. 870 km^2 to 3580 km^2), which accounts to a 4-fold increase (Fig. 7B). This increase is due to a reduction in cultivated agricultural land and, as a consequence, overgrowing of fields and natural reforestation. In addition to forest cover, the area of urban land also increased (from 5.3% to 7.8%). This is caused by the expansion of the private sector and the growth of industry since the mid-1990s. The direct water abstraction (equals water withdraw minus sewage) from the runoff at the Liski gauging section, ranges from -5 to +3.5%. An interesting detail is that at the Liski gauging station, the observed runoff is above the naturalised runoff (calculated natural runoff, without any anthropogenic influence, derived through regression analysis by the State Water Cadastre (1990-2016 yy.). This higher observed flow is due to the additional discharges from sewage withdrawn from wastewater plants, including that from the underground sources, into the river system.

During the historical period of observations (1930-2015), from 3 to 5 prolonged low-flow periods were reported in different parts of the Don basin (Fig. 8). The most extreme low water levels on the Don river at Razdorskaya were observed in the early 1950s, mid-1970s and mid-2000s (Table 2).

The low-flow period of 2007-2016 has the longest duration. Due to the extended period, the runoff deficit volume for the entire low-flow period totals to 55.0 km^3, which is approximately twice the annual volume of the river runoff of the Don River at the Razdorskaya

Fig. 7. Percent of catchment area covered by water bodies (1), urban area (2) and forest (3). Percent of water abstractions from the total runoff (4) and the annual volume of runoff (W, km³) (5) for the catchment area of the Khopyor River - Novokhopyorsk (A) and the Don River - Liski (B)

gauging station (at the river mouth). The low-flow period in the early 1970s is characterized by slightly lower deficit volumes - 42.0 km³. However, the deviation of runoff from the average annual value during the low-flow period of 2007-2016 is only 6.1 km³, which is 1.5 times less than the similar indicator for the low water levels of the 1950s and 1970s. Thus, in terms of the average annual volume and annual deficit these two periods are harsher.

Table 2. Characteristics of the 4 most extreme low-water periods for the gauging station Razdorskaya (at the mouth of the Don River)

Low water period	Duration, years	Average annual volume of runoff for the low water period, km³	Deviation from the average runoff, km³	Runoff deficit for the low water period, km³
1938-1940	2	16.0	4.9	9.8
1949-1951	2	12.7	8.2	16.4
1972-1977	5	12.5	8.4	42.0
2007-2016	9	14.8	6.1	55.0

The occurrence and severity of low-flow periods in the Don Basin are highly spatial heterogenic. The spatio-temporal distribution of the runoff deficit is shown in Fig. 8. Note that some stations in Fig. 8 have an incomplete record. For rivers like the Khopyor and Medvyeditsa River which flow in the eastern part of the Don basin (i.e. left tributaries in flow direction), the most important low-flow period with duration of 5-6 years, occurred in the 1930s. During this period, the runoff deficit on the Medvyeditsa River was higher than that on the Hopyor River (48% and 40% respectively). During the same period, there was a high water deficit on the Chir River (42%) as well.

The low-flow periods in 1938 (according to Fig. 8 for some rivers 1935) - 1940 and 1949-1951 was short at Razdorskaya station (only 2 years), but nevertheless very important in terms of the annual runoff volume accounts 16.0 and 12.7 km^3. The low-flow period from 1972 to 1977 have the same to 1949-1951 averaged annual runoff value (12.5 km^3), but the doubled duration (5 years). Extreme low water levels were observed at all the stations (Fig. 8).

The most extreme and wide-spread low-flow period in the Don basin occurred between 1972 to 1977 with all stations experiencing, to some extent, low runoff values. The most pronounced low-flow period in terms of duration and total deficit was observed on the Krasivaya Mecha River, at the gauging station Don-Kazanskaya and also on the Severskiy Donets River (both right side tributaries). The low-flow situation was slightly better on the left side tributaries of the Don River; namely at the Khoper, Medvyeditsa and Ilovlya. On these rivers, the years experiencing low-flow alternated with years of a medium and high annual runoff. At the same time, the occurrences of the runoff (for all the period of observation) for the extreme low-flow years (1972, 1975, 1976) were much higher (more than 95 %) compared with the others (50 – 80

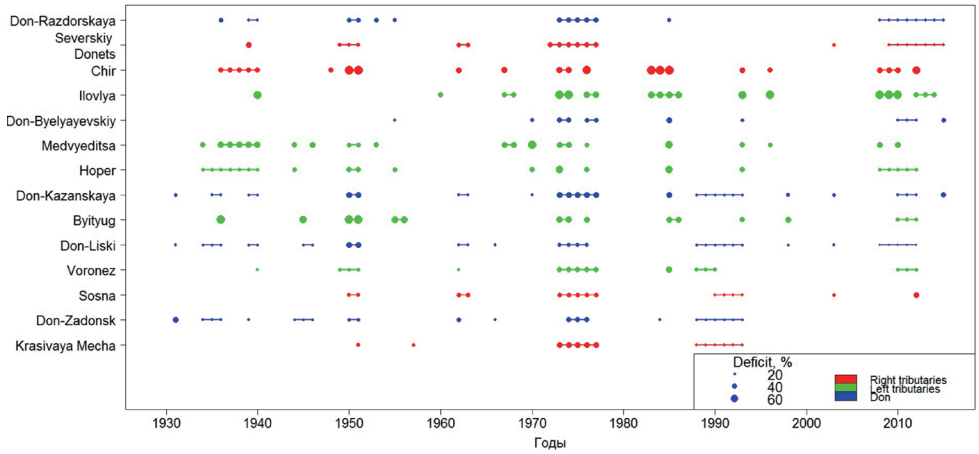

Fig. 8. Volume deficits in the Don basin for the period 1930-2015. Hydrological stations placed at regular intervals on the ordinate in the order from the source (1 – Krasivaya Mecha at Efremov; 2 – Don at Zadonsk; 3 – Sosna at Elets; 4 – Voronezh – at Lipetsk; 5 – Don at Liski; 6 – Bitug at Bobrov; 7 – Don at Kazanskaya; 8 – Khoper at Besplemyanovskiy; 9 – Medvyeditsa at Archedinskaya; 10 – Don at Belyaevskiy; 11 – Ilovlya at Aleksandrovka; 12 – Chir at Oblivskaya; 13 – Seveskiy Donets at Belaya Kalitva; 14 – Don at Razdorskaya) to the mouth , years are on the abscissa, the point size shows the magnitude of the runoff deficit, averaged over each period (the points associated with one period are connected with the line): the larger an icon, the greater was the deficit averaged over that period. Colours indicated the spatial location of the gauging station (Updated from [9])

%). The same alteration was noted for Chir River, one of the largest tributaries to the Tsimlyansk Reservoir. The runoff in 1976 was 67% less than average annual runoff on this river. In general, the runoff of Chir is characterized by high deficit volumes, during low-flow years, with 9 out of 22 low-flow years having less than 50% of the average runoff (occurrences from 80 to 95 %).

In the upper reaches of the Don basin, the period of 1988-1993 was the longest low-flow period observed so far. This low-flow period was especially pronounced on the Krasivaya Mecha River and on the Don River above the station of Khutor Belyaevsky (the gauging stations of Zadonsk, Liski and the Kazanskaya station). There is no long-term low-flow period below the above-mentioned stations during 1988-1993, although the annual runoff in 1993 had very high occurrence (more than 80%) on the rivers Khopyor, Medvyeditsa, Ilovlya and Chir.

The situation in the basin during the most recent low-flow period, is the spatial reverse of the period 1988-1993. In the lower reaches, 2007 can be defined as the beginning of a low-flow period. At the same year, in the upper reaches, a phase of a higher annual flow (with low runoff occurrence 5-10%) is apparent. However, along the Don River, starting from the Liski gauging station and below, there is a continuous water deficit for more than 8 years. At the same time during the whole period 2007-2016, the annual (averaged within low-flow period) deficit is not so high in comparison to the period 1950-1951 and 1972-1977 for the same river (Medvyeditsa, Bityug). The years with low annual flow alternate with years of high annual flow, due to that total deficit of the period is not so high. However, in the lower reaches of the basin, on the Seversky Donets River and the Don River at the gauging station of Razdorskaya, the period 2007-2016 is only characterized by high (more than 90%) annual runoff occurrence values. In some years (2007, 2009), extreme low-flow values observed just for the eastern rivers (i.e. left tributaries), and there is a phase of an increased water content on the western rivers (i.e. right tributaries), which compensates the water deficit in the main river Don.

DISCUSSION

Based on the results obtained in this study, we conclude that the main reason of the extreme low-flow period 2007-2016 in the Don River basin was the combination of several, meteorological conditions. The higher than usual air temperatures that were observed during winter period (plus ~2-4°C) favoured increasing runoff losses in the winter and the pre-spring period from 2007 to 2016. The higher air temperature during winter and the shorter duration of winter had also direct influence on the depth of soil freeze. These three parameters are widely use in forecasting schemes of seasonal and occasional flood wave as well as in modelling (Koren 1988). Warmer conditions in winter lead to shallower frozen soil layer, and additionally, smaller precipitation amounts during fall result in low soil humidity and empty pore space in the soil (Barabanov et al. 2018). Finally, the humidity of soil is small, pore space is filed by the air, and the water inside the soil isn't frozen. In this case the watershed during spring works as a "sponge" and cut significant part of melt water to the infiltration. The same effects widely discussed by Barabanov et al. (2018) for different geographical zones. Small amounts of solid precipitation in winter resulted in thin snow pack and additionally, several transitions through zero °C- dropped the snow thickness to very low values. This mechanism results in increased infiltration and higher groundwater levels (Dzhamalov et al. 2013; Barabanov et al. 2018). This causes the winter discharge in the rivers to increase (Dzhamalov 2013) and the main phase of hydrological year (flood wave by snow melt) to disappear. This lead to infiltration dominating the oth-

er runoff processes. Another, untypical for this natural conditions, process of runoff formation starts to realize (Koren 1988). Small amounts of precipitation during summer and earlier start of the dry season (Dmitreva 2014) resulted in a longer duration and a higher volume of the water deficit.

According to Kireeva (2017), in the Don basin, the evaporative losses from the surface of ponds and reservoirs at the time of the low-flow period in 2007-2016 were about 4-5% of the annual runoff, whereas they reached 13% in the early 1990s. In addition, an increase in the forest cover leads to an increase in water losses through evapotranspiration. Therefore, we can conclude that the input component of the water balance equation is the main reason for the low-flow period.

The low flow periods in the Don basin have several important implications. First, the period 2007-2016 was considered a critical situation and was widely discussed in mass media. The topic was of importance, because the proportion of cultivated agricultural land in the southern part of the catchment is higher than in the north part of the Don basin (Kireeva 2017) and the amount of precipitation is lower during summer as well as snow during winter, which consequently increases the demand for water. The second important factor is the role of the lower reach of the Don River for providing various branches of the water sector: shipping, recreation and industry. Lack of water and falling water levels can cause significant problems for water transport, impede navigation or lead to under load of ships. The third reason for the fact that the long-term low-flow period 2007-2016 in the Don mouth can bring more problems to the population than the same in 1972-1977 in the upper reaches is the largest city (Rostov-on-Don) with one million of inhabitants located in the lower part of the Don basin. The Don river is the main water source for the city and low water levels can lead to interruptions in the water.

SUMMARY AND CONCLUSION

The results of this study show that the low-flow period of 2007-2016 was the highest on record in terms of the duration and the water deficit volume in the Lower Don. Generally, the formation of distinct periods of extreme low-flow is not unusual and can be considered a common feature of the rivers of the Don basin located in the arid climate zone in the southern part of the European Russia. Depending on the part of the basion, four to five long-term low-flow periods were revealed during the period of hydrometric observations (1899-2016).

The most severe periods occurred in the early 1950s and mid-1970s in terms of deviation of the annual runoff volume, during which, the deviation reached 8 km^3, which is equal one third of the total annual runoff. However, the low-flow period of 2007-2016 had the highest water deficit volume. At the gauging section Razdorskaya, the total deficit for the 8-year period was 44.3 km^3, which is equivalent to twice the annual runoff volume of the entire basin. The analysis shows that the tributaries that make the main contribution to the runoff deficit measured at the gauging section Razdorskaya, are varying from year to year. Sometimes the water deficit is more pronounced in the upper reaches, and sometimes in the lower reaches. The long duration of the 2007-2016 low-flow period is the consequence of the combination and superposition of several low-flow periods in different parts of the basin.

According to the analysis performed in this study, the main contribution to low-flow formation was made by unfavourable hydroclimatic conditions due to a combination of several factors during the period 2007-2016. On one hand, at the beginning of the low-flow period, anomalously warm winters were recorded for the region. This contributed to increasing losses of spring runoff due to low soil freezing and higher infiltra-

tion of the melt water, finally, leading to the formation of extremely low spring floods. An increase of days with "thawing conditions" of more than one week lead to a decrease in the amount of solid precipitation, due to spells with positive air temperatures during winter. Solid precipitation decreased by 10-35% throughout the entire basin compared to the reference period (1979-2006). The decrease in the amount of solid precipitation during winter was partially compensated by a higher amount of liquid precipitation during the winter period by 10-30%. The great change for the past 10 years was detected in the amount of liquid precipitation in summer, which decreased by 20-25% (60-120 mm) compared to the reference period. At the same time, the total annual amount of precipitation changed: for example, the precipitation recorded throughout the basin was only 40-60 mm during 2014-2015.

The estimates of the contribution of the transformation of the catchment surface area that were performed for the "pilot" basins of the Khopyor River at Novokhopyorsk and the Don River at Liski showed that the anthropogenic changes in runoff, both the direct (water withdrawal) and the indirect ones (urban growth, reforestation, decrease in field's area) related to the redistribution of land categories, ploughing and reforestation, made a minor contribution to the formation of the low-flow period.

The research presented in this paper gives and overview over the spatial and temporal characteristics of the low-flow periods in the Don Basin over the available record length. The detailed assessment of the 2007-2016 period allowed investigating the meteorological factors contributing to the most recent low situation together with some preliminary assessment of possible human contributions. The results obtained here already provide some important insights in the low-flow characteristics of the region and can aid to inform water management and the development of a low-flow forecasting system. Future studies will perform research beyond these pilot regions, to obtain additional results and test further hypotheses with additional data to gain further insights.

ACKNOWLEDGEMENTS

The study has been carried out with the support of President's Grant No. MK-2331.2017.5 and RFBR Grant in methods of mapping and interpolation of data (Project No. 17-05-41030 RGS_a)

REFERENCES

Alekseevsky N., Frolova N. Safety of water use in conditions of low water level (2011). Water management in Russia: problems, technologies, management, vol. 6, p. 6-17.

Alekseevsky N., Frolova N., Grechushnikova M., Pakhomova O. (2013). Assessment of the negative impact of low water in 2010 on the socio-economic complex of the country. Environmental Management, 3, p. 65-68.

Annual surface and ground water resources, it's use and quality (State Water Cadastre) (1991-2016 yy.). Saint-Petersburg: SPH.

ERA-40 (2005). European Centre for Medium-Range Weather Forecasts Official Website, datasets, data [online]. Available at: http://apps.ecmwf.int/datasets/data/era40-daily/levtype=sfc/ [Accesed 20.11.2018].

ERA-Interim (2005). European Centre for Medium-Range Weather Forecasts Official Website, datasets, data [online]. Available at: http://apps.ecmwf.int/datasets/data/interim-full-daily/levtype=sfc/ [Accesed 20.11.2018].

Barabanov A., Dolgov S., Koronkevich N., Panov V., Petelko A. (2018). Surface runoff and infiltration of the melt water in the soil on the fields in step and forest-step zones of the Russian plain. Pochvovedenie, Vol. 1, 2018, p. 62-69.

Bordi I., Fraedrich K., Sutera A. (2009). Observed drought and wetness trends in Europe: an update. Hydrology and Earth System Sciences: 13, pp. 1519–1530.

code.mpimet.mpg.de (2006). Climate Data Operators [online]. Available at https://code.mpimet.mpg.de/projects/cdo [Accesed 20.11.2018].

code.mpimet.mpg.de (2006). Climate Data Operators Guidelines [online] Available at: https://code.mpimet.mpg.de/projects/cdo/wiki/Cdo#Documentation [Accesed 20.11.2018].

Dee D.P. (2011). The ERA-Interim reanalysis: configuration and performance of the data assimilation system. Quarterly Journal of the Royal Meteorological Society, vol. 137, pp. 553-597.

Dmitrieva V. (2011). Intra-annual and long-term dynamics of seasonal river flow. Arid ecosystems, Vol. 17. No. 2 (47). Pp. 23-32.

Dmitrieva V. (2014). Extreme water content as a factor of disturbance of hydroecological safety in the Upper Don basin. Arid ecosystems, Vol 20, No. 2 (59), p. 12-18.

Dzhamalov R., Frolova N., Kireeva M. (2013). Modern Changes in the Water Regime of the Rivers in the Don Basin. Water Resources, Vol. 40, No. 6, 2013, p. 544-556.

Golubev G., Dronin N. (2004). Geography of Droughts and Food Problems in Russia (1900-2000). Report of the International Project on Global Environmental Change and Its Threat to Food and Water Security in Russia.

Karlin R.N. (2008). Hydrometeorological risks. Saint Petersburg: RHHMI.

Kireeva M.B., Frolova N.L., Rets E.P., Telegina E.A., Telegina A.A., and Ezerova N.N. (2015). The role of seasonal and occasional floods in the origin of extreme hydrological events. Proc. IAHS, 369, pp. 109-113. doi:10.5194/piahs-369-109-2015

Koronkevich N. (1990). Water balance of the Russian Plain and its anthropogenic changes. Moscow: Science.

Mouat D.A., Lancaster J. (2008). Use of remote sensing and GIS to identify vegetation change in the upper San Pedro River watershed. Arizona, Geocarto International: 11:2, 55-67.

Scheme of integrated use and protection of water bodies in the basin of the river Don (2013). Book 1: general characteristics of the river basin, 343 p.

Semenov V.A. (2009). Climate change due to the risk of flooding, flooding and water shortages in the major river basins of Russia. Water problems of large river basins and their solutions. Barnaul, pp. 194-203. (in Russian)

Semenov V.A., Gnilomedov E.V., Salugashviliy R.S., Golubev V.N., Frolov D.M. (2015). Geography and genesis of climate-forced changes of extreme water discharge, floods and droughts for Russian river basin. In Proceedings of RIHMI-WDC, Obninsk, Russia.

Sheeja R., Sabu J., Jaya D., Baiju R. (2011). Land use and land cover changes over a century (1914–2007) in the Neyyar River Basin, Kerala: a remote sensing and GIS approach. International Journal of Digital Earth: 4:3, 258-270, 2011. doi: 10.1080/17538947.2010.493959

Shiklomanov I. (1979). Anthropogenic changes in the water content of rivers Leningrad: Hydrometizdat.

Surface and groundwater resources, their use and quality (1981–2015). St. Petersburg: Hydrometizdat (from 2013 - Es Pe Ha).

Van Lanen H., Laaha G., Kingston D., Gauster T., Ionita M., Vidal J.-P., Vlnas R., Tallaksen L., Stahl K., Hannaford J., Delus C., Fendekova M., Mediero L., Prudhomme C., Rets E., Romanowicz R., Gailliez S., Wong W.K., Adler M.-J., Blauhut V., Caillouet L., Chelcea S., Frolova N., Gudmundsson L., Hanel M., Haslinger K., Kireeva M., Osuch M., Sauquet E., Stagge J. H., and Van Loon A. (2016). Hydrology needed to manage droughts: the 2015 European case. Hydrol. Process., 30: 3097–3104. doi: 10.1002/hyp.10838

Received on November 15th, 2017 Accepted on November 15th, 2018

Emma A. Likhacheva[1*], Larisa A. Nekrasova[1], Mariya E. Kladovschikova[1]
[1] Department of Geomorphology, Institute of Geography, Russian Academy of Sciences, Moscow, Russia
***Corresponding author:** lihacheva@igras.ru

GEOMORPHIC ASSESSMENT OF TERRESTRIAL RESOURCES

ABSTRACT. Building of scientific basis for harmonious exploitation and spatial organization of the economy (land use) is one of the key issues of present-day geography. The study of land resources includes consideration of the relations between economic development, profitability and potential opportunities for further development of the territory, possibility of disturbed lands recovery and returning to the economic turnover, and preservation – all of those things which are necessary for human life worth living. Identification and analysis of land use types and forms is a necessary step of any economic-and-geographic study of a certain territory on the basis of statistical data and field survey. The creation of optimal land use schemes, taking into account the assessment of the conditions for certain types of management placement in given territory, has practical importance.

This paper presents the logical model of the area natural conditions influence on the evolution of urban land, shows the ways of creating the model of comfortable environment, where all types of the place attractiveness – ecological, social and economic – should be balanced.

A constructive formula for the geomorphic assessment of territorial resources includes the synthesis of benefit and profit. That is an engineering and ecologic-and-geomorphic assessment of lands in terms of the convenience for some sort of economic activity, taking into account the ecologic-and-geomorphic restrictions, as well as the economic evaluation of the engineering site preparation, taking into account the availability of recreational and specially protected areas, as well as environmental insurance against adverse processes and phenomena – maintaining of favorable living conditions.

KEY WORDS: ecologic-and-geomorphic assessment, terrestrial resources, land use, natural-and-anthropogenic risk, environmental management, constructive formula, logical model

CITATION: Emma A. Likhacheva, Larisa A. Nekrasova, Mariya E. Kladovschikova (2019) Geomorphic assessment of terrestrial resources. Geography, Environment, Sustainability, Vol.12, No 2, p. 78-86
DOI-10.24057/2071-9388-2018-28

INTRODUCTION

General trend of modern science – greening and harmonious exploitation – requires specification of research, which allows reducing actual knowledge to a certain constructive formula. In order not only to learn how to create anthropogenic-and-geomorphic systems, presenting them as a harmonious combination of natural and artificial components of relief and architecture, but also to manage, use and preserve them (Gerasimov 1985; Gettner 1930; Gorshkov 1998; Demek 1977; Kolbovskiy et al. 2001).

Building of scientific basis for harmonious exploitation and spatial organization of the economy (land use) is one of the key issues of present-day geography (Zvorykin et al. 1988; Simonov et al. 1993; Simonov et al. 2002). The study of land resources from the perspective of assessing the natural environment is a complex procedure, including consideration of the relations between economic development, profitability and potential opportunities for further development of the territory. The possibilities of restoration (attractiveness, value) or disturbed lands returning to the economic turnover should be considered, as well as the preservation of the natural complex as an essential component for human life worth living (Krogius 1979; Lastochkin 1992; Legget 1996; Sen-Mark 1977).

State of the problem

Territorial (land) resources represent a spatial basis for the allocation of economic facilities and population distribution; they are the leading means of production (firstly in agriculture and forestry). The assessment and use of land resources at the state level is based on the Land Code cadastral data and land valuation.

Identification and analysis of land use types and forms is a necessary step of any economic-and-geographic study of a certain territory. It is based on statistical data (Federal Law… 2000) and field survey. The creation of optimal land use schemes on the base of assessment of the conditions for certain types of management placement in given territory, has practical importance. Studies related to agriculture obtained the highest development. The term "land use" specifies the works in systematization and mapping of agricultural types, taking into account local natural and economic conditions (undertaken by English geographer L. Stamp for the first time in 1930) (Varlamov et al. 2006; Sizov 2006; Federal Law… 2000; Federal Law… 2002).

Agenda

Geomorphic assessment of territorial resources is based on the theoretical concepts of the anthropogenic-and-geomorphic system as a special morpholithodynamic system consisting of natural and anthropogenic components (mineral and biological) that are interrelated not only by natural flows of matter, energy and information, but also by the structures of socio-technical management. This is *anthropoecosystem*, complex in time and space. *Morphological and spatial orderliness* determines the engineering properties of the morpholithosystem (and, in particular, the territorial organization), while morphodynamics organization determines the stable functioning (Likhacheva et al. 2002; Likhacheva et al. 2004; Likhacheva 2007).

The tasks requiring geomorphic research are the following:

1. functional zoning of the territory according to the favorable geomorphic conditions for conducting some sort of economic activity;

2. zoning of the territory according to the geotechnical hazard and risk of geomorphic processes development;

3. identification of zones of ecological discomfort, geo-ecological hazard and risk (geochemical, ecologic-hygienic and geophysical), geopathic zones and zones favorable for public health;

4. identification of sanatorium-resort, recreational (including aesthetic) and other resources;

5. determination of priority forms of land use considering their natural potential, as well as their historically established (traditional) economic functions and, most importantly, considering their "geoecological transformation". By this term we define all the deep changes in the morpholithosystem (morphosculpture) – the whole complex of forms, content (properties and composition of the lithogenic base) and the functioning processes changes;

6. modeling, design (creation) of the engineering-natural environment – a stable-equilibrium morpholithosystem, and forecasting its development.

The purpose of the research is to study the "co-creation" of various components in case of the human environment development, as well as to identify the mechanisms of functioning and development on the basis of system analysis.

The system-constructive model of research can be defined as follows: environmental *benefit* – creation of an environment of life = economic *profit* = the continued *preservation* of favorable living conditions (environmental protection). This fine, but rather contradictory and, importantly, hard-to-reach formula determines retrieval route of the *reconciliation* and *elimination* (or reduction) of conflicts between human and nature – "profit" and "preservation of favorable living conditions". This is also an "environmental benefit". The only way is to make preservation (generally "protection of nature") of living environment *profitable* (and therefore to receive income).

People have learned to make profit and to get benefit, yet with causing great damage to nature. That is why various "requirements", regulatory standards and recommendations are being formulated nationwide. In particular, all necessary conditions for "protection of the (human) environment" have been formulated and codified by law in the Russian Federation (Federal Law… 2017).

Protection of the human socio-economic and natural environment (habitats) is a combination of international, state, regional and local administrative-and-economic, technological, political, legal and social activities aimed at ensuring the socio-economic, cultural-and-historical, physical, chemical, biological comfort necessary to preserve human health (protection of landscapes, subsoil, forests, soils, nature, etc.). The list of actions on environmental protection includes its improvement (for human), recultivation, optimization and reclamation (Federal Law… 2017).

Solutions

Typification and land rating for housing, industrial and road development sector is necessary for environmental management system generating, as well as for private economy and agricultural sector management, recreational zones planning in respect of "protective" (valuable) properties of lands, which include scientific, historical-and-cultural, aesthetic, recreational, health-improving and other valuable properties.

The aim of land assessment in old-cultivated areas has an extremely wide range of problems, and its solving should ensure the sustainable use of territorial resources (with the greatest outcome for economy and least damage for nature) and preservation of the engineering, ecological and historical-and-cultural potential of the territories.

These territories have long been attractive for comfort habitable environment creating, because they met the basic human needs, his physical and material capabilities, the development was *economically* profitable. That's why the degree of their development is high enough.

Urban territories show peak concentration of anthropogenic morpholithogenesis. It occurs not only due to purposeful actions, but also under impact of natural

and technogenic-activated processes, which provide *autoregulation* of the system: new relief and *run-off structure* are being formed; new *quality* (geochemical, hydrogeological, etc.) appears. Using P. Velev (1985) glossary, natural morpholithosystem suffers *"metamorphic transformation"* within the urban territory. Herewith stochastic character of development is common to the urbanized morpholithosystem, little-known to natural phenomenon category of "singularity".

A city is human ecosystem, his natural habitat, special *geosystem* – geographical, geological, geophysical, geochemical, and geomorphological. This system is developing and existing according to the *law of natural system development due to environment, due to* substance exchange in the system (entity of the city) and constant substance exchange with environment. This process was defined by P. Velev (1985) as substance exchange *(metabolism)* of organo-mineral (living) system - *"city"*. Natural, anthropogenic and technogenic factors are involved in metabolism, they interact together, being reprocessing and become transforming. New components or metabolites appear as a result of cooperation – technogenic sediments, soils and subsoils (technoliths) with organo-mineral structure (Likhacheva et al. 1997).

A "second nature" is formed on the urban territory with its own microclimate, vegetation, relief and soils, surface water and groundwater, and, what is highly important, with the elements of management.

Modeling of the geosystems operation (both natural and natural-and-anthropogenic), as well as *forecast management*, is the basis for the *management* of territorial resources and natural-and-anthropogenic risks. Using modern methods of data processing (including data on climate change), it is possible to present scenarios for the natural complex development and provide recommendations for land management, for human comfort maintaining, transport infrastructure, resting-places and income provision from land users (subsoil, water, forest users) and other shareholders and insured persons.

The Fig. 1 shows the logical model of the local natural specifics influence on the habitable environment development (and, in particular, on the urban territory). Here you can see the ways of solution the problem of comfortable environment model development, where all types of the local attractiveness – ecological, social and economic – must be balanced (Likhacheva et al. 1997; Forrester 1974).

MONITORING OF URBAN LANDS

Analysis of the existing literature shows, that theoretical and especially methodological foundations of monitoring of urban lands as a specific group within the category of settlement lands, have not been sufficiently issued, which troubles comprehensive monitoring in the frame of activities.

Unfortunately, geomorphological researches is the least considered part of the investigation, whether in environmental monitoring statement or in cadastral valuation of land. Challenges for geomorphological monitoring of urban areas are determined by the needs of relief study, not only as morphogenetic formation, but also as an engineering and environmental factor, as urban planning resource. Relief plays a key role in the urban ecosystem, making a significant impact on the formation of urban ecosystem structure:

1) on the landscape-architectural solutions of urban built-up area;

2) on the construction and management of buildings and facilities, roads and other communications;
3) on sanitary and hygienic conditions (including the formation of physical technogenic fields: noise-induced, vibrational, electromagnetic; geochemical fields, affecting the distribution and concentration of pollutants throughout the urban area, the atmospheric and stream-born transmission, the urban air condition) and generally on the population health.

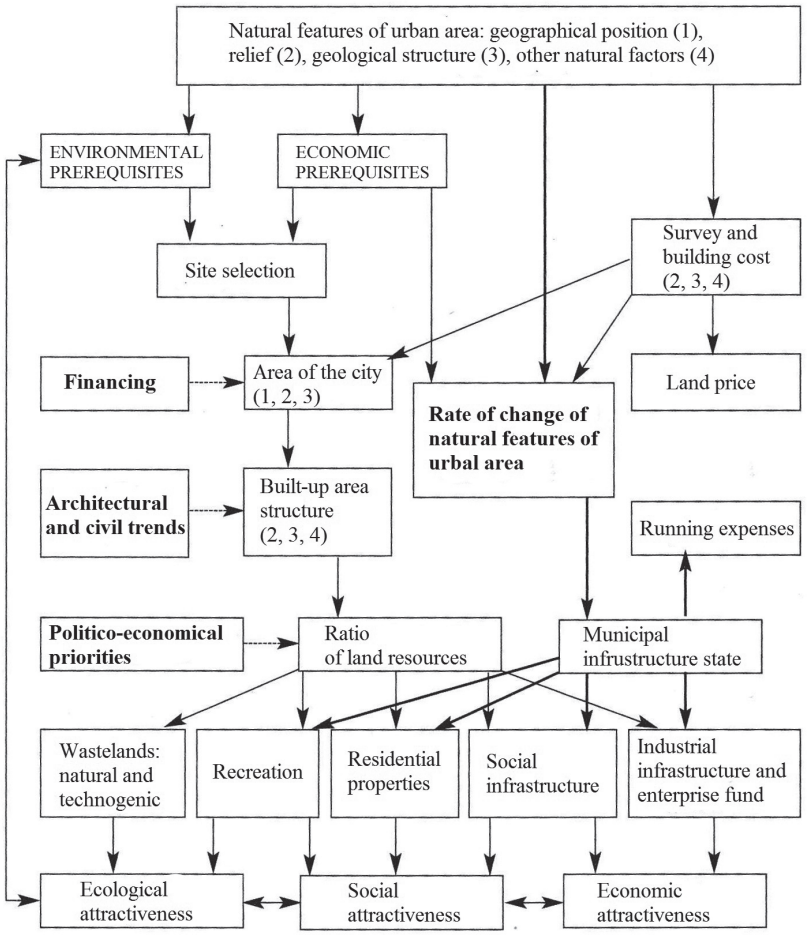

Fig. 1. Outline: logical model of the natural features influence on the anthropoecosystem (1, 2, 3, 4 – the role of natural factors in the descending order of their influence)

Transformations of the morphometric and morphodynamic characteristics of the relief change its functions as a surface that determines land and underground runoff and denudation-accumulation processes development. Inadvertently there are arising conditions for developing processes, compensating disrupted material-energetic balance, for developing natural-technogenic processes. Natural-technogenic processes may also have a negative character, especially after change of economic activity within giver part of urban area (Likhacheva et al. 1997).

Land value in Moscow is high and constantly increasing. To justify the efficient land use, the efficient exploitation of terrestrial compartment and underground space means to consider the land evaluation in efficiency calculations of capital investments, to solve a number of engineering-and-geological, environmental problems, to link the socio-economic and city-planning goals of Moscow development with environmental problems.

The way to solve the above listed challenges is to define the city-planning opportunities of city territory in accordance with their natural resources: the development of scientifically based recommendations for administrative and engineering activities, united by the common name "environmental protection", which can also be termed as harmonious exploitation.

This aim is also pursued by the Moscow Mayor's decree from April 6, 1993, "Towards the Monitoring of Lands in Moscow", which defines the range of necessary observations, primarily for: changing the boundaries of Moscow, administrative-territorial entities, land properties, security and technical zones; land use efficiency; dynamics of urbanization of agricultural exploitation lands, lands of urban forests and green spaces; implementation of landscape-ecological zoning of Moscow territory with allocation of negative processes; state of lands, soil and vegetation cover. These observations had provided studies undertaken by the Department of Land Resources of Moscow, in particular:

1) the subject content of urban lands monitoring as an independent type of scientific-information and operating activities of civil services and specialized organizations have been formulated;

2) an optimal version for the distribution of powers between the executive authorities was proposed, and recommendations for the use of information on the land quality assessing have been given;

3) a basic list of environmental requirements for land use and land users, fixed in the land legal documentation, have been prepared; Atlas of the city lands cadastral valuation was produced;

4) the methodological basis for calculating the size of the monetary equivalent of environmental damage from technogenic processes on the urban lands have been developed, and calculations of damage from littering up and chemical pollution of Moscow lands have been completed; the city already has a Unified Ecological Monitoring System (network of territorial level), observations are conducted over the atmospheric air and surface and groundwater state, karst-suffusion and landslide processes, green spaces, and physical factors of influence (noise);

5) the technological solutions for monitoring the actual use and state of lands by means of remote sensing and new equipment, monitoring of securing the land-legal relations and social processes for Moscow have been recommended (Varlamov et al. 2006; Sizov 2006).

The system of city-forming actions also includes government and public control over the state of the natural environment and the sources of its pollution; protection of natural and cultural monuments, and in the broadest sense – of all material and spiritual living and development conditions of human society and future generations, increase the social standards of living, develop the project environmental impact assessment, databanks creation, organization of monitoring system, and increase the level of urban residents' environmental culture (Shmidt 2013; Kotlyakov and Tishkov 2014; Likhacheva and Bolysov 2017). Huge scientific capability of Moscow, development and implementation of active environmental policy by the Government allow count on major restructuring of the environmental research activities organization of Moscow, which in turn will avoid the environmental disasters in the urban area. These are challenges not only for specialized organizations, but also for academic and higher education institutions (Fig. 2).

DISCUSSION AND CONCLUSION

A constructive formula for the geomorphic assessment of territorial resources includes the synthesis of benefit and profit. That is an engineering and ecologic-and-geomorphic assessment of lands in terms of the convenience for some sort of economic activity, taking into account the ecologic-and-geomorphic restrictions, as well as the economic evaluation of the engineering site preparation, taking into account the availability of recreational and specially protected areas, as well as environmental insurance expenditure against adverse processes and phenomena – maintaining of favorable living conditions:

1) to suggest actions for maintain the evolutionary development of the natural complex, taking into account climate change, natural selection and formation of a new natural-anthropogenic complex based on modeling;

2) to develop assessment criteria of land degradation aiming to determine the optimal complex for recultivation based on modeling.

Generally, a constructive formula of harmonious exploitation > economic development (benefit) > profitability (profit) > the possibility of expanding the economic activity (additional profit) > long-term preservation of favorable living environment (habitat protection).

ACKNOWLEDGEMENTS

The present study was supported by state assignment project № 0148-2019-0005, research, development, and engineering study № AAAA-A19-119021990091-4.

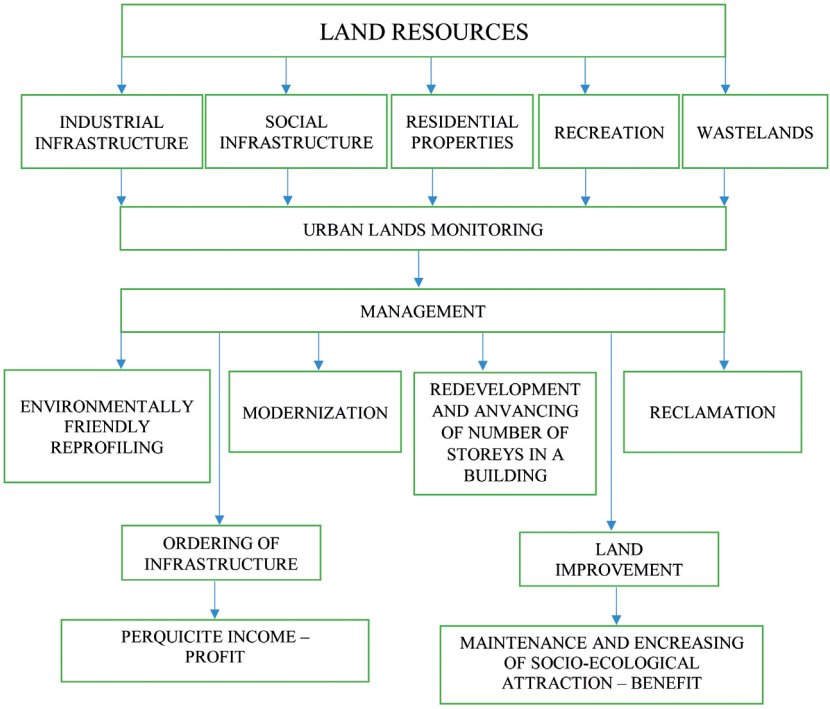

Fig. 2. The scheme of the city land resources management with the benefit and profit on the basis of urban lands monitoring

REFERENCES

Demek Ya. (1977). Theory of systems and landscape research. Moscow: Progress Publ. (in Russian)

Federal Law "Concerning the protection of the Environment" (2002). Consultant Plus. Sure Legal Support Official Website. [online] Available at: http://www.consultant.ru/document/cons_doc_LAW_34823/ [Assessed 1 July 2018]. (in Russian)

Federal Law "Concerning the State Land Cadaster" (2000). Consultant Plus. Sure Legal Support Official Website. [online] Available at: http://www.consultant.ru/document/cons_doc_LAW_25499/ [Assessed 1 July 2018]. (in Russian)

Federal Law "Land Code of the Russian Federation" (2017). Agreement. Contract. Lawyer. Russian Legal Circles Official Website. [online] Available at: https://dogovor-urist.ru/кодексы/земельный_кодекс/ред-01.11.2017/ [Assessed 1 July 2018]. (in Russian)

Forrester D. (1974). Dynamics of the city development. Moscow: Progress Publ. (in Russian)

Gerasimov I.P. (1985). Environmental problems in past, present and future geography. Moscow: Nauka Publ. (in Russian)

Gettner A. (1930). Geography. Its history, essence and methods. Moscow; Leningrad: GIZ Publ. (in Russian)

Gorshkov S.P. (1998). Concept basis of geoecology: Tutorial. Smolensk: Smolensk Humanitarian University Publ. (in Russian)

Kolbovskiy E.Yu. and Morozova V.V. Landscape planning and formation of a protected natural territories networks. Moscow; Yaroslavl: IGRAN and YaPGU Publ. (in Russian)

Kotlyakov V.M. and Tishkov A.A. (2014). Strategic resources and conditions for sustainable development of the Russian Federation and its regions. Moscow: IG RAS Publ. (in Russian with English summary)

Krogius V.R. (1979). City and relief. Moscow: Stroyizdat Publ. (in Russian)

Lastochkin A.M. (1992). Environmental trend in geomorphic researches. In: Engineering geography. Vologda: VFRGO Publ. (in Russian)

Legget R. (1976). Cities and geology. Moscow: Mir Publ. (in Russian)

Likhacheva E.A. (2007). Ecological chronicles of Moscow. Moscow: Media-PRESS (in Russian)

Likhacheva E.A. and Bolysov S.I. (2017). Urban geomorphology: constructive ideas. Moscow: Media-PRESS Publ. (in Russian with English summary and abstracts)

Likhacheva E.A. and Timofeyev D.A. (2002). Relief of human living environment. Moscow: Media-PRESS (in Russian)

Likhacheva E.A. and Timofeyev D.A. (2004). Ecological geomorphology. Reference book. Moscow: Media-PRESS (in Russian)

Likhacheva E.A., Timofeyev D.A., and Zhidkov M.P. (1997). City – Ecosystem. Moscow: IGRAS Publ. (in Russian)

Sen-Mark F. (1977). Socialization of nature. Moscow: Progress Publ. (in Russian)

Shmidt S.O. (2013). Great atlas of Moscow. Moscow: Feoriya Publ. (in Russian)

Simonov Yu.G. and Bolysov S.I. (2002). Methods of geomorphic research: Methodology: Tutorial. Moscow: Aspect-Press Publ. (in Russian)

Simonov Yu.G. and Kruzhalin V.I. (1993). Engineering geomorphology. Moscow: MSU Publ. (in Russian)

Sizov A.P. (2006). Urban lands: quality assessment, monitoring, application of results in land use regulation. Doctoral thesis. Moscow: State University of Land Use Planning. (in Russian)

Varlamov A.A. and Varlamova E.A. (2006). Building of the huge megalopolis lands monitoring system. In: Varlamov A.A., ed., Ecological problems of environmental regional monitoring. Moscow: RANS Publ. Pp. 8-16 (in Russian)

Velev P. (1985). Cities of the future. Moscow: Stroyizdat Publ. (in Russian)

Zvorykin K.V. and Balliyeva R. (1998). Social background of geography and views on its subject. In: Interaction of physical and economic geography. M.: MFRGO Publ. (in Russian)

Received on July 2nd, 2018 Accepted on November 15th, 2018

Safwan A. Mohammed[1*], Riad Qara Fallah[2]
[1] Institution of Land Utilization, Technology and Regional Planning, Faculty of Agricultural and Food Sciences and Environmental Management, University of Debrecen, Debrecen, Hungary
[2] Department of Geography, Faculty of Arts and Humanities, Tishreen University, Lattakia, Syria
***Corresponding author:** safwan@agr.unideb.hu

CLIMATE CHANGE INDICATORS IN ALSHEIKH-BADR BASIN (SYRIA)

ABSTRACT. The trends and variability of climate change were studied through analyzing the trend of change in the annual temperature and rainfall averages during the period (1960 – 2016) in Al-Sheikh Badr Region by using Normal Distribution and De-Martonne index. The results showed a (-189 mm) linear decrease in the general trend of the rainfall, associated with a (+0.9° C) increase in the general trend of the temperature between 1960 and 2016. Also, Normal distribution showed that the probability of extreme temperatures events higher than 17.5°C increased from 3.3% during the period 1960-1990 to 24.8% during the period 1991-2016. While the probability of an extreme annual rainfall (more than 1800 mm) decreases from 5.3% to 4.7%, nevertheless, the probability of rainfall events less than 800mm where increased. Furthermore, there is a significant trend of drought in the studied area, where the De-Martonne index reaches (-10.75) through the period (1960-2016).

KEY WORDS: Climate change, Normal Distribution, De-Martonne Index, the Mediterranean Region

CITATION: Safwan A. Mohammed, Riad Qara Fallah (2019) Climate change indicators in AlSheikh-Badr Basin (Syria). Geography, Environment, Sustainability,
Vol.12, No 2, p. 87-96
DOI-10.24057/2071-9388-2018-63

INTRODUCTION

In this era, climate change has been considered as one of the most global phenomena that affected many ecosystems, resulting in floods, droughts, and rainfall changes. Mediterranean area is considered as one of the most affected regions by climate change (Nouaceur and Mursrescu 2016), as well as, Arab region which already suffers from water scarcity and any changes will lead to catastrophic impact in ecosystems and different economic and social activities.

Syria, which located in the Middle East, has affected badly by climate change (Skaf and Mathbout 2010; Giorgi 2006; Toreti et al. 2016) including gradually declining in average rainfall patterns and increasing average of temperature, which leads to more drought conditions (Åkesson and Falk 2015).

Climate change components had not been widely studied in Syria, Jalab et al. (2014) proved that there is a significant increase in the average annual temperature in the three regions (Latakia, Kasaab and Slenfeh)

in Syria, during the period of analysis 1978-2011. Similarly, Skaf and Mathbout (2010) emphasize the positive trend in dry days number in Syria by using the Effective Drought Index (EDI) during the period 1968-2008, also, Skaf and Saker (2015) analyzed the precipitation characteristics during the period 1960-2010 in six meteorological stations located in the Syrian coastal region, and proved a significant negative trend in annual precipitation in all stations. In a similar vein, Haleme and Qara Fallah (2015) indicated the presence of a decline in the annual rates of rainfall in some stations in Tartous, during the period 1970 – 2010 by using Gamble's distribution. Interestingly, Alsaleh, et al. (2005) indicate that the surface air temperature in Syrian stations seems to be affected by solar cycle and quasi-biennial oscillation as well as the El-Nino southern oscillation with positive trend of annual and seasonal temperature for all studied locations except Latakia during the period from 1955 to 2000. Conversely, Nouaceur and Mursrescu (2016) analyzed rainfall data from three Mediterranean countries (Algeria, Morocco, and Tunisia) and pointed out of the beginning of a gradual return to wetter conditions in these countries, which considered as the first indicator against IPCC reports.

Therefore, the main objective of this research to analyze the trends of climate change components (rainfall and temperature) in Al-Sheikh Badr Region (Syria) during the years 1960-2016, by using Normal Distribution, and De-Martonne index.

MATERIALS AND METHODS

Study area

The research has been conducted in Tartous governorate, in the north of Syria (35° 57′ 40″ and 36o 15′ 55″ East, and 34° 59′ 55″ and 35° 5′ 39″ North; 536 m; Fig. 1).

The entire study area, which located in the coastal region, belongs to the Mediterranean humid or subtropical types of climate, with gradually increasing amount of rainfall, and temperature from the west to the east and decreasing from the higher to the lower slopes of the coastal mountains and from north to south (PAP/RAC 1990). January is the coldest month in the study area, while the hottest month is August. The mean of monthly temperature values increases continuously after January to reach their maximum limit during August, the mean of monthly temperatures varies from 4 to 6° C in January, and from 20 to 22° C in July. The average maximum 31 temperature in the coastal area ranges from 15 to 17° C in January to 28 to 29° C in July. While rainfall distribution and reliability are mainly affected by the seasonal routes of the Atlantic cyclones passing eastwards along the Mediterranean. The rainfall season usually begins in September over the coastal area, and hits the maximum in December through January. The average annual rainfall is 1242.86 mm (COLD 2004). The total area of Sheikh Bader is around 20279 hectares (202.79 km^2). The cultivable area is about 13,250 ha, the main agricultural land use are olive, grapes, green housing, apple, wheat and tobacco. The natural land cover consists mainly of different species such as *Quercus L., Arbutus L., Pinus L., Pistacia L., Rhus cariaria, Prunus L., Ceratonia Siliqua L., Laurus Nobilis., Platanus L. Meanwhile, the main types of shrubs are Spartium junceum L., Micromeria rupestris, Thymus capitatus, Artemisia herba Alba, Myrtus Communis L., Poterium Spinosum L., Inula Viscosa, Calycotome Link, Sorghum halepense, Horolum vulgare, Cynodon dactylon, Juniperus oxycedrus* (Ministry of Agriculture 2015).

The land uses can be classified into 5 classes: natural vegetation cover, agricultural lands, bare land, water bodies and urban areas (COLD 2004). The district of Sheikh Bader comprises 77 villages and 10 extension units spread over those villages. Agriculture is the backbone of the area economy.

Data analysis

To achieve the research goals, climatic data were obtained during the period (1960-2016) from the Directorate of Meteorology - Tartous province. The linear trends of the mean variables (rainfall and temperature) were determined, while the numerical values of the changes in the annual rainfall and temperature were calculated by using Simple Linear Regression by SPSS.

Fig. 1. Location of the study area

After that, Normal distribution was used to analyze the probable density values for the high and low extreme events to determine the impact of it in two ways:

$$f(X)=\frac{1}{\sigma\sqrt{2\pi}}e^{-\frac{1}{2}\left(\frac{x-\bar{x}}{\sigma}\right)^2} \quad (1)$$

Where: $\bar{X}$ is the Average of the event, X is the amount of event, σ is the standard deviation.

For that, mean and standard deviation for the period (1960-2000) were compared to the period (2000-2016) to determine the change in precipitation and temperature within the study area.

The probable density of the variables (temperature and rainfall) for the first period 1960-2000 was calculated on the basis of a value less than 10% of the probability of their occurrence, so that distributed to 5% higher marginal values to the right of the curve, and 5% minimum marginal values on the left of the curve, then the results were compared to the second period 2000-2016, and the differences were calculated.

At the end, The De Martonne aridity index (De Martonne 1926; Croitoru et al. 2013) was calculated as one of the most important indicators to identify dry/humid conditions of different region (Zarghami et al. 2011), which is given by the following equation:

$$IA=\frac{P}{T+10} \quad (2)$$

For monthly index:

$$Ia=\frac{P_m}{t_m+10}\cdot 12 \quad (3)$$

Where: P and T are the annual amount of precipitation and mean annual surface temperature in millimeter and in degree Celsius, respectively.

RESULTS AND DISCUSSION

Temperature Changes (1960-2016)

The general trend of temperature was (+ 0.9)°C linear increase during the period 1960-2016 at the study area, as illustrate in Fig. 2, where it showes a gradual increase since 1970 and a clear higher increase of air temperatures since 2000. These result come along with Lionello et al. (2014) research, where they pointed out the rapidly rising of temperatures in the Mediterranean region through the last decades; which leads to significant upward temperature trends since the 1970s (Lelieveld et al. 2016; Zarenistanak et al. 2014). Additionally, Dubrovsky et al. (2014) analyzed the future climate conditions for the Mediterranean region where the results have shown an increase in temperature in all seasons for all parts of the Mediterranean area.

Rainfall Changes (1960-2016)

The general trend of rainfall was (-189) mm linear decrease during the period 1960-2016 at the study area, as shown in Fig. 3. It is also noted that the period between 1990 and 2000 recorded a significant decrease in rainfall pattern with a minimum value of 591.9 mm.

Deitch et al. (2017) pointed out the downward trends in annual precipitation in the the Mediterranean basin. In addition, De Luis et al. (2009) have proved that there is a decrease in the seasonal and annual precipitation at the Mediterranean Iberian Peninsula (IP) through 1950-2000.

Further, Philandras et al. (2011) emphasis the negative trends of the annual precipitation totals exist in the majority of Mediterranean regions, during the period 1901–2009, which create drier conditions (Kutiel et al., 1996; Turkes, 1998), However, this trend will be expected to continue till 2050 resulting decrease of up to 20% in total annual rainfall (Gonçalves et al., 2014).

Probable density of the high extreme annual temperature (1960-2016)

Analyzing the mean annual temperature in the study area as shown in Fig. 4 indicates that the probability values of temperature generally increased. In addition, the probability of extreme temperatures is higher than +17.5°C increased from +3.3% during the period 1960-1990 to +24.8% during the period 1991-2016 (red curve), with a total estimated probability of increase +21.5%, which is an indicator of warming in the study area.

On contrary, a large decrease in the probability of extreme temperatures less than 16.3°C, can be noted, with the general decrease of the probability from 26.6%

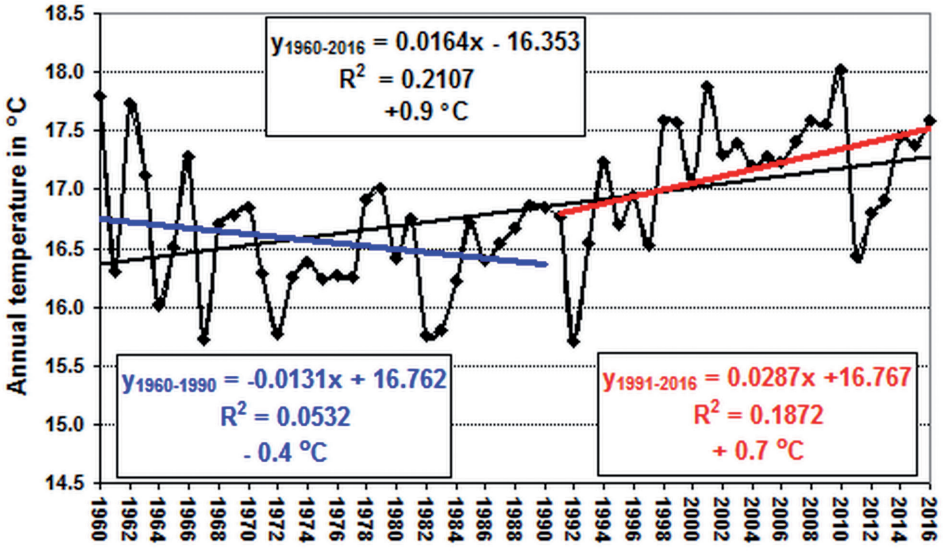

Fig. 2. Trends of annual temperature during the (1960-2016)

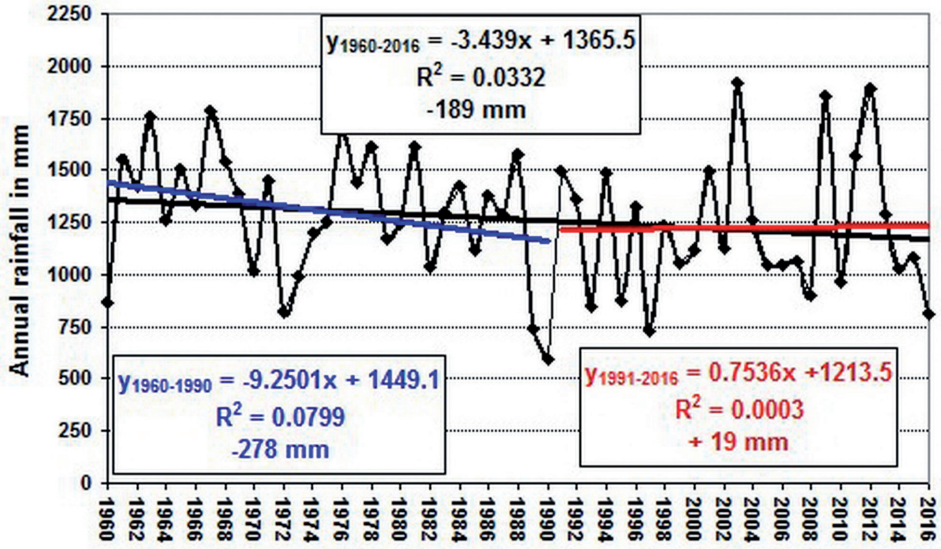

Fig. 3. Trends of annual rainfall amounts during the (1960-2016)

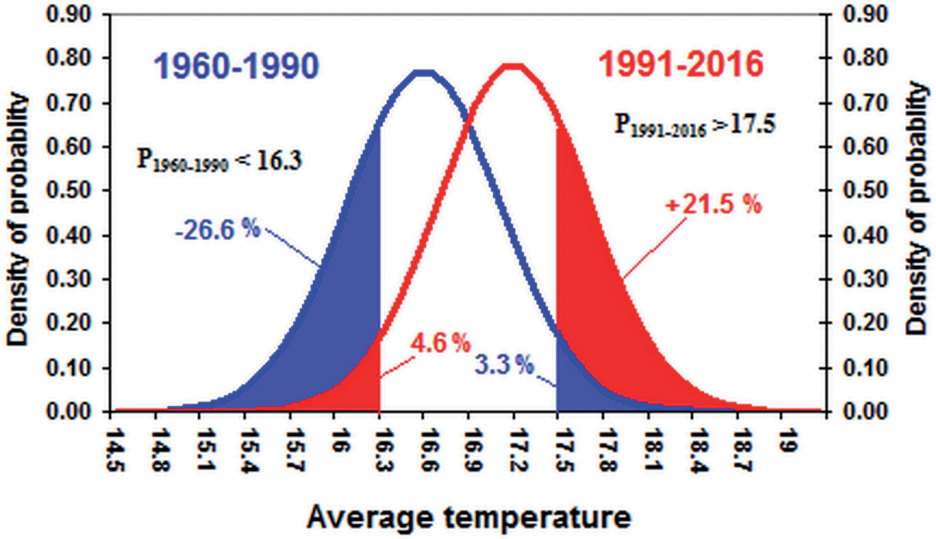

Fig. 4. Average annual mean temperature changes during the period (1991-2016) compared with the period 1960-1990 by using Normal distribution

(blue curve) to 4.6% (red curve). Thus, the probability of extreme temperatures less than 16.3ºC is down by 22%.

Probable density of the high extreme annual Rainfall (1960-2016)

By using Gamble's distribution, the probable values of the rainfall changes during (1991- 2016) compared with (1960-1990) were studied as shown in Fig. 5; which demonstrates an increase in the average rainfall ((less than 800 mm)) from 4.6% during the period 1960-1990 to 10.1% during the period 1990 – 2016 (red line). Moreover, the probability of an extreme annual rainfall (more than 1800 mm) deceased by 0.6%.

De-Martonne aridity index changes (1960-2016)

The De-Martonne aridity index represents the relationship between the temperature and precipitation, which is very important in the arid/humid climate classification.

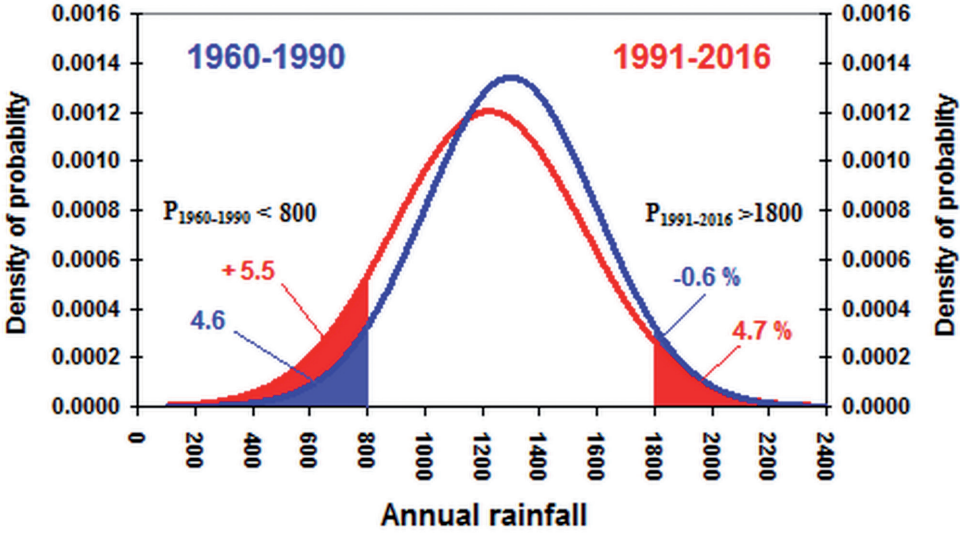

Fig. 5. Average annual rainfall changes during the period (1991-2016) compared with the period 1960-1990 by using Normal distribution

The analysis showed that there was a significant decrease of De-Martonne index by 10.175 during the study period as can be seen in Fig. 6; due to the decrease in the annual rainfall and the increase in the annual average temperature which lead to drought through time (Tanarhte et al. 2012). This was also observed by Mathbout et al. (2018) who reported a significant increase in drought indicators all over Syria through the period 1961-2012, similarly, identify major periods of drought in the Levant from 1998 till 2012. However, statistically, there is no significant change in the period 1960-2000 compared to 2001-2006 as shown in Table 1. And because of the rapid increase in temperature with the variable disturbance of rainfall patterns, many climate models predicted increasing the drought in the Middle East and in Syria (Breisinger et al. 2011).

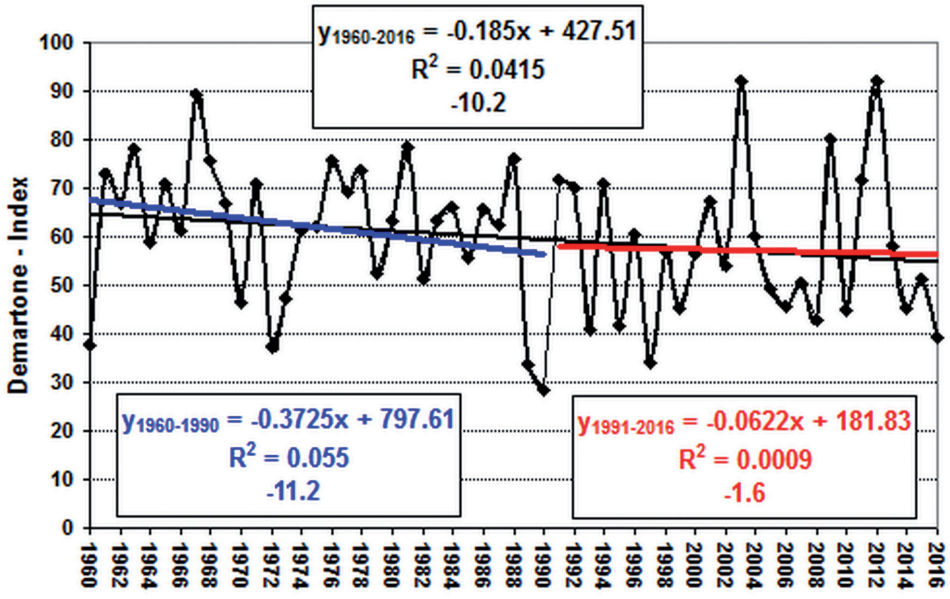

Fig. 6. De-Martonne aridity index changes during the period (1960-2016)

Table 1. The slope in the regression line of temperature, rainfall and De-Martonne aridity index, and the statistical significance of the slope of the regression line

Element	Temperature in °C	Rainfall in mm	De-Martonne Index
Annual change	0.016 +	3.439 -	0.185 -
Trend 1960-2016	0.9 +	189-	10.2-
Sig > 95 %	+	+	+
Average 1960-1990	16.6	1301.1	61.7
Average 1991-2016	17.2	1223.7	57.3
Difference	0.6+	-77.4	-4.4
Sig > 95 %	+	-	-

**Note: The differences among the averages (+) > 95% statistically significant (0) ≤ 95% is not statistically significant*

Generally, climate change become a global issue where the Earth's surface temperature has been increasing from the past century. Many factors such as increased emission of greenhouses gasses, as a result of industrial activities and intensive agriculture are significantly contributed in temperature changes. Also, land use changes which is a direct effect of urbanization that casing urban heat island (UHI) played an important role in climate change (Jorgenson et al. 2019; Comarazamy et al. 2013)

However, there were many indicators of climate change in the Mediterranean region especially in the Middle East (IPCC 2007a; Abu Sada et al. 2015; Zytoon and Shehadeh 2015). Alam and Sharif (2013) conclude that the responsibility of changing in climate in the Middle-East is the global warming which is a result of human interference in the ecosystems (Kousari et al. 2010). Evans (2009) suggested a decrease in storm track activity over the Eastern Mediterranean which is responsible for low rainfall. Similarly, Philandras et al. (2011) suggested that drought conditions and low rainfall in the Mediterranean region are mainly due to positive atmospheric circulation, which lead to move of western winds towards northern Europe causing increased rainfall and temperatures there, while it leads to drier and cooler anomalies in the Mediterranean region (Feidas et al. 2007; Kelley et al. 2015).

CONCLUSIONS

This study aims to analyze some parameters of climate change in Al-Sheikh Badr basin (Syria) during the period (1960-2016). The indicators showed a decrease in rainfall, an increase in temperature and a gradual decrease of De-Martonne aridity index, which will badly affect the ecosystems and different human activities.

For policymakers in Syria, it is important to consider the current and future changes in climatic conditions in order to take steps towards more sustainable natural resource management and water-use efficiency and productivity in agriculture. Furthermore, accelerated steps should be taken towards drought monitoring and early warning systems. Additionally, an assessment should be taken seriously for socio-economic impacts of climate change and their outcomes on different sectors and marginal environments, which should lead to national plans for adaptation to climate change in a multidisciplinary and integrated approach.

REFERENCES

Abu Sada A., Abu-Allaban M., and Al-Malabeh A. (2015). Temporal and Spatial Analysis of Climate Change at Northern Jordanian Badia. Jordan Journal of Earth and Environmental Sciences, 7(2), pp. 87-93.

Åkesson U. and Falk K. (2015). Climate Change in Syria—trends, projections and implications. Background document for SIDA'a development of a results strategy for Syria 2015. Sida's Helpdesk for Environment and Climate Change. SIDA, Stockholm. pp. 43.

Alam S. M. S. and Sharif M. (2013). Assessment of climate change scenario in the Middle-East Region. J Emerg Technol Adv Eng, 3(6), pp. 367-372.

Alsaleh R., Abouzakhem A., Shahawy M., and Eaid E. (2005). Analysis of Seasonal and Annual Variations in Surface Air Temperature in Syria. Damascus University Journal of Agricultural Sciences, 21(1), pp.401–424. (in Arabic).

Breisinger C., Zhu T., Al Riffai P., Nelson G., Robertson R., Funes J., and Verner D. (2011). Global and local economic impacts of climate change in Syria and options for adaptation. International Food Policy Research Institute, Discussion Paper, 1091, 23.

COLD (Land Degradation Monitoring in Lebanon And Syria) (1990). Preliminary study of the integrated plan for the Syrian coastal region. (LIFE TCY/00/INT/00069/MED). Damascus, Syria.

Comarazamy D.E., González J.E., Luvall J.C., Rickman D.L., and Bornstein R.D. (2013). Climate impacts of land-cover and land-use changes in tropical islands under conditions of global climate change. Journal of Climate, 26(5), 1535-1550.

Croitoru A.E., Piticar A., Imbroane A.M., and Burada D.C. (2013). Spatiotemporal distribution of aridity indices based on temperature and precipitation in the extra-Carpathian regions of Romania. Theoretical and applied climatology, 112(3-4), pp. 597-607. DOI: https://doi.org/10.1007/s00704-012-0755-2.

De Luis M., González–Hidalgo J.C., Longares L.A., and Štepánek P. (2009). Seasonal precipitation trends in the Mediterranean Iberian Peninsula in second half of 20th century. International Journal of Climatology: A Journal of the Royal Meteorological Society, 29(9), pp. 1312-1323. DOI: https://doi.org/10.1002/joc.1778.

De Martonne E. (1926). Aréisme et indice artidite. Comptes Rendus de L'Acad Sci, Paris, 182: pp. 1395–1398.

Deitch M.J., Sapundjieff M.J., and Feirer S.T. (2017). Characterizing precipitation variability and trends in the world's Mediterranean-Climate areas. Water, 9(4), pp. 259. DOI: https://doi.org/10.3390/w9040259.

Dubrovský M., Hayes M., Duce P., Trnka M., Svoboda M., and Zara P. (2014). Multi-GCM projections of future drought and climate variability indicators for the Mediterranean region. Regional Environmental Change, 14(5), pp. 1907-1919. DOI: https://doi.org/10.1007/s10113-013-0562-z.

Evans J.P. (2009). 21st century climate change in the Middle East. Climatic Change, 92(3-4), pp. 417-432. DOI: https://doi.org/10.1007/s10584-008-9438-5.

Feidas H., Noulopoulou C., Makrogiannis T., and Bora-Senta E. (2007). Trend analysis of precipitation time series in Greece and their relationship with circulation using surface and satellite data: 1955–2001. Theoretical and Applied Climatology, 87(1-4), pp. 155-177. https://doi.org/10.1007/s00704-006-0200-5.

Giorgi F. (2006). Climate change hot–spots. Geophysical research letters, 33(8). https://doi.org/10.1029/2006GL025734.

Gonçalves M., Barrera-Escoda A., Guerreiro D., Baldasano J.M., and Cunillera, J. (2014). Seasonal to yearly assessment of temperature and precipitation trends in the North Western Mediterranean Basin by dynamical downscaling of climate scenarios at high resolution (1971–2050). Climatic change, 122(1-2), pp. 243-256. DOI: https://doi.org/10.1007/s10584-013-0994-y.

Haleme K. and Fallah R. Q. (2015). Changes of the Rainfalls Rates in Tartous Using Gamble's Distribution. Journal of Geography and Geology, 7(1), PP77-84.

IPCC (Intergovernmental Panel on Climate Change) (2007). Impacts, Adaptation and Vulnerability. Asia Climate Change 2007. Cambridge University Press, Cambridge, UK, 469-506.

Jalab A., Mahfoud I., and Ismaiel F. (2014). Temperature and rainfall changes in Lattakia, kasaab and Slenfeh during 1978-2011. Tishreen University Journal for Research and Scientific Studies - Biological Sciences Series, 36(3), pp. 286-303 (In Arabic).

Jorgenson A.K., Fiske S., Hubacek K., Li J., McGovern T., Rick T., ... and Zycherman A. (2019). Social science perspectives on drivers of and responses to global climate change. Wiley Interdisciplinary Reviews: Climate Change, 10(1), e554.

Kelley C. P., Mohtadi S., Cane M. A., Seager R., and Kushnir Y. (2015). Climate change in the Fertile Crescent and implications of the recent Syrian drought. Proceedings of the National Academy of Sciences, 201421533. DOI: https://doi.org/10.1073/pnas.1421533112.

Kousari M.R., Ekhtesasi M.R., Tazeh M., Naeini M.A.S., and Zarch M.A.A. (2011). An investigation of the Iranian climatic changes by considering the precipitation, temperature, and relative humidity parameters. Theoretical and Applied Climatology, 103(3-4), pp. 321-335. DOI: https://doi.org/10.1007/s00704-010-0304-9.

Kutiel H., Maheras P., and Guika S. (1996). Circulation and extreme rainfall conditions in the eastern Mediterranean during the last century. International Journal of Climatology, 16(1), pp. 73-92. DOI: https://doi.org/10.1002/(SICI)1097-0088(199601)16:1<73::AID-JOC997>3.0.CO;2-G.

Lelieveld J., Proestos Y., Hadjinicolaou P., Tanarhte M., Tyrlis E., and Zittis G. (2016). Strongly increasing heat extremes in the Middle East and North Africa (MENA) in the 21st century. Climatic Change, 137(1-2), pp.245-260. DOI: https://doi.org/10.1007/s10584-016-1665-6.

Lionello P., Abrantes F., Gacic M., Planton S., Trigo R., and Ulbrich U. (2014). The climate of the Mediterranean region: research progress and climate change impacts. DOI: https://doi.org/10.1007/s10113-014-0666-0.

Mathbout S., Lopez-Bustins J. A., Martin-Vide J., Bech J., and Rodrigo F. S. (2018). Spatial and temporal analysis of drought variability at several time scales in Syria during 1961–2012. Atmospheric Research, 200, pp. 153-168. DOI: https://doi.org/10.1016/j.atmosres.2017.09.016.

Ministry of Agriculture (2015). Land use in Syrian. Damascus, Syria.

Mohammed S., Kbibo I., Alshihabi O., and Mahfoud E. (2016). Studying rainfall changes and water erosion of soil by using the WEPP model in Lattakia, Syria. Journal of Agricultural Sciences, 61(4), pp. 375-386. DOI: https://doi.org/10.5539/jgg.v7n1p77.

Nouaceur Z. and Murărescu O. (2016). Rainfall variability and trend analysis of annual rainfall in North Africa. International Journal of Atmospheric Sciences, 2016. DOI: http://dx.doi.org/10.1155/2016/7230450.

PAP/RAC (Regional Activity Centre for Priority Action Programme) (1990). Preliminary study of the integrated plan for the Syrian coastal region, P.7 (CCP/1988-1989/SY/PS). Split, Croatia.

Philandras C.M., Nastos P.T., Kapsomenakis J., Douvis K.C., Tselioudis G., and Zerefos C.S. (2011). Long term precipitation trends and variability within the Mediterranean region. Natural Hazards and Earth System Sciences, 11(12), pp. 3235-3250. DOI: http://dx.doi.org/10.5194/nhess-11-3235-2011.

Skaf M. and Mathbout S. (2010). Drought changes over last five decades in Syria. Economics of drought and drought preparedness in a climate change context, pp. 107-112.

Skaf M. and Saker R. (2015). Changes in seasonal and annual precipitation characteristics in the Syrian coastal region during the period 1960-2010. Tishreen University Journal for Research and Scientific Studies - Biological Sciences Series, 73(2), pp. 218-232. (In Arabic).

Tanarhte M., Hadjinicolaou P., and Lelieveld J. (2012). Intercomparison of temperature and precipitation data sets based on observations in the Mediterranean and the Middle East. Journal of Geophysical Research: Atmospheres, 117(D12). DOI: http://dx.doi.org/10.1029/2011JD017293.

Toreti A., Giannakaki P., and Martius O. (2016). Precipitation extremes in the Mediterranean region and associated upper-level synoptic-scale flow structures. Climate dynamics, 47(5-6), pp. 1925-1941. DOI: http://dx.doi.org/10.1007/s00382-015-2942-1.

Türkeş M. (1998). Influence of geopotential heights, cyclone frequency and Southern Oscillation on rainfall variations in Turkey. International Journal of Climatology: A Journal of the Royal Meteorological Society, 18(6), pp. 649-680. DOI: http://dx.doi.org/10.1002/(SICI)1097-0088(199805)18:6<649::AID-JOC269>3.0.CO;2-3.

Zarenistanak M., Dhorde A.G., and Kripalani R.H. (2014). Temperature analysis over southwest Iran: trends and projections. Theoretical and applied climatology, 116(1-2), pp. 103-117. DOI: https://doi.org/10.1007/s00704-013-0913-1.

Zarghami M., Abdi A., Babaeian I., Hassanzadeh Y., and Kanani R. (2011). Impacts of climate change on runoffs in East Azerbaijan, Iran. Global and Planetary Change, 78(3-4), pp.137-146. DOI: https://doi.org/10.1016/j.gloplacha.2011.06.003.

Zytoon M. and Shehadeh M. (2015). Climate Change Indicators in the North of Jordan. Dirasat: Human and Social Sciences, 42(2), pp. 1467–1486.

Received on August 8th, 2018 Accepted on May 17th, 2019

Maria V. Korneykova[1*], Vladimir A. Myazin[1,2], Lyubov A. Ivanova[1], Nadezhda V. Fokina[1], Vera V. Redkina[1]
[1] Institute of North Industrial Ecology Problems – Subdivision of the Federal Research Centre "Kola Science Centre of Russian Academy of Science", Apatity, Russia
[2] Institute of Russian Academy of Science "Saint-Petersburg Scientific-Research Centre of Ecological Safety", Saint-Petersburg, Russia
*** Corresponding author:** korneykova.maria@mail.ru

DEVELOPMENT AND OPTIMIZATION OF BIOLOGICAL TREATMENT OF QUARRY WATERS FROM MINERAL NITROGEN IN THE SUBARCTIC

ABSTRACT. The new concept of bioremediation of anthropogenic water bodies and quarry wastewaters treatment by phytoextraction and phytotransformation in the Subarctic conditions is presented. This technology is based on transformating the man-caused water reservoirs into nature-like marsh ecosystems. At the first stage, a new patented method for advanced waste treatment using floating bioplate was developed and implemented. After implementing the bioplate, the concentration of ammonium ions in water decreased by 53-90%, nitrate nitrogen reduced by 15-20%. At the second stage, the floating bioplate technology was modified into the highly efficient purificating marsh ecosystem, which allowed to cover the waterbody territory to the greatest possible extent. The technology is based on the creation of phytomats enabling in the accelerated mode to form plant blocks of three different types. They are aimed both at local grassing down, and at swamping deep and shallow areas of sediment ponds. In forming phytomats, two soil substitutional substrates (thermovermiculite and wood sawdust) and regionally-optimized assortment of 24 plant species are used. The proposed technology does not require energy, chemicals and soil components which are scarce in the region. The predominance of natural ecosystem processes in the formed phytocenoses allows to achieve maximum efficiency, and the use of available materials contributes to minimizing the costs of creating and maintaining the system. The introduction of this technology and formation of the artificial phytocenosis with the area of about 30% of the man-caused reservoirs territory made it possible to increase the efficiency of wastewater treating from mineral nitrogen compounds by 22%.

KEY WORDS: bioremediation, sewage quarry, sediment pond, mineral nitrogen compounds, phytocenosis, phytomats

CITATION: Maria V. Korneykova, Vladimir A. Myazin, Lyubov A. Ivanova, Nadezhda V. Fokina, Vera V. Redkina (2019) Development and optimization of biological treatment of quarry waters from mineral nitrogen in the Subarctic. Geography, Environment, Sustainability, Vol.12, No 2, p. 97-105
DOI-10.24057/2071-9388-2019-5

INTRODUCTION

The arctic regions attract attention with their enormous resource potential. This leads to increased environmental problems related to the vulnerability of nature and purification of industrial wastewater from mining enterprises. Ammonium nitrates and additives, such as nitromethane and sodium nitrate, are the main components of the explosives used in drilling and blasting operations at mines. Use of explosives is accompanied by contamination of mine and quarry waters with compounds of the nitrogen group.

So far, alongside physico-chemical and microbiological methods, the approaches based on the use of natural processes occurring in landscape and aquatic ecosystems are thought to be the most promising for cleaning quarry waters of nitrogen compounds (Yakovlev et al. 1985; Vurdova and Fomichev 2001; Birman and Vurdova 2002; Jin et al. 2002; Mattila et al. 2007; Savichev 2008; Ksenofontov 2010; Nefedyeva et al. 2017). To implement these purification methods, constructed wetlands with higher vegetation, substrates, and associated microbial communities are created. They are reliable and effective, do not require energy and chemicals, and do not have an additional negative impact on the environment. Such systems are widely used for post-treatment of sewage water from various pollutants, including mineral nitrogen compounds after primary purification of sewage by mechanical and physicochemical methods (Ran et al. 2004; Stewart et al. 2008; Miranda et al. 2014; Vymazal 2014; Zhang et al. 2014).

The experience of applying this method in Sweden, Finland, Norway, Canada, and Russia shows that constructed wetlands as post-treatment facilities are effective even at low temperatures (Jenssen et al. 1993; Maehlum et al. 1995; Nyquist and Greger 2009). However, the creation and operation of artificial phyto-cleaning systems and plant communities in the northern areas (short vegetation period, prolonged low temperatures, strong winds, and lack of soil resources) are sure to be difficult and requirean individual approach.

The aim of the given research is the development and optimization of biotechnology for post-treatment of quarry waters from nitrogen compounds using phytoremediation in the natural-climatic environment of the Murmansk region, Russia.

MATERIALS AND METHODS

The research was carried out at the settling pond of quarry for iron ore mining in the Murmansk region of Russia. The settling pond was an excavated pond, consisting of two sections, separated by a bulk dam of sandy-gravelly-rocky soil.

Ground and thawed waters, as well as precipitation enter the collection unit at the bottom of the pit. There, they are piped through the pipe system to the first section of the settling pond. Using sedimentation, the sewage is mechanically treated. Later, passing through the dam, the water is cleaned by filtration, adsorption, precipitation, and oxidation-reduction reactions carried out during the life of microorganisms in the filtering stratum. The latest stage for post-treatment of quarry waters from mineral compounds of nitrogen by phytoremediation takes place in the second section of the settling pond. Its depth is not greater than 2 m and is characterized by a frequently changing level of water. From it, the purified water enters a natural watercourse through the collector.

The growth of the coastal strip with local plant species around the pond is very slow; the vegetation occupies an extremely small part of the surface, and the forming groups of plants are thin. The cover is usually in the range from 1–2 to 0.5%. Often, only lone individuals are found.

In the settling pond, vegetation is mainly represented by the coastal-water communities of the helophytes with an insignificant development of the attached and free-floating mono-species of hygrophytic communities. The submerged-water macrophytes are absent.

The development of higher hygrophytic vegetation is impossible in the I-st settling

pond section because of rather muddy water conditions. The bottom cannot be seen from the depth of 0.5 m. Community formation occurs only due to coastal overgrowth by helophytes and temporarily flooded hydrophilic species. In the II-nd settling pond section, the water is less muddy, and the bottom is viewed from the depth of 1.0–1.2 m. However, the bottom of the reservoir is mostly large-stony and strongly cluttered with flooded wood. Aquatic vegetation is found only at the silted and flattened bottom of the coastal shallow. It is represented by mono-species horsetail communities and abundant sedge-cotton grass communities, passing into small coastal sedge marshes.

Due to the use of explosives during iron ore extraction, 5000–6000 kg of nitrates, 30–50 kg of nitrites, and 60–80 kg of ammonium nitrogen are supplied monthly with quarry water to the settling pond. At the beginning of the study, the average content of nitrogen mineral forms in water was: 134.24±10.10 mg/l of nitrates, 0.75±0.18 mg/l of nitrites, and 1.26±0.30 mg/l of ammonium ion. The content of chlorides, sulfates, and iron did not exceed the MPC (maximal permissible concentration). The water pH varied from 7.6 in the I-st section, to 6.8 in the II-nd section, and to 6.6 in the natural water flow.

The analytical work was carried out in the specialized accredited laboratories of INEP KSC RAS (Apatity) and the JSC "Olkon" (Olenegorsk). The water quality indicators were analyzed in accordance with the current standard technical documentation. The content of nitrates was determined by the ionometric method with electrochemical laboratory fluid analyzer "Multitest IPL-102" and measuring electrode Elite-021 (NO3-). The content of nitrites in water was determined by the photometric method with Griess reagent. Determination of ammonium ions was carried out by photometric method with Nessler's reagent.

RESULTS AND DISCUSSION

During the period of 2012 to 2017, we conducted laboratory and field pilot industrial experiments on the phytosystem to inspect wastewater post-treatment for mineral nitrogen compounds.The research was fulfilled in two stages.

The first stage. At this stage, a new patented method for post-treatment of waste quarry waters using the floating bioplate was developed and introduced (Evdokimova et al. 2015). It is represented by the floating clusters of connected frames with biological loading (Fig. 1). It was experimentally established that the bioplate area should be at least 40% of the total area of the treated reservoir for more rapid and effective treatment of the reservoir from nitrogen compounds (Evdokimova et al. 2016).

Fig. 1. Floating clusters of bioplate

As the result of using the floating bioplate with higher vegetation in the course of 3 years, its viability and possibility for absorbing nitrogen compounds, mostly ammonium and nitrite forms, and in a lesser degree nitrate forms, are shown (Table 1).

Table 1. The content of mineral nitrogen compounds in the settling pond water in 2013-2016, mg/l

Date	NH_4+		NO_3–		NO_2–	
	I section	Collector	I section	Collector	I section	Collector
27.06.2013	1.29±0.07	1.10±0.08	155.3±11.2	153.1±10.8	0.73±0.06	0.17±0.02
10.07.2013	0.26±0.02	0.07±0.01	133.0±9.5	137.2±9.6	1.06±0.07	0.55±0.05
09.10.2013	3.30±0.19	2.04±0.15	107.9±7.6	95.0±6.9	0.91±0.07	0.80±0.07
09.07.2014	1.51±0.09	0.38±0.08	138.5±9.8	127.3±9.2	0.63±0.05	0.57±0.04
16.09.2014	3.62±0.18	0.52±0.07	178.4±12.5	180.1±12.6	0.41±0.05	0.37±0.03
02.10.2014	1.50±0.08	0.35±0.05	128.6±9.1	109.7±7.9	0.36±0.04	0.14±0.01
01.07.2015	4.20±0.21	0.45±0.06	168.2±12.5	157.4±11.2	0.67±0.05	0.55±0.06
29.07.2015	1.47±0.11	0.42±0.08	157.8±11.4	150.5±10.5	0.58±0.06	0.41±0.02
09.10.2015	2.81±0.14	0.63±0.12	241.1±17.1	230.1±17.2	0.71±0.05	0.40±0.03
06.06.2016	3.30±0.15	0.46±0.05	131.4±9.2	150.5±9.7	0.68±0.05	0.35±0.03
26.07.2016	8.92±0.48	6.45±0.51	203.9±14.3	206.9±14.6	1.23±0.09	1.40±0.12
19.09.2016	9.30±0.67	6.90±0.45	214.6±12.6	165.4±11.7	1.00±0.08	1.10±0.11

**Note: "–" – was not defined*

Prior to starting research, ammonium ions decreased by 15% in the second section from the initial content in first section of settling pond. After the bioplate introduction, their content decreased by 53–90%. The nitrate nitrogen concentration in the water decreased by 15–20% after the bioplate construction.

Further observations revealed that the floating bioplate allowed the post-treatment to be carried out exclusively in the deep-water areas of the settling pond. In these circumstances, the coastal strip, dam, shoal, and backwaters were not involved into the process. The swamping of these areas would help to increase the pond cover area with plants significantly and accelerate the restoration succession at the site.

The second stage. The goal of this stage was to modify the floating bioplate into a more efficient phytoremediation ecosystem, allowing maximum coverage of the territory. The research was carried out in 2017. The basis of the development was the technology of creating phytomats, which allowed forming plant communities of different types.

A phytomate is a plastic mesh bag with the dimensions of 0.4 x 0.7 m. Of the mixture, 12.5 dm^3 consisted of sawdust and thermovermiculite. It was taken in the ratio of 4:1 (by volume), and 50 g of the grass mixture was placed into the bag. This technology allowed to form of phytomats up to 10 cm in height and an area of about 0.3 m^2 each. (Fig. 2). The composition of grass mixture included seeds of the grasses, which intensively grow in the Murmansk region, on sandy-stony soils: *Agropyron intermedium* (Host.) Beauv., *Elytrigia repens* (L.) Desv. ex Nevski, *Festuca rubra* L., *Phleum pratense*

L., *Leymus arenarius* (L) Hochst., *Polygonum weyrichii* Fr. Schmidt, and *Bistorta vivipara* (L.) Delarbre. The manufactured goods can be stored in a dry state for a long period of time and transported to any distance.

To create phytomats, two types of substrates were used. The first substrate is small-fractioned thermovermiculite from the Kovdor deposit obtained by the electric roasting method (Ivanova and Kotelnikov 2006; Ivanova 2010). The second substrate is sawdust. All the used substrates were not the source of secondary pollution that was established by the laboratory studies.

Thermovermiculite and sawdust are known to have high air, moisture capacity, and sorption. They provide optimal conditions (humidity, aeration, and temperature) for the assured, rapid, and harmonious germination of seeds included in phytomate composition. They also are conducive to intensive growth and development of plants in subsequent stages of ontogeny. They enhance the purifying capacity of the phytosystem not only due to sorption properties, but also as the result of consuming mineral nitrogen compounds by microorganisms, which transforms plant materials.

The main purpose of phytomates is creating high-quality artificial phytocenoses (plant blocks) of 3 types:

- *Plant blocks of type I* are for sodding sandy-gravel coastal strips, slopes of filtering dams, and other land areas lacking natural fertile soils. These blocks transform these territories into phyto-barriers (Fig. 3A). After the phytomates have been spread out, they are moistened (5 liters of water/1 phytomate) to start the process of seed germination. The initial germination of seeds in the phytomats occurs on the 5th–7th day, and the mass germination takes place on the 10th–13th day. Throughout the whole period of phytomate functioning, the organic-mineral-vegetable base continues to work as a filter and nutrient layer.

- *Plant blocks of type II* are for creating plant communities in the backwater or shallows. The nutrient organic-mineral substrate

Fig. 2. The plastic mesh bags consist of sawdust, thermovermiculite, and seeds mixture

becomes the basis for strengthening and growing plants at the bottom (Fig. 3b). The phytomats are spread out in groups and submerged partially into water. If the air temperature is favorable, the germination of seeds will be observed on the 7th day. At this point, different types of hygrophytes and hydrophytes in the form of prepared seedlings, cuttings, or adult plants can be introduced in to phytomates. In such conditions, plants take root within 3–5 days and quickly grow at the bottom of the pond.

- *Plant blocks of type III* are for originating plant communities in the deep-water sites of the ponds (more than 0.5 m). Phytomats are placed on the floating constructions, which ensures their retention and partial submerging into water (Fig. 3c). The floating bioplate, which was used in our earlier work, can serve as an example of such a construction.

The efficiency of quarry water treatment depends to a large extent on the adequate choice of the plant species. There were 24 types of plants used as the main plants of cenosis: *Typha latifolia L., Carex sp., Eryophorum angustifolium Honck* = E. *polystachion* L., *Eriophorum vaginatum* L., *Menyanthes trifoliate* L., *Comarum palustre* L., *Calla palustris* L., *Caltha palustris* L., *Equisetum fluviatile* L., *Equisetum palustre* L., *Salix phylicifolia* L., *Salix caprea* L., *Sphagnum sp., Lemna minor* L., *Hippuris sp., Ranunculus repens* L., *Agropyron intermedium* (Host.) Beauv., *Elytrigia repens* (L.) Desv. ex Nevski, *Festuca rubra* L., *Phleum pratense* L., *Leymus arenarius* (L) Hochst., *Polygonum weyrichii* Fr. Schmidt, *Tussilago farfara* L., and *Bistorta vivipara* (L.) Delarbre.

Efficiency assessment of the suggested technology. In the course of monitoring the content of mineral forms of nitrogen in the settling pond water after introducing the proposed technology, the following results were obtained (Table 2).

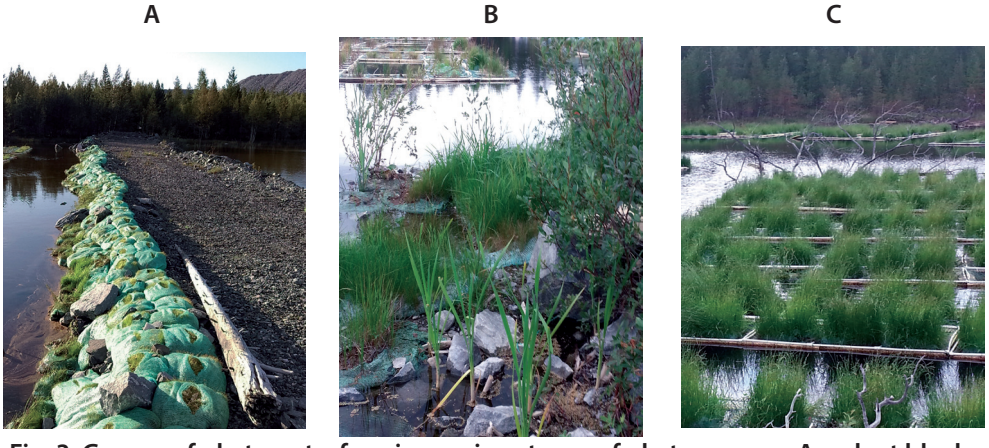

Fig. 3. Groups of phytomate, forming various types of phytocenoses: A – plant blocks of type I; B – plant blocks of type II; C – plant blocks of type III

Table 2. Nitrate content in waste water in 2017, mg/l

Place of sampling	01.06.	20.06.	06.07.	14.07.	04.08.	30.08.	26.09.
	NO^{3-}						
I section	90.5±9.4	112.5±11.9	100.3±12.0	100.7±11.3	124.1±9.1	112.1±9.8	125.5±12.3
II section	11.6±0.8	95.8±6.7	93.1±6.8	90.2±8.2	120.0±10.2	103.2±8.5	111.5±10.1
Collector	12.2±0.9	84.0±5.9	85.3±5.9	80.6±6.4	116.0±9.4	106.9±10.5	108.5±9.2
Natural stream	16.5±1.2	31.5±2.2	42.6±4.5	45.5±5.1	68.2±8.5	59.3±5.8	70.6±7.5

As the result of dilution during intensive snowmelt, research indicated the nitrate concentration decreased. Subsequently, the decreased concentration of nitrate ions was not significant and amounted to 10–25% of the initial level. In the natural watercourse, the nitrate concentration decreased to values not exceeding or equal to MPC (45 mg/l) in June–July; in August–September, it exceeded the MPC by 30–50%.
On average, during the observation period, the nitrate concentration in the II section water was 84.8±14.9 mg/l, which exceeded the established value of MPC by 2 times. The ammonium and nitrite ions concentrations in the II section water of the settling pond were below MPC values.

In the course of the work, we noted that the increase of the delay of water in the settling tank increased, so the duration of contact with water and coastal vegetation resulted in a marked decrease in the concentration of nitrate ions.

The study of the nitrate ions content in plants revealed their predominant accumulation in the roots of plants growing on the bioplato, compared with the green biomass (Table 3).

Generally, throughout the study period, the efficiency of clearing quarry waters increased by 22% (Table 4).

CONCLUSIONS

This multi-year research-based, low-cost technology has been developed for the transformation of man-caused water bodies into a nature-like wetland ecosystem for the after-treatment of waste quarry waters from mineral nitrogen compounds. The technology is based on the use of phytomats, allowing an accelerated creation of different plant block combinations for landscapes with different moisturizing (coastal areas, backwater or shallows).

The proposed purification system is based on natural mechanisms using aborigine species of higher plants and substrates-soil substitutes (thermovermiculite and wood sawdust); it does not require the use of the

Table 3. Nitrate content in plant roots, mg/kg

Plant species	Nitrate content in plant roots	
	Plants from natural wetlands	Plants from constructed wetlands
Cómarum palústre L.	67.05	195.52
Eryophorum angustifolium Honck	79.78	154.12
Salix phylicifolia L.	77.96	95.25

Table 4. Efficiency of waste water treatment in the settling pond

	2013	2014	2015	2016	2017
Constructed wetlands area, m^2 (%)	360 (7.5)	660 (13.75)	960 (20)	1260 (26.25)	1560 (32.5)
Concentration of nitrates*, mg/l	135.12±10.78	169.74±34.16	175.82±14.14	171.00±12.37	84.8±14.9
Efficiency of wastewater treatment, %	0	3.4	5.3	8.6	22.5

*Note: * - the average value for the investigated vegetation period in the collector of the settling pond*

energy, chemicals, and scarce soil components in the region. Predominance of natural ecosystem processes in the formed phytocenoses allows for maximum efficiency, and the use of cheap materials allows for the minimization of costs for creation and maintenance. Over the entire period of research, the efficiency of quarry waters treatment averaged 22% with a 30% coverage of the man-caused reservoir with phytomats.

This research is significant because it proposes an integrated approach to forming nature-like wetland ecosystems for wastewater treatment. This has been the first time it was implemented in the practice of existing mining enterprises in the extreme conditions of the subarctic region.

ACKNOWLEDGEMENTS

This work was carried out with the financial and technical support of the JSC "Olkon" (the Olenegorsk Mining and Processing Plant).

REFERENCES

Birman Yu., Vurdova N. (2002). Engineering protection of the environment. Purification of waters. Recycling. Moscow: ASV (in Russian).

Evdokimova G.A., Ivanova, L. A., Myazin, V. A. (2015). Device for biological treatment of waste water. Patent RU 2560631 C1. Date of publication: 20.08.2015. Bull. 23 (in Russian).

Evdokimova G.A., Ivanova L.A., Mozgova N.P., Myazin V.A., Fokina N.V. (2016). Floating bioplato for purification of waste quarry waters from mineral nitrogen compounds in the Arctic. Journal of Environmental Science and Health, Part A, 51(10), pp. 833-838.

Ivanova L.A., Kotelnikov V.A. (2006). Perspectives of hydroponic plant growing in the Murmansk region. Apatity: KSC RAS (in Russian).

Ivanova L.A. (2010). The method of creating an environmentally cleaner coating and a nutrient medium for its cultivation. Patent RU 2393665 C1. Date of publication: 10.07.2010. Bull. 2 (in Russian).

Jenssen P., Maehlum T., Krogstad T. (1993). Potential use of Constructed Wetlands for Wastewater Treatment in Northern Environments. Water Science Techniques, 28(10), pp. 149-157.

Jin G., Kelley T., Freeman M., Callahan M. (2002). Removal of N, P, BOD5 and Coliform in Pilot-Scale Constructed Wetland Systems. International Journal of Phytoremediation, 4(2), pp. 127-141. DOI: 10.1080/15226510208500078.

Ksenofontov B.S. (2010). Flotation treatment of water, waste and soil. Moscow: New Technologies (in Russian).

Maehlum T., Jenssen P., Warner, W.S. (1995). Cold-climate constructed wetlands. Water Science and Technology, 32(3), pp. 95-101. DOI: 10.2166/wst.1995.0130.

Mattila K., Zaitsev G. Langwaldt J. (2007). Biological removal of nutrients from mine waters. Final report. Rovaniemi: Finnish Forest Research Institute.

Miranda M.G., Galvan A., Romero L. (2014). Nitrate Removal Efficiency with Hydrophytes of Los Reyes Aztecas Lake Water, Mexico. Journal of Water Resource and Protection, 6, pp. 945-950. DOI: 10.4236/jwarp.2014.611089.

Nefedyeva E.E., Sivolobova N.O., Kravtsov M.V., Shaykhiyev I.G. (2017). The post-treatment of wastewater using phytoremediation. Bulletin of the technological university, 20(10), pp. 145-148 (in Russian).

Nyquist J., Greger M. (2009). A field study of constructed wetlands for preventing and treating acid mine drainage. Ecological engineering, 35, pp. 630-642. DOI: 10.1016/j.ecoleng.2008.10.018.

Ran N., Agami M., Oron G. (2004). A pilot study of constructed wetlands using duckweed (Lemna gibba L.) for treatment of domestic primary effluent in Israel. Water Research, 38(9), pp. 2241-2248. DOI: 10.1016/j.watres.2004.01.043.

Savichev O.G. (2008). Biological treatment of wastewater using wading biogeocoenoses. Bulletin of Tomsk Polytechnic University, 312(1), pp. 69-74 (in Russian).

Stewart F.M., Mulholland T., Cunningham A.B., Kania B.G., Osterlund M.T. (2008). Floating islands as an alternative to constructed wetlands for treatment of excess nutrients from agricultural and municipal wastes – results of laboratory-scale tests. Land Contamination and Reclamation, 16(1), pp. 25-33. DOI 10.2462/09670513.874.

Yakovlev S.V., Karelin Ya.A., Laskov Yu.M., Voronov Yu.V. (1985). Industrial wastewater treatment. Moscow: Stroyizdat (in Russian).

Vurdova N.G., Fomichev V.T. (2001). Electro dialysis of natural and waste water. Moscow: ASV (in Russian).

Vymazal J. (2014). Constructed wetlands for treatment of industrial wastewaters: A review. Ecological Engineering, 73, pp. 724-751. DOI: 10.1016/j.ecoleng.2014.09.034.

Zhang D.Q., Jinadasa K.B.S.N., Gersberg R.M., Liu Y., Ng W.J., Tan S.K. (2014). Application of constructed wetlands for wastewater treatment in developing countries. A review of recent developments (2000–2013). Journal of Environmental Management, 141, pp. 116-131. DOI: 10.1016/j.jenvman.2014.03.015.

Received on January 15th, 2019 Accepted on May 17th, 2019

Amir Mor-Mussery[1*], Shimshon Shuker[2] and Eli Zaady[2]
[1] Department of Soil and Water Sciences, Faculty of Agriculture, Hebrew University, Jerusalem, Israel
[2] Volcani Agriculture Research Centre (ARO), Rishon LeTsiyon, Israel
*** Corresponding author:** amir.mussery@gmail.com

NEW APPROACH FOR SUSTAINABLE AND PROFITABLE GRAZING SYSTEMS IN ARID OPEN LANDS OF THE NORTHERN NEGEV DESERT (ISRAEL)

ABSTRACT. In the past, most of the open lands of arid areas were used as rangelands because of the pivotal role of grazing in the life of the indigenous populace. Currently, because of the competition between grazing and other types of land management (crops' breeding, urbanisation, etc.) and the seemingly destructive effect of the grazing on the ecosystem, only a reduced part of the open lands is used for grazing. Even in the lands that are allocated to pasture, many restricting' legislations have been enforced by the authorities. Consequently, these policies have resulted in the dramatic reduction in the profits of the herd owners and a drastic decrease in the rate of grazing, which resulted by ecological catastrophes such as wide spread of fires and invasion of exotic species. In order to achieve a sustainable and profitable utilization of these open lands, we used an alternative approach, which based on the physical interactions of the animals with the ecosystem. This scheme takes into consideration the physical interactions of the bred animals with the ecosystem there, the statutory state of the lands, and the social patterns of the indigenous farmers, as parameters for a holistic solution for arid lands.

KEY WORDS: animals' physical interaction model, open lands, sustainable and profitable grazing system

CITATION: Amir Mor-Mussery, Shimshon Shuker and Eli Zaady (2019) New approach for sustainable and profitable grazing systems in arid open lands of the northern Negev desert (Israel). Geography, Environment, Sustainability,
Vol.12, No 2, p. 106-127
DOI-10.24057/2071-9388-2019-15

INTRODUCTION

Since ancient times, grazing play a very important function for the local population of the northern Negev. Grazing was their major source of employment and income. Scenes from the shepherds' lives are mentioned all over the holy scriptures of the main monotheistic religions (the Bible, New Testament, and the Quran) (Bodenheimer 1960; Stewart 1979). In these scriptures, the grazing and the animals serve, not only, as a food resource for the shepherds' families but also as an indicator of the shepherds' wealth, symbols of peace making, and treaties among people. In addition, herd management considered an educational tool for acquiring good manners. Never-

theless, the grazing areas were mostly frontier lands far from human settlements ('for every shepherd is an abomination unto the Egyptians') (Genesis chapter 46, line 34). Grazing restrictions were also legislated: 'It was prohibited to grow ruminants in the holy land' (Babylon Talmud, Baba Qama, chapter 70, page 2). In fact, the first murder mentioned in the Bible was due to the dispute between a crop breeder and a shepherd (Genesis, chapter 4). Such an attitude led to the destruction of ecosystems and an increase in the social alienation of the shepherds, particularly those whose major source of income was grazing. This attitude, which correlates grazing to ecosystem degradation, is still widely spread in the minds of politicians, land managers, researchers and the public, translated by the municipalities into over-regulation and restrictions on the herd owners, which causes a drastic decrease in their profits and a lack of wiliness by them to breed animals on pasture (Winter 2000). The reduced grazer density in the open lands has led to ecological catastrophes such as fires (Archibald et al. 2005).

Lately, several studies have demonstrated the positive impact of controlled grazing on the sustainable management of open areas, and even their rehabilitation efficiency in cases of degraded areas caused by inadequate agriculture practices such as intense tillage (Papanastasis 2009; Yurista 2012). Nevertheless, these data are partial, unorganised, and based mainly on theories. In order to suggest a substitutable grazing system, the existing grazing patterns of the northern Negev will be reviewed together with novel findings regarding the animal–ecosystem interrelations.

THE NORTHERN NEGEV AND ITS' CURRENT GRAZING SYSTEM

The basic terms that model any grazing system are the land statutory state, the bred animals on pasture, and the herd owners' social patterns.

The statutory state of the northern Negev open lands

Since the foundation of the state of Israel until 1978, the rangelands in the northern Negev were statutory defined as 'public' or 'private-undefined property', which allowed each herd owner to enter and use the land without limitations. This led to many disagreements on the use of these lands between the herd owners themselves and the municipalities. Ecologically it raised the overgrazing phenomena in a large part of the rangelands (Zeligman et al. 2016). Only after long legislation processes, parts of the lands were allocated to urbanisation, while the remaining were nationalised. Some of the open lands were leased to Kibbutzim (cooperative settlements), and others were given to KKL (Keren Kayemet L'Israel) for afforestation (from 1978, KKL leased a part of her areas for seasonal grazing). The remaining areas were defined as open lands, which were allocated to the Bedouin farmers, the local people of these areas) for yearly use. Parts of the allocated lands are used for rangelands, while others are used for rotational rain-fed cereals, breeding, and grazing, Fig.1. After the cereal seeds' collection season (defined from the end of summer until autumn, i.e. July–October), the straws are collected into buckets for sell or used for fallow grazing (Le Hougrou 2009; Ingram and Hunt 2015). In some cases, when the rainfall is not homogenous and inter-sessional forecasts claim that drought is predicted, the Bedouin farmers prefer to transport the herds to the fields even before the fallow season, a practice which was observed, as an example, in the summer of 2017. Altogether, the open lands are intensively cultivated for rain-fed cereals and used for grazing on a yearly basis, without a multi-year plan (Alassaf et al. 2012; Roncoli et al. 2012; Abdulrashid 2013).

Animals bred on pasture supply in the northern Negev

Historically, four animal species have been bred in the northern Negev, including the bulls, ruminants (cattle, goats, and sheep), and camels. The bulls mainly belong to the

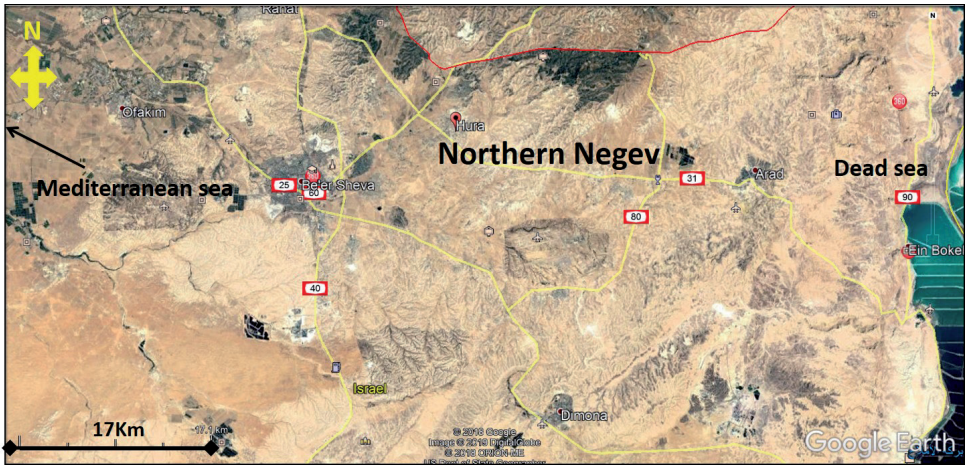

Fig. 1. The northern Negev open lands. A hilly and highly incised area due to long term and intensive agriculture utilization

species Bos Taurus with an estimated number of several thousand animals. A cattle herd contains 10–20 animals bred mainly for meat (data from Israel Grazing Authority, IGA). The ruminants are mostly goats (Capra hirctus mambrica) and sheep (Ovis aries musimon) that are mostly grazed together. Several herd owners have noted that their goats' role in the herd is to lead the sheep to the rangeland and back to their enclosure. The total number of ruminants in the northern Negev is estimated to be 250 000–300 000. The goats' ratio from the total grazed ruminants is 4% (Olsvig-Whittaker et al. 2006). The goats bred in Israel belong to the Negev-Baladi and Shami species' types and are bred mainly for the dairy industry. The sheep belong mostly to the Awasi species' type, and they are bred mainly for meat. The average ruminant herd contains 100–150 animals (Zeligman et al. 2016). The ruminant herds and the cattle are generally brought to the rangeland twice a day (early in morning: 06:00–10:00), and in the evening (16:00–19:00), mainly in the late spring and at the end of summer, i.e. April–September (personal data from local breeders). The fourth group of grazers are the camels, mostly belonging to Camelus dromedaries. As opposed to the other grazers, the camels are brought to the rangeland for several days or weeks before getting back to the enclosure. Their total number in the Negev is 3000 to 5000 herds; their herds are small, less than 10 in number, and they are bred for their milk and meat (Engelhardt et al. 1989).

The social patterns of the sepherds

In the past, most of the Bedouin families in the Negev relied on grazing as their main source of income. The adults were the herd managers, the women dealt with the milking and cheese making, while the young helped with the grazing and gained experience in herd management. Today, most of the herd owners are older than 50 years of age, while the women and young prefer more profitable occupations. Some herd owners rent illegal and inexperienced shepherds, which leads to additive ecological damage to the rangelands by improper practices. Others prefer to breed their herds in an enclosure or to limit open grazing only to the spring season only for the sake of convenience.

THE INTERACTIONS OF ANIMALS WITH THE ECOSYSTEM

The main models that are correlating the grazing intensity and the ecosystem are the compensatory, over grazing and the 'Intermediate Grazing Optimisation-IGO (Oba et al. 2001). The Compensatory model describes mostly ecosystem resist to grazing as ones settled with invaded species (Parker et al. 2006) (Fig.2). The steep decrease of the overgrazing model reflects species, which are highly sensitive to overgrazing (Villarreal-Barajas and Martorell, 2009). Nevertheless, the IGO model is been considered as the most

Fig. 2. The grazing animals in the northern Negev. A. Camels herd, Wadi Atir farm (31°16'16.64"N, 56°34'11.80"E), northern Negev, February 2011; B. Cattle herd, Ramot Menashe, March 2015. C. Ruminant herd (composed of goats and sheep), Eshtamoa Basin, February 2014. D. Ruminant herd dispatch linearly along the rangeland to reduce damage to the ecosystem, Eshtamoa Basin, northern Negev, February 2014, Photos: Amir Mor-Mussery

comprehensive one and includes both of them in its' different phases (Oba et al. 2001). Additional model is based on the physical effects of the animal on the ecosystem.

The IGO model

The correlation between the grazing intensity and the ecosystem's vegetation is been commonly described as a parabola. This scheme defines 'Intermediate Grazing Optimisation', which is composed of several phases (Oba et al. 2001; Doole and Romera 2013). Until the first turnover value, the grazing intensity does not affect the pasture edibility, which implies less edible species and reduced amounts. From the second turnover value, the increased grazing intensity causes an enhancement of pasture edibility. From the third turnover value, a negative effects are exists between the grazing intensity and the pasture edibility, as shown in Fig. 3.

The IGO model suffers from the following drawbacks, when applied to the study of the ecosystem states in the arid areas:

a. The meadows-oriented model is based on the studies of meadows with a mostly homogenous vegetal cover, while arid areas are characterised by patchy forms (shrubs or other ecosystem engineers that create small soil patches with low vegetal cover) (Mor-Mussery et al. 2015). Therefore, any scheme correlating the grazing and the vegetation in the arid areas must treat the patches and the matrices separately.

b. Wide parts of the open lands in arid regions have been defined as fragmented landforms because of the intensive erosion processes (Shi and Shao 2000). Thus, some of these landforms are more or less accessible to the animals, resulting in varying vegetation characteristics (Shi and Shao 2000).

c. Even under a given grazing intensity regime, the effects on the vegetation (and the whole ecosystem) may vary (for example, shrubs' browsing may accelerate the growth of fresh canopy parts, and the trampling may damage the patches' productivity; Schleuning et al. 2015).

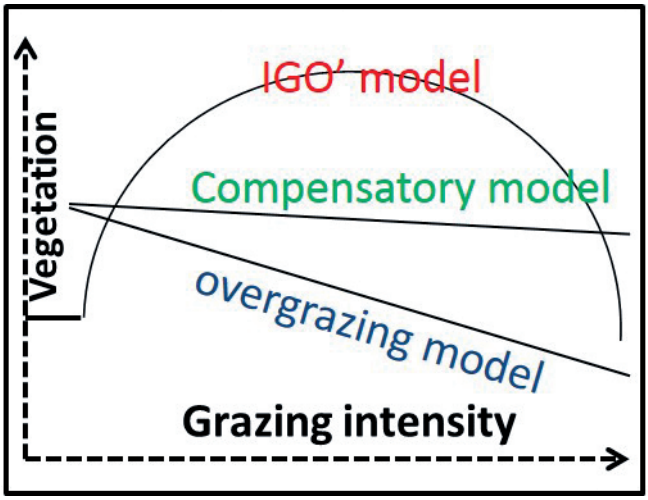

Fig. 3. Correlation between grazing intensity and vegetation patterns. The «Compensatory», «Overgrazing» and 'Intermediate Grazing Optimisation' models (Oba et al. 2001). 'Grazing intensity' denotes the number of the animals per plot, number of grazing sets in a year, etc.; 'Vegetation' defines the vegetation richness as amount, species biodiversity, etc

The animals' physical interactions model

Due to abovementioned drawbacks of the common scheme, in this study, we used an alternative scheme, which is based on the physical interaction modes of the animals and the ecosystem and analysed the factors that influence these physical interactions.

The main effects of the animals on the ecosystem are the trampling, vegetation harvesting, and excrement outlaying (Greenwood and McKenzie, 2001), as shown in Fig. 4.

These interactions influence the physical, chemical, and microbial characteristics of the soil in the rangelands (McNaughton et al. 1998; Sankaran and Augustine 2004; Savadogo et al. 2007). In turn, via feedback loops, these characteristics influence the productivity of the rangeland and its suitability for continuous use in cultivation. The factors that influence the intensity of these interactions can be grouped into animal, herd size, grazing timing and period, rangeland abiotic and vegetation state, and the herd owner's operations.

Animal: This group of parameters includes the species (Gamfeldt et al. 2008; Baker

Fig. 4. The physical effects of the animal on the ecosystem. A. Effect of flora harvesting on A. victoriae canopy, Chiran area, northern Negev, March 2015. B. Flora patches cut off due to ruminant trampling (B) as compared to the conserved area near the Chiran area (B*), northern Negev, March 2015. C. Reduced vegetation coverage due to concentrated ruminants' manure, Wadi Attir (31°16'16.64"N, 56°34'11.80"E), northern Negev, January 2017. Photos: Amir Mor-Mussery

et al. 2006(, type (Gamfeldt et al. 2008(, gender (Verdú et al. 2004), physiological state (Parsons et al. 1994), and travelling patterns (Duffy et al. 2003).

Herd: This group includes three parameters: herd size (Parsons et al. 1994), composition (Parsons et al. 1994), and travelling and distribution patterns (Duffy et al. 2003).

Grazing timing: This group includes three parameters: period (Fleischner 1994), duration, and intensity (number of grazing sets per unit time; Taylor et al. 1993).

Rangeland vegetation: This group includes three comprehensive parameters: vegetation composition (shrubs, perennials, cereals, broad leaves, etc.), physiological parameters (plant growth rate, blooming, drying out, etc.) (Tueller 2012), and the 'vegetation stability' — a parameter which defines the ability of the natural species to resist the invasion of exotic species (Clarke et al. 2005; Miki and Kondoh 2002).

Rangeland abiotic patterns: This group of parameters includes the climate characteristics (mainly the rainfall patterns; Kincaid and Williams 1966), landscape' patterns (Wondzell and Ludwig 1995), and soil properties (Wondzell and Ludwig 1995).

Herd owner's operations. The most important parameter of this group is the herd owner's personality; nevertheless, different social patterns such as origin, gender, and age may influence the operational grazing (preference of grazing vs. breeding in enclosure, grouped vs. spread, etc.) and consequently, the interactions with the ecosystem (Corner 1991; Fernandez-Gimenez, 1999).

The animals' physical interactions with the ecosystem in the northern Negev

In order to determine in the northern Negev open lands, the effects of the different grazing factors on the intensity of the animal' effects we interviewed 10 local Bedouin sheperds on the factors presented in Section Using Toma et al. (2016) methodology, per each factor the data from the herd owner translated into four conceptual intensity levels:

'H' (High effect): State which describes productivity change two folds higher (or lower) than the state in the previous year.

'M' (Moderate effect): State correlated to a productivity change of 50%–200% as compared to the previous year.

'L' (Low effect): State of productivity change of 25%–50% as compared to the previous year.

'Min' (Minor impact): State of productivity change of less than 25% as compared to the previous year.

One has to take into consideration that a factor's influence based on the existing state of the land in the northern Negev (climate, grazer species, etc.), therefore, elsewhere, the influence may be different. The findings are presented in the conceptual equation Eq. 1.

$$Trampling = Animal^{M-L} * Herd^{M-L} * Timing^{M} * *Vegetation^{L-H} * Abiotic^{Min} * Social^{H}$$

$$V.harvesting = Animal^{L-H} * Herd^{L-H} * Timing^{M} * *Vegetation^{L-H} * Abiotic^{Min} * Social^{M}$$

$$E.spreading = Animal^{L-M} * Herd^{L-H} * Timing^{M} * *Vegetation^{L-H} * Abiotic^{Min} * Social^{L}$$

where X^{H} - high, X^{M} - moderate, X^{L} - low, X^{Min} - minor effect grades; V. harvesting - vegetation harvesting; E. spreading - excrement spreading.

SUSTAINABLE GRAZING SYSTEM OF THE NORTHERN NEGEV OPEN LANDS

In order to establish a sustainable grazing scheme in the northern Negev, we will refer to the land state and cultivation management, in-field management practices, and pasture enhancement practices. The data are based on recent publications and the unpublished data collected by the authors.

Land state and cultivation management
Rangeland privatisation

As stressed previously, wide parts of the northern Negev open lands are 'public'. Nevertheless, in these lands, several privatisation schemes have been carried out along the years. In the 80's of the previous century, 59 areas in the Negev were allocated to private farmers for sustainable management as rangelands. The limitations of the privatisation terms, un-regularised state of the farms, and lack of supervision from the authorities led the farmers to rely on grazing as a secondary source of income, if at all (the main uses of the farmlands were tourism and medicinal plant cultivation). This state damaged in many cases the ecosystem productivity. An example is presented in Fig. 5.

Additional privatisation trials are conducted on seasonally or yearly rangelands' allocation to herd owners. Nevertheless, because of insufficient enforcement and lack of supervision on the existing state of the rangelands, wide parts of these privatised areas are continuously degraded (Olsvig-Whittaker et al. 2006; Hahazni-Cohen 2011).

Cultivation rotation

One of the most documented practices for long-term sustainable management of open lands in the northern Negev is the fallow period, years in which the land is not processed, neither grazed nor tilled. In the past, the recommended ratio between the grazing years and the fallow ones was 6:1, defined also by Shmita (Antal et al. 2016). However, currently, because of the global climate changes and the use of intensive cultivation, additional fallow years needed for a sustainable multi-year grazing set (Abubakar 1996). An example for the influence of conservation (prevention of grazing) on loess area in Project wadi Attir (PWA) presented in Fig. 6.

Recent studies that took place at the Wadi Atir farm in the northern Negev showed that four years of continuous fallow management caused an exponential growth of herbaceous biomass of up to two-fold as compared to the grazed area (Mor-Mussery et al. 2017). At the Oren-Aren family farm, after 20 years of partial conservation (1.1 ha per ruminant, preventing grazing at vegetation germination, etc.), the herbaceous biomass weight was nine-fold higher than that of the adjacent unsupervised area (0.09 vs. 0.01 Kg m^{-2}, Leu et al. 2014) (see Fig. 7).

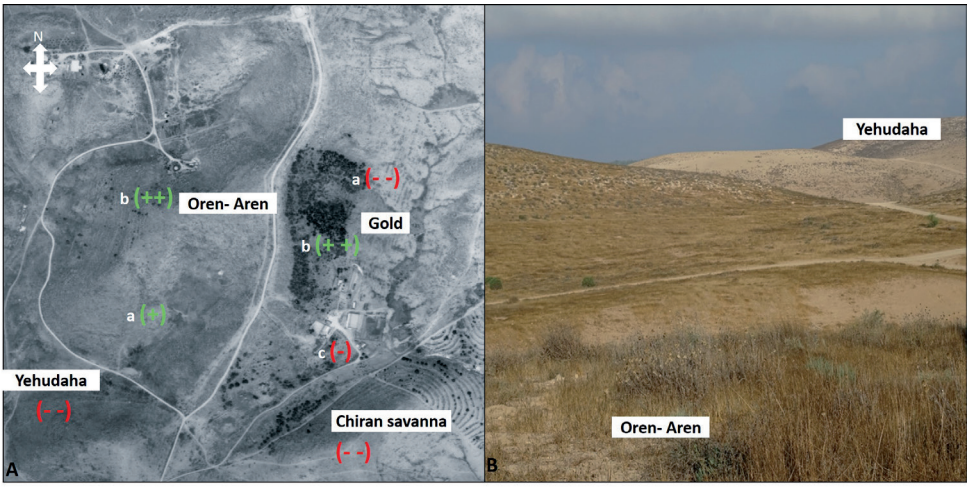

Fig. 5. Influences of privatisation on biomass in Chiran farms (31°19'17.46"N, 57°34'22.19"), northern Negev. A. Effects of land management on biomass production on Chiran farms, northern Negev: 'influence' levels: destructive (leads to degradation) '-', highly destructive '- -', and rehabilitative '++'. B. Differences in biomass cover between Oren-Aren and Yehudah farms, May 2016

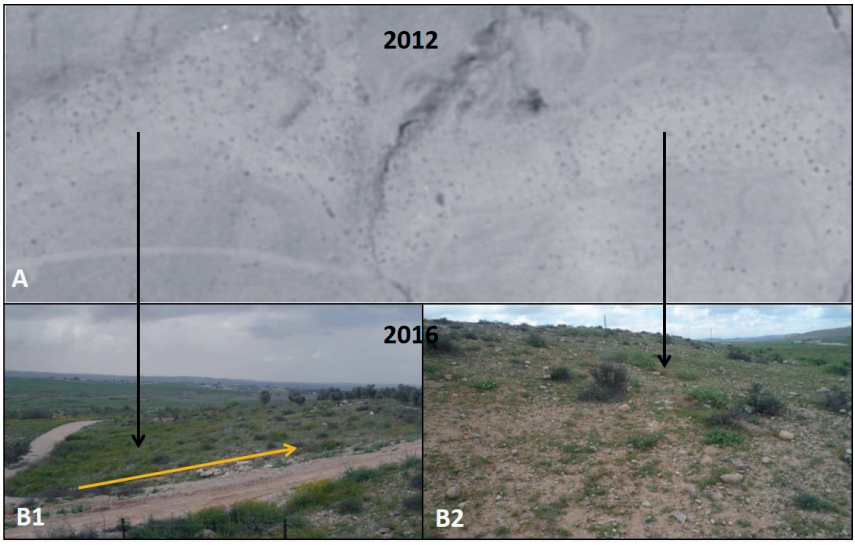

Fig. 6. Influence of continuous prevention of grazing on the vegetation state in the Wadi Atir area between 2012 and 2016 (31°16'16.64"N, 56°34'11.80"E). A. Air photograph from 2012, describing the degraded state of the rocky ground before conservation. B(1). A rehabilitation processes of the conserved rocky ground, expressed by a gradual increase in the vegetative cover downhill. B(2) Homogenous and low vegetation cover in the overgrazed rocky ground. Photo Amir Mor-Mussery

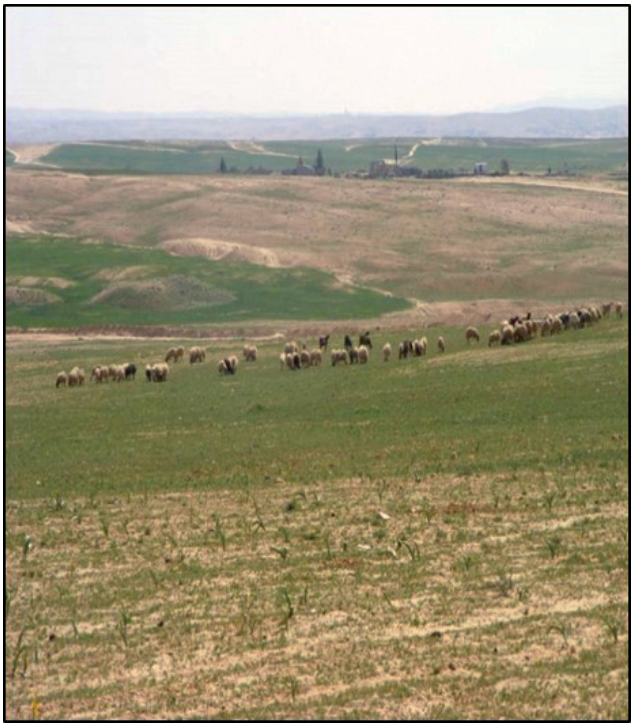

Fig. 7. Combined crop–livestock regime in the northern Negev (2016, Chiran area). The improper ruminant herding of crop fields (combination of multi-year monoculture wheat cultivation; ruminant herding during crop germination and after tillage) leads to drastic soil erosion and incision. Photo Stefan Leu

Most of the open lands in the northern areas are cultivated according to the combined stock-rain-fed cereals scheme (Perevolotsky and Seligman 1998) as follows: soil tilling in September–October and sowing in October–November. In case of the hay use as a feed it is produced from green wheat normally in April after the end of rainy season. In case when the grain is used it is harvested between May and June. During the fallow season, the animal herds are brought to the field for grazing. In drought years such as 2017, grazing starts as early as February–March without grain harvesting (Abdulrashid 2013; Ingram and Hunt 2015). The final decision on cultivation is based on the observed rainfall patterns or short-term meteorological forecasts and not on multiyear plans (Alassaf et al. 2012; Roncoli et al. 2012). The PWA (Project Wadi Attir) area is continuously cultivated with rain-fed wheat, except during the droughts. This cultivation scheme, which is repeated yearly, enhances degradation processes expressed by soil fertility, productivity decrease, and landform erosion (Sainju et al. 2011). The separation of the grazing sets from the crop cultivation reduces tillage and can thus enhance sustainability. For example, Thornton and Herrero (2001) described a decrease of 40% in the external nitrogen required for fertilisation once the combined scheme is applied. Descheemaeker et al. (2010) described a decrease of 25% in the need for additive irrigation (due to better infiltration of the rainfall, higher microbial activity, better CO2 fixation, and reduction in soil erosion). Nevertheless, comprehensive studies that will take into account the animals, soil, and climate need to be carried out in the Negev for increased pasture amounts (Herrero et al. 2010).

Possible sustainable practices

Based on the previously published data and our observations, the recommended guidelines for grazing in the Negev open lands are as follows:

a. Preventing or reducing the grazing intensities in the rangeland, when wide apart from the vegetation in the germination stage (Oesterheld and Sala 1990).

b. Spreading the animals in the rangeland or moving them rotationally between the pasture plots for preventing continuant grazing in the same locations, mainly during the vegetation growth period (Williams and Hall 1994; Encinias and Smallidge 2010).

c. Adjusting the animal to the pasture species' composition, for example, in the case of massive amounts of cereals, cattle may be preferred (Vesk and Westoby 2001).

d. Adjusting the grazing to the vegetation patterns. The main types of vegetation cover are grasslands and shrublands. In a shrubland, the shrubs establish soil patches with dense **biomass coverage**. These patches are the key factors for the vegetation growth in the whole area; therefore, any grazing scheme has to prevent severe damage to the patches (Butt 2010; Jakoby et al. 2010), while in the grasslands, this problem does not exist.

Pasture enhancement practices

Conservation

The state of almost all the open lands in the northern Negev is defined as 'degraded' because of continuous mismanagement by repeated tilling and grazing without fertilizer input, fertility, or grazing management (Helman et al. 2014; Weissmann and Shnerb 2014). The common way to increase the pasture amounts is based on conservation and leaving the land to restore its' vegetation coverage, processes that last 5–10 years (Leu et al. 2014). Nevertheless, the main drawbacks of this practice is its' long-term continuation and the reduced profits for the farmer in these years (Perrings et al. 2014). The Bedouins in Israel have a relatively low income as compared to the other populations; therefore, relying on conservation practices alone may not be practical for them.

Manure spreading

One of the common methods to increase rangeland productivity in the northern

Negev rangelands is the spreading of animal manure, obtained mostly from enclosures. The manure is dissimilated by microorganisms into soluble nutrients that are absorbed by the vegetation and enhance its growth and development (Ayan et al. 2010). Nevertheless, improper spreading can lead to the percolation of nutrients to the underground water (Madison et al. 2016), enhanced soil salinisation (Hao and Chang 2003), accelerated changes in the composition of the natural species such as enhanced propagation and growth of exotic species (Lu et al. 2010), and even accelerated soil erosion (Gilley and Risse 2000). The following parameters must been taken into account with respect to manure spreading (Williams 1999).

a. Manure source: The excrements of different animals and the enclosure beds have a considerable effect on the chemical composition of the manure and its assimilation rate (Kuepper 2000; Khan et al. 2008).

b. Timing: The most crucial factor for manure assimilation is the wetting. In rangelands, wetting is achieved artificially by irrigation, but in the northern Negev, it is mostly achieved by the rain water, which is highly heterogeneous. On the one hand, the long duration of unwetted manure may decelerate the vegetation development (Dewes 1996); on the other hand, massive amounts of manure, usually in the middle of winter, may lead to ground water contamination (Kuepper 2000). In general, the best timing for manure spreading is autumn or the beginning of the winter as during these periods, a low and prolonged assimilation of the manure into the soil takes place (Madison et al. 2016).

c. Soil thickness and landform patterns: In thick soils exposed to soil erosion and inclination higher than 12%, one has to use a thin manure layer to prevent its being swept away (MPCA 2012; Madison et al. 2016).

The effects of different manure spreading schemes presented in Fig. 8

Fig. 8(A) shows the differences between two rain-fed wheat fields. One of them was shallow tilled with a homogenous spread of cattle manure in autumn, while the other was cultivated without manure spreading. Fig. 8(B) shows improper manure spreading, which manifests in the lack of a vegetation cover due to the thin manure layer, which can lead to the leakage of nutrients into the low soil layers.

In the past, the herd owners in the Negev used to wander with their herds along the Negev rangelands and at night to establish temporary enclosures in the field. Based on the principles of these observations, several studies suggested the spatial location of these temporary enclosures in order to use them to fertilise the whole area (Verdoodt et al. 2010; Kigomo and Muturi

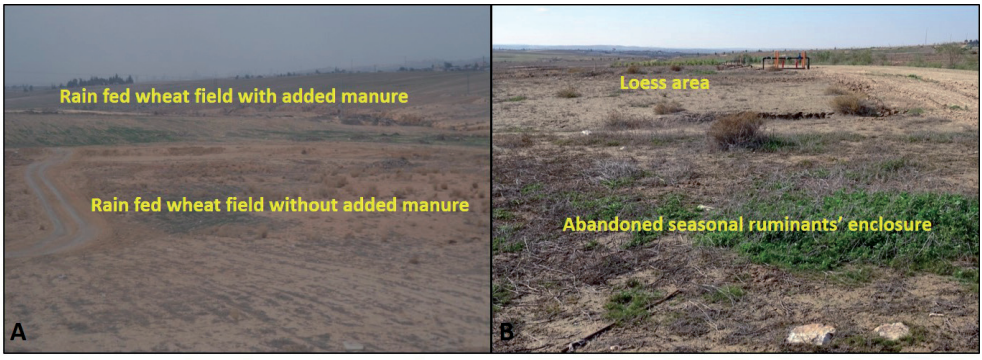

Fig. 8. Effect of manure spreading and abandoned seasonal enclosure on soil productivity. A. The impact of homogenous manure spreading on rainfed cultured cereals field, vs. un-spread one. Attir heals area (31o16'16.64" N, 56034'11.79"E), January 2017; B. The impact of abandoned seasonal enclosure on herbaceous cover vs. adjacent open area, Project Wadi Attir, February 2015. Photos Amir Mor-Mussery

2013). Nowadays, the reduced size of the rangelands, their fragmentation for other land uses, and grazing restrictions enforce the herd owners to take their herds from the permanent enclosure to the rangeland and return them at night. This makes the fertilisation based on the spatial location of the seasonal enclosures less practical.

Rangeland reseeding

An additional tool for enhanced herbaceous biomass is reseeding the rangeland with natural species of grazing importance (high edibility, rapid growth, etc.). The enriched seedbank creates a dense cover of the selected species (Grantz et al. 1997) in addition to enhancing pasture utilisation. For example, a herd owner from the Arzog Bedouin village claimed that a mix of *Triticum aestivum* and natural species in each reseeding set enhanced the ruminants' health, which resulted in increased profits for him. Examples for rangelands reseedings presented in Fig. 9.

This reseeding practice may also stabilise the landform by reducing the negative influences of monoculture cereal breeding (Vasta et al. 2008). Nevertheless, the selection of the seeds must be done with caution in order to prevent the spreading of exotic species (Rejmánek and Richardson 1996). In the northern Negev, several species have become invasive because of improper reseeding such as *Atriplex holocarpa F. Muell* (Dufour-Dror 2012) and Chloris gavana (Ng'weno et al. 2010; Dufour-Dror 2012).

Savanisation

Savanisation for enhanced pasture, defined additionally as 'silvi-pasture', has been documented in the northern Negev and other arid areas (Rai et al. 1999; Clason 1995). Several factors may influence the pasture amounts and properties, including the soil, landform, the animals, and the climate. The savanna trees affect the pasture in two ways: the canopy as the food source and the formation of understory vegetal patterns (mostly linked to the 'tree–grass' correlations; Dohn et al. 2013).

a. Tree canopy as pasture resource

The physiological state of the animals is also important; for example, milking animals prefer to consume vegetal parts enriched with nitrogen (Cabiddu et al. 1999). The accessibility of the canopy to the animal is determined by the tree and animal parameters, as shown in Fig. 10.

b. Trees' understory vegetation as pasture resource

Many parameters determine the effect of the tree on its understory vegetation (tree–grass interactions). The common theory, defined additionally by the competition/facilitation ratio (C/F ratio) (Dohn et al. 2013), claims that the tree–grass

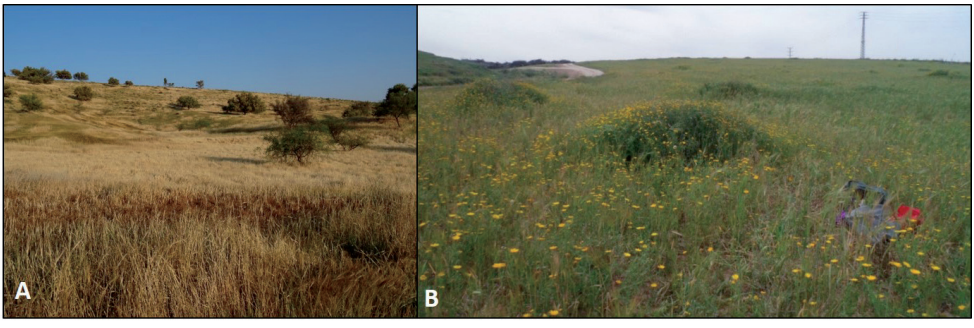

Fig. 9. Influence of rangeland reseeding on herbaceous biomass. A. Reseeded rangeland with wheat for increasing pasture, Yattir farm, March 2016. B. Cultivated field composed from autumn wheat and natural flora seeds for better pasture (mainly Chrysanthemum coronarium), Arzog 2015 (31°24'39.12"N, 47°34'33.57"E). *The noticeable wheat crowns all over the Arzog fields are attributed to the enhanced ant nesting underneath. Photo Amir Mor-Musser

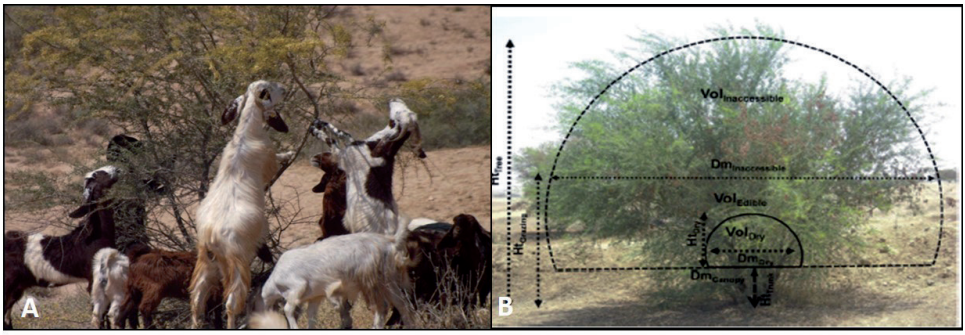

Fig. 10. Accumulation of available tree canopy volume for grazing. A. Goats eating the A. victoriae flowers. B. Scheme for evaluating the edible canopy part of a given savanna tree (based on Mor-Mussery et al. 2013). DmInaccessable- canopy diameter not accessible to the animal; VolInaccessable- canopy volume not accessible to the animal; DmDry dry part diameter surrounding the bole, which is not edible for the animal; DmDry- dry part volume surrounding the bole, which is not edible for the animal; HtDry- dry part height surrounding the bole, which is not edible for the animal; HtTrunk- trunk height; HtTree- tree total height; and DmCanopy- total diameter of the tree. Photos Amir Mor-Mussery

interactions are influenced by the ratio between two opposite processes. One is the 'competition' for resources, such as water, nutrients, or closeness to the roots, and the other is facilitation, which describes the ability of the tree to encourage the vegetation growth underneath its' canopy. The resulting understory vegetation patterns such as biomass weight and species biodiversity are determined by the ratio between these processes (Fig. 11).

The first and foremost parameter having effect on the C/F ratio is the stressor intensity. Anthropogenic effects such as dense tree plantings and a wide canopy may be considered as intense stressors that might reduce the understory vegetation (Sankaran et al. 2004; Dohn et al. 2013). Recent studies in the northern Negev have demonstrated that the C/F ratio theory is not comprehensive as the same stressor intensity may have different outcomes in the case of different species (Fig. 10A and B). In addition, dense planting may not only increase the understory vegetation but also affect the area between the trees' canopy (Fig. 10C). In summary, in many cases, the use of several savanna tree species, such as *Acacia victoriae*, may accelerate the vegetation growth and pasture usability of open lands.

PRINCIPLES FOR A SUSTAINABLE AND PROFITABLE GRAZING SYSTEM IN THE NORTHERN NEGEV

The current study describes a wide range of influences on the interactions of the animals and the ecosystem of the northern Negev open lands. In order to rehabilitate these lands and establish a sustainable and profitable grazing system, several groups must be involved, such as the authorities, the local herd owners, and scientific institutes. Nevertheless, the prerequisite for a successful grazing system in the northern Negev is a change in the attitude. Since the establishment of the state of Israel and even before it, the public and the policy makers viewed grazing as an 'unnecessary economic sector', because of the belief that grazing is destructive to the environment. This attitude led to a statutory change of many open lands from grazing to other uses and severe anti-grazing legislation. In turn, this attitude forced the herd owners to get imported food, which made the animal breeding, in many cases, unprofitable (Nevo 2013). The decrease in the animal grazing in the open lands (Zeligman et al. 2016) led to a decreased number of grazers, which in turn increased the unemployment in the Bedouin sector (Meir 1984). Besides the social effects, the decrease in the number of grazers in the open lands led to an increase in the number of fires (Perrings

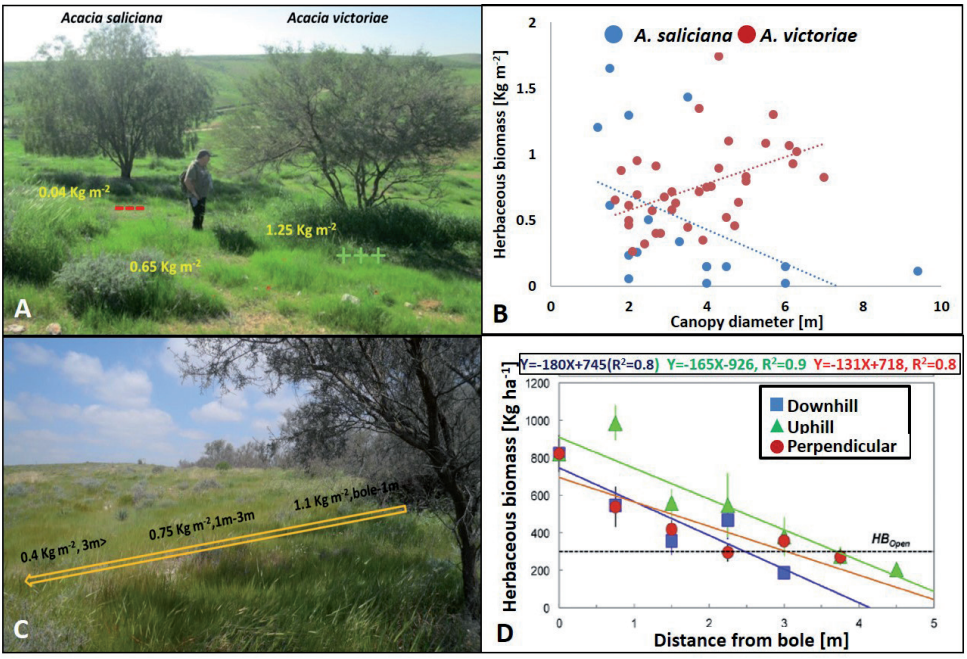

Fig. 11. Trees' influence on understory herbaceous pasture. All plots managed with the same grazing regime. A. Effect of different savanna tree species on the understory herbaceous biomass (March 2016) (Acacia victoriae accelerates the annuals growth underneath its canopy, while A. saliciana suppresses it). B. Effects of different canopy sizes on the understory herbaceous cover of savanna trees (Helman et al. 2017) (A. vicotriae canopy size is positively correlated to the understory vegetal cover, while that of A. saliciana is negatively correlated). C. Dense planting of Acacia victoriae encourages vegetal growth outside the trees' canopy area (photographed by A. Mor-Mussery in the Chiran area, 2016). D. The relative location of the tree trunk on the hill slope affects the vegetal biomass underneath (Mor-Mussry et al. 2017). Photos Amir Mor-Mussery

and Walker 1997) and the propagation of exotic species (Brunson and Tanaka 2011). The policy makers must realise that planned grazing is not only ecosystem friendly but also crucial for a sustainable and profitable management of open lands and will enhance the rehabilitation of the degraded ones (Papanastasis 2009; Yurista 2012). In order to achieve this goal, a collaboration among the authorities, local herd owners, and scientific institutes must be established on the basis of the scheme illustrated in Fig. 12.

CONCLUSION

In this paper, we presented a comprehensive view of the grazing system of the open lands in the Northern Negev, based on its' unique soil, vegetation, landscape and the indigenous farmers patterns. The scheme separates the interactions of the animal with the ecosystem, which enables better planning of adequate and sustainable utilization even in degraded open lands that are mostly been considered as 'edgy' and uncultivated. Nevertheless, the scheme requires a consistent cooperation among the farmers, municipalities and research institutes. Although the scheme studied on the northern Negev patterns, its' principles and its' suggested management plan could be adjusted for most of the open lands across the globe.

ACKNOWLEDGEMENTS

The authors wish to thank Sheich El Salam from Arzog fields, the managers of Wadi Attir farms; Noam Oren from the Yattir family farms; and Dr. David Helman for his assistance.

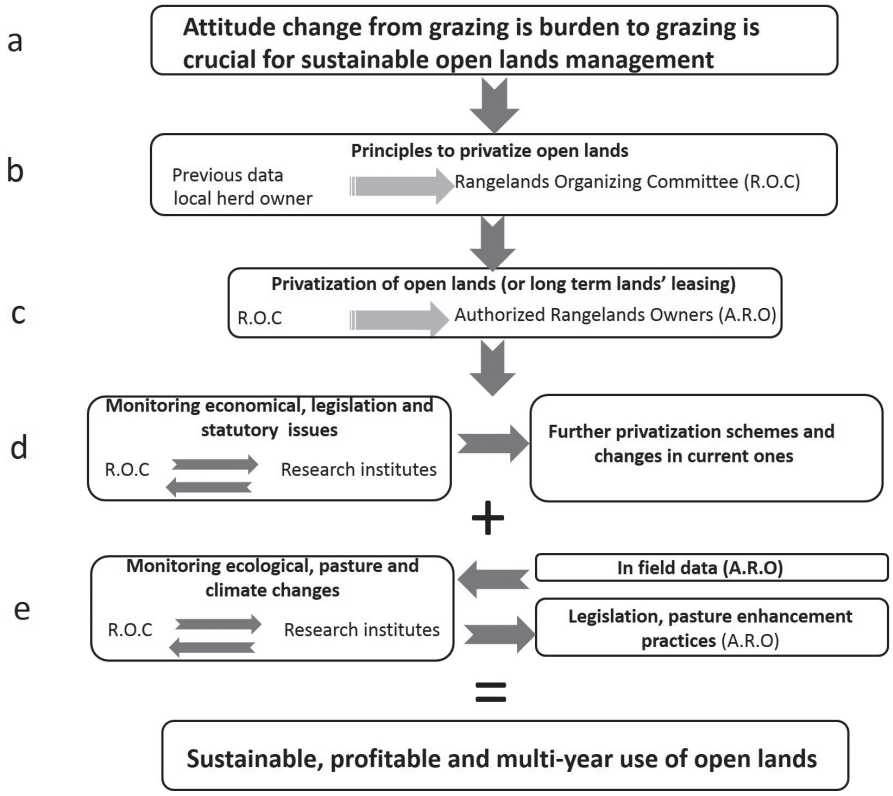

Fig. 12. Summarised scheme for sustainable rangeland management in the northern Negev open lands. A. Basic requirement of an attitude change from 'grazing is a burden' to 'grazing is crucial for successive open lands' functioning'. B. Determination of privatisation schemes for open lands on the basis of the social patterns of the local herd owners by the rangeland organising committee (R.O.C). C. Based on the determined privatisation schemes, the R.O.C allocates the open lands to authorised local herd owners (A.R.O). D. Continuous knowledge transfer between scientific institutes and the R.O.C, regarding economic and procedural issues and translation of the knowledge into further privatisation schemes or modification of the existing ones. E. Parallel to 'D', knowledge transfer of infield data from the A.R.O to the R.O.C, which will be analysed by research institutes and be translated into seasonal legislation and guidelines for the A.R.O. After several years of continuant implementation, it will lead to a sustainable and profitable utilisation of the open land.

REFERENCES

Antal J., Bullitt-Jonas M., DeChristopher T., Friedman R. S. M., Miller L. W., Murad M. M. and McKanan D. (2016). Spiritual and Sustainable: Religion Responds to Climate Change. CrossCurrents, 66(1), 70-91.

Abdulrashid L. (2013). Sustainability of indigenous knowledge in seasonal rainfall. Electronic version available online at: www.ijac.org.uk/images/frontImages/gallery/Vol._2_No._4_April_2013/4.pdf

Abubakar S. M. (1996). Rehabilitation of degraded lands by means of fallowing in a semi-arid area of northern Nigeria. Land Degradation and Development, 7(2), 133-144.

Akuja T., Avni Y., Zaady E. and Gutterman Y. (2001). Soil erosion effects as indicators of desertification processes in the Northern Negev Desert. In Soil Erosion (p. 595). American Society of Agricultural and Biological Engineers.

Alassaf A., Majdalwai M. and Nawash O. (2011). Factors affecting farmers' decision to continue farm activity in marginal areas of Jordan. African Journal of Agricultural Research, 6(12), 2755-2760.

Allen V.G., Baker M.T., Segarra E. and Brown C.P. (2007). Integrated irrigated crop–livestock systems in dry climates. Agronomy Journal, 99(2), 346-360.

Archibald S., Bond W.J., Stock W. D. and Fairbanks D. H. K. (2005). Shaping the landscape: fire–grazer interactions in an African savanna. Ecological applications, 15(1), 96-109

Avalgon D., Kumisreachick S., Nian I., Zligman N. (2014). Pasture and its use in the planted forests of KKL in Israel central spaciousness. Forest 13:18-26 (Hebrew).

Ayan I., Mut H., Onal-Asci O., Basaran U. and Acar Z. (2010). Effect of manure application on the chemical composition and nutritive value of rangeland hay. Journal of Animal and Veterinary Advances, 9(13), 1852-1857.

Bakker J.P., Olff H., Willems J.H. and Zobel M. (1996). Why do we need permanent plots in the study of long-term vegetation dynamics? Journal of Vegetation Science, 7(2), 147-156.

Bakker E.S., Ritchie M.E., Olff H., Milchunas D.G. and Knops J. M. (2006). Herbivore impact on grassland plant diversity depends on habitat productivity and herbivore size. Ecology letters, 9(7), 780-788.

Beatley J.C. (1974). Phenological events and their environmental triggers in Mojave Desert ecosystems. Ecology, 55(4), 856-863.

Beyers J.L. (2009). Non-native and native seeding. Fire effects on soils and restoration strategies. En eld, NH: Science Publishers, 321-336.

Bibalani G.H., Golshani A.A., Zahedi S.S. and Bazhrang Z. (2007). Soil stabilizing characteristics of rangelands vegetation in Northwest Iran (Misho Rangelands protected location of Shabestar). Asian Journal of Plant Sciences, 6(6), 1020-1023

Blaser W.J., Sitters J., Hart S.P., Edward P.J. and Olde Venterink H. (2013). Facilitative or competitive effects of woody plants on understory vegetation depend on N-fixation, canopy shape and rainfall. Journal of Ecology, 101(6), 1598-1603.

Bodenheimer F.S. (1960). Animal and man in bible lands [Text] (Vol. 2). Brill Archive.

Bohlen P.J. and House G. (Eds.). (2009). Sustainable agroecosystem management: integrating ecology, economics, and society. CRC Press.

Boogaard B.K., Oosting S.J., Bock B.B. and Wiskerke J.S.C. (2011). The sociocultural sustainability of livestock farming: an inquiry into social perceptions of dairy farming animal, 5(09), 1458-1466.

Brunson M.W. and Tanaka J. (2011). Economic and social impacts of wildfires and invasive plants in American deserts: lessons from the Great Basin. Rangeland Ecology and Management, 64(5), 463-470.

Butt B. (2010). Pastoral resource access and utilization: quantifying the spatial and temporal relationships between livestock mobility, density and biomass availability in southern Kenya. Land Degradation and Development, 21(6), 520-539.

Christie E.K. (Ed.) (1981). Desertification of Arid and Semiarid Natural Grazing Lands. School of Australian Environmental Studies, Griffith University.

Clarke P.J., Latz P.K. and Albrecht D.E. (2005). Long-term changes in semi-arid vegetation: Invasion of an exotic perennial grass has larger effects than rainfall variability. Journal of Vegetation Science, 16(2), pp. 23

Clason T.R. (1995). Economic implications of silvipastures on southern pine plantations. Agroforestry Systems, 29(3), 227-238.

Conner J.R. (1991). Social and economic influences on grazing management. Grazing Management-an ecological perspective. Timber Press, Inc. Portland, Oregon, pp.191-199.7-248.

de Faccio Carvalho P.C., Anghinoni I., de Moraes A., de Souza E.D., Sulc R.M., Lang C.R., et al. and de Lima Wesp C. (2010). Managing grazing animals to achieve nutrient cycling and soil improvement in no-till integrated systems. Nutrient Cycling in Agroecosystems, 88(2), 259-273.

Descheemaeker K., Amede T. and Haileslassie A. (2010). Improving water productivity in mixed crop–livestock farming systems of sub-Saharan Africa. Agricultural water management, 97(5), 579-586.

Dewes T. (1996). Effect of pH, temperature, amount of litter and storage density on ammonia emissions from stable manure. The Journal of Agricultural Science, 127(04), 501-509.

Dohn J., Dembélé F., Karembé M., Moustakas A., Amévor K.A. and Hanan N.P. (2013). Tree effects on grass growth in savannas: competition, facilitation and the stress-gradient hypothesis. Journal of Ecology, 101(1), 202-209.

Doole G.J. and Romera A.J. (2013). Detailed description of grazing systems using nonlinear optimisation methods: a model of a pasture-based New Zealand dairy farm. Agricultural Systems, 122, 33-41.

Dufour-Dror J.M. (2012). Alien invasive plants in Israel. Middle East Nature Conservation Promotion Association.

Duffy J., Paul Richardson J. and Canuel E.A. (2003). Grazer diversity effects on ecosystem functioning in seagrass beds. Ecology letters, 6(7), pp.637-645.

Encinias M. and Smallidge S. (2010). Developing a grazing system for arid climates. Circular 649 NM State University

Engelhardt W.V., Rutagwenda T., Lechner-Doll M., Kaske M. and Schultka W. (1989). Comparative aspects of ruminants and camels grazing on a thornbush savannah pasture. In feeding strategies for improving productivity of ruminant livestock in developing countries

Fernandez-Gimenez M.E. (1999). Reconsidering the role of absentee herd owners: a view from Mongolia. Human Ecology, 27(1), pp.1-27.

Fleischner T.L. (1994). Ecological costs of livestock grazing in western North America. Conservation biology, 8(3), 629-644.

Foster D., Swanson F. Aber J., Burke I., Brokaw N., Tilman D. and Knapp A. (2003). The importance of land-use legacies to ecology and conservation. AIBS Bulletin, 53(1), 77-88.

Fynn R.W.S. and O'connor T.G. (2000). Effect of stocking rate and rainfall on rangeland dynamics and cattle performance in a semi-arid savanna, South Africa. Journal of Applied Ecology, 37(3), 491-507.

Gamfeldt L., Hillebrand H. and Jonsson P.R. (2008). Multiple functions increase the importance of biodiversity for overall ecosystem functioning. Ecology, 89(5), pp.1223-1231.

Gilley J.E. and Risse L. M. (2000). Runoff and soil loss as affected by the application of manure. Transactions of the ASAE, 43(6), 1583.

Grantz D.A., Vaughn D.L., Farber R., Kim B., Zeldin M., VanCuren T. and Campbell R. (1998). Seeding native plants to restore desert farmland and mitigate fugitive dust and PM10. Journal of Environmental Quality, 27(5), 1209-1218.

Greenwood K.L. and McKenzie B.M. (2001). Grazing effects on soil physical properties and the consequences for pastures: a review. Australian Journal of Experimental Agriculture, 41(8), 1231-1250.

Grenier L. (1998). Working with indigenous knowledge: A guide for researchers. IDRC

Hahazni-Cohen (2001). Strategic Grazing, combating with invasions to rangelands in Israel,policy document. Hebrew University of Jerusalem press. Electronic version: public-policy.huji.ac.il/.upload/PolicyPaperA/Sarah_Hatzeni.pdf (Hebrew)

Helman D., .Mor-Mussery A., Lensky I.M. and Leu S. (2014). Detecting changes in biomass productivity in different land management regimes in drylands using satellite-derived vegetation index. Soil Use and Management 30(1): 32-39.

Hernanz J.L., López R., Navarrete L. and Sanchez-Giron V. (2002). Long-term effects of tillage systems and rotations on soil structural stability and organic carbon stratification in semiarid central Spain. Soil and Tillage Research, 66(2), 129-141.

Herrero M., Thornton P.K., Notenbaert A.M., Wood S., Msangi S., Freeman H.A., et al. and Lynam J. (2010). Smart investments in sustainable food production: revisiting mixed crop-livestock systems. Science, 327(5967), 822-825.

Hilimire K. (2011). Integrated crop/livestock agriculture in the United States: A review. Journal of Sustainable Agriculture, 35(4), 376-393.

Hobbs N.T., Galvin K.A., Stokes C.J., Lackett J.M., Ash A.J., Boone R.B., et al. and Thornton P. K. (2008). Fragmentation of rangelands: implications for humans, animals, and landscapes. Global Environmental Change, 18(4), 776-785.

Ingram S.E. and Hunt C. H. (2015). Traditional Arid Lands Agriculture. Understanding the Past for the Future. The university of Arizona press.

Jakoby O., Quaas M. F., Müller B., Baumgärtner S. and Frank, K. (2014). How do individual farmers' objectives influence the evaluation of rangeland management strategies under a variable climate?. Journal of applied ecology, 51(2), 483-493.

Khan H. Z., Malik M.A. and Saleem M. F. (2008). Effect of rate and source of organic material on the production potential of spring maize (Zea mays L.). Pakistan Journal of Agriculture Science, 45(1), 40-43.

Kigomo J.N. and Muturi G.M. (2013). Impacts of enclosures in rehabilitation of degraded rangelands of Turkana County, Kenya. Journal of Ecology and the Natural Environment, 5(7), 165-171.

Kincaid D.R. and Williams G. (1966). Rainfall effects on soil surface characteristics following range improvement treatments. Journal of Range Management, pp.346-351.

Kressel G.M., Ben-David J., Rabi'a K.A. and Bedouin N. (1991). Changes in the land usage by the negev bedouin since the mid-19th century. The intra-tribal perspective. Nomadic Peoples, 28-55.

Kuepper G. (2000). Manures for organic crop production. ATTRA.

Lázaro R., Rodrigo F.S., Gutiérrez L., Domingo F. and Puigdefábregas J. (2001). Analysis of a 30-year rainfall record (1967–1997) in semi–arid SE Spain for implications on vegetation. Journal of arid environments, 48(3), 373-395.

Le Hougrou H.N. (2009). Long-term dynamics in arid-land vegetation and ecosystems of North Africa. Arid Land Ecosystems: Volume 2, Structure, Functioning and Management, 2, 357.

Lesorogol C. K. (2008). Land Privatization and Pastoralist Well-being in Kenya. Development and Change, 39(2), 309-331.

Leu S., Mor-Mussery A. and Budovsky A. (2014). The effects of long time conservation of heavily grazed shrubland: A case study in the Northern Negev, Israel. Environmental management, 54(2), 309-319.

Lu J., Zhu L., Hu G. and Wu J. (2010). Integrating animal manure-based bioenergy production with invasive species control: A case study at Tongren Pig Farm in China. Biomass and bioenergy, 34(6), 821-827.

Madison F., Kelling K., Massie L., Ward Good L. (2016). Guidelines for applying manure to cropland and pasture in Wisconsin

McNaughton S.J.R.W. Ruess, and Seagle S.W. (1988). «Large mammals and process dynamics in African ecosystems.» BioScience 38, no. 11 (1988): 794-800.

Meir A. (1984). Demographic transition among the Negev Beduin in Israel and its planning implications. Socio-Economic Planning Sciences, 18(6), 399-409.

Miki T. and Kondoh M. (2002). Feedbacks between nutrient cycling and vegetation predict plant species coexistence and invasion. Ecology Letters, 5(5), pp.624-633.

Mor-Mussery A., Leu S. and Budovsky A. (2013). Modeling the optimal grazing regime of Acacia victoriae silvopasture in the Northern Negev, Israel. Journal of arid environments, 94, 27-36.

Mor-Mussery A., Helman D., Leu S., Budovsky A. (2016). Modeling herbaceous productivity considering subcanopy zone effect in drylands savannah: The case study of Yatir farm in the Negev drylands. Journal of Arid Environments, 124, 60-64.

Mor Mussery A., Helman D., Ben Eli M. and Leu S. (2017). Restoration of degraded arid farmland at Project Wadi Attir: Impact of conservation on biological productivity and soil organic matter, EGU General Assembly Vienna (Lecture' abstract).

Mottet A., Ladet S., Coqué N. and Gibon A. (2006). Agricultural land-use change and its drivers in mountain landscapes: A case study in the Pyrenees. Agriculture, ecosystems and environment, 114(2), 296-310.

MPCA (Minnesota Pollution Control Agency) (2012). Manure application rate guide. Electronic version: www.pca.state.mn.us/sites/default/files/wq-f6-26.pdf

Nevo (2013). Legislation list 1.1.2013 (Hebrew)

Ng'weno C. C. Mwasi S.M. and Kairu J. K. (2010). Distribution, density and impact of invasive plants in Lake Nakuru National Park, Kenya. African Journal of Ecology, 48(4), 905-913.

Oba G., Vetaas O.R. and Stenseth N.C. (2001). Relationships between biomass and plant species richness in arid-zone grazing lands. Journal of Applied Ecology, 38(4), 836-845.

O'connor T.G. and Roux P.W. (1995). Vegetation changes (1949-71) in a semi-arid, grassy dwarf shrubland in the Karoo, South Africa: influence of rainfall variability and grazing by sheep. Journal of Applied Ecology, 612-626.

Oesterheld M. and Sala O.E. (1990). Effects of grazing on seedling establishment: the role of seed and safe-site availability. Journal of Vegetation Science, 1(3), 353-358.

Olsvig-Whittaker L., Frankenberg E., Perevolotsky A. and Ungar E.D. (2006). Grazing, overgrazing and conservation: Changing concepts and practices in the Negev rangelands. Science et changements planétaires/Sécheresse, 17(1), 195-199.

Pakeman R.J., Hulme P.D., Torvell L. and Fisher J. M. (2003). Rehabilitation of degraded dry heather [Calluna vulgaris (L.) Hull] moorland by controlled sheep grazing. Biological Conservation, 114(3), 389-400.

Papanastasis V.P. (2009). Restoration of degraded grazing lands through grazing management: Can it work? Restoration Ecology, 17(4), 441-445.

Parker, J. D., Burkepile, D. E., and Hay, M. E. (2006). Opposing effects of native and exotic herbivores on plant invasions. Science, 311(5766), 1459-1461.

Parsons A.J., Newman J. A., Penning P. D., Harvey A. and Orr R.J. (1994). Diet preference of sheep: effects of recent diet, physiological state and species abundance. Journal of animal ecology, 465-478.

Payton R.W., Barr J. J. F., Martin A., Sillitoe P., Deckers J. F., Gowing J. W., … and Zuberi M. I. (2003). Contrasting approaches to integrating indigenous knowledge about soils and scientific soil survey in East Africa and Bangladesh. Geoderma, 111(3), 355-386

Perrings C.A. and Walker B. (1997). Biodiversity, resilience and the control of ecological-economic systems: the case of fire-driven rangelands. Ecological Economics, 22(1), 73-83.

Perrings C.A. (Ed.) (2012). Biodiversity Conservation: Problems and Policies. Papers from the Biodiversity Programme Beijer International Institute of Ecological Economics Royal Swedish Academy of Sciences (Vol. 4). Springer Science and Business Media

Phillips A., Heucke J., Dorgers B. and O'Reilly G. (2001). Co-grazing cattle and camels. A report for the Rural Industries Research and Development Corporation

Pieper R.D. (1990). Overstory-understory relations in pinyon-juniper woodlands in New Mexico. Journal of Range Management, 413-415.

Pilgrim D.H., Chapman T.G., Doran D.G. (1988). Problems of rainfall-runoff modelling in arid and semiarid regions. Hydrological Sciences Journal 33(4), 379-400.

Pretty J. N. (1994). Alternative systems of inquiry for a sustainable agriculture. IDS bulletin, 25(2), 37-49.

Pugnaire F.I. and Lázaro R. (2000). Seed bank and understorey species composition in a semi-arid environment: the effect of shrub age and rainfall. Annals of Botany, 86(4), 807-813.

Rai P., Solanki K.R. and Rao G.R. (1999). Silvipasture research in India-a review. Indian Journal of Agroforestry, 1(2), 107-120.

Rejmánek M. and Richardson D.M. (1996). What attributes make some plant species more invasive? Ecology, 77(6), 1655-1661.

Roncoli C., Ingram K. and Kirshen P. (2002). Reading the rains: local knowledge and rainfall forecasting in Burkina Faso. Society and Natural Resources, 15(5), 409-427.

Sabo K.E., Hart S.C., Sieg C.H. and Bailey J. D. (2008). Tradeoffs in overstory and understory aboveground net primary productivity in southwestern ponderosa pine stands. Forest Science, 54(4), 408-416.

Sainju U.M., Lenssen A.W., Goosey H. B., Snyder E. and Hatfield P. G. (2011). Sheep grazing in a wheat–fallow system affects dryland soil properties and grain yield. Soil Science Society of America Journal, 75(5), 1789-1798.

Sankaran M. and Augustine D.J. (2004). Large herbivores suppress decomposer abundance in a semiarid grazing ecosystem. Ecology, 85(4), pp.1052-1061.

Savadogo P., Sawadogo L. and Tiveau D.(2007). Effects of grazing intensity and prescribed fire on soil physical and hydrological properties and pasture yield in the savanna woodlands of Burkina Faso. Agriculture, Ecosystems and Environment, 118(1), pp.80-92.

Schleuning M., Fründ J. and Garcia D. (2015). Predicting ecosystem functions from biodiversity and mutualistic networks: an extension of trait-based concepts to plant–animal interactions. Ecography, 38(4), 380-392.

Schuster J.L. (1964). Root development of native plants under three grazing intensities. Ecology, 45(1), pp.63-70.

Shelef O., Soloway E. and Rachmilevitch S. (2014). Introduction and domestication of woody plants for sustainable agriculture in desert areas. In EGU General Assembly Conference Abstracts (Vol. 16, p. 11829).

Shi, H. and Shao M. (2000). Soil and water loss from the Loess Plateau in China. Journal of Arid Environments, 45(1), 9-20.

Stewart P.J. (1979). Islamic law as a factor in grazing management: the pilgrimage sacrifice. The Commonwealth Forestry Review, 27-31.

Takala T., Tahvanainen T. and Kouki J. (2012). Can re-establishment of cattle grazing restore bryophyte diversity in abandoned mesic semi-natural grasslands? Biodiversity and conservation, 21(4), 981-992.

Taylor Jr.C.A., Brooks T.D. and Garza N.E. (1993). Effects of short duration and high-intensity, low-frequency grazing systems on forage production and composition. Journal of Range Management, 118-121.

Thornton P. K., Herrero M. (2001). Integrated crop–livestock simulation models for scenario analysis and impact assessment. Agricultural Systems, 70(2), 581-602.

Toma L., Barnes A. P., Sutherland L. A., Thomson S., Burnett F., and Mathews K. (2016). Impact of information transfer on farmers' uptake of innovative crop technologies: a structural equation model applied to survey data. The Journal of Technology Transfer, 1-18.

Tracy B.F. and Zhang Y. (2008). Soil compaction, corn yield response, and soil nutrient pool dynamics within an integrated crop-livestock system in Illinois.

Tueller P.T. (Ed.). (2012). Vegetation science applications for rangeland analysis and management (Vol. 14). Springer Science and Business Media.-Crop Science, 48(3), 1211-1218.

Van de Fliert E. and Braun A. R. (2002). Conceptualizing integrative, farmer participatory research for sustainable agriculture: From opportunities to impact. Agriculture and Human Values, 19(1), 25-38.

Verdoodt A., Mureithi S.M. and Van Ranst E. (2010). Impacts of management and enclosure age on recovery of the herbaceous rangeland vegetation in semi-arid Kenya. Journal of Arid Environments, 74(9), 1066-1073.

Vasta V., Nudda A., Cannas A., Lanza M. and Priolo A. (2008). Alternative feed resources and their effects on the quality of meat and milk from small ruminants. Animal Feed Science and Technology, 147(1), 223-246.

Veenendaal E.M., Ernst W.H.O. and Modise G.S. (1996). Effect of seasonal rainfall pattern on seedling emergence and establishment of grasses in a savanna in south-eastern Botswana. Journal of Arid Environments, 32(3), 305-317.

Verdú M., Villar-Salvador P. and García-Fayos P. (2004). Gender effects on the post-facilitation performance of two dioecious Juniperus species. Functional Ecology, 18(1), pp.87-93.

Vesk, P. A. and Westoby M. (2001). Predicting plant species' responses to grazing. Journal of Applied Ecology, 38(5), 897-909.

Villarreal-Barajas, T. and Martorell C. (2009). Species-specific disturbance tolerance, competition and positive interactions along an anthropogenic disturbance gradient. Journal of Vegetation Science, 20(6), 1027-1040.

Weissmann H., Shnerb N.M. (2014). Stochastic desertification. EPL (Europhysics Letters), 106(2), 28004.

Wijdenes D.O., Poesen J., Vandekerckhove L. and De Luna E. (1997). Chiselling effects on the vertical distribution of rock fragments in the tilled layer of a Mediterranean soil. Soil and Tillage Research, 44(1), 55-66.

Williams J.C. and Hall M.H. (1994). Four steps for rotational grazing. Agronomy facts, 43,1-4. Available in electronic version: http://www.forages.psu.edu/agfacts/agfact43.pdf

Williams T. O. (1999). Factors influencing manure application by farmers in semi-arid West Africa. Nutrient Cycling in Agroecosystems, 55(1), 15-22.

Winter M. (2000). Strong policy or weak policy? The environmental impact of the 1992 reforms to the CAP arable regime in Great Britain. Journal of Rural Studies, 16(1), 47-59.

Wondzell S. and Ludwig J.A. (1995). Community dynamics of desert grasslands: influences of climate, landforms, and soils. Journal of Vegetation Science, 6(3), pp.377-390.

Yurita D. (2012). This year first. Grants for beduin shepherds which will graze their herd in openlands for preventing forests from fires, Ministry of Agriculture, internal news. www.moag.gov.il/yhidotmisrad/dovrut/publication/2012/pages/Bedouin_shepherd_grants.aspx

Zeligman N., Unger D.U., Hankin Z., Zaadye E. and Pravalotzky A. (2016). On vegetation, animals and people, on grazing management in Israel. Nekudat Chen press (published in Hebrew).

Zheng Y., Xie Z., Gao Y., Shimizu H., Jiang L. and Yu Y. (2003). Ecological restoration in northern China: germination characteristics of nine key species in relation to air seeding. Belgian Journal of Botany, 129-138.

Received on February 3rd, 2019 Accepted on May 17th, 2019

Elena Yu. Novenko[1], Pavel E. Tarasov[2], Alexander V. Olchev[1]
[1] Faculty of Geography, Lomonosov Moscow State University, Moscow, Russia
[2] Institute of Geological Sciences, Section of Paleontology, Freie Universitat Berlin, Berlin, Germany

SPECIAL ISSUE «CLIMATE-VEGETATION INTERACTION: NATURAL PROCESSES VERSUS HUMAN IMPACT»

With the last decades of globally documented climate change, concern is growing that it will have widespread impact on the world's environments and human populations (IPCC 2014). Comprehensive studies of vegetation–atmosphere interaction at different spatial (from ecosystem to regional and global scales) and temporal scales are nowadays an important challenge in geography, ecology and climatology. There are numerous factors and multiple pathways that control the interaction of land surface, vegetation and the atmosphere. It is well known that the weather and climatic characteristics (e.g. air temperature, solar radiation and precipitation) influence significantly plant growth and primary production (Woodward, 1987). In turn, the vegetation via various feedback mechanisms (e.g. CO_2 uptake and release, surface albedo, evapotranspiration) affect the local, regional, and, to some extent, global weather and climate conditions (Bonan et al. 1992; Bathiany et al. 2010). Despite the many available studies and reports documenting the various pathways of climate-vegetation interactions, there is a broad spectrum of unresolved scientific questions. In particular it is still not clear

- how the different vegetation types respond to changes of environmental conditions (including anomalous weather conditions) in different geographical regions;
- how plants have responded in the past to changing climates and how the different vegetation types will respond to projected climate change in the 21st century;
- how forest disturbances influence the local and regional climate conditions;
- what is the effect of deforestation and afforestation processes on regional and global climate and weather conditions.

Looking for the answers to these crucial research questions was the main goal of the experimental and modeling studies presented in the session of the IGU Commission of Environment Evolution at the Thematic Conference of the International Geographical Union (IGU) that was held 4-6 June 2018 in Moscow, Russia and dedicated to the centennial of the Institute of Geography of the Russian Academy of Sciences.

The special issue «Climate-vegetation interaction: natural processes versus human impact» discusses a wide range of scientific problems presented in this meeting including the human–vegetation and vegetation–climate interactions in the past, present and future, natural and anthropogenic impacts on forest and grassland ecosystems, effects of forest disturbances on green house gas (GHG) fluxes and the climate system, long-term variability of GHG exchange in forest ecosystems, etc.

Four papers presented in this special issue introduce the novel research achievements in Holocene landscape dynamics, climate changes and human activity in different regions. They show a diversity of Northern Eurasian landscapes from Central Europe to

the Russian Far East. Considering landscape and vegetation variability across a broad array of geographical conditions allows us to gain insight into past climate–vegetation interactions from a global perspective.

New evidences of the Late glacial and Early Holocene environments and human occupation in Brandenburg (eastern Germany) are presented in the paper of Kobe et al. (this issue). The authors suggest that climate changes during the Younger Dryas interval (12.9–11.7 ka BP) led neither to substantial deforestation nor spread of tundra vegetation. This idea supports the concept that the Younger Dryas cooling was mainly observed over the winter months, while summers remained comparably warm and allowed a much broader (than initially believed) spread of cold-tolerant boreal tree species.

The paper of Novenko et al. (this issue) provides a reconstruction of the Holocene climatic moisture conditions in the central part of European Russia. Surface moisture conditions were reconstructed using the climate moisture index, aridity index and dryness index of Budyko based on evidence for the mean annual temperature and precipitation in the north-west of the Mid-Russian Upland inferred from pollen records. The authors show that the surface moisture conditions in the study region during the Holocene are characterized by a large variability. Periods of mild temperature and moderately wet conditions were followed by dry periods, which resulted in significant changes in palaeoenvironments.

Borisova and Panin (this issue) investigated in their project a peat-lacustrine sedimentary section on the shore of Lake Tere-Khol (Tuva, southern Siberia). The late Holocene climatic changes in the Tere-Khol basin were reconstructed using pollen records. The authors suggest that the general tendency towards climate cooling and aridification included alternation of dry-wet and cold-warm epochs with a duration of several centuries. An overview of a large number of regional and global climatic reconstructions inferred from different proxies presented in this article show that climate variability in the Tere-Khol basin largely corresponds to the Holocene climate dynamics in the Altai-Sayan region and activity of the Asian monsoon.

Environmental history and climate changes in the southern Sikhote-Alin Mountains (Russian Far East) over the past 5.4 ka are discussed in the paper of Razjigaeva et al. (this issue). The authors demonstrate the response of regional vegetation and fire frequencies to minor climatic fluctuations. The cooling and warming phases revealed from pollen and diatom data of the studied peatland are in good agreement with global paleoclimatic events.

The study of Mor-Mussery et al. (this issue) examines the grazing system of the northern Negev desert in Israel. The authors suggest a new approach for sustainable and profitable grazing systems in arid open lands that is based on soil, vegetation, landscape and the indigenous farmer patterns. The key principles and suggested management plan could be obviously adopted for most of the open arid regions across the globe.

Several papers in the Special Issue are dealing with the temporal variability of the carbon dioxide (CO_2) and water vapor fluxes between tropical and boreal forest ecosystems and the atmosphere. In the paper of Avilov et al. (this issue) the CO_2 emission from the soil surface in a seasonally dry tropical forest in southern Vietnam was investigated. It shows significant soil heterogeneity caused mainly by different biotic factors including the distribution of fine roots and amount of decaying residues and litter on the soil surface. Detected spots with extremely high CO_2 emission can be explained by local insect activity in the upper soil horizons.

The paper of Gushchina et al. (this issue) shows new experimental results illustrating the influence of the very strong El Niño Southern Oscillation (ENSO) event of 2015–16 on local and regional meteorological conditions, as well as on energy and CO_2 fluxes in a mountainous primary tropical rainforest in Indonesia. The study is based on ERA-Interim reanalysis data as well as long-term meteorological and eddy covariance flux measurements in the tropical rainforest in the southern part of the Lore Lindu National Park in Central Sulawesi, Indonesia. Results showed that the El Niño event led to a strong increase of incoming monthly solar radiation and air temperature and consequently to a strong increase of surface evapotranspiration and decrease of net CO_2 uptake. Taking into account a very high contribution of tropical rainforests to the global budget of atmospheric GHG, the detected strong influence of ENSO on water and carbon dioxide exchange between tropical forests and the atmosphere can help to better understand the modern dynamics of GHG in the atmosphere and to improve our ability to predict their possible future changes.

The effect of clear-cutting on forest microclimate, energy, water and CO_2 fluxes in boreal forests is investigated in the paper of Mamkin et al. (this issue). Continuous three-year-long flux measurements at a recently clear-cut area situated at the southern boundary of the boreal forest zone in the western part of Russia showed a relatively low interannual variability of energy fluxes and net CO_2 exchange that were governed mainly by both local weather conditions and amount of regenerated vegetation in the clear-cut area. The energy budget is characterized by higher daily and monthly latent heat fluxes throughout the entire period of measurements. The obtained rates of net ecosystem exchange of CO_2 are consistent with the hypothesis that clear-cutting turns forest ecosystems from a CO_2 sink to a CO_2 source for the atmosphere for several years after logging. Results of modeling experiments using a three-dimensional model showed a very strong influence of vegetation heterogeneity on spatial air flow patterns and atmospheric fluxes that should be taken into account in any flux measurement campaigns conducted over or within a non-uniform plant canopy.

The paper of Sukhoveeva and Karelin (this issue) provides the retrospective analysis of the major components of the carbon cycle in agrolandscapes under land use changes in the Central Forest zone of European Russia. For the analysis six administrative regions (three areas with unchanged arable land structure in the Kaluga, Moscow and Yaroslavl regions, and three areas with changed crop rotation in the Kostroma, Smolensk and Twer regions) were selected. The results provided by using the process-based DNDC (DeNitrification-DeComposition) model showed that all investigated agrolandscapes functioned over the growing season as a net carbon sink and accumulated carbon from the atmosphere into plant biomass. The dynamics of organic carbon in soil under growing crops is also depended on organic fertilizers. It is shown that the cumulative rates of net ecosystem exchange and soil respiration had decreased during the last 30 years mainly due to reduction of arable land area.

The net ecosystem exchange (NEE) of CO_2, gross primary production and ecosystem respiration variability of a ridge-hollow oligotrophic Mukhrino peat bog situated in the Middle Taiga Zone in West Siberia (Russia) were investigated in the paper of Dyukarev et al. (this issue). The model of NEE to describe the influence of different ambient factors on NEE and to estimate the total carbon budget of the peat bog over the growing season was also suggested. Results showed that the Mukhrino peat bog acted over the growing seasons of 2017-2018 as a carbon sink. Moreover, it was found that the monthly NEE rates at the hollows exceeded the NEE rates at the ridge sites.

The study provided by Tiralla et al. (this issue) shows the importance of adequate estimations of surface emissivity for the appropriate model parameterization of energy

and matter fluxes between the forest and the atmosphere. In this study, the emissivity of the five broadleaf tree species *Acer pseudoplatanus, Fagus sylvatica, Fraxinus excelsior, Populus simonii* and *Populus candicans* were determined under laboratory conditions in a controlled-climate chamber. The data were used to examine the effects of surface emissivity changes on radiative, sensible and latent energy fluxes of the Hainich forest in Central Germany. The results showed that the energy fluxes and surface temperature increased with a decrease in emissivity, whereas net CO_2 exchange decreased, due to respiration losses resulting from the temperature increase. Overall, the findings indicate that the dependency of energy and matter fluxes on surface emissivity changes is non-linear. The study therefore provides important basics for the correct application of variable leaf emissivity in energy budget modeling and thus to a better estimation of the contribution of forest ecosystems to the climate.

Effects of land use and forest cover changes in the central part of the East European plain on regional weather conditions was investigated in the study provided by Nikitin et al. (this issue). For the modeling experiments two extreme land-use change scenarios imitating total deforestation and afforestation were used. Modeling results conducted for the year 2016 showed that deforestation results in an increase of the annual temperature range by 0.6º C and in reduction of the annual precipitation amount by 35 mm. On the other hand, afforestation leads to decrease of annual temperature range by 0.3° C and growth of precipitation amount by 15 mm. Moreover, it was shown that the deforestation led to higher frequencies of stronger wind speeds, whereas the afforestation had opposite effects.

The last paper of Ivanova et al (this issue) analyses the phenological development of the bird cherry (*Prunus padus L.*) in the Yekaterinburg city as a part of the large-scale project "A Single Phenological Day". It was revealed the slowing of the bird cherry development in the city areas situated close to large water reservoirs. Moreover, it was shown that the bird cherry trees growing inside large industrial areas, on the contrary, developed much faster.

All results presented in the special issue can be considered as a basis for fruitful collaboration of different research teams within the international scientific community investigating environment evolution and interaction of plant ecosystems and the atmosphere in different geographical regions.

REFERENCES

Bathiany S., Claussen M., Brovkin V., Raddatz T., Gayler V. (2010). Combined biogeophysical and biogeochemical effects of large-scale forest cover changes in the MPI earth system model. Biogeosciences, 7, pp. 1383–1399.

Bonan G.B., Pollard D., Thompson S.L. (1992). Effects of boreal forest vegetation on global climate. Nature, 359, pp. 716–718.

IPCC 2014: Climate Change (2014). Synthesis Report. Contribution of Working Groups I, II and III to the Fifth Assessment Report of the Intergovernmental Panel on Climate Change (Core Writing Team, R. K. Pachauri & L. A. Meyer (eds.)). Geneva: IPCC.

Woodward F.I. (1987). Climate and plant distribution. Cambridge: Cambridge University Press.

Franziska Kobe[1], Martin K. Bittner[1], Christian Leipe[1,2], Philipp Hoelzmann[3], Tengwen Long[4], Mayke Wagner[5], Romy Zibulski[1], Pavel E. Tarasov[1*]
[1] Institute of Geological Sciences, Paleontology, Freie Universität Berlin, Berlin, Germany
[2] Institute for Space-Earth Environmental Research (ISEE), Nagoya University, Nagoya, Japan
[3] Institute of Geographical Sciences, Physical Geography, Freie Universität Berlin, Berlin, Germany
[4] School of Geographical Sciences, University of Nottingham Ningbo China, Ningbo, China
[5] Eurasia Department and Beijing Branch Office, German Archaeological Institute, Berlin, Germany
***Corresponding author:** ptarasov@zedat.fu-berlin.de

LATEGLACIAL AND EARLY HOLOCENE ENVIRONMENTS AND HUMAN OCCUPATION IN BRANDENBURG, EASTERN GERMANY

ABSTRACT. The paper reports on the results of the pollen, plant macrofossil and geochemical analyses and the AMS ^{14}C-based chronology of the «Rüdersdorf» outcrop situated east of Berlin in Brandenburg (Germany). The postglacial landscape changed from an open one to generally forested by ca. 14 cal. kyr BP. Woody plants (mainly birch and pine) contributed up to 85% to the pollen assemblages ca. 13.4–12.5 cal. kyr BP. The subsequent Younger Dryas (YD) interval is characterized by a decrease in arboreal pollen (AP) to 75% but led neither to substantial deforestation nor spread of tundra vegetation. This supports the concept that the YD cooling was mainly limited to the winter months, while summers remained comparably warm and allowed much broader (than initially believed) spread of cold-tolerant boreal trees. Further support for this theory comes from the fact that the relatively low AP values persisted until ca. 10.6 cal. kyr BP, when the «hazel phase» of the regional vegetation succession began. The postglacial hunter-gatherer occupation is archaeologically confirmed in Brandenburg since ca. 13 cal. kyr BP, i.e. much later than in the western part of Germany and ca. 1000 years after the major amelioration in the Rüdersdorf environmental record.

KEY WORDS: pollen analysis, plant macrofossils, sediment geochemistry, AMS ^{14}C dating, vegetation, climate change

CITATION: Franziska Kobe, Martin K. Bittner, Christian Leipe, Philipp Hoelzmann, Tengwen Long, Mayke Wagner, Romy Zibulski, Pavel E. Tarasov (2019) Lateglacial and early Holocene environments and human occupation in Brandenburg, eastern Germany. Geography, Environment, Sustainability, Vol.12, No 2, p. 132-147
DOI-10.24057/2071-9388-2018-50

INTRODUCTION

In the recent decades of globally documented climate warming, concern is growing that it will have widespread impact on the world's environments and human populations (IPCC 2014). However, these future impacts are poorly constrained by ecosystem models and direct observations. Therefore, reconstruction of possible effects of past climatic changes on vegetation, animal and human population dynamics remains one of the key tasks of palaeoenvironmental research. In particular, multidisciplinary studies of ecosystem transformations, which occurred in response to global warming during the Lateglacial-Holocene transition ca. 15–8 thousand calendar years before present (cal. kyr BP) and was of comparable magnitude to climatic change predicted for the next hundred years, are of increasing importance.

The environmental response of European terrestrial and limnic ecosystems to the distinct climatic fluctuations at the end of the last glaciation varied both in time and space, depending on local and regional climatic conditions and on the distance to the Atlantic Ocean and adjacent ice sheets (Wohlfarth et al. 2007). Palaeoenvironmental and palaeoecological reconstructions of the response to these climatic fluctuations remain hampered by problems inherent with ^{14}C dating (de Klerk 2002; Litt et al. 2009) and limited by the availability of high-resolution Lateglacial and early Holocene terrestrial records from many regions. Although new investigations are now emerging from different regions offering the possibility to address these issues in greater detail, there are many areas (even within Europe), where understanding Lateglacial and early Holocene climatic and environmental conditions requires more in-depth studies (Tarasov et al. 2018) in order to be robustly correlated with reference environmental archives across Eurasia (e.g. Namiotko et al. 2015; Stebich et al. 2009, 2015; Schlolaut et al. 2017).

The landscapes of the Federal States Berlin and Brandenburg in eastern Germany are part of the North German plains and lowlands predominantly formed by Weichselian glacial and periglacial processes. The area includes many lakes and peatlands, the deposits of which are important palaeoecological archives. Palynological studies into Lateglacial and early Holocene vegetation history are numerous (e.g. Behre et al. 1996 and references therein), however, would greatly benefit from higher temporal resolution and better chronological control (de Klerk 2002). A misbalance in the dating quality is particularly noticeable when comparing Lateglacial and early Holocene environmental archives from the eastern part of Germany with annually laminated lacustrine sediments from the Eifel maars in the southwestern part (Sirocko 2009).

To contribute in filling this gap, we performed a multi-proxy palaeoenvironmental study of a Lateglacial to early Holocene sedimentary section from Rüdersdorf near Berlin (Fig. 1a, b). The area is best known for its unique Triassic limestone deposits, which represents the largest geological outcrop of the Mesozoic in northern Germany (Schroeder 2015). The limestone exploitation in the Rüdersdorf quarry (Fig. 1c) requires removal of relatively thin Weichselian glacial and postglacial sediments covering the Triassic layers. These works allow rescue of well-preserved sections composed of Lateglacial–early Holocene limnic-telmatic sediments (Fig. 1d). The outcrop "Paddenluch" (Fig. 1c) has been intensively studied for faunal and macrobotanical remains and ^{14}C-dated using Accelerator Mass Spectrometry (AMS) to the Lateglacial and Holocene intervals (Kossler 2010). Our current study reports results of the pollen, plant macrofossil and geochemical analyses and the AMS ^{14}C dating of the "Rüdersdorf" outcrop situated ca. 650 m west of the Paddenluch (Fig. 1c). In the accompanying discussion we address the following issues: (i) the local and regional environments during the Younger Dryas (YD) interval (ca. 12.7–11.6 cal. kyr BP); (ii) the onset of the "hazel phase" in the vegetation development; and (iii) the postglacial environments and hunter-gatherer occupation.

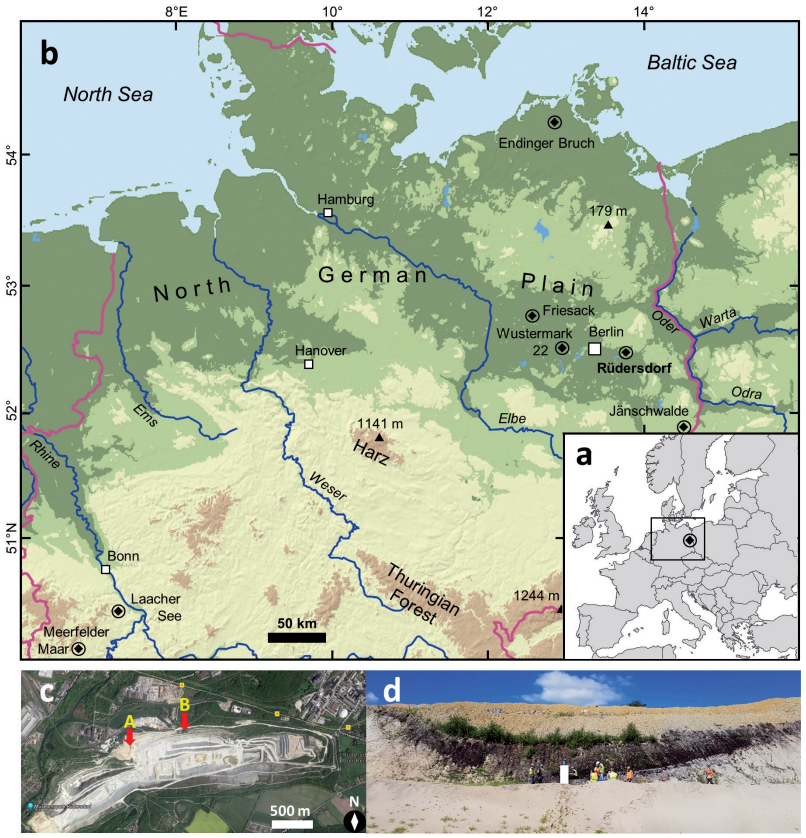

Fig. 1. a) Location of the Rüdersdorf site in central Europe; b) topographic map of northern Germany indicating positions of the key sites discussed in the text; c) aerial image of the Rüdersdorf limestone quarry and locations of the Rüdersdorf (arrow A) and Paddenluch (arrow B) outcrops; d) photo of the Rüdersdorf outcrop and the sampled section (white column) representing the Lateglacial–early Holocene interval

SITE SETTING AND REGIONAL ENVIRONMENTS

The study site (52°29'N, 13°48'E, ca. 30 m a.s.l.) is located in the northern part of the active limestone quarry in Rüdersdorf operated by the CEMEX OstZement GmbH Werk Rüdersdorf. The quarry is situated approximately 30 km southeast of Berlin on the ground moraine of the Barnim Plateau, just north of the Warsaw-Berlin glacial valley (Schroeder 2015). The major Weichselian ice extent in the study area occurred during the Brandenburg Phase prior to ca. 21 cal. kyr BP (Hardt and Böse 2018). The retreat and melting of the glaciers left sandy soils and a complex system of rivers and lakes. The end moraines of the Frankfurt Stage are documented north of Rüdersdorf suggesting that the area was already free of permanent ice after ca. 18.4 cal. kyr BP (Schroeder 2015). Although exact dates are still under debates (e.g. Hardt and Böse 2018), the AMS-dated remains of *Armeria maritima* (sea thrift) from the Paddenluch outcrop show that the area was undoubtedly ice-free (including dead ice in kettle holes) and vegetated by ca. 15 cal. kyr BP (Kossler 2010). The Rüdersdorf outcrop analyzed here likely represents one of the shallow water lakes that appeared in topographic depressions on the fluvio-glacial surface of the Barnim Plateau at about the same time.

The modern climate of the area is sub-continental within an oceanic-continental transitional zone (Behre et al. 1996). It is characterized by a mean January temperature of –0.7°C, a mean July temperature of

18°C, and an annual precipitation of about 580 mm (ca. 65% of this sum falls during the vegetative period). The study area is situated within the temperate deciduous forest biome zone, although located very close to the western margin of the cool mixed forest zone (Prentice et al. 1996). Therefore, vegetation cover of the Barnim region consists of diverse temperate deciduous and cool mixed forest taxa, with *Pinus sylvestris* (Scots pine), *Fagus sylvatica* (beech) and *Quercus* spp. (oak) being dominant.

MATERIALS AND METHODS

The Rüdersdorf outcrop (Fig. 1d) was sampled on Sunday April 9, 2017. The limited amount of time allowed for sampling in this area of the quarry to which access is usually prohibited, the steep slope of the outcrop and groundwater outflow complicated the fieldwork. The samples (each consisting of 4-cm-thick sediment sequences) were continuously taken from the lower 156 cm of the cleaned sedimentary section (Fig. 2a), packed in plastic bags and stored in the refrigerator. The sampled section consists of a minerogenic lower part with fine sand (156–132 cm) and an upper part with partly laminated calcareous gyttja, silt and clay (132–124 cm), organic gyttja (124–103 cm), peaty gyttja (101–66 cm) and black peat (above 66 cm). The interval between 101 and 103 cm contains a 1–2 cm thick yellowish sediment layer, the Laacher See Tephra (LST) that has been also identified in the Paddenluch section (Kossler 2010). This ash is named after a caldera lake in the Eifel region in western Germany (Fig. 1b), about 500 km southwest of Rüdersdorf. The last eruption of the Laacher See Volcano has been securely dated to 12,937±23 cal. yr BP (Bronk Ramsey et al. 2015) and the LST is an important chronological marker of supra-regional importance. Visible plant macrofossils (i.e. small twigs) were also hand-picked from the cleaned surface of the section for AMS dating.

The eight AMS ^{14}C dates on short-lived terrestrial plant macrofossils were generated in the Poznan Radiocarbon Laboratory and used together with the known age of the LST to construct a robust age model for the analyzed sediment sequence. All obtained ^{14}C dates (Table 1) were converted into calendar ages using the OxCal v.4.3.2 software package (Bronk Ramsey 1995) and the IntCal13 calibration curve (Reimer et al. 2013). We adopted a Poisson process Bayesian depositional model (Bronk Ramsey 2008) to investigate the sequence's age-depth relationship using information from these ^{14}C dates, the known age of LST layer, the key lithological boundaries (LBs) and the estimated minimum age (ca. 11,500 cal. yr BP) for the Lateglacial-Holocene transition (ca. 74 cm) based on pollen and geochemistry data (Fig. 2). The OxCal command *Boundary*() was used to model the selected LBs. The critical values for the agreement index and convergence index in the model were set to, respectively, 60% and 95% (Bronk Ramsey 1995). The reconstructed curve was further smoothed by a quadratic regression between the two variables (i.e. modelled calibrated age and depth), in order to minimise influences by individual ^{14}C dating anomalies and to focus on the overall rate of deposition.

A multi-disciplinary approach, including palynological, geochemical and plant macrofossil analyses, was applied to the sediment samples in order to reconstruct local to regional environmental dynamics.

Basic geochemical parameters such as elemental analysis of TIC (total inorganic carbon), TOC (total organic carbon) and TN (total nitrogen) as well as determination of major elements (Fig. 3) by ICP-OES (inductively coupled plasma optical emission spectrometer) on the base of an aqua regia extraction (DIN EN 2001) were conducted for all collected samples. The main mineralogic components were determined by XRD (X-ray diffraction). The XRD-results (Fig. 3) are expressed in counts per second (cps), which reflects semi-quantitatively the proportion of the minerals. These common analyses are described in detail in Vogel et al. (2016).

Extraction of pollen, fern spores and other non-pollen palynomorphs (NPPs) was performed according to the protocol described in Leipe et al. (2018). The protocol

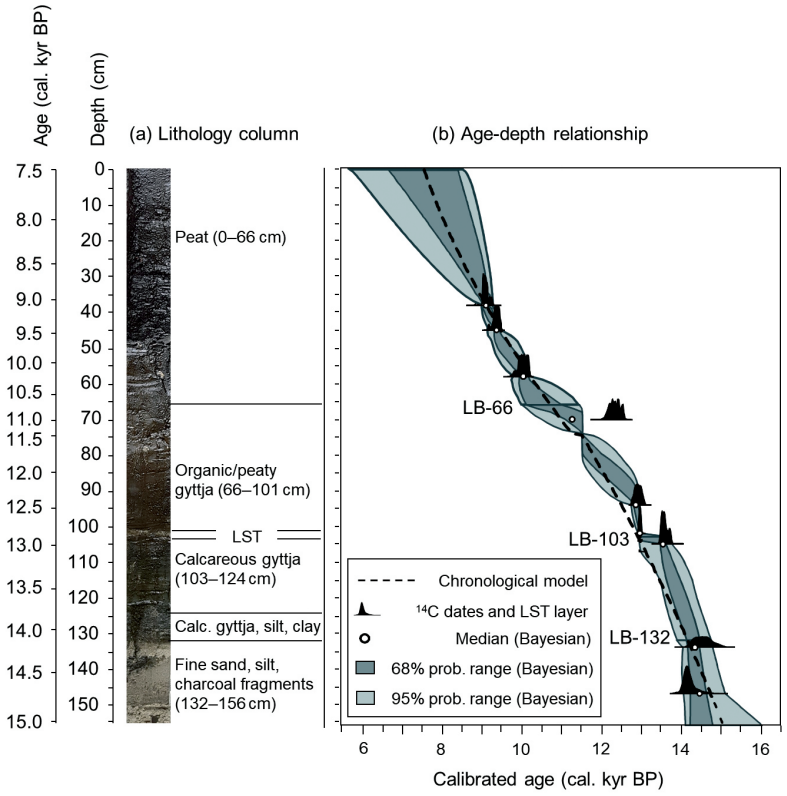

Fig. 2. a) Lithology column and b) age-depth model of the Rüdersdorf section based on the ^{14}C dates (Table 1) and key lithological boundaries (LBs)

Table 1. ^{14}C dates and calibrated ages for the Rüdersdorf section

Sample Nr./ Lab. Nr.	Dated material	Composite depth, cm	^{14}C Date, uncal. yr BP	Calibrated age (unmodelled), cal. yr BP (OxCal v.4.3.2)
RU-I-9/ Poz-91180	twig fragment	147	12240 ± 70 BP	68.2% probability 14257BP (68.2%) 14025BP 95.4% probability 14563BP (95.4%) 13927BP
RU-I-20-24/ Poz-96975	twig fragment	134	12420 ± 70 BP	68.2% probability 14711BP (68.2%) 14279BP 95.4% probability 14948BP (95.4%) 14162BP
RU-I-51/ Poz-91181	twig fragment	105	11740 ± 60 BP	68.2% probability 13696BP (2.2%) 13685BP 13610BP (66.0%) 13465BP 95.4% probability 13725BP (95.4%) 13452BP
Laacher See Tephra (LST)	tephra	101-103	–	12937± 23 cal. yr BP (after Bronk Ramsey et al., 2015)

RU-I-60-64/ Poz-96669	twig fragment	94	11030 ± 60 BP	68.2% probability 12984BP (68.2%) 12811BP 95.4% probability 13044BP (95.4%) 12744BP
RU-I-84-88/ Poz-96976	twig fragment	70	10430 ± 60 BP	68.2% probability 12518BP (6.5%) 12488BP 12425BP (16.0%) 12366BP 12358BP (33.6%) 12227BP 12213BP (12.2%) 12160BP 95.4% probability 12541BP (95.4%) 12089BP
RU-II-6/ Poz-91182	twig fragment	58	8890 ± 50 BP	68.2% probability 10156BP (13.9%) 10114BP 10088BP (54.3%) 9921BP 95.4% probability 10191BP (88.7%) 9883BP 9878BP (1.4%) 9861BP 9849BP (5.3%) 9785BP
RU-II-19/ Poz-91183	twig fragment	45	8330 ± 50 BP	68.2% probability 9430BP (68.2%) 9295BP 95.4% probability 9473BP (90.4%) 9237BP 9222BP (1.3%) 9205BP 9176BP (3.7%) 9142BP
RU-II-24-28/ Poz-91186	twig fragment	38	8130 ± 50 BP	68.2% probability 9122BP (68.2%) 9009BP 95.4% probability 9255BP (95.4%) 8992BP

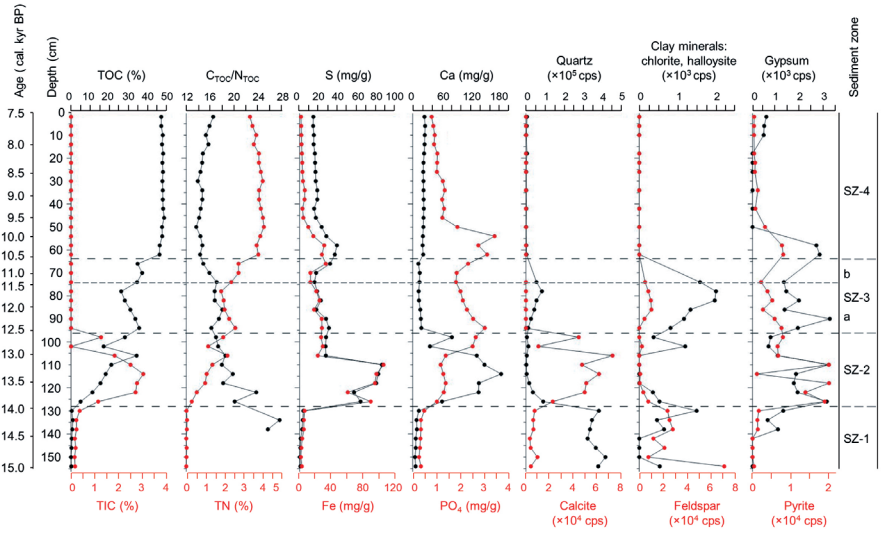

Fig. 3. Rüdersdorf sediment geochemistry for the main components discussed in the text. The XRD-results are expressed in counts per second (cps)

includes treatment of 0.5 gram of sediment with 10% HCl, 10% KOH, dense media separation using sodium polytungstate (SPT) at a density of 2.1, and acetolysis. Dense media separation using non-toxic SPT serves for isolating the pollen fraction from siliceous and other heavier sediment particles and is particularly recommended instead of extremely dangerous HF treatment often utilized by palynologists to digest siliceous matter. In order to estimate pollen concentrations, we added a known quantity of exotic *Lycopodium clavatum* marker spores to each sample prior to lab preparation following Stockmarr (1971). Pollen and NPPs were counted using a light microscope with magnification ×400–600 and taxonomically identified with the help of regional pollen atlases (Beug 2004; Demske et al. 2013 and references therein) and the institute's reference collection. For all analyzed fossil pollen samples, calculated pollen percentages refer to the sum of terrestrial pollen grains. Other counted taxa percentages, including pollen of aquatic plants, spores of ferns and algae remains were calculated using the total terrestrial pollen sum plus the sum of palynomorphs in the respective group. Tilia version 1.7.16 software (Grimm 2011) was used for calculating pollen and NPP taxa percentages and drawing the diagrams.

Plant macrofossils (i.e. remains of plants that are visible by naked eye with a median size of 0.5 to 2 mm) were selected and used for AMS ^{14}C dating and for palaeoecological interpretations. Sediment samples were treated with 10% H_2O_2 over night and then washed through a 125 µm sieve. Plant macrofossils were picked from the residue using a binocular microscope. Identification was performed using published literature (van Geel 1978; Kossler 2010 and references therein) and a reference collection at the Alfred Wegener Institute for Polar and Marine Research (Potsdam). Specimens were photographed using a Keyence VHX-1000 digital microscope and a ZEISS SUPRATM 40 VP Ultra Scanning Electron Microscope (SEM). To examine oospores of Characeae at the SEM, specimens were dehydrated in a graded ethanol series (10%, 30%, 50%, 70%, 100%), dried on a metal stage and coated.

RESULTS AND INTERPRETATONS

Age-depth model

The age-depth model for the analyzed Rüdersdorf section (Fig. 2a) is presented in Fig. 2b. In general, estimated ages for the uppermost peat section (66–0 cm) and lowermost sand/silt section (156–132 cm) fit well with the determined ^{14}C dates. There seems to be, however, a certain level of mismatch between ^{14}C dates within the gyttja section (132–66 cm) and the adopted model. Fortunately, the LST layer provides a unique control point to determine the mismatch. It turns out that the ^{14}C dates in the section are probably older than their depositional contexts. Anomalies are not rare in ^{14}C dating (Long et al. 2016) and one in twenty radiocarbon dates can be expected to be either younger or older than its age of deposition (Bronk Ramsey 2009). In any case, introducing quadratic regression to focus on the overall rate of deposition helped establishing a model in which the influence of single anomalous datings is minimized.

Sediment geochemistry

The sediment geochemistry (Fig. 3) reveals four sediment units/zones that are mainly reflected by changes in the contents of the organic substance (TOC), calcite (TIC, Ca concentration), iron and sulfur (Fe, S) as well as in varying mineralogical components (mainly quartz, calcite, pyrite, and gypsum).

SZ-1 (156–128 cm, ca. 15,030–13,970 cal. yr BP) reflects almost organic-free pure siliclasts (quartz, feldspars, and partly clay minerals) that represent the Lateglacial sands and silts deposited at a time when the water table had not yet inundated the Rüdersdorf topographical depression. High C/N values (up to 28) also point to low input of mainly terrestrial organic matter.

SZ-2 (128–96 cm, ca. 13,970–12,560 cal. yr BP) is characterized by increasing TOC (up to 34,4%), calcite (up to 24%) and lowered quartz and feldspar proportions but peaking Fe and S contents due to the appear-

ance of pyrite. The rising groundwater table reached the depression and a lake formed, as shown by the production of organic substance. As the C/N value decreases towards the top, an increase in water plants and algae contribute to the organic substance produced in the lake. The relatively high gypsum peaks in the XRD-diagrams reflect the local geology including gypsum deposits. The parallel trend of Fe and S throughout the entire section points out that pyrite formed authigenically. Calcite probably formed during summer when temperature and biological production were highest.

SZ-3 (96–64 cm, ca. 12,560–10,570 cal. yr BP) is characterized by high TOC (26.3 to 37.3%) and phosphate contents, but missing presence of calcite. Probably the organic production increased with lowered water depth and the high organic content dissolved formerly present calcite in the sediments (Dean 1999). The increased quartz and clay mineral (chlorite and halloysite) contents point to an increased aeolian detrital input from the catchment. This sediment zone represents a shallowing lake that steadily transforms into a lowland fen/moor.

At SZ-4 (64–0 cm, ca. 10,570–7540 cal. yr BP) the Rüdersdorf depression reached a state when peat was formed as shown by TOC contents between 46.4–48.8%, that would represent organic substance well above 80%. Minerogenic components are almost absent and also gypsum shows only low contents reflecting low input of groundwater. However, the C/N ratios around 14 represent a mixture between organic matter produced by subhydric algae and terrestrial plants – typical for a lowland fen/moor.

Micro- and macrofossil remains

Results of the palynological investigation are shown in a simplified pollen diagram (Fig. 4). Five local pollen zones (LPZ) objectively defined with the help of CONISS represent most important changes in the pollen assemblages and in regional and local environments between ca. 15 and 8 cal. kyr BP.

The lowermost LPZ-1 (156–128 cm, ca. 15,030–13,970 cal. yr BP) reveals very low pollen concentration suggesting quick sedimentation and/or sparse vegetation cover. Arboreal pollen (AP) taxa percentages are low indicating a generally open landscape. The most distinctive taxa are

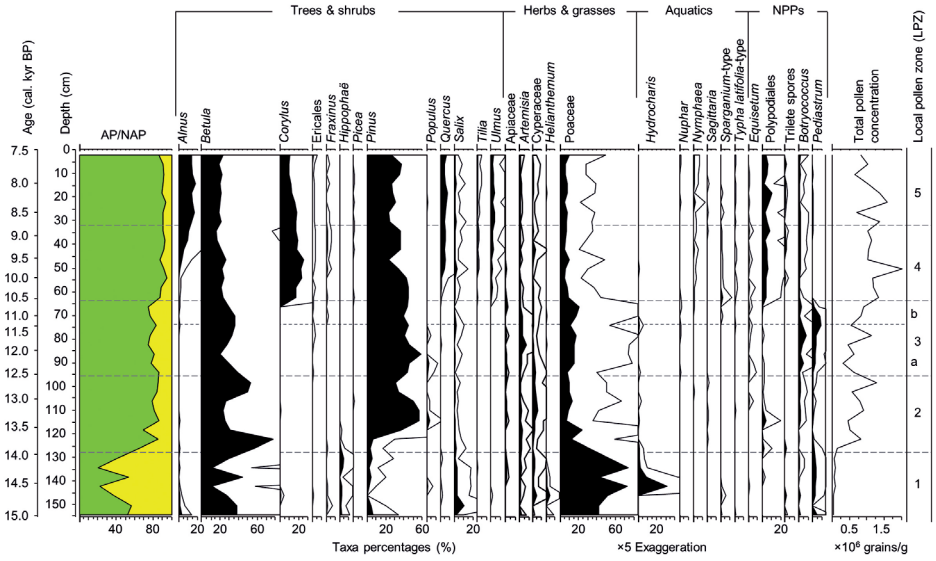

Fig. 4. Percentage diagram showing simplified results of the palynological analysis of the Rüdersdorf section

Betula, Salix and *Hippophäe,* suggesting that riparian tree and shrub communities with birches, willows and sea buckthorn grew close to the site. Low percentages of *Pinus* likely represent air transport from more distant region to the south. Among the non-arboreal pollen (NAP) taxa, Poaceae, likely representing coastal grass vegetation, absolutely predominates. *Hydrocharis* (frogbit) and *Pediastrum* green algae colonies represent relatively shallow and quiet aquatic environments. Identifiable plant macrofossils were not found in this zone but twig fragments collected from 147 and 134 cm (Table 1) likely represent willow or sea buckthorns growing near the site.

LPZ-2 (128–96 cm, ca. 13,970–12,560 cal. yr BP) is characterized by a noticeable increase in pollen concentrations and high AP contents (up to 85%) indicating a dense vegetation cover and high proportions of woody plants in the study area. Pines and birches are major pollen contributors. The NAP taxa composition is relatively rich representing meadow vegetation. Virtual disappearance of *Hydrocharis* pollen and higher proportions of fern spores likely indicate a shallow lake or pond. The macrofossil assemblage from 128–124 cm (ca. 13,970–13,800 cal. yr BP) reveals remains of *Gasterosteus aculeatus* (three-spined stickleback). This small fish prefers slow-flowing water bodies (fresh, brackish or saline) with areas of emerging vegetation. *Hippuris vulgaris* (mare's tail) fruits also suggest submerged or littoral growth in carbonate-rich stagnant or slow-flowing water and summer temperatures above 13°C. Poorly preserved *Betula* sp. seeds indicate presence of birches in the local vegetation. *Daphnia pulex* (the most common species of water flea) ephippia remains stand for a winter or dry-season resting stage and may indicate stress associated with the Lateglacial climate and small-pool environments.

LPZ-3 (96–64 cm, ca. 12,560–10,570 cal. yr BP) reveals a small-scale decrease in the pollen concentrations and AP values (to 75%), which coincides with a relative increase in Poaceae and *Artemisia* percentages, suggesting a decrease in the regional tree cover and local spread of grass and wormwood communities, which may indicate climate deterioration and seasonally drier environments, particularly obvious in the lower part of this zone, prior to ca. 11,650 cal. yr BP. The sediment from 68–64 cm (ca. 10,830–10,570 cal. yr BP) reveals fruits of *Groenlandia densa* (opposite-leaved pondweed). It occurs in flowing and stagnant waters, but prefers warm summer conditions, in agreement with the early Holocene dates. *Betula* seeds were also found in the sediment.

LPZ-4 (64–32 cm, ca. 10,570–8790 cal. yr BP) demonstrates a return to very high pollen concentrations and AP percentages reaching 95%. *Corylus* (hazel) dominates this zone together with *Pinus* and *Betula* suggesting that regional climate became significantly warmer. Appearance of *Quercus, Ulmus, Tilia, Alnus* and some other temperate deciduous taxa supports this interpretation and indicates the development of species-rich temperate deciduous forests with oak, elm, lime and alder trees and abundant hazel shrubs in the understory layer. Noticeable increase in Polypodiaceae spores in this zone suggests development of a fern cover and mire environments. The macrofossil assemblage from 52–48 cm (ca. 9850–9600 cal. yr BP) reveals remains of submerged plants, e.g. *Nymphaea alba* (white water lily) and *Ceratophyllum demersum* (rigid hornwort) preferring slowly flowing to stagnant warm and eutrophic waters, and littoral community members, e.g. *Carex pseudocyperus* (cyperus sedge) and *Scirpus lacustris* (lakeshore bulrush). This suggests that the site was flooded, at least seasonally or periodically. On the other hand, needles and bark of *Pinus sylvestris* and catkins of *Betula pendula* and *B. pubescens* indicate the presence of tree birch and pine in the near vicinity during the entire telmatic phase.

LPZ-5 (32–0 cm, ca. 8790–7540 cal. yr BP) differs from the previous LPZ-4 by higher proportions of temperate deciduous trees and a moderate decrease in hazel percentages. This change may indicate the development of canopy trees leading to a relatively sparsely vegetated understory. Abundant fern spores indicate local

mire environments. On the other hand, the presence (even in low quantities) of pollen of aquatic plants may indicate proximity of the sampled site to a shallow water body.

DISCUSSION

The Younger Dryas landscape at Rüdersdorf

The YD palynozone in Germany is dated to ca. 12,680–11,590 cal. yr BP based on varve counting in the sediment cores from the Eifel maar lakes (Litt et al. 2007). As the most recent and longest of several interruptions of the gradual warming of the Earth's climate since the end of the Last Glacial Maximum, the YD signifies a last return to glacial conditions before the onset of the Holocene. The YD cold oscillation is named after the indicator alpine-tundra herbaceous plant *Dryas octopetala* (white dryad), as its leaves were typically found in the Lateglacial sediments of Denmark and southern Sweden. Due to the scarcity of annually laminated lake sediments precise allocation (and dating) of the YD in the lacustrine sequences across the world proved to be a non-easy task (e.g. Stebich et al. 2009; Tarasov et al. 2018 and references therein). The long-year discussion of presence/absence of woods in different parts of Europe during the YD and the role of woody plants in the Lateglacial vegetation cover cannot be adequately resolved without secure chronological control. In eastern Germany, the reference pollen record from Tegeler See (Berlin), for example, has been reported as representing the entire Lateglacial-Holocene interval (Behre et al. 1996). However, this assumption is based on three conventional ^{14}C age determinations, with the oldest dating within the Boreal phase of the Holocene. Noticeably for the Lateglacial chronology issue, of the 12 ^{14}C dates from the five palynologically investigated sections in the Endinger Bruch, northeastern Germany, 10 revealed either too young or too old ages (de Klerk 2002).

Kossler (2010) reported a series of 10 AMS ^{14}C age determinations based on seeds and leaves of terrestrial plants from the Paddenluch and reliably established the chronological frame of the YD in the analyzed section. The macrofossil analysis of the YD sediments in the Paddenluch provided results, which do not support a treeless character of the surrounding landscape. The presence of tree birches (*Betula pubescens* and *B. pendula*), Scots pine, aspen (*Populus tremula*) and willow remains, on the one hand, and the absence of the characteristic tundra elements in the macrofossil record, on the other hand, disagree with the reconstruction of tundra or a park-tundra landscape in Brandenburg during the YD (see Kossler 2010, for discussion and references). The pollen record from the Rüdersdorf section presented here corroborates the plant macrofossil record, suggesting that pine and birch woods were rather common in the Brandenburg area during the YD. This, in turn, indicates rather warm summer temperatures in mid-latitude Central Europe and supports climate model simulations suggesting mean July temperatures in the study region as high as 15–16°C during the YD (Renssen and Isarin 1997 ; Schenk et al. 2018). The results from Rüdersdorf and from other areas across northern Eurasia (e.g. Stebich et al. 2009; Werner et al. 2010) demonstrate that the pronounced YD cooling was mainly limited to the winter months, while summers remained comparably warm, thus promoting growth and much broader (than initially believed) spread of cold-tolerant boreal summergreen and eurythermic conifer tree and shrub taxa (Kossler 2010; Werner et al. 2010).

The onset of the "hazel phase" in the records from western and eastern Germany

Corylus avellana (common hazel) is a species of hazel native to Europe and characteristic for the cool temperate deciduous tree/shrub plant functional type, contributing to a number of forest biomes in the temperate climate zone. Wind-pollinated hazel is one of the great pollen producers; therefore, *Corylus* is a common constituent of European pollen diagrams. In the pollen records from Germany it shows a well-recognized maximum during the early Holocene (e.g. Behre et al. 1996). However, an

asynchronous onset of the *Corylus* phase in the southern (southwestern) and northern (northeastern) parts of Germany has been presented (Sirocko 2009) suggesting substantial differences in climatic/environmental conditions and in availability of this important economic plant for Mesolithic hunter-gatherers. In the most accurately dated pollen records from Holzmaar and Meerfelder Maar (Fig. 1b) in the Eifel region (Litt et al. 2009) the *Corylus* percentages grow from a few to almost 80% of the total pollen sum between ca. 11,000 and 10,500 varve yr BP and maximal values persist until ca. 9000 varve yr BP. In the Rüdersdorf pollen record, the maximum values are much lower (i.e. 25%) and similar to other pollen records from Brandenburg, i.e. 30% in the Tegeler See diagram (Behre et al. 1996). As approved by the AMS dates from the Rüdersdorf section, the maximum values of *Corylus* pollen occurred ca. 9800–9300 cal. yr BP, i.e. much later than in the Eifel. However, the first rapid increase in *Corylus* pollen percentages up to 15% in the Rüdersdorf section dates to around 10,500 cal. yr BP. Bearing this in mind, the early Holocene pattern of hazel spread in the two regions becomes much more similar.

Postglacial environments and hunter-gatherer occupation of Brandenburg

The retreat of the Weichselian ice sheet and the development of a sparse vegetation cover in the Rüdersdorf area by ca. 15 cal. kyr BP have been proved with the help of palaeobotanical data and AMS ^{14}C dating (Kossler 2010). Since then, the area, rich in lakes, ponds and rivers, was a potential summer grazing ground for herds of migrating herbivores (i.e. reindeers and horses) and numerous water birds. Thus, it would have been also attractive for the hunter-gatherers of that time, at least during the summer months. However, presence of Late Paleolithic people in Brandenburg has been archaeologically proved only since ca. 13 cal. kyr BP (Bönisch 2014), i.e. much later than in the western part of Germany (Sirocko 2009) and ca. 1000 years after the major amelioration in the Rüdersdorf environmental record. Investigations reported by Oppenheimer (2011) suggest that the initial eruption of the Laacher See Volcano took place in late spring or early summer, but volcanic activity continued for several weeks or months leaving near the crater over 50-m-thick tephra deposits exterminating all plants and animals within a distance of ca. 60 km to the northeast and ca. 40 km to the southeast. Tephra deposits from the eruption dammed the Rhine, creating a lake ca. 140 km^2 in areal extent (Schmincke et al. 1999). Riede (2008) suggested that the eruption also had a dramatic impact on forager demography all along the northern periphery of the Lateglacial settlement area and precipitated archaeologically visible cultural change. The area most affected by the fallout, the Thuringian Basin, appears to have been largely depopulated, whereas populations in southwest Germany and France increased. Whether the hunter-gatherer population movement to the area of northeastern Germany was (at least partly) stimulated by the catastrophic explosion of the Laacher See Volcano remains an interesting topic for future studies.

The first traces of postglacial hunter-gatherers in Brandenburg fall within the Allerød interstadial (13,350–12,680 varve yr BP; Litt et al. 2007) and postdates the onset of the Lateglacial warming during the Meiendorf interstadial (14,450–13,800 varve yr BP; Litt et al. 2007). The environmental situation during the second part of the Lateglacial must have been not much different from that of the end of the penultimate Saale glaciation, about 130 kyr BP, which the oldest Neanderthal stone tools recently discovered in Jänschwalde, Brandenburg (Fig. 1b), have been assigned to (Bönisch 2014). Animal bones and plant remains associated with the finds show that at that time (i.e. ca. 2 kyr before the onset of the penultimate Eemian interglacial) there was a water-rich valley covered by open boreal forest vegetation inhabited by large mammals such as wolf, horse, elk and bison (Bönisch 2014). The Late Paleolithic people living in Brandenburg by the end of the Lateglacial could also rely on a rich fauna, as revealed by the abundant fossil vertebrate remains from the archaeological site Wustermark

22 (Fig. 1b) west of Berlin (Gramsch et al. 2013). The list of identified species dated to ca. 13.6–11.5 cal. kyr BP includes elk and reindeer (abundant bone remains), but also wild horse, roe deer, aurochs, beaver, brown bear, wolf and wild boar. However, bones of pike are the most numerous indicating that fish was also an important component of the human diet (Gramsch et al. 2013). A further evidence of fishing as a part of the subsistence strategy of the Late Paleolithic groups comes from the fishhooks made of bone material found in the YD layers of Wustermark 22 (Gramsch et al. 2013). Pike, which is also present in the macrofossil assemblage of the Paddenluch dated to ca. 14–13 cal. kyr BP (Kossler 2010), has been the most frequent fish species in the Late Paleolithic to Early and Late Mesolithic archaeological sites in northern Central Europe (Cziesla 2004).

Early to Late Mesolithic hunter-gatherer occupation in Brandenburg was reconstructed in detail by excavating the multilayered site Friesack 4 northwest of Berlin (Fig. 1b). During the entire period from ca. 11 to 7.8 cal. kyr BP hunter-gatherers repeatedly visited this lake shore site, as documented by approximately 100 archaeological layers, about 140,000 Mesolithic and 18,000 Neolithic stone artifacts, thousands of animal bones and plant remains (Gehlen 2009). Bone and antler artifacts, the remains of Mesolithic fishing nets and abundant shells of hazelnut indicate a very broad subsistence strategy, including hunting of a great number of forest and water animals, birds and turtles, but also fishing and collecting edible nuts and berries during the early Holocene (Gramsch 2000).

CONCLUSIONS

The results of the multi-proxy study of the limnic-telmatic sedimentary section from Rüdersdorf near Berlin presented in the current study allow the following conclusions. The postglacial landscape in the study area changed from predominantly open and sparsely vegetated to generally forested by about 14 cal. kyr BP, as suggested by a high proportion of AP (mainly birch and pine) contributing up to 85% to the pollen assemblages ca. 13.4–12.5 cal. kyr BP. A minor decrease in AP (75%) and a more pronounced one in pollen concentration occurred during the YD. This opening of the vegetation cover corroborates the higher aeolian detrital input suggested by the sediment geochemistry. However, pollen and plant macrofossils do not suggest either substantial deforestation or spread of tundra. This corroborates recent dendrochronological records from Brandenburg and suggests relatively warm YD summers that allowed much broader than initially believed spread of cold-tolerant and drought-resistant boreal trees, such as pines. The relatively low AP values persisted until ca. 10.6 cal. kyr BP, i.e. the early Holocene, when the climate improved significantly and promoted major spread of hazel in the regional forests. The postglacial hunter-gatherer occupation in Brandenburg is archaeologically confirmed since ca. 13 cal. kyr BP, i.e. much later than in the western part of Germany and ca. 1000 years after the major amelioration observed in the Rüdersdorf environmental record.

ACKNOWLEDGEMENTS

We are particularly thankful to Geologist Jördis Hofmann from the Museumspark Rüdersdorf for her great help in organizing sampling, getting all necessary permissions and spending several Sundays at the outcrop with us. Richard Henneberg, Pascal Olschewski and Ennie Schulz (all FU Berlin) are acknowledged for their assistance in the fieldwork and PD Dr. Ralf Milke (FU Berlin) for his help in identification of the LST.

This work contributes to the project «Individual life histories in long-term culture change: Holocene hunter-gatherers in Northern Eurasia» (SSHRC Partnership Grant Number 895-2018-1004).

REFERENCES

Behre K.E., Brande A., Küster H. and Rösch M. (1996). Germany. In: B.E. Berglund, H.J.B. Birks, M. Ralska-Jasiewiczowa and H.E. Wright, eds., Palaeoecological Events During the Last 15000 Years: Regional Syntheses of Palaeoecological Studies of Lakes and Mires in Europe. Chichester: John Wiley & Sons, pp. 507–551.

Beug H.-J. (2004). Leitfaden der Pollenbestimmung: für Mitteleuropa und angrenzende Gebiete. München: Pfeil.

Bönisch E. (2014). Versunkene Welt der Altsteinzeit und Tiefbau über Tage - Einführung zum Archäologie-Report 2011/12. In: F. Schopper, ed., Arbeitsberichte zur Bodendenkmalpflege in Brandenburg Band 27: Ausgrabungen im Niederlausitzer Braunkohlenrevier 2011/2012. Wünsdorf: Brandenburgisches Landesamt für Denkmalpflege und archäologisches Landesmuseum, pp. 7–43.

Bronk Ramsey C. (1995). Radiocarbon calibration and analysis of stratigraphy: the OxCal program. Radiocarbon 37(2), 425–430.

Bronk Ramsey C. (2008). Deposition models for chronological records. Quaternary Science Reviews 27, 42–60.

Bronk Ramsey C. (2009). Dealing with outliers and offsets in radiocarbon dating. Radiocarbon 51 (3), 1023–1045.

Bronk Ramsey C., Albert P.G., Blockley S.P.E., Hardiman M., Housley R.A., Lane C.S., Lee S., Matthews I.P., Smith V.C. and Lowe J.J. (2015). Improved age estimates for key Late Quaternary European tephra horizons in the RESET lattice. Quaternary Science Reviews 118, 18–32.

Cziesla E. (2004). Late Upper Palaeolithic and Mesolithic cultural continuity – or: bone and antler objects from the Havelland. In: T. Terberger and B.V. Eriksen, eds., Hunters in a Changing World. Environment and Archaeology of the Pleistocene–Holocene Transition (ca. 11000–9000 B.C.) in Northern Central Europe. Rahden, Westfalen: Marie Leidorf Publisher, pp. 165–182.

Dean W.E. (1999). The carbon cycle and biogeochemical dynamics in lake sediments. Journal of Paleolimnology 21, 375–393.

de Klerk P. (2002). Changing vegetation patterns in the Endinger Bruch area (Vorpommern, NE Germany) during the Weichselian Lateglacial and Early Holocene. Review of Palaeobotany and Palynology 119, 275–309.

Demske D., Tarasov P.E., Nakagawa T. and Suigetsu 2006 Project Members (2013). Atlas of pollen, spores and further non-pollen palynomorphs recorded in the glacial-interglacial late Quaternary sediments of Lake Suigetsu, central Japan. Quaternary International 290–291, 164–238.

DIN EN (2001). DIN EN 13346, April 2001. Charakterisierung von Schlämmen – Bestimmung von Spurenelementen und Phosphor – Extraktionsverfahren mit Königswasser; Deutsche Fassung EN 13346: 2000. Berlin: Beuth Verlag.

Gehlen B. (2009). A microlith sequence from Friesack 4, Brandenburg, and the Mesolithic in Germany. In: P. Crombé, M. Van Strydonck, J. Sergant, M. Boudin and M. Bats, eds., Chronology and Evolution within the Mesolithic of North-West Europe. Proceedings of an International Meeting, Brussels, May 30th-June 1st 2007. Cambridge: Cambridge Scholars Publishing, pp. 363–393.

Gramsch B. (2000). Friesack: Letzte Jäger und Sammler in Brandenburg. Jahrbuch RGZM 47, 51–96.

Gramsch B., Beran J., Hanik S. and Sommer R.S. (2013). A Palaeolithic fishhook made of ivory and the earliest fishhook tradition in Europe. Journal of Archaeological Science 40, 2458–2463.

Grimm E.C. (2011). Tilia 1.7.16 Software. Springfield, IL: Illinois State Museum, Research and Collection Center.

Hardt J. and Böse M. (2018). The timing of the Weichselian Pomeranian ice marginal position south of the Baltic Sea: A critical review of morphological and geochronological results. Quaternary International 478, 51–58.

IPCC 2014: Climate Change (2014). Synthesis Report. Contribution of Working Groups I, II and III to the Fifth Assessment Report of the Intergovernmental Panel on Climate Change (Core Writing Team, R. K. Pachauri & L. A. Meyer (eds.)). Geneva: IPCC.

Kossler A. (2010). Faunen und Floren der limnisch-telmatischen Schichtenfolge des Paddenluchs (Brandenburg, Rüdersdorf) vom ausgehenden weichselhochglazial bis ins Holozän: Aussagen zu Paläomilieu und Klimabedingungen. Berliner paläobiologische Abhandlungen 11, 1–422.

Leipe C., Kobe F., Müller S. (2018) Testing the performance of sodium polytungstate and lithium heteropolytungstate as non-toxic dense media for pollen extraction from lake and peat sediment samples. Quaternary International, published online, https://doi.org/10.1016/j.quaint.2018.01.029.

Litt T., Behre K.-E., Meyer K.-D., Stephan H.-J. and Wansa S. (2007). Stratigraphische Begriffe für das Quartär des norddeutschen Vereisungsgebietes. Eiszeitalter und Gegenwart 56 (1–2), 7–65.

Litt T., Schölzel C., Kühl N. and Brauer A. (2009). Vegetation and climate history in the Westeifel Volcanic Field (Germany) during the past 11000 years based on annually laminated lacustrine maar sediments. Boreas 38, 679–690.

Long T., Hunt C.O. and Taylor D. (2016). Radiocarbon anomalies suggest late onset of agricultural intensification in the catchment of the southern part of the Yangtze Delta, China. Catena 147, 586–594.

Namiotko T., Danielopol D.L., von Grafenstein U., Lauterbach S., Brauer A., Andersen N., Hüls M., Milecka K., Baltanás A., Geiger W. and DecLakes Participants (2015). Palaeoecology of Late Glacial and Holocene profundal Ostracoda of pre-Alpine lake Mondsee (Austria) – A base for further (palaeo-) biological research. Palaeogeography, Palaeoclimatology, Palaeoecology 419, 23–36.

Oppenheimer C. (2011). Eruptions that shook the world. Cambridge: Cambridge University Press.

Prentice I.C., Guiot J., Huntley B., Jolly D. and Cheddadi R. (1996). Reconstructing biomes from palaeoecological data: a general method and its application to European pollen data at 0 and 6 ka. Climate Dynamics 12, 185–194.

Reimer P.J., Bard E., Bayliss A., Beck J.W., Blackwell P.G., Bronk Ramsey C., Buck C.E., Cheng H., Edwards R.L., Friedrich M., Grootes P.M., Guilderson T.P., Haflidason H., Hajdas I., Hatté C., Heaton T.J., Hoffmann D.L., Hogg A.G., Hughen K.A., Kaiser K.F., Kromer B., Manning S.W., Niu M., Reimer R.W., Richards D.A., Scott E.M., Southon J.R., Staff R.A., Turney C.S.M. and van der Plicht J. (2013). IntCal13 and MARINE13 radiocarbon age calibration curves 0–50,000 years cal BP. Radiocarbon 55, 1869–1887.

Renssen H. and Isarin R.F.B. (1997). Surface temperature in NW Europe during the Younger Dryas: AGCM simulation compared with temperature reconstructions. Climate Dynamics 14, 33–44.

Riede F. (2008). The Laacher See-eruption (12,920 BP) and material culture change at the end of the Allerød in Northern Europe. Journal of Archaeological Science 35, 591–599.

Schenk F., Väliranta M., Muschitiello F., Tarasov L., Heikkilä M., Björck S., Brandefelt J., Johansson A., Näslund J.-O. and Wohlfarth B. (2018). Warm summers during the Younger Dryas cold reversal. Nature Communications 9, doi:10.1038/s41467-018-04071-5.

Schlolaut G., Brauer A., Nakagawa T., Lamb H.F., Tyler J.T., Staff R.A., Marshall M.H., Bronk Ramsey C., Bryant C.L. and Tarasov P.E. (2017). Evidence for a bi-partition of the Younger Dryas Stadial in East Asia associated with inversed climate characteristics compared to Europe. Scientific Reports 7, doi:10.1038/srep44983.

Schmincke H.-U., Park C. and Harms E. (1999). Evolution and environmental impacts of the eruption of Laacher See Volcano (Germany) 12,900 a BP. Quaternary International 61, 61–72.

Schroeder J.H. (2015). Rüdersdorf bei Berlin – der Kalkstein-Tagebau: Geo-Glanzpunkt in Brandenburg: ein Blick in die Erdgeschichte – etwa 245 Millionen Jahre zurück. Berlin: Selbstverlag Geowissenschaftler in Berlin und Brandenburg e.V.

Sirocko F. (2009). Wetter, Klima, Menschheitsentwicklung: Von der Eiszeit bis ins 21. Jahrhundert. Stuttgart: Konrad Theiss Verlag.

Stebich M., Mingram J., Han J. and Liu J. (2009). Late Pleistocene spread of (cool-)temperate forests in Northeast China and climate changes synchronous with the North Atlantic region. Global and Planetary Change 65, 56–70.

Stebich M., Rehfeld K., Schlütz F., Tarasov P.E., Liu J. and Mingram J. (2015). Holocene vegetation and climate dynamics of NE China based on the pollen record from Sihailongwan Maar Lake. Quaternary Science Reviews 124, 275–289.

Stockmarr J. (1971). Tablets with spores used in absolute pollen analysis. Pollen et Spores 13, 614–621.

Tarasov P.E., Savelieva L.A., Long T. and Leipe C. (2018). Postglacial vegetation and climate history and traces of early human impact and agriculture in the present-day cool mixed forest zone of European Russia. Quaternary International, published online. https://doi.org/10.1016/j.quaint.2018.02.029.

van Geel B. (1978). A palaeoecological study of Holocene peat bog sections in Germany and the Netherlands, based on the analysis of pollen, spores and macro- and microscopic remains of fungi, algae, cormophytes and animals. Review of Palaeobotany and Palynology 25, 1–120.

Vogel S., Märker M., Rellini I., Hoelzmann P., Wulf S., Robinson M., Steinhübel L., Di Maio G., Imperatore C., Kastenmeier P., Liebmann L., Esposito D. and Seiler F. (2016). From a stratigraphic sequence to a landscape evolution model - Late Pleistocene and Holocene volcanism, soil formation and land use in the shade of Mount Vesuvius (Italy). Quaternary International 394, 155–179.

Werner K., Tarasov P.E., Andreev A.A., Müller S., Kienast F., Zech M., Zech W. and Diekmann B. (2010). A 12.5-ka history of vegetation dynamics and mire development with evidence of the Younger Dryas larch presence in the Verkhoyansk Mountains, East Siberia, Russia. Boreas 39, 56–68.

Wohlfarth B., Lacourse T., Bennike O., Subetto D., Tarasov P., Demidov I., Filimonova L. and Sapelko T. (2007). Climatic and environmental changes in northwestern Russia between 15,000 and 8000 cal yr BP: a review. Quaternary Science Reviews 26, 1871–1883.

Received on September 19th, 2018 Accepted on November 15th, 2018

Olga K. Borisova[1*], Andrei V. Panin[1,2]
[1] Institute of Geography, Russian Academy of Sciences, Moscow, Russia
[2] Lomonosov Moscow State University, Moscow, Russia
*** Corresponding author:** olgakborisova@gmail.com

MULTICENTENNIAL CLIMATIC CHANGES IN THE TERE-KHOL BASIN, SOUTHERN SIBERIA, DURING THE LATE HOLOCENE

ABSTRACT. Pollen analysis was carried out on an 80-cm sedimentary section on the shore of Lake Tere-Khol (southeastern Tuva). The section consists of peat overlapping lake loams and covers the last 2800 years. The alternation of dry-wet and cold-warm epochs has been established, and changes in heat and moisture occurred non-simultaneously. The first half of the studied interval, from 2.8 to 1.35 kyr BP was relatively arid and warmer on average. Against this background, temperature fluctuations occurred: relatively cold intervals 2.8–2.6 and 2.05–1.7 kyr BP and relatively warm 2.6-2.05 and 1.7-1.35 kyr BP. The next time interval 1.35-0.7 kyr BP was relatively humid. Against this background, the temperatures varied from cold 1.35-1.1 kyr BP to relatively warm 1.1–0.7 kyr BP. The last 700 years have been relatively cold with a short warming from 400 to 250 years ago. This period included a relatively dry interval 700–400 years ago and more humid climate in the last 400 years. The established climate variability largely corresponds to other climate reconstructions in the Altai-Sayan region. The general cooling trend corresponds to an astronomically determined trend towards a decrease in solar radiation in temperate latitudes of the Northern Hemisphere, and the centennial temperature fluctuations detected against this background correspond well to changes in solar activity reconstructed from 14C production and the concentration of cosmogenic isotopes in Greenland ice. Against the general tendency towards aridization, alternating wet and dry phases correspond well to changes in the activity of the Asian monsoon, established by the oxygen-isotope composition of speleothems in South China.

KEY WORDS: Late Holocene, short-term climate changes, Little Ice Age, Medieval Warm Period, pollen analysis, south-eastern Tuva

CITATION: Olga K. Borisova, Andrei V. Panin (2019) Multicentennial Climatic Changes In The Tere-Khol Basin, Southern Siberia, During The Late Holocene. Geography, Environment, Sustainability, Vol.12, No 2, p. 148-161
DOI-10.24057/2071-9388-2018-64

INTRODUCTION

Many paleoclimatic studies over the last two decades have addressed the natural climate variability during the present Holocene interglacial (Mann and Jones 2003; Mayewsky et al. 2004; Wanner et al. 2008; Marcott et al. 2013; and other). They reconstructed the mean surface air temperature, using a variety of land and marine-based proxy data from all around the world. Overall, the pattern of temperatures shows a rapid rise at the beginning of the Holocene, warm conditions until the middle of the Holocene,

and a cooling trend over the last 5000 years. Figure 1a shows an example of temperature anomalies record for the Northern Hemisphere reconstructed by Marcott et al. 2013 for the past 11,300 years. According to this reconstruction, the Early-Middle Holocene (11.3 to 5.0 calibrated kyr BP) warm interval was followed by ~0.7°C cooling through the second half of the Holocene (after 5.0 kyr BP), culminating in the coolest temperatures of the Holocene during the Little Ice Age, about 200 years ago.

Comparison of reconstructions of multicentennial-scale temperature oscillations over the Late Holocene reveals agreement on major climatic episodes, such as the 'Medieval Warm Period' and 'Little Ice Age', but substantial difference in reconstructed temperature amplitude. Thus, reconstruction of the mean Northern Hemisphere temperatures for the past two thousand years by Moberg et al. (2005) shows much larger multicentennial-scale variability than most previous multi-proxy reconstructions, including that by Mann and Jones (2003) (Fig. 1b, c). According to Moberg et al. (2005), high temperatures, similar to those observed in the 20th century before 1990, occurred around 1000-900 years ago, and minimum temperatures that were about 0.7°C below the average of 1961-90 occurred about 400 years ago. This reconstruction suggests significant adjustments to the idea of the climate stability of the Late Holocene. As this large natural variability is likely to continue in future, reconstructing the Late Holocene climate is essential for better understanding of climate variability, and provides necessary background knowledge for improving predictions of future climate changes.

Estimating the global or macroregional changes of the humidity of climate during the Holocene represent an even more complicated problem than that of temperature, as the regional variation is very large. Based on palynological data, M.P. Grichuk (1960) worked out a general scheme of the humidity changes during an interglacial, including the Holocene. According to this scheme, within the warm middle part of each interglacial, the earlier *thermoxerotic* (drier), and the later *thermohygrotic* (more humid) phases can be distinguished, their boundary corresponding to the maximum warming (the interglacial optimum). On the whole, this pattern corresponds rather well to the reconstructed changes in heat and moisture supply during the Holocene in various large regions of northern Eurasia by Khotinski (1977).

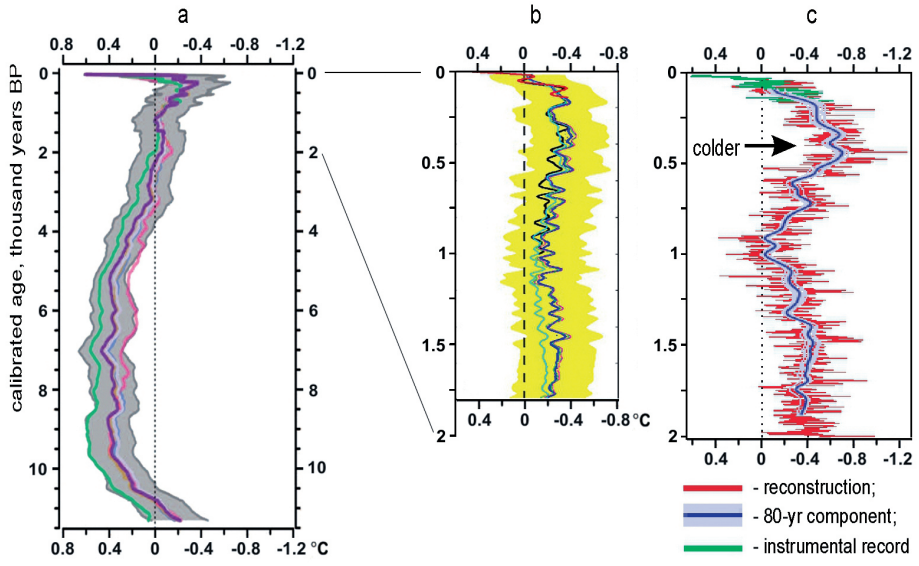

Fig. 1. Northern Hemisphere temperature reconstructions (a) Marcott et al. 2013; (b) Mann and Jones 2003; (c) Moberg et al. (2005). Temperature anomalies in a, b and c are with respect to the 1961–90 average shown by dashed line

The large fluctuations in lake levels, monsoon activity, and regional humidity registered in paleorecords from different regions indicate a considerable short-term variability of the hydrological cycle during the Holocene. Mayewski et al. (2004) concluded that the episodes of rapid climate cooling in high latitudes of both hemispheres within the Holocene were mainly characterized by an intensification of atmospheric circulation and increasing aridity in low latitudes, as the distribution of moisture-bearing winds in the monsoon regions and the carrying capacity for moisture in the atmosphere altered dramatically.

Climate changes in the mountain regions of Southern Siberia and in the adjacent regions during the Holocene

The mountainous areas of southern Siberia (Altai, Sayan and Tuva) are a key region for the analysis of the Holocene climatic changes in Eurasia due to their central location in the continent. They reflect the long-term dynamics of the main pressure fields in the Northern Hemisphere (changes in the depth of the Icelandic Low and the strength of the Siberian anticyclone), associated with the strengthening/ weakening of the Westerlies and the Asian monsoon (Tarasov et al. 2000; Mayewski et al. 2004).

Over the past decades, detailed data on landscape and climate changes during the Holocene have been obtained in the Altai-Sayan region and in adjacent areas of Central Asia.

In the East Sayan Mts., a decrease of temperatures and an increase in the continentality of climate started after 5.5 kyr BP (Bezrukova et al. 2016). The authors explain these changes by weakening of the summer Asian monsoon, strengthening of the Westerlies, and the decrease of summer insolation. Further cooling accompanied by an increase in the aridity occurred in the region about 2.5 kyr BP (Bezrukova et al. 2016). In the southwestern Tuva, the arid climate of the Early Holocene (12-11 kyr BP) has been followed by warming and increasing humidity, which persisted until 5.5-5.0 kyr BP. Later, a process of replacement of forest formations by steppe vegetation caused by cooling and increasing aridity is registered, especially pronounced after 2.0 kyr BP (Blyakharchuk et al. 2007; Blyakharchuk 2008). Analyses of Chironomidae composition in the sediments of the Ak-Khol and Grusha lakes in Tuva indicate four main climatic phases during the Holocene: cold and dry phase 12.1-8.5 kyr BP, warm and dry phase 8.5-5.9 kyr BP, cold and humid phase 5.9-1.8 kyr BP, and cold and dry phase during the last 1.8 thousand years (Ilyashuk and Ilyashuk 2007). Based on the palynological data, Tchebakova et al. (2009) distinguished the following main climatic phases for the Altai-Sayan mountainous region: cold and dry early Holocene, warm and humid climate 8.0-5.3 kyr BP, followed by cooling and drying, so that at app. 3.2 kyr BP the climate was both colder and dryer than the modern one.

In the regions adjacent to the Sayan and Tuva, similar climatic changes were reconstructed for the Holocene, including the most humid conditions in the middle Holocene and increasing aridity in the late Holocene. Thus, based on the multi-proxy studies of the Hoton-Nur basin in northwest Mongolia, Tarasov et al. (2000) and Rudaya et al. (2009) reconstructed an increase in humidity of climate 10.0-10.5 kyr BP, when a transition from steppe to forest steppe occurred in the area, and the beginning of rapid aridization at about 4 kyr BP. In the Baikal region, the transition from more humid conditions to more arid and continental climate took place 6-7 kyr BP (Bezrukova et al. 2014; Reshetova et al. 2013; Sharova et al. 2015). A somewhat different sequence of climate changes was reconstructed for the area west of the Baikal Lake. According to the palynological data on the Khall lake sediments (Bezrukova et al. 2013), 5 to 4 kyr BP the precipitation in the region was higher than today. A subsequent aridization reached its maximum approximately 2.5 kyr BP. Dry conditions persisted there during the entire Late Holocene, with the only increase in humidity 700 to 450 years ago. Dirksen et al.

(2007) reconstructed changes in humidity of climate during the Holocene using pollen data on the sediments of two lakes in the Minusinsk depression and on the Yenisei River floodplain. They distinguished two main phases, a dryer early one 11.7-7.6 kyr BP, and a later more humid phase after 7.6 kyr BP. Within the latter, two relatively dry intervals were identified: 3.6-2.8 kyr BP and 1.5 kyr BP – present (Dirksen et al. 2007).

Therefore, according to the majority of reconstructions, within the mountain regions of Southern Siberia and in the adjacent region of Central Asia three main climatic phases can be distinguished within the Holocene. The Early Holocene was characterized by low temperatures and humidity; the Middle Holocene climate was both the warmest and the most humid. The time of transition to the third phase differs considerably over the larger area, but in the Altai, Sayan, and Tuva Mts. the climate amelioration of the Middle Holocene gave way to a cooling along with increasing continentality and aridity in the last 5.5-5.0 kyr BP. These processes became especially pronounced after 2.0 kyr BP. They brought about the decline of forest and a greater spread of steppe vegetation.
However, the data on short-term climatic oscillations in the late Holocene for this territory are still scarce.

STUDY AREA

Physiography and vegetation

A promising method for studying landscape and climatic changes of the multicentennial rank is a detailed pollen analysis of sediments with a stable accumulation regime, with high contents and good preservation of microfossils, reliably dated by radiocarbon method. As a research object, we chose a section of the lake and mire sediments at the shore of the Tere-Khol Lake in southeastern Tuva (Fig. 2).

Tere-Khol Lake is situated in the intermountain depression of the same name (50°37´N, 97°24´E). The bottom of the Tere-Khol depression lies at the height of about 1300 m above sea level, within the belt of mountain larch and larch-Siberian pine forests. The Tere-Khol depression is located at the transition between the forest and steppe zones, near the southern boundary of the permafrost. Permafrost exists in the bottom of the Tere-Khol basin due to the average annual temperature of -6°C, severity and low snowiness of winters. Part of the basin around the lake and along the rivers flowing from it is paludified and covered by reed, sedge and grass swamps and shrub thickets (mainly of *Salix* spp.). Larch forests of *Larix sibirica* with well-developed shrub and grass layers, as well as meadows, stretch along rivers and streams. Spruce-larch forests cover the southern shore of the lake. The slopes of the mountains surrounding the Tere-Khol depression are occupied with larch forests with the participation of *Pinus sibirica*. In the lower parts of the steep southern slopes and on well-drained patches of the bottom of the depression, steppe communities with rich species composition of forbs are developed (Sobolevskaya 1950). The upper limit of the belt of Siberian pine-larch forests on the Sangilen ridge, lying to the south of the depression, is situated at altitudes of 2200-2300 m above sea level (Koropachinski 1975). Above this belt the mountain tundra with areas of subalpine shrubs and alpine meadows occur.

Panin et al. (2012) studied the history of the development of the Tere-Khol Lake in the Holocene. Based on the multi-proxy data on lake sediments, they distinguished three intervals of high water level and three intervals of low water level, including the one from 2000 to 100 years ago, corresponding to the maximum aridity of climate for the entire Holocene. Overall, the 20th century was marked by a greater water supply to the lake. N.S. Bolikhovskaya performed a pilot palynological study of the upper 120 cm of the Tere-Khol Lake sediments accumulated since approximately 6 kyr BP (Bolikhovskaya and Panin, 2008). The composition of the pollen spectra indicate predominance of mountain taiga similar to the modern vegetation in the Tere-Khol depression. Changes in participation of species characteristic of subalpine and mountain steppe communities reflect short-term changes in temperature and humidity.

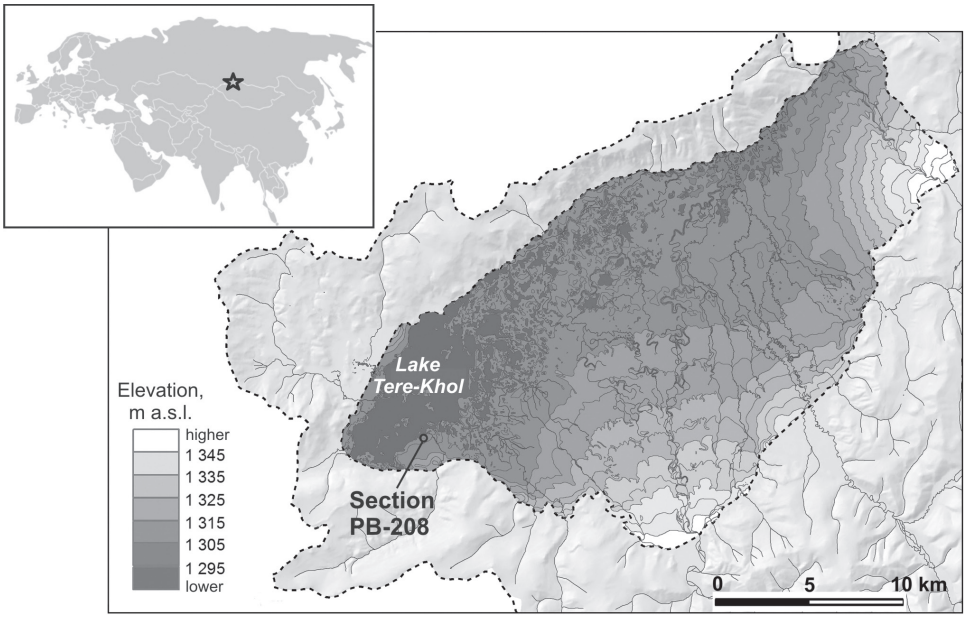

Fig. 2. Location map of Lake Tere-Khol and section PB-208

Unfortunately, the shallowness of the lake (average and maximum water depth are 0.6 m and 2.0 m respectively) provides conditions for its freezing to bottom during the most severe winters. Therefore, the upper part of lacustrine deposits may have been subject to repeated freeze/thaw cycles in the past that could cause sediment mixing. That is why the lacustrine sediments cannot provide a reliable archive for detailed reconstructions of the Late Holocene.

Study site

To study the Late Holocene environmental changes, we selected section PB-208 (50.61032N, 97.40346E) located 50 m from the southern bank of Lake Tere-Khol 1.5 m above its water level (Fig. 2).

In the upper part, section PB-208 includes dark-brown highly decomposed grass and sedge peat with abundant fragmented and entire shells of terrestrial Gastropods without visible mineral admixture, except for a single interlayer containing fragments of schist 6x3x0.3 cm at the depth of 32 cm. The debris were probably brought to the site by lake ice during a spring flood. Total thickness of peat is 49 cm. Underlying deposits are lacustrine sandy silt. Below the depth of 80 cm sediments are permanently frozen.

METHODS

26 samples from section PB-208, 1 cm thick each, at 2 to 3 cm intervals, were subsampled for pollen analysis and processed using the pollen extraction technique of Grichuk (1940): the processing included heavy liquid (cadmium iodine) separation. A minimum of 400 pollen grains and spores per sample was counted. Relative frequencies of pollen of trees and shrubs were calculated based upon the arboreal pollen sum (AP) to make it easier to trace changes in the composition of forest and shrub communities. Pollen percentages of herbaceous plants were based upon the non-arboreal pollen sum (NAP), and those of aquatic plants were based upon the total terrestrial pollen sum, as well as percentages of spores.

Geochronology of the section was established by radiocarbon method (Table 1). Three accelerated mass-spectrometry (AMS) dates on macrofossils and one AMS date on total carbon (TOC) from lacustrine silts were produced in the Institute of Geography RAS (lab index IGANAMS). At the base of peat layer, one scintillation date was provided by the Saint-Petersburg University laboratory (index LU). The dates have been calibrated using OxCal v 4.3.2 (Bronk Ramsey, 2017) and IntCal13 atmospheric curve

(Reimer et al. 2013). Age-depth model was calculated and visualized in OxCal v 4.3.2 (Bronk Ramsey, 2017).

RESULTS

The series of radiocarbon dates from section PB-208 (Table 1) permitted to construct the age-depth model (Fig. 3), which shows that the accumulation of peat below the depth of 10 cm and underlying sandy loam occurred at a rather constant rate of 0.27 mm/yr (26.7 cm per 1000 years). Extrapolation of this rate to the bottom of the section (80 cm) provides the estimation of the total duration of sedimentation at 2.8 thousand years.

Table 1. Radiocarbon dates and calibrated ages for the PB-208 section

Depth, cm	Dated material	^{14}C age	Cal BP* ±1σ	Cal BC/AD, yr	Lab. No.
9.5	plant macrofossils	40±20	75±60	AD 1875±60	IGANAMS-5170
25.5	plant macrofossils	670±20	625±40	AD 1325±40	IGANAMS-5171
38.5	plant macrofossils	1160±20	1085±55	AD 865±55	IGANAMS-5172
48-49	peat	1680±100	1595±120	AD 355±120	Lu-6052
57.5	gyttja (TOC)	1950±20	1900±25	AD 50±25	IGANAMS-5173

**counting from AD 1950*

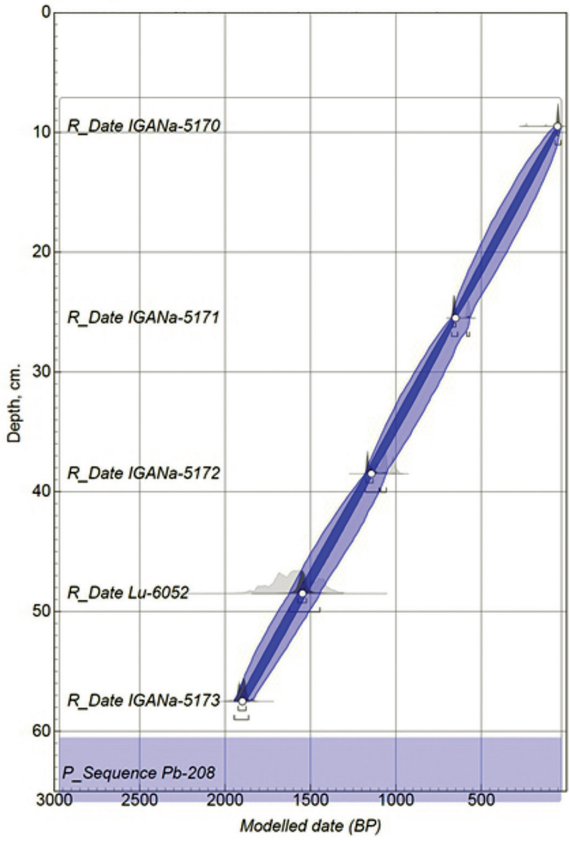

Fig. 3. Age-depth model for the PB-208 section

Based on the changes in the composition of the pollen spectra in section PB-208, we identified six local pollen zones (LPZ) (Fig. 4).

Among arboreal pollen (AP), *Pinus sibirica* and *P. sylvestris* pollen dominate. The latter does not grow in the Tere-Khol depression; the part of its modern range closest to the site is about 100 km to the north (Sokolov et al. 1977). Pollen of *Abies sibirica* occur in minor quantities throughout the entire sequence. Its present geographical range in Tuva is similar to that of Scots pine. Pollen contents of spruce are relatively stable (5-7% of AP) and are adequate to the role of *Picea obovata* in the local vegetation, where it participate larch and mixed taiga forests.

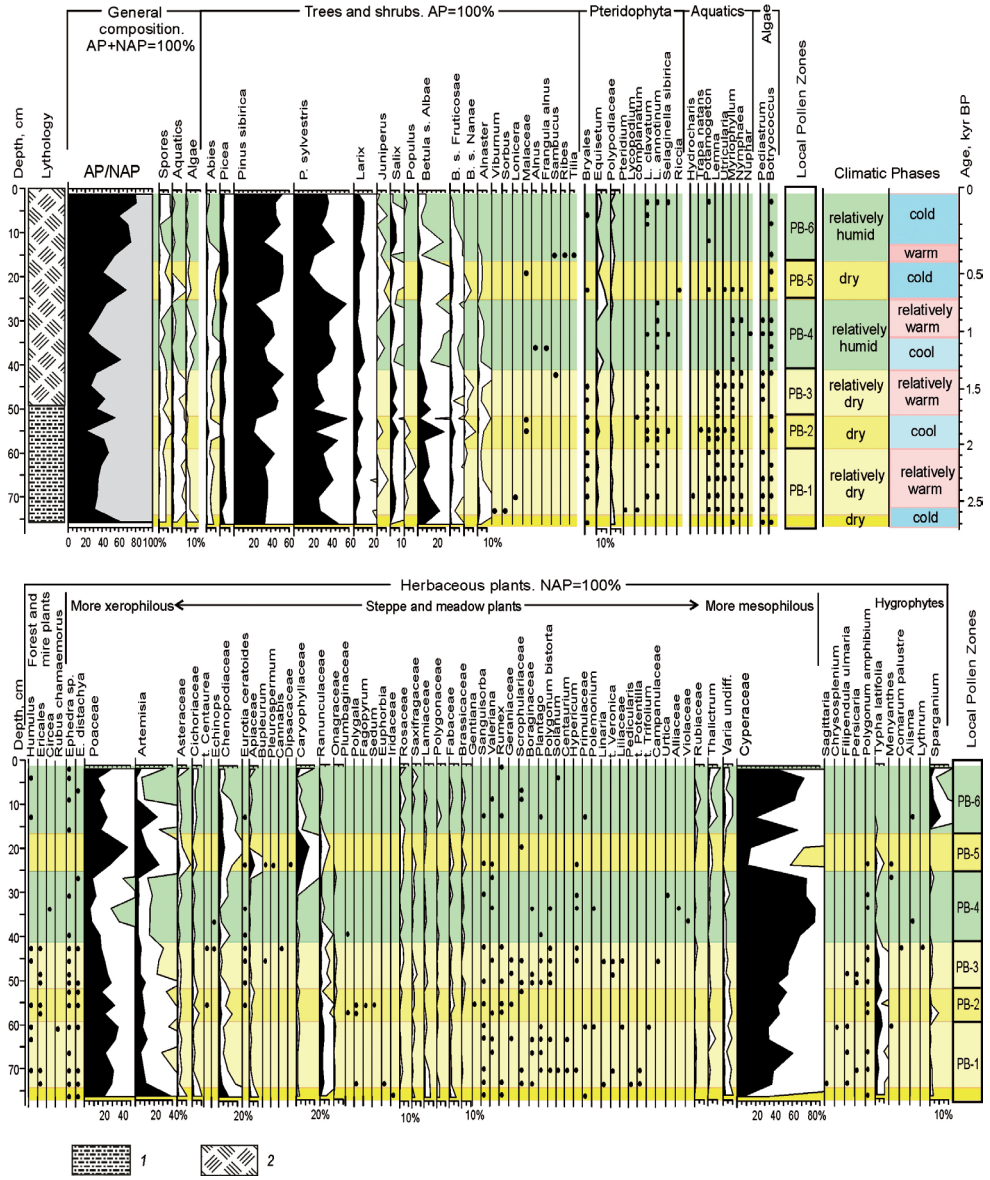

Fig. 4. Section PB-208 percentage pollen diagram. Clear curves represent x5 exaggeration of base curves. Analyses by O. Borisova. 1 – silt and sandy silt deposits, 2 – grass and sedge peat

Low resistance of larch pollen to deterioration in the sediments is probably the main cause of relatively low percentages of *Larix* in pollen spectra. The content of *Larix* pollen in the surface sample of section PB-208 is only 5% of AP, although *L. sibirica* dominates in the forests on the slopes of the Tere-Khol depression. In general, the composition of pollen and spores throughout the section reflects a predominance of mountain taiga similar to modern vegetation in this area. Changes in the abundance of pollen of the main forest-forming species (*Larix, Pinus sibirica, Picea, Betula* sect. *Albae,* etc.), in combination with pollen of microthermal shrubs (*Betula* sect. *Fruticosae, Alnaster fruticosus, Juniperus* spp., etc.), or more thermophilous species of trees and shrubs, allow tracing the altitudinal shifts of the vegetation belts caused by relative warming or cooling.

In the layers with the highest abundance of the non-arboreal pollen (NAP) (up to 40-60%), 60-75% belong to Cyperaceae family, which is probably locally produced by species of sedges growing on the waterlogged ground along the water margin. Poaceae pollen is also abundant (20-30% of NAP). The presence of phytoliths of the characteristic shape suggests that a considerable part of the grass pollen in the lower, sandy clay part of the section might belong to reed (*Phragmites communis*), still widely spread on the shores of the Tere-Khol Lake. Among NAP, there are quite high contents of Chenopodiaceae and *Artemisia*. Presence of pollen of typical xerophytes (*Ephedra, Eurotia ceratoides, Polygala,* etc.) indicate that there were mountain steppe communities on south-facing slopes. A great variety of NAP species indicates that during drier phases, meadows and meadow-steppes occupied larger part of the depression than at present. During the relatively humid phases, the participation of more mesophilous herbaceous plants in the steppe communities increased.

The presence of pollen of aquatic plants typical of stagnant and weakly flowing shallow lakes (*Lemna, Myriophyllum, Potamogeton, Utricularia, Nymphaea,* etc.), algae (*Pediastrum* and *Botryococcus*), and various hygrophytes (*Typha latifolia, Sparganium, Polygonum amphibium* and other) in LPZ PB-1-3 indicates that the accumulation of sediments took place in the coastal part of the lake, which at that time extended farther inland at the site. Changes in the composition of the pollen of hydro- and hygrophytes reflect the process of shallowing and overgrowing of the marginal part of the lake and the formation of the mire, where about 1.7 kyr BP the accumulation of peat has begun.

The composition of AP in LPZ PB 1-3 suggests that larch forests occupied then not only the slopes of the Tere-Khol depression, but also a considerable part of its bottom. On the sufficiently humid and fertile soil, spruce participated in these forests. Siberian pine grew in the upper part of the mountain forest belt, as at the present time. The role of tree birch in the taiga forest composition was then greater than at present. Along the rivers, on the margins of the mires, and in the forest undergrowth, *Betula* sect. *Fruticosae* and, more seldom, *Alnaster fruticosus*, occurred. Pollen of these microthermal shrubs could be transported to the site from the subalpine belt of the Sangilen mountains. Rare pollen grains of *B.* sect. *Nanae*, yet another shrub which grows in the subalpine and alpine belts, occur in the lower part of section PB-208.

In the upper part of the section (LPZ PB-4-6), the pollen percentage of tree birch, characteristic of the lower part of the forest belt in the region, decreases, while the amount of larch pollen increases. The pollen content of *Pinus sibirica*, which forms the upper treeline in the mountains of the region, also increases. In this part of the section, the pollen of *Juniperus* is constantly present. Both species of juniper, characteristic of the region (*J. sibirica* and *J. pseudosabina*), grow in subalpine Siberian pine and larch woodlands and on stony patches in high mountains. Overall, these changes are indicative of the colder conditions compare to the lower part of the section.

LPZ PB-4 is characterized by the largest

content of *Pinus sylvestris* pollen, the increase of Cyperaceae pollen (up to 80% of NAP) and diversity of forbs, as well as by the presence of pollen of mesophilous arboreal species (*Alnus* and *Frangula*). Relatively thermophilous aquatic plants, such as *Nymphaea* and *Nuphar*, also occurred at the site.

At the transition from LPZ PB-4 to PB-5, the proportion of Cyperaceae pollen decreased sharply (to 15% от NAP), and the pollen of *Artemisia* and Poaceae reached their highest abundances for the entire sequence. The proportion of Chenopodiaceae, Asteraceae, Apiaceae, Caryophyllaceae, and Ranunculaceae also increased. Within LPZ PB-5, pollen of typical steppe xerophytes (*Eurotia ceratoides, Bupleurum,* and *Pleurospermum*) occur. Larch pollen curve decline, while pollen of *Betula* sect. *Nanae* and *Alnaster fruticosus* is registered here again. Probably, the water content at the mire decreased, as of the plants growing on the waterlogged peaty ground only pollen of *Sparganium, Alisma plantago-aquatica* and *Equisetum* spores are found in this layer. These changes in pollen spectra indicate dry and cold conditions and increasing role of the mountain steppe communities at the site.

In the lower part of LPZ PB-6, rare pollen grains of relatively thermophile shrubs *Sambucus* and *Ribes*), as well as a single pollen grain of *Tilia*, were registered. The proportion of AP reaches its maximum for the entire sequence – 80% of the total terrestrial pollen. In the upper part of the zone, pollen curves of *Abies, Picea*, and *Betula* sect. *Albae* decline. The role of Siberian pine in the larch communities increased, as suggested by the highest proportion of *Pinus sibirica* pollen for the entire sequence (up to 50% of AP). Cyperaceae pollen contents rise again almost to the level of LPZ PB-4, while percentages of *Artemisia* decrease sharply. Pollen of meadow and steppe herbaceous plants of Caryophyllaceae, Asteraceae, Apiaceae, Cichoriaceae, Rosaceae, and other families occur in this layer, but the diversity of forbs here is lower than in LPZ PB-1-3. Proportion of *Artemisia* pollen in LPZ PB-6 is up to 5% of NAP; rare pollen grains of Chenopodiaceae and *Ephedra* are also registered there. Of plants growing on the moist ground, pollen of *Sparganium* and *Alisma plantago-aquatica*, as well as spores of *Equisetum* and club moss species, *Lycopodium clavatum* and *L. annotinum,* are found.

DISCUSSION AND CONCLUSIONS

The boundary position of the site in combination with altitudinal belts and exposure differences in vegetation associated with the mountain relief of the surrounding area lead to a distinct reflection of low-amplitude and short-term climatic variations in the composition of pollen spectra.

Changes in vegetation in the Tere-Khol depression and surrounding mountains over the last 2.8 thousand years, reconstructed from the palynological data on section PB-208, reflect the alternation of wetter and drier phases and relative warmings/coolings lasting several hundred years each, which occurred against the general background of cold and dry climate of the Late Holocene. The formation of deposits in the lower part of the section (up to about 1350 yr BP) occurred in more arid conditions than modern ones. The drier phases several hundred years long were at the same time colder, which means an increase in the continentality of climate during these intervals. The most dry and cold conditions are reconstructed for the earliest part of the sequence (LPZ PB-1, 2.8-2.6 kyr BP).

At the time of peat accumulation in the upper part of the section (LPZ PB-4-6) (1350 yr BP – present), the reconstructed conditions were generally colder than during the previous part of the Late Holocene. During this period, the correspondence of the phases of cooling and drying mentioned above altered: the cooler intervals partly corresponded to relatively moist conditions. The duration of warm phases decreased with increasing differences between warm and cold intervals. The most pronounced dry and

cold phase was from 700 to 400 yr BP (LPZ PB-5). This interval separated two relatively warm and humid phases: from 1100 to 700 yr BP and from 400 to 250 yr BP. The lessening of the climate continentality during the warm phases is emphasized by the largest content of *Pinus sylvestris* pollen, by the presence of pollen of mesophilous shrubs and forbs. In the last 250 years, there has been a new cooling, although it was not accompanied by noticeable aridization. The composition of the pollen spectra in LPZ PB-6 shows that the modern climate differs from the cryoxerotic phase 700-400 years ago by less seasonality and slightly higher humidity of climate.

Thus, changes in the vegetation cover in the Tere-Khol depression and in surrounding mountains over the last 2.8 thousand years, reconstructed from the palynological data from section PB-208, reflect the alternation of wetter and drier phases, as well as relatively warm and cold phases, that were several hundred years long, in the context of the cold dry climate of the Late Holocene (see Fig. 4).

Comparison of the short-term oscillations reconstructed for the Tere-Khol depression (SE Tuva mountains) with other reconstructions obtained for the Late Holocene in the Altai-Sayan-Tuva region shows certain common features. Thus, palynological data on the Uzun-Kol Lake situated in the central Altai (Blyakharchuk et al. 2004) indicate an arid phase 1.7 to 1.3 kyr BP and the cooling accompanied by drying after 700 years ago. The climate reconstructions based on the Lake Teletskoye pollen record (NE Altai Mts) (Rudaya et al. 2016) show that a short period of cooling occurred between 1.4 and 1.3 kyr BP. Lower July temperatures are also reconstructed for 0.55-0.2 kyr BP; however, a general cooling trend that led to this minimum began about 0.85-0.8 kyr BP. Blyakharchuk and Chernova (2013), based on the palynological data on the Lugovoe Mire in the West Sayan Mts, reconstructed two dry intervals, 2.2-1.5 kyr BP and 0.7-0.2 kyr BP. These dry phases are similar to the ones reconstructed in this study for SE Tuva. Agatova et al. (2012) identified two main stages of the glaciers' advance in the SE Altai Mts: 2.3-1.7 kyr BP and 0.7-0.15 kyr BP. They pointed out that the thermal minimum in the middle of 19th century was the greatest in the last millennium. The beginning of *pingo* formation in the Chuya Depression in central Altai is dated to 2.25 kyr BP (Blyakharchuk et al. 2004), thus indicating the Late Holocene stage of permafrost aggradation.

The warmings/coolings and oscillations of humidity reconstructed from the palynological data on section PB-208 are depicted in Figure 5 on the time-scale to facilitate their comparison with the temperature reconstruction for the Northern Hemisphere by Moberg et al. (2005) and with the proxy-data, which reflect both the short-term climate changes and their probable drivers.

According to the estimations of Northern Hemisphere mean temperature variations by Moberg et al. (2005), the highest temperature for the past two thousand years was reached between AD 1000 and 1100, during the so-called "Medieval Warm Period", and the greatest cooling occurred around AD 1600, during the "Little Ice Age" (Fig. 5a). Based on the similarity of the paleotemperature curves and changes in the intensity of solar radiation reconstructed from the contents of 14C and 10Be isotopes (Wanner et al. 2008), it can be assumed that the temperature fluctuations were mainly due to the changes in solar activity (Fig. 5c). Bond et al. (2001) demonstrated that ice rafted debris (IRD) were deposited in the North Atlantic by southerly drifting icebergs. Higher IRD numbers indicate cooler time intervals, often called "Bond events" (Fig. 5d).

Warm/cold fluctuations, reconstructed from palynological data on section PB-208, are similar to those described above in their direction, duration and time of manifestation, but less pronounced.

Comparison of paleoclimate records with climate forcing time series suggests that changes in insolation related both to Earth's orbital variations and to solar

variability played a central role in the global scale changes in climate of the Holocene (Mayewski et al. 2004). Solar variability (fluctuations in solar output) superimposed on long-term changes in insolation (Bond et al. 2001; Mayewski et al. 2004) seems to be the most likely forcing mechanism for the rapid climate changes.

Data on changes in the isotope composition of oxygen in the calcite of stalagmite from the Dongge cave in southern China (Wang et al. 2005) with a high (up to one-year) time resolution show that, apart from the decrease of the monsoon strength from 7.0 to 0.5 kyr BP, separate episodes of a particularly severe fall in the Asian monsoon activity occurred in phase with the ice-rafting events in the North Atlantic (Wang et al. 2005; Wanner et al. 2008). The relatively humid/dry phases inferred from the PB-208 pollen record, which manifested themselves against the general background of climate aridization in the mountainous regions of southern Siberia in the Late Holocene, correspond fairly well to the phases of Asian monsoon strengthening/weakening.

ACKNOWLEDGMENTS

This study contributes to the Russian Academy of Sciences Fundamental Research Program, State Task 0148-2019-0005 and to the Russian Foundation for Basic Research Project 19-05-00863.

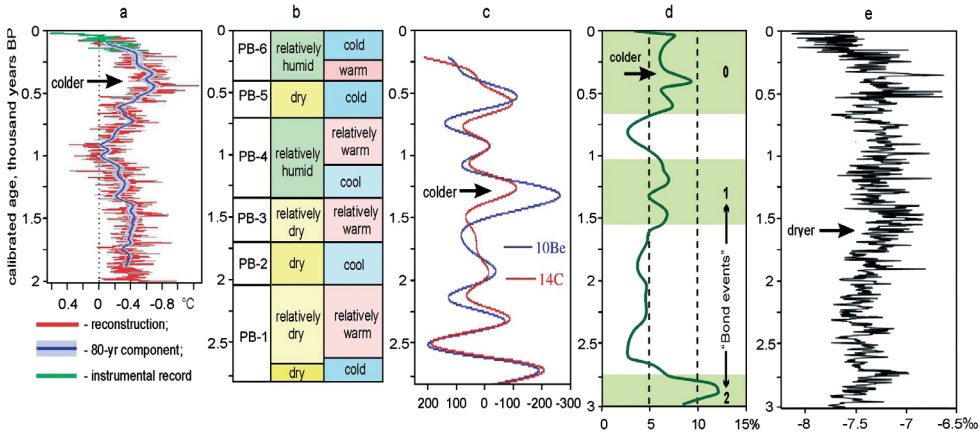

Fig. 5. Short-term climatic oscillations in the late Holocene indicated by different paleodata. a. Multi-proxy reconstruction of Northern Hemisphere mean temperature variations AD 1–1979 with its >80-yr component AD 133–1925, and the instrumental record (Moberg et al. 2005); b. Fluctuations in temperature and humidity inferred from palynological data on section PB-208; c. Reconstructions of the solar activity (in relative units) based on ^{10}Be concentrations measured in the GRIP ice core and ^{14}C production rate (Wanner et al. 2008); d. Changes in the quantity of the ice rafted debris in North Atlantic (Bond et al. 2001); e. Oxygen isotope record from Dongge Cave speleothem in southern China (Wang et al. 2005)

REFERENCES

Agatova A.R., Nazarov A.N., Nepop R.K., and Rodnight H. (2012). Holocene glacier fluctuations and climate changes in the southeastern part of the Russian Altai (South Siberia) based on a radiocarbon chronology. Quaternary Science Reviews 43, 74–93.

Bezrukova E.V., Belov A.V., Letunova P.P., and Kulagina N.V. (2014). The response of the environment of the Angara-Lena Plateau to global climate change in the Holocene. Russian Geology and Geophysics 55 (4) pp. 463–471.

Bezrukova E.V., Letunova P.P., Kulagina N.V., Sharova O.G. (2013). Environment and landscape's reconstruction of the Priolkhon region based on the data of lacustrine sediments. Evraziya v Kainozoe. Stratigrafiya, Paleoekologiya, Kul'tury, vol. 2, pp. 19–25 (in Russian).

Bezrukova E.V., Schetnikov A.A., Kuzmin M.I., Sharova O.G., Kulagina N.V., Letunova P.P., Ivanov E.V., Krainov M.A., Kerber E.V., Filinov I.A., and Levina O.V. (2016). First data on changes in the environment and climate of the Zhombolok volcanic district (Eastern Sayan) in the middle-late Holocene. Doklady Akademii nauk 468 (3), pp. 323–327 (in Russian).

Blyakharchuk T.A. (2008). Reconstructing the vegetation of forest and alpine-steppe landscapes in the southwestern part of Tuva since the Late Glacial period till the present. Geography and Natural Resources 29 (1), pp. 57–62.

Blyakharchuk T.A., Wright H.E., Borodavko P.S., van der Knaap W.O., and Ammann B. (2004). Late-glacial and Holocene vegetational changes on the Ulagan high-mountain plateau, Altai Mountains, southern Siberia. Palaeogeography, Palaeoclimatology, Palaeoecology 209, pp. 259–279.

Blyakharchuk T.A., Wright H.E., Borodavko P.S., van der Knaap W.O., and Ammann B. (2007). Late Glacial and Holocene vegetational history of the Altai Mountains (southwestern Tuva Republic, Siberia). Palaeogeography, Palaeoclimatology, Palaeoecology 245, pp. 518–534.

Blyakharchuk T.A. and Chernova N.A. (2013). Vegetation and climate in the Western Sayan Mts, according to pollen data from Lugovoe Mire as a background for prehistoric cultural change in southern Middle Siberia. Quaternary Science Reviews 75, pp. 22–42.

Bolykhovskaya N.S. and Panin A.V. (2008). Dynamics of the vegetation cover in the Tere-Khol depression (southeastern Tuva) in the second half of the Holocene. Palynology: Stratigraphy and geoecology. Proceedings XII All-Russian Palynological Conference, Sept. 29 – Oct. 4, 2008, St. Petersburg, vol. II. VNIGRI, St. Petersburg, pp. 69-75 (in Russian).

Bond G., Kromer B., Beer J., Muscheler R., Evans M., Showers W., Hoffmann S., Lotti-Bond R., Hajdas I., and Bonani G. (2001). Persistent solar influence on North Atlantic climate during the Holocene. Science 294, pp. 2130–2136.

Bronk Ramsey C. (2017). Methods for summarizing radiocarbon datasets. Radiocarbon 59 (2), pp.1809–1833.

Dirksen V.G., van Geel B., Koulkova M.A., Zaitseva G.I., Sementsov A.A., Scott E.M., Cook G.T., van der Plicht J., Lebedeva L.M., Bourova N.D., and Bokovenko N.A. (2007). Chronology of Holocene climate and vegetation changes and their connection to cultural dynamics in Southern Siberia. Radiocarbon 49 (2), pp.1103–1121.

Grichuk M.P. (1960). General features of the history of nature of the middle part of the Yenisei and Ob basins and their significance for the Quaternary sediment stratigraphy. In: Materialy po istorii Krasnoyarskogo kraya. Gosgeoltekhizdat, Moscow, pp. 57–64 (in Russian).

Grichuk V.P. (1940). Method of treatment of the sediments poor in organic remains for the pollen analysis). Problemy Fizicheskoi Geografii 8, pp. 53–58 (in Russian).

Ilyashuk B.P. and Ilyashuk E.A. 2007. Chironomid record of Late Quaternary climatic and environmental changes from two sites in Central Asia (Tuva Republic, Russia) – local, regional or global causes? Quaternary Science Reviews 26, pp. 705–731.

Khotinski N.A. (1977). Holocene of North Eurasia. Nauka, Moscow (in Russian).

Koropachinski I.Yu. (1975). Dendroflora of the Altai-Sayan mountain region. Nauka SO, Novosibirsk (in Russian).

Mann M.E. and Jones P.D. (2003). Global surface temperatures over the past two millennia, Geophysical Research Letters 30 (15), 1820.

Marcott S.A., Shakun J.D., Clark P.U., and Mix A.C. (2013). A Reconstruction of Regional and Global Temperature for the Past 11,300 Years. Science 339, pp. 1198-1201.

Mayewski P.A., Rohling E.E., Stager J.C., Karlén W., Maasch K.A., Meeker L.D., Meyerson E.A., Gasse F., van Kreveld S., Holmgren K., Lee-Thorp J., Rosqvist G., Rack F., Staubwasser M., Schneider R.R., and Steig E.J. (2004). Holocene climate variability. Quaternary Research 62 (3), pp. 243–255.

Moberg A., Sonechkin D.M., Holmgren K., Datsenko N.M., and Karlén W. (2005). Highly variable Northern Hemisphere temperatures reconstructed from low- and high-resolution proxy data. Nature 433, pp. 613–617.

Panin A.V., Bronnikova M.A., Uspenskaya O.N., Arzhantseva I.A., Konstantinov E.A., Koshurnikov A.V., Selezneva E.V., Fuzeina Y.N., and Sheremetskaya E.D. (2012). Doklady Earth Sciences 446 (2), pp. 1204–1210.

Reimer P.J., Bard E., Bayliss A., Beck J.W., Blackwell P.G., Bronk Ramsey C., Buck C.E., Cheng H., Edwards R.L., Friedrich M., Grootes P.M., Guilderson T.P., Haflidason H., Hajdas I., Hatté C., Heaton T.J., Hoffmann D.L., Hogg A.G., Hughen K.A., Kaiser K.F., Kromer B., Manning S.W., Niu M., Reimer R.W., Richards D.A., Scott E.M., Southon J.R., Staff R.A., Turney C.S.M., and van der Plicht J. (2013). IntCal13 and Marine13 radiocarbon age calibration curves 0-50,000 years cal BP. Radiocarbon 55, 1869–1887.

Reshetova S.A., Ptitsyn A.B., Bezrukova E.V., Panizzo V., Henderson E., Daryin A.V., and Kalugin I.A. (2013). Vegetation of Central Transbaikalia in the Late Glacial and Holocene. Geografiya i Prirodnye Resursy 34 (2), pp. 172–178 (in Russian).

Rudaya N., Tarasov P., Dorofeyuk N., Solovieva N., Kalugin I., Andreev A., Daryin A., Diekmann B., Riedel F., Tserendash N., and Wagner M. (2009). Holocene environments and climate in the Mongolian Altai reconstructed from the Hoton-Nur pollen and diatom records: a step towards better understanding climate dynamics in Central Asia. Quaternary Science Reviews 28, pp. 540–554.

Rudaya N., Nazarova L., Novenko E., Andreev A., Kalugin I., Daryin A., Babich V., Li H.-C., and Shilov P. (2016). Quantitative reconstructions of mid- to late Holocene climate and vegetation in the northeastern Altai Mountains recorded in lake Teletskoye. Global and Planetary Change 141, pp. 12–24.

Sharova O.G., Bezrukova E.V., Letunova P.P., Kulagina N.V., Schetnikov A.A., Filinov I.A., Ivanov E.V., and Levina O.V. (2015). Vegetation and Climate of the Tankhoi Foothill Plain (Lake Baikal Southern Shore) over the Late Glacial and Holocene. Izvestiya Irkutskogo Gosudarstvennogo Universiteta. Seriya: Geoarkheologiya. Etnologiya. Antropologiya 11, pp. 86–102 (in Russian).

Sobolevskaya K.A. (1950). The vegetation of Tuva. AN SSSR Publ., Novosibirsk, 139 pp. (in Russian).

Sokolov S.Ya., Svyazeva O.A., and Kubli V.A. (1977). Distribution of trees and shrubs of the USSR, vol. 1. Nauka, Leningrad (in Russian).

Tarasov P., Dorofeyuk N., and Metel'tseva E. (2000). Holocene vegetation and climate changes in Hoton-Nur basin, northwest Mongolia. Boreas 29 (2), pp. 117–126.

Tchebakova N.M., Blyakharchuk T.A., and Parfenova E.I. (2009). Reconstruction and prediction of climate and vegetation change in the Holocene in the Altai-Sayan mountains, Central Asia. Environmental Research Letters 4 (4), 045025.

Wang Y., Cheng H., Edwards R.L., He Y., Kong X., An Z., Wu J., Kelly M.J., Dykoski C.A., and Li X. (2005). The Holocene Asian monsoon: links to solar changes and North Atlantic climate. Science 308, pp. 854–857.

Wanner H., Beer J., Bütikofer J., Crowley T.J., Cubasch U., Flückiger J., Goosse H., Grosjean M., Joos F., Kaplan J.O., Küttel M., Müller S.A., Prentice I.C., Solomina O., Stocker T.F., Tarasov P., Wagner M., and Widmann M. (2008). Mid- to Late Holocene climate change: an overview. Quaternary Science Reviews 27 (19-20), pp. 1791–1828.

Received on February 1st, 2019 Accepted on May 17th, 2019

Nadezhda G. Razjigaeva[1*], Larisa A. Ganzey[1], Ludmila M. Mokhova[1], Tatiana R. Makarova[1], Ekaterina P. Kudryavtseva[1], Alexander M. Panichev[1], Khikmat A. Arslanov[2]

[1] Pacific Geographical Institute FEB RAS, Vladivostok, Russia

[2] St.-Petersburg State University, St.-Petersburg, Russia

*** Corresponding author:** nadyar@tigdvo.ru

CLIMATE AND HUMAN IMPACT ON VEGETATION IN THE UPPER PART OF THE USSURI RIVER BASIN IN LATE HOLOCENE, RUSSIAN FAR EAST

ABSTRACT. Changes in vegetation in the southern Sikhote-Alin Mountains, which are in the upper reaches of the Ussuri R., are shown respond to minor climatic fluctuations over the past 5.4 ka. The largest mountain, Muta mire, chosen for paleoenvironmental reconstructions, is located within the main regional watershed. The studies include diatoms and pollen analyses. Chronology is based on radiocarbon dating and position of B-Tm tephra of the Millennium eruption of Baitoushan volcano. The cooling and warming reconstructed from the regional data correlate with global paleoclimatic events. The regional humidity changes notably along with the temperature fluctuations. Fire chronology was established and its significance for vegetation was estimated. Periods of frequent forest fires coincided with reduced moisture supply during cooling events. The analysis performed revealed a considerable human impact on the vegetation in the 20th century.

KEY WORDS: vegetation, climate changes, anthropogenic factor, forest fires, late Holocene, Sikhote-Alin

CITATION: Nadezhda G. Razjigaeva, Larisa A. Ganzey, Ludmila M. Mokhova, Tatiana R. Makarova, Ekaterina P. Kudryavtseva, Alexander M. Panichev, Khikmat A. Arslanov (2019) Climate And Human Impact On Vegetation In The Upper Part Of The Ussuri River Basin In Late Holocene, Russian Far East. Geography, Environment, Sustainability,
Vol.12, No 2, p. 162-172
DOI-10.24057/2071-9388-2018-44

INTRODUCTION

Short-term climate fluctuations are among the leading factors that controlled the landscape evolution in the late Holocene. In Primorye, human contribution to landscape changes started at the end of the 19th century when the first settlers started land cultivation. These processes included deforestation, forest fires, housebuilding, agricultural land use, and mining. Secondary forests and shrub communities increased in importance (Kurentsova 1973). Geoarcheological data provided evidence of the human impact on the environments having longer history than formerly recognized (Vostretsov 2009). The earlier settlement of the region

since the late Neolithic led to environment transformation but, the scale of the changes was incomparable with modern impact.

The present paper is intended to display the response of mountain and river valley landscapes with late Holocene climate changes, and to find relative significance of natural and anthropogenic factors in the vegetation evolution.

The upper reaches of the Ussuri R., in the «Zov Tigra» National Park, have been chosen as the site of paleoenvironmental reconstructions (Fig. 1). The studies were concentrated on the Muta mire, the most extensive swamp (10×3 km) in the Sikhote-Alin mountains. The mire occupies a flat watershed separating the Ussuri River from the Milogradovka River basin, flowing into the Sea of Japan. The flattened, divide surface resulted from the river causing regressive erosion during a previous Pleistocene cold phase (Korotky 2010).

The reconstructions are based on a section in the northwest area of the mire. The biostratigraphic studies included diatom and pollen analysis. The methods and results were described in detail (Razjigaeva et al. 2018). Small charcoals and burnt cells of plants have been counted. The age determinations were based on radiocarbon dates obtained at St. Petersburg State University and on tephrostratigraphy. The radiocarbon dates were calibrated by OxCal 4.2 and IntCal13 curve (https://c14.arch.ox.ac.uk). The tephra was identified with microprobe analysis of volcanic glass studied in V.G. Khlopin Radium Institute, St.-Petersburg.

REGIONAL SETTING

The upper Ussuri River flows across an intermountain depression. The ridges surrounding the mire display a distinct altitudinal zonation: 1) Korean pine (Pinus koraiensis)–broadleaf forests: 530–800 m; 2) Korean pine–spruce–fir forests: 800–1100 m; 3) spruce–fir forests: 1000-1550 m; 4) woodland of Erman's birch and shrub pine: 1550–1700 m; 5) 'goltsy' and alpine tundra: above 1700 m (Kiselev and Kudryavtseva 1992). The mire is confined to 550–600 m a.s.l. The largest part of the mire is covered with open relict larch forest (*Larix olgensis*, Fig. 2), which is one of the largest (5000 hectares) in the Sikhote-Alin (Shishkin 1933).

The forests in the Ussuri valley have been disturbed by repeated fires (1924, 1929, the mid-1980s) (National… 2014). Traces of fire in the late 18th century, 1936, 1941, and 1948 were found on the Oblachnaya Mt. (Kiselev and Kudryavtseva 1992). The oldest fire could be climate-controlled; fires in the 20th century occurred due to human activities.

Ussuri River valley colonization began late in the 19th century. Settlements persisted until the mid-20th century and have been replaced by forb meadow. In the

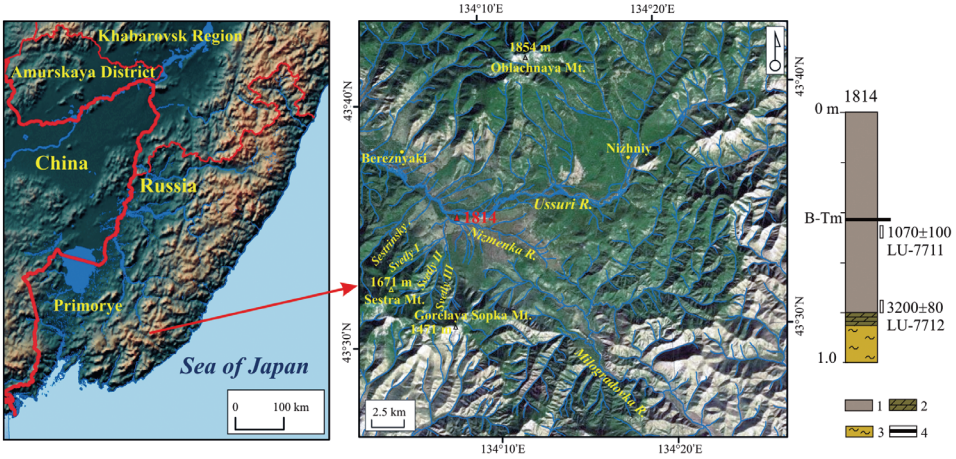

Fig. 1. Study area with position and construction of peatbog section

1950s-1970s, the region was explored for the geological surveys. The territory south of the mire was not subjected to human impact. Forest cutting continued from the 1970s until 2008 (National… 2014). The secondary forests are noted for a wide occurrence of Betula platyphylla.

The regional climate is continental with some monsoon features. The mean annual temperature is +0.4°C, the coldest month is January (–21.3°C) the warmest month is July (+18.1°C). The frost-free period is no more than 100 days. Mean annual precipitation is 760 mm, 80% of total falling during the warm period. The snow cover (from 5 to 67 cm) persists for 152 days. Northwest winds are dominant in winter (70%) compared to south-eastern in summer (39%). Foggy days are up to 52 per year (National… 2014).

RESULTS

Vegetation of the studied area

This area is larch forest with *Betula platyphylla*. The forest age may be estimated ~300-350 years. The understory includes *Betula ovalifolia, Alnus hirsuta* and *Ledum palustre*. The *Vaccinium uliginosum*, *Lonicera caerulea, Rubus arcticus* and *Rhododoccum vitis-idaea* occupy small hummocks. The grass is poorly developed (*Maianthemum bifolium, Galium boreale; Carex disperma, C. globularis, C. loliacea, C. minuta)*. The moss layer is dominated by *Sphagnum squarrosum with S. girgensohnii, S. angustifolium* and *Alaucomnium palustre. Oxycoccus microcarpus* is common on the mosses.

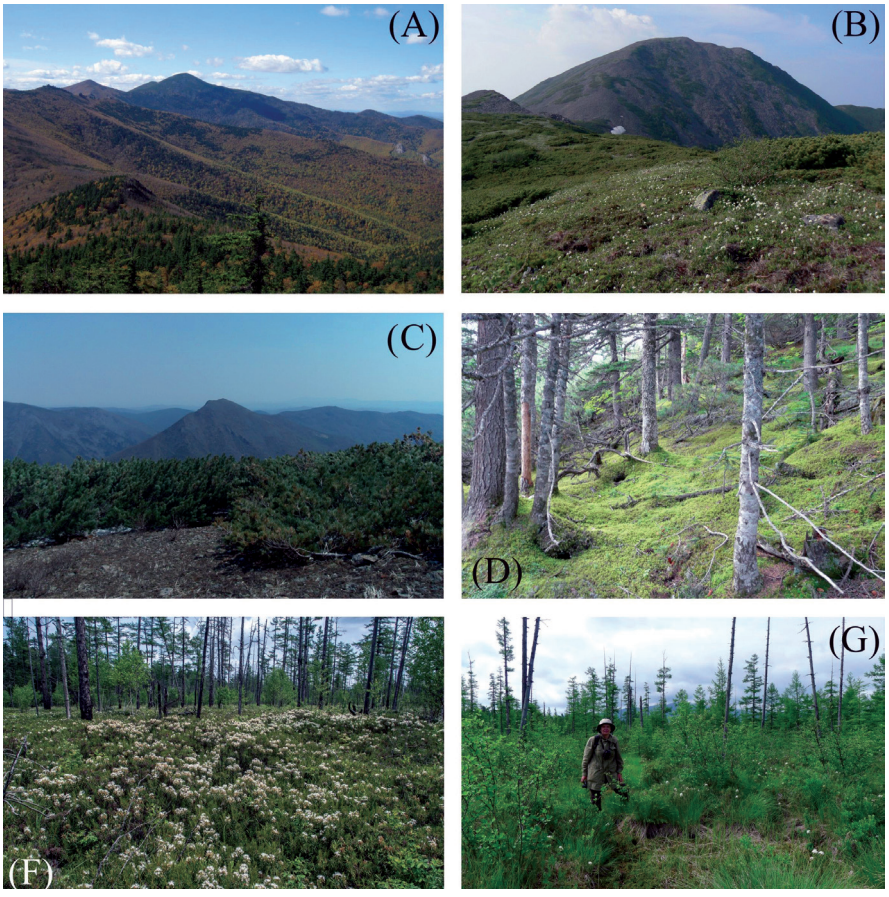

Fig. 2. Landscapes of Sikhote Alin: A– Ridge between Gorelaya Sopka and Sestra Mts., B –shrub pine and alpine tundra, Oblachnaya Mt., C – shrub pine near Snezhnaya Mt., D – fir-spruce forest, Oblachnaya Mt. (Photos of Yu. I. Bersenev); F, G – Muta mire

The age and accumulation rate of the peat

The lower part of the peat (0.35–0.80 m) is dark brown, compact, fairly decomposed, with herb remains. The upper part consists of yellowish-brown loose sphagnum peat (0.10–0.35 m) and moss mat (0–0.10 m). The base of the peat was dated at 3200±80 yr BP (3430±100 cal yr BP), LU-7712. A tephra horizon is correlatable with B-Tm tephra of the caldera-forming eruption of Baitoushan volcano in 946/947 AD (Chen et al. 2016). The tephra age is supported by ^{14}C date 1070±100 yr BP (1000±120 cal yr BP), LU-7711 obtained from the underlying peat. At the beginning the peat accumulation rate was 0.14 mm/yr; during the last millennium the rate rose to 0.35 mm/yr.

Changes in humidity

The diatom distribution permits distinguishing 9 stages in mire evolution which were controlled by the changes in atmospheric precipitation (Fig. 3, 4).

3780–3430 yr BP. Beginning of surface waterlogging and development of a shallow oligotrophic-dystrophic pond. Cosmopolitan *Eunotia praerupta* typical of northern bogs and mountain shallow lakes prevail, its optimal pH is 7.05.

3430–3080 yr BP. Moisture decreased. Benthic species most common. The dominant are benthic *Pinnularia crucifera*, and epiphyte *Eunotia glacialis,* typical of shallow ponds in the northern latitudes and in mountains. Planktonic and epiphytes – inhabitants of current water were brought by floods.

3080–2735 yr BP. Moisture supply reduced. Increasing proportion of *Pinnularia borealis* and *Hantzschia amphioxys* suggests occasional drought periods. Species brought by floods are decreased.

2735–2040 yr BP. The aridity is growing, as suggested by a low proportion of diatoms.

2040–1000 yr BP. The swamp gains water supply. The number of species indicating the overgrowth of the moss bog is increasing. The pH value most favorable for the dominant species is 5.6-6.5. Planktonic diatoms, presumably brought by strong floods, are more numerous.

1000–715 yr BP. The dominants inhabit hygrophilic mosses. On sphagnum bogs *Eunotia paludosa* prefers relatively dryer habitats (Nováková and Pouličková 2004). The peat bog rose above the ground water table and the role of atmospheric moisture

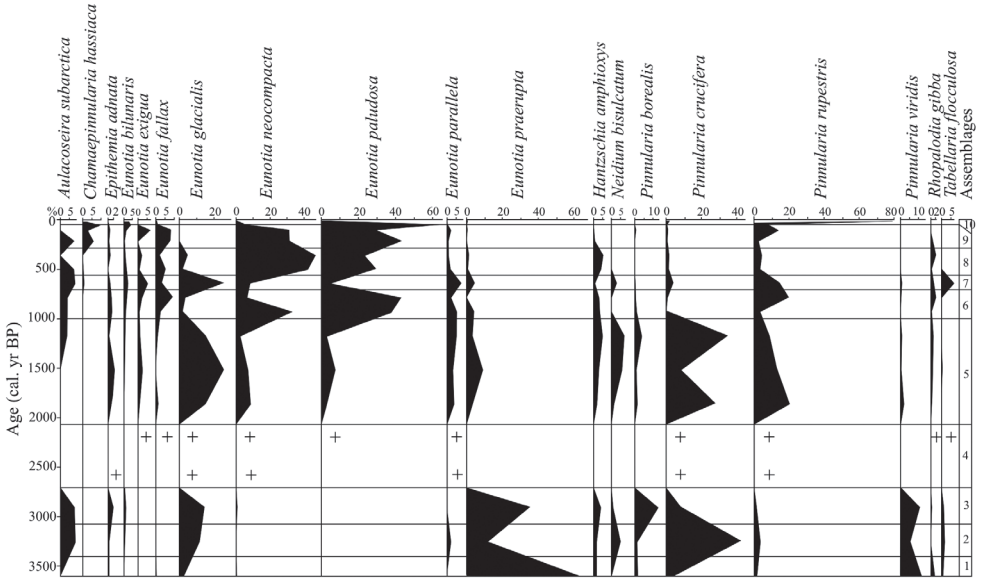

Fig. 3. Diatom percentage diagram of Muta peatbog plotted against the chronology

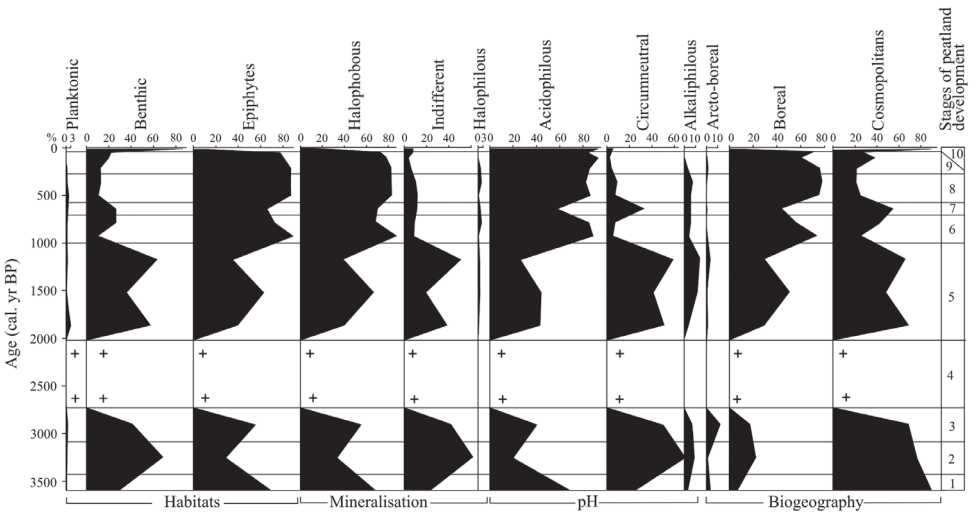

Fig. 4. Distribution of ecological groups of diatoms plotted against the chronology

supply increased.

715–570 yr BP. The environment became wetter and colder, open water patches rose in number and area. Hydrophilic diatoms increase in proportion, particularly those typical for oligotrophic ponds in the north and on mountains.

570–290 yr BP. Values of pH decreased to ~5.6. Planktonic *Aulacoseira granulata, A. italica, A. subarctica* were possibly brought to the mire during floods.

270 yr BP – the mid-20th century. The moisture supply is somewhat reduced. The species characteristic of flowing water disappeared. The usual inhabitants of moss bogs occur.

The late 20th – early 21st centuries. The moisture supply to the swamp increased. Proportions of *Eunotia bilunaris*, the species choosing wet sphagnum areas with pH 3.5, increase. *Pinnularia rupestris* increased rapidly. Usually this species becomes dominant in wetter places on sphagnum bogs (Nováková and Pouličková 2004).

Phases in the vegetation development

were reconstructed accordingly the pollen zones identified in the section (Fig. 5).

5410-4120 yr BP. The lower boundary of the coniferous forests was lower than modern ranges, possibly due to cooler climate than present. A wide occurrence of ferns may be attributed to forest fires. There was a short episode identified when fir pollen was proportion higher. At present, forests dominated by *Abies nephrolepis* occur in

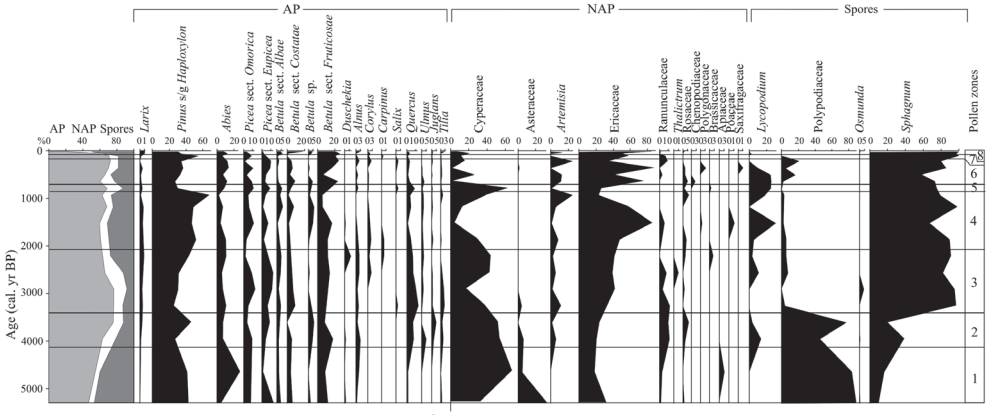

Fig. 5. Pollen percentage diagram of Muta peatbog plotted against the chronology

the upper forest zone only (Kiselev and Kudryavtseva 1992). It is possible that, those forests became widespread at the swamp periphery Pollen data indicates a development of sedge marsh with *Betula ovalifolia*. Wet meadows occurred in small patches.

4120-3430 yr BP. The swamp was encircled with forests of Korean pine and broadleaf trees, with fern cover. Valley forests had an abundance of walnut, elm, and alder. Spruce began to dominate in the dark coniferous forests. The second half of the interval was marked by increasing expansion of larch over the swamp. Sedge communities with Rosaceae and Ranunculaceae were dominant. The pollen of Rosaceae could have been partly transported from surrounding slopes. In the ground cover of coniferous-broadleaf forests Ranunculaceae was widely presented.

3430–2040 yr BP. The vegetation evolved further under conditions of decreasing temperature and moisture. *Picea koraiensis* increased in river valleys forests. Proportion of dark coniferous increased ~3025-2215 yr BP. Birch became more important in the forests, while the floodplain was actively overgrowing with willow. Hazel acquired a greater importance in the undergrowth. *Artemisia* was rising notably, which is a the plant usually found in dry forests of Korean pine with oak, and predominantly oak forests. Pollen of *Artemisia lagocephala* could be brought from stone taluses in the upper slopes. Brassicaceae pollen makes its appearance on the river banks. A cooling period accompanied with drying was recorded ~2620–2215 yr BP and was marked by *Betula ovalifolia* and Ericaceae increasing. The swamp began to be overgrown with larch and *Sphagnum*. *Duschekia* pollen indicates that the area of shrub alder (and possibly, of shrub pine) expanded at that time. The presence of *Carpinus* pollen suggests increasing intensity of southern winds at the beginning of summer. At present, the northern limit of *Carpinus cordata* is 40-50 km to the south.

2040–860 yr BP. Forests of Korean pine with broadleaf trees were dominant at elevations of ~500–600 m a.s.l. Sedges and sagebrush could also grow in the dry forests. The river terraces appear to be occupied by moist forests of Korean pine with elm, linden, and walnut. The lower boundary of spruce and fir forests was shifted upwards. In the swamp, the sedge presence was drastically reduced, while heather became more common; proportion of Ranunculaceae decreased, sagebrush expands on taluses.

860–715 yr BP. The environments became more favorable for broadleaf (primarily, oak) and white birch forests, which possibly replaced those of broadleaf trees and Korean pine. A reduced population of Korean pine could be the result of forest fires during the previous dryer interval. The subsequent increase in humidity favored an enlargement of fir-spruce. Alder forests and willow thickets developed in the valley. An increased humidity is suggested by a sharp increase in sedge content.

715–140 yr BP. Coniferous forests became dominant. The upper limit of the broadleaf–Korean pine forests went down below 500 m a.s.l. Oak apparently disappeared from the slopes surrounding the swamp. Willow and alder were still common in valley forests, and *Betula ovalifolia* and heather shrubs grew in the swamp. Presence of Saxifragaceae pollen suggests a wide occurrence of golets and stone streams on the mountain slopes. The source of pollen could be *Chrysosplenium* sp. which is typical of wet habitats near rivers. A high proportion of *Artemisia* pollen may be due to a wide occurrence of stone rivers spread over the territory until now. Slope processes were typically activated during coolings in the Holocene (Korotky et al. 1997). Chenopodiaceae pollen could be brought from either sandy banks or dry slopes.

The late 19th – early 20th centuries. Before an active cultivation of the Ussuri valley, the Korean pine forests were widespread in the region. The presence of *Carpinus* pollen agrees with prevalence of southern winds in early summer.

Since the 1950s the process of secondary forest development in places of tree cutting and fires is recorded in pollen assemblages

by lower AP content and a steep rise of the *Betula* pollen proportion. A reduced content of Korean pine and dark coniferous pollen seems to exhibit the timber cutter preferences with Korean pine, spruce and fir being cut first. Less spruce pollen could be partly attributed to the trees drying up (National… 2014). The broadleaf pollen content increases (up to 6%), though it is less than during the earlier warm phases. The oak pollen was most likely brought by wind from the Milogradovka basin, where *Quercus mongolica* is widely distributed up to 650 m a.s.l.

DISCUSSION

Climatic control of vegetation development

Small-magnitude Holocene climatic changes are receiving much attention (Borisova 2014; Mayewski et al. 2004; Wanner et al. 2008; 2011), as they present the most probable analogies to environmental changes that can be expected in the future under conditions of differing climatic trends. The warm intervals may be considered possible scenarios of the environmental evolution under conditions of global warming (Climates… 2010), while the latter seems to be the principal modern trend in the climatic regime of the Far East (Lobanov et al. 2014). The data obtained from regional responses to global events deserve special attention, as well as important information on the mountain landscape changes in response to minor climatic fluctuations.

The multi-proxy studies of peat revealed a considerable sensitivity of the upper Ussuri environments to the climate changes. This can be attributable to the altitudinal position of the mire and also to the swamp hydrological regime related to its position on a vast and flat watershed. The swamp was fed mostly by atmospheric precipitation, with groundwater being of secondary importance.

The wetlands became widely distributed since ~ 4120 yr BP. The swamp development due to warm and wet climate was recorded on the plateaus of the southern Sikhote-Alin, on large landslides surfaces, in river valleys, and on the coasts of the Sea of Japan (Korotky et al. 1997; Razzhigaeva et al. 2016a; 2017). It is possible that, the peat accumulation began earlier in the central part of the Muta mire where the peat layer is 1.5 m thick (Zhudova 1967). Sizeable portions of watershed could be eroded in the middle Holocene, when the river discharge was greater (Korotky et al. 1997).

There were several episodes of cooling and warming recorded in the peat and underlying loam during the late Holocene, which influenced the dynamics of wetland and mountain plant communities.

One of most important paleoclimatic event was global cooling ~5410–5170 yr BP occurrence (Borisova 2014), which was distinctly pronounced on the southern Far East (Korotky et al. 1997). As with other regions of East Asia (Wanner et al. 2011), it was marked by a decrease in the mean annual precipitation (by 100 mm below the present value); mean annual temperatures on the sea coast were 1–1.5°C below those of today (Korotky et al. 1997). The lower boundary of the coniferous forests near the Muta area was at least 100-150 m below its position at present.

The cooling correlate with the global cold event of ~2800-2600 yr BP was associated with low solar activity (Borisova 2014; Mayewski et al. 2004; Wanner et al. 2008, 2011) and did not result in considerable changes within the Korean pine – broadleaf forest belt at elevations of ~500 m a.s.l., apart from reduced proportion of broadleaf species in the forests. An increase in dark conifer pollen suggests a lowering of the fir-spruce forest boundary. As in studies of peatlands on the Shkotovskoe plateau, expansion of dark coniferous forests occurred then at ~700–750 m a.s.l. (Razzhigaeva et al. 2016a). The interval of ~3080–2735 yr BP was marked by drying, with forest fires becoming common in the region. The pyrogenic factor could partly account for a wide distribution of the shrub birch on the swamp (~2735–2390 yr BP) and birch and hazel on the mountain slopes. The maximum aridity on the swamp during

~2735–2040 yr BP was typical of the Far East south (Korotky et al. 1997; Razzhigaeva et al. 2016a, 2016b, 2017). Taking into consideration the ecological optimum of *Larix olgensis* (hygromesophytic plant, more thermophile than other larchs of the Far East (Urusov et al. 2007), it may be supposed that the sum of temperatures ≥10°C was no less than 1600°C, and the annual rainfall was at least 600 mm/year. A decrease of rainfall was particularly characteristic of Eastern Asia monsoon during that cooling period (Wanner et al. 2008, 2011).

The global cooling during ~1750–1350 yr BP was noted for abrupt and negative anomalies of temperature (Wanner et al. 2011). It was one of longest-lasting cold intervals in the late Holocene. In the Upper Ussuri R. basin, the role of Korean pine increased, and Korean pine-broadleaf forests were dominant at elevations of ~500-600 m a.s.l. It is quite possible that a part of the pollen identified as *Pinus* s/g *Haploxylon* could belong to the shrub pine that became more common above the tree line. The swamp became wetter and mosses were actively overgrowing it. Occasional findings of planktonic diatoms suggest episodes of floods. Two extreme floods have been dated at ~1640±70 yr BP and 1430±70 yr BP on the marine coast (Razzhigaeva et al. 2016b).

The Little Ice Age was noted for considerable changes in the forests in the Upper Ussuri basin when the dark coniferous forest zone expanded, along with open spaces on the mountain slopes. Broadleaf species reduced drastically and in all probability, oak disappeared completely from that part of the basin. Slope processes seem to become more active while stone streams and screes were widespread. Sphagnum mosses were widely distributed on the mire. As concluded from the diatom composition, the beginning of the Little Ice Age (715–570 yr BP) was the coldest period, which agrees with the data on the Sikhote-Alin (Razzhigaeva et al. 2016b; 2017). Strong floods happened in the upper reaches of the Ussuri ~715–430 yr BP.

Pronounced warming occurred in the region during the Subboreal optimum – a global climatic event (Borisova 2014). In the Primorye its magnitude was close to the Holocene optimum, though it was shorter. The mean annual temperature was 2.5-3°C above that of today (Korotky et al. 1997). In the Sea of Japan region the period was distinct for highly active summer monsoons (Yi 2011; van Soelen et al. 2016) and intensified cyclonic activity, including typhoons with heavy rains.

About 4120 yr BP the upper boundary of broadleaf forests with Korean pine was approximately 100-150 m above present-day position. Oak was common in the forests. Walnut, elm, and alder were widely spread in valley forests. On Shkotovskoe Plateau polydominant broadleaf forests with Korean pine and Korean pine–broadleaf forests occurred at ≥700–750 m a.s.l. (Razzhigaeva et al. 2016a). In the upper reaches of the Ussuri R. such vegetation persisted up to 3430 yr BP, in spite of lowered temperature (Korotky et al. 1997); although it is worthy of note that the time was close to the beginning of the global cooling ~3300–2500 yr BP (Wanner et al. 2011).

A short-term warm phase at the beginning of the Subatlantic has not been recognized in the upper reaches of the Ussuri R., though it is easily identifiable on the Shkotovskoe Plateau and on the coasts of Primorye (Razzhigaeva et al. 2016a, 2016b; Mikishin et al. 2008).

At the Medieval Warm Period, forests of Korean pine were widespread in mountains. A growing population of that species was recorded in other regions of the Primorye (Razzjigaeva et al. 2016a). A higher proportion of broadleaf trees in the forests has been recorded by the end of the Little Holocene Optimum. Mountain slopes around the swamp were overgrown with forests of oak and white birch. Increased presence of broadleaved trees, first of all oak, was noted in the south Primorye coasts at the end of the warm phase (950–790 yr BP). The Medieval optimum in the Ussuri upper reaches was noted for intensive floods, as witnessed by bogs diatom data.

Chronology of paleofires

An irregular distribution of charcoal fragments and burnt cells of plants over the peat section suggests a few periods with high frequency of forest fires. These were intervals ~3780–3430, 3080–2735, 2390–2040, and 1690–1000 yr BP. The intervals marked by fires correlate with regional chronology of pyrogenic events, which are confined to periods of droughts (mostly also to coolings). As to the neighboring regions of the Sikhote-Alin, the intervals of frequent fires were as follows: on the Sergeevskoe Plateau ~3670–3310 yr BP, 2620–2210 yr BP, 2130–1920 yr BP, 1600–1180 yr BP, 980–390 yr BP; on the Kit Bay coasts ~3800-3660 yr BP, 3380-3240, and 1430 yr BP (Razzhigaeva et al. 2016a; 2017).

Unlike other regions, no traces of forest fires datable to the Middle Ages have been found on Muta mire. It is possible that the swamp was inundated at that time. The anthropogenic factor was minor, as the environments in the intermountain depression were not favorable for human settlement during the Little Ice Age. Traces of fire activity in the upper part of the section are most probably attributable to the 1924 fire. A vast burnt area on the swamp with *Betula platyphylla* and *Alnus hirsuta* was studied in 1946 (Zhudova 1967). Fire in the mid-1980s destroyed forested area between Sestrinsky and Svetly creeks (National… 2014), though hardly damaged the Muta mire.

Significance of the human impact

A peat layer dated to ~1690–1350 yr BP appeared to contain *Ambrosia* pollen, which may be considered as a sign ancient human presence and its effect on the vegetation. The *Ambrosia* pollen presence in the Holocene sequences in Primorye is usually associated with the early man appearance and considered to be a sign of practiced agriculture (Kudryavtseva et al. 2018). Archeological sites of the paleo-metal epoch have been found in the Milogradovka R. upper reaches (National… 2014). At that time, the inner regions of Primorye were brought under cultivation by the Krownovskaya culture – bearers practicing agriculture (Vostretsov 2009).

The birch forests in the upper reaches of the Ussuri R. are young formations that existed as a result of area cultivation in the second half of the 20th century. Among the causes of their appearance were man-induced fires and forest felling; the primary objects of felling were Korean pine and dark conifers.

CONCLUSIONS

1. The wetland vegetation, as well as valley and mountain landscapes in the upper Ussuri basin, underwent considerable transformations through the last 5.4 ka with their dynamics being mostly controlled by climate.

2. This data allowed identification of cooling and warming periods that exerted primary control over the vegetation evolution. Both the temperature and the moisture supply were subject to noticeable changes. The flat surface was waterlogged at the beginning of the late Holocene, under conditions of higher temperature and humidity as compared with the present. The identified intervals of utter aridity coincided mostly with coolings.

3. Fires were one of the factors of change in biotic components. As shown from the data on the age of fires, the periods of increased frequency mostly coincided with reduced moisture supply during cooler periods.

4. The man-induced transformation of environments in the upper Ussuri reaches occurred in the 20th century. All the earlier changes in landscapes may be attributed to natural causes.

ACKNOWLEDGEMENTS

The authors are grateful to Yu.I. Bersenev for his help in the field studies, to N.P. Domra (FSC of Land Diversity FEB RAS, Vladivostok) for the sample preparation to pollen analysis.

The work was performed with financial support from RFBR, grant 15-05-00171, and from research program "Far East", FEB RAS, project 15–I–6–097.

REFERENCES

Borisova O.K. (2014). Landscape-climatic changes at Holocene. Izv. of Russian Academy of Sciences. Geographical Series, 2, pp. 5-20. (in Russian with English summary).

Chen X-Y., Blockley S.P.E., Tarasov P.E., Xu Y.-G., McLean D., Tomlinson E.L., Albert P.G., Liu J.-Q., Müller S., Wagner M., and Menzies M.A. (2016). Clarifying the distal to proximal tephrochronology of the Millennium (B-Tm) eruption, Changbaishan Volcano, northeast China. Quat. Geochronology, 33, pp. 61-75, doi:0.1016/j.quageo.2016.02.003.

Climates and Landscapes of Northern Eurasia under Conditions of Global Warming. Retrospective Analysis and Scenarios. (2010). Moscow: GEOS. (in Russian with English summary).

Kiselev A.N. and Kudryavtseva E.P. (1992). High mountain vegetation of South Primorye. Moscow: Nauka. (in Russian).

Korotky A.M. (2010). Reconfiguration of the river system in the Primorye: causes, mechanisms, influence on geomorphologic processes. Geomorphology, 2, pp. 78-91. (in Russian with English summary).

Korotky A.M., Grebennikova T.A., Pushkar' V.S., Razzhigaeva N.G., Volkov V.G., Ganzey L.A., Mokhova L.M., Bazarova V.B., and Makarova T.R. (1997). Climatic changes in the Southern Russian Far East during Late Pleistocene-Holocene. Bull. FEB RAS, 3, pp. 121-143. (in Russian with English summary).

Kudryavtseva E.P., Bazarova V.B., Lyashchevskaya M.C., and Mokhova L.M. (2018). Modern distribution of Ambrosia artemisiifolia and its presence in Holocene deposits of the Primorskii Krai (South of the Far East). In: P.Ya. Baklanov, ed., Geosystems in Northeast Asia. Types, current state and development prospects. Vladivostok: PGI FEB RAS, pp. 176-183. (in Russian with English summary).

Kurentsova G.E. (1973). Natural and anthropogenic changes of vegetation of Primorye and Southern Priamur'e. Novosibirsk: Nauka. (in Russian).

Lobanov V.B., Danchenkov M.A., Luchin E.V., Mezentseva L.I., Ponomarev V.I., Sokolov O.V., Trusenkova O.O., Ustinova E.I., Ushakova R.N., and Khen G.B. (2014). Far East of Russia. In: V.V. Yasuykevich, ed., Second estimation report about climate changes and its impact on the territory of Russian Federation. Moscow: Rosgidromet, pp. 684-743. (in Russian).

Mayewski P.A., Rohling E.E., Stager J.C., Karlén W., Maasch K.A., Meeker L.D., Meyerson E.A., Gasse F., van Kreveld S., Holmgren K., Lee-Thorp J., Rosqvist G., Rack F., Staubwasser M., Schneider R.R., and Steig E.J. (2004). Holocene climate variability. Quaternary Research, 62, pp. 243-255, doi:10.1016/j.yqres.2004.07.001.

Mikishin Yu.A., Petrenko T.I., Gvozdeva I.G., Popov A.N., Kuzmin Ya.V., Rakov V.A., and Gorbarenko S.A. (2008). Holocene of the coast of South Western Primorye. Scientific Review, 1, pp. 8-27 (in Russian).

National Park "Zov Tigra". (2014). Vladivostok: Dalnauka.

Nováková J. and Pouličková A. (2004). Moss diatom (Bacillariophyceae) flora of the Nature Reserve Adrspassko-Teplicke Rocks (Czech Republic). Czech Phycology, 4, pp. 75-86.

Razjigaeva N.G., Ganzey L.A., Mokhova L.M., Makarova T.R., Panichev A.M., Kudryavtseva E.P., and Arslanov Kh.A. (2018). Muta Area as a Natural Archive of the Environmental Changes (National Park « Zov Tigra», Russia). Biodiversity and Environment of Protected Areas, 1, pp. 37-70. (in Russian with English summary).

Razzhigaeva N.G., Ganzey L.A., Mokhova L.M., Makarova T.P., Panichev A.M., Kudryavtseva E.P., Arslanov Kh.A., Maksimov F.E., and Starikova A.A. (2016a). The Development of Landscapes of the Shkotovo Plateau of Sikhote-Alin in the Late Holocene. Izv. Ross. Akad. Nauk. Ser. Geogr., 3, pp. 65–80. (in Russian with English summary).

Razzhigaeva N.G., Ganzey L.A., Grebennikova T.A., Mokhova L.M., Kudryavtseva E.P., Arslanov Kh.A., Maksimov F.E., and Starikova A.A. (2016b). Changes of the landscapes of coasts and mountains surrounding Kit Bay (Eastern Primorye) in middle-late Holocene. Geogr. and Natural Resources, 3, pp. 141-151. (in Russian with English summary).

Razzhigaeva N.G., Ganzey L.A., Grebbennikova T.A., Kopoteva T.A., Mokhova L.M., Panichev A.M., Kudryavtseva E.P., Arslanov Kh.A., Maksimov F.E., Petrov A.Yu., and Klimin M.A. (2017). Environmental changes recorded in deposits of the Izyubrinye Solontsi Lake, Sikhote-Alin. Contemporary problems of ecology, 4, pp. 441-453, doi:10.1134/S1995425517040096.

Shishkin I.K. (1933). To the knowledge of larch Olginskaya (*Larix olgensis* A. Henry). Botanical J. USSR, 18, pp. 162–210. (in Russian).

van Soelen E.E., Ohkouchi N., Suga H., Damsté J.S.S., and Reichart G-J. (2016). A late Holocene molecular hydrogen isotope record of the East Asian Summer Monsoon in Southwest Japan. Quaternary Research, 86(3), pp. 287-294, doi:10.1016/j.yqres.2016.07.005.

Urusov, V.M., Lobanova, I.I., and Varchenko, L.I. (2007). Conifers of Russian Far East – Valuable Object of the Study, Protection, Breeding and Use. Vladivostok: Dalnauka. (in Russian).

Vostretsov Yu.E. (2009). First cultivators in the coast of the Peter the Great Bay. Bulletin of Novosibirsk State University. Series History, Philology, 8(3), pp. 113-120. (in Russian with English summary).

Wanner H., Beer J., Bütikofer J., Crowley T.J.,Cubasch U., Fluckiger J., Goosse H., Grosjean M., Joos F., Kaplan J.O., Kuttel M., Muller S.A., Prentice I.C., Solomina O., Stocker T.F., Tarasov P., Wagner M., and Widmann M. (2008). Mid- to Late Holocene climate change: an overview. Quaternary Science Reviews, 27, pp. 1791-1828, doi:10.1016/j.quascirev.2011.07.010.

Wanner H., Solomina O., Grosjean M., Ritz S.P., and Jetel M. (2011). Structure and origin of Holocene cold events. Quaternary Science Reviews, 30, pp. 3109-3123, doi:10.1016/j.quascirev.2008.06.013.

Yi S. (2011). Holocene vegetation response to East Asian monsoonal changes in South Korea. In: J. Blanco, H. Kheradmand, eds., Climate Change – Geophysical Foundation and Ecological Effects. Rijeka: InTech, pp. 157-178, doi:10.5772/23920.

Zhudova P.P. (1967). Vegetation and flora of Sudzukhinsky State Reserve of Primorye. Bulletin of Sikhote-Alin State Reserve, 4, pp. 3–245. (in Russian).

Received on August 24th, 2018 Accepted on May 17th, 2019

Vitaly K. Avilov[1,3*], Dmitry G. Ivanov[1,3], Konstantin K. Avilov[2], Ivan P. Kotlov[1,3], Nguyen Van Thinh[3], Do Phong Luu[3] and Julia A. Kurbatova[1]
[1] A.N. Severtsov Institute of Ecology and Evolution RAS, Moscow, Russia
[2] Marchuk Institute for Numerical Mathematics RAS, Moscow, Russia
[3] Joint Russian-Vietnamese tropical research center, Soutern branch, Ho Chi Minh city, Vietnam
*** Corresponding author:** vit.avilov@gmail.com

HOT SPOTS OF SOIL RESPIRATION IN A SEASONALLY DRY TROPICAL FOREST IN SOUTHERN VIETNAM: A BRIEF STUDY OF SPATIAL DISTRIBUTION

ABSTRACT. Many studies report asymmetrical spatial distribution of soil respiration caused by presence of areas with significantly higher emission rates (so-called *hot spots*). For seasonally dry tropical forest soil respiration was measured on 1 ha plot with 20m, 5m and 1 m scale in the first half of dry season. 457 measurements made in 9 series at 54 sampling points. The results suggest that lognormal spatial distribution model appears to be much more supported rather than the normal one. A statistical method proposed for estimation the mean value and its confidence interval of lognormally distributed data. The mean emission rate E(R_s) for the lognormal distribution amounted to 4.28 μmol m^{-2} s^{-1}, the 95% confidence interval is 3.93 to 4.76 μmol m^{-2} s^{-1}. However, the standard sample mean can be used as an estimator of the mean of lognormally distributed values of soil respiration if their coefficient of variance remains approximately the same as in our study (CV=0.35). Based on the data obtained and literature sources, recommendations are given on the number of sampling points for estimating the spatial average value with a given accuracy

KEY WORDS: soil respiration, carbon emission, hot spots, tropical forest, spatial variability, sample size

CITATION: Vitaly K. Avilov, Dmitry G. Ivanov, Konstantin K. Avilov, Ivan P. Kotlov, Nguyen Van Thinh, Do Phong Luu and Julia A. Kurbatova (2019) Hot spots of soil respiration in a seasonally dry tropical forest in southern Vietnam: a brief study of spatial distribution. Geography, Environment, Sustainability,
Vol.12, No 2, p. 173-182
DOI-10.24057/2071-9388-2018-87

INTRODUCTION

Tropical forests contain about 40% of the global vegetation carbon and are responsible for about 50% of terrestrial gross primary production. Owing to their large C stocks and budgets, tropical forests can affect the global C balance, and hence potentially play an important role in climate change, despite only covering 12% of the total land

surface (FAO 2001). Seasonal forests represent 43% of the total tropical forest area, which is comparable with that of tropical rainforests.

In tropical forest ecosystems, the eddy covariance method has improved our understanding of ecosystem carbon cycle processes (e.g. Yamamoto et al. 2005; Kumagai et al. 2006; Kosugi et al. 2008). However, this method can provide unreliable nocturnal CO_2 fluxes under low wind speed conditions (Baldocchi 2003), which can be used as a proxy for ecosystem respiration; thus, alternative chamber methods for measuring respiration are still important for understanding the processes of carbon flow in relation to climate change (Kume at al. 2013).

Soil CO_2 efflux (syn. soil respiration, R_s) is the sum of multiple processes in rhizosphere, bacteria and fungi, soil fauna, litter decomposing organisms respiration and other, and many factors affect each of these components. Although soil temperature and soil water content are considered as primary drivers of soil respiration, coincidence of secondary factors (such as root biomass, organic carbon content, insect nests (Lopes de Gerenyu et al. 2015)) can cause emission values considerably exceeding surrounding background, which makes soil respiration a process of high spatial and temporal variability. Areas with significantly higher emission rates are generally recognized as hot spots (McClain et al. 2003). Several problems may appear when estimating spatial average value of soil respiration. Due to insufficient sampling, the *hot spots* can be not taken into account at all, or they could be treated as a measurement artifact and discarded.

Soil respiration hot spots can be considered as *ecosystem control points* – points (spatial or temporal) where the exchange rate is of sufficient magnitude or ubiquity to affect dynamics of the ecosystem (Bernhardt 2017). With this approach, investigating the properties of soil respiraton hotspots can lead to a better understanding of ecosystem processes.

Aim of this study was evaluation of spatial variability of soil CO_2 efflux in seasonally dry tropical forest, describing magnitude, size and temporal behavior of hotspots and estimation of optimum amount of sampling for further studies.

STUDY AREA

The study has been carried out in semi-deciduous tropical forest of Cat Tien national park (a part of the Dong Nai Biosphere Reserve) located in Dong Nai province, Vietnam (Fig. 1). The mean annual temperature, measured on Dong Xoai meteorological station approx. 57 km WNW from the study site in 1981 – 2010 was 26.4 °C with annual variation of monthly averages within 4°C, mean annual rainfall amounts to 2518 mm (Deshcherevskaya

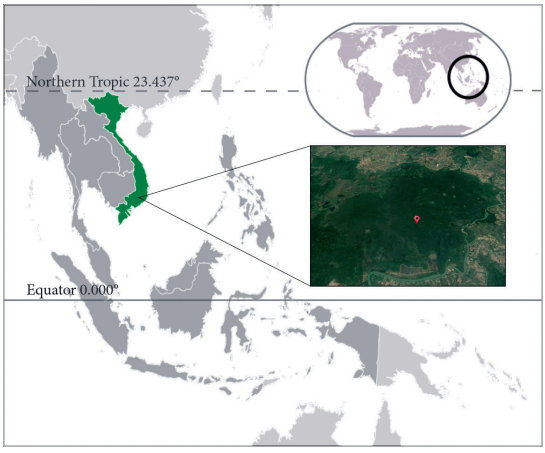

Fig. 1. Location of the study site (satellite image credits: CNES/Airbus 2018, DigitalGlobe 2018)

et al. 2013). Climate of the region described as tropical monsoon (Am) by Köppen climate classification, which characterized by pronounced dry season, which lasts from December to March: mean total rainfall for this period makes only 5% of the annual amount. The forest dominant deciduous tree species are *Lagestroemia caluculata, Tetrameles nudiflora, Hopea odorata, Ficus spp* (Kuznetsov and Kuznrtsova 2011). Forest understory is abundant and evergreen, with minor grass cover. Soil of the study site is very dark brown (7.5YR 2.5/2 by Munsell color system) andisol with negligible color variation among study area. Organic carbon content in upper layer (0-20 cm) is 5.34%, nitrogen content is 0.44%, pH is 5.56 (Okolelova et al. 2014).

MATERIALS AND METHODS

Sampling design

A measurement site of 1ha (100 x 100 m) was established in 50 meters south from NCT flux tower (Kurbatova et al. 2013; NCT – AsiaFlux. [Online]) with a zero point (SW corner) at 11.440309°N, 107.400072°E. The measurement points were placed on 3 different scales (Fig. 2): in the center of each 20x20 m subplot (n=25), then one random subplot was partitioned with 5 x 5 m grid and sampling points were placed on the intersections of the grid (n=25), the final scale was a small transect of 4 sampling points, placed with 1 m interval between two points of 5 x 5 m scale (n=6).

The measurements of soil respiration were repeated in 9 series with 6-8 days interval during December 2017 to February 2018. Each of the series has been measured in two days: on first day each of 25 points of the 100x100m plot has been measured and rest of the points measured the next day. The measurements of each day were taken between 9 am and 12 pm, one time per measuring point. At each sampling point a PVC collar of 250mm diameter was installed with depth of about 3-5 cm below ground and height of 5 cm above, tree litter was not removed from the collars. First measurements were taken 10 days after the collars installation. Soil respiration was measured with non-steady state closed loop chamber method using custom-made respirometer based on LI-820 infrared gas analyzer (LI-COR inc., USA). The measuring chamber (Fig. 3) was of hemispherical shape 2.8 l in volume. Air intake was mounted at the top of the hemisphere, and the air return flow was distributed around the base perimeter, which made it possible to avoid the use of a fan and the consequent excessive turbulence inside the chamber. Air-tight connection to the collar was realized using a thin rubber sealing ring. CO_2 concentration values were logged with 1 Hz rate during each 120 seconds-long measurement.

Air temperature inside the measuring chamber was registered for every CO_2 efflux measurement to estimate molar volume. Soil temperature and volumetric water content were measured along with CO_2

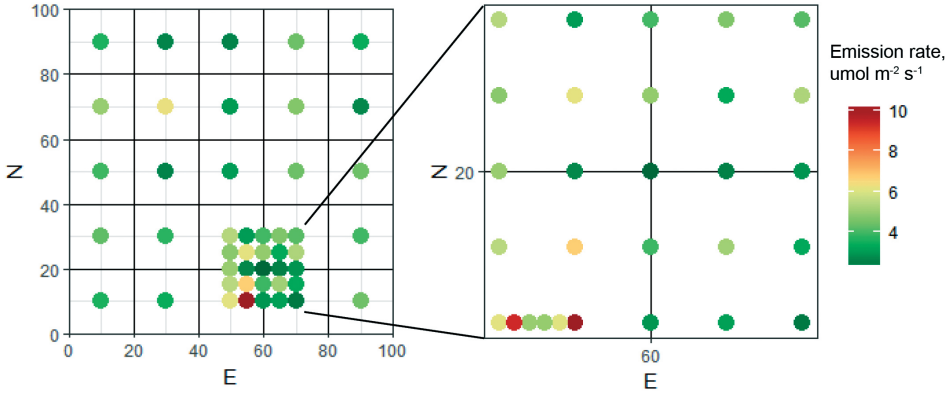

Fig. 2. Sampling design and time-averaged values of soil CO_2 emission, µmol m^{-2} s^{-1} (shown in color gradient). The numbers on axes represent distances to North and East from a zero point in meters

efflux measurement in close proximity to the chamber. Soil temperature was measured at 2-5 cm depth using Checktemp-1 digital thermometer (Hanna instruments, USA). Soil volumetric water content was measured using electrical conductivity meter 5TE (Decagon Devices, Inc., USA). Due to the sensor failure, soil water content was measured only during first 4 series.

The method for calculation of CO_2 efflux rate was similar to one used in commercial soil gas flux system LI-8100A (LI-COR inc., USA). CO_2 concentration values from a first few seconds of a measurement were discarded due to disturbances caused by installation of the chamber. However, CO_2 growth rate was estimated at the moment of chamber installation by approximation of good data with a gradient diffusion equation (Healy et al. 1996) using *TableCurve2D* software:
Where *C'(t)* is the instantaneous chamber

$$C' = C'_x + (C'_0 - C'_x) * e^{-(a*(t-t_0))}$$

CO_2 mole fraction, *C0'* is the value of *C'(t)* when the chamber installed, and *Cx'* is a parameter that defines the asymptote, all in µmol CO_2/mol air (ppm); a is a parameter that defines the curvature of the fit (s^{-1}). The *Cx'*, a and t_0 parameters yielded by the regression were used to estimate CO_2 concentration growth rate at the moment $t = t_0$: Then CO_2 efflux rate was calculated:

$$\left.\frac{dC'}{dt}\right|_{t=t_0} = a(C'_x - C'_0)$$

Where R_s is soil respiration rate (µmol * m^{-2} * s^{-1}), Vch is the volume of measuring chamber(m^3), Sch is the area covered with the chamber (m^2) and Vm is the molar volume for temperature measured inside the chamber (m^3).

$$R_s = \left.\frac{dC'}{dt}\right|_{t=t_0} * \frac{V_{ch}}{V_m} * \frac{1}{S_{ch}}$$

Statistical methods

To make distribution of R_s values from each measurement series comparable, the temporal trend was removed: we calculated the median value in each trial (M_i,i=1,...,9), and the median of all values in the dataset (M_{all}). Then, for each trial (i=1,...,9) the detrended data were calculated as

$$\widetilde{R}_s = R_s - M_i + M_{all}$$

Hot spots were defined as outliers by Tukey's criteria (Tukey 1977) as it was done by other authors for defining geochemical phenomena (Kessel et al. 1993; Ohashi 2007). A sampling point was defined as a hot spot in the given measurement series when: $R_s > Q_3 + 1.5*IQR$, where Q_1 and Q_3 are 25th and 75th percentiles and IQR= Q_3 - Q_1 is the interquartile range of the deterended dataset.

The spatial dependence was analyzed by applying gammavariance technique (Bachmaier et al. 2011; Cressie 1993) with variogram function in "gstat" R package v.1.1-6 (Pebesma 2004).

Four normality tests were used (Lilliefors test, Anderson-Darling test, Kolmogorov-Smirnov test, and Jarque-Bera test) on both the original data and log-transformed data (testing for lognormal distribution).

Assuming that the time-averaged CO_2

Fig. 3. Measuring chamber (left) and a collar at one of the sampling points (right)

emission rates at different spatial locations are independent and follow lognormal distribution, the mean emission rate ($E(R_S)$) was estimated using the method by Shen, Brown and Zhi (Shen et al. 2006):
where X_i=LogRs_i

$$E(R_S) = \exp\left(\overline{X} + \frac{(n-1)S^2}{2(n+4)(n-1)+3S^2}\right)$$

is log-transformed data,
is the sample mean of X,

$$\overline{X} = \sum_{i=1}^{n} X_i / n$$

is the sample sum of squared deviations of

$$S^2 = \sum_{i=1}^{n} (X_i - \overline{X})^2$$

X, and n is the size of the sample. The bootstrap confidence interval (CI) for $E(R_S)$ was generated with 10^5 simulated samples.

To estimate the number of test sites required to measure the mean CO_2 emission rate with given precision, we studied the properties of the bootstrap CI by Shen et al. (2006).

If R_S is a lognormally distributed random variable, X=logR_S is normally distributed with mean μ and standard deviation (SD) σ. The dimensionless parameter σ is related to the coefficient of variation of R_S:
where $CV=SD(R_S)/E(R_S)$ is the coefficient of

$$\sigma = \sqrt{\log(CV^2+1)}$$

variation of Z.

From CI formulas in (Shen et.al. 2006) it can be shown that the relative width of the CI $[c_1,c_2]$ for $E(R_S)$
is a function of σ and n only. At the same

$$RWCI = \frac{c_2 - c_1}{E(R_S)}$$

time, *RWCI* may be considered as a measure of relative precision of estimation of $E(R_S)$. Thus, if and target *RWCI* are given, it is possible to estimate the required sample size n.

RESULTS AND DISCUSSION

The natural distribution of detrended soil respiration values displayed an asymmetrical distribution with the tail of higher values (Fig. 4). The obtained normality tests' p-values for time-averaged data are 0.1859, 0.0046, 0.6126, <0.001 for the original data and >0.5, 0.5029, 0.9345, >0.5 for the log-transformed data (L, AD, KS, and JB tests respectively). Although only two tests reject normality of the original data at 5% significance level, lognormality of the data appears to be much more supported.

The mean emission rate $E(R_S)$ for the lognormal distribution amounted to 4.28 μmol m-2 s-1, the 95% confidence interval is 3.93 to 4.76 μmol m^{-2} s^{-1}. The relative width of the confidence interval (RWCI) is 0.195. The median rate amounted to 3.95 μmol m^{-2} s^{-1} which is 12% lower than estimated mean value. The standard sample average, which suggests normal distribution, amounted to 4.31 μmol m-2 s-1 , with confidence interval in 3.88 – 4.74 μmol m-2 s-1 and RWCI of 0.20, which is quite close to the results of lognormal distribution Thus, we may state that the standard sample mean can be used as an estimator of the mean of lognormally distributed values of soil respiration if their coefficient of variance remains approximately the same as in our study (CV=0.35). However, in the case of much more expressed hotspots (i.e. as described for methane emissions, denitrification and other processes by Bernhardt (2017)), these estimates may differ significantly, and the use of our proposed method for estimating the average of the lognormal distribution will be reasonable.

The results of the individual measurement series are shown in Table A.1.

There was no significant overall trend in R_S during the measurement campaign (slope <0.03 μmol m^{-2} s^{-1} per day). Some hot spots were stable in time, while some appeared only once or twice, and some points oppositely reacted to the same change in conditions. Our data shown no statistical dependence of soil respiration on temperature (linear model R^2 < 0.006, p-value: 0.11)

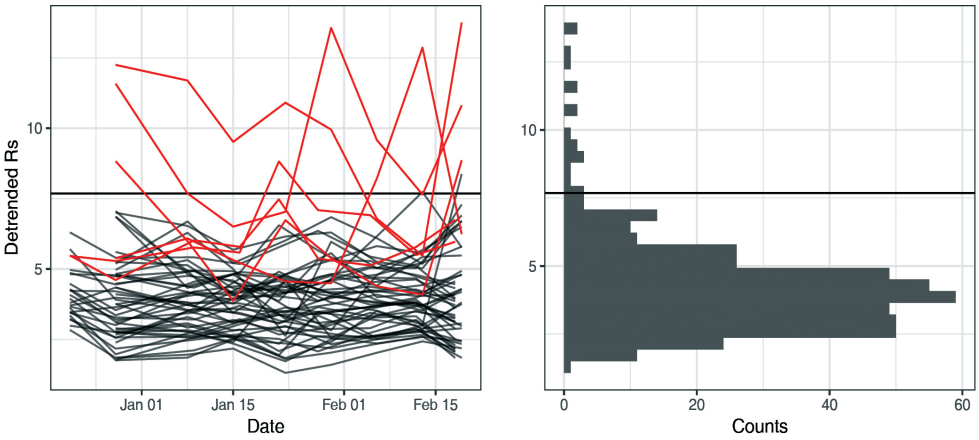

Fig. 4. Left plot: variation of soil respiration rate on individual sampling points along the measurement campaign. Trend of spatial median fluctuation is removed (median values of each measurement series are corrected to the common median value). The black lines represent sampling points with no hot moments detected. Right plot: frequency distributon of detrended soil respiration values (n=486). The horizontal black line on both plots shows the Tukey`s outlier criteria

and soil moisture (linear model R^2 >0.03, p-value: 0.04), and we suggest that none of these factors determine abnormally high emission values. Thus, it can be argued that observed soil respiration hotspots are of a different nature, and each detected hotspot may be due to different factors and react differently to the same change in environmental conditions.

The spatial dependence analysis didn't show any systematic behavior described by theoretical models (linear, spherical, exponential, Gaussian, and power law). This can serve as the evidence of heterogenous nature of time-averaged CO_2 efflux values or a hypothesis that the scale of spatial variation of soil CO_2 efflux at our site was smaller than double minimal distance between sampling points, i.e. less than 2 meters. Two-sample *t-test* showed statistically different mean values of two most expressed hotspots with any surrounded sampling point within 2 meter radius.

The time-averaged soil respiration values obtaineded at 54 sampling points produce standard deviation of log-transformed values σ=0.3433 (with corresponding 95% confidence interval $CV(Z)$=0.3537). In order to estimate the possible range of σ, we fetched data from four other studies of tropical forests in Southeast Asia (Ohashi 2007; Katayama 2009; Kosugi 2007; Adachi 2009) in the form of sample means and sample SDs (20 sets of data in total, with varying conditions and sample sizes). The data were used to calculate rough estimations of CVs (because sample means and sample SDs are very biased estimators of true means and SDs of lognormal distributions), and, in turn, to calculate rough estimations of . The minimal observed σ was 0.2576, the maximum one was 0.5847, with a peak of frequency near to our σ=0.3433. So we decided to explore the range $\sigma \in [0.15; 0.75]$.

The calculated RWCIs for various and n are shown in Fig. 5. Every value was calculated using 105 simulated samples in the bootstrapping procedure. The graphs may be used for estimating the required sample size if target RWCI is known and is estimated in a pilot study or assumed from literature data.

For σ=0.35, which can be considered as typical, some RCWI values were tabulated (Table 1):

These values clearly show that sampling design which includes 5-10 spatial probes may produce estimates very far from the true mean CO_2 emission rates.

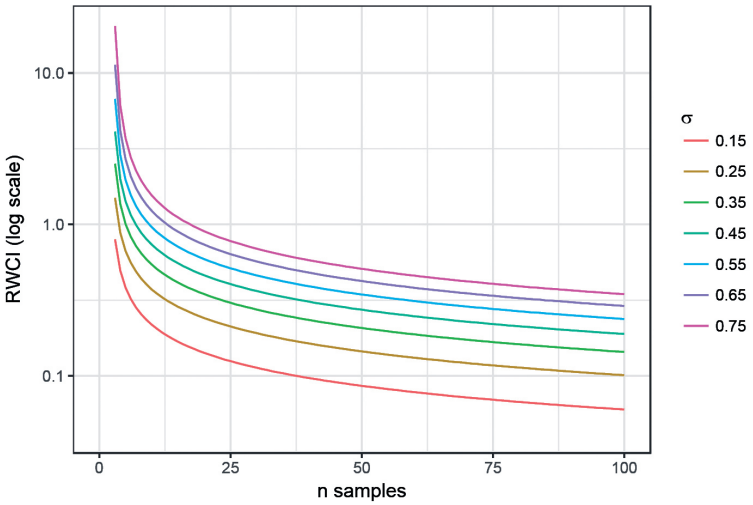

Fig. 5. Relative width of the 95% confidence interval for the mean of lognormally distributed variable Z as a function of its σ=SD(logZ) parameter and sample size n

Table 1. Relative widths of 95% confidence intervals for σ=0.35 . Lognormal distribution is assumed

n	3	5	10	20	30	40	50	60	70
$RWCI_{\sigma=0.35}$	2.488	1.005	0.542	0.346	0.274	0.234	0.207	0.188	0.173

CONCLUSIONS

Soil respiration rate in a seasonally dry tropical forest is highly variable in space, due to the small size of zones with significantly higher rates (hot spots). Spatial distribution of this parameter rejects normality tests, and lognormal distribution is much more supported by the statistical tests. However, we may state that the standard sample mean can be used as an estimator of the mean of lognormally distributed values of soil respiration if their coefficient of variance remains approximately the same as in our study (CV=0.35).

Hotspots apparently have a heterogenous nature, some of them are more stable than another ones. The stable hot spots can be explained by higher root biomass and leaf area index (LAI), the presence of decaying residues or areas of higher soil gas permeability. Rarely distributed short-term hot spots can be caused by insect activity. The detected hotspots apparently have a size of no more than 2 meters.

Assuming the lognormal nature of the distribution of soil respiration and the variability observed in our study and other literature sources, it may be proposed to make at least 20 spatially independent samples to obtain an estimate of the soil respiration with relative width of 95% confidence interval of no more than 0.35 of the estimated mean.

ACKNOWLEDGEMENTS

The study was funded by RFBR and Russian Geographical Society according to the research project № 17-05-41127 and partially was supported the Presidium of the Russian academy of sciences, Programs № 51 «Climate change: causes, risks, consequences, problems of adaptation and regulation» and № 41 "Biodiversity of natural systems and biological resources of Russia"

REFERENCES

Adachi M., Ishida A., Bunyavejchewin S., Okuda T., & Koizumi H. (2009). Spatial and temporal variation in soil respiration in a seasonally dry tropical forest, Thailand. Journal of Tropical Ecology, 25(05), 531. doi:10.1017/S026646740999006X.

AsiaFlux.net (2018). Asia Flux Official Website. [online] Available at: http://asiaflux.net/index.php?page_id=86 [Accessed 31 Dec 2018].

Bachmaier M. & Backes M. (2011). Variogram or semivariogram? Variance or semivariance? Allan variance or introducing a new term? Mathematical Geosciences, 43(6), 735–740.

Baldocchi DD. (2003). Assessing the eddy covariance technique for evaluating carbon dioxide exchange rates of ecosystems: past, present and future. Global Change Biology 9: 479–492.

Bernhardt E. S., Blaszczak J. R., Ficken C. D., Fork M. L., Kaiser K. E. & Seybold, E. C. (2017). Control Points in Ecosystems : Moving Beyond the Hot Spot Hot Moment Concept. Ecosystems, 20(4), 665–682. doi:10.1007/s10021-016-0103-y.

Cressie N.A.C. (1993). Statistics for Spatial Data, Wiley.

Deshcherevskaya O.A., Avilov V.K., Dinh B.D., Tran C.H., & Kurbatova J.A. (2013). Modern climate of the Cát Tiên National Park (Southern Vietnam): Climatological data for ecological studies. Izvestiya, Atmospheric and Oceanic Physics, 49(8), 819–838. doi:10.1134/S0001433813080021.

FAO (Food and Agriculture Organization) (2001). Global Forest Resources Assessment 2000—Main Report. FAO Forestry Paper 140, Rome.

Katayama A., Kume T., Komatsu H., Ohashi M., Nakagawa M., Yamashita M. et al. (2009). Effect of forest structure on the spatial variation in soil respiration in a Bornean tropical rainforest. Agricultural and Forest Meteorology, 149(10), 1666–1673. doi:10.1016/j.agrformet.2009.05.007.

Kessel C., D. J. Pennock, and R. E. Farrell (1993). Seasonal variations in denitrification and nitrous oxide evolution at the landscape scale, Soil Sci. Soc. Am. J., 57, 988–995.

Kosugi Y., Takanashi S., Ohkubo S., Matsuo N., Tani M., Mitani T., Tsutsumi D., Abdul Rahim N. (2008). CO2 exchange of a tropical rainforest at Pasoh in Peninsular Malaysia. Agricultural and Forest Meteorology 148: 439–452.

Kosugi Y., Mitani T., Itoh M., Noguchi S., Tani M., Matsuo N. et al. (2007). Spatial and temporal variation in soil respiration in a Southeast Asian tropical rainforest. Agricultural and Forest Meteorology, 147(1–2), 35–47. doi:10.1016/j.agrformet.2007.06.005.

Kumagai T., Ichie T., Yoshimura M., Yamashita M., Kenzo T., Saitoh T.M., Ohashi M., Suzuki M., Koike T., Komatsu H. (2006). Modeling CO2 exchange over a Bornean tropical rain forest using measured vertical and horizontal variations in leaf-level physiological parameters and leaf area densities. Journal of Geophysical Research 111: D10107. DOI: 10.1029/2005JD006676.

Kume T., Tanaka N., Yoshifuji N., & Chatchai T. (2013). Soil respiration in response to year-to-year variations in rainfall in a tropical seasonal forest in northern Thailand. Ecohydrology, 6(1), 134–141. Available at: http://onlinelibrary.wiley.com/doi/10.1002/eco.1253/full.

Kuznetsov A.N., Kuznetsova S.P. (2011). Forest vegetation: species composition and stand structure. In: A.V. Tuonov, ed., Structure and functions of soil organisms in a tropical monsoon forest (Cat Tien national park, southern Vietnam). Moscow: KMK scientific press ltd., pp. 16-43 (in Russian with English summary).

Lopes de Gerenyu V.O., Anichkin A.E., Avilov V.K., Kuznetsov A.N., & Kurganova I.N. (2015). Termites as a factor of spatial differentiation of CO2 fluxes from the soils of monsoon tropical forests in southern Vietnam. Eurasian Soil Science, 48(2). doi:10.1134/S1064229315020088.

McClain M. E., Boyer E. W., Dent C. L., Gergel S. E., Grimm N. B., Groffman P. M. et al. (2003). Biogeochemical hot spots and hot moments at the interface of terrestrial and aquatic ecosystems. Ecosystems, 6(4), 301–312.

Ohashi M., Kume T., Yamane S., & Suzuki M. (2007). Hot spots of soil respiration in an Asian tropical rainforest. Geophysical research letters, 34(8), L08705. doi:10.1029/2007GL029587.

Okolelova A.A., Van T.N. & Avilov V.C. (2014). Properties of basic types of soils in the Dong Nai biosphere reserve (south Vietnam). Belgogrod State University Scientific Bulletin: Natural Sciences, (27).

Pebesma E.J. (2004). Multivariable geostatistics in S: the gstat package. Computers \& Geosciences, 30: 683-691.

Shen H., Brown L.D., & Zhi H. (2006). Efficient estimation of log–normal means with application to pharmacokinetic data. Statistics in medicine, 25(17), 3023-3038.

Tukey J.W. (1977). Exploratory Data Analysis. Addison-Wesley. ISBN 978-0-201-07616-5. OCLC 3058187.

Yamamoto S., Saigusa N., Gamo M., Fujinuma Y., Inoue G., Hirano T. (2005). Findings through the AsiaFlux network and a view toward future. Journal of Geographical Society 15: 142–148.

Received on December 31st, 2018 Accepted on May 17th, 2019

Appendix A

Table A.1. Values of soil respiration rate, obtained in different series, μmol m-2 s-1. SD is standard deviation of mean, E(Z) is estimation of mean RS based on lognormal distribution. CI low and CI high are 95%confidence intervals of E(Z), JB-test is Jarque-Bera test

Series	Meas. date	n	Min	Max	Median	Mean	SD	E(Z)	CI low	CI high	RWCI	JB-test p-value for Z	JB-test p-value for log(Z)	Mean Ts, ℃	Mean VWC, m^3/m^3
1	2017 -12-21	25	1.79	5.26	2.90	3.10	0.91	3.08	2.77	3.52	0.24	0.131	0.500	27.3	0.22
2	2017 -12-28	54	2.24	12.73	4.42	4.77	2.14	4.72	4.28	5.35	0.23	≤ 0.001	0.213	29.7	0.21
3	2018 -01-08	54	2.04	11.88	4.13	4.41	1.68	4.38	4.02	4.87	0.20	≤ 0.001	0.435	28.8	0.22
4	2018 -01-15	54	1.85	9.19	3.62	3.67	1.28	3.65	3.36	4.04	0.18	≤ 0.001	0.500	28.1	0.19
5	2018 -01-23	54	2.20	11.79	4.83	5.00	1.81	4.97	4.57	5.52	0.19	≤ 0.001	0.500	25.2	0.27*
6	2018 -01-30	54	2.14	14.11	4.49	4.80	2.00	4.76	4.35	5.31	0.20	≤ 0.001	0.048	25.2	0.25*
7	2018 -02-06	54	1.49	9.05	3.41	3.67	1.49	3.65	3.31	4.12	0.22	0.002	0.500	22.2	0.18*
8	2018 -02-13	54	1.55	11.98	3.06	3.41	1.68	3.36	3.04	3.82	0.23	≤ 0.001	0.043	22.5	0.17*
9	2018- 02-19	54	2.42	14.34	4.53	5.10	2.35	5.05	4.55	5.75	0.24	≤ 0.001	0.254	24.8	0.17*

** the data fetched from NCT flux tower in 50-150 m away from the measured points*

Daria Gushchina[1], Florian Heimsch[2], Alexander Osipov[1], Tania June[3], Abdul Rauf[4], Heiner Kreilein[2], Oleg Panferov[5], Alexander Olchev[1*], Alexander Knohl[2]

[1] Faculty of Geography, Moscow State University, Moscow, Russia
[2] Bioclimatology, University of Goettingen, Goettingen, Germany
[3] Bogor Agricultural University, Department of Geophysics and Meteorology, Bogor, Indonesia
[4] Universitas Tadulako, Palu, Indonesia
[5] Department of Climatology and Climate Protection, Faculty of Life Sciences and Engineering, University of Applied Sciences, Bingen am Rhein, Germany
*** Corresponding author:** aoltche@gmail.com

EFFECTS OF THE 2015–2016 EL NIÑO EVENT ON ENERGY AND CO_2 FLUXES OF A TROPICAL RAINFOREST IN CENTRAL SULAWESI, INDONESIA

ABSTRACT. The influence of the very strong 2015–16 El Niño event on local and regional meteorological conditions, as well as on energy and CO_2 fluxes in a mountainous primary tropical rainforest was investigated using ERA-Interim reanalysis data as well as meteorological and eddy covariance flux measurements from Central Sulawesi in Indonesia. The El Niño event led to a strong increase of incoming monthly solar radiation and air temperature, simultaneously with the increasing Niño4 index. Monthly precipitation first strongly decreased and then increased reaching a maximum in 3–4 months after El Niño culmination. Ecosystem respiration increased while gross primary production showed only a weak response to the El Niño event resulting in a positive anomaly of net ecosystem CO_2 exchange (reduced CO_2 uptake). The changes of key meteorological parameters and fluxes caused by the strong El Niño event of 2015–16 differed from the effects of moderate El Niño events observed during the period 2003-2008, where net ecosystem CO_2 exchange remained largely unaffected. In contrast to earlier moderate El Niño events, the strong El Niño 2015–16 affected mostly the air temperature resulting in a weakening of the net carbon sink at the rainforest site in Central Sulawesi, Indonesia.

KEY WORDS: El Niño Southern Oscillation, Niño4, tropical rainforest, eddy covariance flux measurements, energy and CO_2 fluxes

CITATION: Daria Gushchina, Florian Heimsch, Alexander Osipov, Tania June, Abdul Rauf, Heiner Kreilein, Oleg Panferov, Alexander Olchev, Alexander Knohl (2019) Effects Of The 2015–2016 El Niño Event On Energy And CO_2 Fluxes Of A Tropical Rainforest In Central Sulawesi, Indonesia. Geography, Environment, Sustainability,
Vol.12, No 2, p. 183-196
DOI-10.24057/2071-9388-2018-88

INTRODUCTION

The contribution of tropical rainforests to the global budget of atmospheric greenhouse gases (GHG), their possible influence on the climate system and their sensitivity to environmental changes are key topics of numerous modeling and experimental studies (Grace et al. 1995; Malhi et al. 2007, 2010; Le Quéré et al. 2015). Tropical forests cover large areas of the Earth's surface and they are characterized by a large diversity. Their growth and development are governed by various factors including the regional climatic conditions, landscape properties and soil characteristics (FAO 2016). Representative information about possible responses of tropical forest ecosystems to changing environmental conditions can help to obtain new knowledge about possible future dynamics of tropical forest ecosystems in different geographical regions as well as to describe the possible effects of vegetation and land-use changes in tropical regions on local and regional climate conditions.

South-East (SE) Asia hosts some of the oldest, intact rainforests on Earth (Corlett and Primack 2006). They still cover vast areas in the region and are characterized by a large biological diversity and high species richness (Myers et al. 2000). A high deforestation rate due to widespread logging over the last decades in the region leads, however, to degradation of the primary rainforests and to reduction of their extension (FAO 2016; Hansen et al. 2013). During the last decades, rainforest in SE Asia were the objects of intensive aggregated studies of ecosystem - atmosphere interactions (Ibrom et al. 2007; Ichii et al. 2017). Nevertheless, considerable parts of primary tropical rainforests in remote areas, far away from administrative centers and human settlements, are still very poorly investigated in respect to their sensitivity to changes of environmental conditions and their contributions to the global and regional budgets of GHG in the atmosphere.

Recent scientific assessments indicated that the tropical rainforests of SE Asia are highly sensitive to the effects of large-scale atmospheric and oceanic modes such as El Niño-Southern Oscillation, Indian Ocean Dipole, Madden-Julian Oscillation (Hirano et al. 2007; Olchev et al. 2015). El Niño-Southern Oscillation (ENSO) is associated with quasi-periodic fluctuations in sea surface temperature (SST) in the central and eastern parts of the Equatorial Pacific and atmospheric pressure fluctuations between the eastern and western tropical Pacific. It has significant influence on the weather and climatic conditions both in the tropical Pacific region and through teleconnections at mid and high latitudes (Trenberth et al. 1998; Diaz et al. 2001; Zheleznova and Gushchina 2015, 2016). The warm phase (or event) of ENSO, termed El Niño, is characterized by positive SST anomalies located either in the Eastern (conventional event) or Central (Modoki event) Pacific (Ashok et al. 2007). The ocean warming is associated with a well pronounced shift of the Walker circulation to the east, resulting in strong convection and abundant precipitation over the Central and Eastern Pacific as well as in decreasing cloudiness and precipitation in Western Pacific areas, including the islands of the Indonesian archipelago and Northern and Eastern Australia (Gushchina et al. 1997; Dewitte et al. 2002). The decreasing cloudiness in the Western Pacific leads to increased solar radiation and air temperature.

To describe possible effects of ENSO events on CO_2- and H_2O-exchange between the land surface and the atmosphere, studies for various Western Pacific regions were carried out during the last decades (Feely et al. 1999; Olchev et al. 2015). Most of them, however, analyzed relatively weak El Niño events due to the absence of strong El Niño events between 1998 and 2015.

The main goal of this study is therefore to describe possible effects of the very strong 2015–2016 El Niño event (warm phase of ENSO) on energy, water, and CO_2 fluxes in the Western Pacific at the example of mountainous old-growth tropical rainforest growing in Central Sulawesi, Indonesia.

MATERIAL AND METHODS

Study area

The tropical rainforest selected for the study is situated near the village Bariri in the southern part of the Lore Lindu National Park in Central Sulawesi in Indonesia (1°39.47'S and 120°10.41'E or UTM 51S 185482.0 m East and 9816523.0 m North) (Fig. 1). The site is located on a large plateau with a size of several kilometers, about 1440 m above sea level. The area is surrounded by mountain chains surmounting the plane by another 300 m to 400 m. A 70 m high micrometeorological tower is installed on the site and equipped with meteorological and gas-exchange measuring sensors. Within 500 m around the tower the elevation varies between 1390 and 1430 meters (Ibrom et al. 2007; Olchev el al. 2015).

The area is influenced by the intertropical convergence zone (ITCZ) and it is characterized by a humid climate with low temperature range throughout the year (the mean monthly air temperature varies between 19.4°C and 19.7°C). It belongs to the tropical wet (or rainforest) climate (*Af*) according to the Köppen-Geiger climate classification (Chen and Chen 2013; Olchev el al. 2015) and to the equatorial type of climate - according to the climate classification suggested by Alisov (Alisov 1954). The mean annual precipitation rate exceeds 2000 mm with May to October exhibiting drier conditions than the rest of the year (Ibrom et al. 2007; Olchev et al. 2015).

The vegetation cover at the site is characterized by a large diversity. There are more than 90 different tree species per hectare (Ibrom et al. 2007). Among the dominant species are *Castanopsis accuminatissima* BL. (29%), *Canarium vulgare Leenh.* (18%) and Ficus spec. (9.5%). The density of trees, with diameter at breast height (DBH) larger than 0.1 m, is about 550 trees ha^{-1}. Additionally there is more than a 10-fold larger number of smaller trees with a stem diameter lower than 0.1 m. Leaf area index (LAI) is about 7.2 m^2 m^{-2}. LAI was estimated using an indirect hemispherical photography method. The height of the trees, with DBH >0.1 m, varies between 12 m and 36 m with the mean of 21 m (Ibrom et al. 2007).

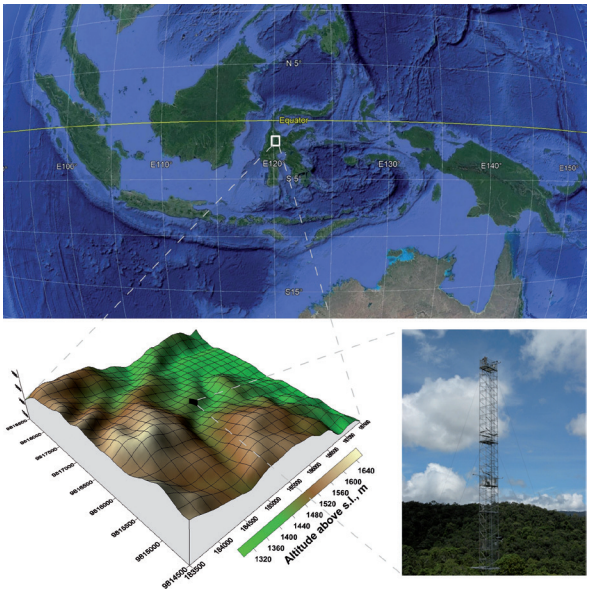

Fig. 1. Geographical location (source: Google maps), surface topography of the Bariri site and a photo of the meteorological tower for long-term observations of the energy, water, and CO_2 fluxes between land surface and the atmosphere. The surface topography map was created using ASTER GDEM version 2 data set (https://asterweb.jpl.nasa.gov/gdem.asp)

Reanalysis data

Various reanalysis products are used to document the anomalies of meteorological and oceanic parameters observed in the study area during the 2015–16 El Niño. Monthly net solar radiation, air temperature and wind at the 850 hPa level are obtained from the ERA-Interim reanalysis (Dee et al. 2011) with the grid spacing of 2.5°×2.5°. To derive monthly SST the Extended Reconstructed Sea Surface Temperature version 4 (ERSST.v4) archive is used (grid spacing of 2°×2°). Precipitation anomalies are calculated from the GPCP archive (Huffman et al. 2009), with the grid spacing of 2.5°×2.5°. Anomalies are calculated respectively to the mean seasonal cycle averaged over 1979–2014 period. Niño3 (SST anomalies averaged over 150°W-90°W and 5°S-5°N) and Niño4 (SST anomalies averaged over 160°E-150°W and 5°S-5°N) indices are obtained from https://www.esrl.noaa.gov/psd/gcos_wgsp/Timeseries/.

Flux measurements in the tropical rainforest

Measurements of CO_2 and H_2O fluxes are carried out at the Bariri site since 2003 (Falk et al. 2005; Ibrom et al. 2007, 2008; Panferov et al. 2009). Eddy covariance equipment for flux measurements is installed on a meteorological tower of 70 m height at the 48 m level, i.e. ca. 12 m above the maximum tree height. The measuring system consists of a three-dimensional sonic anemometer (USA-1, Metek, Germany) and an open-path CO_2 and H_2O infrared gas analyzer (IRGA, LI-7500A, Li-Cor, USA). The system is solar powered and entirely self-sustaining. It has been proven to run unattended over a period of several months. Post-field data processing of eddy covariance flux estimates was carried out strictly according to established recommendations for raw data analysis including despiking, block averaging, and 2D coordinate rotation (Aubinet et al. 2012). Negative fluxes indicate a flux towards the land surface (uptake), positive fluxes a flux towards the atmosphere (release). For filling the gaps in the measured Net Ecosystem Exchange (*NEE*), sensible and latent heat flux records as well as to quantify Gross Primary Production (*GPP*), Net Primary Production (*NPP*) and Ecosystem respiration (*RE*) the process-based Mixfor-SVAT model (Olchev et al. 2002; 2008, 2015) was used.

Mixfor-SVAT is a one-dimensional model of the energy, H_2O and CO_2 exchange between vertically structured mono- or multi-specific forest stands and the atmosphere. The key advantage of the model is its ability to describe seasonal and daily patterns of CO_2 and H_2O fluxes at individual tree and entire ecosystem levels and to estimate the contributions of soil, forest understorey, and various tree species of overstorey into total ecosystem fluxes while taking into account individual biophysical properties and responses of tree species to changes in environmental conditions. The model also allows taking into account the non-steady-state water transport in the trees, rainfall interception, dew generation, turbulence and convection flows within the canopy and plant canopy energy storage (Olchev et al. 2015).

Data analysis

To estimate the possible impacts of ENSO events on energy, water, and CO_2 fluxes in the tropical rainforest at the Bariri site the meteorological and flux data measured in the periods from 2003 to 2008 and from 2013 to 2017 were analyzed. The periods were chosen due to the small amount of gaps in the time series data. The period between 2003 and 2008 contains several warm ENSO events of moderate intensity. The period 2013–2017 contains one of the strongest warm events during the last several decades – the El Niño of 2015–16.

Statistical analysis included both simple correlation and cross-correlation analysis (Chatfield 2004). Correlation coefficients are calculated between the Niño4 index and the deviations of smoothed mean monthly (moving average ±3 months) values of meteorological parameters and atmospheric fluxes from their monthly averages over the entire considered period (2003–2008, 2013–2017). The deviations were calculated according to the approach

described by Olchev et al (2015). Cross-correlation analysis was used to take into account possible forward and backward time shifts of maximal anomalies of meteorological parameters and energy, water, and CO_2 fluxes in respect to time of the El Niño culmination.

RESULTS AND DISCUSSION

The El Niño event of 2015–2016 was one of the strongest ever recorded with the amplitude comparable to the extreme events of 1982–1983 and 1997–1998 (Santoso et al. 2017). The values of Niño3 and Niño4 indices reached in 2015–2016 values of 2.65°C and 1.59°C, respectively, that exceeds the corresponding values of SST anomalies observed in 1982–83 and 1997–98 for Niño4 region (Fig. 2c). Reanalysis data show that the area of positive anomalies of SST persisted over the Central and Eastern Pacific from June 2015 up to May 2016 and it was associated with strong westerly wind anomalies spreading up to 120°W in the ENSO culmination phase (Fig. 2a).

The extreme SST and atmosphere circulation anomalies induced a strong remote response over the entire equatorial Pacific region and resulted in significant changes in temperature and precipitation fields. In the area of our study site in Central Sulawesi, Indonesia, this episode was manifested in positive temperature anomalies that exceeded 1°C during the culmination phase and it remained above the mean until the fall season of 2016 (Fig. 3c-d). Decreased precipitation over Sulawesi was observed from April 2015 to February 2016 (Fig. 3e-f). Similar trends were also revealed from data obtained at Bariri site (Fig. 4a-b). The easterly shift of the convection zone resulted also in higher solar radiation over Indonesia during summer and fall of 2015 and winter of 2015–2016 with a maximum in the period from September to November 2015 (Fig. 3a, 4a).

The comparisons of the 2013–17 time series of the mean monthly deviations of meteorological parameters measured at the tower in Bariri with anomalies calculated for the study area from reanalysis data showed that the deviations of solar radiation, air temperature and precipitation in 2015–16 from the mean values observed during the entire period of instrumental measurements at the experimental site are very well correlated with the anomalies obtained from reanalysis. From March 2015 up to October 2016 air temperature (*T*) exceeded the mean temperature of 2003–2017 (Fig. 5a). Precipitation (*P*) remained lower than

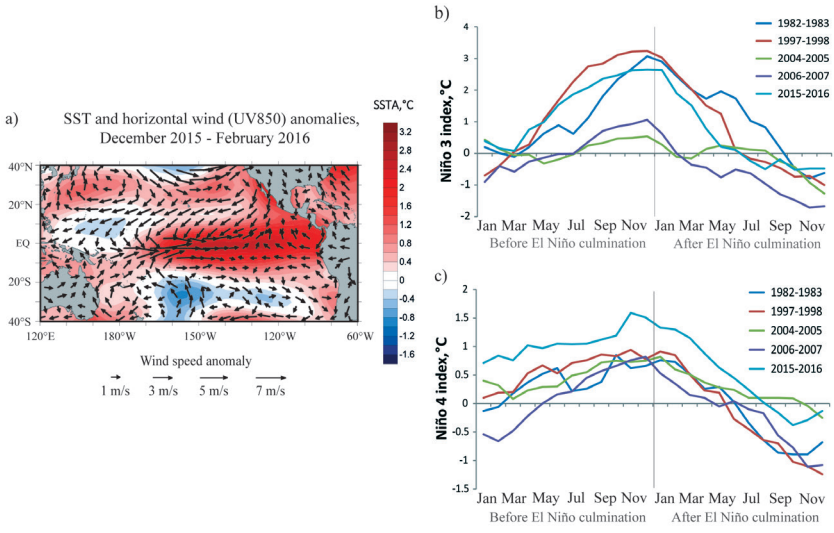

Fig. 2. (a) Anomalies of sea surface temperature and wind at 850 hPa for the culmination phase of the El Niño 2015/2016 (December 2015 - February 2016), (b) the Niño3 index, and (c) the Niño4 index evolution during the strongest El Niño events since 1980s

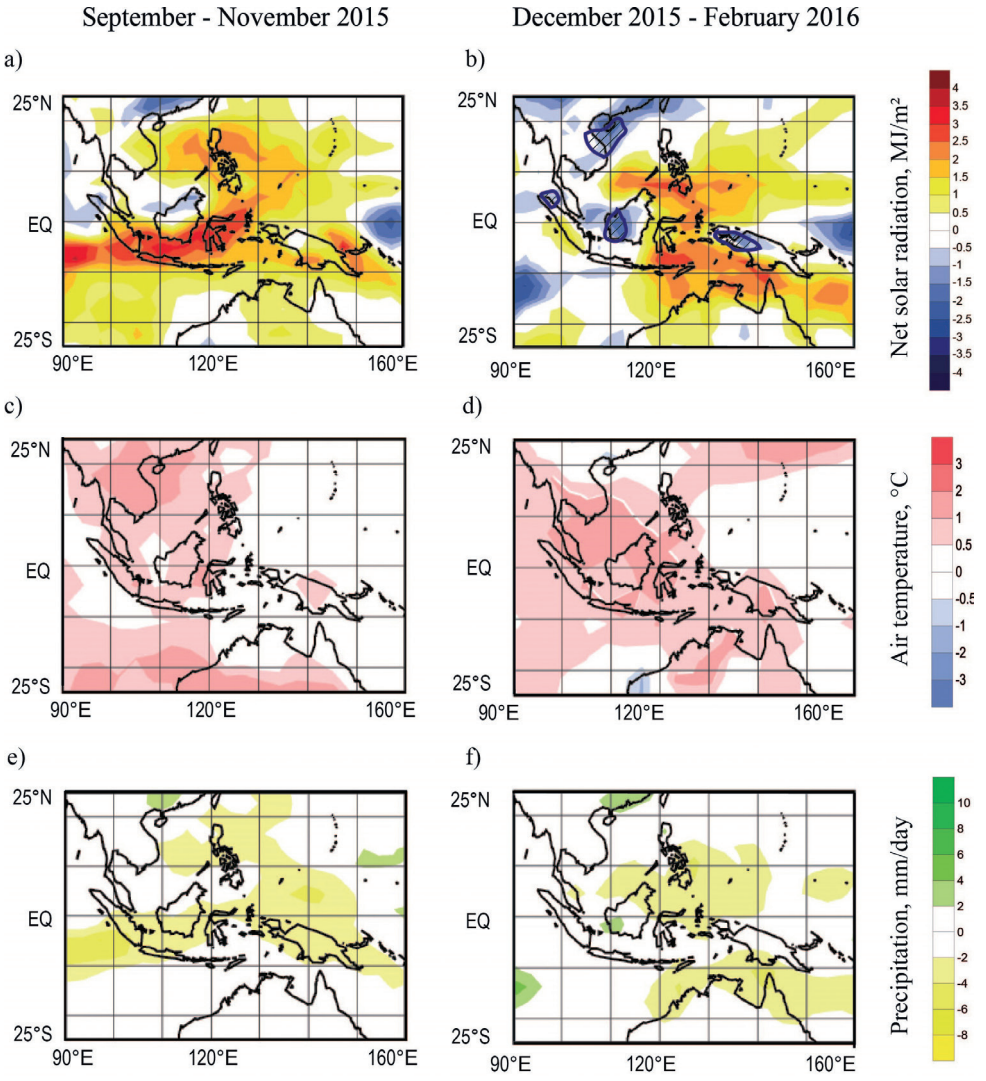

Fig. 3. Anomalies of (a, b) surface net solar radiation, (c, d) near-surface air temperature and (e, f) precipitation during the development (left panel) and the peak (right panel) of the El Niño 2015/2016

the mean values until November 2015 and exceeded them in the El Niño culmination phase (Fig. 5b). The temporal variability of water vapor pressure (*e*) is characterized by insignificant variations during the El Niño development that are interrupted shortly before the El Niño peak and manifested in a fast growth of *e* simultaneously with *P* increasing (Fig. 4b,5b). The deviations of incoming solar radiation (*G*) and net radiation (*Rn*) from mean values have two peaks before and after El Niño culmination: in August-September 2015 and March-April 2016, respectively (Fig. 5a,e).

Monthly *NEE* and *RE* rates increase during the El Niño development, and the deviations from the means reached their maximum values almost simultaneously with the peak of the event (Fig. 5c-d). NPP exhibits negative anomalies during the El Niño of 2015–2016, while GPP shows a small, but consistent growth during the whole period from 2013 to 2017 (Fig. 4c-d, 5c-d). LE rate reaches maximum values about two months prior to the El Niño peak and suddenly decreases in the culmination and decaying phases (Fig. 4e, 5e). It can be explained by joint effects of positive cor-

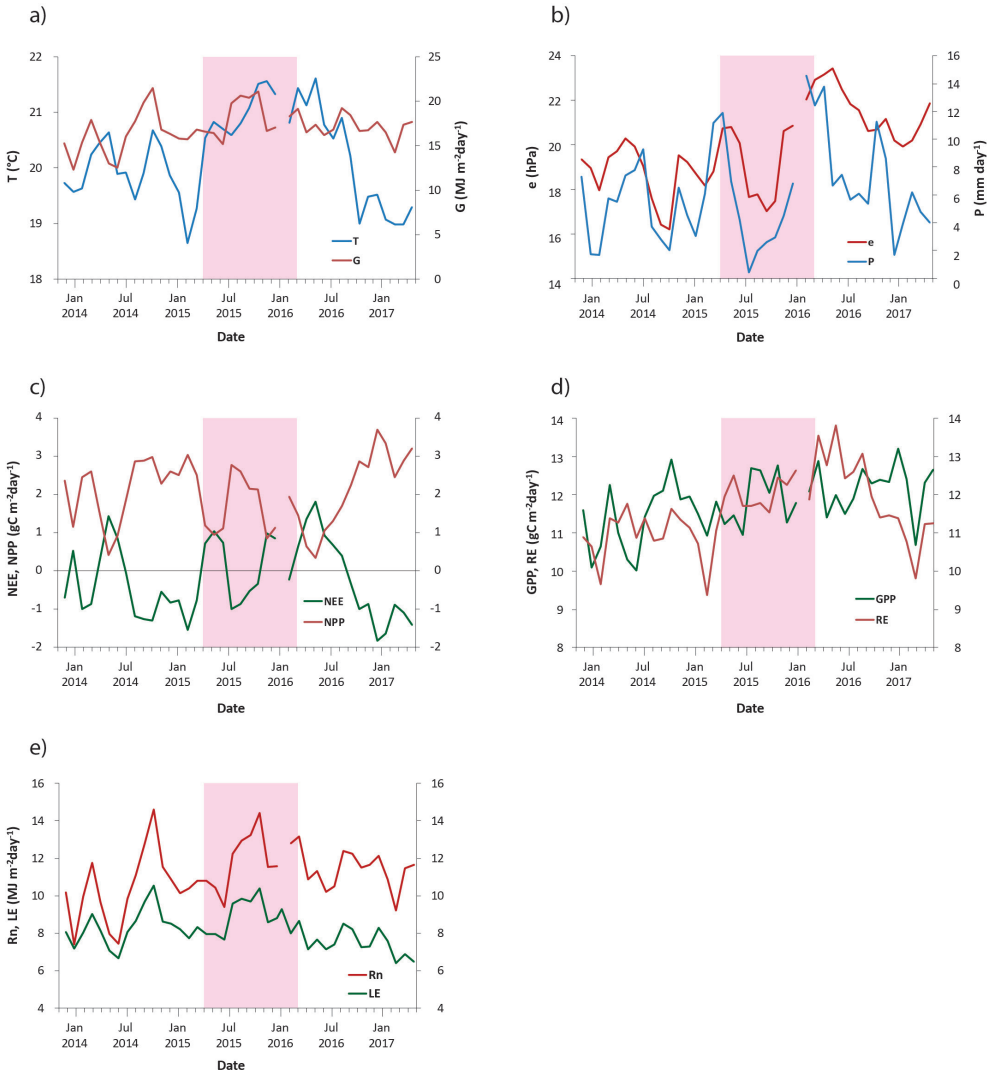

Fig. 4. Temporal variability of (a) *T* (°C) and *G* (MJ m^{-2} day^{-1}), (b) *e* (hPa) and *P* (mm day^{-1}), (c) *NEE* (gC m^{-2} day^{-1}) and *NPP* (gC m^{-2} day^{-1}), (d) *GPP* (gC m^{-2} day^{-1}) and *RE* (gC m^{-2} day^{-1}), (*e*) *Rn* (MJ m^{-2} day^{-1}) and *LE* (MJ m^{-2} day^{-1}) for the measurement period from December 2013 to April 2017 at the Bariri site. Pink rectangle indicates the period of the El Niño (Niño4 >1.0°C) from April 2015 to March 2016

relations of ΔLE with ΔT (r=0.64, p<0.05) and with ΔG (r=0.49, p<0.05) as well as of negative correlation of ΔLE with Δe (r=-0.48, p<0.05).

In order to analyze the response of energy and CO_2 fluxes in the tropical rainforest in Central Sulawesi to ENSO associated anomalies a lag cross correlation analysis is provided (Fig. 6). The cross-correlation analysis shows that NEE and RE rates have similar relationship with ENSO indices: they are negatively correlated before and positively correlated after El Niño peak with maximum at -9 and 4 month lags, respectively. Therefore, NEE and RE are suppressed during the El Niño development phase and intensified after the ENSO culmination. The latter may be considered as a response to the high air temperature observed during the El Niño culmination phase (the maximum positive correlation of ΔT with Niño4 index falls on the same time lag as for ΔRE). Taking into account that *GPP* is not influenced by the

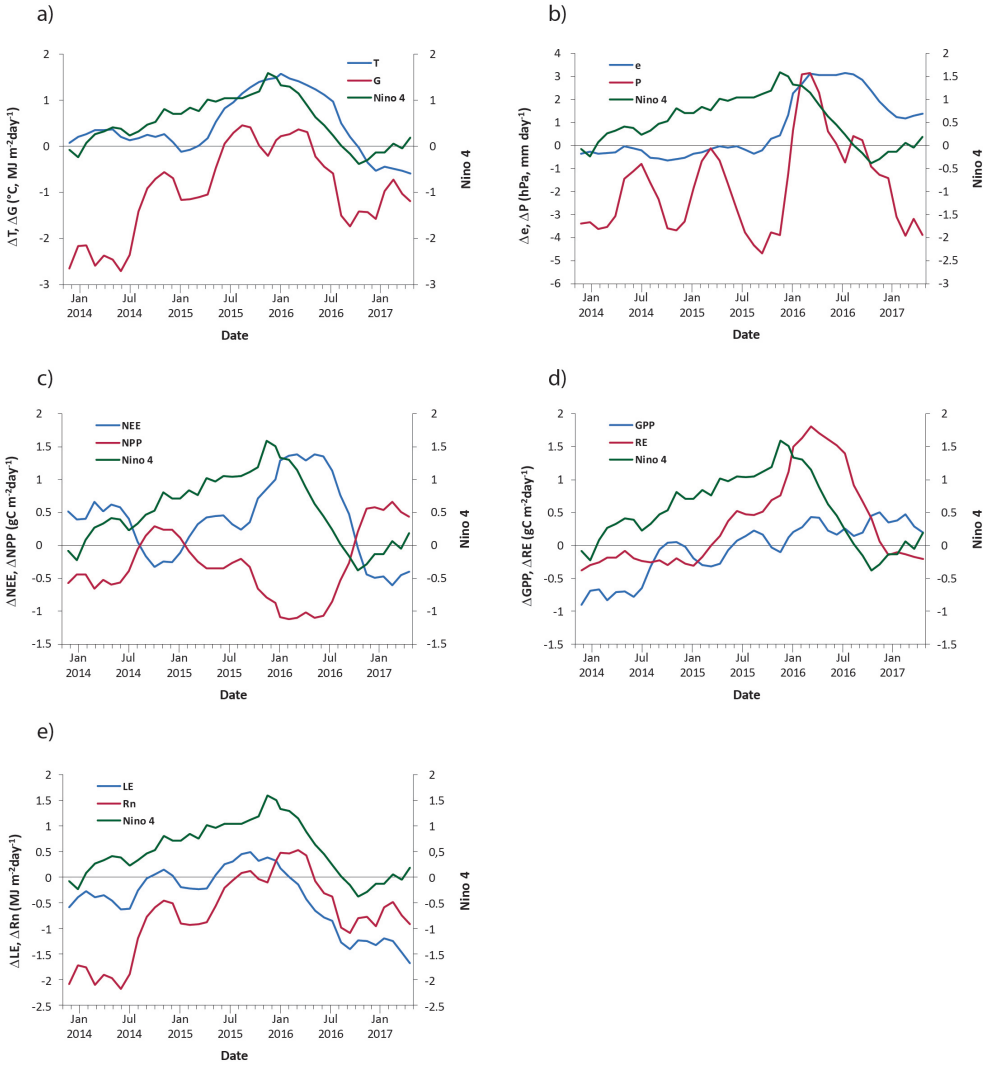

Fig. 5. Deviations from 2003–2017 means of *T* (*ΔT*, °C), *G* (*ΔG*, MJ m^{-2} day^{-1}), *P* (*ΔP*, mm day^{-1}), *e* (*Δe*, hPa), *LE* (*ΔLE*, MJ m^{-2} day^{-1}), *Rn* (*ΔRn*, MJ m^{-2} day^{-1}), *GPP* (*ΔGPP*, gC m^{-2} day^{-1})), *RE* (*ΔRE*, gC m^{-2} day^{-1}), *NEE* (*ΔNEE*, gC m^{-2} day-^{1}) and *NPP* (*ΔNPP*, gC m^{-2} day^{-1}) values at the Bariri site and SST anomalies in Niño4 region (°C)

El Niño of 2015–2016 in a straightforward manner and *ΔGPP* is not correlated with Niño4, a relatively high correlation of *ΔNEE* with Niño4 can be explained by a prevailing contribution of *RE* change into *NEE* variability. The temperature variation is connected in turn with solar radiation anomalies that preceded the air temperature anomaly by 3 months and reached their maximum at the El Niño peak. The same relationships with Niño4 index are observed for Δe and ΔP values suggesting that anomalously high temperature during 2015–2016 El Niño acts as a major influencing factor of observed anomalous conditions. The *LE* anomalies are mostly governed by changes of solar radiation which is supported by the same lag-correlation functions for *ΔG* and *ΔLE*.

Analysis of temporal variability of *ΔNPP* shows that it changed in an opposite phase with *ΔNEE*, *ΔGPP* and *ΔRE* (Fig. 5, 6). *ΔNPP* is positively correlated with Niño4 before the El Niño appearance and negatively correlated at El Niño culmination and its decaying

phases. Notably *ΔNPP* is also in antiphase with temperature changes. The temporal variability of *NPP* usually coincides with the *GPP* pattern and is mainly influenced by *G* and *T* variability. It is likely that the *ΔNPP* reduction after El Niño culmination can be explained, on the one hand, by a very low sensitivity of *GPP* of the tropical rainforest to changes of Niño4 index in the period of the El Niño of 2015–2016 and, on the other hand, by high contribution of *T* variations to the changes of forest canopy autotrophic respiration.

The El Niño of 2015–2016 was classified as a conventional event with some features of Modoki at the mature phase (Osipov and Gushchina 2018). In this context we compared the responses of energy, water and CO_2 fluxes to the El Niño event of 2015–16 with flux anomalies observed during the moderate El Niños of 2004–05 and 2006–07 which were classified as Modoki events.

Comparison results show that the correlation of *ΔG* and *ΔRn* with Niño4 index are quite similar for both periods, however in 2003–08 the *ΔG* and *ΔRn* leads Niño4 by 3 months while in 2013–17 they are almost varied in the same phase. This is due to the fact that Rn and *G* growth during Modoki events occurs earlier in the seasonal cycle as compared to the conventional ENSO event. The *ΔLE* variability is mainly influenced by solar radiation changes, and therefore has a similar pattern for both periods. Maximum correlation between *ΔLE* and Niño4 index in 2003–08 is observed 2 months prior El Niño culmination and its response to Niño4 well agreed with re-

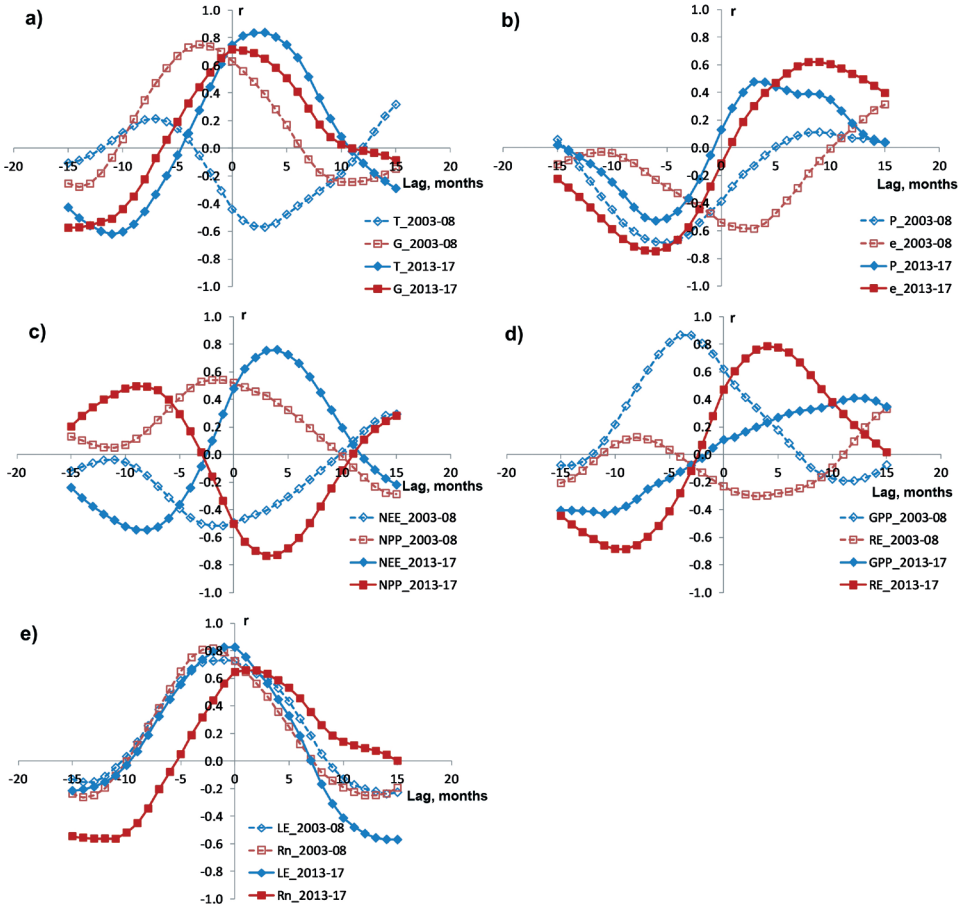

Fig. 6. Cross-correlation (r) functions between *ΔT, ΔG, ΔP, Δe, ΔLE, ΔRn, ΔGPP, ΔRE, ΔNEE* and *ΔNPP* values and Niño4 index. Solid lines – correlation for period from 2013 to 2017, dashed lines for 2003–2008 period

sponses of *Rn* and *G* to Niño4 oscillations. Precipitation is strongly suppressed before El Niño peaks and increases after its culmination for all observed events. Noteworthy a weaker positive correlation between precipitation and Niño4 was observed in 2003–08 as compared to 2013–17. This effect may result from different decaying rate of conventional and Modoki events. The 2015–16 event decayed very quickly and passed to La Niña conditions, associated with extremely high precipitation in the western Pacific, in spring 2016. Whereas the Modoki events (observed in period 2003-08) are usually characterized by a longer decaying phase.

In contrast to solar radiation the air temperature and water vapor pressure anomalies are differently correlated with Niño4 index in 2003-08 and 2013-17 periods. The *ΔT* values follow the *ΔG* growth in 2015-16 and they are positively correlated with Niño4, while during Modoki events of 2003-08 the *T* deviations were always negative and did not exceed -0.5°C (Oltchev et al. 2015). This led to the negative *ΔT* and Niño4 correlation during the entire period of 2003-08 (Fig. 6). As a consequence, ΔRE in 2003-08 was predominantly negative and was negatively correlated with Niño4. Very high correlation of *ΔGPP* and Niño4, and very weak negative correlation of ΔRE and Niño4 resulted in a clearly manifested negative correlation of *ΔNEE* and Niño4 in 2003-08 in contrast to the period from 2013 to 2017, that is characterized by a very weak correlation between *ΔGPP* and Niño4 and in turn a very well manifested positive correlation between *ΔNEE* and Niño4 (Fig. 6). The difference in temporal patterns of *Δe* and Niño4 index in 2003-08 and 2013-17 could result from various air temperature and precipitation responses to the SST oscillation in Niño4 region.

The *NPP* and *RE* responses to the El Niño event are also strongly different in periods of 2003-08 and 2013-17. In 2003-08 *NPP* is mainly influenced by *ΔG*, which was tightly related to Niño4 variability whereas the temperature changes during this period were relatively low causing the small sensitivity of NPP to temperature. In 2015-16 we observed a weak dependence of *ΔGPP* on Niño4 which resulted in a prevailing dependence of *ΔNPP* on T oscillations and, as it was already mentioned, in a negative correlation between *ΔNPP* and Niño4 at culmination and mature phases of the El Niño 2015-16. The different responses of *ΔRE* to Niño4 changes are influenced by different effects of various types of ENSO of different intensity on the pattern of *ΔT* in equatorial Pacific. The El Niño 2015-16 is characterized by a clearly manifested dependence of *ΔT* on Niño4 variation whereas in the period from 2003 to 2008 such relation is insignificant.

The present study focuses on the analysis of possible effects of the 2015-16 El Niño event on the temporal variability of key meteorological parameters and energy, water, and CO_2 fluxes in a tropical rainforest ecosystem. Possible uncertainties of flux estimations provided by the eddy covariance technique (caused by e.g. low turbulence, rainfall events, etc.) were not considered. To derive the flux responses to El Niño intensity we analyze monthly flux deviations from long-term mean fluxes obtained at the experimental site since 2003. Effect of flux measurement uncertainties on monthly flux deviations in this case is relatively small and can be neglected.

CONCLUSIONS

The results of long-term eddy covariance flux measurements in a tropical rainforest in Central Sulawesi showed a very strong influence of the El Niño event of 2015–16 on local and regional meteorological conditions, energy, water, and CO_2 fluxes. The El Niño influence is manifested in a strong increase of incoming solar radiation, low precipitation, and high air temperature that reach their extreme values, or maximum and minimum values. Maximum of low precipitation - is not quite adequate values quite simultaneously with the Niño4 index. Monthly precipitation reached maximum about 3–4 months after El Niño culmination. Increased incoming solar radiation, net radiation and surface temperature resulted in a strong increase of *LE* (surface evapotranspiration) that reached its maxi-

mum about two months before the El Niño peak. *RE* showed a continuous increase simultaneously with air temperature growth resulting in a positive anomaly of NEE (reduced CO_2 uptake). The *GPP* rate is characterized by a very low sensitivity to Niño4 changes and had no impact on *NEE* rates. Low sensitivity of *GPP* to Niño4 also resulted in a negative anomaly of *NPP* that varied in reversed phase with *NEE*.

The discovered tropical rainforest responses (key meteorological parameters as well as energy, water, and CO_2 fluxes) to the El Niño 2015–16 forcing are different from the ones during the moderate El Niño events of 2003–08. The main difference is the strong relationship between air temperature and Niño4 index during 2015–16 that was not observed during 2003–08. As a consequence, the sensitivity of *RE* to Niño4 during the period of 2003–08 was very low in contrast to the well manifested dependence of *RE* on Niño4 during the period of 2015–16. High *RE* was the main driver of CO_2 uptake reduction (decrease of NEE), as well as decrease of NPP during the El Niño phenomenon of 2015–16. No differences in relationships between *LE* and Niño4 for the analyzed periods with El Niño of different intensities were found. It can be assumed that the different sensitivity of the energy, water, and CO_2 fluxes of the tropical rainforest ecosystem to El Niño events is due to intensities intensity of meteorological anomalies that were observed in the region during the considered period. It can be expected that anomalies of key meteorological parameters (e.g. temperature, precipitation, solar radiation) with different intensity may result in opposite effects on the CO_2 and energy fluxes.

ACKNOWLEDGEMENTS

The study was supported by the German Research Foundation (DFG) under the projects "Stability of Rainforest Margins in Indonesia", STORMA (Collaborative German-Indonesian Research Center CRC 552), "Ecological and Socioeconomic Functions of Tropical Lowland Rainforest Transformation Systems (Sumatra, Indonesia)" (Collaborative German-Indonesian Research Center CRC 990) and "BaririFlux" (KN 582/8-1), as well as by Lomonosov Moscow State University (grant No. AAAA-A16-116032810086-4). The authors would like to thank Pak Dudin, Pak Ore, Ibu Aiyen Tjoa, Dietmar Fellert and Edgar Tunsch for assistance with field measurements.

REFERENCES

Alisov B.P. (1954). Die Klimate der Erde. Berlin: Deutscher Verlag der Wissenschaften. 277 pp.

Aubinet M., Vesala T. and Papale D. (2012). Eddy covariance. A practical guide to measurement and data analysis. Springer. 438 pp.

Ashok K., Behera S. K., Rao S. A., Weng H., Yamagata T. (2007). El Niño Modoki and its possible teleconnection. Journal of Geophysical Research, 112, C11007.

Chatfield C. (2004). The Analysis of Time series, An Introduction, 6th ed. New York: Chapman & Hall/CRC, 333 pp.

Chen D. and Chen H.W. (2013) Using the Koppen classification to quantify climate variation and change: An example for 1901-2010. Environmental Development, 6, pp. 69-79

Ciais P., Piao S.-L., Cadule P., Friedlingstein P., and Chedin A. (2009). Variability and recent trends in the African terrestrial carbon balance. Biogeosciences, 6, pp. 1935-1948.

Corlett R., Primack R. (2006). Tropical rainforests and the need for cross-continental comparisons. Trends in Ecology and Evolution, 21 (2), pp. 104–110.

Grace J., Lloyd J., McIntyre J., Miranda A., Meir P., Miranda H., Nobre C., Moncrieff J.B., Massheder J.M., Malhi Y., Wright I. and Gash J.C. (1995). Carbon dioxide uptake by an undisturbed tropical rain forest in south-west Amazonia, 1992 to 1993. Science, 270, pp. 778-780.

Dee D.P. , Uppala S.M. , Simmons A.J. , Berrisford P., Poli P., Kobayashi S., Andrae U., Balmaseda M.A. , Balsamo G., Bauer P., Bechtold P., Beljaars A.C.M. , van de Berg L., Bidlot J., Bormann N., Delsol C., Dragani R., Fuentes M., Geer A.J., Haimberger L., Healy S.B., Hersbach H., Hólm E.V., Isaksen L., Kållberg P., Köhler M., Matricardi M. , McNally A P. , Monge-Sanz B.M., Morcrette J.-J., Park B.-K., Peubey C., de Rosnay P. , Tavolato C., Thépaut J.-N., Vitart F. (2011). The ERA-Interim reanalysis: configuration and performance of the data assimilation system. Quarterly Journal of the Royal Meteorological Society, 137(656), pp. 553–597. https://doi.org/10.1002/qj.828.

Dewitte B., Gushchina D., du Penhoat Y., Lakeev S. (2002). On the importance of subsurface variability for ENSO simulation and prediction with intermediate coupled models of the tropical pacific: A case study for the 1997-1998 El Niño. Geophysical Research Letters, 29(14). https://doi.org/10.1029/2001GL014452.

Diaz H.F., Hoerling M.P., and Eischeid J. K. (2001). ENSO variability, teleconnections and climate change, Int. J. Climatol., 21, pp.1845– 1862, https://doi.org/10.1002/joc.631.

Falk U., Ibrom A., Kreilein H., Oltchev A., Gravenhorst G. (2005). Energy and water fluxes above a cacao agroforestry system in Central Sulawesi, Indonesia, indicate effects of land-use change on local climate. Meteorologische Zeitschrift, 14(2), pp. 219-225.

Feely R.A., Wanninkhof R., Takahashi T., and Tans P. (1999). Influence of El Niño on the equatorial Pacific contribution to atmospheric CO_2 accumulation. Nature, 398, pp. 597-601.

Food and Agriculture Organization of the United Nations. Global Forest Resources Assessment 2015: How are the world's forests changing? (Second Edition). (2016). Rome. 54 pp.

Grace J., Lloyd J., McIntyre J., Miranda A.C., Meir P., Miranda H.S., Nobre C., Moncrieff J., Massheder J., Malhi Y., Wright I., Gash J. (1995). Carbon dioxide uptake by an undisturbed tropical rain in Southwest Amazonia, 1992 to 1993. Science, 270(5237), pp. 778-780.

Gushchina D.Y, Petrosyants M.A., Semenov E.K. (1997). An empirical model of tropical tropospheric circulation during ENSO. part II. Analysis of evolution of circulation characteristics. Russian Meteorology and Hydrology, 2, pp. 8–18.

Hansen M.C., Potapov P.V., Moore R., Hancher M., Turubanova S.A., Tyukavina A., Thau D., Stehman S.V., Goetz S.J., Loveland T.R., Kommareddy A., Egorov A., Chini L., Justice C.O., Townshend J.R.G. (2013). High-Resolution Global Maps of 21st-Century Forest Cover Change. Science, vol. 342 (6160), pp. 850-853. https://doi.org/10.1126/science.1244693.

Hirano T., Segah H., Harada T., Limin S., June T., Hirata R., Osaki, M. (2007) Carbon dioxide balance of a tropical peat swamp forest in Kalimantan, Indonesia. Glob. Change Biol., 13, pp. 412–425.

Huffman G.J, Adler R.F., Bolvin D.T., Gu G. (2009). Improving the global precipitation record: GPCP Version 2.1. Geophys. Res. Lett., 36, L17808. https://doi.org/10.1029/ 2009GL040000.

Ibrom A., Olchev A., June T., Ross T., Kreilein H., Falk U., Merklein J., Twele A., Rakkibu G., Grote S., Rauf A. and Gravenhorst G. (2007). Effects of land-use change on matter and energy exchange between ecosystems in the rain forest margin and the atmosphere. In The stability of tropical rainforest margins: Linking ecological, economic and social constraints. Eds. Tscharntke T., Leuschner C., Zeller M., Guhardja E. and Bidin A., Springer Verlag, Berlin, pp. 463 – 492.

Ibrom A., Oltchev A., June T., Kreilein H., Rakkibu G., Ross Th., Panferov O., Gravenhorst G. (2008) Variation in photosynthetic light-use efficiency in a mountainous tropical rain forest in Indonesia. Tree Physiol., 28, pp. 499–508

Ichii K., Ueyama M., Kondo M., Saigusa N., Kim J., Alberto M.C., Ardö J., Euskirchen E.S., Kang M., Hirano T., Joiner J., Kobayashi H., Marchesini L.B., Merbold L., Miyata A., Saitoh T.M., Takagi K., Varlagin A., Bret-Harte M.S., Kitamura K., Kosugi Y., Kotani A., Kumar K., Li S.G., Machimura T., Matsuura Y., Mizoguchi Y., Ohta T., Mukherjee S., Yanagi Y., Yasuda Y., Zhang Y., Zhao F. (2017). New data-driven estimation of terrestrial CO2 fluxes in Asia using a standardized database of eddy covariance measurements, remote sensing data, and support vector regression. Journal of Geophysical Research Biogeosciences, 122, pp. 767-795.

Le Quéré C., Moriarty R., Andrew R.M., Peters G.P., Ciais P., Friedlingstein P., Jones S.D., Sitch S., Tans P., Arneth A., Boden T.A., Bopp L., Bozec Y., Canadell J.G., Chevallier F., Cosca C.E., Harris I., Hoppema M., Houghton R.A., House J.I., Jain A., Johannessen T., Kato E., Keeling R.F., Kitidis V., Klein Goldewijk K., Koven C., Landa C.S., Landschützer P., Lenton A., Lima I.D., Marland G., Mathis J.T., Metzl N., Nojiri Y., Olsen A., Ono T., Peters W., Pfeil B., Poulter B., Raupach M.R., Regnier P., Rödenbeck C., Saito S., Salisbury J.E., Schuster U., Schwinger J., Séférian R., Segschneider J., Steinhoff T., Stocker B.D., Sutton A.J., Takahashi T., Tilbrook B., van der Werf G.R., Viovy N., Wang Y.-P., Wanninkhof R.; Wiltshire A., Zeng N. (2015). Global carbon budget 2014. Earth System Science Data, 7(1), pp. 47–85.

Malhi Y., Mateus J., Migliavacca M., Misson L., Montagnani L., Moncrieff J., Moors E., Munger J.W., Nikinmaa E., Ollinger S.V., Pita G., Rebmann C., Roupsard O., Saigusa N., Sanz M.J., Seufert G., Sierra C., Smith M.-L., Tang J., Valentini R., Vesala T. and Janssens I.A. (2007). CO2 balance of boreal, temperate, and tropical forests derived from a global database. Global Change Biology, 13(12), pp. 2509-2537.

Malhi Y. (2010). The carbon balance of tropical forest regions, 1990–2005. Current Opinion in Environmental Sustainability, 2(4), pp. 237–244.

Myers N., Mittermeier R.A., Mittermeier C.G., da Fonseca G.A.B., Kent J. (2000) Biodiversity hotspots for conservation priorities. Nature, 403, pp. 853-858. https://doi.org/10.1038/35002501.

Oltchev A., Cermak J., Nadezhdina N., Tatarinov F., Tishenko A., Ibrom A., Gravenhorst G. (2002). Transpiration of a mixed forest stand: field measurements and simulation using SVAT models. Boreal Environmental Reserach, 7(4) , pp. 389-397.

Olchev A., Ibrom A., Ross T., Falk U., Rakkibu G., Radler K., Grote S., Kreilein H., Gravenhorst G. (2008). A modelling approach for simulation of water and carbon dioxide exchange between multi-species tropical rain forest and the atmosphere. J. Ecological Modelling, 212, pp. 122–130.

Olchev A., Ibrom A., Panferov O., Gushchina D., Kreilein H., Popov V., Propastin P., June T., Rauf A., Gravenhorst G., and Knohl A. (2015). Response of CO2 and H2O fluxes in a mountainous tropical rainforest in equatorial Indonesia to El Niño events. Biogeosciences, 12, pp. 6655-6667.

Osipov A. and Gushchina D. (2018). El Nino 2015/2016: evolution, mechanisms, and concomitant remote anomalies. Fundamental and applied climatology (in Russian), 3, pp. 54-81.

Panferov O., Ibrom I., Kreilein H., Oltchev A., Rauf A., June T., Gravenhorst G. and Knohl A. (2009). Between deforestation and climate impact: the Bariri Flux tower site in the primary montane rainforest of Central Sulawesi, Indonesia. The Newsletter of FLUXNET. 2(3), pp. 17-19.

Santoso A., McPhaden M.J., and Cai W. (2017). The defining characteristics of ENSO extremes and the strong 2015/2016 El Niño. Reviews of Geophysics, 55, pp. 1079–1129. https://doi.org/10.1002/2017RG000560.

Trenberth K.E., Branstator G.W., Karoly D., Kumar A., Lau N.-C., and Ropelewski C. (1997). The definition of El Nino. Bulletin of the American Meteorological Society, 78(12), pp. 2771-2777.

Zheleznova I.V., Gushchina D.Y. (2015). The response of global atmospheric circulation to two types of El Niño. Russian Meteorology and Hydrology, 40(3), pp. 170-179.

Zheleznova I. V., Gushchina D. Y. (2016). Circulation anomalies in the atmospheric centers of action during the Eastern Pacific and Central Pacific El Niño. Russian Meteorology and Hydrology, 41 (11-12), pp. 760–769.

Received on December 31st, 2018 Accepted on May 17th, 2019

Vadim V. Mamkin[1*], Yulia V. Mukhartova[2], Maria S. Diachenko and Julia A. Kurbatova[1]
[1] A.N. Severtsov Institute of Ecology and Evolution, Russian Academy of Sciences, Moscow, Russia
[2] Faculty of Physics, Moscow State University, Moscow, Russia
*** Corresponding author:** vadimmamkin@gmail.com

THREE-YEAR VARIABILITY OF ENERGY AND CARBON DIOXIDE FLUXES AT CLEAR-CUT FOREST SITE IN THE EUROPEAN SOUTHERN TAIGA

ABSTRACT. Forest clearing strongly influences the energy, water and greenhouse gas exchange at the land surface - atmosphere interface. To estimate effects of clear cutting on sensible (*H*), latent heat (*LE*) and CO_2 fluxes the continuous eddy covariance measurements were provided at the recently clear-cut area situated in the western part of Russia from spring 2016 to the end of 2018. The possible effects of surrounding forest on the air flow disturbances and on the spatial pattern of horizontal advection terms within the selected clear-cut area were investigated using a process-based 3D momentum, energy and CO_2 exchange model. The modeling results showed a very low contribution of horizontal advection term into total turbulent momentum fluxes at flux tower location in case of the southern wind direction. The results of field flux measurements indicated a strong inter- and intra-annual variability of energy and CO_2 fluxes. The energy budget is characterized by higher daily and monthly *LE* fluxes throughout the entire period of measurements excepting the first two months after timber harvest. The mean Bowen ratio ($\beta=H/LE$) was 0.52 in 2016, 0.30 - in 2017 and 0.35 - in 2018. Analysis of CO_2 fluxes during the first year following harvest showed that the monthly CO_2 release at the clear-cut area consistently exceeded the CO2 uptake rates. The mean net ecosystem exchange (*NEE*) in the period was 3.3±1.3 $gC \cdot m^{-2} \cdot d^{-1}$. During the second and the third years of the flux measurements the clear-cut was also a prevailed sink of CO_2 for the atmosphere excepting short periods in June and in the first part of July when daily CO_2 uptake was higher than CO_2 release rates. The mean *NEE* rates averaged for the entire warm period of corresponding years were 1.2±2.3 $gC \cdot m^{-2} \cdot d^{-1}$ in 2017 and 2.8±2.5 $gC \cdot m^{-2} \cdot d^{-1}$ in 2018, respectively. The mean ratio between gross primary production (*GPP*) and ecosystem respiration (*TER*) was 0.58 in 2016, 0.84 - in 2017 and 0.74 - in 2018.

KEY WORDS: clear-cut, eddy covariance, southern taiga, net ecosystem exchange, energy fluxes, 3D hydrodynamic model

CITATION: Vadim V. Mamkin, Yulia V. Mukhartova, Maria S. Diachenko, Julia A. Kurbatova (2019) Three-Year Variability Of Energy And Carbon Dioxide Fluxes At Clear-Cut Forest Site In The European Southern Taiga. Geography, Environment, Sustainability,
Vol.12, No 2, p. 197-212
DOI-10.24057/2071-9388-2019-13

INTRODUCTION

Clear-cutting is one of the most widespread logging practice, which can substantially transform energy, water vapor and CO_2 exchange between forest ecosystems and the atmosphere and affect the climate system at multiple scales. Effects of different logging practices as well as natural forest disturbances on vegetation-atmosphere interaction is a key topic of various experimental and modeling studies provided over the recent decades (Amiro et al. 2010; Masek and Collatz 2006; Olchev et al. 2009; Radler et al. 2010; Coursolle et al. 2012; Ma et al. 2013; Molchanov et al. 2017). Clear-cutting influences surface albedo, net radiation, surface roughness and consequently the energy flux partitioning into sensible (H), latent (*LE*) and soil heat fluxes (McCaughey 1985; Amiro 2001; Rannik et al. 2002; Kowalski et al. 2003). Amiro et al. (2006) and Williams et al. (2013) reported on significant decrease of evapotranspiration rate at clear-cut sites that can be observed during several years after logging. At the same time some studies showed that the Bowen ratio (β=*H/LE*) at the clear-cut sites can be quickly recovered (within one growing season) to pre-disturbance values (Matthews et al. 2017). Most of the recent studies focused on effects of clear-cutting on ecosystem-atmosphere interaction were dedicated to analysis of CO_2 balance changes in forest ecosystems induced by the clear-cut harvesting (Amiro et al. 2010; Aguilos et al. 2014; Grant et al. 2010; Paul-Limoges et al. 2015; Rodrigues et al. 2010; etc.). Numerous studies reported that clear-cutting lead to forest ecosystem change from CO_2 sink to CO_2 source in annual or growing season balances. Aggregated analysis of FLUXNET data sets for territory of the USA and Canada provided by Amiro et al. (2010) showed that forest ecosystems after clear-cutting require usually about 20 years to restore their ability to be a CO_2 sink in the annual balance. The time that is necessary for ecosystem after logging to reach a compensation point between carbon uptake and release rates is varied depending on local climate and geographical conditions. Also, most of available studies use a hypothesis that clear-cutting lead to the substantial decrease of gross primary production (*GPP*). The ecosystem respiration (*TER*) rate in general doesn't change substantially after the forest disturbance mainly due to rapid compensation of the decreased autotrophic respiration contribution into *TER* by increased heterotrophic one (Amiro et al. 2010; Paul-Limoges et al. 2015; Williams et al. 2014).

Most of previous experimental studies were performed at disturbed forest ecosystems in North America and Europe but effects of clear-cutting on ecosystem-atmosphere exchange in Russian boreal forests are still very poorly investigated and represented in a couple of experimental and modeling studies only (e.g. Machimura et al. 2008; Mamkin et al. 2016, 2019; Molchanov et al. 2017). Boreal forests cover large areas in Russia and they are very sensitive to different natural and anthropogenic disturbances (Zamolodchikov et al. 2017). It makes very necessary to investigate the consequences of the forest disturbances for biogeophysical and biogeochemical climate regulation functions of the forest ecosystems, first of all in the context of prediction the carbon balance of Russian forests and their influence on climate system. To derive the long-term variability of CO_2 fluxes in forest ecosystems an eddy covariance measuring technique is mainly used (Aubinet et al. 2012; Burba et al. 2013). The eddy covariance flux measurements are usually provided in undisturbed forest ecosystems over uniform vegetation canopy. The forest damaging can obviously lead to strong air flow disturbances that make very difficult the application of eddy covariance techniques for the flux measurements in such areas. Vegetation heterogeneity can lead to disruption of the basic assumptions used in the method and hence, to large uncertainties in measured fluxes. To improve the accuracy of the energy, water vapor and greenhouse gas (GHG) flux estimates the effects of non-homogeneous canopy should be taken into account in the flux analysis (Belcher et al. 2011). During the last time the influence of the clear-cuts on the air flows has been investigated using mathematical models in several studies (e.g. Frank and Ruck 2008; Sogachev et al. 2005;

Mamkin et al. 2016; Levashova et al. 2017). Within the framework of our study the temporal variability of the energy, water vapor and CO_2 fluxes during the three growing seasons following harvest using continuous eddy covariance flux measurements was analyzed and the possible influence of forest edges on the air flows within the clear-cut using 3D hydrodynamic turbulent exchange model was assessed.

METHODS

Site description

The flux measurements were performed at the recently clear-cut forest ecosystem in the sustainable management zone of the Central Forest Biosphere Reserve (CFBR) in Tver region in the western part of Russia (56.44° N, 33.05° E, 250 m a.s.l.) (Fig. 1). CFBR is located in the south-western part of Valdai Hills and its territory belongs to the humid continental climate zone (Dfb type according to the Köppen-Geiger classification scheme) (Peel et al. 2007; Kuricheva et al. 2017). The Climate Moisture Index (*CMI*) (Willmott and Feddema 1992), calculated as the ratio between annual precipitation and potential evapotranspiration, ranged between 0.3-0.4 that corresponded to moderately wet surface moisture conditions (Novenko et al. 2018). The forest vegetation is consisted of typical species of southern taiga e.g. Norway spruce (Picea abies), European white birch (*Betula pubescens*) and Eurasian aspen (*Populus tremula*) (Knohl et al. 2002).

The area of experimental clear-cut site is about 4.5 ha and it is situated at a flat plain with well-drained sod-pale podzolics soils. Organic carbon content in the upper soil horizons varied between 2.73 and 5.79%. It is surrounded by mixed forest stand with Norway spruce (*Picea abies*), European white birch (*Betula pendula*) and Eurasian aspen (*Populus tremula*). The site was clear-felled in March-April 2016. After logging the large amount of harvest residuals, stumps and litter were remained on the ground (Mamkin et al. 2016, 2019). During the first months after logging the site was free of any vegetation. Active vegetation regeneration started after the ground defrosting in the second half of April. In June-August the vegetation was mainly represented by herbaceous vegetation with dominated starwort (*Stellaria graminea*), sow-tit (*Fragaria vesca*) and wood-sour (*Oxalis acetosella*), as well as by a small number of juvenile aspen (*Populus tremula*). In the first half of August the leaf area index (*LAI*) of vegetation increased to 2.5 $m^2 \cdot m^{-2}$ and the grassy and woody vegetation reached 70-90 cm height while the height of the surrounding forest

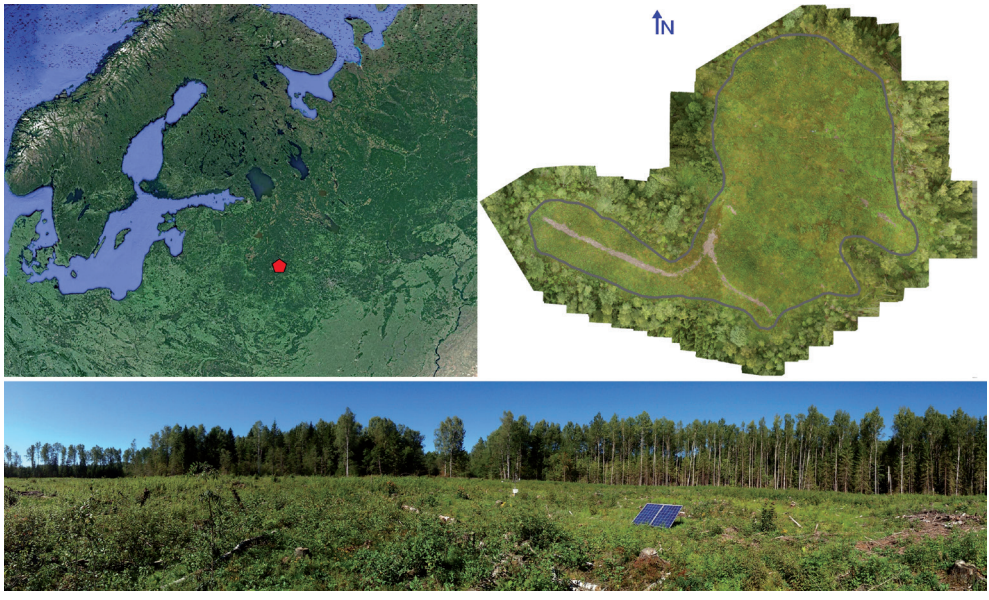

Fig. 1. Geographical location, aerial photo and panoramic view of the clear-cut area (Aug. 2016)

varied from 18 to 22 m (Mamkin et al. 2019).

During the winter 2016-2017 all juvenile trees were completely destructed by wild animals. Therefore, at the beginning of the growing season 2017 *LAI* was again close to 0 $m^2 \cdot m^{-2}$. The vegetation cover in summer 2017 was very diverse and represented by different types of both grassy and woody plants. The woody vegetation was mainly represented by juvenile aspen (*Populus tremula*), European alder (Alnus glutinosa), rowan-tree (*Sorbus aucuparia*), Norway maple (*Acer platanoides*) and red raspberry (*Rubus idaeus*). A herbaceous vegetation is composed mainly of grasswort (*Cerastium arvense*), sow-tit (*Fragaria vesca*), water avens (*Geum rivale*), common rush (*Juncus effusus*) and honeysweet (*Filipendula ulmaria*). The growth rate of juvenile trees in 2017 was very slow whereas their growth rate in 2018 was significantly higher and comparable with high growth rate observed in summer 2016. In the second half of June 2018 LAI at the clear-cut reached the maximum value - 3.7 $m^2 \cdot m^{-2}$.

Meteorological and eddy-covariance flux measurements

The 3 m tower for flux measurements at the clear-cut site was installed immediately after the timber harvest in April 2016. The tower location was chosen taking into account the dominating southern wind direction in spring and summer (Mamkin et al. 2016). The eddy covariance equipment includes open-path CO_2/H_2O gas analyzer LI-7500A (LI-COR Inc., USA) and 3-D ultrasonic anemometer WindMaster Pro (Gill Instruments, UK). The instruments were mounted on the tower at the height of 2.4 m above the ground.

The air temperature, relative humidity and precipitation rates were measured by the weather transmitter WXT 520 (Vaisala Inc., Finland) that was installed at the height of 2 m above the ground. Global and reflected short-wave solar radiation as well as long-wave incoming and outgoing radiation was measured using 4-component radiometer NR01 (Hukseflux Thermal Sensors, The Netherlands) at the height of 1.9 m. To obtain the temperature and volumetric water content (SWC) of the upper soil layer four reflectometers CS655 (Campbell Sci. Inc., USA) were installed around the tower in the soil at the 10 cm depth. Soil heat flux was measured using three heat flux sensors HFP01SC (Hukseflux Thermal Sensors, The Netherlands) installed in the soil at the 5 cm depth.

The eddy covariance data was sampled at the frequency of 10 Hz using Analyzer interface unit LI-7550 (LI-COR Inc., USA). Meteorological parameters were collected with data logger CR3000 (Campbell Sci. Inc., USA) at the frequency of 0.1 Hz and averaged over 30 - min time intervals. The Eastern European time (UTC+2) was used for data storage. The data acquisition by most of the sensors started in 2016 on 7 April and continued until 18 October. The soil temperature and volumetric water content measurements started on 19 May 2016, and the soil heat flux measurements started on 3 August 2016. In 2017 all measurements continued since 6 May to 15 November. In 2018 the measurements started on 4 February and continued until the end of the year.

Data post-processing

All steps of data post-processing were performed according to guidelines for data analysis (Aubinet et al. 2012; Burba et al. 2013). Flux calculation from the raw data was carried out for 30-min time intervals using EddyPro data processing software (LI-COR Inc., USA), with implementing of all necessary corrections and statistical tests. The footprint characteristics were estimated using the model suggested by Kljun et al. (2004). Quality check included 0-2 flag policy (Mauder and Foken 2006). The fluxes were determined with corresponding storage terms that was estimated according to Migliavacca et al. (2009). After data post-processing all fluxes with flag 2, as well as the fluxes with flag 0 and 1, containing the spikes and measured under e.g. rainfall and dew events, weak turbulence and low wind, were removed from the final data sets. The u*-filtering procedure was implemented for estimation of net ecosystem exchange (*NEE)* of CO_2. The mean threshold values of *u** were 0.086 $m \cdot s^{-1}$ for 2016, 0.197 $m \cdot s^{-1}$ - for 2017 and 0.064 $m \cdot s^{-1}$ - for 2018, respectively. The *u**-filtering, gap filling of the flux data and partitioning of *NEE* into *TER* and *GPP* was per-

formed using REddy proc online tool (Wutzler et al. 2018).

A three-dimensional hydrodynamic model for momentum, water vapor and carbon dioxide exchange between a non-uniform land surface and the atmosphere

A three-dimensional (3D) hydrodynamic model uses a 1.5-order closure scheme and it is based on a system of averaged Navier-Stokes and continuity equations for the mean wind speed components, as well as on the reaction-advection-diffusion equation for H_2O and CO_2 transfer within the atmospheric surface layer (Garratt 1992; Wyngaard 2010; Mukhartova et al. 2015). The 3D wind speed components,

$$\vec{V} = \vec{V}(x,y,z,t), \vec{V} = \{u,v,w\}$$

and concentration of any green house gases (GHG), e.g. CO_2, $c = c(x,y,z,t)$, are considered as functions of horizontal coordinates *x, y*, and vertical coordinate *z*, where *x* is the coordinate along the prevailed wind direction, and *z* is equal to the height above the ground surface. The model uses Reynolds's decomposition and expresses the wind speed and concentrations of any considered GHG as sums of their mean values and deviations:

$$\vec{V} = \overline{\vec{V}} + \vec{V}'$$

and $c = \bar{c} + c'$,

where $\overline{\vec{V}} = \{\bar{u}, \bar{v}, \bar{w}\}$ and $\bar{c}$ are mean values of corresponding parameters, $\vec{V'} = \{u', v', w'\}$ and *c'* - their deviations. In case of neutral atmospheric stratification the averaged Navier-Stokes and continuity equations can be written as:

$$\frac{\partial \overline{\vec{V}}}{\partial t} + (\overline{\vec{V}}, \nabla)\overline{\vec{V}} = -\frac{1}{\rho_0}\nabla \delta P - \left(\frac{\partial}{\partial x}\overline{u'\vec{V}'} + \frac{\partial}{\partial y}\overline{v'\vec{V}'} + \right.$$

$$\left. + \frac{\partial}{\partial z}\overline{w'\vec{V}'} \right) + \vec{F}^{cor} + \vec{F}^{d}, \quad div\overline{\vec{V}} = 0,$$

where ρ_0 is the density of dry air, δP is the mean pressure deviation from the hydrostatic distribution, $\vec{F}^{cor}$ and $\vec{F}^{d}$ are the Coriolis and drag force acting within the vegetation cover. The Coriolis force components can be written as:

$$\vec{F}^{cor} = -2\Omega\vec{\eta} \cdot \overline{\vec{V}}$$

where Ω is angular velocity of the Earth rotation ($7.29 \cdot 10^{-5}$ rad s^{-1}) and $\vec{\eta}$ is the unit vector along the axis of rotation. Taking into account the significance of the term $\eta_Z = \sin\psi$ (ψ is the geographic latitude), the components of $\vec{F}^{cor}$ can be written as:

$$F_x^{cor} = f \cdot \bar{v},\ F_y^{cor} = -f \cdot \bar{u},\ F_Z^{cor} = 0,\ f = 2\Omega\sin\psi$$

The drag force can be expressed as follows:

$$\vec{F}^{d} = -c_d \cdot LAD\left|\overline{\vec{V}}\right| \cdot \overline{\vec{V}}$$

where c_d is the dimensionless drag coefficient (we assume in our study that c_d=0.4), *LAD* is the leaf area density ($m^2 \cdot m^{-3}$), that describes the total area of vegetation elements (leaves, branches, tree trunks) per unit volume.

The 1.5-closure scheme assumes that the turbulent fluxes can be expressed using the turbulent kinetic energy *E* and turbulent exchange coefficient *K* as follows:

$$\overline{u'u'} = \frac{2}{3}E - 2K\frac{\partial \bar{u}}{\partial x},\ \overline{v'v'} = \frac{2}{3}E - 2K\frac{\partial \bar{v}}{\partial y},$$

$$\overline{w'w'} = \frac{2}{3}E - 2K\frac{\partial \bar{w}}{\partial z},$$

$$\overline{u'v'} = -K\left(\frac{\partial \bar{u}}{\partial y} + \frac{\partial \bar{v}}{\partial x}\right), \overline{u'w'} = -K\left(\frac{\partial \bar{u}}{\partial z} + \frac{\partial \bar{w}}{\partial x}\right),$$

$$\overline{v'w'} = -K\left(\frac{\partial \bar{v}}{\partial z} + \frac{\partial \bar{w}}{\partial y}\right),$$

$$E = \frac{1}{2}\left\{\overline{(u')^2} + \overline{(v')^2} + \overline{(w')^2}\right\},\ K = C_\mu \frac{E^2}{\varepsilon}$$

where C_μ is a dimensionless model parameter, and ε is the dissipation rate for turbulent kinetic energy.

The values of *E* and ε are found from the system of differential equations (Sogachev and Panferov 2006; Mukhartova et al. 2017; Olchev et al. 2017):

$$\frac{\partial E}{\partial t} + (\overline{\vec{V}}, \nabla)E = div\left(\frac{K}{\sigma_E}\nabla E\right) + P_E - \varepsilon,$$

$$\frac{\partial \varphi}{\partial t} + (\overline{\vec{V}}, \nabla)\varphi = div\left(\frac{K}{\sigma_\varphi}\nabla \varphi\right) + \frac{\varphi}{E}\left(C_{\varphi 1} \cdot P_E - C_{\varphi 2} \cdot \varepsilon\right) + \Delta_\varphi,$$

where φ ($\varphi = \varepsilon \cdot E^{-1}$) is the supplemented function characterizing the scale of turbulence. The dimensionless constants $\sigma_E = \sigma_\varphi = 2$ introduce the Prandtl number for turbulent

kinetic energy and turbulent Schmidt number for the function φ, respectively. The function P_E describes the shear generation of turbulent kinetic energy and can be expressed as:

$$P_E = \left\{ \left(\overline{u'u'}\frac{\partial \overline{u}}{\partial x} + \overline{u'v'}\frac{\partial \overline{u}}{\partial y} + \overline{u'w'}\frac{\partial \overline{u}}{\partial z} \right) + \left(\overline{v'u'}\frac{\partial \overline{v}}{\partial x} + \overline{v'v'}\frac{\partial \overline{v}}{\partial y} + \overline{v'w'}\frac{\partial \overline{v}}{\partial z} \right) + \left(\overline{w'u'}\frac{\partial \overline{w}}{\partial x} + \overline{w'v'}\frac{\partial \overline{w}}{\partial y} + \overline{w'w'}\frac{\partial \overline{w}}{\partial z} \right) \right\}$$

The coefficients $C_{\varphi 1}$=0.52 and $C_{\varphi 2}$=0.8 are model constants. The term $\Delta\varphi$ describes the increase of energy dissipation caused by air flow interaction with vegetation elements. In the first approximation it can be expressed as follows:

$$\Delta\varphi = 12 \cdot \sqrt{C_\mu} \cdot (C_{\varphi 2} - C_{\varphi 1}) \cdot c_d \cdot LAD \cdot \left|\vec{V}\right| \cdot \varphi$$

RESULTS AND DISCUSSION

Meteorological conditions

The three year measuring period from spring 2016 to the end of 2018 is characterized by various weather conditions (Fig. 2). Mean air temperature for the measurement period of 2016 was 12.9°C, 11.6°C - for 2017 and 13.4°C - for 2018. The precipitation amount for corresponding periods of measurements was 404.2 mm, 455.2 mm and 383.4 mm, respectively. Total amount of incoming solar radiation in the measurement period in 2016 was 2247 MJ·m^{-2}. Due to prevailed cloudy weather conditions in summer 2017 the total amount of incoming solar radiation in the period from May to October 2017 was some smaller than in 2016 - 2087 MJ·m^{-2}. The summer of 2018 is characterized by sunny weather conditions and incoming solar radiation reached maximum values for period from May to October - 2413 MJ·m^{-2}. The temporal variability of albedo at the clear-cut area was closely depended on vegetation dynamics. In 2016 albedo grew from 11% in May to 26 % in August. In 2017 the vegetation cover was denser and higher that resulted in lower day-to-day variation of albedo. The maximal albedo values in 2017 were observed in June (about 30%) and the minimums in October (about 14%). Mean daily albedo variation for corresponding period in 2018 changed from 28% in May to 18% in October.

The soil temperature at the depth of 10 cm changed from 6.4 to 20.4 °C in 2016 (since 19 May), from 4.6 to 16.4 °C - in 2017, and from 6.7 to 17.9 °C - in 2018. Due to active vegetation regeneration in 2017 and 2018 the daily soil temperature range in the periods was some lower than in 2016. The *SWC* variability was characterized by relatively small variations between 0.36 and 0.43 m^3·m^{-3} in 2016, between 0.37 to 0.49 m^3·m^{-3} in 2017 and between 0.29 and 0.42 m^3·m^{-3} in 2018.

Modelling of the wind field and turbulent patterns within the clear-cut area

To describe the spatial pattern of wind speeds and atmospheric fluxes, as well as to estimate the possible influence of forest edges on the air flows at the flux tower location the 3D hydrodynamic turbulent exchange model was applied. The main attention in our modeling experiments was paid to descriptions of the 3D wind and flux distributions within and

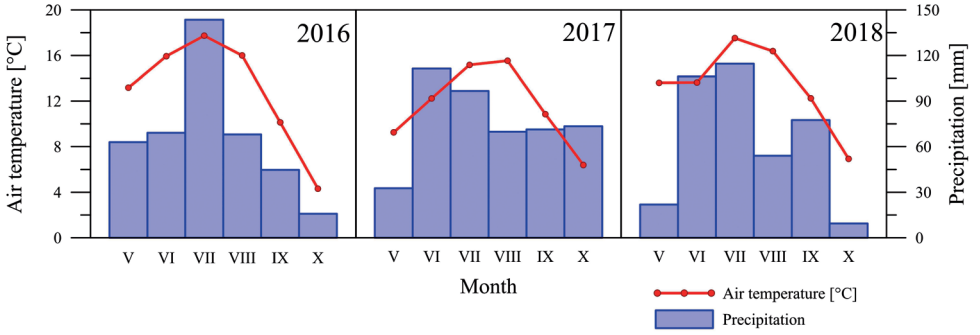

Fig. 2. Monthly mean air temperature at 2 m height and monthly precipitation amount for the period from May to October 2016, 2017 and 2018 respectively

around the clear-cut area under different wind directions and thermal stratifications of the atmosphere.

Analysis of the spatial variability of horizontal and vertical wind speed components showed significant heterogeneity of the air flows within and around the clear cut area. It is also enhanced by complex shape of the clear-cut boundary (Fig. 1). Results of numerical experiments showed that the largest effect of the clear-cut on the air flows is mainly appeared along the windward forest edge whereas at the leeward forest edge this effect is less pronounced (Fig. 3). The leeward part of the clear-cut is characterized by prevailed downward air flows (with negative *w*) whereas the upward air flows (*w* is positive) are appeared at its windward part (Fig. 3). It is very important to point out that the vertical wind velocity around the tower location as well as its horizontal gradient at 3-4 m height above the ground surface was relatively small (close to 0 $m \cdot s^{-1}$) (Fig. 3c) that can be used as one of criteria indicating sufficient reestablishing of the air flow at tower location after its disturbance at the leeward forest edge.

To estimate effects of the air flow disturbances at forest edges to wind and turbulent conditions within the clear-cut area we also analyzed the spatial patterns of the horizontal and vertical momentum fluxes. Negligible horizontal turbulent flux is a requirement for representative eddy covariance measurements. Fig. 4 shows an example of vertical distribution of momentum fluxes along profile crossing the clear-cut are from south to north and passing through the tower location. Maximum horizontal turbulent fluxes are detected at leeward part of the clear-cut area and at windward forest edge. Moreover the high anomalies of horizontal turbulent fluxes are also observed above the clear-cut area in the atmospheric layers higher than 20-30 meters above the ground. Area of minimum (close to zero) horizontal turbulent fluxes is situated in the northern (windward) part of the clear-cut and its boundaries overlap the flux tower location (Fig. 4a). Analysis of vertical turbulent fluxes along selected profile at the height of flux tower is also showed their very low variability at the tower location. All these factors confirm obviously the representativeness of provided eddy covariance flux measurements under southern wind directions. In case of the northern winds the influence of the forest edge on wind and turbulence patterns at flux tower location is much higher that can obviously lead to significant uncertainties in flux estimations using the eddy covariance technique.

Temporal variability of energy fluxes

Analysis of the eddy covariance flux data showed that the monthly *LE* fluxes exceeded *H* fluxes during the entire three-year period of flux measurements (Fig. 5). The total *LE* fluxes integrated over the period from 06 May to 18 October are also higher than total sums of *H* fluxes (Table 1). The temporal variability of *H* fluxes is mainly influenced by changes of global radiation. The daily *H* fluxes are usually reached maximum values in May and in the first half of June (8 $MJ \cdot m^{-2} \cdot d^{-1}$ in 2016, 5.9 $MJ \cdot m^{-2} \cdot d^{-1}$ in 2017, and 6.6 $MJ \cdot m^{-2} \cdot d^{-1}$ in 2018) and minimums (-1 $MJ \cdot m^{-2} \cdot d^{-1}$ in 2016, -0.2 $MJ \cdot m^{-2} \cdot d^{-1}$ in 2017 and -1.6 $MJ \cdot m^{-2} \cdot d^{-1}$ in 2018) in October, respectively. Seasonal variability of the *LE* fluxes is mainly influenced by the changes of global radiation and vegetation dynamics at the clear-cut area. In 2016 *LE* varied between 1.7 and 8.9 $MJ \cdot m^{-2} \cdot d^{-1}$. Maximal values were observed in the second half of July when *LAI* reached its maximum values (4.5 $m^2 \cdot m^{-2}$). The maximal values of *LE* were observed in the second half of June 2017 (10.8 $MJ \cdot m^{-2} \cdot d^{-1}$) and in the first half of June 2018 (11.8 $MJ \cdot m^{-2} \cdot d^{-1}$), respectively.

The differences in seasonal courses of the *H* and *LE* fluxes can be well characterized by variations of the Bowen ratio *(β=H/LE)*. In all years of flux measurements *β* decreased from May to September and increased slightly in October. The mean monthly *β* in 2016 reached 1.4, whereas it doesn't exceed 0.9 in 2017 and 0.7 in 2018. Maximum values of *β* in 2016 were observed mainly

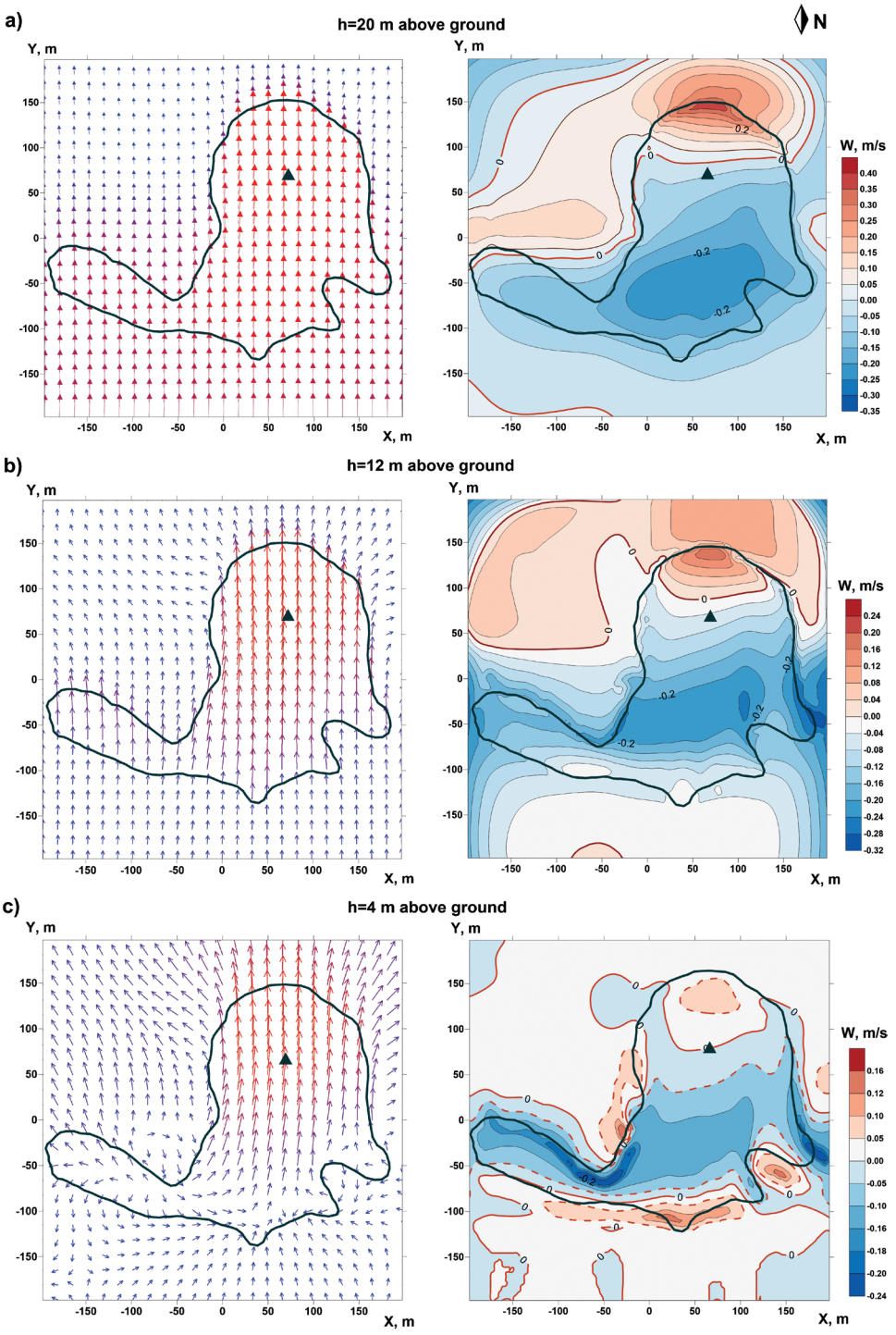

Fig. 3. Horizontal (*u,v*) (left) and vertical (*w*) (right) wind components within and around the clear-cut area under neutral thermal atmospheric stratification, and prevailed (southern) wind direction at the heights 20 m (a), 12 m (b) and 4 m (c) above ground surface. The dark green line denotes the clear-cut edge and the black triangle shows the tower location

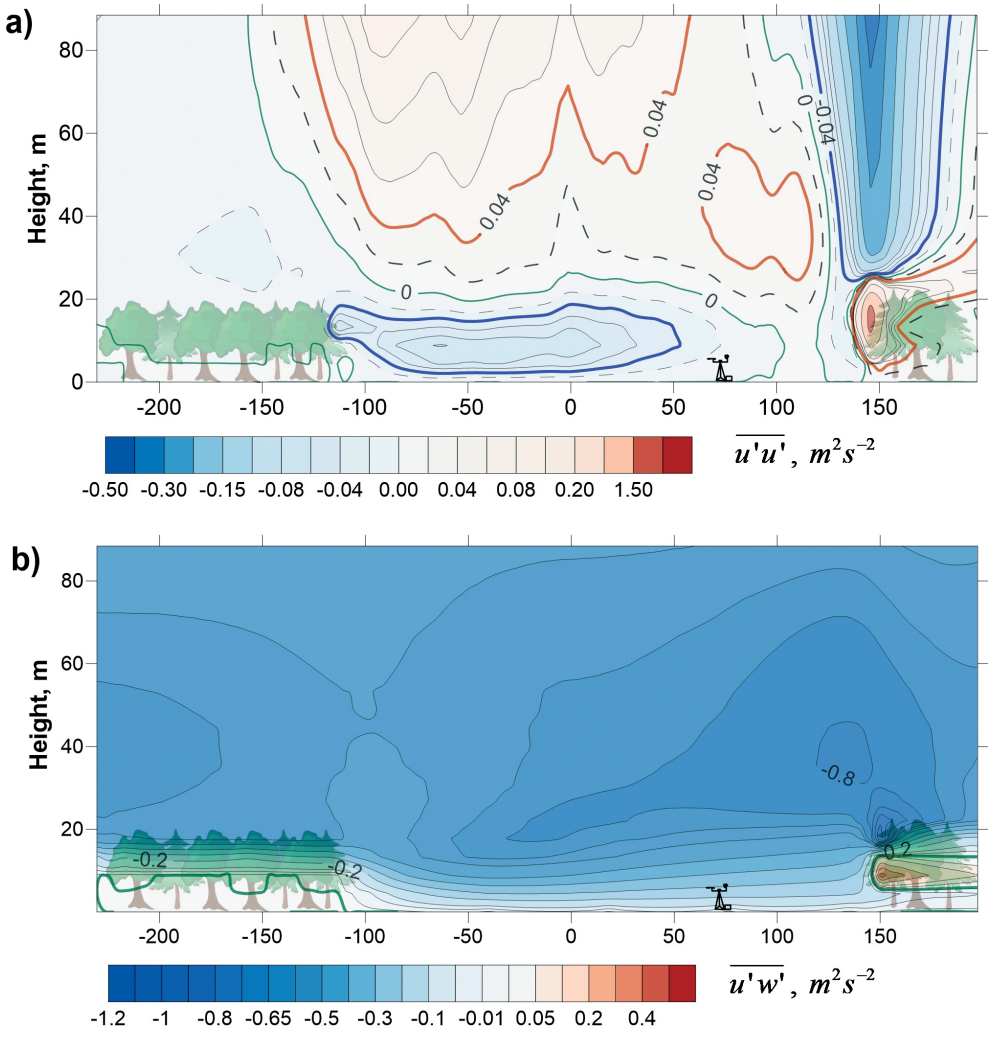

Fig. 4. Horizontal $\overline{u'u'} = -2K\frac{\partial \bar{u}}{\partial x}$ **(a) and vertical** $\overline{u'w'} = -K\left(\frac{\partial \bar{u}}{\partial z} + \frac{\partial \bar{w}}{\partial x}\right)$ **(b) momentum flux distributions along a profile crossing the clear-cut in the south-north direction**

due to the lack of vegetation cover (after timber harvesting) in May and June. Since July β decreased to 0.3 and was quite invariable until the beginning of September. Similar trends with maximum of β in May were observed also in springs of 2017 and 2018. The summer variability of β in 2017 and 2018 was mainly governed by weather conditions and it was also relatively small. β varied in the periods between 0.1 and 0.5. The mean β for the measuring period in 2016 was 0.5, in 2017 - 0.3 and in 2018 - 0.4 (Table 1).

It is important to point out that the lowest values of *LE* were measured during the first year after the timber harvest. The previously conducted comparisons of the energy fluxes in undisturbed forest and at the clear-cut area (Mamkin et al. 2019) showed that the clear-cutting led to decrease of *LE* by 30% in the first growing season following harvest. Moreover, the H also decreased due to the harvesting by 22%. The decreasing trend in turbulent energy fluxes due to clear-cutting can be explained by increased albedo and consequently reduced surface

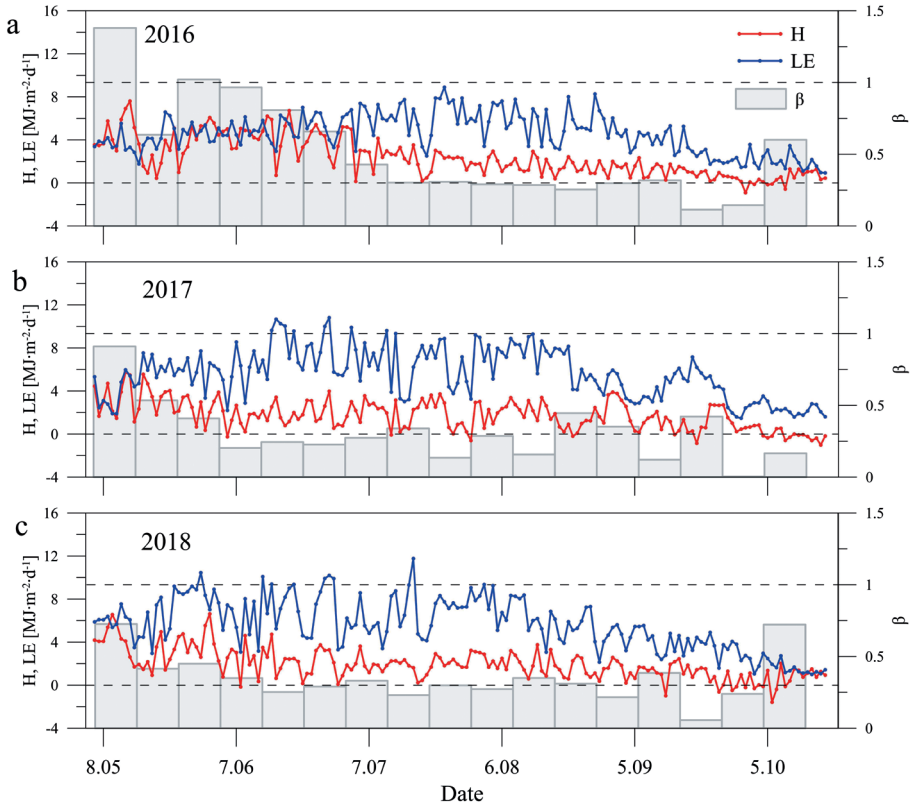

Fig. 5. Temporal variability of daily sensible (*H*) and latent (*LE*) heat fluxes, and the Bowen ratio (*β*) for the period (06.05-18.10) in 2016 (a), 2017 (b) and 2018 (c)

available energy (available energy is a difference between net radiation and sum of soil heat flux and canopy energy storage term). It should be also taken into account that the low *LAI* values influence the transpiration and evapotranspiration rates. Moreover, the comparison showed that in spite of lower *H* and *LE* fluxes measured at the clear-cut site the mean seasonal *β* for the clear-cut and undisturbed forest was almost the same (Mamkin et al. 2019).

In year 2017 and 2018 *LE* grew by ~20% following active regeneration of grassy and woody vegetation at the clear-cut area, and *β* decreased from 0.52 to 0.30-0.35. The main differences between *LE* fluxes were observed between the first and the second years after the harvest although the weather conditions in the second and the third years were more contrasting. Fast recovery of *β* value to pre-disturbance values have been discussed in several studies (e.g. Amiro et al. 2006; Matthews et al. 2017; Williams et al. 2013). Particularly, Williams et al. (2013) also reported about decreased summer and autumn *H* and increased *LE* for period from the first to the third years following harvest at the clear-cut of Norway spruce (Picea abies) forest in Massachussets (USA).

Temporal variability of CO_2 fluxes

Assessment of the temporal variability of *NEE* over the entire period of flux measurements at the clear-cut area showed that the CO_2 fluxes are characterized by a large variability mainly governed by weather conditions (first of all, incoming solar radiation, air temperature) and amount of regenerated photosynthesizing vegetation (Fig. 6). In 2016 the daily sums of *NEE* were persistently positive (clear-cut acted as a CO_2 source for the atmosphere) and varied between 0.8 and 7.2 $gC \cdot m^{-2} \cdot d^{-1}$. The cumulative sum of *NEE* for the entire period of measurements was 553 $gC \cdot m^{-2}$ (3.3±1.3

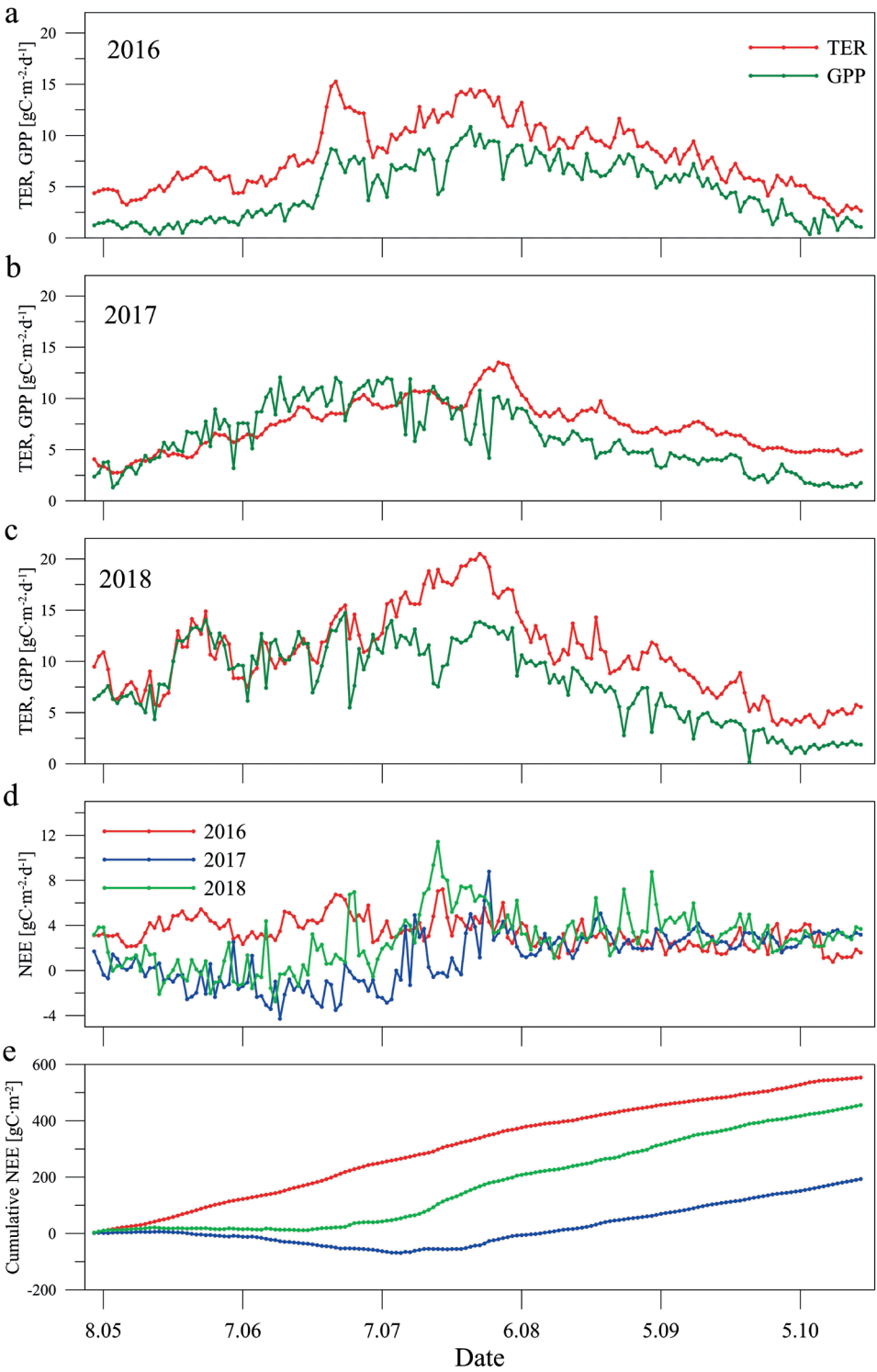

Fig. 6. Mean daily sums of total ecosystem respiration (*TER*) and gross primary production (*GPP*) in (a) 2016, (b) 2017 and (c) 2018, as well as mean daily sums of *NEE* (d) and cumulative *NEE* (e) at the clear-cut site in 2016, 2017 and 2018

gC·m^{-2}·d^{-1}). The growing season of 2017 is characterized by higher CO_2 uptake (*GPP*). During the period from May to June the daily *GPP* rates were higher than *TER* rates (*NEE* is negative) and the clear-cut ecosystem for a short two-month period acted as a CO_2 sink for the atmosphere. At the same time the total growing season *NEE* rate was still positive - 193 gC·m^{-2} (1.2±2.3 gC·m^{-2}·d^{-1}). In 2018 the total seasonal *NEE* grew to 456 gC·m^{-2} (2.8±2.5 gC·m^{-2}·d^{-1}) and negative values of daily *NEE* (*GPP* higher than *TER*) were estimated only in May and in the first half of June. It should be pointed out that the minimum daily NEE in 2018 was only -2.8 gC·m^{-2}·d^{-1} in contrast to 2017 when the minimum *NEE* was -4.3 gC·m^{-2}·d^{-1}. Such effects can be explained by higher *TER* rates in 2018 due to higher air temperatures. Maximal daily *NEE* reached 8.8 gC·m^{-2}·d^{-1} in 2017 and 11.4 gC·m^{-2}·d^{-1} in 2018, respectively. The maximum *NEE* rates are usually observed in July.

As it was already mentioned the *NEE* rate is strongly depended on the difference between *GPP* and *TER*. In 2016 *GPP* and *TER* rates had similar shapes of seasonal courses. The maximum rates of *GPP* and *TER* reached in July - 10.8 gC·m^{-2}·d^{-1} and 15.3 gC·m^{-2}·d^{-1}, respectively. In 2017 and 2018 maximum values of *GPP* were observed in June (12.1 gC·m^{-2}·d^{-1} in 2017 and 14.7 gC·m^{-2}·d^{-1} in 2018) whereas *TER* reached maximum rates in July similarly to 2016 (13.7 gC·m^{-2}·d^{-1} in 2017 and 20.5 gC·m^{-2}·d^{-1} in 2018). Cumulative sums of *GPP* for growing seasons were 778 gC·m^{-2} in 2016, 1021 gC·m^{-2} in 2017 and 1322 gC·m^{-2} in 2018, while cumulative sums of *TER* were 1331 gC·m^{-2} in 2016, 1214 gC·m^{-2} in 2017 and 1778 gC·m^{-2} in 2018, respectively. Therefore, the *NEE* increase in 2018 was observed under the grown *GPP* and can be explained by high values of *TER* in 2018. The mean ratios of *GPP/TER* during the period of flux measurements from May to October were 0.58 in 2016, 0.84 in 2017 and 0.74 in 2018.

The cumulative *NEE* for the period from May to October was positive in each year of the flux measurements, which is consistent with the results of the previous studies, obtained in other boreal and sub-boreal post clear-cut forest ecosystems of the young successional stages (Amiro et al. 2010; Augilos et al. 2014; Grant et al. 2010). It is mainly governed by *GPP/TER* ratio that is varied in our study between 0.1-0.9. The *GPP/TER* ratio is usually grown with vegetation recovery but this process can be interrupted by the short-term periods of *GPP/TER* decreasing caused by changes of key meteorological parameters (e.g. the high air temperature in 2018 resulted in strong increase of *TER* rate and decrease of *NEE*). The same effects were observed by Paul-Limoges et al. (2015) between the second and the third years following harvest at the Douglas-fir clear-cut in the Vancouver island in Canada and by Pypker and Fredeen (2002) between 5th and 6th years at the spruce-fir clear-cut

Table 1. Cumulative sums of energy fluxes, evapotranspiration (ET), and CO_2 fluxes at the clear-cut for the period from 06 May to 18 Oct in 2016, 2017 and 2018

Variable	2016	2017	2018
H [MJ·m^{-2}]	389.6	287.8	322.9
LE [MJ·m^{-2}]	755.4	927.6	924.2
ET [mm]	302.2	371.0	369.7
β	0.52	0.30	0.35
NEE [gC·m^{-2}]	553.4	193.3	456.0
GPP [gC·m^{-2}]	777.5	1020.5	1322.3
TER [gC·m^{-2}]	1330.9	1213.7	1778.3
GPP/TER	0.58	0.84	0.74

in British Columbia (Canada). Paul-Limoges et al. (2015) explained increasing the *TER* rate by large biomass at the clear-cut site. Pypker and Fredeen (2002) is also discussed such effect and tried to connect it with the changes in soil temperature and soil moisture conditions.

The temporal variability of CO_2 fluxes measured at various post-clear felled ecosystems are influenced by local weather and climate conditions, as well as by dominating vegetation species. The most available estimations of *NEE* rate for boreal and temperate clear-cut forest ecosystems during the first 8 years after the harvest varies between 0.2 to 6.2 $gC \cdot m^{-2} \cdot d^{-1}$ (Mamkin et al. 2019). In various biomes the estimates of limiting factors controlling *NEE* and its components can be very different. For example (Gao et al. 2015) reported that the clear-cut of poplar (*Populus dettoides*) in subtropical China became a CO_2 sink at the end of the first growing season following harvest. It is obvious that to explain adequately the temporal and spatial variation of *NEE* rate, effect of all possible factors that control *GPP* and *TER* rates at the clear-cut (including analysis of environmental condition, vegetation and soil properties, biomass of debris, etc.) should be investigated within aggregated experimental and modeling studies.

CONCLUSIONS

The results of our experimental and modeling studies showed a strong influence of clear-cutting on the energy and water vapor fluxes between forest ecosystem and the atmosphere. It is manifested in disturbance of the spatial air flow patterns, in change of microclimatological conditions and the energy and CO_2 fluxes. Decreased net radiation and higher albedo in summer period are resulted in lower *LE* and *H* fluxes. Sufficient soil moisture and regenerated vegetation promote higher *LE* fluxes comparing with *H* ones. Obtained *NEE* dynamics are consistent with the hypothesis that clear-cutting turns forest ecosystems from CO_2 sink to CO_2 source for the atmosphere for several years after logging. *NEE* was reached maximal values in the first year after the harvest and minimal - in the second one. *GPP* increased from the first to the third year while the *TER* decreased in the second and increased in the third year, respectively. Variability of *GPP/TER* ratio is well corresponded to results obtained in other post-clear felled boreal forest ecosystems of the young successional stages. Representativeness of our eddy covariance flux measurements were controlled by results of numerical experiments using a 3D hydrodynamic model. It was shown that the area at tower location under prevailed southern wind direction is characterized by low horizontal and vertical momentum fluxes as well as by small horizontal gradient of the vertical wind speed component. Disturbing effect of the forest edges on our flux measurements can be therefore neglected. The results obtained in the present study can be applicable for predicting the influence of deforestation on the regional weather conditions in boreal ecozone and for estimating its consequences for the climate system.

ACKNOWLEDGEMENTS

The study was funded by the RFBR and Russian Geographical Society according to the research project № 17-05-41127. It was also partially supported by the Presidium of the Russian Academy of Sciences (programs № 51 «Climate change: causes, risks, consequences, problems of adaptation and regulation» and № 41 "Biodiversity of natural systems and biological resources of Russia".

REFERENCES

Aguilos M., Takagi K., Liang N., Ueyama M., Fukuzawa K., Nomura M., Kishida O., Fukazawa T., Takahashi H., Kotsuka C., Sakai R., Ito K., Watanabe Y., Fujinuma Y., Takahashi Y., Muragama T., Saigusa N., Sakai R. (2014). Dynamics of ecosystem carbon balance recovering from a clear-cutting in a cool-temperate forest. Agric. For. Meteorol., 197, pp. 26-39.

Amiro B. D., Barr A. G., Black T. A., Iwashita H., Kljun N., McCaughey J. H., Morgenstern K., Murayama S., Nesic Z., Orchansky A. L., Saigusa N. (2006). Carbon, energy and water fluxes at mature and disturbed forest sites, Saskatchewan, Canada. Agric. For. Meteorol., 136, pp. 237-251.

Amiro B. D., Barr A. G., Barr J. G., Black T. A., Bracho R., Brown M., Chen J., Clark K. L., Davis K. J., Desai A. R., Dore S., Engel V., Fuentes J. D., Goldstein A. H., Goulden M. L., Kolb T. E., Lavigne M. B., Law B. E., Margolis H. A., Martin T., McCaughey J. H., Misson L. , Montes–Helu M., Noormets A., Randerson J. T., Starr G., Xiao J. (2010). Ecosystem carbon dioxide fluxes after disturbance in forests of North America. J. Geophys. Res. 115, G00K02.

Aubinet M., Vesala T. and Papale D. (2012). Eddy Covariance: A Practical Guide to Measurement and Data Analysis, Dordrecht, The Netherlands, Springer

Burba G. (2013). Eddy covariance method for scientific, industrial, agricultural and regulatory applications: A field book on measuring ecosystem gas exchange and areal emission rates. LI-COR Biosciences

Coursolle C., Margolis H. A., Giasson M. A., Bernier P. Y., Amiro B. D., Arain M. A., Barr A.G., Black T.A., Goulden M.L., McCaughey J.H., Chen J. M., Dunn A.L., Grant R.F., Lafleur P.M. (2012). Influence of stand age on the magnitude and seasonality of carbon fluxes in Canadian forests. Agric. For. Meteorol. 165, pp. 136-148.

Garratt J.R. (1992). The atmospheric boundary layer. Cambridge: Cambridge University press.

Grant R. F., Barr A. G., Black T. A., Margolis H. A., McCaughey J. H., Trofymow J. A. (2010). Net ecosystem productivity of temperate and boreal forests after clearcutting - a Fluxnet–Canada measurement and modelling synthesis. Tellus Ser. B, 62(5), pp. 475-496.

Kljun, N., Calanca P., Rotach M. W., Schmid H. P. (2004). A simple parameterisation for flux footprint predictions Boundary Layer Meteorol. 112, pp. 503-523

Knohl A., Kolle O., Minayeva T. Y., Milyukova I. M., Vygodskaya N. N., Foken T., Schulze E. D. (2002). Carbon dioxide exchange of a Russian boreal forest after disturbance by wind throw. Global Change Biol, 8(3), pp. 231-246.

Kowalski S., Sartore M., Burlett R., Berbigier P., Loustau D. (2003). The annual carbon budget of a French pine forest (Pinus pinaster) following harvest. Global Change Biol., 9(7), pp. 1051-1065.

Kurbatova J., Li C., Varlagin A., Xiao X., Vygodskaya N. (2008). Modeling carbon dynamics in two adjacent spruce forests with different soil conditions in Russia. Biogeosciences 5, pp. 969–980.

Kuricheva O., Mamkin V., Sandlersky R., Puzachenko J., Varlagin A., Kurbatova J. (2017). Radiative entropy production along the paludification gradient in the Southern Taiga. Entropy, 19(1), p. 43.

Levashova N. T., Muhartova J. V., Olchev A.V. (2017) Two approaches to describing the turbulent exchange within the atmospheric surface layer. Mathematical Models and Computer Simulations, 9(6), pp. 697–707

Ma Y., Geng Y., Huang Y., Shi Y., Niklaus P.A., Jin-Sheng B.S. (2013). Effect of clear-cutting silviculture on soil respiration in a subtropical forest of China. Journal of Plant Ecology 6(5), pp. 335-348.

Masek J.G., and Collatz G.J. (2006). Estimating forest carbon fluxes in a disturbed southeastern landscape: Integration of remote sensing, forest inventory, and biogeochemical modeling. Journal of Geophysical Research: Biogeosciences 111, G01006.

Machimura T., Kobayashi Y., Hirano T., Lopez L., Fukuda M., Fedorov A. N. (2005). Change of carbon dioxide budget during three years after deforestation in eastern Siberian larch forest. J. Agric. Meteorol., 60(5), pp. 653-656.

Mamkin V., Kurbatova J., Avilov V., Mukhartova Y., Krupenko A., Ivanov D., Levashova N., Olchev A. (2016). Changes in net ecosystem exchange of CO2, latent and sensible heat fluxes in a recently clear-cut spruce forest in western Russia: results from an experimental and modeling analysis. Environ. Res. Lett., 11(12), p. 125012.

Mamkin V., Kurbatova J., Avilov V., Ivanov D., Kuricheva O., Varlagin A., Yaseneva I., Olchev A. (2019) Energy and CO2 exchange in an undisturbed spruce forest and clear-cut in the southern taiga. Agricultural and Forest Meteorology 265, pp. 252–268.

Matthews B., Mayer M., Katzensteiner K., Godbold D. L., Schume, H. (2017). Turbulent energy and carbon dioxide exchange along an early–successional windthrow chronosequence in the European Alps. Agric. For. Meteorol. 232 (15), pp. 576-594

Mauder M., Foken T. (2006). Impact of post-field data processing on eddy covariance flux estimates and energy balance closure. Meteorologische Zeitschrift, 15, pp. 597-609.

Migliavacca M., Meroni M., Manca G., Matteucci G., Montagnani L., Grassi G., Zenone T., Teobaldelli M., Goded I., Colombo R., Seufert G. (2009). Seasonal and interannual patterns of carbon and water fluxes of a poplar plantation under peculiar eco-climatic conditions. Agr. For. Meteorol. 149, pp. 1460–1476

Molchanov A.G., Kurbatova Yu. A., Olchev A.V., (2017). Effect of Clear-Cutting on Soil CO2 Emission. Biology Bulletin, 44 (2), pp. 218-223.

Mukhartova Yu. V., Levashova N. T., Olchev A. V., Shapkina N. E. (2015) Application of a 2D model for describing the turbulent transfer of CO2 in a spatially heterogeneous vegetation cover. Moscow University Physics Bulletin, 70(1), pp. 14-21

Mukhartova Yu.V., Krupenko A.S., Mangura P.A., Levashova N.T. (2017). A two-dimensional hydrodynamic model of turbulent transfer of CO2 and H2O over a heterogeneous land surface. IOP Conf. Ser.: Earth Environ. Sci. 107, p. 012103.

Novenko E., Tsyganov A.N., Olchev A.V. (2018) Palaeoecological data as a tool to predict possible future vegetation changes in the boreal forest zone of European Russia: a case study from the Central Forest Biosphere Reserve. IOP Conf. Series: Earth and Environmental Science, 107, p. 012104

Olchev A., Radler K., Sogachev A., Panferov O., Gravenhorst G. (2009). Application of a three-dimensional model for assessing effects of small clear-cuttings on radiation and soil temperature. Ecol. Modell., 220(21), pp. 3046-3056.

Olchev A.V., Mukhartova Yu.V., Levashova N.T., Volkova E.M., Ryzhova M.S., Mangura P.A. (2017). The Influence of the Spatial Heterogeneity of Vegetation Cover and Surface Topography on Vertical CO2 Fluxes within the Atmospheric Surface Layer. Izvestiya, Atmospheric and Oceanic Physics, 53(5), pp. 539-549.

Paul-Limoges E., Black T. A., Christen A., Nesic Z., Jassal R. S., (2015). Effect of clearcut harvesting on the carbon balance of a Douglas-fir forest. Agric. For. Meteorol. 203, pp. 30-42.

Peel M.C., Finlayson B.L., McMahon T.A. (2007). Updated world map of the Koppen-Geiger climate classification. Hydrol. Earth. Syst. Sci., 11, pp. 1633–1644.

Pypker T. G., Fredeen A. L., (2002). Ecosystem CO2 flux over two growing seasons for a sub-Boreal clearcut 5 and 6 years after harvest. Agric. For. Meteorol, 114(1-2), pp. 15-30.

Radler K., Oltchev A., Panferov O., Klinck U., Gravenhorst G. (2010). Radiation and temperature responses to a small clear-cut in a spruce forest. The Open Geography Journal 3, pp. 103-114.

Rodrigues A., Pita G., Mateus J., Kurz-Besson C., Casquilho M., Cerasoli S., Pereira J. (2011). Eight years of continuous carbon fluxes measurements in a Portuguese eucalypt stand under two main events: Drought and felling. Agricultural and Forest Meteorology, 151(4), pp. 493-507.

Sogachev A., Panferov O. (2006). Modification of two-equation models to account for plant drag. Bound. Lay. Meteorol. 121(2), pp. 229-266.

Williams C. A., Vanderhoof M. K., Khomik M., Ghimire B. (2014). Post–clearcut dynamics of carbon, water and energy exchanges in a midlatitude temperate, deciduous broadleaf forest environment. Global Change Biol., 20(3), pp. 992-1007.

Willmott C.J. and Feddema J.J., (1992). A more rational climatic moisture index. Professional Geographer 44, pp. 84-88.

Wutzler T., Lucas-Moffat A., Migliavacca M., Knauer J., Sickel K., Šigut L., Menzer O., Reichstein, M. (2018). Basic and extensible post-processing of eddy covariance flux data with REddyProc, Biogeosciences, 15, pp. 5015-5030.

Wyngaard J. C. (2010). Turbulence in the Atmosphere. Cambridge: Cambridge University press.

Zamolodchikov D. G., Grabovskii V. I., Shulyak P. P., Chestnykh, O. V. (2017). Recent decrease in carbon sink to Russian forests. Doklady Biological Sciences 476(1), pp. 200-202.

Received on January 31st, 2019 Accepted on May 17th, 2019

Olga E. Sukhoveeva[1*], Dmitry V. Karelin[1,2]
[1] Institute of Geography, Russian Academy of Sciences, Moscow, Russia
[2] Center for Problems of Ecology and Productivity of Forests, Russian Academy of Sciences, Moscow, Russia
*** Corresponding author:** olgasukhoveeva@gmail.com

APPLICATION OF THE DENITRIFICATION-DECOMPOSITION (DNDC) MODEL TO RETROSPECTIVE ANALYSIS OF THE CARBON CYCLE COMPONENTS IN AGROLANDSCAPES OF THE CENTRAL FOREST ZONE OF EUROPEAN RUSSIA

ABSTRACT. The retrospective dynamics of major components of the carbon cycle under land use changes in the Central Forest zone of European Russia was investigated. This area is known as one of the most important agricultural and economical regions of the country. We applied the process-based simulation model DNDC (DeNitrification-DeComposition) recommended by UNCCC and world widely used. In this study the DNDC model was parameterized for Russian arable soils using official statistical information and data taken from published sources. Three main carbon variables in agrolandscapes were modelled: soil organic carbon, soil respiration, and net ecosystem exchange over the period of 1990-2017. For the analysis six administrative regions were selected: three with unchanged (permanent) arable land structure (Kaluga, Moscow, and Yaroslavl), and other three with changed crop rotation (Kostroma, Smolensk, and Tver). All regions in the study are characterized by homogeneous soil cover and similar cultivated crops. The results of the modelling were verified using the data from field CO_2 fluxes observations in the European part of Russia. In growing season, the agrolandscapes function as a net carbon sink and accumulate C from the atmosphere into plant biomass. The dynamics of organic carbon in soil under growing crops depends on organic fertilizers in cultivation technologies, and if they aren't inputted, soil loses carbon. During the last 30 years the cumulative rates of net ecosystem exchange and soil respiration had decreased mostly due to reduction of arable land area. CO_2 emission and soil organic carbon losses are the most important controls of land degradation. Based on the dynamic patterns of CO_2 fluxes, the regions of the Central Forest zone could be separated into two groups. The group with central location characterized by intensive soil respiration and high rate of accumulation of organic carbon in soil, whereas peripheral group characterized by losses of soil organic carbon and low rates of soil respiration. According to the modelling, within the period of observations the inter-annual changes of carbon fluxes are mainly controlled by rising air temperature and heat supply, variable precipitation, and increasing concentration of CO_2 in the atmosphere. Among human activity the most important are change of arable land area and decreasing amount of fertilizers.

KEY WORDS: Carbon dioxide, Land Degradation Neutrality, Net Ecosystem Exchange, simulation modelling, soil organic carbon, soil respiration

CITATION: Olga E. Sukhoveeva, Dmitry V. Karelin (2019) Application of the DeNitrification-DeComposition (DNDC) model to retrospective analysis of the carbon cycle components in agrolandscapes of the Central Forest zone of European Russia. Geography, Environment, Sustainability,
Vol.12, No 2, p. 213-226
DOI-10.24057/2071-9388-2018-85

INTRODUCTION

Mathematical methods and simulation modelling are widely used in geography and global ecology. Some of these models are focus on the cycles of nitrogen and carbon as the most important biogeochemical elements. They proved to be effective to solve specific agricultural goals such as to forecast and create the programs for reduction of Greenhouse Gases (GHG) fluxes and emissions from soils to the atmosphere under anthropogenic impact, to develop recommendations for proper use of agricultural technologies for sustainable land use, and to decrease losses of yields or soil organic carbon due to unfavorable environmental conditions.

The UN Convention to Combat Desertification considers the dynamics and balance of soil organic content as one of the most important indicators of the recent concept namely Land Degradation Neutrality (LDN), which is in turn a key for achieving LDN target defined in the Sustainable Development Goal 15.3 (UNCCD 2015). The UN Framework Convention on Climate Change (1992-2018) admits that models can be used as an alternative instrument to the IPCC methods for estimation of GHG emission from agriculture if being adapted for different countries and environmental conditions (Estimation of emissions from agriculture 2004; Report of the 38th meeting 2012).

In these documents, among the numerous biogeochemical models for estimation of GHG emission from agriculture, DNDC model (DeNitrification-DeComposition) is declared as the most suitable. It is the only model officially used at national level. Advantages of the model are free access, friendly and simple interface, diurnal format of modelling, taking into account both natural and anthropogenic factors, complex and diverse structure of output fluxes including different components of the carbon and nitrogen cycles.

The model DNDC is successfully applied for different regions and types of land use in 14 countries (Bolan et al. 2004). Impressive results in modelling of GHG emissions were obtained in Asia (Frolking et al. 2004; Pathak et al. 2005; Li et al. 2005), USA (Li 2008), Canada (Yadav and Wang, 2017; Guest et al. 2017), and Australia (Chen et al. 2013). Moreover, this model had been used in several international projects for estimation of organic matter and the nitrogen cycle in arable soils (Giltrap et al. 2010; Leip et al. 2008; Rosenstock et al. 2016). In the last years in Russia some authors used the model for analysis of nitrous oxide emission from soil under vegetables (Buchkina et al. 2007; Balashov et al. 2014) and CO_2 emission from forest and wetland ecosystems (Kurbatova et al. 2009). But it wasn't applied for estimation of CO_2 fluxes in Russian agrolandscapes yet.

In our previous study (Sukhoveeva 2018) internal parameters of the model were parametrized according to Russian arable soils specificities. The database for modelling included meteorological parameters, soil cover, crops characteristics, and features of anthropogenic activity (tillage, fertilization, crops yields etc.) in agrolandscapes. In this research we focused on DNDC simulation modelling of the retrospective dynamics of components of the

carbon cycle due to land use changes in European part of Russia.

MATERIALS AND METHODS

DNDC is a process-based computer simulation model of the carbon and nitrogen cycling in agricultural ecosystems (Li et al. 1992). Its block structure consists of three subunits: thermo-hydrological, nitrogen (DeNitrification) and carbon (DeComposition). The model requires a large amount of input data and highly depends on their quality. Its parameters are climatic variables (daily maximum and minimum air temperatures and precipitations), soil characteristics (soil texture, pH, bulk density, soil organic carbon, C/N ratio, litter/humads/humus), and agricultural variables (days of sowing and harvesting, yields, biomass production, biomass fractions, C/N ratio in biomass, data and method of tiling, data and amount of fertilizers, data of manure amendment and content of C and N in it). Besides it uses many assumptions on the controls of GHG emissions per soil type.
The Central Forest zone is one the most valuable agricultural and economical areas of European Russia (Fig. 1). It includes 12 administrative units: Bryansk, Ivanovo, Kaluga, Kostroma, Moscow, Orel, Ryazan, Smolensk, Tver, Tula, Vladimir, Yaroslavl regions, and Moscow-city. Sod-podzolic soils are spread most widely in these regions. According to Köppen's classification, climate in these regions is the warm summer variant of the humid continental climate (Chen and Chen 2013), temperate climate according to Alisov's classification.

Three main characteristics of the carbon budget in agrolandscapes were modelled:
• soil organic carbon dynamics as difference between initial and final soil organic carbon content per year,
• soil respiration consisting of root and microbial fluxes,
• Net Ecosystem Exchange (NEE) – difference between Gross Primary Production (i.e. photosynthesis) and Ecosystem Respiration (i.e. sum of aboveground plant respiration and soil respiration).

Taking into account soil type and growing crops in different administrative units, we distinguished 20 agrolandscapes (Table 1). Totally we run 560 modelling experiments over the period of 1990-2017 (28 years). Finally, 3920 values of the carbon cycle components had been used, when creating maps.

At the preliminary stage of modelling we created a database on agroclimatic re-

Fig. 1. Administrative units (in green) of the Central Forest zone of Russia

Table 1. Matrix of CO_2 fluxes modelling in the Central Forest zone of European Russia

Soil type	Crops / Regions	Winter wheat	Winter rye	Barley	Oat	Potato	Structure of arable lands
Sod-podzolics, mainly rather shallow podzolics, Umbric Albeluvisols Abruptic	Kostroma	–	–	+	+	–	Changed
	Yaroslavl	–	–	+	+	+	Unchanged
Sod-podzolics, mainly shallow and non-deep podzolics, Umbric Albeluvisols Abruptic	Moscow	+	–	+	–	+	
	Kaluga	+	–	+	+	+	
	Smolensk	–	+	+	+	–	Changed
	Tver	–	–	+	+	–	

courses of the Central Forest zone. Weather data were provided by Russian Institute of Hydro-Meteorological Information – World Data Center (http://meteo.ru/data) from 16 weather stations. Soil cover characteristics were defined through the Unified State Register of Soil Resources of Russia (2014). Only prevalent soil types covered more than 30% of regions territory were included into the analysis.

Degree-days required for a crop to reach maturity and water demand for cultivated in European Russia varieties were corrected with use of open access sources. Due to the lack of information on particular dates of sowing, harvesting, plowing, input of fertilizers, and other cultivation operations, the average dates and periods for agricultural techniques, recommended by Ministry of agriculture were inputted into the model.

List of growing crops and its yields were summarized from information of Federal State Statistical Service (https://fedstat.ru/). Data on crop fertilizing was obtained from Statistics bulletin "Application of fertilizers for the harvest and works for chemical land melioration" over the period 1990-2017.

Due to the information available, the duration of the analyzed period was 28 years. For better comparison this period was separated into four 7-years intervals, which correspond with the main social and economic changes in the country.

In our study, the structure of arable land and crop rotations were assumed to stay unchanged if they meet the following requirements:

- List of growing crops hadn't been changed during the period 1990-2017,
- Each crop covered more than 5% of territory.

RESULTS

At the preliminary stage of the analysis, six administrative regions in the Central Forest zone of European Russia were chosen: Kaluga, Kostroma, Moscow, Smolensk, Tver, and Yaroslavl regions. They are characterized by homogeneous soil type and the same growing crops. Open access to weather data was also critical in that choice.

The most common soil type in the zone is sod-podzolic – Umbric Albeluvisols Abruptic (WRB 2006), Eutric Podzoluvisols (FAO 1988): sod-podzolic, mainly shallow and non-deep podzolics, and sod-podzolics, mainly rather shallow podzolics. These soil types cover more than 30% of territory in corresponding regions (Table 1).

It was also found that the most important crops cultivated in all regions in the study are spring grain crops: barley and oat, as well as potato. Besides, in the southern part of the Central Forest zone predominate winter grain crops such as wheat

and rye. In Kaluga, Moscow, and Yaroslavl regions arable land structure is rather stable, with no changes in the list of grown crops during the last 28 years. In contrast, in Kostroma, Smolensk, and Tver regions, areas of each crop vary significantly.

Other regions of the Central Forest zone were excluded from the analysis either due to excessively non-homogeneous soil cover (Bryansk, Ryazan, Tula regions), or the lack of open access meteorological data (Vladimir, Ivanovo, Orel regions).
It is usual that existing official information includes some omissions and uncertainness:

- Official statistical data is averaged on a base of administrative units,
- Boundaries and areas of soil types do not match the administrative division,
- It is not known what soil types are tillaged,
- It is not clear what territories and soil types are occupied by each crop,
- Crop rotations, i.e. spatial and temporal replacement of crops, are unknown,
- Varieties of crops and their requirements to environmental conditions are unknown,
- Arable land area and crops areas are changed.

In this study the soil organic carbon dynamics depends on features of growing crops and input of fertilizers. In the northern regions as Kostroma and Tver, such spring grain crops as barley and oat are dominated (Fig. 2), and the losses of organic carbon from soil are typical due to absence of organic fertilizers in cropping technologies (Fig. 3). But for the last 10-15 years the intensity of agriculture, crops yields, and amount of fertilizers had greatly increased, resulting in less carbon losses.

Similarly, according to the modelling the observed dynamics of CO_2 fluxes depends on input of fertilizers, yield changes, and rise of CO_2 concentration in the atmosphere.

Kostroma, Smolensk, and Tver regions are characterized by decrease of soil respiration in 1990s and following increase in 2010s (Fig. 4). Curiously, it was found that in Tver region the rates of soil respiration were less than 1.0 t C ha^{-1} yr^{-1} during the 28-years period of modelling. This is mostly due to low intensity of agricultural technologies, i.e. small amounts of inputting fertilizers, little plant biomass, and low temperatures as compared to other regions in the study. And vice versa, in Moscow, Kaluga, and Yaroslavl regions,

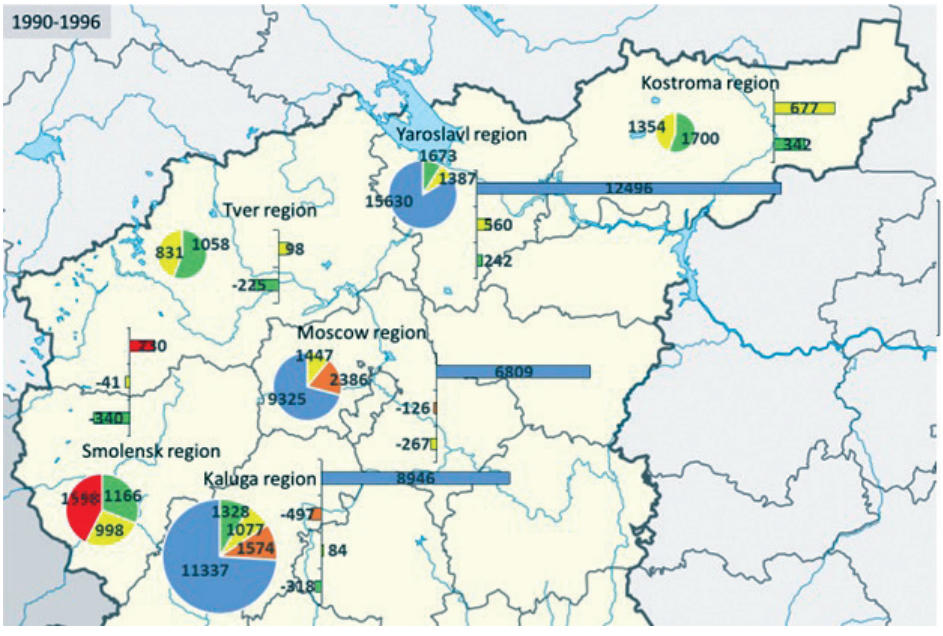

2a

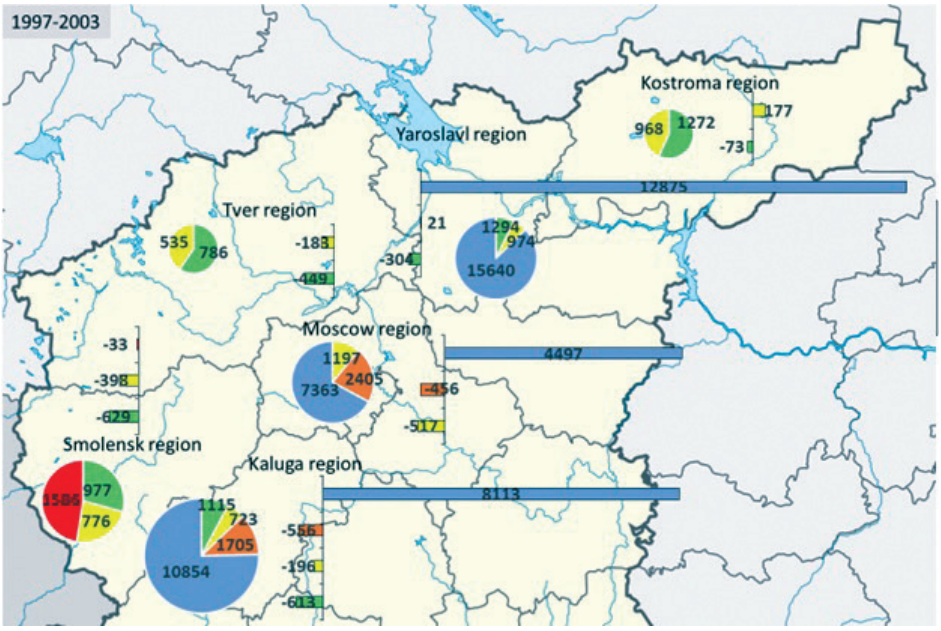
1997-2003
Kostroma region
Yaroslavl region
Tver region
Moscow region
Smolensk region
Kaluga region
968
1272
177
-731
12875
21
1294
974
15640
-304
535
786
-183
-449
-33
-398
-629
1197
2405
7363
4497
-456
-517
977
776
1586
1115
723
1705
10854
8113
-556
-196
-613

2b

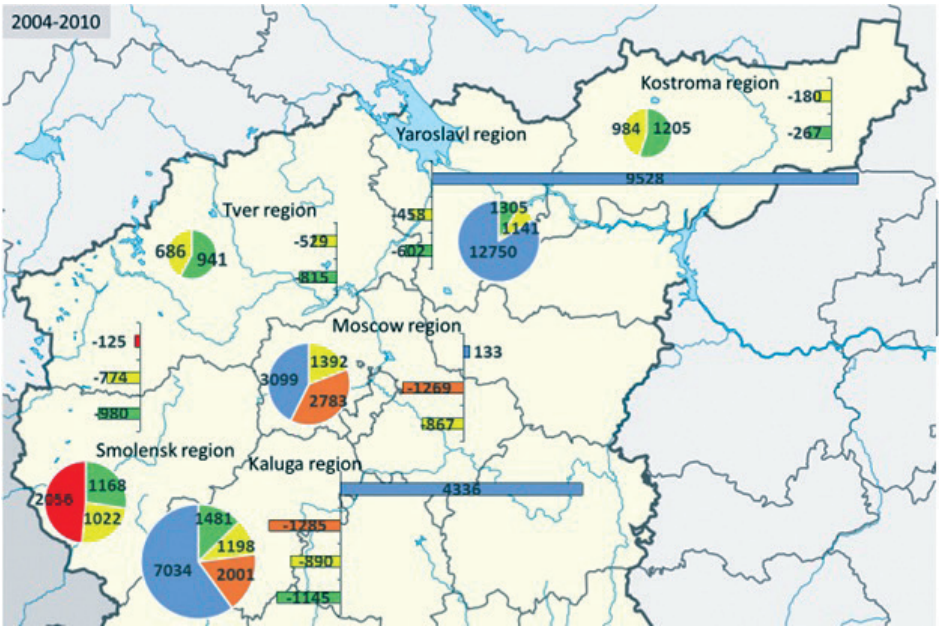
2004-2010
Kostroma region
Yaroslavl region
Tver region
Moscow region
Smolensk region
Kaluga region
984
1205
-180
-267
9528
458
1305
1141
12750
-602
686
941
-529
-815
-125
-774
-980
1392
3099
2783
133
-1269
-867
1168
1022
2656
1481
1198
7034
2001
4336
-1285
-890
-1145

2c

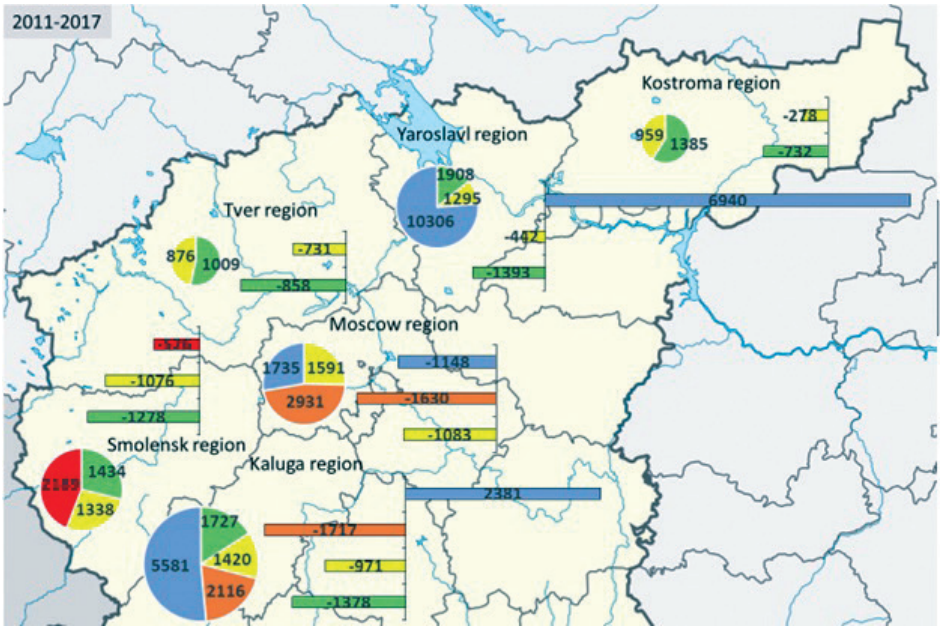

2d

Fluxes of CO_2
Soil respiration
Net ecosystem exchange

Crops
Oat
Barley
Winter wheat
Winter rye
Potato

Fig. 2. Annual values of CO_2 fluxes in agrolandscapes of the European Russia by crops and regions by 7-years intervals, kg C ha^{-1} yr^{-1}

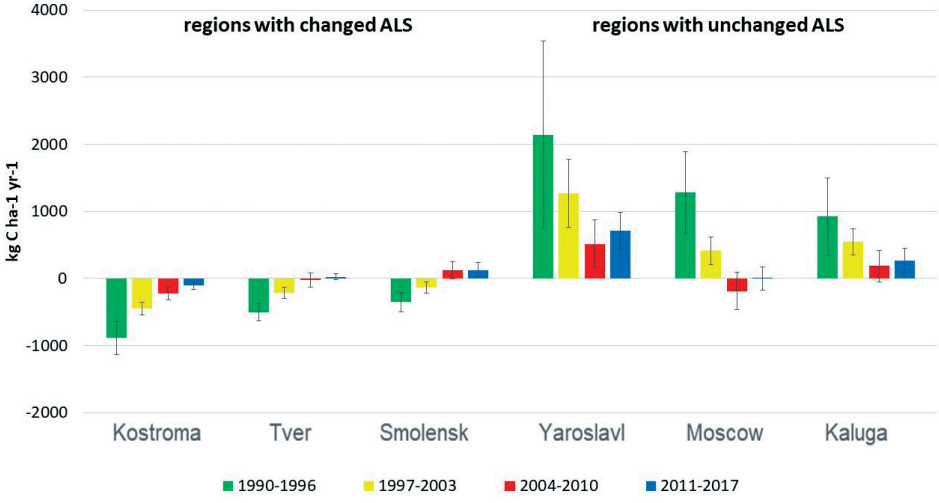

Fig. 3. Spatiotemporal mean annual dynamics of soil organic carbon in agrolandscapes of the studied regions of European Russia by 7-years intervals. Here and on other figures: ALS – arable land structure, means with standard deviations are given

highly productive crops such as winter wheat and potato are grown (Fig. 2). They are characterized by use of great amount of fertilizers in cropping technologies, resulting in general accumulation of carbon in soils. But in the last decades in these regions carbon deposition and rate of soil respiration were reducing due to decrease of fertilizers input.

Cumulative soil respiration decreased due to reduction of arable soil area in these regions in general (Fig. 5). Its mean rates were equal to 800-1400 kt C ha^{-1} yr^{-1} in 1990-1996 and 200-300 kt C ha^{-1} yr^{-1} in 2011-2017.

And during the observed period the carbon balance in agroecosystems was changed between the net source of CO_2 to the atmosphere and sequestration (Fig. 6). Thus, ecosystems of the zone in 1990-2003 acted as the net source of carbon (400-800 kt C ha^{-1} yr^{-1}), whereas in 2004-2017 NEE firstly became close to zero and then the ecosystems were a carbon sink during vegetative period (Fig. 7).

Finally, based upon the direction and intensity of CO_2 fluxes, geographical location, and the degree of anthropogenic impact, the agrolandscapes of the Central Forest zone of European Russia could be separated into two large administrative groups:

• "Central" – Moscow, Kaluga, Yaroslavl regions – intensive agriculture (including winter wheat and potato cropping), stable structure of arable land and agricultural production, prevailing accumulation of organic carbon in soil (0-2.0 t C ha^{-1} yr^{-1}), high rate of soil respiration (2.0-6.0 t C ha^{-1} yr^{-1});

• "Peripheral" – Kostroma, Smolensk, and Tver regions – small number of crops, extensive agriculture, losses of soil organic carbon (0-0.9 t C ha^{-1} yr^{-1}), low rate of soil respiration (< 2 t C ha^{-1} yr^{-1}).

DISCUSSION

In our previous study it had been proved that the parametrized DNDC model is rather effective to estimate components of the carbon cycle in European part of Russia (Sukhoveeva 2018). For verification of the adapted DNDC model to Russian conditions, the data from two field sites were used. Namely seasonal and annual CO_2 emissions were estimated in Kursk and Moscow regions. The results of ANOVA showed that the mean measured and calculated values of emissions were not significantly different (calculated F-criteria were less than critical F-criteria).

Medium positive correlation was also found between the observed and modelled CO_2 fluxes. Thus, in Kursk region the Pearson coefficients correlations between measured and modelled values of soil res-

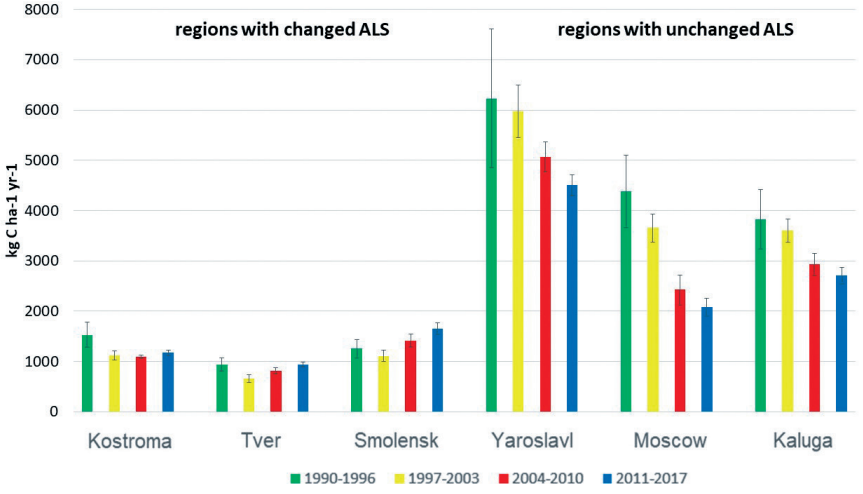

Fig. 4. Spatiotemporal annual dynamics of soil respiration in agrolandscapes of the studied regions of European Russia by 7-years intervals

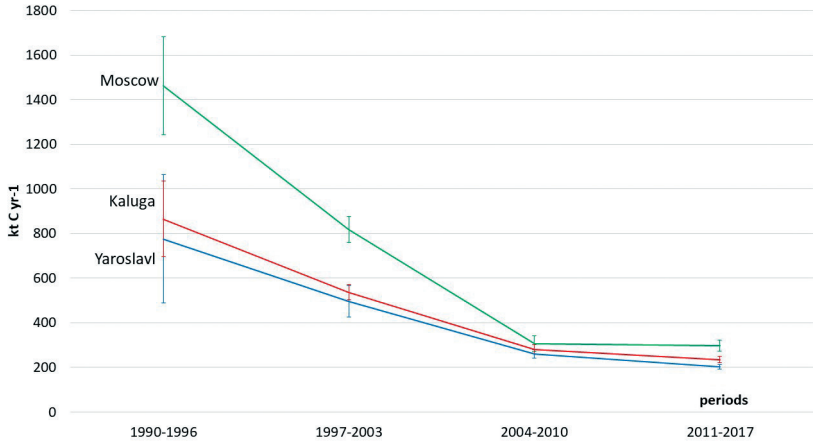

Fig. 5. Modelled cumulative annual rates of soil respiration in the regions haracterized by unchanged arable land structure by 7-years intervals

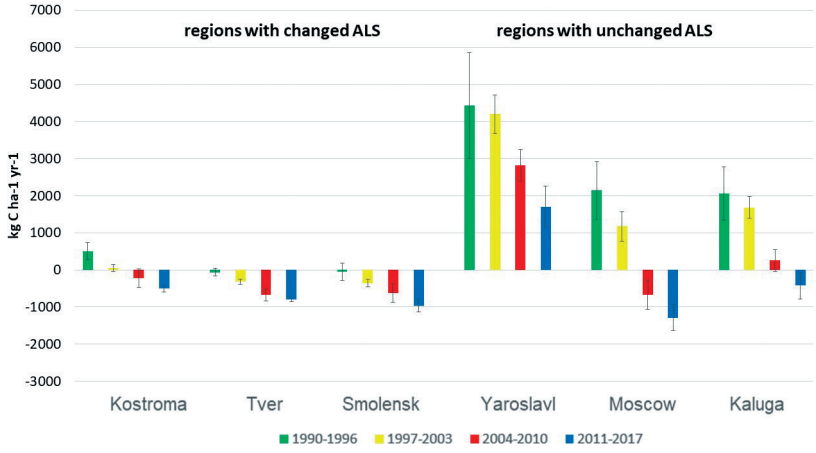

Fig. 6. Spatiotemporal mean annual dynamics of Net Ecosystem Exchange in agrolandscapes of the studied regions of the European Russia by 7-years intervals

Fig. 7. Modelled cumulative values of Net Ecosystem Exchange in the regions characterized by unchanged arable land structure by 7-years intervals

piration were equal to $r_p = 0.662$, $P = 0.005$ for sunflower, $r_p = 0.533$, $P = 0.028$ for barley, $r_p = 0.531$, $P = 0.028$ for winter wheat, and $r_p = 0.300$, $P = 0.259$ for potato, respectively. In Moscow region the correlation between field measured and modelled values of soil respiration was equal to $r_p = 0.582$, $P < 0.001$ for cereal-fallow crop rotation ($r_p = 0.546$, $P < 0.001$ for winter wheat and $r_p = 0.723$, $P < 0.001$ for fallow, respectively) (Sukhoveeva 2018).

Besides verification of the model was performed by published information on CO_2 emission and carbon balance in arable soils in Moscow, Orel, and Vladimir regions (Table 2). In all cases the measured annual values were inside the interval of predicted by the model ones. Also, the ratios between major CO_2 fluxes were checked with winter wheat taken as example. Modelled ratio of respiration to photosynthesis (0.34-0.36) was similar to ratio in laboratory experiment (0.35-0.60) (Gifford, 1995). The modelled and measured relative inputs of root and microbial respiration were also corresponding to each other (0,33 : 0,67 by the model and 0,34-0,38 : 0,62-0,66 by the field experiment) (Kurganova, 2010). There aren't field experiments for measuring NEE in Russia that's why this CO_2 flux hadn't been used for verification of the model.

Generally arable soils are losing organic carbon and, in this study, anthropogenic impact was also found to be the most important for soil C exchange. This conclusion has been confirmed widely (Kolchugina et al. 1995; Lal 2004; Semenov et al. 2008; Larionova et al. 2010; Kosolapov et al. 2015).

Table2. Verification of the model DNDC in the Central Forest zone of European Russia on the base of published results of field measurements

Para meters	Annual C balance in soil, kg C ha^{-1} yr^{-1}			Annual CO_2 emission from soil, kg C ha^{-1} yr^{-1}					
Model values	162,6-277,7	-248… - 55 Without fertilizers	+4988-+6111 With fertilizers	2258-3664	7420-8196	701-2540	6658-7709	427-800 Without fertilizers	1307–4074 With fertilizers
Field values	250	-1004	+6016	3304	7850	788-3066	3767-9899	1753	3019
Crops	Crop rotation winter wheat – fallow	Potato		Crop rotation winter wheat – fallow	Winter wheat	Fallow	Barley	Potato	
Region	Pushchino, experiment of Institute of physical-chemical and biological problems of soil science RAS	Vladimir, Long-term experiment of Institute of organic fertilizer and peat		Pushchino, experiment of Institute of physical-chemical and biological problems of soil science RAS	Orel, western part	Moscow, Long-term experiment of Timiriazev academy		Vladimir, Long-term experiment of Institute of organic fertilizer and peat	
Period, yr	2000-2004	2004-2014		2000-2004	2013	2005-2008		2004-2014	
References	Sapronov, 2008	Lukin, 2015		Sapronov, 2008	Karelin et al., 2017	Chistotin and Safonov, 2016		Lukin, 2015	

In all studied regions the dynamics of soil organic carbon storage in agrolandscapes was negative, especially under annual crops. Therefore, both emissions and carbon net accumulation rates in soil were decreased. Similar observations were made by Fedorov (2017); in his research broad-scale changes in land use (substitution of arable lands by grasslands and pastures) followed by declining fertilizers input, resulted in decrease of both CO_2 soil emission and net carbon accumulation from the atmosphere. Moreover, source pattern of net ecosystem exchange resulted from soil organic carbon losses and further degradation of agroecosystems (Kirschbaum and Mueller 2001).

Variability of modelled estimates could be evaluated by standard deviation or coefficient of variation.

The smallest standard deviations were found for Tver region < 100 kg C m^{-2} yr^{-1}. This is correct for barley and oat cultivated in this region, and for all carbon fluxes taken into account: soil respiration, soil organic carbon, and net ecosystem exchange. The biggest standard deviations were obtained for potato > 1000 kg C m^{-2} yr^{-1} also for three major CO_2 fluxes in the regions characterized by unchanged arable lands structure (Kaluga, Moscow, Yaroslavl).

The smallest coefficients of variation (less than 8%) were found for soil organic carbon and NEE in the agrolandscapes of Yaroslavl and Kostroma regions, where barley and oat are cultivated. Whereas the greatest coefficients of variation (more than 150%) are characteristic for soil organic carbon under grain crops in Moscow and Kaluga regions.

Two the most probable factors influencing instability of the carbon cycle components are climate change, including temperature increase, and further rise of CO_2 concentration in the atmosphere at the rate of 3 ppm per year, according to WMO message (WMO 2017). Thus, during the last four decades, under the most expressed climate changes due to Global Warming events, the strong increase in heat supply in the Central Forest zone was observed (Sukhoveeva 2016). During that period both mean annual (+0.3 °C/10 yr) and mean monthly (+0.9 °C/10 yr) air temperatures were rising. This was also true for the trends of positive degree-days (+48 °C/10 yr) and longevity of vegetative periods. Sum of precipitation (monthly trend 5 mm/10 yr, annual trend 30 mm/10 yr) and moisture supply in vegetative period enhanced, too, but they became unstable.

Hopefully the results of this study will provide help to create recommendations (i) to decrease losses of yields due to unfavorable environmental conditions, (ii) to reduce GHG emissions from arable soils to the atmosphere due to land use practices, and (iii) to promote carbon sequestration through sustainable land management practices targeting on the LDN achievement (Sanz et al. 2017).

CONCLUSIONS

The DNDC model has been successfully applied for simulation of the carbon cycle components in agrolandscapes of the Central Forest zone in European Russia. The dynamics of soil respiration, net ecosystem exchange, and soil organic carbon content in arable lands were estimated over the 28-yr period (1990-2017) to evaluate how carbon fluxes and stocks depend on geographical location and administrative belonging. Spatial and temporal variations of CO_2 fluxes were plotted and mapped for arable soils in administrative regions characterized by homogeneous soil type and the same growing crops. According to the results of the study, the regions of the Central Forest zone of European Russia were separated into two groups. Central regions are characterized by intensive soil respiration and accumulation of organic carbon in soil, whereas peripheral ones are characterized by losses of soil organic carbon and low rates of soil respiration. At present the agrolandscapes of the Central Forest zone during vegetative season are functioning as carbon sinks and accumulate carbon from the atmosphere into plant biomass. In soil under growing crops organic carbon is absorbing, if organic fertilizers are present

in cultivate technologies, but under technologies without organic fertilizers, soil loses carbon. In Moscow, Kaluga, and Yaroslavl regions characterized by unchanged crop rotations, both rate of cumulative soil respiration and net ecosystem exchange are decreasing due to reduction of arable land area during the last 28 years.

ACKNOWLEDGEMENTS

Modelling dynamics of soil organic carbon, soil respiration, and net ecosystem exchange was performed for the Project of Russian Science Foundation № 18-17-00178; agroclimatic recourses and local climate change in the Central Forest zone were evaluated for Fundamental scientific research theme № 0148-2018-0006 (renewed № 0148-2019-0009) and Program of Presidium of RAS № 51 (№ 0148-2018-0036)

REFERENCES

Balashov E., Buchkina N., Rizhiya E., and Farkas C.S. (2014). Field validation of DNDC and SWAP models for temperature and water content of loamy and sandy loam spodosols. International agrophysics, 28 (2), pp. 133-142.

Bolan N.S., Saggar S., Luo J., Bhandral R., and Singh J. (2004). Gaseous emissions of nitrogen from grazed pastures: processes, measurements and modeling, environmental implications, and mitigation. Advances in agronomy, 84, pp. 38-120.

Buchkina N.P., Balashov E.V., Rizhiya E.Y., and Li C. (2007). Application of DNDC model for Russian agro-ecosystems. In: Denitrification: a challenge for pure and applied science. Book of abstracts. University of Aberdeen, pp. 17.

Chen C., Chen D., Pan J., and Lam S.K. (2013). Application of the denitrification-decomposition model to predict carbon dioxide emissions under alternative straw retention methods. Scientific World Journal, 25, pp. 851-901. DOI: 10.1155/2013/851901.

Chen D. and Chen H.W. (2013). Using the Köppen classification to quantify climate variation and change: an example for 1901-2010. Environmental Development, 6, pp. 69-79.

Chistotin M.V. and Safonov A.F. (2016). Temporal patterns of respiration of an agro-sod-podzolic soil as controlled by organic matter content and meteorological factors. Problemy agrokhimii i ekologii, 3, pp. 52-58. (in Russian)

Estimation of emissions from agriculture. (2004). United Nations framework convention on climate change. FCCC/SBSTA/2004/INF.4. GE.04–61454. – Bonn: UNFCCC, 28 May 2004. Available at: http://unfccc.int/resource/docs/2004/sbsta/inf04.pdf. [Accessed 1 Dec. 2018].

FAO-Unesc. (1988). Soil Map of the World. Revised Legend. World Resources Report, 60. Rome: FAO.

Fedorov B.G. (2017). Russian carbon balance. Moscow: Scientific consultant (in Russian).

Frolking S., Li C., Braswell R., and Fuglestvedt J. (2004). Short- and long-term greenhouse gas and radiative forcing impacts of changing water management in Asian rice paddies. Global Change Biology, 10 (7), pp. 1180-1196.

Gifford R.M. (1995). Whole plant respiration and photosynthesis of wheat under increased CO2 concentration and temperature: long-term vs. short-term distinctions for modelling. Global Change Biology, 1, pp. 385-396.

Giltrap D.L., Li C., and Saggar S. (2010). DNDC: a process-based model of greenhouse gas fluxes from agricultural soils. Agriculture, Ecosystems & Environment, 136 (3-4), pp. 292-300.

Guest G., Kröbel R., Grant B., Smith W., Sansoulet J., Pattey E., Desjardins R., Jégo G., Tremblay N., and Tremblay G. (2017). Model comparison of soil processes in eastern Canada using DayCent, DNDC and STICS. Nutrient Cycling in Agroecosystems, 109 (3), pp. 211–232.

Karelin D.V., Goryachkin S.V., Kudikov A.V., Lunin V.N., Dolgikh A.V., Lyuri D.I., and Lopes de Gerenu V.O. (2017). Changes in carbon pool and CO2 emission in the course of postagrogenic succession on gray soils (Luvic Phaeozems) in European Russia. Eurasian Soil Science, 50 (5), pp. 559-572. DOI: 10.7868/80032180X17050070

Kirschbaum M.U.F. and Mueller R. (2001). Net Ecosystem Exchange. – Australia: Cooperative Research Centre for Greenhouse Accounting.

Kolchugina T.P., Vinson T.S., Gaston G.G., Rozhkov V.A., and Schlentner S.F. (1995). Carbon pools, fluxes, and sequestration potential in soil of the Former Soviet Union. In: R. Lal, J. Kimble, E. Levine, B.A. Stewart, ed., Soil Management and greenhouse effect. Boca Raton, London, Tokyo: Lewis Publishers, pp. 25-40.

Kosolapov V.M., Trofimov I.A., Trofimova L.S., and Yakovleva E.P. (2015). Agrolandscapes of Central Cernozem area. Zoning and management. Moscow: Nauka (in Russian).

Kurbatova J. Li C. Varlagin A. Xiao X., and Vygodskaya N. (2008). Modeling carbon dynamics in two adjacent spruce forests with different soil conditions in Russia. Biogeosciences, 5, pp. 969-980.

Kurganova I.N. (2010). Emission and balance of carbon dioxide in terrestrial ecosystems of Russia: doctor thesis. Pushchino: IFXiBPP RAN. (in Russian)

Lal R. (2004). Soil carbon sequestration to mitigate climate change. Geoderma, 123 (1-2), pp. 1-22. DOI: 10.1016/j.geoderma.2004.01.032.

Larionova A.A., Kurganova I.N., De Gerenyu V.O.L., Zolotareva B.N., Yevdokimov I.V., and Kudeyarov V.N. (2010). Carbon dioxide emission from agrogrey soils under climate change. Eurasian soil science, 43 (2), pp. 168-176. DOI: 10.1134/S1064229310020067 (in Russian)

Leip A., Marci G., Koeble R., Kempen M., Britz W., and Li C. (2008). Linking an economic model for European agriculture with a mechanistic model to estimate nitrogen and carbon losses from arable soils in Europe. Biogeosciences, 5, pp. 73-94.

Li C., Frolking S., and Frolking T.A. (1992). A model of nitrous oxide evolution from soil driven by rainfall events: 1. Model structure and sensitivity. Journal of geophysical research, 97 (D9), pp. 9759-9776.

Li C., Frolking S., Xiao X., Moore III B., Boles S., Qiu J., Huang Y., Salas W., and Sass R. (2005). Modeling impacts of farming management alternatives on CO_2, CH_4, and N_2O emissions: A case study for water management of rice agriculture of China. Global Biogeochemical Cycles, 19 (3), GB3010. DOI: 10.1029/2004GB002341.

Li C. (2008). Modeling soil organic carbon sequestration potential with modeling approach. In: Simulation of Soil Organic Carbon Storage and Changes in Agricultural Cropland in China and Its Impact on Food Security. China Meteorological Press.

Lukin S.M. (2015). Carbon dioxide emission in potato agrocenosis on sod-podzolic sandy soils. Vladimirskii zemledelets, 3-4 (74), pp. 22-23. (in Russian)

Pathak H., Li C., and Wassmann R. (2005). Greenhouse gas emissions from India rice fields: calibration and upscaling using the DNDC model. Biogeosciences, 2 (2), pp. 113-123.

Report of the thirty-eighth meeting of the small-scale working group (2012). Bonn: CDM SSC WG.

Rosenstock T.S., Rufino M.C., Butterbach-Bahl K., Wollenberg E., and Richards M. (2016). Methods for measuring greenhouse gas balances and evaluating mitigation options in smallholder agriculture. USA: Springer.

Sanz M.J., de Vente J., Chotte J.-L., Bernoux M., Kust G., Ruiz I., Almagro M., Alloza J.-A., Vallejo R., Castillo V., Hebel A., and Akhtar-Schuster M. (2017). Sustainable Land Management contribution to successful land-based climate change adaptation and mitigation. In: A Report of the Science-Policy Interface. Bonn: UNCCD.

Sapronov D.V. (2008). Long-term dynamics of CO_2 emission from grey forest and sod-podzolic soils: PhD thesis. Pushchino: IFHiBPP RAN. (in Russian)

Semenov V.M., Ivannikova L.A., Kuznetsova T.V., Semenova N.A., and Tulina A.S. (2008). Mineralization of organic matter and the carbon sequestration capacity of zonal soils. Eurasian soil science, 41 (7), pp. 717-730. DOI: 10.1134/S1064229308070065 (in Russian)

Sukhoveeva O.E. (2016). Changes of climatic conditions and agroclimatic recourses in Central Non-Cernozem zone. Proceedings of Voronezh State University. Series: Geography. Geoecology, 4, pp. 41-49. (in Russian)

Sukhoveeva O.E. (2018). Evaluation of spatiotemporal variability of CO_2 fluxes in agrolandscapes of European Russia on the base of simulation modelling: PhD thesis. Moscow: Institute of Geography RAS. (in Russian)

UNCCD. (2015). Science policy brief, 1.

Unified state register of soil recourses of Russia. Versa 1.0. (2014). Moscow: Soils institute.

WMO. (2017). Greenhouse Gas Bulletin, 13.

World reference base for soil resources. (2006). IUSS Working Group. World Soil Resources Reports, 103. Rome: FAO.

Yadav D. and Wang J. (2017). Modelling carbon dioxide emissions from agricultural soils in Canada. Environmental Pollution, 230, pp. 1040-1049. DOI: 10.1016/j.envpol.2017.07.066.

Received on Dec 31st 2018 Accepted on May 17th 2019

Egor A. Dyukarev[*1,2], Evgeniy A. Godovnikov[1], Dmitriy V. Karpov[1], Sergey A. Kurakov[2], Elena D. Lapshina[1], Ilya V. Filippov[1], Nina V. Filippova[1], Evgeniy A. Zarov[1]
[1]Yugra State University, Khanty-Mansiysk, Russia
[2]Institute of Monitoring of Climatic and Ecological System of the Siberian Branch Russian Academy of Sciences, Tomsk, Russia
*** Corresponding author:** dekot@mail.ru

NET ECOSYSTEM EXCHANGE, GROSS PRIMARY PRODUCTION AND ECOSYSTEM RESPIRATION IN RIDGE-HOLLOW COMPLEX AT MUKHRINO BOG

ABSTRACT. The continuous field measurements of net ecosystem exchange (NEE) of CO_2 were provided at ridge-hollow oligotrophic bog in the Middle Taiga Zone of West Siberia, Russia in 2017-2018. The model of net ecosystem exchange of CO_2 was suggested to describe the influence of different environmental factors on NEE and to estimate the total carbon budget of the bog over the growing season. The model uses air and soil temperature, incoming photosynthetically active radiation (PAR) and water table depth, as the key factors influencing gross primary production (GPP) and ecosystem respiration (ER). The model coefficients were calibrated using the data collected by automated soil CO_2 flux system with two transparent long-term chambers placed at large hollow and small ridge sites.
Experimental and modeling results showed that the Mukhrino bog acted over the study period as a carbon sink, with an average NEE of –87.7 gC m^{-2} at the hollow site and –50.2 gC m^{-2} at the ridge site. GPP was – 344.8 and –228.5 gC m^{-2} whereas ER was 287.6 and 140.9 gC m^{-2} at ridge and hollow sites, respectively. Despite of a large difference in NEE estimates between 2017 and 2018 the growing season variability of NEE were quite similar.

KEY WORDS: carbon dioxide, net ecosystem exchange, peatlands, ridge-hollow complex, ecosystem respiration, gross primary production

CITATION: Egor Dyukarev, Evgeniy Godovnikov, Dmitriy Karpov, Sergey Kurakov, Elena Lapshina, Ilya Filippov, Nina Filippova, Evgeniy Zarov (2019) Net Ecosystem Exchange, Gross Primary Production And Ecosystem Respiration In Ridge-Hollow Complex At Mukhrino Bog. Geography, Environment, Sustainability,
Vol.12, No 2, p. 227-244
DOI-10.24057/2071-9388-2018-77

INTRODUCTION

Peatland ecosystems play a significant role in the global carbon cycle, being sources and sinks of greenhouse gases (GHG) (Ciais et al. 2013; Rydin and Jeglum 2015). Despite covering a relatively small part of the Earth surface (about 3%), peatlands store a large amount of organic matter that is ranged between 500 and 700 billion tonnes of C (Page and Baird 2016; Leifeld and Menichetti 2018). In West Siberia peatlands occupy over 30% of the area (Terentieva et al. 2016; Dyukarev et al. 2011; Sheng et al. 2004). According to IPCC estimates (Ciais et al. 2013) the contribution of natural mires into total natural methane emissions ranged between 61 and 82%. The intensity of GHG fluxes is controlled by different factors including the hydrological and thermal regime of the peat deposit (Naumov 2009; Sasakawa et al. 2012; Helfter et al. 2015; Molchanov 2015; Walker et al. 2016; Glagolev et al. 2017; Veretennikova and Dyukarev 2017; Leroy et al. 2017).

The gaseous exchange between the atmosphere and the peatlands is governed by photosynthetic fixation of CO_2 from the atmosphere and by soil and vegetation respiration losses of CO_2. The balance between them is known as the net ecosystem exchange (NEE) of CO_2 (Bubier et al. 2003; Olchev et al. 2009; Golovatskaya and Dyukarev 2012; Helfer et al. 2015). The other major gaseous emission of C into the atmosphere is accounts for methane (CH_4), which is produced via anoxic decay of the soil organic matter (Saunois et al. 2016). The loss of C into the fluvial system occurs via export of dissolved and particulate organic carbon, and dissolved gases (CO_2 and CH_4). The rise in surface air temperature (Zhaojun et al. 2011; Baird et al. 2012) and the lowering of water levels causes peat drying, increase of temperature and aeration, which contributes to the intense of greenhouse gas emissions (Baird et al. 2012; The second assessment report… 2014). Peatland ecosystems in different years can also serve as both a source and a sink of carbon (Golovatskaya et al. 2008; Panzaoo et al. 2017). The variety of direct and inverse relationships existing between the components of the peatlands and the surrounding areas indicates a complex nonlinear impact of peatlands on the environment in different geographic, climatic, and geomorphological conditions (Peatlands of West Siberia 1976; Vomperskiy 1994; Ratcliffe et al. 2017; Webster et al. 2018). The quantitative estimation of the rate of carbon exchange between peatlands and the atmosphere, as well as the revealing of environmental factors affecting carbon exchange, is an important scientific issue (Sheng et al. 2004; Kabanov 2015).

High-precision measurements of carbon and GHG fluxes obtained using standardised methodologies are important for our understanding C cycle within and across ecosystems. (see Franz et al. 2018; Pavelka et al. 2018). The study of the hydrological and ecological mechanisms controlling peatland response to climate changes is critical to predict potential feedbacks on the global C cycle (Baird et al. 2012; The second assessment report… 2014). Recent field studies indicated that the peatland C balance represents a net C sink in intact peatlands in Canada (Wu et al. 2010; Munir et al. 2014; Webster et al. 2018), China (Zhu et al. 2015; Zhou et al. 2009), Finland (Laine et al. 2019; Minkkinen et al. 2018), Ireland (Swenson et al. 2019), Scotland (Helfter et al. 2015), Germany (Günther et al. 2017), France (Leroy et al. 2017), Poland (Acosta et al. 2017), New Zealand (Campbell et al. 2014), East (Runkle et al. 2013; Fleischer et al. 2016; Eckhardt et al. 2018; Davydov et al. 2018) and Western part of Russia (Kurbatova et al. 2009; Kurganova et al. 2011; Molchanov 2015; Ivanov et al. 2017).

Modelling approaches are useful to divide the observed NEE into gross primary production (GPP) and total ecosystem respiration (ER) components, since it provides a better diagnostic of ecosystem processes and their regulating factors (Falge et al. 2001; Widlowski et al. 2011). Carbon balance models are used to quantify the contribution of different environmental factors to GPP, ER and NEE variability, and to calculate daily and annual carbon bud-

gets using the gap-filled time series. Partitioning of the NEE into GPP and ER is also needed for better understanding of interannual and spatial variability of the carbon fluxes (Sokolov et al. 2019). The fundamental ecosystem processes (including photosynthesis and respiration) are common to mires and other terrestrial ecosystems, so changes in photosynthetically active radiation (PAR), air temperature (Ta), and precipitation may affect the C cycle in peatlands, e.g. due to alterations of the growing season length, water and energy budget, vegetation composition and water table levels (WTL) (Yurova et al. 2007; Humphreys and Lafleur 2011, Grant et al 2012, Campbell et al. 2014; Molchanov and Olchev 2016; Eckhardt et al. 2018).

The main purpose of this study is to asses CO_2 exchange fluxes in oligotrophic peatland complex at the Middle Taiga Zone in West Siberia using field chamber measurements and developed mathematical model of NEE.

MATERIALS AND METHODS

The field measurements were provided on the international scientific field station "Mukhrino" (Yugra State University, Khanty-Mansijsk) founded in 2009 (Lapshina et al. 2015). The field station is a part of the International Network for Terrestrial Research and Monitoring in the Arctic (INTERACT, eu-interact.org) and is actively used by Russian and foreign scientists for studies of the functioning of mire ecosystems. Over the past years, the Mukhrino bog was the main object of numerous experimental study of GHG fluxes (Glagolev et al. 2011; Alekseychik et al. 2017), geochemistry and physical, chemical, and biochemical properties of peat (Stepanova and Pokrovsky 2011; Szajdak et al. 2016), mire hydrology (Bleuten and Filippov 2008), and microbiology including mycology (Filippova et al. 2015).

The Mukhrino bog (60°54´N, 68°42´E) is located at the eastern terrace of the Irtysh River 20 km to the south from the point of its confluence with the Ob River, in the middle taiga zone of the West Siberian Lowland (Alekseychik et al. 2017). The climate of the region is a subarctic or boreal (Dfc) according to Köppen–Geiger climate classification with long cold winters and short warm summers. Mean annual temperature at Khanty-Mansijsk weather station for period 1983-2013 is –0.7° C, annual precipitation is 526 mm, sunshine duration is 1845 hours (Grebenuk and Kuznetsova 2012).

Pine bogs and ridge–hollow complexes are dominant at the boundaries of the Mukhrino peatbog. The vegetation is represented by rare pine trees and shrubs, dense herbaceous vegetation and mosses. Tree cover is mainly represented by stunted *Pinus sylvestris*. The dwarf shrub layer consists of *Ledum palustre*, *Andromeda polifolia*, *Chamaedaphne calyculata, Vaccinium vitis-idaea, Vaccinium uliginosum*, and *Oxycoccus palustris*. Herbs are represented by *Rubus chamaemorus* and a few tiny species of sundews (*Drosera anglica, D. intermedia, D. rotundifolia*). *Carex limosa, Eriophorum vaginatum, Scheuchzeria palustris* are widespread within oligotrophic hollows of ridge–hollow complexes. The moss layer consists of sphagnum mosses such as *S. fuscum, S. lindbergii, S. balticum, S. papillosum, S. angustifolium, S. magellanicum, S. jensenii*, etc. The area fractions of open water, hollows, and ridges within a 200 m radius around the observation site are 1, 67, and 32% (Alekseychik et al. 2017). Automated monitoring of carbon dioxide fluxes at oligotrophic ridge-hollow complex was performed in 2017-2018 using the portable atmospheric soil measuring system (ASMS) with two transparent chambers. Automated chambers were placed at a large hollow and a small ridge. ASMS is able to measure and record simultaneously the following environmental parameters: air temperature (Ta) and humidity (RH) (at height of 2 m above the ground and at the ground surface), PAR (incoming solar radiation in the 400-700 nm spectral range), carbon dioxide content and water vapor pressure in the air samples. The system includes a two-channel gas analyzer Li-7000 (Li-COR Biogeosciences, USA) and two measuring chambers with a volume of 120 l. The chambers are closed for 5

minutes every hour (or 3 hours in 2017) to provide the flux measurement. The rest of the time they remain open. The air for a sample is continuously pumped through the chamber and the gas analyzer during the observation period using diaphragm pump 7006ZVR (Gardner Denver Thomas GmbH, Germany) with flow rate about 2 l/minute. The measurements of the concentration of CO_2 and H_2O, Ta, RH and PAR are continuously stored in the ASMS and transferred to the web-server. The observation data were downloaded from server and processed using specially created software modules. Real-time ground water depth monitoring was conducted using a pressure transducer (Mini-diver DL501, Van Essen Instruments, Netherlands) submerged into a water at a fixed level under the surface.

The automated system operated in a measuring mode from July to August in 2017, and from May to October in 2018. The flux of CO_2 was calculated using a specialized software module developed in the Matlab R2014b (MathWorks, USA) using a linear model for changing the concentration in the chambers during the first two minutes of data sampling. Totally about 500 observations of fluxes were made at each experimental site in 2017 and more than 2500 observations - in 2018, respectively.

Mathematical modelling

To obtain continuous data records, to extrapolate them to other periods when experimental data are missing and to calculate the annual carbon budget of the ecosystem, a model of total ecosystem carbon exchange was proposed (Dyukarev 2017). The measured total NEE (Fig.1) was partitioned into the incoming (GPP) and expenditure (ER) components (Mäkelä et al. 2004; Laine et al. 2009; Kandel et al. 2013; Campbell et al. 2015).

$$NEE = ER - GPP; \quad (1)$$

$$GPP = f_W \times f_{PAR}; \quad (2)$$

$$ER = f_W \times f_T; \quad (3)$$

GPP is defined as the total amount of the carbon fixed in the process of photosynthesis by plants in an ecosystem, while NEE refers to GPP minus ER. ER is the result of plants and soil respiration, where soil respiration is the sum of autotrophic respiration (roots) and heterotrophic respiration (soil biota).

It is well known that the photosynthetic response under low light intensities is characterized by a linear response and photosynthetic saturation is observed at high light intensities (Pessarakli 2005). A rectangular hyperbolic function f_{PAR} (4) is used for the light response of NEE in daytime (Mäkelä et al. 2004; Laine et al. 2009).

$$f_{PAR} = \alpha \times PAR \times G_m / (\alpha \times PAR + G_m); \quad (4)$$

where α is the initial slope of the light response curve at low light (photosynthetic efficiency) (mg μmol^{-1}), G_m is the theoretical maximum rate of photosynthesis at infinite PAR (photosynthetic capacity) (mg m^{-2} h^{-1}). Carbon dioxide fluxes are given in mg of CO_2 per m^2 per hour. PAR is measured in μmol m^{-2} s^{-1}. Possible GPP limitation at high air temperatures was not accounted.

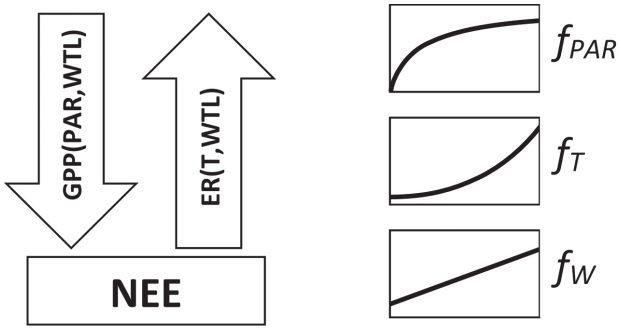

Fig. 1. Schematic representation of CO_2 fluxes (1-3) and shapes of environmental response curves (4-5)

The total ecosystem respiration was modelled using an exponential equation f_T (5) widely used for explanation of ER variation (Kandel et al. 2013; Campbell et al. 2015). The shapes of functional dependence of C fluxes from environmental variables are shown in Fig. 1.

$$f_T = E_0 \times exp(k_T \times T_a); \quad (5)$$

where Ta is air temperature (°C), E_0 is the reference ecosystem respiration (mg m^{-2} h^{-1}) at $T_a = 0$°C and $WTL = 0$, k_T is coefficient describing the respiration temperature response (°C^{-1}).

The rate of photosynthesis and respiration of *Sphagnum* mosses are well correlated with peat moisture (Molchanov and Olchev 2016; Taylor et al. 2016). Changes in water table depth strongly influence GPP (Grant et al. 2012; Pugh et al. 2018), ER (Helfter et al. 2015), and heterotrophic respiration (Eckhardt et al. 2018). Additional factor f_W (6) characterises the influence of WTL on GPP and ER fluxes and can be expressed in a simple linear form:

$$f_W = 1 + k_W \times WTL; \quad (6)$$

where k_W is a parameter of sensitivity of GPP and ER to variation of WTL (cm^{-1}).

NEE is negative when the value of GPP exceeds the ER value and there is a net removal of carbon dioxide from the atmosphere. NEE is positive when the ER value exceeds the GPP value and the carbon dioxide is released from the ecosystem into the atmosphere.

The model has been calibrated using all available data set on carbon dioxide fluxes in 2017 and 2018. Two-step procedure of model calibration was developed to estimate model parameters. At the first step, model parameters were calculated for each studied site (ridge and hollow) using all the available data for 2017-2018. At the second step, k_T, G_m, k_W were fixed and the E_0 and α were calculated for each month of the study period separately. Multi-objective optimization procedure was performed in the Matlab software using *fminsearch* function. The minimum of the unconstrained multivariable function was found using derivative-free optimization method (Lagarias et al. 1998). Root-mean-square error was used as a minimizing function (Dyukarev 2017).

RESULTS AND DISCUSSION

Environmental conditions

During the study period (May – October 2017 and 2018) environmental conditions characterized by large seasonal and diurnal variability (Fig. 2). Minimum air temperature (–7.4 °C) was observed at 4:00 a.m. (local time) on October 23, 2018. Maximum value the air temperature (+ 32.3 °C) reached at 14:00 on July 12, 2018. Rapid temperature raise with a daily mean temperature above 10 °C occurs after June 1. The monthly mean air temperature of June 2017 was 16.4 °C, the mean air temperature of June 2018 was 14.2 °C. Monthly air temperatures in 2018 were slightly lower than in 2017, except July and October. July air temperatures were 18.3 °C and 19.1 °C in 2017 and 2018, respectively. October 2018 was extremely warm with mean air temperature 3.9 °C, when mean temperature in October 2017 was 0 °C.

The maximal values of incoming PAR (up to 1861 μmol m^{-2} s^{-1}) were observed in the middle of a day (at 11:00 on June 26, 2018). Daily maximal incoming solar radiation increased from May to mid-June. Mean monthly PAR in June were 1384 and 1571 μmol m^{-2} s^{-1} in 2017 and 2018, respectively. Minimal PAR values were observed in October: 355 and 425 μmol m^{-2} s^{-1} for 2017 and 2018, respectively. The daily averaged PAR in May-July in 2017 were somewhat higher than in 2018, whereas the daily PAR in August-October were higher in 2018 than in 2017.

The depth of the water table level is gradually decreased from the early spring after snowmelt to the end of summer (Fig. 2). Rapid rise of WTL occurs after heavy rains. The total amount of precipitation over the growing season in 2018 (315 mm) was higher than in 2017 (288 mm) and it is resulted in higher WTL in 2018.

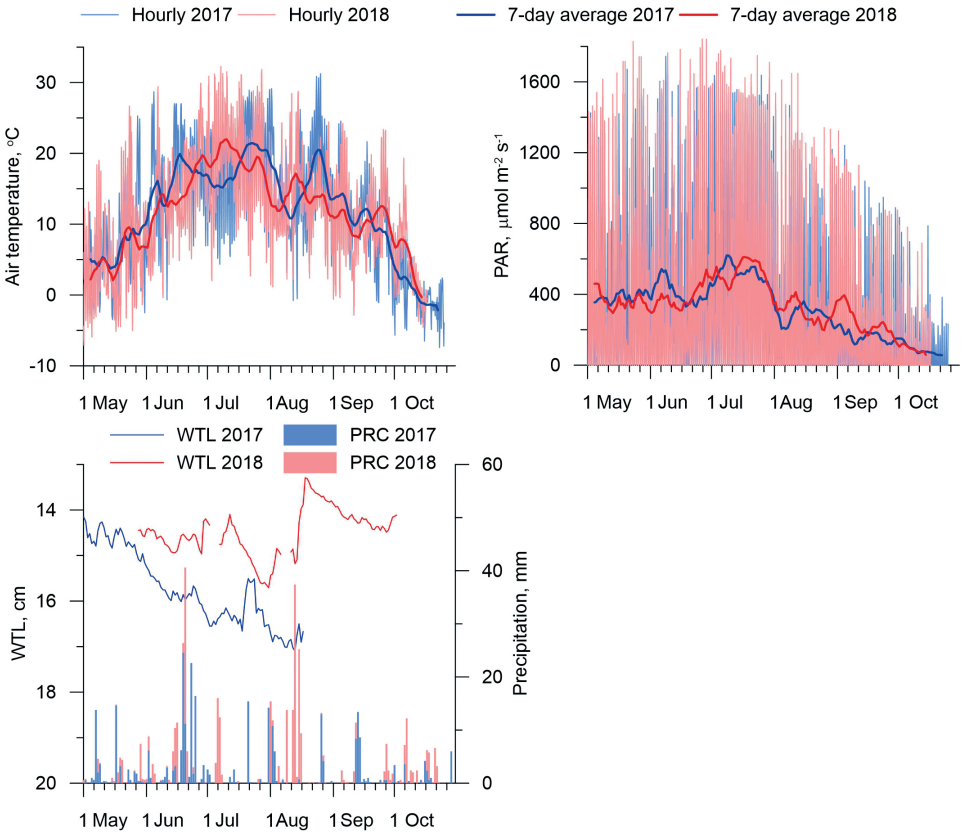

Fig. 2. Seasonal variations of the air temperature (T_a), photosynthetically active radiation (PAR), water table level (WTL) and precipitation (PRC) in May-October 2017 and 2018. Thin lines show hourly data, bold lines show 7-days running average values

Carbon dioxide fluxes

Monthly averaged diurnal variations of the CO_2 fluxes for different months and their standard deviations are shown in Fig.3. A diurnal course of fluxes is quite similar for entire period of measurements. The daily pattern of carbon dioxide fluxes is characterized by a clear maximum at night hours (from 11 p.m to 1 a.m.) when CO_2 is released into the atmosphere, and minimum from 10 a.m. to 1 p.m., when CO_2 uptake by plants exceeds the ecosystem respiration (Golovatskaya, Dyukarev, 2011). Night hours are characterized by positive fluxes whereas negative fluxes are observed from early morning (4 – 6 a.m.) until late evening (6 – 8 p.m.).

The NEE rate changed the sign from positive (release) to negative (uptake) in May even at low air temperatures and remained in the time at relatively low level. CO_2 fluxes increased during the first half of summer whereas GPP and ER reached maximum values at mid-July. ER in August-October is lower than in mid-summer due to decreased air and soil temperatures, but it is higher than at the beginning of the growing season because of a large amount of plant litter and mortmass.

The diurnal pattern of measured CO_2 fluxes on the hollow site in different summer months of 2017, does not vary significantly (Fig. 3). The ridge site is characterized in turn by a slightly decreased CO_2 absorption before noon and increased nocturnal emission from June to August. The early spring in 2017 resulted in a long growing season and, consequently, early onset of the development of vascular plants.

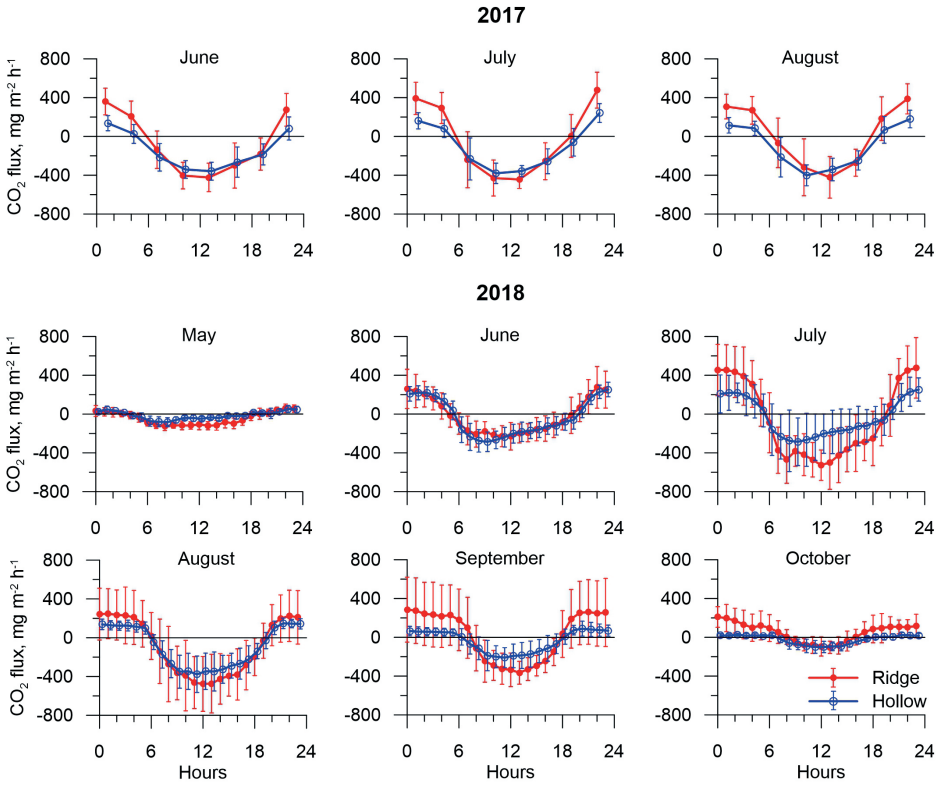

Fig. 3. Monthly averaged diurnal variations of CO_2 fluxes measured at ridge and hollow sites at Mukhrino bog in June-August 2017 and May-October 2018. (Dots – average values, vertical whiskers – standard deviations)

Maximal diurnal variation of fluxes is typical for July, when diurnal range of the fluxes reached 622 and 1004 mg m-2 h^{-1} at hollow and ridge sites, respectively. In May and October 2018, diurnal dynamics of fluxes was very smoothed and characterized by lowered diurnal amplitude. The amplitude of diurnal variations of the CO_2 fluxes in September was 127 and 313 mg m^{-2} h^{-1} at hollow and ridge sites, respectively.

Dwarf shrubs and herbs available at the ridge site are characterized by higher green biomass than sedge at the hollow site. Therefore, both CO_2 uptake and emission fluxes at the ridge site have higher absolute NEE values during the entire growing season, excepting May.

Obtained results are well agreed with measured fluxes at peatlands in other geographical regions. In particular, NEE at peatbog in the south taiga in the European part of Russia (Ivanov et al., 2017) in summer period 2014 was positive (+200 mg m^{-2} h^{-1}) at hummocks and negative (-79 mg m^{-2} h^{-1}) at hollow sites. Under very dry and hot weather conditions in year 2015, CO_2 balance in hummock and hollow was positive with NEE reached +220 and +31 mg m^{-2} h^{-1}, respectively. Ecosystem respiration was significantly higher (300-700 mg m^{-2} h^{-1}) than the ER rates obtained in our study. According to our estimates, CO_2 emission at the ridge site was 2–4 times higher in comparison with estimations in a forested peatbog of the southern taiga in West Siberia (Golovatskaya and Dyukarev 2012). NEE measured in a patterned peatland in Ireland (Laine et al., 2006) have showed, that the absolute flux rates were some higher at hummocks and lower at hollows. The daytime average NEE at the sites were –1700 and –330 mg m^{-2} h^{-1} at hummock and hollow; and the average night time fluxes were +300 and +50 mg m^{-2} h^{-1}, respectively.

Model calibration

The adequate projection of carbon cycle by an ecosystem-level model requires accurate calibration of model input parameters (Wu et al. 2010). The NEE rate measured by automated system was partitioned into ecosystem respiration ER and GPP using suggested NEE model. At the first step of the model calibration all available observation data for the years 2017 and 2018 were used. The 3299 and 3190 observations were used in total for each experimental site (ridge and hollow).

The results of calibration showed a great difference between key model parameters for both experimental sites. The temperature sensitivity coefficient (k_T) for ER rate for the ridge site was about two times smaller than for the hollow site, but at the same time the reference respiration (E_0) at the ridge site was 5.4 times higher (Table 1). The photosynthetic efficiency (α) and photosynthetic capacity (G_m) obtained for the ridge site were about 1.7 times higher than corresponding parameter for the hollow site, likely due to difference in green biomass amount. The effect of WTL on CO_2 fluxes at the hollow site was higher comparing with the ridge site. The model calibrated for the whole data set allows reproducing adequately the fast diurnal variations of CO_2 fluxes, but the projected diurnal variations are significantly lower than the variation obtained from observation data. Mean error (difference between modeled and observed data) was small resulting in high correlation between simulated and observed fluxes ($R>0.94$, $R^2>0.84$, significant at $p<0.05$), although the mean absolute error (MAE) was quite high (Table 1).

In the second step of the model calibration, k_T, G_m and k_W were taken to be constant and equal to the values obtained after the first calibration step (Table 2). The parameters E_0 and α were calculated for each month of the study period separately. The number of observations used for model calibration varies from 110 in June 2017 to 661 in September 2018.

The parameters α and E_0 increase during the growing season simultaneously with plant biomass development until the mid-summer (Table 2). The maximum values of photosynthetic efficiency (5.14 mg μmol^{-1}) were obtained for July 2018 at the ridge site. The maximum values of α for the hollow site were by 20-60% lower than for the ridge. Seasonal course of photosynthetic efficiency is well pronounced and α value for May is significantly lower than α value for middle of the growing season, and about two times lower than the value for the end of the season (October).

Table 1. Calibration step 1. NEE model parameters for ridge and hollow sites. (n - number of observations, G_m, α, k_T, E_0, kW – model parameters, R^2 – determination coefficient, ME – mean error, MAE - mean absolute error)

	Ridge	Hollow
n	3299	3190
G_m, $mg\ m^{-2}\ h^{-1}$	885.4	548.9
α, mg μmol^{-1}	2.08	1.13
k_T, $^oC^{-1}$	0.038	0.091
E_0, $mg\ m^{-2}\ h^{-1}$	126.3	23.5
k_W, cm^{-1}	0.01	0.03
R^2	0.85	0.84
ME, $mg\ m^{-2}\ h^{-1}$	-5.99	-7.92
MAE, $mg\ m^{-2}\ h^{-1}$	65.0	42.3

Table 2. Calibration step 2. NEE model parameters for ridge and hollow sites (*n* - number of observations, *a*, E_0 – model parameters, MAE - mean absolute error)

		Ridge				Hollow			
		n	*a*, mg μmol^{-1}	E_0, mg m^{-2} h^{-1}	*MAE*, mg m^{-2} h^{-1}	*n*	*a*, mg μmol^{-1}	E_0, mg m^{-2} h^{-1}	MAE, mg m^{-2} h^{-1}
2017	June	110	3.31	189.9	25.8	110	1.78	32.9	16.5
	July	204	3.71	190.0	31.1	201	1.79	24.8	30.5
	August	183	2.46	164.2	21.5	161	1.65	28.3	28.0
2018	May	220	0.19	17.6	16.8	209	0.08	7.7	19.5
	June	535	0.94	111.9	36.3	523	0.75	30.1	24.3
	July	545	5.14	186.1	27.8	490	3.11	36.2	21.9
	August	558	2.45	116.8	33.1	561	1.90	33.2	16.1
	September	661	2.36	146.6	35.2	655	0.61	20.7	14.8
	October	253	0.73	75.5	25.6	250	0.33	8.4	10.6
Projected parameters									
2017	May	–	0.63	56.4	–	–	0.27	11.7	–
	September	–	1.19	87.4	–	–	0.57	17.4	–
	October	–	0.23	27.7	–	–	0.08	6.2	–

The ER rate growth is mainly influenced by increased autotrophic respiration rates due to raised biomass amount and increased soil temperatures. E_0 for the hollow site was significantly smaller than the value at the ridge site due to lower biomass amount and reduced contribution of leaf and root respiration.

The model parameters *a* and E_0 for ridge and hollow sites were related with monthly air temperature T_m using exponential model:

$a\ (Ridge) = 0.22\ exp(0.16 \times T_m),\ R^2 = 0.69;$
$a\ (Hollow) = 0.08\ exp(0.19 \times T_m),\ R^2 = 0.79;$
$E_0\ (Ridge) = 27.15\ exp(0.11 \times T_m),\ R^2 = 0.61;$
$E_0\ (Hollow) = 6.06\ exp(0.10 \times T_m),\ R^2 = 0.82.$

These equations were used for projection of *a* and E_0 for May, September and October 2017 taking into account monthly air temperatures (Table 2).

Monthly CO_2 fluxes

Time series of gap-filled modeled ER, GPP and NEE fluxes were integrated for each month of the study period. Annual variability of monthly carbon fluxes for ridge and hollow sites is shown in Fig 4. The largest ER efflux was measured in July 2017 at the ridge site - 97.3 gC m^{-2}. Respiration rate at the hollow site reached maximum values in July too, and they were somewhat lower than at the ridge site – 42.1 gC m^{-2}. In May, the total respiration at both sites were similar and does not exceed 17.9 gC m^{-2} in 2018 and 5.6 gC m-2 in 2017 because of lower temperatures. June and August were characterized by moderate respiration fluxes ranging between 13.8 and 75.0 gC m^{-2}. The more intense emission was obtained for the ridge site where various vascular species strongly contribute to autotrophic part of respiration and thicker acrotelm layer promotes aerobic

decomposition of plant residuals. The ER rate in September and October was still high at the ridge site but because of low GPP the ridge acted as a source of CO_2 for the atmosphere.

The recovery of photosynthetic activity of peatbog vegetation began in 2017 in early spring and the GPP rate reached rather high values in May – 20.7 and 43.4 gC m^{-2} for hollow and ridge sites, respectively. Due to late spring in 2018 the GPP values in May was essentially lower for both sites – 2.7 and 7.1 gC m^{-2} for hollow and ridge sites, respectively. GPP reached its maximum rates in July – 120.3 gC m^{-2} at the ridge site and 91.3 gC m^{-2} at the hollow site. June and August of 2017 and 2018 are characterized by lower values of GPP because of lower PAR values (see Fig.2). The hollow site is characterized by faster autumn decrease of GPP comparing with ridge site.

The ratio of GPP to ER is used to estimate the fraction of assimilated carbon that was consumed by the plants (Falge et al., 2002). Analysis of the GPP/ER ratio for the entire measuring period showed that the ratio was 1.2 for the ridge site and 1.6 for the hollow site respectively. Both sites acted as a sink of carbon dioxide from the atmosphere.

The largest variations of carbon fluxes were observed at the ridge site, where seasonal maximums in absolute values of ER and GPP significantly exceed the corresponding values at the hollow site. The hollow site has smoother fluxes dynamics and lower absolute values of ER and GPP. Despite of the found differences in GPP and ER between both sites, monthly NEE was higher at the hollow site. Summer month rates of NEE at the hollow site varied from -0.3 to -40.7 gC m^{-2} in 2017 and from +0.5 to -27.0 gC m^{-2} in 2018, whereas at the ridge site NEE changed from +1.8 to -25.4 gC m^{-2} in 2017 and from +14.0 to -23.5 gC m^{-2} in 2018. The maximal carbon uptake occurred in July at both sites. Small positive NEE values (up to 14.0 gC m^{-2}) were obtained for June and October 2018 at the ridge site and for May and June 2018 at the hollow site, respectively.

The growing season cumulative NEE, calculated by integrating the monthly averaged diurnal NEE rates for period from May to September was –78.5 and –121.6 gC m^{-2} in 2017 for ridge and hollow sites, respectively. Results show that amount of captured CO_2 from the atmosphere for both experimental sites was lower for year 2018 than for the same period in 2017. While the cumulative NEE rate for ridge site was –21.9, for hollow site it reached –53.8 gC m^{-2}. The most significant decrease in NEE at the hollow site from 2017 to 2018 occurs mainly due to decrease in GPP from 257.3 to 199.8 gC m^{-2}, and insignificant rise in ER rates from 135.7 to 146.0 gC m^{-2}. High-

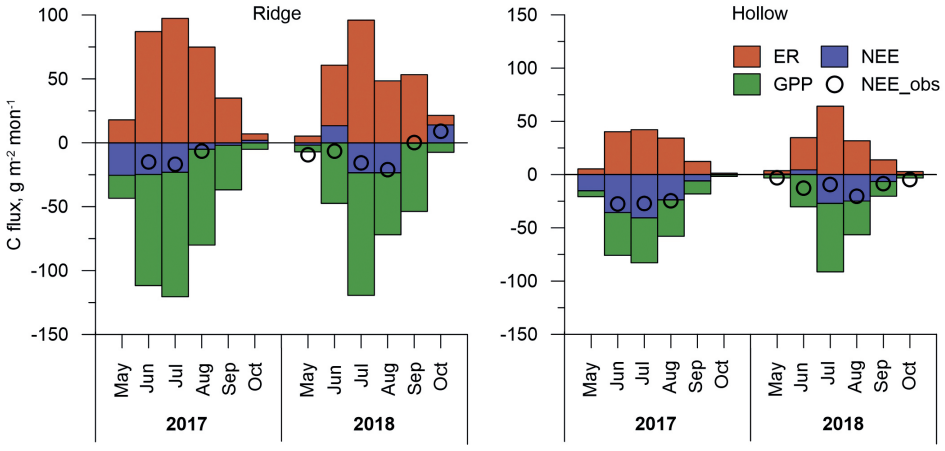

Fig. 4. Monthly carbon dioxide fluxes at the ridge and hollow sites at Mukhrino bog in 2017 and 2018. Circles show NEE observations, bars – model estimations for ER, GPP and NEE

er values of NEE in 2018 at the ridge site were obviously related with smaller values of the both GPP and ER rates. Whereas ER rate at the ridge site decreased from 317.3 to 257.9 gC m^{-2}, GPP falls down from 395.8 to 293.8 gC m^{-2}.

Over the two years of flux measurements, the average annual uptake of CO_2 was 87.7 gC m^{-2} at the hollow and 50.2 gC m^{-2} at the ridge site at Mukhrino bog and the NEE rates were quite similar to findings at other peatland sites. In particular, two years of measurements of CO_2 fluxes in the Stordalen palsa mire (a nutrient poor permafrost peatland) in Sweden showed that the mire was a net sink of carbon, with average annual uptake of –46 gC m^{-2} per year (Olefeldt et al. 2012). The results of two years flux measurements in a boreal minerogenic oligotrophic mire in northern Sweden (Nilsson et al., 2008) showed the peatbog was also a net carbon sink with annual net uptake of about –55 gC m^{-2}. McVeigh et al. (2014) reported about the average 10-years annual CO_2 uptake of –55.7 ± 18.9 gC m^{-2} in Atlantic blanket bog in Glencar, southwest Ireland. The results of 11 year flux measurements in a temperate lowland peatland in central Scotland (Helfter et al. 2015) showed a very high variation of annual NEE rate that is ranged between –5.2 and –36.9 gC m^{-2} yr^{-1}.

The differences in microtopographic features between hummocks and hollows and its statistically significant influence on the total ER, but not on GPP, were found by Wu et al. (2010) at ombrotrophic MerBlue bog. NEE rates estimated at the hummock and hollow sites were –66 ÷ +19 gC m^{-2} yr^{-1} and –146 ÷ –260 gC m^{-2} yr^{-1}, respectively. The chamber estimates of NEE at patterned blanked bog (Laine et al. 2006) found that the annual NEE of the driest peatbog sites was about 130% larger than the NEE rate at the wet sites, indicating a large spatial variation that can be found in NEE rates within a quite uniform peatbog ecosystem.

CONCLUSION

The results of field measurements of CO_2 fluxes at ridge-hollow complex bog in combination with suggested mathematical model allowed us to estimate adequately the NEE, ER and GPP rates for ridge and hollow sites at oligotrophic bog in Middle Taiga Zone of West Siberia. The cumulative CO_2 uptake rates exceed cumulative respiration rates at both experimental sites. The two year average growing season NEE at the hollow site was 1.7 times higher (87.7 gC m^{-2}) than at the ridge site (50.2 gC m^{-2}). GPP and ER rates at the ridge site were higher than at the hollow site. The influence of key environmental factors (air temperature, incoming photosynthetically active radiation and water table depth) on CO_2 fluxes at each ecosystem was very different. It is claimed by differences in model parameters describing ER and GPP response to changed ambient characteristics. The suggested NEE model is a promising tool to describe the NEE partitioning into GPP and ER, and to better understand the biogeochemical processes in mire ecosystems in order to find new possibilities to extrapolate the data of local observations to peatland ecosystems of Western Siberia.

ACKNOWLEDGMENTS

This study was supported by the project AAAA-A17-117013050031-8 and grant 13-01-20/39 of the Yugra State University. The field works at Mukhrino field station was funded by Russian Fund for Basic Researches and Government of the Khanty-Mansiysk Autonomous region according to the research project 18-44-860017.

REFERENCES

Acosta M., Juszczak R., Chojnicki B., Pavelka M., Havránková K., Lesny J., Krupková L., Urbaniak M., Machačová K., Olejnik J. (2017). CO_2 Fluxes from Different Vegetation Communities on a Peatland Ecosystem. Wetlands, V.37, N.3, pp. 423–435. https://doi.org/10.1007/s13157-017-0878-4.

Alekseychik P., Mammarella I., Karpov D., Dengel S., Terentieva I., Sabrekov A., Glagolev M., Lapshina E.D. (2017). Net ecosystem exchange and energy fluxes measured with the eddy covariance technique in a western Siberian bog. Atmos. Chem. Phys., V.17, pp. 9333-9345, https://doi.org/10.5194/acp-17-9333-2017.

Baird A., Belyea L., Comas X., Reeve A., Slater L. (2013). Carbon Cycling in Northern Peatlands. Geophysical Monograph Series. AGU pp. 297.

Bleuten W., Filippov I. (2008). Hydrology of mire ecosystems in central West Siberia: the Mukhrino Field Station, in Transactions of UNESCO department of Yugorsky State University "Dynamics of environment and global climate change" ed. Lapshina, E. D., Novosibirsk, NSU, pp. 208–224.

Bubier J.L., Crill P.M., Mosedale A., Frolking S., Linder E. (2003). Peatland responses to varying interannual moisture conditions as measured by automatic CO_2 chambers. Glob. Biogeochem Cycles. V.17. N.2, p.1066. https://doi.org/10.1029/2002GB001946.

Campbell D.I., Smith J., Goodrich J.P., Wall A.M., Schipper L.A. (2014). Year-round growing conditions explains large CO_2 sink strength in a New Zealand raised peat bog. Agricultural and Forest Meteorology, V.192–193, pp.59–68. https://doi.org/10.1016/j.agrformet.2014.03.003.

Campbell D.I., Wall A.M., Nieveen J.P., Schipper L.A. (2015). Variations in CO_2 exchange for dairy farms with year-round rotational grazing on drained peatlands. Agric. Ecosyst. Environ. V.202, pp.68–78. http://dx.doi.org/10.1016/j.agee.2014.12.019.

Ciais P., Sabine C., Bala, G., Bopp, L., Brovkin, V., Canadell, J., Chhabra, A., DeFries, R., Galloway, J., Heimann, M., Jones, C., Le Quéré, C., Myneni, R.B., Piao, S., Thornton, P. (2013). Carbon and Other Biogeochemical Cycles. In: Climate Change 2013: The Physical Science Basis. Contribution of Working Group I to the Fifth Assessment Report of the Intergovernmental Panel on Climate Change [Stocker, T.F., Qin, D., Plattner, G.-K., Tignor, M., Allen, S.K., Boschung, J., Nauels, A., Xia, Y., Bex, V., Midgley, P.M. (eds.)]. Cambridge University Press, Cambridge, United Kingdom and New York, NY, USA.

Davydov D.K., Dyachkova A.V., Fofonov A.V., Maksyutov S.S., Dyukarev E.A., Smirnov S.V., Glagolev M.V. (2018). Measurements of methane and carbon dioxide fluxes from wetland ecosystems of the Southern Taiga of West Siberia. Proceedings of SPIE - The International Society for Optical Engineering. V.10833, 1083389.

Dyukarev E.A. (2017). Partitioning of net ecosystem exchange using chamber measurements data from bare soil and vegetated sites. Agricultural and Forest Meteorology. V.239, pp. 236-248. https://doi.org/10.1016/j.agrformet.2017.03.011.

Dyukarev E.A., Golovatskaya E.A., Duchkov A.D., Kazantsev S.A. (2009). Temperature monitoring in Bakchar bog (West Siberia). Russian Geology and Geophysics, N.6, pp. 745-754. https://doi.org/10.1016/j.rgg.2008.08.010.

Dyukarev E.A., Pologova N.N., Dyukarev A.G, Golovatskaya E.A. (2011). Forest cover disturbances in the South Taiga of Western Siberia. Environ. Res. Lett. V.6, N.3, 035203 9pp. https://doi.org/10.1088/1748-9326/6/3/035203.

Eckhardt T., Knoblauch C., Kutzbach L., Simpson G., Abakumov E., and Pfeiffer E.-M. (2018). Partitioning CO_2 net ecosystem exchange fluxes on the microsite scale in the Lena River Delta, Siberia, Biogeosciences Discuss., https://doi.org/10.5194/bg-2018-311, in review.

Falge E., Baldocchi D., Olson R., Anthoni P., Aubinet M., Bernhofer C., Burba G., Ceulemans R., Clement R., Dolman H., Granier A., Gross P., Grünwald T., Hollinger D., Jensen N.-O., Katul G., Keronen P., Kowalski A., Ta Lai C., Law B.E., Meyers T., Moncrieff J., Moors E., Munger J.W., Pilegaard K., Rannik Ü., Rebmann C., Suyker A., Tenhunen J., Tu K., Verma S., Vesala T., Wilson K., Wofsy S. (2001). Gap filling strategies for defensible annual sums of net ecosystem exchange. Agric. For. Meteorol. V.107, pp.43–69. https://doi.org/10.1016/S0168-1923(00)00225-2.

Filippova N.V., Bulyonkova T.M. Lapshina, E.D. (2015). Fleshy fungi forays in the vicinities of the YSU Mukhrino field station (Western Siberia). Environ. Dyn. Glob. Clim. Change, V.6, pp.3–31. http://dx.doi.org/10.17816/edgcc613-31.

Fleischer E., Khashimov I., Hölzel N., Klemm O. (2016). Carbon exchange fluxes over peatlands in Western Siberia : Possible feedback between land-use change and climate change. Science of the Total Environment. V.545–546, pp. 424–433. https://doi.org/10.1016/j.scitotenv.2015.12.073.

Franz D., Acosta M., Altimir N., Arriga N., Arrouays D., Aubinet M. et al. (2018). Towards long-term standardised carbon and greenhouse gas observations for monitoring Europe´s terrestrial ecosystems: a review. International Agrophysics. V.32, N.4, pp. 439-455. https://doi.org/10.1515/intag-2017-0039.

Glagolev M., Kleptsova I., Filippov I., Maksyutov S., Machida T. (2011). Regional methane emission from West Siberia mire landscapes. Environ. Res. Lett., V.6, pp. 045214, https://doi.org/10.1088/1748-9326/6/4/045214.

Glagolev M.V., Ilyasov D.V., Terentyeva I.E., Sabrekov A.F., Krasnov O.A., Maksyutov Sh.Sh. (2017). Methane and carbon dioxide fluxes in the waterlogged forests of Western Siberian southern and middle taiga subzones. Optika Atmosfery i Okeana. V.30, N. 04, pp. 301–309 (in Russian).

Golovatskaya E.A., Dyukarev E.A. (2011). Seasonal and diurnal dynamics of CO_2 emission from oligotrophic peat soil surface. Russian Meteorology and Hydrology. N.6, pp.84-93. https://link.springer.com/article/10.3103%2FS1068373911060094.

Golovatskaya E.A. and Dyukarev E.A. (2012). The influence of environmental factors on the CO_2 emission from the surface of oligotrophic peat soils in West Siberia. Eurasian Soil Science Journal. N.6, pp. 658–667. https://link.springer.com/article/10.1134/S106422931206004X.

Golovatskaya E.A., Dyukarev E.A., Ippolitov I.I., Kabanov M.V. (2008). Influence of landscape and hydrometeorological conditions on CO_2 emission in peatland ecosystems. Doklady Earth Sciences. N.4, pp.1-4.

Grant R.F., Desai A.R., Sulman B.N. (2012). Modelling contrasting responses of wetland productivity to changes in water table depth. Biogeosciences, V.9, N.11, pp.4215–4231. https://doi.org/10.5194/bg-9-4215-2012.

Grebenyuk G.N., Kuznetsova V.P. (2012). Modern climate dynamics and phenological variability of northern territories. Fundamental research, N.11-5, pp. 1063-1077 (in Russian).

Günther A., Jurasinski G., Albrecht K., Gaudig G., Krebs M., Glatzel S. (2017) Greenhouse gas balance of an establishing Sphagnum culture on a former bog grassland in Germany. Mires and Peat. V.20, pp. 1-16. https://doi.org/10.19189/MaP.2015.OMB.210.

Helfter C., Campbell C., Dinsmore K.J., Drewer J., Coyle M., Anderson M., Skiba U., Nemitz E., Sutton M.A. (2015). Drivers of long-term variability in CO_2 net ecosystem exchange in a temperate peatland. Biogeosciences, V.12, N.6, pp.1799–1811. https://doi.org/10.5194/bg-12-1799-2015.

Humphreys E.R., Lafleur P.M. (2011). Does earlier snowmelt lead to greater CO_2 sequestration in two low arctic tundra ecosystems? Geophys. Res. Lett. V.38, N.5, L09703. https://doi.org/10.1029/2011GL047339.

Ivanov D.G., Avilov V.K., Kurbatova Y.A. (2017). CO_2 fluxes at south taiga bog in the European part of Russia in summer. Contemporary Problems of Ecology. V.10, N.2, pp. 97–104. https://doi.org/10.1134/s1995425517020056.

Kabanov M.V. (2015). Regional climate-regulating factors in Western Siberia Geography and Natural Sciences. V.3, pp. 207-113.

Kandel T.P., Elsgaard L., Larke, P.E. (2013). Measurement and modelling of CO_2 flux from a drained fen peatland cultivated with reed canary grass and spring barley. GCB Bioenergy. V.5, pp. 548-561. https://doi.org/10.1111/gcbb.12020.

Kurbatova J., Li C., Tatarinov F., Varlagin A., Shalukhina N., Olchev A. (2009). Modeling of the carbon dioxide fluxes in European Russia peat bogs. Environmental Research Letters, V.4, N.4, 045022. https://doi.org/10.1088/1748-9326/4/4/045022.

Kurganova I.N., Lopes de Gerenyu V.O. L., Petrov A.S., Myakshina T.N., Sapronov D.V., Ableeva V. A., Kudeyarov V. N. (2011). Effect of the observed climate changes and extreme weather phenomena on the emission component of the carbon cycle in different ecosystems of the southern taiga zone. Doklady Biological Sciences, V.441, N.1, pp. 412-416. https://doi.org/10.1134/S0012496611060214.

Lagarias J.C., Reeds J.A., Wright M.H., Wright P.E. (1998). Convergence properties of the nelder-mead simplex method in low dimensions. SIAM Journal of Optimization, V.9, N.1, pp. 112–147.

Laine A., Riutta T., Juutinen S., Valiranta M., Tuittila E.S. (2009). Acknowledging the spatial heterogeneity in modelling/reconstructing carbon dioxide exchange in a northern aapa mire. Ecol. Modell. V.220, pp.2646–2655. https://doi.org/10.1016/j.ecolmodel.2009.06.047.

Laine A.M., Mehtätalo L., Tolvanen A., Frolking S., Tuittila E.S. (2019). Impacts of drainage, restoration and warming on boreal wetland greenhouse gas fluxes Sci. Total Environ., V.647 pp. 169-181, https://doi.org/10.1016/j.scitotenv.2018.07.390.

Lapshina E.D., Alexeychik P., Dengel S., Filippova N.V., Zarov E.A., Filippov I.V., Terentyeva I.E., Sabrekov A.F., Solomin Y.R., Karpov D.V., Mammarella I. (2015). A new peatland research station in the center of West Siberia: description of infrastructure and research activities. Report series in aerosol science. pp. 236-240. http://www.atm.helsinki.fi/faar/reportseries/rs-180.pdf.

Leifeld J., Menichetti L. (2018). The underappreciated potential of peatlands in global climate change mitigation stratigies, Nat. Commun., V.9, pp.1071, https://doi.org/10.1038/s41467-018-03406- 6.

Leroy F., Gogo S., Guimbaud C., Bernard-Jannin L., Hu Z., Laggoun-Défarge F. (2017). Vegetation composition controls temperature sensitivity of CO_2 and CH_4 emissions and DOC concentration in peatlands. Soil Biology and Biochemistry, V.107, pp.164–167. https://doi.org/10.1016/j.soilbio.2017.01.005.

Mäkelä A., Hari P., Berninger F., Hänninen H., Nikinmaa E. (2004). Acclimation of photosynthetic capacity in Scots pine to the annual cycle of temperature. Tree Physiol. V.24, N.4, pp. 369–376. https://www.ncbi.nlm.nih.gov/pubmed/14757576.

McVeigh P., Sottocornola M., Foley N., Leahy P., Kiely G. (2014). Meteorological and functional response partitioning to explain interannual variability of CO_2 exchange at an Irish Atlantic blanket bog. Agricultural and Forest Meteorology V.194, pp. 8–19. https://doi.org/10.1016/j.agrformet.2014.01.017.

Minkkinen K., Ojanen P., Penttilä T., Aurela M., Laurila T., Tuovinen J.-P., Lohila A. (2018). Persistent carbon sink at a boreal drained bog forest. Biogeosciences. V.15, N.11, pp. 3603–3624. https://doi.org/10.5194/bg-15-3603-2018.

Molchanov A.G. (2015). Gas exchange in sphagnum mosses at different near-surface groundwater levels. Russian Journal of Ecology. V.46, N.3. pp. 230-235. https://doi.org/10.7868/s0367059715030063.

Molchanov A.G., Olchev A.V. (2016) Model of CO_2 exchange in a sphagnum peat bog. Computer research and modelling. V.8. N.2. pp. 369-377.

Munir T.M., Xu B., Perkins M., Strack M. (2014). Responses of carbon dioxide flux and plant biomass to water table drawdown in a treed peatland in Northern Alberta: A climate change perspective. Biogeosciences. V.11, N.3, pp. 807–820. https://doi.org/10.5194/bg-11-807-2014.

Naumov A.V. (2009). Soil respiration. Novosibirsk, Izd SO RAN. P. 208.

Nilsson M., Sagerfors J., Buffam I., Laudon H., Eriksson T., Grelle A., Klemedtsson L., Weslien P., Lindroth A. (2008). Contemporary carbon accumulation in a boreal oligotrophic minerogenic mire – a significant sink after accounting for all C-fluxes. Global Change Biol. 14 (10), 2317–2332. https://doi.org/10.1111/j.1365-2486.2008.01654.x.

Olefeldt D., Roulet N.T., Bergeron O., Crill P., Bäckstrand K., Christensen T.R. (2012). Net carbon accumulation of a high-latitude permafrost palsa mire similar to permafrost-free peatlands. Geophys. Res. Lett. 39, L03501 https://doi.org/10.1029/2011GL050355.

Olchev A., Novenko E., Desherevskaya O., Krasnorutskaya K., Kurbatova J. (2009). Effects of climatic changes on carbon dioxide and water vapor fluxes in boreal forest ecosystems of European part of Russia. Environmental Research Letters, V.4, N.4, 045007 https://doi.org/10.1088/1748-9326/4/4/045007.

Page S., Baird A. (2016). Peatlands and global change: response and resilience, Ann. Rev. Environ. Resour., V.41, pp.35–57.

Parazoo N.C., Koven C.D., Lawrence D.M., Romanovsky V. Miller C.E. (2017) Detecting the permafrost carbon feedback: Talik formation and increased cold-season respiration as precursors to sink-to-source transitions. The Cryosphere, https://doi.org/10.5194/tc-2017-189.

Pavelka M., Acosta M., Kiese R., Altimir N., Brümmer C., Crill P., Darenova E., Fuß R., Gielen B., Graf A., Klemedtsson L., Lohila A., Longdoz B., Lindroth A., Nilsson M., Jiménez S., Merbold L., Montagnani L., Peichl M., Pihlatie M., Pumpanen J., Ortiz P., Silvennoinen H., Skiba U., Vestin P., Weslien P., Janous D., Kutsch, W. (2018). Standardisation of chamber technique for CO_2, N_2O and CH_4 fluxes measurements from terrestrial ecosystems. International Agrophysics, V.32, N.4, pp.569–587. https://doi.org/10.1515/intag-2017-0045.

Peatlands of West Siberia (1976). Their composition and hydrological regime. Leningrad, Hydrometeoizdat. P. 615.

Pessarakli M. (2005). Handbook of Photosynthesis. Taylor & Francis Group. P.928.

Pugh C. A., Reed D. E., Desai A. R., Sulman B. N. (2018). Wetland flux controls: how does interacting water table levels and temperature influence carbon dioxide and methane fluxes in northern Wisconsin? Biogeochemistry, V.137, N.1–2, pp. 15–25. https://doi.org/10.1007/s10533-017-0414-x.

Ratcliffe J.L., Creevy A., Andersen R., Zarov E., Gaffney P., Taggart M.A., Mazei Y., Tsyganov A.N., Rowson J.G., Lapshina E.D., Payne R.J. (2017). Ecological and environmental transition across the forested-to-open bog ecotone in a west Siberian peatland Science of the Total Environment. V.607-608, pp.816-828. https://doi.org/10.1016/j.scitotenv.2017.06.276.

Runkle B.R.K., Sachs T., Wille C., Pfeiffer E.-M., Kutzbach L. (2013). Bulk partitioning the growing season net ecosystem exchange of CO_2 in Siberian tundra reveals the seasonality of its carbon sequestration strength. Biogeosciences. V.10, pp.1337-1349. https://doi.org/10.5194/bg-10-1337-2013, 2013.

Rydin H., Jeglum J. (2015). The Biology of Peatlands. Oxford. Univ. Press., pp. 400.

Sasakawa M., Ito A., Machida T., Tsuda N., Niwa Y., Davydov D., Fofonov A., Arshinov M. (2012). Annual variation of CH_4 emissions from the middle taiga in West Siberian Lowland (2005-2009): A case of high CH_4 flux and precipitation rate in the summer of 2007. Tellus, Series B: Chemical and Physical Meteorology, V.64, N.1, pp.1–10. https://doi.org/10.3402/tellusb.v64i0.17514.

Saunois M., Bousquet P., Poulter B., Peregon A., Ciais P., Canadell J. G., Dlugokencky E. J., Etiope G., Bastviken D., Houweling S., Janssens-Maenhout G., Tubiello F. N., Castaldi S., Jackson R. B., Alexe M., Arora V. K., Beerling D. J., Bergamaschi P., Blake D. R., Brailsford G., Brovkin V., Bruhwiler L., Crevoisier C., Crill P., Covey K., Curry C., Frankenberg C., Gedney N., Höglund-Isaksson L., Ishizawa M., Ito A., Joos F., Kim H.-S., Kleinen T., Krummel P., Lamarque J.-F., Langenfelds R., Locatelli R., Machida T., Maksyutov S., McDonald K. C., Marshall J., Melton J. R., Morino I., Naik V., O'Doherty S., Parmentier F.-J. W., Patra P. K., Peng C., Peng S., Peters G. P., Pison I., Prigent C., Prinn R., Ramonet M., Riley W. J., Saito M., Santini M., Schroeder R., Simpson I. J., Spahni R., Steele P., Takizawa A., Thornton B. F., Tian H., Tohjima Y., Viovy N., Voulgarakis A., van Weele M., van der Werf G. R., Weiss R., Wiedinmyer C., Wilton D. J., Wiltshire A., Worthy D., Wunch D., Xu X., Yoshida Y., Zhang B., Zhang Z., Zhu Q. (2016). The global methane budget 2000–2012, Earth Syst. Sci. Data, V.8, pp.697-751. https://doi.org/10.5194/essd-8-697-2016.

Sheng Y., Smith L.C., MacDonald G.M., Kremenetski K.V., Frey K.E., Velichko A.A., Lee M., Beilman D.W., Dubinin P. (2004). A high–resolution GIS–based inventory of the west Siberian peat carbon pool. Global Biogeochemical Cycles. V.18, p.GB3004.

Sokolov A.V., Mamkin V.V., Avilov V.K., Tarasov D.L., Kurbatova J.A., Olchev A.V. (2019). Application of a balanced identification method for gap-filling in CO_2 flux data in a sphagnum peat bog. Computer research and modelling. V.11, N.1, pp.153-171. https://doi.org/10.20537/2076-7633-2019-11-1-153-171.

Stepanova V.A., Pokrovsky O.S. (2011). Macroelement composition of raised bogs peat in the middle taiga of Western Siberia (the bog complex Mukhrino), Tomsk State University Bulletin. V.352, pp.211–214, (in Russian).

Swenson M.M., Regan S., Bremmers D.T.H., Lawless J., Saunders M., Gill L.W. (2019). Carbon balance of a restored and cutover raised bog: implications for restoration and comparison to global trends. Biogeosciences. V.16, pp.713-731, https://doi.org/10.5194/bg-16-713-2019.

Szajdak L.W., Lapshina E.D., Gaca W., Styla K., Meysner T., Szczepanski M., Zarov E.A. (2016). Physical, chemical and biochemical properties of Western Siberia Sphagnum and Carex peat soils, Environ. Dyn. Glob. Clim. Change, V.7, pp. 13–25. http://dx.doi.org/10.17816/edgcc7213-25

Taylor N., Price J., Strack M. (2016). Hydrological controls on productivity of regenerating Sphagnum in a cutover peatland. Ecohydrology, V.9, N.6, pp. 1017–1027. https://doi.org/10.1002/eco.1699.

Terentieva I. E., Glagolev M. V., Lapshina E. D., Sabrekov A. F., Maksyutov S. (2016). Mapping of West Siberian taiga wetland complexes using Landsat imagery: implications for methane emissions, Biogeosciences, V.13, pp.4615-4626, https://doi.org/10.5194/bg-13-4615-2016.

The second assessment report of Roshydromet on climate change and their consequences on the territory of the Russian Federation (2014). Federal service for Hydrometeorology and environmental monitoring. pp. 605.

Veretennikova E.E. and Dyukarev E.A. (2017). Diurnal variations in methane emissions from West Siberia peatlands in summer. Russian Meteorology and Hydrology. V.42, N.5, pp. 319-326. https://link.springer.com/article/10.3103/S1068373917050077.

Vomperskiy S.E. (1994). The role of peatlands in carbon cycling, in Biogeocenotic features of peatlands and their rational exploitation. Moscow, Nauka, pp. 5-37.

Walker T.N., Garnett M.H., Ward S.E., Oakley S., Bardgett R. D., Ostle N. J. (2016). Vascular plants promote ancient peatland carbon loss with climate warming. Global Change Biology, V.22, N.5, pp. 1880–1889. https://doi.org/10.1111/gcb.13213.

Webster K.L., Bhatti J.S., Thompson D.K., Nelson S.A., Shaw C.H., Bona K.A., Hayne S.L., Kurz W.A. (2018). Spatially-integrated estimates of net ecosystem exchange and methane fluxes from Canadian peatlands. Carbon Balance and Management, V.13, N.1. https://doi.org/10.1186/s13021-018-0105-5.

Widlowski J.-L., Pinty B., Clerici M., Dai Y., De Kauwe M., de Ridder K., Kallel A., Kobayashi H., Lavergne T., NiMeister W., Olchev A., Quaife T., Wang S., Yang W., Yang Y., Yuan H. (2011). RAMI4PILPS: An intercomparison of formulations for the partitioning of solar radiation in land surface models. Journal of Geophysical Research: Biogeosciences, V.116, N.2. https://doi.org/10.1029/2010JG001511.

Wu J., Roulet N.T., Moore T.R., Lafleur P., Humphreys E. (2010). Dealing with microtopography of an ombrotrophic bog for simulating ecosystem-level CO_2 exchanges. Ecological Modelling. V.222, N.4, pp. 1038–1047. https://doi.org/10.1016/j.ecolmodel.2010.07.015.

Yurova A., Wolf A., Sagerfors J., Nilsson M. (2007). Variations in net ecosystem exchange of carbon dioxide in a boreal mire: Modeling mechanisms linked to water table position. Journal of Geophysical Research: Biogeosciences, V.112, N.2, G02025. https://doi.org/10.1029/2006JG000342.

Zhaojun B., Joosten H., Hongkai L., Gaolin Z., Xingxing Z., Jinze M., Jing Z. (2011). The response of peatlands to climate warming: A review. Acta Ecologica Sinica, V.31, N.3, pp.157–162. https://doi.org/10.1016/j.chnaes.2011.03.006.

Zhou L., Zhou G., Jia Q. (2009). Annual cycle of CO_2 exchange over a reed (Phragmites australis) wetland in Northeast China. Aquatic Botany, V.91, N.2, pp. 91–98. https://doi.org/10.1016/j.aquabot.2009.03.002.

Zhu X., Song C., Swarenzenski C.M., Guo Y., Zhang X., Wang J. (2015). Ecosystem-atmosphere exchange of CO2 in a temperate herbaceous peatland in the Sanjiang Plain of northeast China. Ecological Engineering, V.75, pp. 16–23. https://doi.org/10.1016/j.ecoleng.2014.11.035.

Received on Dec 16th 2018 Accepted on May 17th, 2019

Nina Tiralla[1*], Oleg Panferov[2], Heinrich Kreilein[1], Alexander Olchev[3,4], Ashehad A. Ali[1] and Alexander Knohl[1]
[1] University of Goettingen, Bioclimatology, Göttingen, Germany
[2] University of Applied Sciences Bingen, Dept. of Life Sciences and Engineering, Bingen, Germany
[3] Moscow State University, Faculty of Geography, Moscow, Russia
[4] Severtsov Institute of Ecology and Evolution, Russian Academy of Sciences, Moscow, Russia
*** Corresponding author:** ntirall1@gwdg.de

QUANTIFICATION OF LEAF EMISSIVITIES OF FOREST SPECIES: EFFECTS ON MODELLED ENERGY AND MATTER FLUXES IN FOREST ECOSYSTEMS

ABSTRACT. Climate change has distinct regional and local differences in its impacts on the land surface. One of the important parameters determining the climate change signal is the emissivity (ε) of the surface. In forest-climate interactions, the leaf surface emissivity plays a decisive role. The accurate determination of leaf emissivities is crucial for the appropriate interpretation of measured energy and matter fluxes between the forest and the atmosphere. In this study, we quantified the emissivity of the five broadleaf tree species *Acer pseudoplatanus, Fagus sylvatica, Fraxinus excelsior, Populus simonii* and *Populus candicans*. Measurements of leaf surface temperatures were conducted under laboratory conditions in a controlled-climate chamber within the temperature range of +8 °C and +32 °C. Based on these measurements, broadband leaf emissivities ε (ε for the spectral range of 8-14 µm) were calculated. Average $\varepsilon_{8\text{-}14\ \mu m}$ was 0.958±0.002 for all species with very little variation among species. In a second step, the soil-vegetation-atmosphere transfer model 'MixFor-SVAT' was applied to examine the effects of ε changes on radiative, sensible and latent energy fluxes of the Hainich forest in Central Germany. Model experiments were driven by meteorological data measured at the Hainich site. The simulations were forced with the calculated ε value as well as with minimum and maximum values obtained from the literature. Significant effects of ε changes were detected. The strongest effect was identified for the sensible heat flux with a sensitivity of 20.7 % per 1 % ε change. Thus, the variability of ε should be considered in climate change studies.

KEY WORDS: Leaf emissivity, matter flux, energy flux, MixFor-SVAT

CITATION: Nina Tiralla, Oleg Panferov, Heinrich Kreilein, Alexander Olchev, Ashehad A. Ali, Alexander Knohl (2019) Quantification of leaf emissivities of forest species: Effects on modelled energy and matter fluxes in forest ecosystems. Geography, Environment, Sustainability,
Vol.12, No 2, p. 245-258
DOI-10.24057/2071-9388-2018-86

INTRODUCTION

Impacts of climate change on regional as well as on local scales differ spatially substantially. Some of the reasons for this spatial variability is local and regional as land use and land cover differences as well land use changes, which bring along variations in surface properties (Pielke et al. 2011). The impact of forest specific land use changes such as anthropogenic deforestation and the effect of forest biomes in general on climate is extensively discussed in the scientific literature (Alkama and Cecatti 2016; Snyder et al. 2004 among many others). The strength of the forest-climate interactions and the magnitude of the contribution of the forest to climate variability and to climate change depends strongly on forest properties such as canopy structure, albedo, and surface roughness (Bonan 2008). One of the important forest parameters is the surface emission coefficient or emissivity (ε), which determines the radiation emission via the Stefan-Boltzmann law, and thus directly affects net radiation. That in turn regulates the radiative cooling and warming of the surface, and thus determines surface temperatures, which affect the local and regional climate (Sabajo et al. 2017). Information on surface emissivity is crucial for an accurate interpretation of measured energy and matter fluxes between forest and the atmosphere, for the interpretation of remote sensing data and for an appropriate parameterization of biomes in land surface models (Jin and Liang 2006).

For almost two decades, several studies have focused on estimating specified emissivity values for different land covers and plant functional types (da Luz and Crowley 2007; Jin and Liang 2006; Valor and Caselles 1996). However, there is no consensus on how to measure emissivity accurately because emissivity of forested surfaces may vary with surface properties such as tree species composition, plant growth stage, surface roughness, leaf area index and water content (Zhou et al. 2008). Aside from that, the emissivity of a forest canopy as a whole differs from that of individual leaves. This is also true for monocultures, since the canopy emissivity is defined by a composition of different surfaces such as the ones of leaves, stems, understory plants and soil and it is also affected by the "cavity effect" (Jin and Liang 2006; Fuchs and Tanner 1966). For the direct estimation of broadband emissivity in the 8-13 µm wavelength band ($\varepsilon_{8\text{-}13\mu m}$) of individual leaves, Fuchs and Tanner (1966) used infrared (IR)-thermometer and 0.08 mm iron-constantan thermocouples inserted into leaves of tobacco and snap bean to measure their leaf surface temperature. They obtained $\varepsilon_{8\text{-}13\mu m}$ values of 0.971±0.002 and 0.957±0.005, respectively. For dense canopies of tall sudangrass and alfalfa, Fuchs and Tanner (1966) identified canopy emissivities of 0.976 and 0.977, respectively. A similar, but more advanced approach in terms of reproducibility, was made by Idso et al. (1969), who found $\varepsilon_{8\text{-}13\mu m}$ values between 0.969 and 0.977 for different forest species (Table 1). Leaf emissivity values measured in forests and horticulture (Chen 2015; Lopez et al. 2012; Rahkonen and Jokela 2003; Arp and Phinney 1980) are summarized in Table A.1 of the Appendix.

The estimation of ε by remote sensing is more complicated, since it additionally requires information on the surface temperature at the particular moment of the satellite or airborne measurement. Considering this, the remote sensing study by Valor and Caselles (1996) used indirect estimations of emissivity. They estimated the emissivity of the spectral region between 10.5 to 12.5 µm using satellite measurements of infrared radiation and normalized difference vegetation index (NDVI). Da Luz and Crowley (2007) estimated spectral emissivity of forest leaves, ε_λ, with spectral measurements. However, their approach was ground based - under laboratory conditions and in the field. In their study, surface temperature was approximated indirectly through an iterative method also used in Horton et al. (1998). Da Luz and Crowley (2007) showed that the ε_λ of forest tree species varies considerably in the spectral region of 8 to 13 µm: for American beech (*Fagus grandifolia*) from 0.94 to 0.97 and for red maple (*Acer rubrum*) from 0.942 to 0.973. To evaluate

Table 1. Leaf emissivities (ε ± s.d.) of different forest species

Species	ε	References
Acer rubrum	0.942 - 0.973	Da Luz & Crowley (2007)
Catalpa speciosa	0.938 - 0.973	Da Luz & Crowley (2007)
Cornus florida	0.962 - 0.985	Da Luz & Crowley (2007)
Fagus grandifolia	0.940 - 0.970	Da Luz & Crowley (2007)
Hedera helix var. Algerian	0.969 ± 0.005	Idso et al. (1969)
Ligustrum vulgare cv.Japanese	0.964 ± 0.003	Idso et al. (1969)
Liriodendron tulipifera	0.948 - 0.973	Da Luz & Crowley (2007)
Morus alba	0.976 ± 0.008	Idso et al. (1969)
Populus fremontii	0.977 ± 0.004	Idso et al. (1969)
Prunus serotina	0.945 - 0.967	Da Luz & Crowley (2007)

the effects of ε variability on climate modelling results, Jin and Liang (2006) converted the spectral emissivities, ε_{λ}, obtained from the remote sensing platform MODIS into the broadband emissivity, $\varepsilon_{8\text{-}13\mu m}$. They investigated the effect of measured vs. fixed emissivity values onto the climate by using the Community Land Model, CLM2. The main focus of those sensitivity studies was the comparison of radiation, sensible and latent energy fluxes under following assumptions: 1) the default ε value of 0.96 for bare soil and 0.97 for vegetation and 2) under an estimated value of 0.9 for bare soil, keeping 0.97 for vegetation-covered regions. The results of the global simulations show surface temperature changes of ±1 °C (January 1998) for the offline CLM simulation and up to 1.5 °C temperature decrease for the coupled CAM2-CLM2 simulation. Furthermore, changes of the sensible heat flux (new value minus control run) were -1 Wm^{-2} to +5 Wm^{-2}. Due to the fact that the highest sensitivity to ε values was identified for desert areas, a separate run was performed for Tucson, Arizona, for the year 1993. The results showed changes of daily surface temperatures up to 10 °C and changes of diurnal sensible and latent heat fluxes up to 50 Wm^{-2}, whereas the changes in sensible heat were always positive (Jin and Liang 2006).

These findings show that the poorly constrained value of emissivity substantially contributes to uncertainties in land surface models and thus to a quantification of climate change signals. Consequently, it is necessary to estimate the emissivity as accurate as possible and to cover many different land surfaces and plant species.

Thus, our goals are (1) to measure the broadband emissivities $\varepsilon_{8\text{-}14\ \mu m}$ of five different broadleaf tree species by using a direct approach similar to that of Fuchs and Tanner (1966), i.e. applying infrared-pyrometer and thermocouples onto leaf surfaces, and (2) to integrate the measured emissivity into a modeling framework (MixFor-SVAT) and investigate the sensitivity of modeled variables (outgoing longwave radiation, net radiative balance, latent and sensible heat fluxes, canopy temperature and net ecosystem exchange) to changes in emissivity.

MATERIAL AND METHODS

Study site

The Hainich tower site in Central Germany serves as reference site for this study. It is located within the southern part of the 'Hainich National Park' (51°04'46"N, 10°27'08"E, 440 m a.s.l.) in suboceanic/subcontinental climate (Knohl et al. 2003). At the Hainich flux tower,

measurements of carbon dioxide, water vapor and energy fluxes between the forest and the atmosphere as well as microclimate in the forest are made. The flux tower is placed in an old unmanaged mixed beech forest with a highly heterogeneous age class distribution ranging from 0 to 250 years and a maximum height varying between 30 and 35 m. The forest is dominated by European beech (*Fagus sylvatica*) with 65 %, codominated by the secondary tree species European ash (*Fraxinus excelsius*) with 25 %, followed by maple (*Acer pseudoplatanus* and *A. platanoides*) with 7 %. Several other deciduous and coniferous species are interspersed (Anthoni et al. 2004). The maximum leaf area index is 5.0 m^2 m^{-2} (Knohl et al. 2003). The Hainich tower site (DE-Hai) is apart of the European Integrated Carbon Observation network (ICOS, https://www.icos-ri.eu/) and the global eddy covariance station network FLUXNET (http://fluxnet.fluxdata.org/).

Instrumentation

For the direct estimations of $\varepsilon_{8\text{-}14\,\mu m}$ of the chosen tree species, we applied a direct method similar to that of Fuchs and Tanner (1966). The surface temperature of leaves was measured simultaneously by means of digital infrared pyrometers (IN510-N, Omega Engineering Inc., Deckenpfronn, Germany) and thermocouples inserted under the skin of the leaves. The IN510-N had a default emission factor of $\varepsilon_{IR} = 0.95$, a 2:1 field of view and a spectral range of 8 µm to 14 µm. We used two types of thermocouples; type K (NiCr-Ni, DIN class 1, Ø: 0.08 mm, TC Direct, Mönchengladbach, Germany) and type T (Cu-CuNi, Ø: 0.2 mm, TC Direct, Mönchengladbach, Germany). Temperatures were continuously logged using two eight–channel RedLab USB TC measuring units (Meilhaus Electronic GmbH, Alling, Germany). For the calibration of the thermocouples, a reference thermo-meter (Hg thermometer, 0.01 °C resolution, Karl Schneider & Sohn oHG, Wertheim, Germany) was used. The ambient conditions, air temperature and air humidity, were measured by a thermo-hygrometer (Hygroclip with ROTRONIC HYGROMER® IN-1 and PT100 1/3 DIN Klasse B, Rotronic, Ettlingen, Germany) with an accuracy of ±0.8 %rh and ±0.2 K. For data recording, a data logger (CR 1000, Campbell Scientific Ltd., Logan, UT, USA) was used. Thermocouple measurements were performed every second and averaged over the period of one minute, whereas pyrometer measurements happened at a minutely base. The readings of the reference thermometer were done manually with a frequency of 20 minutes.

Calibrations

Thermocouples: We carried out calibration of the thermocouples in distilled water by means of a close-system water bath. The insulated container was surrounded by a heating film and contained a magnetic stirrer. The thermocouples were calibrated against a reference mercury thermometer within the range of +7 °C and +43 °C. To perform the calibration at low temperatures, several ice cubes were put into the water. Then the water with ice warmed up at room temperature. For temperatures higher than room's temperature, we heated up the water by means of the heating film. After that it continuously cooled down itself at room temperature. We repeatedly performed these calibration runs. Based on the calibration data, we calculated a linear calibration function for each sensor respectively. After the calibration, the thermocouples do not differ significantly under α=0.05.

Digital infrared-pyrometer: To obtain the absolute calibration, we took one random pyrometer to calibrate it against the calibration source IRS-350 (Voltcraft®, Conrad Electronics, Wernberg-Köblitz, Germany). This reference pyrometer was then used for the cross-calibration of the other four pyrometers deployed during the experiment. We carried out the cross-calibration in a climate chamber by using an open-system water bath filled with distilled water ($\varepsilon = 0.96$ at 20 °C according to Wolfe and Zissis 1978). The chamber was repeatedly heated up and cooled down within the range of +8 °C to +30 °C. Using these results, we calculated a linear calibration function for each sensor, which resulted in an absolute error range of ±0.4 °C.

Measurements

For the quantification of the species specific leaf emissivities, we chose *Populus simonii*

and *Populus candicans* additionally to the dominant tree species of the Hainich site for the experimental setup.

The experimental study was carried out under stable climatic conditions in a climate chamber with temperature thresholds of +8 °C and +32 °C reflecting the range of temperatures at the Hainich site during the growing season. The experiments were performed for each of the chosen tree species separately. We put a minimum of 3 young trees of one species into the chamber. The surface temperature of a leaf was measured with a digital infrared pyrometer and two thermocouples: type K and type T. In case of the populous species, we also measured both, the adaxial and abaxial sides, of the leaves. The pyrometers were placed vertically in a distance of 4 cm above the leaf, whereas both thermocouples were directly affixed on the leaf surface right next to each other. Ambient air temperature and air humidity were recorded. We performed the experiments at absolute darkness, in order to avoid disturbance by short-wave radiation, for several days in a row; meanwhile the chamber temperature was continuously heated up and down within the range of 10 °C to 30 °C. The heating process was carried out in 5° C steps (5 hours) with 7 hours stabilising breaks in between. The broadband emissivities, $\varepsilon_{8\text{-}14\mu m}$, of each leaf (from hereon called emissivity) were then calculated from the comparison of directly measured and radiative leaf temperatures based on the Stefan-Boltzmann law (eq. (1)).

$$\varepsilon_{leaf} = \frac{Tsur_{IR}^4 \times \varepsilon_{IR}}{Tsur_{Tc}^4}$$

where:
$Tsur_{IR}$ is surface temperature measured with IR-pyrometer (8-14 µm spectral range),
$Tsur_{TC}$ is surface temperature measured with thermocouples,
ε_{IR} is default emission factor (s. Material and Methods).

Modelling

We applied the model MixFor-SVAT to determine the effect of emissivity variations on mass and energy exchange at a local scale. The model experiments with MixFor-SVAT were performed with the static broadband emissivity obtained in our present study ($\varepsilon_{8\text{-}14\mu m}$ = 0.958) as well as with the minima (ε = 0.94) and maxima (ε = 0.97) leaf emissivity for forest tree species found in scientific literature (da Luz and Crowley 2007). The model simulations were driven by meteorological data (air temperature, water vapor pressure, wind speed, precipitation rate, and global radiation) of the Hainich tower site for the years 2008 and 2009. MixFor-SVAT calculates the energy and matter fluxes between the atmos-phere and the forest, including downward longwave radiation. As indicator parameters, outgoing longwave radiation (LRup [Wm^{-2}]), net radiative balance (Rn [Wm^{-2}]), latent (LE [Wm^{-2}]) and sensible (H [Wm^{-2}]) heat fluxes, canopy temperature (Tc [°C]), net ecosystem exchange (NEE [$\mu molCO_2 m^{-2} s^{-1}$]) and the physical storage term of soil heat flux and canopy storage (PS [Wm^{-2}]) were selected.

MixFor-SVAT is a one-dimensional process based soil-vegetation-atmosphere transfer (SVAT) model, enabling the description of radiation transfer, plant transpiration and water uptake, as well as the turbulent exchange of carbon dioxide, sensible and latent heat between mono- and multi-species forest stands and the atmospheric surface layer (Olchev et al. 2008; Falge et al. 2005; Olchev et al. 2002). The plant canopy is assumed to be horizontally uniform and vertically structured. For the simulation of exchange processes, MixFor-SVAT uses a detailed description of biophysical properties of the different tree species such as the mean tree height, crown shape, leaf area density distribution, tree diameter at breast height, leaf stomatal conductance, parameters describing the photosynthesis and respiration including the kinetic properties of Rubisco, the dependence of electron transport on incoming photosynthetically active radiation, rate of dark respiration and others. The model is modularized and describes the following processes: radiative transfer (shortwave and longwave radiation), turbulent exchange of momentum, sensible heat, H_2O and CO_2 within and above a forest canopy, soil heat and water dynamics, plant water use, precipitation interception and net- and gross ecosystem production. The simulation procedure of the radiative transfer in a plant canopy takes into account

the different optical and structural properties of various tree species as well as annual leaf area index changes regulated by tree phenology (e.g. date of emergence of leaves, the onset of leaf fall, etc.). The broadband emissivity in the model is assumed to be constant for all vegetation types (ε = 0.96). The longwave radiation absorption is calculated according to Kirchhoff's law (α = ε). The calculation of the radiation energy, water and CO_2 fluxes for Hainich forest were provided with a time step of 30 minutes. Maximum tree height in the forest canopy was assumed to be 31m and the maximum LAI of the forest canopy as 6.06 m^2 m^{-2}. Gaps in the NEE, LE and H measurement records were filled using an approach based on a process-based MixFor-SVAT model (Olchev et al. 2015). MixFor-SVAT well simulated the observed surface fluxes, e.g. net radiation (R^2 = 0.96, slope = 0.996, p < 0.001).

RESULTS

Quantification of leaf emissivities for different tree species

Direct leaf surface temperature measurements using the T and K type thermocouples showed very good agreement with a temperature difference of less than 0.001 °C indicating no systematic differences between both thermocouples types. Leaf temperature measured with the infrared pyrometer was strongly linearly correlated to the direct measurements using thermocouples (p < 0.001 for all sensors). The measured broadband ε of the five investigated species varied only slightly (Table 2, Table A.1). The highest leaf emissivity is 0.960±0.003 for *Fagus sylvatica* and the lowest 0.954±0.003 for *Populus simonii*. The mean calculated emissivity of all species is 0.958 with a standard deviation of 0.002. According to Dunn's Multiple Comparison Test, there are only significant differences between the emissivites of *Populus simonii* (ε = 0.954) and the non-populous species. No temperature dependencies of the leaf emissivity could be detected within the investigated range of +8 to +32 °C: $\varepsilon_{8\text{-}14\mu m}$ varied by ±0.0026.

Effects of a change in emissivity on the energy and matter fluxes at a local scale

Three MixFor-SVAT simulations with a static broadband ε of 0.94, 0.958 (our mean value) and 0.97, respectively, were performed for the Hainich tower site for the period of 2008 and 2009. As seen in figure 1, mean annual values of LRup increase with an increase in broadband emissivity, whereas the mean annual values of Rn, Tc, LE, H and NEE decrease. The same trend can be observed for both years. However, the results indicate that the responses of the fluxes are non-linear.

While the differences between the respective values of both years seem to be similar for most parameters, the decrease of LE and Rn in 2009 is slightly stronger than in 2008. One possible reason for this is the higher amount of incoming shortwave radiation in 2008 which compensates the longwave emission losses - the shortwave radiation balance in 2008 was in average 8 Wm^{-2} higher than in 2009.

The comparison of modelled and measured

Table 2. Leaf emissivity (ε) of five different broadleaf species

Tree species	ε
Acer pseudoplatanus	0.959 ± 0.003 a
Fagus sylvatica	0.960 ± 0.003 a
Fraxinus excelsior	0.958 ± 0.002 a
Populus candicans	0.957 ± 0.003 ab
Populus simonii	0.954 ± 0.003 b
total	0.958 ± 0.002

**Emissivities are displayed as mean ± s.d.. Groups sharing the same letter are not significantly different (p < 0.05, Dunn's Multiple Comparison Test).*

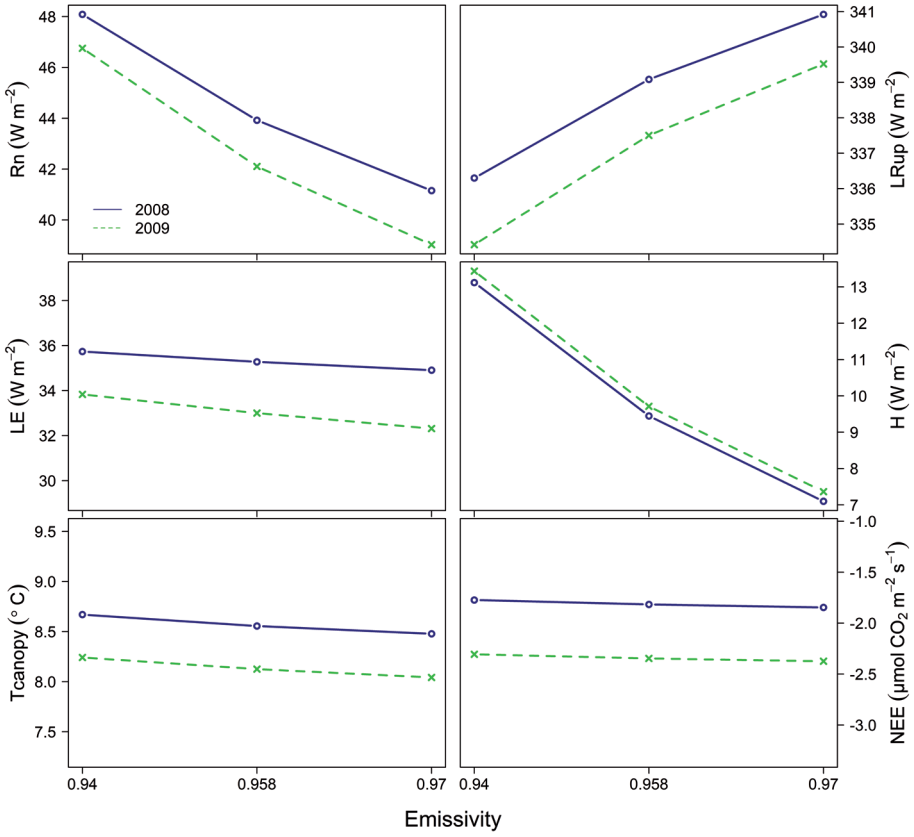

Fig.1. Dependency of energy and matter fluxes on changes in broadband emissivity. Mean annual values of the net radiative balance (Rn), outgoing longwave radiation (LRup), canopy temperature (Tcanopy), latent heat (LE), sensible heat (H) fluxes and net ecosystem exchange (NEE) calculated according to MixFor-SVAT model runs with ε = 0.94, ε = 0.958 (our mean value) and ε = 0.97 for the years 2008 and 2009

data (Table 3) shows that in the case of LRup, Rn and NEE, measured data are higher than the modelled ones for 2008 and 2009. In 2008, measured H data are higher than modelled ones, whereas they are similar for 2009. On the contrary, for LE the measured data for 2008 are below the modelled data and for 2009 they are similar. The measured and the modelled canopy temperatures agree well for both years.

The relative changes of fluxes are shown

Table 3. Comparison of measured and MixFor-SVAT-modelled energy and matter fluxes

	year	Rn [Wm^{-2}]	LE [Wm^{-2}]	H [Wm^{-2}]	NEE [µmol CO_2 m^{-2}s^{-1}]	LRup [Wm^{-2}]	Tc [°C]
MixFor-SVAT	2008	48.09 - 41.15	35.75 - 34.1	13.12 - 7.1	-1.77 – -1.85	336.3 - 340.92	8.7 - 8.48
measured	2008	60.35	31.6	20.47	-1.66	355.92	8.65
MixFor-SVAT	2009	46.75 - 39.03	33.83 - 32.31	13.44 - 7.36	-2.31 – -2.37	334.42 - 339.52	8.2 - 8.04
measured	2009	60.85	33.79	13.18	-1.95	355.58	8.31

**MixFor-SVAT-modelled data are given as ranges due to simulations with emissivities of ε= 0.94, ε= 0.958 and ε= 0.97*

in Fig. 2. The flux values obtained with the mean emissivity measured in the present study (0.958) are taken as reference. The relative changes are calculated as
The relative changes were estimated for

$$\Delta Flux = \frac{(Flux - Flux_{Ref})}{Flux_{Ref}} \times 100\% \quad (2)$$

above calculated indicators and additionally for PS.

For 2008, the largest relative difference is found for the sensible heat flux. A decrease of 0.018 in emissivity (ε = 0.94) results in an increase of H, indicating a sensitivity of 20.7 % per 1 % of ε change. The change from 0.958 to 0.97 (0.012) causes a decrease of H, denoting a relative sensitivity of -19.9 % per 1 % of ε change. All other fluxes show less sensitivity to ε. For Rn, a decrease of 0.018 in emissivity produces an expected increase of radiative balance, implying a relative sensitivity of 5.0 % per 1 % of ε change. An increase in emissivity to 0.97 leads to a decrease in Rn, showing a relative sensitivity of -5.0 % per 1 % of ε change. A decrease of ε to 0.94 generates a relative PS decrease, indicating a sensitivity of -2.4 % per 1 % of ε change. The change from 0.958 to 0.97 leads to an increase of PS, denoting a relative sensitivity of 4.6 % per 1 % of ε change. The responses of the other fluxes show a relative sensitivity below 1.5 %.

In 2009, the changes of fluxes are similar. Here, the largest relative difference is detected for sensible heat, caused by a decrease in emissivity to ε = 0.94, implying a sensitivity of 20.4 % per 1 % of ε change. The emissivity increase of 0.012 generates an H decrease, implying a relative sensitivity of -19.3 % per 1 % of ε change. In op-

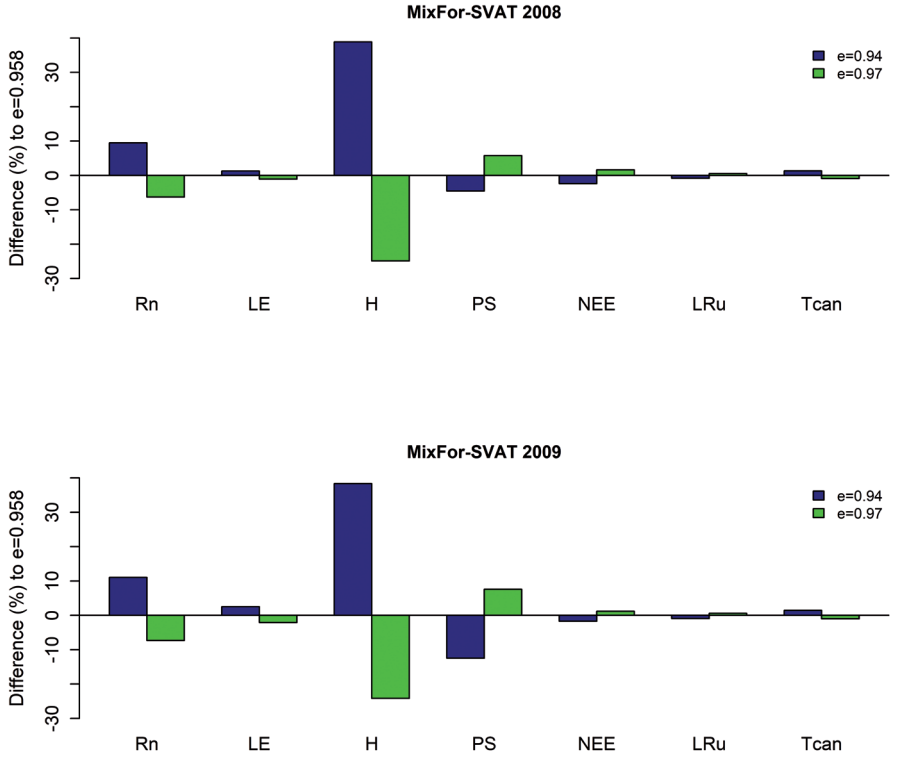

Fig.2. Effects of ε changes on the radiative, sensible and latent energy fluxes of Hainich forest. Relative changes of energy fluxes Rn, LE, H, LRup, PS as well as of NEE and Tc to changes in emissivity based on MixFor-SVAT model simulations with emissivities of ε = 0.94, ε = 0.958 and ε = 0.97 for the years 2008 and 2009. The flux values calculated with ε=0.958 are taken as the reference. The relative changes are based on mean annual fluxes and calculated according to equation (2)

posite to 2008, Rn and PS show a similar relative change to emissivity changes in 2009. A decrease of ε from 0.958 to 0.94 leads to a relative PS decrease, indicating a sensitivity of -6.6 % per 1 % of ε change. The change from 0.958 to 0.97 causes an increase of PS, denoting a relative sensitivity of 6.0 % per 1 % of ε change. For Rn, a decrease of 0.018 in emissivity produces a relative increase, implying a relative sensitivity of 5.9 % per 1% of ε change. An increase in emissivity to 0.97 leads to an Rn decrease, standing for a sensitivity of -5.8 % per 1 % of ε change. All other fluxes show less response to ε; below 2.0 % relative sensitivity. These results indicate that the responses of fluxes to the changes of emissivity are non-linear.

DISCUSSION

So far, only a few studies have been carried out to directly determine broadband emissivities of leaves for forest species resulting in values ranging from 0.94 to 0.97. The leaf emissivities calculated in this study are also within this range (0.958±0.002). No statistically significant differences among species were found except for *Populus simonii* (Table 2). The question is whether this variability has any considerable effect on energy and matter fluxes, and thus, on local and regional climate in forests as was described by Jin and Liang (2006) by means of the coupled atmosphere land surface model CAM2-CLM2 for the emissivity of bare soil (0.9 instead of 0.96). The MixFor-SVAT model applied in this study produced reliable results, well agreeing with the measurements. With increasing ε, the value of LRup increases since more longwave radiation is emitted with higher ε according to the Stefan-Boltzmann law. When more longwave radiation is lost from the surface, Rn is decreasing as all other fluxes of the radiation budget (incoming shortwave radiation, reflected shortwave radiation and incoming longwave radiation from the atmosphere) are not affected – however, a higher proportion of the incoming longwave radiation will be absorbed (ε = α, Kirchhoff's law). At the same time, the surface temperature will decrease leading to a lower sensible heat fluxes as well as lower latent heat fluxes. With the decreasing surface temperature, also respiration and photosynthesis are decreasing. As respiration decreases faster than photosynthesis, the net CO_2 uptake is increasing (more negative net ecosystem exchange). The differences in relative changes (Fig. 2) are a consequence of the absolute change and the magnitude of the annual mean fluxes. The annual mean fluxes of H are low due to the negative values at night and wintertime and thus resulting in the largest relative changes. The model, therefore, shows plausible ecosystem responses and can be used for the experiments. The effect of emissivity changes on fluxes found in the present study is considerable, although the absolute values of daily mean changes of fluxes are slightly lower than in Jin and Liang (2006) for desert areas - up to 50 Wm^{-2}. The differences between ε = 0.94 and 0.97 results in changes of daily fluxes up to 16.8 Wm^{-2} for Rn, 13.3 Wm^{-2} for LE, 19.7 Wm^{-2} for H and -10.9 Wm^{-2} for LRup. The responses of the system are, thus, quite comparable despite of the different models used for the studies. The lower differences in our study could be explained by the smaller change of ε. The changes of daily Tc are, however, comparable with Jin and Liang (2006) - up to 1.1 °C. The response of daily NEE to the ε variability is considerable - up to 0.5 µmol C $m^{-2}s^{-1}$ or 5 kg per day and ha. Moreover, the short time responses at 30 min scales (not shown by Jin and Liang) are even stronger - up to -82.1 Wm^{-2} for Rn, 113.8 Wm^{-2} for LE and 178.3 Wm^{-2} for H. The hourly variability of LRup is of similar order as the daily one, up to -13.9 Wm^{-2}. The differences in Tc and NEE are also very large: between -2 and 0.5 °C and up to 5.5 µmol C $m^{-2}s^{-1}$ (2.4 kg C $ha^{-1}h^{-1}$). Thus, the variability of ε should be taken into account in climate change studies. Hence, not only the soil emissivity but also the exact values of leaf emissivities for forest species are crucial information for the better estimation of the contribution of forest ecosystems to climate processes and to climate change. The simple approximation of ε is difficult since the dependence of fluxes on ε is non-linear, as demonstrated in this study. Moreover, it should be noted that the responses obtained in this study are the di-

rect, "momentarily" ones, as they do not include feedbacks of the climate system to changes in the underlying surface. It is, therefore, recommended to repeat the simulations with a coupled model as in the study of Jin and Liang (2006).

CONCLUSION

In the present study, we quantified the broadband leaf emissivities $\varepsilon_{8\text{-}14\mu m}$ of the forest species' *Acer pseudoplatanus, Fagus sylvatica, Fraxinus excelsior, Populus simonii* and *Populus candicans*. The results showed that the interspecies variability of leaf emissivities is very low – the obtained mean value across all species is $\varepsilon = 0.958$ (± 0.002). A statistically significant difference was found for Populus simonii. Our results demonstrate that emissivity changes have significant impacts on modelled energy and matter fluxes. Energy fluxes and surface temperature increased with a decrease in emissivity, whereas NEE decreased, due to respiration losses resulting from the temperature increase. The strongest effect was identified for the sensible heat flux with a sensitivity of 20.7 % per 1 % of ε change. Overall, the findings indicate that the dependency of energy and matter fluxes on ε changes are non-linear.

Revealing directly measured leaf emissivities of the five forest species', this study provides important basics for the correct application of variable leaf emissivity in energy budget modelling and thus to a better estimation of the contribution of forest ecosystems to the climate. Additionally, the application of the obtained emissivity values in MixFor-SVAT showed, that there are strong effects of emissivity changes on radiative, sensible and latent energy fluxes. Therefore, it is recommended to consider the variability of ε in climate change studies. Further research should be implemented to extend the knowledge on the forest climate interaction by obtaining information on forest species specific leaf emissivities.

ACKNOWLEDGEMENTS

This study was financially supported by the Deutsche Forschungsgemeinschaft (DFG) (KN 582/6-1) and the Deutsche Bundesstiftung Umwelt (DBU) (20014/352). We are indebted to Andreas Teichmann, Sara Nicke-Mühlfeit, Frank Tiedemann, Dietmar Fellert and Stefan Schütz (University of Göttingen). Measurements at the Hainich tower site were supported by the German Federal Ministry of Education and Research (BMBF) as part of the European Integrated Carbon Observation System (ICOS) and by the Deutsche Forschungsgemeinschaft (INST 186/1118-1 FUGG).

REFERENCES

Alkama R. and Cescatti A. (2016). Biophysical climate impacts of recent changes in global forest cover. Science, 351, pp. 600-604. https://doi.org/10.1126/science.aac8083.

Anthoni P.M., Knohl A., Rebmann C., Freibauer A., Mund M., Ziegler W., Kolle O. and Schulze E.D. (2004). Forest and agricultural land-use-dependent CO_2 exchange in Thuringia, Germany. Global Change Biology, 10, pp. 2005-2019. doi: 10.1111/j.1365-2486.2004.00863.x.

Bonan G.B. (2008). Forests and Climate Change: Forcings, Feedbacks, and the Climate Benefits of Forests. Science, 320 (5882), pp. 1444-1449. doi: 10.1126/science.1155121.

Chen C. (2015). Determining the leaf emissivity of three crops by infrared thermometry. Sensors, 15(5), pp. 11387-11401. doi:10.3390/s150511387.

Da Luz B.R. and Crowley J.K. (2007). Spectral reflectance and emissivity features of broad leaf plants: Prospects for remote sensing in the thermal infrared (8.0 –14.0 µm). Remote Sensing of Environment, 109(4), pp. 393-405.

Falge E., Reth S., Brüggemann N, Butterbach-Bahl K., Goldberg V., Oltchev A., Schaaf S., Spindler G., Stiller B., Queck R., Köstner B. and Bernhofer C. (2005). Comparison of surface energy exchange models with eddy flux data in forest and grassland ecosystems of Germany. Ecological Modelling, 188, pp. 174-216.

Fuchs M. and Tanner C.B. (1966). Infrared thermometry of vegetation. Agronomy Journal, 58, pp. 597-601.

Horton K.A., Johnson J.R. and Lucey P.G. (1998). Infrared measurements of pristine and disturbed soils 2. Environmental effects and field data reduction. Remote Sensing of Environment, 64(1), pp. 47-52.

Idso S.B., Jackson R.D., Ehrler W.L. and Mitchell S.T. (1969). A Method for Determination of Infrared Emittance of Leaves. Ecology, 50, pp. 899-902. doi:10.2307/1933705.

Jin, M. and Liang S. (2006). An improved land surface emissivity parameter for land surface models using global remote sensing observations. Journal of Climate, 19(12), pp. 2867-2881.

Knohl A., Schulze E.D., Kolle O. and Buchmann N. (2003). Large carbon uptake by an unmanaged 250-year-old deciduous forest in Central Germany. Agricultural and Forest Meteorology, 118, pp. 151-167.

Lopez A., Molina-Aiz F.D., Valera D.L. and Peña A. (2012). Determining the emissivity of the leaves of nine horticultural crops by means of infrared thermography. Scientia Horticulturae, 137, pp. 49-58.

Oltchev A., Cermak J., Nadezhdina N., Tatarinov F., Tishenko A., Ibrom A. and Gravenhorst G. (2002). Transpiration of a mixed forest stand: field measurements and simulation using SVAT models. Boreal Environmental Research, 7(4), pp. 389-397.

Olchev A., Ibrom A., Ross T., Falk U., Rakkibu G., Radler K., Grote S., Kreilein H. and Gravenhorst G. (2008). A modelling approach for simulation of water and carbon dioxide exchange between multi species tropical rain forest and the atmosphere. Ecological Modelling, 212, 122-130.

Olchev A., Ibrom A., Panferov O., Gushchina D., Kreilein H., Popov V., Propastin P., June T., Rauf A., Gravenhorst G., Knohl A. (2015). Response of CO_2 and H_2O fluxes in a mountainous tropical rainforest in equatorial Indonesia to El Niño events. Biogeosciences, 12, pp. 6655-6667.

Pielke R.A., Pitman A., Niyogi D., Mahmood R., McAlpine C., Hossain F., Goldewijk K.K., Nair U., Betts R., Fall S., Reichstein M., Kabat P., Noblet N. (2011). Land use/land cover changes and climate: modeling analysis and observational evidence. WIREs Climate Change, 2, pp. 828-850. doi:10.1002/wcc.144.

Rahkonen J. and Jokela H. (2003). Infrared radiometry for measuring plant leaf temperature during thermal weed control treatment. Biosystems Engineering, 86, pp. 257-266.

Sabajo C.R., le Maire G., June T., Meijide A., Roupsard O. and Knohl A. (2017). Expansion of oil palm and other cash crops causes an increase of the land surface temperature in the Jambi province in Indonesia. Biogeosciences, 14, pp. 4619-4635. doi.org/10.5194/bg-14-4619-2017.

Snyder P.K., Delire C. and Foley J. (2004). Evaluating the influence of different vegetation biomes on the global climate. Climate Dynamics, 23, pp. 279-302.

Valor E. and Caselles V. (1996). Mapping Land Surface Emissivity from NDVI: Application to European, African, and South American Areas. Remote Sensing of Environment, 57, pp. 167-184.

Wolfe W.L. and Zissis G.J. (1978). The Infrared Handbook. Washington DC, Environmental Research Institute of Michigan.

Zhou L., Dickinson R., Dirmeyer P., Chen, H., Dai D. and Tian Y. (2008). Asymmetric response of maximum and minimum temperatures to soil emissivity change over the Northern African Sahel in a GCM. Geophysical Research Letters, 35, L05402. doi:10.1029/2007GL032953.

Received on Dec 31st 2018 Accepted on May 17th 2019

Appendix

Table A.1. Leaf emissivities (ε ± s.d.) of different plant species

species	ε	s.d.	reference
Hedera helix var. *Algerian*	0.969	0.005	Idso et al. (1969)
Acer pseudoplatanus	0.959	0.003	Tiralla et al. (2019)*
Acer rubrum	0.942 - 0.973		Da Luz & Crowley (2007)
Aralia seboldi	0.968	0.006	Idso et al. (1969)
Brassicca rapa L.	0.980	0.010	Rahkonen & Jakela (2003)
Capsicum annuum	0.978	0.008	Lopez et al. (2012)
Capsicum frutescens cv. Long Green	0.979	0.005	Idso et al. (1969)
Carica papaya	0.988	0.002	Idso et al. (1969)
Catalpa speciosa	0.938 - 0.973		Da Luz & Crowley (2007)
Cereus bridges II	0.973	0.001	Idso et al. (1969)
Citrullus lanatus Thunb.	0.981	0.009	Lopez et al. (2012)
Citrus aurantium	0.972	0.008	Idso et al. (1969)
Citrus jambhiri	0.975	0.008	Idso et al. (1969)

Cocculus laurifolius	0.973	0.003	Idso et al. (1969)
Cordyline terminalis	0.967	0.003	Idso et al. (1969)
Cornus florida	0.962 - 0.985		Da Luz & Crowley (2007)
Cucumis melo L.	0.978	0.006	Lopez et al. (2012)
Cucumis sativus L.	0.983	0.008	Lopez et al. (2012)
Cucurbita pepo L.	0.985	0.007	Lopez et al. (2012)
Fagus grandifolia	0.940 - 0.970		Da Luz & Crowley (2007)
Fagus sylvatica	0.960	0.003	Tiralla et al. (2019)*
Fraxinus excelsior	0.958	0.002	Tiralla et al. (2019)*
Gossypium barbadense cv. Pima S-4	0.979	0.008	Idso et al. (1969)
Gossypium hirsutum cv. Deltapine 16	0.964	0.007	Idso et al. (1969)
Gossypium hirsutum cv. Hopicala	0.967	0.011	Idso et al. (1969)
Hedera helix var. Algerian	0.969	0.005	Idso et al. (1969)
Ligustrum vulgare cv. Japanese	0.964	0.003	Idso et al. (1969)
Liriodendron tulipifera	0.948 - 0.973		Da Luz & Crowley (2007)
Lophocereus schottii	0.973	0.004	Idso et al. (1969)
Lycopersicon esculentum cv. Pearson Improved	0.982	0.004	Idso et al. (1969)
Lycopersicum esculentum	0.980	0.010	Lopez et al. (2012)
Morus alba	0.976	0.008	Idso et al. (1969)
Nicotiana tabacum	0.971	0.002	Fuchs & Tanner (1966)
Nicotiana tabacum	0.972	0.006	Idso et al. (1969)
Nymphaea odorata	0.957	0.006	Idso et al. (1969)
Opuntia basilaris	0.978	0.002	Idso et al. (1969)
Opuntia engelmannii	0.961	0.004	Idso et al. (1969)
Opuntia ficus indica	0.957	0.002	Idso et al. (1969)
Opuntia linguiformis	0.965	0.001	Idso et al. (1969)
Opuntia orbiculate	0.710	0.006	Idso et al. (1969)
Opuntia rufida	0.977	0.002	Idso et al. (1969)

Opuntia santa rita	0.969	0.002	Idso et al. (1969)
Pachira macrocarpa	0.985	0.005	Chen (2015)
Paphiopedilum var. Michael Koopowitz	0.981	0.007	Chen (2015)
Pelargonium domesticum var. Martha Washington	0.992	0.002	Idso et al. (1969)
Persea drymifolia	0.979	0.009	Idso et al. (1969)
Phalaenopsis var. Taisuco Anna (mature leaves)	0.981	0.010	Chen (2015)
Phalaenopsis var. Taisuco Anna (young leaves)	0.978	0.009	Chen (2015)
Phaseolus coccineus	0.983	0.005	Lopez et al. (2012)
Phaseolus vulgaris cv. Bountiful (center leaflet)	0.938	0.008	Idso et al. (1969)
Phaseolus vulgaris cv. Bountiful (lateral leaflet)	0.964	0.005	Idso et al. (1969)
Phaseolus vulgaris L.	0.983	0.006	Lopez et al. (2012)
Phaseolus vulgaris L.	0.957	0.005	Fuchs & Tanner (1966)
Philodendron selloum	0.990	0.010	Idso et al. (1969)
Populus candicans	0.957	0.003	Tiralla et al. (2019)*
Populus fremontii	0.977	0.004	Idso et al. (1969)
Populus simonii	0.954	0.003	Tiralla et al. (2019)*
Prunus serotina	0.945 - 0.967		Da Luz & Crowley (2007)
Rosa	0.993	0.006	Idso et al. (1969)
Saccharum officinarum	0.995	0.004	Idso et al. (1969)
Solanum melongena L.	0.973	0.007	Lopez et al. (2012)
Sonchus arvensis	0.980	0.010	Rahkonen & Jakela (2003)
Zea mays cv. Mexican June	0.944	0.004	Idso et al. (1969)

** this study*

Mikhail A. Nikitin[1], Ekaterina V. Tatarinovich[1,2], Inna A. Rozinkina[1] and Andrei E. Nikitin[1]
[1] Hydrometeorological Research Center of Russian Federation, Moscow, Russia
[2] Faculty of Geography, Moscow State University, Moscow, Russia
*** Corresponding author:** arhin@yandex.ru

EFFECTS OF DEFORESTATION AND AFFORESTATION IN THE CENTRAL PART OF THE EAST EUROPEAN PLAIN ON REGIONAL WEATHER CONDITIONS

ABSTRACT. Forest vegetation can affect the climate and weather patterns in multiple ways. What are the main mechanisms of such influence and how the land-use and vegetation changes may affect the weather and climate conditions in different geographical regions are still not quite clear. In our study, the possible impact of land use and forest cover changes in the central part of the East European plain on regional meteorological conditions was investigated using the regional COSMO model. In our modeling experiments we used two extreme land-use change scenarios imitating total deforestation and afforestation of experimental area located between 55° and 59ºN and 28° and 37°E in the central part of the East European plain. Modeling results conducted for the year 2016 showed that deforestation results in increase of the temperature difference between summer and winter months by up to 0.6ºC and in reduction of the annual precipitation by 35 mm. On the contrary, afforestation leads to decrease of the annual temperature range by 0.3° C and to growth of annual precipitation by 15 mm. Moreover, the deforestation results in higher frequencies of stronger winds and lower number of fog events, while the afforestation leads to opposite effects. Analysis of the Khromov and Gorchinsky indexes of continentality showed that the deforestation of the selected experimental area may lead to increase of the climate continentality in the study region, whereas the afforestation results in milder climate conditions.

KEY WORDS: deforestation, afforestation, COSMO, numerical experiments, air temperature, precipitation, fog frequency

CITATION: Mikhail A. Nikitin, Ekaterina V. Tatarinovich, Inna A. Rozinkina and Andrei E. Nikitin (2019) Effects of deforestation and afforestation in the central part of the East European plain on regional weather conditions. Geography, Environment, Sustainability, Vol.12, No 2, p. 259-272
DOI-10.24057/2071-9388-2019-12

INTRODUCTION

There are numerous factors and multiple pathways that control the interaction of forest vegetation and the atmosphere at various temporal and spatial scales. It is well known that the weather and climatic characteristics (e.g. air temperature, incoming solar radiation, latent and sensible heat fluxes, and precipitation) influence significantly the forest growth and primary production (Whittaker 1975; Woodward 1987). In turn, forests via the various feedback mechanisms (emission and absorption of CO_2, albedo, evapotranspiration, precipitation interception) affect the local, regional, and, to some extent, global weather and climate conditions (Bonan et al. 1992; Brovkin et al. 2009; Bathiany et al. 2010). Any forest disturbances can influence surface albedo, net radiation, sensible and latent heat, and CO_2 fluxes between the land surface and atmosphere, and can substantially affect climate conditions from local to global scales (Kulmala et al. 2014; Seidl et al. 2014; Mamkin et al. 2019). These feedback mechanisms were investigated over the last decades in many experimental and modeling studies (Nobre et al. 1991; Bonan et al. 1992; Carlson and Groot 1997; Pielke et al. 2007; Olchev et al. 2009; Brovkin et al. 2009; Anav et al. 2010; Bathiany et al. 2010; Kulmala et al. 2014; Mamkin et al. 2016, 2019). They showed a large diversity of feedbacks of forest and land use changes on local and regional weather conditions that could not be explained without deep understanding of all available relationships and effects arising between atmospheric and the land surface processes. For such scientific tasks, the mathematical models of different scales and complexity can be a very effective tool. The key factors influencing the accuracy of the model projections are the land surface heterogeneity, lack of necessary experimental data, and multiple simplifications still used in mathematical models in description of the land surface - atmosphere interaction. The main goal of the study is to derive the possible impact of land use and forest cover changes in the central part of the East European plain on regional meteorological conditions using the regional weather forecast COSMO model.

METHODS

General description of the COSMO model

To investigate the impact of deforestation and afforestation processes on regional meteorological conditions we used the non-hydrostatic limited area weather forecast COSMO (the Consortium for Small-Scale Modeling) model. This model is based on the key equations of hydro- and thermodynamic, allowing one to describe adequately air flows in a fully compressible, non-hydrostatic, moist atmosphere. In this assumption, the atmosphere is considered as a multi-component continuum that is composed of dry air, water vapor and water in liquid and solid states. The model is based on basic equations providing the conservation of momentum, mass and energy. These equations are written in form of budget conservation. All equations are formulated for rotated geographical coordinates. A height-based terrain-following coordinate system is also used. The model variables are staggered on an Arakawa-C/Lorenz grid with scalar defined at the centre of a grid and wind velocity components defined on the corresponded box faces (Doms and Baldauf 2018). COSMO includes subgrid-scale parameterizations of different physical processes such as atmospheric turbulence, convection and cloud formation, radiative transfer, energy and water fluxes at ground surface, heat and water exchange in different soil horizons, etc.

The weather forecast COSMO model is accepted by the Central Methodical Committee of the Russian Hydrometeorological Services as the main mesoscale regional short-range atmospheric model (up to three model days) for short-term weather prediction. The operational weather forecasts are produced for the territory of Russia with a grid spacing ranged from 1.1 to 13.2 km (Rivin et al. 2015).

The module TERRA integrated into the COSMO model is used to describe the processes at the land surface - atmosphere interface. It includes the soil module com-

bined with a simplified heat and water transfer schemes, parameterizations of the radiation fluxes at the land surface, and the annual cycles of vegetation parameters. TERRA allows describing the rainfall and snow accumulation, dew and rime formation, evapotranspiration and surface runoff. Besides, the module includes parameterizations of water infiltration, percolation, and capillary movement in different soil layers, as well as water phase transition processes. The ground surface temperature and water content are calculated in the model for eight soil, subsoil and parent rock layers of different thickness down to the depth of 14.58 m. It is assumed that the ground surface is characterized by different morphological properties and can be roughly divided into the following types: ice, stony surface, sand, loamy sand, fertile soil, loam, clay, and peat. Each surface type is characterized by unique assemblage of specific parameters characterizing the soil physical properties, including thermal conductivity, field capacity, minimum infiltration rate, soil porosity, soil albedo, etc.

To derive the possible impact of open water reservoir on regional atmospheric processes a one-dimensional parametric fresh-water lake model, built into the COSMO model (FLAKE, Mironov 2008) is used. To adjust the water temperature and depth of mixed layer close to real values during the modeling experiment, the so-called "cold start" procedure is used. The method uses the following assumptions: no ice on the lake surface, temperature of mixed layer is equal to surface temperature that can be taken from ICON data archive, temperature of bottom layer is assumed to be equal to temperature at maximum water density (3.98°C). The "cold start" procedure is recommended to be used in spring and autumn – after the ice and snow melts, or before freezing over when the lakes have thermal stratification close to neutral. In this case, the model characteristics obtained during the "cold start" procedure would quicker come to better agreement with observational data.

External parameters describing land use and vegetation properties such as vegetation type, fraction of forest cover, root depth, maximum and minimum values of leaf area index and others, are taken from global datasets: GLOBCOVER, GLC2000 and GLCC (Asensio et al. 2018).

Thus, the COSMO model has a reasonable scheme of land surface parameterization, which is characterized by a set of key parameters for different soil and vegetation types (apart of morphometric characteristics such as coastline and surface topography) that allows to describe the possible influence of land surface on regional weather processes.

Strategy and scenarios of modeling experiments

For our numerical experiments we used the COSMO-Ru-NWR (North–West Russia) configuration of the COSMO model with horizontal grid spacing of about 6.6 km. The modeling domain (1848×1452 km) covers the entire northern part of European Russia, the eastern part of Belarus and some parts of Eastern European and Northern European countries. The central part of the modeling domain stretched from 55° to 59°N and from 28° to 37°E was taken as experimental area where the scenarios of the land surface deforestation and afforestation were simulated (Fig. 1). This area is covered with forest, which occupies up to 60.7% of the territory. At the same time, this area is covered with relatively dense network of meteorological stations, which allows analyzing the quality of our numerical experiments.

For modeling experiments, the period from November 1, 2015 at 00:00 UTC to December 31, 2016 (the full year plus two-month spin-up period) was selected to assess the impact of forest cover changes on meteorological conditions. Two-month spin-up period was used to adjust the thermal regime of big number of large (Ladoga and Onega lakes, Rybinsk reservoir) and small freshwater reservoirs that are available within the selected modeling domain.

The meteorological conditions during selected 2016 year were characterized by di-

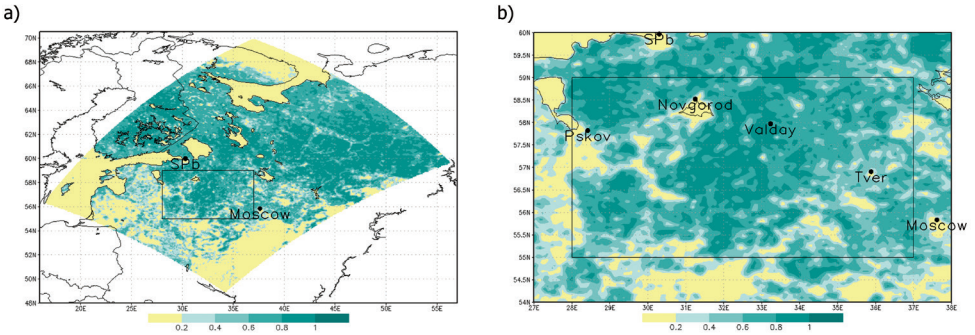

Fig. 1. The forest distribution within the selected modeling domain. The depth of green color indicates the fraction of forest cover (both evergreen and broad-leaved tree species). Black rectangle marks the boundary of experimental area

verse weather conditions and were close to long-term climatic mean values. According to COSMO-Ru-NWR estimations, the mean annual temperature of 2016 for the selected experimental area was about 5.3°C and annual precipitation was close to 848 mm.

The initial and boundary conditions of our modeling experiments with COSMO-Ru-NWR were taken from ICON global model (13 km grid spacing) of the German Meteorological Service (DWD). In the experiments, "spectral nudging" of meteorological fields, enabled in COSMO modeling system, was not used. It allowed us to pay attention to the response of the model to change of ground surface characteristics. The boundary conditions were renewed each three hours. The initial conditions were not renewed, and the model started once for the entire period of simulation. Results of model runs were recorded with 1-hour time step.

The calculations were carried out using the climatic version of the COSMO model with daily update of key land surface and vegetation parameters such as root depth, leaf area index, sea (water reservoir) surface temperature, etc. The special software module for recalculating the current leaf area index (LAI) and root depth of different plant species from specified minimum and maximum values of these parameters depending on the day of the year were used. Three numerical experiments were conducted in our study using the configuration COSMO-Ru-NWR: reference (control) experiment describing the regional weather conditions under present land-use conditions and two experiments imitating the total deforestation and afforestation of the experimental area.

Reference experiment assumes the present distribution of broad leaved and coniferous forest types within the selected experimental area (55° – 59° N, 28° – 37° E). The present forest cover within the experimental area is about 60.7%. The fraction of coniferous forests is 25.5% and deciduous species is 35.2%. LAI is specified in dependence on different forest types. It is assumed that it is varied in winter between 0.2 and 1.2 m^2m^{-2}, and in summer – between 3 and 3.5 m^2m^{-2}, respectively. Root depth is specified for each vegetation types and ranged from 0.3 m to 0.7 m.

Deforestation experiment imitates the total forest clearing at entire experimental area. We assumed that all cleared areas are covered by grassy vegetation. Their LAI in the area reaches maximum values in summer months and do not exceed 2.5 m^2m^{-2}. The root depth of grassy vegetation is assumed to be 0.3 m.

Afforestation experiment assumes complete cessation of agricultural and industrial activity in the region and widespread forest recovery. Taking into account a very slow regeneration rate of coniferous tree species we assume that all areas previously covered with grassy vegetation are completely occupied with deciduous trees. LAI value for each day of the year is

determined as a maximum value from all available LAI values within the modeling domain. The plant root depth is assumed to be the same as in the reference experiment.

Data analysis

To derive the possible effects of forest cover changes on regional weather conditions we analyzed the difference between monthly mean values of the key meteorological parameters predicted for scenarios imitating total deforestation and afforestation and monthly values obtained for reference experiment assuming the present land use and forest structure.

To estimate effects of deforestation and afforestation on regional patterns of wind speed and fog occurrence we analyzed the temporal variability of these parameters for all available meteorological stations situated within the experimental area.

To estimate the climate continentality in our study we used two indexes (*CI*), suggested by Khromov and Gorchinsky (Khromov and Mamontova 1974; Kireeva-Ginenko et al. 2017). The index of continentality suggested by Gorchinsky is calculated as:

$$K = 1.7A / \sin\varphi - 20.4$$

According to Khromov *CI* can be calculated as:

$$K = (A - 5.4\sin\varphi) / A$$

where, *A* is annual range of the air temperature, and φ is latitude. The annual range of the air temperature is calculated as a difference of monthly mean air temperatures in July and January. Since the experimental area has a long north-to-south extension we used for our calculations the latitude of the parallel crossing the central part of our experimental area (57° N).

To analyze the surface moisture conditions we used the hydro-thermal coefficient (HTC) suggested by Selyaninov (Selyaninov 1928; Khromov and Mamontova 1974). It is calculated as:

$$K = 10 \times P / \sum t$$

where ∑t – the sum of mean daily temperatures during the period when it exceeds +10°C, *P* – total precipitation in mm for the same period. Under very wet surface moisture conditions *K* is higher than 2.0. When *K* is varied between 1.0 and 2.0 the surface moisture conditions can be classified as moderately wet. The moderately dry surface moisture conditions are characterized by *K* below 1.0, and very dry – by *K* below 0.4.

RESULTS AND DISCUSSION

The results of conducted numerical experiments showed significant influence of forest cover changes on regional and local weather conditions within both the selected experimental area and the entire modeling domain. It is traced in changes of spatial patterns of the air temperature, precipitation rate, wind speed, fog intensity and frequency.

The influence of forest cover change on the air temperature

Effect of forest cover change on the air temperature is determined by various factors including surface albedo, roughness, net radiation, evapotranspiration rate, etc. Their aggregated influence leads to opposite trends of the air temperature changes for cold and warm seasons of the year. Results of the modeling experiments show that deforestation processes result in lower winter and spring temperatures and in higher summer temperature (Table 1). The largest difference in mean monthly air temperature (at 2 m) between scenarios imitating forest cover changes and the reference experiment was detected in spring. In March the temperature difference between reference and deforestation experiments was -0.6° C (averaged for entire experimental area), whereas the temperature difference between reference and afforestation experiment was positive and some smaller in absolute range – +0.3°C. Such difference is most likely could be explained by various surface albedo and different rates of snow melting at open and forested areas. Whereas the air temperature in January for experiment imitating

total deforestation was 0.4°C lower than for the reference experiment, the air temperature in July under the same scenario was already 0.3°C higher than the temperature in the reference experiment.

Afforestation processes result in opposite effects: the air temperature of January was 0.2°C higher, and in July 0.1°C lower than in the reference experiment, respectively.

The obtained results also show that the deforestation results in an increase of the annual air temperature range (+0.6 °C), whereas afforestation leads to its decreasing (-0.3 °C). Analysis of continentality indexes shows that deforestation slightly increases the climate continentality, whereas afforestation leads to milder climate conditions (Table 2).

Similar numerical experiments provided using the COSMO model to derive the air temperature responses to forest cover changes for the same experimental area during the warm period of 2010 (Kuz'mina et al. 2017a, b; Olchev et al. 2018) showed that deforestation leads to much higher increase of the air temperature in summer months. It was shown, in particular, that the total deforestation of experimental area under weather conditions of July 2010 resulted in increase of the mean monthly temperature up to 1.6°C. The total afforestation under weather conditions of 2010 resulted vice versa in temperature decrease by about 0.7°C (Kuz'mina et al. 2017a, b). We can expect that such strong temperature response to forest cover changes might be explained by anomalously hot and dry weather conditions observed in the European part of Russia in summer 2010.

Comparisons of obtained results with similar numerical experiments provided using other models showed their good agreement. In particular the similar temperature trends were detected during the modeling experiments imitating complete deforestation of the large forest areas situated north of 45°N with the earth system model of the Max Planck Institute for Meteorology (MPI-ESM) (Bathiany et al. 2010).

Table 1. Mean monthly air temperature at 2 m and total precipitation within experimental area modeled for control experiment and experiments imitating total deforestation and afforestation

Month	Air temperature at 2 m (°C)			Precipitation (mm month^{-1})		
	Reference	Deforestation	Afforestation	Reference	Deforestation	Afforestation
1	-10.6	-10.9 (-0.3)	-10.4 (+0.2)	76.4	74.4 (-2.0)	77.6 (+1.2)
2	-2.1	-2.3 (-0.2)	-2.0 (+0.1)	57.4	53.2 (-4.2)	59.4 (+2.0)
3	-2.2	-2.8 (-0.6)	-1.9 (+0.3)	46.2	43.1 (-3.1)	48.1 (+1.9)
4	5.2	4.8 (-0.4)	5.3 (+0.1)	73.0	69.7 (-3.3)	74.4 (+1.4)
5	13.6	13.8 (+0.2)	13.5 (-0.1)	50.2	48.3 (-1.9)	50.7 (+0.5)
6	17.2	17.8 (+0.6)	17.0 (-0.2)	61.7	57.4 (-4.3)	63.0 (+1.3)
7	19.0	19.3 (+0.3)	18.9 (-0.1)	138.5	133.5 (-5.0)	140.0 (+1.5)
8	17.1	17.2 (+0.1)	16.9 (-0.2)	83.5	81.3 (-2.2)	84.4 (+0.9)
9	11.2	11.2 (0.0)	11.1 (-0.1)	40.2	39.1 (-0.3)	40.7 (+0.5)
10	2.5	2.5 (0.0)	2.5 (0.0)	69.3	67.4 (-1.9)	70.1 (+0.8)
11	-3.6	-3.7 (-0.1)	-3.5 (+0.1)	97.2	93.7 (-3.5)	99.0 (+1.8)
12	-4.0	-4.1 (-0.1)	-4.0 (0.0)	54.6	52.2 (-2.4)	56.0 (+1.4)
Year	5.3	5.2 (-0.1)	5.3 (0.0)	848.2	813.3 (-34.9)	863.3 (+15.1)

Table 2. Continentality index for the experimental area calculated using Khromov's and Gorchinsky's equations for reference experiment and experiments imitating total deforestation and afforestation

	Reference	Deforestation	Afforestation
Gorchinsky CI	39.62	40.84	39.01
Khromov CI	0.847	0.850	0.845

The spatial pattern of the air temperature changes due to forest cover change is influenced by an ensemble of different factors including local land use properties and regional circulation processes. Figure 2 shows examples of the spatial patterns of the air temperature changes that can be detected in the case of total deforestation of experimental area in January and July 2016. In January, the air temperature difference between deforestation and reference experiments is predominantly manifested within the experimental area only. Such tendency can be mainly explained by influence of deforestation on surface albedo as well as by weak circulation activity observed within the modeling domain during the second half of winter. In July, the change in air temperature is evident within the entire modeling domain that is mainly governed by high cyclone activity and high intensity of meridional and zonal air mass transfer. Analysis of the influence of afforestation on the spatial temperature pattern indicates the similar features.

It is noteworthy that the most significant changes of surface air temperature caused by forest cover changes are observed in the central part (in July - in the central and eastern parts) of the experimental area. The temperature changes observed outside of the experimental area borders were influenced mainly by prevailing wind directions in lower and middle troposphere.

Effects of forest cover change on precipitation

The influence of forest cover change on precipitation is characterized by very mosaic spatial patterns both within and outside of the experimental area (Fig. 3), as well as by uniformly distributed trend of precipitation changes throughout the entire year (Table 1). In January, maximum precipitation changes are detected within the experimental area, while in July they were spread over the entire modeling domain. The difference between annual precipitation for scenario imitating the total deforestation of experimental area and the reference experiment is -35 mm (precipitation decreased from 848.0 to 813.3 mm and the difference does therefore not exceed 5% of annual precipitation amount). Vice verse, in the case of afforestation experiment precipitation is higher than in the reference experiment in all months of the year. Absolute range of the changes is some smaller than for deforestation scenario not exceeding 15 mm.

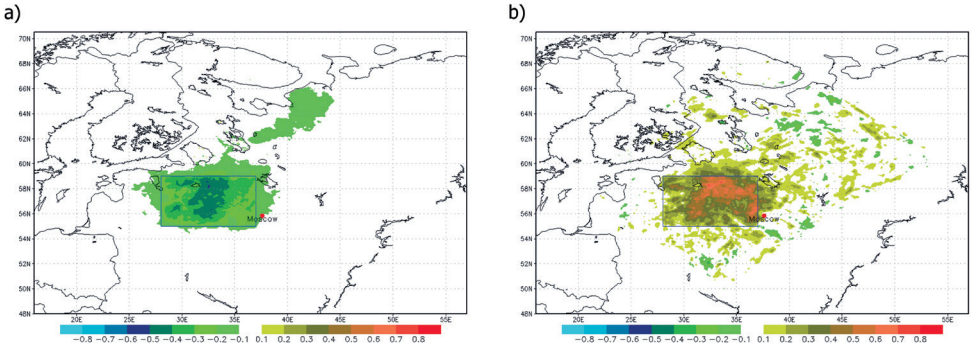

Fig. 2. The spatial patterns of the air temperature difference (at 2 m) between scenario imitating total deforestation of the experimental area and the reference experiment in (a) January and (b) July of 2016

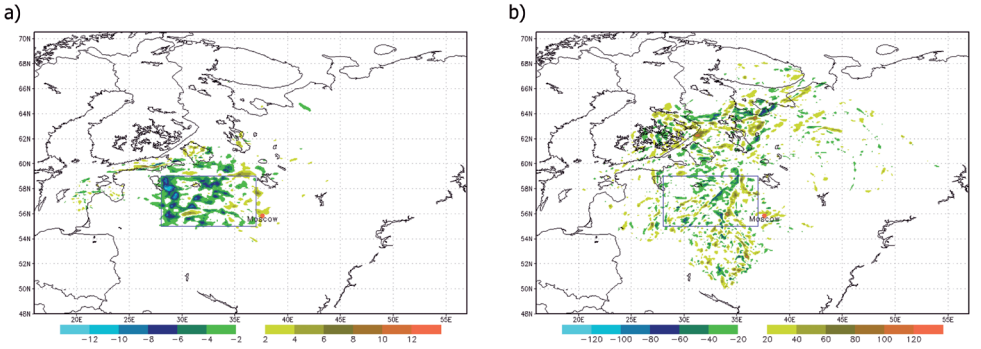

Fig. 3. Differences in precipitation amount between scenario imitating the total deforestation of the experimental area and the reference experiment in January (a) and July (b) 2016

Analysis of surface moisture conditions within the modeling domain using HTC index showed that in 2016 it ranged within the experimental area between 1.0 and 2.5 that corresponds to moderately wet moisture conditions (Fig. 4).

The response of HTC index to forest cover change is observed over the entire modeling domain (Fig. 4b), and in different regions this response has the different signs. Despite of a variety of HTC responses to forest clearing, at local scale the deforestation processes lead to increase of surface dryness, whereas the afforestation results in opposite effects. The difference of HTC values between deforestation and afforestation experiments reaches -0.4, and in some regions even -0.6. The highest changes of HTC are observed in the central and northern parts of the modeling domain, whereas in its western part the projected changes are relatively small.

The influence of forest cover change on wind speed and fog frequency

Forest cover change and wind speed

To derive the possible effects of forest cover changes on regional weather conditions we also considered the possible changes of wind speed pattern and the frequency of high wind speeds due to deforestation and afforestation taking into account their significant influence on regional agriculture, forestry and population.

Numerical experiments showed that deforestation results in significant growth of the mean wind speeds and the number of days with strong wind speed (>8 m/s) within the experimental area (Table 3). In particular, under scenario imitating the total deforestation of experimental area the number of the days with strong wind speed is increased in Valdai station from 1 to 35. Afforestation vise versa leads to decrease of the mean wind speeds and number of days with strong wind.

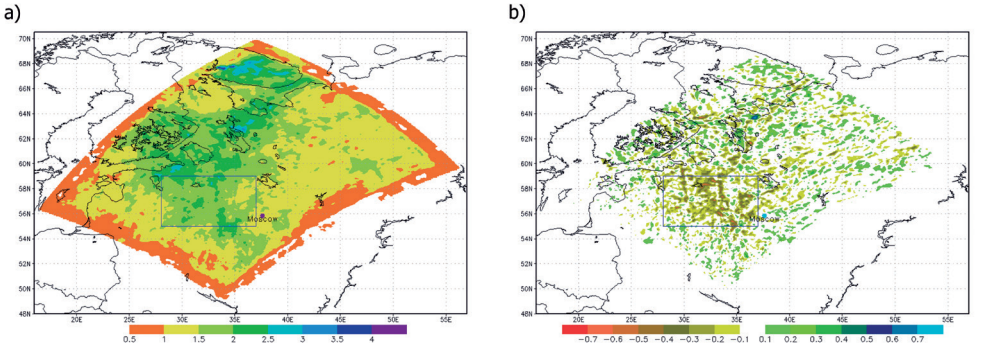

Fig. 4. The spatial pattern of Selyaninov hydro-thermal coefficient, HTC (Selyaninov, 1928) in reference experiment for year 2016 (a) and the difference between HTC values estimated for deforestation and afforestation scenarios (b)

Table 3. The number of days with strong wind speed (> 8 m/s) for 4 stations within the experimental area for the reference, deforestation, and afforestation experiments for the period from May to September of 2016. The differences between the deforestation/afforestation and reference experiments are shown in brackets

Number of days with wind speed > 8 m/s			
Station	Reference	Deforestation	Afforestation
Valdai	1	35 (+34)	1 (0)
Novgorod	9	29 (+20)	1 (–8)
Pskov	5	25 (+20)	3 (–2)
Tver	5	16 (+11)	0 (–5)

Forest cover change and fog occurrence

To analyze the main features of fog formation under land-use and forest cover changes, in the first step we compared the dew point variability for reference and deforestation/afforestation scenarios. Results showed that the changes of monthly mean dew point values are quite similar to variation of precipitation rate (Table 4). Under deforestation conditions during all months of the year 2016 dew point tended to decrease, whereas under afforestation scenario it increased, and these changes were some lower than in the case of deforestation scenario. Analysis of the spatial patterns of dew point differences between the reference and forest cover change scenarios showed significant heterogeneity for the coldest and warmest half of the year. The changes projected for winter months are significantly higher than the changes of dew point in summer months (Fig. 5). It can be also pointed out that the dew point changes during the summer months are spread into the entire modeling domain and characterized by mosaic structure with positive and negative deviations whereas the changes of dew point in winter months are always negative and manifested mainly within the experimental area.

Table 4. Monthly mean dew points at 2 m within the experimental area in the reference experiment and in the experiments imitating total deforestation and afforestation

Months	Dew point at 2 m level		
	Reference	Deforestation	Afforestation
1	–12.3	–12.7 (–0.4)	–12.1 (+0.2)
2	–3.0	–3.3 (–0.3)	–2.9 (+0.1)
3	–3.6	–4.3 (–0.7)	–3.3 (+0.3)
4	3.0	2.6 (–0.4)	3.1 (+0.1)
5	7.5	7.5 (0.0)	7.6 (+0.1)
6	10.7	9.9 (–0.8)	10.9 (+0.2)
7	15.3	15.1 (–0.2)	15.4 (0.1)
8	13.6	13.5 (–0.1)	13.7 (+0.1)
9	7.9	7.9 (0.0)	7.9 (0.0)
10	1.0	0.9 (–0.1)	1.0 (0.0)
11	–4.5	–4.7 (–0.2)	–4.4 (+0.1)
12	–4.8	–5.0 (–0.2)	–4.8 (0.0)
Year	2.6	2.3 (–0.3)	2.7 (+0.1)

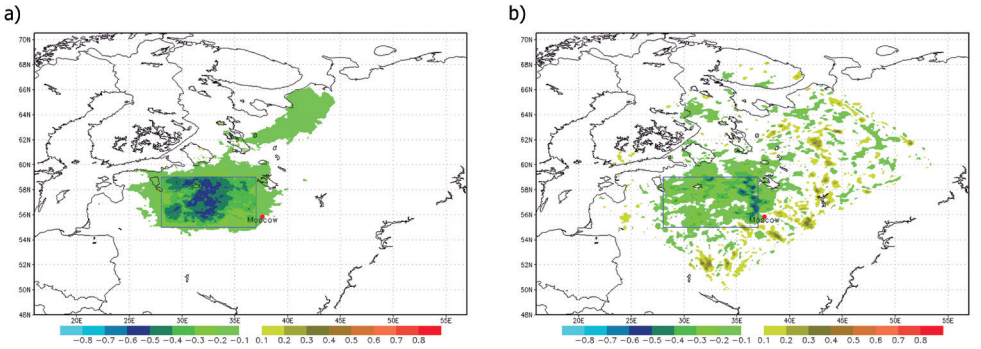

Fig. 5. Difference of monthly mean dew points at 2 m between deforestation and reference experiments in January (a) and July (b), 2016

The results of dew point analysis can be effectively used to explain the changes of spatial pattern of fog occurrence caused by deforestation and afforestation processes. The COSMO model assumes that the fog can occur if the cloudiness sinks in the lowest model level, and its intensity is quantified in octs ranging from 0 to 8. Relative humidity in the corresponding atmospheric layer is considered as a criterion to quantify the fog intensity. It is assumed that all values lower than 8 octs correspond to weather conditions that are favorable for the fog formation. The intensity of fogs equal to 8 octs is assumed as the maximum probability of fog events with the highest intensity. During the warm season of 2016 (from May to September) in deforestation experiment the frequency of favorable conditions for fog formation is decreased, whereas in afforestation experiment – it is increased. The same tendency is observed for fogs of maximum intensity (equal to 8 octs).

Taking into account the main features of the trend for fog number of maximum intensity (8 octs), reproducing by the model for different forest cover change experiments for all months of 2016 (Fig. 6), it is very important to point out that the dependence of the dense fog probability on relative humidity looks a little bit ambiguous. It is obvious that accurate prediction of fog intensity requires accurate description of all key processes influencing fogging processes and it is clear that it cannot be reduced by a direct dependence on relative humidity only. Thus, Fig. 6 shows that in all months of the cold period of 2016 there is no pronounced increase in fog numbers under afforestation experiment in respect to the experiment imitating total deforestation, while the number of simulated fogs in both experiments noticeably increased in relation to the warmest half of the year. The latter indicates an increase in the frequency of weather con-

Table 5. Number of favorable conditions for fog formation for four meteorological stations situated within the experimental area in the reference experiment and in the experiments imitating afforestation and deforestation during the period from May to September, 2016. In the brackets the fog number differences between the deforestation/afforestation and the reference experiments are shown

	Number of favorable situations for fog formation			Number of fogs (8 octs)		
Station	Reference	Deforestation	Afforestation	Reference	Deforestation	Afforestation
Valdai	73	69 (–4)	91 (+18)	21	16 (–5)	20 (–1)
Novgorod	58	41 (–17)	72 (+14)	9	7 (–2)	10 (+1)
Pskov	32	25 (–7)	50 (+18)	7	5 (–2)	15 (+8)
Tver	34	30 (–4)	51 (+17)	7	5 (–2)	8 (+1)

Fig. 6. Number of modeled fogs (8 octs) at meteorological stations within the experimental area (indicated by station indexes) in the deforestation (red color) and afforestation (green color) experiments for different months of 2016

ditions that are favorable for fog formation in the winter period. It can be also resulted from, for example, an underestimation of the surface air temperature, leading to the occurrence of radiation fogs, or an increase in the number of advective fogs. However, these hypotheses require further aggregated studies using both experimental data and modeling experiments.

CONCLUSION

The numerical experiments conducted with the COSMO model for experimental area situated in the central part of the East European plain for the reference period from January to December 2016 showed significant influence of forest cover changes on regional meteorological conditions. It was shown that deforestation results in decrease of the air temperature in cold half of the year and in increase – in summer time. The afforestation results in opposite effects. An increase of annual temperature range in the case of total deforestation of experimental area is about 0.6°C and it can lead to small increase of climate continentality. In the case of afforestation the decrease of annual temperature range is about 0.3°C that promotes the milder climate conditions. Analysis of changes in precipitation under different forest cover change scenarios showed that deforestation leads to relatively small decrease of the annual precipitation by 35 mm, whereas afforestation leads to increase of precipitation by 15 mm. It can be expected that deforestation leads to drier climate conditions that in the long-term perspective can influence the rate of forest recovery, species composition and biodiversity.

It is very important to mention that the forest cover change influences a broad spectrum of meteorological conditions. The numerical experiments showed that deforestation processes lead to higher frequency of the days with strong wind speed and lower frequency of fog events especially of the highest intensity. In the case of afforestation, the number of days with high wind speed is changed insignificantly, whereas the fog frequency is significantly grown.

It should also be pointed out that all obtained results are well agreed with a number of numerical experiments conducted using global scale models (e.g. Brovkin et al, 2009). At the same time, it is obvious that such studies should be continued using the models of different scales and complexity as well as using experimental data to derive the whole spectrum of possible responses of regional and global weather conditions on forest cover changes.

ACKNOWLEDGEMENTS

This study was supported by the grant of the Russian Science Foundation (Grant 14-14-00956). The project is also associated with the Northern Eurasia Earth Science Partnership Initiative (NEESPI).

REFERENCES

Anav A., Ruti P.M., Artale V., Valentini R. (2010). Modelling the effects of land-cover changes on surface climate in the Mediterranean region. Clim. Res., [online] 41(2), pp. 91–104. Available at: https://doi.org/10.3354/cr00841 [Accessed 22 Jan. 2019].

Asensio H., Massmer M., Liithi D., Osterried K. (2018). External Parameters for Numerical Weather Prediction and Climate Application [online]. Available at: http://www.cosmo-model.org/content/support/software/ethz/extpar-userManual-v5.0.pdf [Accessed 10 Apr. 2019].

Bathiany S., Claussen M., Brovkin V., Raddatz T., Gayler V. (2010). Combined biogeophysical and biogeochemical effects of large-scale forest cover changes in the MPI earth system model. Biogeosciences, [online] 7, pp. 1383–1399. Available at: https://doi.org/10.5194/bg-7-1383-2010 [Accessed 22 Jan. 2019].

Bonan G.B., Pollard D., Thompson S.L. (1992). Effects of boreal forest vegetation on global climate. Nature, 359, pp. 716–718.

Brovkin V., Raddatz T., Reick C.H., Claussen M., Gayler V. (2009). Global biogeophysical interactions between forest and climate. Geophysical Research Letters, [online] 36, L07405. Available at: https://doi.org/10.1029/2009GL037543 [Accessed 22 Jan. 2019].

Carlson D.W., Groot A. (1997). Microclimate of clear-cut, forest interior and small openings in trembling aspen forest. Agricultural and Forest Meteorology, [online] 87, pp. 313–329. Available at: https://doi.org/10.1016/S0168-1923(95)02305-4 [Accessed 22 Jan. 2019].

Doms G., Baldauf M. (2018). A description of the Nonhydrostatic Regional COSMO-Model. Part I: Dynamics and Numerics [online]. Available at: http://www.cosmo-model.org/content/model/documentation/core/cosmoDyncsNumcs.pdf [Accessed 23 Jan. 2019].

Kireeva-Ginenko I.A., Novikova E.P., Chumeikina A.S. (2017). Analysis and valuation of continentality index in the Central-Chernozem area for last 30 years. Progress in contemporary natural sciences, [online] No. 7, pp. 76–80 (in Russian). Available at: http://www.natural-sciences.ru/ru/article/view?id=36481 [Accessed 22 Jan. 2019].

Khromov S.P. and Mamontova L.I. (1974). Meteorological dictionary. Leningrad, USSR: Gidrometizdat (in Russian).

Kulmala L., Aaltonen H., Berninger F., Kieloaho A.J., Levula J., Bäck J., Hari P., Kolari P., Korhonen J.F.J., Kulmala M., Nikinmaa E., Pihlatie M., Vesala T., Pumpanen J. (2014). Changes in biogeochemistry and carbon fluxes in a boreal forest after the clear-cutting and partial burning of slash. Agricultural and Forest Meteorology, [online] 188, pp. 33–44. Available at: https://doi.org/10.1016/j.agrformet.2013.12.003 [Accessed 22 Jan. 2019].

Kuz'mina E.V., Olchev A.V., Nikitin M.A., Rozinkina I.A., Rivin G.S. (2017a). Impact of forest coverage variations in the central regions of the European Russia on the regional meteorological conditions: assessment with application of climate version of COSMO model. In: A.V. Olchev, ed., Forests of the European territory of Russia in condition of changing climate, 1st ed. Moscow, Russia: Community of scientific publications KMK, pp. 230–272 (in Russian).

Kuz'mina E.V., Ol'chev A.V., Rozinkina I.A., Rivin G.S., Nikitin M.A. (2017b). Application of the COSMO-CLM mesoscale model to assess the effects of forest cover changes on regional weather conditions in the European part of Russia. Russian Meteorology and Hydrology, 42(9), pp. 574–581.

Mamkin V., Kurbatova J., Avilov V., Mukhartova Y., Krupenko A., Ivanov D., Levashova N., Olchev A. (2016). Changes in net ecosystem exchange of CO_2, latent and sensible heat fluxes in a recently clear-cut spruce forest in western Russia: results from an experimental and modeling analysis. Environ. Res. Lett., 11(12), 125012.

Mamkin V., Kurbatova J., Avilov V., Ivanov D., Kuricheva O., Varlagin A., Yaseneva I., Olchev A. (2019). Energy and CO2 exchange in an undisturbed spruce forest and clear-cut in the Southern Taiga. Agricultural and Forest Meteorology, 265, pp. 252–268. Available at: https://doi.org/10.1016/j.agrformet.2018.11.018 [Accessed 22 Jan. 2019].

Mironov D.V. (2008). Parameterization of lakes in numerical weather prediction. Description of a lake model. COSMO Technical Report, No. 11. Offenbach am Main, Germany: Deutscher Wetterdienst.

Nobre C.A., Sellers P.J., Shukla J. (1991). Amazonian deforestation and regional climate change. J. Clim., [online] 4, pp. 957–988. Available at: https://doi.org/10.1175/1520-0442(1991)004<0957:ADARCC>2.0.CO;2 [Accessed 22 Jan. 2019].

Olchev A., Radler K., Sogachev A., Panferov O., Gravenhorst G. (2009). Application of a three-dimensional model for assessing effects of small clear-cuttings on radiation and soil temperature. J. Ecol. Modell., [online] 220, pp. 3046–3056. Available at: https://doi.org/10.1016/j.ecolmodel.2009.02.004 [Accessed 22 Jan. 2019].

Olchev A.V., Rozinkina I.A., Kuzmina E.V., Nikitin M.A., Rivin G.S. (2018). Influence of forest cover changes on regional weather conditions: estimations using the mesoscale model COSMO. IOP Conf. Series: Earth and Environmental Science, 107, P. 012105-012105.

Pielke R.A., Adegoke J., Beltran-Przekurat A., Hiemstra C.A., Lin J., Nair U.S., Niyogi D., Nobis T.E. (2007). An overview of regional land-use and landcover impacts on rainfall. Tellus B: Chemical and Physical Meteorology, [online] 59, pp. 587–601. Available at: https://doi.org/10.1111/j.1600-0889.2007.00251.x [Accessed 22 Jan. 2019].

Rivin G.S., Rozinkina I.A., Vil'fand R.M., Alferov D.Yu., Astakhova E.D., Blinov D.V., Bundel' A.Yu., Kazakova E.V., Kirsanov A.A., Nikitin M.A., Perov V.L., Surkova G.V., Revokatova A.P., Shatunova M.V., and Chumakov M.M. (2015). The COSMO-Ru system of nonhydrostatic mesoscale short-range weather forecasting of the Hydrometcenter of Russia: The second stage of implementation and development. Russian Meteorology and Hydrology, 40(6), pp. 400–410.

Seidl R., Schelhaas M.J., Rammer W., Verkerk P.J. (2014). Increasing forest disturbances in Europe and their impact on carbon storage. Nat. Clim. Chang., 4(9), pp. 806–810.

Selyaninov G.T. (1928). About climate agricultural estimation. Proceedings on Agricultural Meteorology, 20, pp. 165–177.

Woodward F.I. (1987). Climate and plant distribution. Cambridge: Cambridge University Press.

Whittaker R.H. (1975). Communities and Ecosystems. New York: MacMillan.

Received on Jan 29th 2019 Accepted on May 17th 2019

Uliya R. Ivanova[1]*, Nataliya V. Skok[1] and Oksana V. Yantser[1]
[1] Ural State Pedagogical University, Yekaterinburg, Russia
*** Corresponding author:** miss.nocentra@list.ru

SPATIAL HETEROGENEITY IN PHENOLOGICAL DEVELOPMENT OF *PRUNUS PADUS* L. IN THE YEKATERINBURG CITY

ABSTRACT. The possible impact of the climate changes on vegetation is a key topic of various research studies in geography and ecology. In this study we tried to provide a «one-time survey» of the phenological development of *Prunus padus L*. in the Yekaterinburg city as a part of the large-scale project "A Single Phenological Day" and show the data on a map. The registration of a seasonal development of bird cherry was provided annually in the years of 2012-2018 on one and the same date in the city of Yekaterinburg, on 15 May. Yekaterinburg is the largest city located on the eastern foothills of the Middle Urals, Russia. The city has residential areas, parks, water reservoirs, as well as large industrial facilities that affect microclimatic conditions, resulting in an increase of the temperatures. Such microclimatic heterogeneity results in uneven development of bird cherry in spring. It was revealed the slowing of the bird cherry development in the areas situated close to large water reservoirs. At the same time bird cherry trees growing inside large industrial areas, on the contrary, developed much faster. The development rates of *Prunus padus L*. also differed though years: in years with dry and warm weather during the period of late April - early May the vegetation began earlier.

KEY WORDS: phenology, urban vegetation, *Prunus padus L*., The Nationwide Phenology Day

CITATION: Uliya R. Ivanova, Nataliya V. Skok and Oksana V. Yantser (2019) Spatial Heterogeneity In Phenological Development Of *Prunus Padus* L. In The Yekaterinburg City. Geography, Environment, Sustainability,
Vol.12, No 2, p. 273-281
DOI-10.24057/2071-9388-2018-84

INTRODUCTION

The study of the spatial and temporal variability of seasonal nature phenomena is very important issue of modern geography and landscape ecology. In particular, the study of variability and inter-annual fluctuation in vegetation phenology is one of the simplest and low-cost approach to analyze changing weather and climate conditions. The timing of the onset of seasonal phenomena allows to indicate local and regional changes in climatic variables affecting plant development over growing season.

The concept of global phenology monitoring was formulated first in 1977 by Vladimir Batmanov (Yantser et al. 2010), the founder of the Ural phenological school. This idea was based on simultaneously registering the stage of seasonal development of a certain distinct species by numerous observers on a wide geographical area. The object of study (as *Prunus padus L*. in our researches) should be widespread, well-known and easily observed. Due to the insufficiency of the theoretical and methodological background this approach for a long time remained theoretical. In 2000, the several research teams of the Ural phenological school began to develop methods for global phenological observations (Kupriyanova 2010), however, this process was delayed, and only by 2012 the idea of V.A. Batmanov was turned into a global research project – The Nationwide Phenology Day (NPD).

Since 2018, the Russian scientists carry out the observations in almost all regions of the research object distribution in natural growth conditions (Yantser 2018). The teams involved in the observations are extremely diverse: from research scientists to junior schoolchildren.

The retrospective analysis of geographic and biological research suggests that with using phenological observations is possible to specify the degree of influence of the urban microclimate on the timing of the onset of seasonal phenomena. Within the framework of the project «NPD» we have attempted to visualize the influence of urban and suburban environment on vegetation.

The seasonal phenomena and effects of climate changes on plant and animal phenology are studied in different climatic regions from a variety of perspectives. The academics have a lot of publications devoted to the effect of climate change on the phenology of plants and animals. Among them, regional scale studies prevail, such as the reaction of some tree species to changes in the thermal conditions in the French Alps (Asse et al. 2018); phenological observations of the Betula genus in Europe (Siljamo et al. 2008), the studies of the generative cycle (flowering) in the Canadian subarctic ecosystems.

The seasonal development of plants is studied from both perspectives: plant physiology and ecology (Cleland et al. 2007; Clark et al. 2014), and geography. The studies was mainly focused on researches of species-specific responses of plants to climatic changes in the Northern Hemisphere (Minin 2002, 2006; Golubyatnikov 2009; Grebenyuk and Kuznetsova 2012; Soloviev 2015; König et al. 2018), also was studied the interannual variability of seasonal phenomena in relation to air temperature (Menzel and Sparks 2007), early spring index (Schwartz 1990), phenology of flowering plants (Tooke and Battey 2010), influence of some environmental factors on individual phenophases of woody plants (Penuelas 2001; Kulygin 2001; Körner and Basler 2010), as well as plant response and climate phenology (Richardson et al. 2013).

It was investigated the differences in the onset of seasonal processes both in natural conditions and in the urban areas (Kuklina and Danchenko 2009; Gorton et al. 2018); features of phenophases in large cities (Kulagin and Nikolaeva 2014; Ufimtseva and Terekhina 2017) and the effect of artificial lighting on plant development. Modeling and forecasting of seasonal processes are less studied issues, however, they hold a specific place as a

promising direction. Scientists pay much attention to the methodological issues of the organization of phenological networks in various territories and their data processing (Visser and Both 2005; Kane and Beery 2009; Denny et al. 2014; Gerst et al. 2016).

MATERIAL AND METHODS

For the 40-year period from 1890 to 1930 the average date of *Prunus padus L*. blossoming shifted from was May 24 to May 19 (Batmanov 1952). Currently the average monthly spring temperatures are much higher than during the mentioned period, and thus, we decided to select May 15 for the uniform phenology observations. *Prunus padus L*. was selected as a uniform study species. The blooming of *Prunus padus L*. marks the beginning of the last period of spring and is often accompanied by a temperature drop and a stable rise in average temperatures (Minin and Voskova 2014). The number of observers exceeds several hundred people thought the county. To ensure a distinct registration we have developed a simple list of phenological states with a number code. Each phenophase has its own digital characteristic. For example, "code 1" is representing the winter dormancy phase, "code 2" - gemmation phase, "3" – the budding phase, etc.

To identify the peculiarities of the seasonal dynamics of the species in urban areas, phenological surveys were carried out in Yekaterinburg and its surroundings. The observer was asked to choose a *Prunus padus L*. tree or bush as a constant observation object for several years and to describe its phenological state each year on May 15, using the corresponding number code and to report to the Scientific and Educational Phenological Center.

Yekaterinburg is a big city situated in the eastern foothills of the Urals. The climate of the region is moderately continental. The mean annual temperature equals +3.0°C, mean temperatures of January and July are -12.6°C, and +19.0°C corresponsive. The annual temperature range reaches 33°C. Mean annual precipitation is about 540 mm. In general, the climate is characterized by long winters (up to 5 months) with stable snow cover in winter time, short transitional seasons, late springs and early autumn frosts, short frost-free periods (110–120 days), short summers (70–94 days); the timing of the transitional seasons is not stabile. Spring is characterized by warm and cold periods, that are associated with the meridional atmosphere circulation clearly manifested on the eastern macro slope of the Urals. The air temperature in the daytime can rise to + 24°C, and drop below 0 at night.

The microclimatic data was studied in the 1970s by the Sverdlovsk (former name of Yekaterinburg) weather control and environmental monitoring service made a series of field meteorological observations within the city boundaries and in its suburbs (Morokov and Shver 1981) within the city at seven plots. All observation points can be divided into several types depending on location: weather stations, parks, squares, lawns, city ponds and residential areas. Studies of the temperature dynamics in the "city-suburb" gradient show that the temperatures in the central regions of the city are higher than those in the outskirts by 0.2-0.6°C on average throughout the year; sometimes reaching up to 5°C. The vegetation rates depend on the moisture content in the soil after the spring snowmelt. In the second half of spring, due to the predominantly anticyclonic weather character, the rainfall level is low influencing the rates of *Prunus padus L*. seasonal development.

RESULTS AND DISCUSSION

Based on the previously mentioned researches we calculated the average score within a period of seven years for each object. We plotted these scores on the map of the city of Yekaterinburg in accordance with the location of the observation points (Fig. 1).

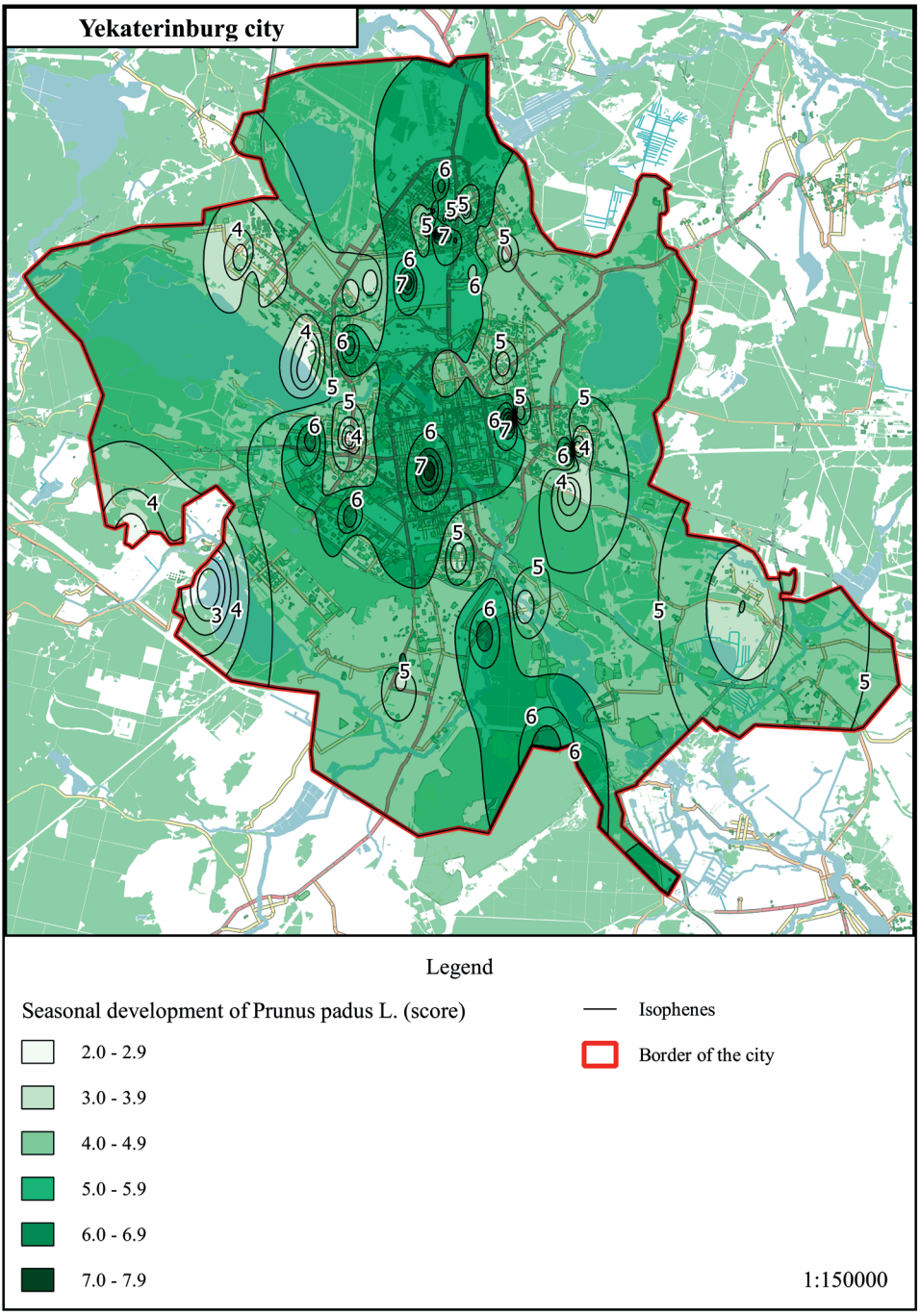

Fig. 1. The map of the average phenological state of *Prunus padus* L. as of May 15 in Yekaterinburg

We compared the average rate of phenological development in the city and its deviations from the multiyear average, as well as meteorological indicators that may influence spring development of the studied species (Table 1) thus receiving data on the temporal variability of vegetation period of *Prunus padus L*. in spring on the territory of Yekaterinburg.

The map clearly shows the lag in the outskirts of the city in relation to its center (Fig. 1). These results correspond with the results of the microclimatic observations (Morokov and Shver 1981). The most densely populated central and northern regions of Yekaterinburg are characterized by the earliest vegetation phases. The high points in terms of vegetation in the north of the city are driven by the area of heat above the large industrial area of Uralmash. According to meteorological observations, Uralmash region is warmer than the city center by 1.5°C, and the suburbs by 3-4°C. The lag was recorded near such large waterbodies as – Shartash and Shuvakish lakes and Verkh-Isetsky pond, as well as in the marshy southwest, east and southeast of the city. The lakes of the city produce a greenhouse effect at night and anti-greenhouse effect in daytime. Since they are cited in deep valleys, their effect extends only to 200-300 m of the coastal strip. The cold air stagnation adds to the effect.

The observations have shown that the temperature of lawns and areas with a natural coating is 2-2.5°C lower than the temperature around city squares. This is confirmed by the highest rates of phenological development of *Prunus padus L*. around them. The district of the Uktussky Mountains, located in the southeast of the city, is colder than the center by 3-4°C. This is confirmed by the fact that the vegetation scores of *Prunus padus L*. here are 1 point lower than in the city center.

The results of the studies of the vegetative period of *Prunus padus L*. are presented in Table 1. The long-term average phenological score on May 15 is 6.5. In the years

Table 1. Dynamics of phenoclimatic indicators for the period 2012-2018 in Yekaterinburg

Year	2012	2013	2014	2015	2016	2017	2018
Average of phenological development	7.8	6.5	8.2	7.0	7.8	5.8	2.3
Deviation from the multiyear average	-1.3	0.0	-1.7	-0.5	-1.3	+0.7	+4.2
First day with average daily air temperature above 0°C	19.03	16.03	09.03	10.03	25.03	21.02	03.04
Date of steady transition of average daily air temperature to positive values	02.04	03.04	12.04	31.03	25.03	06.04	03.04
∑ of air temperatures >0°C	431.6	299.9	323.0	318.2	379.4	310.8	213.8
∑ of air temperatures >+5°C	402.3	273.0	303.2	241.5	322.6	277.2	158.6
∑ of precipitation from 01.11 to 15.05 (mm)	138.1	236.4	230.5	142.0	210.3	188.2	148.6
∑ of precipitation from 01.05 to 15.05 (mm)	23.8	16.9	17.6	32.4	3.3	11.1	7.7
The average temperature of the first half of May (°C)	10.9	9.5	14.5	11.3	9.5	9.4	8.0

characterized by the greatest amount of accumulated heat and small amount of precipitation early vegetation is registered. In most cases the crucial factors are the arrival of heat in the first half of May and low rates of precipitation. Minimal deviations in the phenological development of *Prunus padus L*. were recorded in years with meteorological parameters close to the mean ones. The greatest delay in vegetation of *Prunus Padus L* relative to the average score at the NPD date was recorded in year 2018 -4.2 points. This was driven by the significant lag of all temperature characteristics and the latest transition of the average daily temperature to positive values within the last 7 years. Although 2014 was the most advanced in terms of phenological development, it was not characterized by the earliest transition of average daily temperature to positive values and had moderate amounts of accumulated heat. There was quite a large amount of precipitation in the first half of May. The significant increase in air temperature at the beginning of the second decade of May (to 16–24°C) had a decisive influence on the acceleration of the phenological development of the *Prunus padus L*.

CONCLUSION

The urban environment has a significant impact on the spatial and temporal structure of the seasonal development of *Prunus padus L*. The obtained results revealed the large differences in the timing of the *Prunus padus L*. growing season in the urban (artificial) and suburban (natural) environments. Such results resemble with the results of similar studies obtained particularly for two species of birch in the city of Tomsk (Kuklina 2009). Thus, we can conclude that in the cities vegetation begins earlier than in the suburbs of both birch, and bird cherry. The higher temperatures of the central areas od the city drive faster development of the *Prunus padus L*., especially in highly populated areas. Warm temperature periods during late April-early May along with the dry weather conditions trigger early *Prunus padus L*. seasonal development. We plan to continue the study in order to reveal shifts in *Prunus padus L*. spring seasonal development. The further study of suburban-urban differences in the vegetation period on will reveal the spatial characteristics of plant phenology. With the accumulation of data, the results of this study can help in a detailed understanding of the time shifts in plant phenology under the influence of climate change. Also, the calculation of the developmental anomalies of *Prunus padus L*. in days is more explicit and promising.

REFERENCES

Asse D., Chuine I., Vitasse Y., Yoccoz N., Delpierre N., Badeau V., Delestrade A., Randin C. (2018). Warmer winters reduce the advance of tree spring phenology induced by warmer springs in the Alps. Agricultural and Forest Meteorology, 252, pp. 220–230. doi:10.1016/j.agrformet.2018.01.030.

Batmanov V.A. (1952). Nature calendar of Sverdlovsk and its environs. Sverdlovsk. 95 p. (in Russian).

Bennie J., Davies T., Cruse D., Bell F., Gaston K. (2018). Artificial light at night alters grassland vegetation species composition and phenology. Journal of Applied Ecology, 55, pp. 442–450. doi:10.1111/1365-2664.12927.

Caffarra A., Donnelly A., Chuine I. (2011). Modelling the timing of Betula pubescens budburst. II. Integrating complex effects of photoperiod into process-based models. Climate Research, 46, pp. 159–170. doi:10.3354/cr00983.

Clark J., Melillo J., Mohan J., Salk C. (2014). The seasonal timing of warming that controls onset of the growing season. Global Change Biology, 20, pp. 1136–1145. doi:10.1111/gcb.12420.

Cleland E., Chuine I., Menzel A., Mooney H., Schwartz M. (2007). Shifting plant phenology in response to global change. Trends in Ecology and Evolution, 22, pp. 357–365. doi:10.1016/j.tree.2007.04.003.

Crepinsek Z., Kajfez-Bogataj L., Bergant K. (2006). Modelling of wheather variability effect on fitophenology. Ecological Modelling, 194, pp. 256–265.

Denny E., Gerst K., Miller-Rushing A., Tierney G., Crimmins T., Enquist C., Guertin P., Rosemartin A., Schwartz M., Thomas K., Weltzin J. (2014). Standardized phenology monitoring methods to track plant and animal activity for science and resource management applications. International Journal of Biometeorology, 58, pp. 591–601. doi:10.1007/s00484-014-0789-5.

Gerst K., Kellermann J., Enquist C., Rosemartin A., Denny E. (2016). Estimating the onset of spring from a complex phenology database: trade-offs across geographic scales. International journal of biometeorology, 60, pp. 391–400. doi:10.1007/s00484-015-1036-4.

Golubyatnikov L.L. (2009). The impact of climate change on the vegetation cover of Russian regions In: Skvortsov E.V., Rogova T.V. (eds.): Environment and Sustainable Development of Regions: New Methods and Research Technologies. Volume III: Modeling in the Protection of the Environment. General Ecology and Biodiversity Conservation. Kazan: "Brig". (in Russian).

Gorton A., Moeller D., Tiffin P. (2018). Little plant, big city: A test of adaptation to urban environments in common ragweed (Ambrosia artemisiifolia) In: Proceedings of the Royal Society B: Biological Sciences. The Royal Society. Available at: http:// http://rspb.royalsocietypublishing.org/ [Accessed 3 Okt. 2018].

Grebenyuk G.N. and Kuznetsova V.P. (2012). Modern dynamics of climate and phenological change of northern territories. Fundamental research, 11, pp. 1063–1077. (in Russian with English summary).

Hopkins G., Gaston K., Visser M., Elgar M., Jones T. (2018). Artificial light at night as a driver of evolution across urban-rural landscapes. Frontiers in Ecology and the Environment, 16, pp. 472–479. doi:10.1002/fee.1828.

Kane J. and Beery K. (2009). Phenology of Plants at the Kleinstu ck Preserve Kalamazoo College.

König P., Tautenhahn S., Cornelissen J., Kattge J., Bönisch G., Römermann C. (2018). Advances in flowering phenology across the Northern Hemisphere are explained by functional traits. Global Ecology and Biogeography, 27, pp. 310–321. doi:10.1111/geb.12696.

Körner C. and Basler D. (2010): Phenology under global warming. Science, 327, pp. 1461–1462. doi:10.1126/science.1186473.

Kuklina T.E. and Danchenko A.M. (2009). Autumn development BETULA PENDULA ROTH AND BETULA PUBESCENS ERHR. in the landscaping of the city of Tomsk and the suburbs. Tomsk State University Journal, № 322, pp. 239–242. (in Russian).

Kulagin A.A. and Nikolaev V.V. (2014). Spring phenorhythms of birch (BETULA PENDULA ROTH), growing in the city of Ufa (republic of Bashkortostan). Bulletin of Bashkir University. Biology, 19, pp. 1228–1231. (in Russian with English summary).

Kulygin A.A. (2001). Role of Temperature Factor in Fruit Ripening of Wood Plants. Bulletin of higher educational institutions. Lesnoy zhurnal, № 5-6, pp. 7–10. (in Russian with English summary).

Kupriyanova M.K. (2010). V.A. Batmanov - the founder of a new direction in phenology. In: The Modern State of Phenology and the Prospects of Its Development. pp. 42–56. (in Russian).

Lessard-Therrien M., Bolmgren K., Davies T. (2014). Predicting flowering phenology in a subarctic plant community. Botany, 92, pp. 749–756. doi:10.1139/cjb-2014-0026.

Massetti L. (2018). Assessing the impact of street lighting on Platanus x acerifolia phenology. Urban Forestry and Urban Greening, 34, pp. 71–77. doi:10.1016/j.ufug.2018.05.015.

Menzel A. and Sparks T. (2007). Temperature and Plant Development: Phenology and Seasonality In: Plant Growth and Climate Change. pp. 70–95.

Minin A.A. (2002). Trees and birds on climate change. Chemistry and life, № 2, pp. 38–42. (in Russian)

Minin A.A. (2006). Ecosystems of the Amur basin under climate warming: experience of nature reserves In: The Impact of Climate Change on the Amur River Basin Ecosystems. WWF Russia, Moskow, pp. 17–22. (in Russian).

Minin A.A. and Voskova A.V. (2014): Homeostatic responses of plants to modern climate change: Spatial and phenological aspects. Russian Journal of Developmental Biology, Volume 45, pp. 162–169. (in Russian with English summary).

Morokov V.V. and Shver C.A. (1981). The climate of Sverdlovsk. Leningrad: Ural UGKS. (in Russian).

Penuelas J. (2001). Phenology: Responses to a Warming World. Science, 294, pp. 793–795. doi:10.1126/science.1066860.

Richardson A., Keenan T., Migliavacca M., Ryu Y., Sonnentag O., Toomey M. (2013). Climate change, phenology, and phenological control of vegetation feedbacks to the climate system. Agricultural and Forest Meteorology, 169, pp. 156–173. doi:10.1016/j.agrformet.2012.09.012.

Schwartz M. (1990). Detecting the onset of spring: a possible application of phenological models.

Siljamo P., Sofiev M., Ranta H., Linkosalo T., Kubin E., Ahas R., Genikhovich E., Jatczak K., Jato V., Nekovář J., Minin A., Severova E., Shalaboda V. (2008). Representativeness of point-wise phenological betula data collected in different parts of Europe. Global Ecology and Biogeography, 17, pp. 489–502. doi:10.1111/j.1466-8238.2008.00383.x.

Soloviev A.N. (2015). Climatogenic and anthropogenic dynamics of biota in the changing environmental conditions of the east of the Russian Plain. Abstract of the Dissert ... Doctor of Biological Sciences. Petrozavodsk: All-Russian Research Institute of Hunting and Animal Farming named after Professor B.M. Zhitkov, 47 p. (in Russian)

Tooke F. and Battey N. (2010). Temperate flowering phenology. Journal of Experimental Botany, 61, pp. 2853–2862. doi:10.1093/jxb/erq165.

Ufimtseva M.D. and Terekhina N.V. (2017). Assessment of the ecological status of the central district (saint-petersburg) on the basis of ecophytoindication. Vestnik of Saint-Petersburg University. Earth Sciences, Volume 62, pp. 209–217. doi:10.21638/11701/spbu07.2017.206. (in Russian with English summary).

Visser M. and Both C. (2005). Shifts in phenology due to global climate change: the need for a yardstick. Proceedings of the Royal Society B: Biological Sciences, 272, pp. 2561–2569. doi:10.1098/rspb.2005.3356.

Yantser O.V. (2018). Spring development of bird cherry on the territory of Russia (results of a Single phenological day) In: Chronicle of Nature of Russia: Phenology. Proceedings of I Intern. Phenological School-Seminar in the Central Forest State Natural Biosphere Reserve Reserve. Velikiye Luki, pp. 218–222. (in Russian).

Yantser O.V., Skok N.V., Terentyeva E.Y. (2010). Unpublished work on phenology V.A. Batmanova with comments from members of the phenological section of the Russian Geographical Society. Yekaterinburg. (in Russian with English summary).

Received on Dec 31st, 2018 Accepted on May 17th, 2019

AUTHOR GUIDELINES

1. Authors are encouraged to submit high-quality, original work: scientific papers according to the scope of the Journal. reviews (only solicited) and brief articles.

2. Papers are accepted in English. Either British or American English spelling and punctuation may be used.

3. All authors of an article are asked to indicate their names (with one forename in full for each author, other forenames being given as initials followed by the surname) and the name and full postal address (including postal code) of the affiliation where the work was done. If there is more than one institution involved in the work, authors' names should be linked to the appropriate institutions by the use of 1, 2, 3 etc superscript. Telephone and fax numbers and e-mail addresses of the authors could be published as well. One author should be identified as a Corresponding Author. The e-mail address of the corresponding author will be published, unless requested otherwise.

EXAMPLE:

Ivan I. Ivanov[1], Anton A. Petrov[1*], David H. Smith[2]
[1]University/Organization name, Street, City, ZIP-code, Country
[2]University/Organization name, Street, City, ZIP-code, Country
*** Corresponding author:** example@example.com

4. The GES Journal style is to include information about the author(s) of an article. Therefore we encourage the authors to submit their portrait photos and short CVs (up to 100 words).

5. Article structure should contain further sections:
   • Abstract.
   • Keywords (Immediately after the abstract, provide a maximum of 6 keywords, avoiding general and plural terms and multiple concepts (avoid, for example, 'and', 'of'). Be sparing with abbreviations: only abbreviations firmly established in the field may be eligible. These keywords will be used for indexing purposes.).
   • Introduction (State the objectives of the work and provide an adequate background, avoiding a detailed literature survey or a summary of the results.).
   • Material and methods (Provide sufficient details to allow the work to be reproduced by an independent researcher. Methods that are already published should be summarized, and indicated by a reference. If quoting directly from a previously published method, use quotation marks and also cite the source. Any modifications to existing methods should also be described.
   • Results (Results should be clear and concise.).
   • Discussion (This should explore the significance of the results of the work, not repeat them. A combined Results and Discussion section is often appropriate. Avoid extensive citations and discussion of published literature.).
   • Conclusions (The main conclusions of the study may be presented in a short Conclusions section, which may stand alone or form a subsection of a Discussion or Results and Discussion section.).
   • Acknowledgements (List here those individuals who provided help during the research and funds which provided financial support of your research.).
   • References (Make a list of references according to guidance provided below).
   • Appendices (If there is more than one appendix, they should be identified as A, B, etc.

Formulae and equations in appendices should be given separate numbering: Eq. (A.1), Eq. (A.2), etc.; in a subsequent appendix, Eq. (B.1) and so on. Similarly for tables and figures: Table A.1; Fig. A.1, etc.).

6. Sections and sub-sections shouldn't be numbered, but divided into sub-levels. If you would like to refer to a particular section, name it without any numbers (for example: see "Materials and methods")

7. Math equations should be submitted as editable text and not as images (use appropriate tool in text editor). Present simple formulae in line with normal text where possible and use the solidus (/) instead of a horizontal line for small fractional terms, e.g., X/Y. In principle, variables are to be presented in italics. Number consecutively any equations that have to be displayed separately from the text (if referred to explicitly in the text).

8. Figures and figure captions. Number the illustrations according to their sequence in the text. Regardless of the application used, when your figure is finalized, please 'save as' or convert the images to one of the following formats: TIFF, JPG. Supply files that are optimized for screen use. **The resolution should be at least 300 dpi**. Besides inserting figures into your manuscript, you must also upload appropriate files during paper submission. Ensure that each illustration has a caption. A caption should comprise a brief title (not on the figure itself) and a description of the illustration beginning from "Fig. 1…" (note: no any dots in the end of the capture!). Keep text in the illustrations themselves to a minimum but explain all symbols and abbreviations used.

Example of referring to the figure in text: (Fig. 1)
Example of figure caption: Fig. 1. The distribution of the family Monimiaceae

9. Tables. Please submit tables as editable text and not as images. Tables can be placed either next to the relevant text in the article, or on separate page(s) at the end. Number tables consecutively in accordance with their appearance in the text, place table caption above the table body and place any table notes below the body. Be sparing in the use of tables and ensure that the data presented in them do not duplicate results described elsewhere in the article. Please avoid using vertical rules and shading in table cells.

Example of table caption: Table 1. Case studies and used methods

10. The optimum size of a manuscript is about 3,000–5,000 words. Under the decision (or request) of the Editorial Board methodological and problem articles or reviews up to 8,000–10,000 words long can be accepted.

11. To facilitate the editorial assessment and reviewing process authors should submit "full" electronic version of their manuscript with embedded figures of "screen" quality as a **PDF or DOC file.**

12. We encourage authors to list three potential expert reviewers in their field. The Editorial Board will view these names as suggestions only.

13. Original reviews of submitted manuscripts remain deposited for 3 years.

SCIENTIFIC AND PRACTICAL PEER-REVIEWED JOURNAL "GEOGRAPHY, ENVIRONMENT, SUSTAINABILITY"

No. 02 (v. 12) 2019

FOUNDERS OF THE MAGAZINE: Russian Geographical Society, Faculty of Geography, Lomonosov Moscow State University and Institute of Geography of the Russian Academy of Sciences

The magazine is published with financial support of the Russian Geographical Society.

The magazine is registered in Federal service on supervision of observance of the legislation in sphere of mass communications and protection of a cultural heritage. The certificate of registration: ПИ № ФС77-67752, 2016, December 21.

PUBLISHER
Russian Geographical Society
Moscow, 109012 Russia
Novaya ploshchad, 10, korp. 2
Phone 8-800-700-18-45
E-mail: press@rgo.ru
www.rgo.ru/en

EDITORIAL OFFICE
Lomonosov Moscow State University
Moscow 119991 Russia
Leninskie Gory,
Faculty of Geography, 1806a
Phone 7-495-9391552
Fax 7-495-9391552
E-mail: ges-journal@geogr.msu.ru
www.ges.rgo.ru

DESIGN & PRINTING
Agency «CONNECT»
Moscow, 117452,
Artekovskaya str., 9, korp. 1
Phone: +7 (495) 955-91-53
E-mail: info@connect-adv.ru

Sent into print 04.06.2019
Order N gi219

Format 70 ½ 100 cm/16
11,4 p. sh.
Digital print
Circulation 20 ex.